Advances in Experimental Medicine and Biology 756

Mieczyslaw Pokorski *Editor*

Respiratory Regulation - The Molecular Approach

Springer

Respiratory Regulation - The Molecular Approach

Advances in Experimental Medicine and Biology

For further volumes:
http://www.springer.com/series/5584

Mieczyslaw Pokorski
Editor

Respiratory Regulation - The Molecular Approach

Springer

Editor
Mieczyslaw Pokorski
Department of Respiratory Research
Polish Academy of Sciences
Medical Research Center
Warsaw, Poland

ISSN 0065-2598
ISBN 978-94-007-4548-3 ISBN 978-94-007-4549-0 (eBook)
DOI 10.1007/978-94-007-4549-0
Springer Dordrecht Heidelberg New York London

Library of Congress Control Number: 2012943591

Printed on acid-free paper

Springer is part of Springer Science+Business Media (www.springer.com)

Preface

The book contains the chapters related to the molecular issues of respiratory regulation. The research presented herein was communicated and discussed at the International Conference 'Advances in Pneumology' which was held in Bonn, Germany, on June 17–18, 2011. The chapters are a selection of peer-reviewed manuscripts, mostly original research work, to demonstrate the topics discussed at the conference. Experimental pathophysiology research often seems not very interesting or even useful from the clinical standpoint. This basic research, however, meticulously builds up on previous studies and lays the foundation for clinical advances. The conference is thought as a merge between basic and clinical research concerning respiratory medicine, neural and chemical respiratory regulation, and the mutual relationship between respiration and other neurobiological functions. The essential topics of interest include a wide range of issues, most notably molecular aspects related to gene polymorphism underlying various diseases, cardiovascular-respiratory disorders, infections and inflammatory conditions exemplified by asthma and chronic obstructive pulmonary disease (COPD), respiratory allergy and cough, and immunology. In the chapters presented in this volume the cutting-edge knowledge is communicated and discussed by prominent experts in the areas of science outlined above. I want to thank the invited speakers and other presenters at the conference, as well as the authors and reviewers of the chapters; their contributions certainly will enhance the value of this volume. The clinical advances cannot be reached without the continual efforts to understand the underlying mechanisms of diseases.

The 2011 conference was the fruit of many collaborative efforts. The Local Organizing Committee was headed by Dr. Rüdiger Siekmeier of the Federal Institute for Drugs and Medical Devices (BfArM) in Bonn, Germany. I am indebted to him for his efforts and to all those who extended a helping hand and advice in the organization, in particular Prof. Dr. med. Kurt Rasche of HELIOS Klinikum Wuppertal Lungenzentrum, Klinik für Pneumologie, Allergologie, Schlaf- und Beatmungsmedizin and Anke Hastenrath of Wuppertal, and Dr. Tadeusz M. Zielonka of Warsaw Medical University and the Polish Respiratory Society in Warsaw, Poland.

I also want to thank the non-profit research and academic institution which kindly cooperated and supported the organization of the conference and the publication of this book; in particular the Medical Research Center of the Polish Academy of Sciences in Warsaw, the Polish Respiratory Society, and the Rhein-Ruhr-Stiftung in Essen. Finally, I am also grateful to Max Haring, Ph.D. and Tanja van Gaans of Springer for their expert management of the production process of this book.

Warsaw, Poland — Mieczyslaw Pokorski

Contents

Chapter 1
Neutrophil Extracellular Trap in Human Diseases

Magdalena Arazna, Michal P. Pruchniak, Katarzyna Zycinska, and Urszula Demkow

Abstract NETosis is a unique death pathway that differs from apoptosis and necrosis and depends on the generation of reactive oxygen species (ROS) by NADPH oxidase. During this process, neutrophil extracellular traps (NETs) are created. NETs are extracellular structures composed of chromatin and variety of proteins from cells granules that bind and kill microorganisms. Recently, novel functions of NET have been proposed. It seems that neutrophil traps play an essential role during autoimmunity. They can induce and exacerbate diseases based on immune system malfunction.

Keywords NETosis • Neutrophil extracellular trap • Autoimmune disease • Immunity • Neoplasms

1.1 Introduction

Neutrophils are the most abundant group of cells specialized in defense against pathogens such as bacteria, fungi, and protozoa. They are one of the first responders among inflammatory cells during infections. They migrate towards blood stream to the site of inflammation in response to chemical agents in the process called chemotaxis. After migration to infection site, they act in synergy with several other cells amplifying inflammatory reactions. They synthesize and release specific cytokines which activate endothelial cells, macrophages, and mast cells. However, the main task of neutrophils is to attack microorganisms with the use of their unique repertoire of activities: phagocytosis, degranulation and generation of reactive oxygen species (ROS). It is very important that after elimination of inflammatory factor, neutrophils should be safely removed as it is necessary to keep cellular homeostasis under physiologic conditions. Apoptosis is a physiologic suicide mechanism contributing to cells removal from inflamed tissue. This effect inhibits releasing hazardous intracellular contents. Recently, a new microbicidal mechanism has been described. NETosis is a unique cell death distinct

M. Arazna (✉) • M.P. Pruchniak • U. Demkow
Department of Laboratory Diagnostic and Clinical Immunology of Developmental Age,
Warsaw Medical University, 24 Marszalkowska St, 00-576 Warsaw, Poland
e-mail: magdaarazna@gmail.com

K. Zycinska
Department of Family Medicine, Internal and Metabolic Diseases, Warsaw Medical University,
Systemic Vasculitis Outpatient Clinic, Czerniakowski Hospital, Warsaw, Poland

M. Pokorski (ed.), *Respiratory Regulation - The Molecular Approach*,
Advances in Experimental Medicine and Biology 756, DOI 10.1007/978-94-007-4549-0_1,

from necrosis and apoptosis. This phenomenon was observed in human, bovine, and fish neutrophils (Brinkmann et al. 2004; Köckritz-Blickwede and Nizet 2009; Villanueva et al. 2011; Yousefi et al. 2009). In this mechanism, neutrophils die after releasing 'neutrophil extracellular traps' (NETs), a web-like structure. Mast cells, eosinophils, and plant cells also are able to form extracellular traps (Köckritz-Blickwede and Nizet 2009; Papayannopoulos at al. 2010). Probably, mast cells play more important role than neutrophils in the web formation, during allergic disease (Köckritz-Blickwede and Nizet 2009).

1.2 Characterization of Neutrophil Extracellular Traps

NETs are composed of granular and nuclear constituents of neutrophils (Wartha et al. 2007). Most of proteins and enzymes which act inside the web originate from primary, secondary and tertiary granules. The most common enzymes are elastase, cathepsin G, myeloperoxidase, proteinase-3, bactericidal permeability increasing protein, lactofferin, gelatinase (Wartha et al. 2007; Soehnlein 2009; Li et al. 2010). They cause death of bacteria or at least inhibit their growth. The nuclear components are chromatin fibers and histones (h1, h2a, h2b, h3, h4) (Wartha et al. 2007). The first one creates a backbone on which proteinaceous effectors can reside. No membrane fragments, membrane proteins, and cytoplasmic markers are present in this structure (Wartha et al. 2007). In 2004, Brinkmann et al. (2004) using electron microscopy observed and measured all structures for the first time. They noted that DNA stretches have a diameter of 15–17 nm and a globular protein creates specific domains of around 25 nm. Due to its size, they might aggregate to larger elements of diameters of up to 50 nm. DNase causes disintegration of these unique structures (Wartha et al. 2007). The major components of mast cell extracellular traps are DNA, histones, and mast cell-specific granule proteins such as tryptase. It is important that DNase alone is not sufficient to dismantle NET. In addition, myeloperoxidase can cause degradation of tryptase (Köckritz-Blickwede and Nizet 2009). The origin of DNA in neutrophils and mast cell is nuclear. After releasing the chromatin neutrophils die. Eosinophils form this structure from mitochondrial DNA, although they survive after catapulting their genetic material. Moreover, they react faster, as they need only a few seconds to form a web (Köckritz-Blickwede and Nizet 2009).

The release of NETs can be stimulated by bacteria, fungi, protozoa, and some mediators (e.g., interleukin-8, lipopolysaccharide (LPS), phorbol esters (PMA), and hydrogen peroxide). Also, complement factor (Li et al. 2010) in synergy with GM-CSF or interferon γ/α (INF- γ/α) may play a crucial role in this process. Direct exposure to a variety of different microbial pathogens, both Gram-positive and Gram-negative bacteria, such as *Staphylococcus aureus, Streptococcus pyogenes, Pseudomonas aeruginosa, Mycobacterium tuberculosis, Escherichia coli*, or *Leishmania amazonesis* is sufficient to trigger NET formation (Brinkmann et al. 2004; Köckritz-Blickwede and Nizet 2009; Ramos-Kichik et al. 2009; Urban et al. 2006). Also, fungi like *Candida albicans* stimulate neutrophils in the same manner. Depending on the target, neutrophils extracellular traps act in two ways. They can simply immobilize microorganisms or kill them after capturing. These processes can be blocked pharmacologically by cytochalasin D or by DNase enzyme. Only mature and non-defective granulocytes may express the functional machinery required for the transduction of indispensable signals for NET generation. Depending on the stimulator, the time frame to form NETs varies from 10 min to 4 h. After bacterial stimulation or activator such as phorbol esters, NETs are released within 2–4 h, but neutrophils activated by platelet cells stimulated with LPS, react faster (Köckritz-Blickwede and Nizet 2009).

The role of ROS in innate immunity was recognized for the first time in phagocytes undergoing a 'respiratory burst' upon activation. This process is connected with the superoxide-generating enzyme NADPH oxidase (Nox2). This enzyme is essential for microbial killing and till now, lack of its function was only related to enhanced susceptibility to microbial infections (Rada and Leto 2008).

New evidence strongly indicates that creation of NETs is associated with ROS. It has been noted that hereditary dysfunction of NADPH oxidase prevents neutrophils from creating extracellular traps. Also, a pharmacological influence on ROS enzymes blocks NETosis. As above mentioned, NET formation requires reduced NADPH oxidase activity. Marcos et al. (2010) postulated that chemokine receptors (CXCR) can be related during NETosis. Their studies have shown that promotion of CXCR1, but not CXCR2, signaling pathways provokes the neutrophil trap formation. Whereas CXCR1 stimulate ROS production, CXCR2 have no effect on NADPH oxidase activity and generation of ROS, so it strongly indicates a tight relationship between ROS and NETosis. However, how do ROS promote NET formation remains still unclear (Villanueva et al. 2011; Marcos et al. 2010).

NETs are an important component of immune defense, especially in severe infections. This mechanism is implicated in the pathogenesis of sepsis and autoimmunity (Papayannopoulos at al. 2010). Research describes NETs in the course of appendicitis, pre-eclampsia, systemic lupus erythematosus (SLE), chronic granulomatous disease, small vessels vasculitis, or intestinal spirochetosis (Wartha et al. 2007; Köckritz-Blickwede and Nizet 2009). There is increasing evidence that NETs play an important role in noninfectious diseases. For example recent studies show a commitment of these structures during insemination (Wartha et al. 2007). Sperm cells are caught and clogged into web in female reproductive system, which prevents conception. Recently, more bacterial virulence factors and their defense systems have been identified. Pathogens can resist NET-mediated killing by adding positive charge to their cell surface (Wartha et al. 2007). They can produce a special outer capsule, which reduces bacterial trapping and generate DNases or variety of other enzymes which are able to digest NET structures (Wartha et al. 2007; Köckritz-Blickwede and Nizet 2009). For example, *Streptococcus pneumoniae* causes NET degradation by DNase EndA. Moreover, these bacteria produce capsules rich in D-analynated lipoteichoic acids (LTA) which modify the surface charge; thus this structure prevents entrapment by extracellular traps (Köckritz-Blickwede and Nizet 2009).

1.3 NETs in Neoplasm of Developmental Age

Neoplasms of developmental age account for 0.5–2.0% all cancers causes in human population. Clinical manifestation, progression rate and genetic predisposition are different in children compared with adults. Leukemia, due to maturation arrest and uncontrolled proliferation of cells in bone marrow, is the most common pediatric neoplastic disease. Acute lymphocytic leukemia (ALL) approaches 80% of leukemia cases in children (Bleyer 1990). ALL leads to the accumulation of malignant lymphoblasts in bone marrow and peripheral blood. Acute myeloid leukemia (AML) and acute non-lymphoblastic leukemia (ANLL) occur rarely.

The diagnosis of leukemia relies on immunocytochemistry, immunophenotyping, cytogenetics, and gene rearrangement detection. Nowadays, there are many innovative, specific molecular and cellular techniques to confirm the diagnosis. The improved sensitivity of applied tests has made possible to establish an early presence pathological cells in bone marrow and peripheral blood.

Leukemia is the most common cause of disease-related death in childhood. The patients with acute leukemia are at high risk for infections complications (Hirotsu and Akatsuka 1991; Maranda et al. 2010). Serious, life threatening infections remain a major cause of morbidity and mortality in this group of patients. In 1970–1990 large scale clinical trials regarding therapy in ALL reported that 90% of patients die within 4 years. In the 1990s, more than 70% of all children with ALL, who were younger than 10 years at the time of diagnosis, reached a complete and durable remission due to modern therapy. Nowadays, in the group of children with acute lymphocytic leukemia, the mortality rate from infection during chemotherapy is around 1–3% (Hirotsu and Akatsuka 1991). Neutropenia, the use of corticosteroids, broad spectrum antibiotics, central venous lines, presence of mucositis, and surgery procedures are among common underlying causes of infections in leukemic

patients (Hirotsu and Akatsuka 1991; Klaassen et al. 2000). Furthermore, other factors such as impaired functional capabilities of neutrophils may contribute to severe infections before and after chemotherapy. Several studies have shown the presence of defective neutrophil function (i.e., ROS formation) in patients with acute leukemia (Hubel et al. 1999). However most of them were performed in adult population and only a few in children, who usually undergo more intensive chemotherapy compared with adults.

Multidrug chemotherapy combinations are standard regiments in the treatment of leukemia in children significantly improving survival of patients. Chemotherapeutic agents act by the multiple mechanism, including incorporation into DNA and inhibition of DNA replication, cell membrane damage or free radical generation (Bleyer 1990). Invasive infections are the common complications of chemotherapy in leukemic children. To-date, no study has been undertaken to explore if NET formation is defective in patients with acute leukemias and how this mechanism is altered by chemotherapy.

NET formation is initiated by the production of ROS. ROS constitute an essential signal leading to the induction of unique cell death program connected with NETs (Köckritz-Blickwede and Nizet 2009; Yousefi et al. 2009). This is a physiologic suicide mechanism for elimination of neutrophils from inflamed tissue and it has been named NETosis. Oxidative burst may be hampered by chemotherapeutic agents, bacterial products and inflammatory mediators released by leukemic blasts and tumor infiltrating immune cells. Interference with ROS generation by chemotherapeutic agents may block the formation of the web. Moreover, NET formation requires fully mature neutrophils, thus immature or defective neutrophils released from leukemic bone marrow may not express the functional machinery required for the transduction of external signals (Martinelli et al. 2004). The negatively charged DNA backbone of NETs also provides a framework for the activation of the contact system, including serum-derived serine proteases, factor XI, factor XII, and plasma kallikrein, together with the non-enzymatic high-molecular-weight-cofactor and kininogen (Oehmcke et al. 2009). NETs also produced after platelet-mediated neutrophil activation and the accumulation of NETs and their component proteases may promote vascular endothelial injury and ischemia (Clark et al. 2007; Oehmcke et al. 2009). These events may contribute to cardiovascular complication including thrombosis in leukemic patients.

The immune system is a complex and decentralized machinery present in multicellular organisms and is composed of many types of proteins, cells, organs, and tissues. Its main goal is to provide a generic and immediate defense against pathogens like bacteria, fungi, and protozoa. In addition, it can identify and destroy tumor or virus carrying cells. Due to its complex nature every disorder can provoke different reaction: autoimmune diseases, immunodeficiency, cancer, or inflammatory diseases (Beck and Gail 2007).

1.4 NETs in Autoimmunity

Autoimmunity is defined as a failure in self-recognition of the body. This kind of failure of immune regulation is responsible for autoimmune diseases. During immune system malfunction, a variety of antibodies attack host structures. Not only do these antibodies influence in a direct manner various body parts, but they also can recruit cytotoxic T cells which multiply devastating effect. Recently, it has been postulated that NETs can be related to autoimmune diseases either through the initiation or propagation of the disease (Papayannopoulos and Zychlinsky 2009). In this paper we will focus on two immune-related syndromes: ANCA-associated vasculitis and systemic lupus erythematosus.

Anti-neutrophil cytoplasmic antibodies (ANCA)-associated vasculitis (AAV) is a life threatening autoimmune disease characterized by necrotizing vasculitis of small and medium sized vessels. Pathogenesis of AAV is complex, with a number of overlapping effector limbs. ANCAs are of major importance for disease and cause vasculitis interacting with neutrophils upon specific triggers

(Ozaki 2007; Jennette and Falk 1998; van Rossum et al. 2005; Wilde et al. 2010). ANCAs with specificity for either proteinase-3 (PR3-ANCA) in Wegener's granulomatosis or myeloperoxidase (MPO-ANCA) in Churg-Strauss syndrome are a hallmark of AAV and had a pivotal role in disease development (Gómez-Puerta et al. 2009; Wilde et al. 2010; van Rossum et al. 2005). ANCAs themselves are thought to be pathogenic (Ozaki 2007). Furthermore, ANCAs promote deregulation of neutrophils and monocytes facilitating endothelial damage. The endothelium is also activated and neutrophil adherence is enhanced. The initial damage leads to a cascade of reactions resulting in leucocyte tissue infiltration (Gómez-Puerta et al. 2009). T-cell driven granuloma formation and further damage. ANCAs bind to neutrophils and endothelial cells having differential but synergistic effects on both cell types (Wilde et al. 2010). ANCAs bind to membrane-bound PR3/MPO on neutrophils. This interaction with ANCAs results in activation and finally in release of cytotoxic superoxide and serine proteases (such as PR3). Membrane-bound MPO-PR3 is expressed constitutively by neutrophils and can be enhanced by proinflammatory cytokines, such as tumor necrosis factor alpha (TNF-α) and interferon-γ (INF-γ). Priming of neutrophils also enhances adhesion to endothelial cells along with a further increase of membrane MPO/PR3 expression (van Rossum et al. 2005; Rarok et al. 2003). Thus, deregulation occurs in close contact with the vascular endothelium, resulting in vasculitic damage. The interaction of ANCAs with endothelial cells enhances expression of adhesion molecules like E/P- selectin and vascular cell adhesion molecule (Ara et al. 2001). In the late 1980s, it was discovered that PR3 was the main antigen for cytoplasmic-ANCA, whereas MPO was shown to be the antigenic target of perinuclear-ANCA in patients with vasculitis. Recent findings bring up a new hypothesis on the induction of ANCAs by immune responses against Gram-positive or Gram-negative bacteria. Pathogens like *Staphylococcus aureus* bear genetic sequences that are complementary to the human PR3 gene pointing to an exogenous origin of cPR3 transcripts. Chronic nasal carriage of *S. aureus* has been demonstrated to increase the risk for disease relapse. T cells are also usually found within granulomas in lesions present in AAV (Stegeman et al. 1994; Tadema et al. 2010). Elevated levels of markers of T-cell activity, such as soluble interleukin-2 (IL-2) receptor, neopterin and soluble CD30 as measured in the circulation have been shown to be associated with disease activity (Wilde et al. 2010; Schmidt et al. 1992).

As above mentioned, the anti-neutrophil cytoplasmic autoantibodies formed during small-vessel vasculitis have major effects upon neutrophils; thus they can be potent NETosis inductors. Two types of ANCA antibodies are abundant in AVV. c-ANCA are specific for the serine proteinase-3. pANCA called MPO-ANCA type has specificity for myeloperoxidase. The interaction of p-ANCA and c-ANCA with neutrophils surface results in the production of ROS (Papayannopoulos and Zychlinsky 2009; Kallenberg 2010). Due to the fact that production of ROS plays an essential role in the neutrophil traps-creation pathway, it is believed that ANCA are strongly associated with continuous NETs formation. Moreover, microbial factors, in particular *Staphylococcus aureus* and Gram-negative bacteria, simultaneously with anti-neutrophil cytoplasmic autoantibodies seem to be involved in AVV induction (Kallenberg 2010). On the other hand, it has been shown that NET can occur in an autoinflammatory structure in the absence of microbial infection. Unfortunately, the basic mechanism that includes exacerbation of AVV and neutrophil extracellular traps is still not known (Kessenbrock et al. 2009).

Systemic lupus erythematosus (SLE) is a chronic systemic autoimmune connective tissue disease characterized by various manifestations often demonstrating a waxing-waning course. It is a Type III hypersensitivity reaction caused by antibody-immune complex formation (Ballestar et al. 2006; Rahman and Isenberg 2008). SLE does run in families, but no single casual gene has been identified. Genes which contain risk variants for SLE are IRF5, PTPN22 (Orozco et al. 2011; Rahman and Isenberg 2008). The second mechanism may be due to environmental factors such as viruses and bacteria (Sebastiani and Galeazzi 2009). Many patients with SLE exhibit symptoms that involve skin and joints, other symptoms of SLE vary widely between patients. SLE most often harms the heart, lungs, liver, kidneys and nervous system. The course of the disease is unpredictable, with periods of

illness (flares) alternating with remissions (Rahman and Isenberg 2008). The disease occurs nine times more often in women than in men, especially in women in child-bearing years ages 15–35 and is also more common in those of non-European descent (Krishnan and Hubert 2006; Tandon et al. 2004). Serologic markers play an important role in the assessment of disease activity in SLE, including assessment of anti-double-stranded DNA and complement levels. Serological markers are critical for the understanding of the pathogenesis of the disease. Serologic markers have an imperfect correlation with disease activity and cannot substitute alone for a direct assessment of clinical benefit (Rahman and Isenberg 2008). Antinuclear antibody (ANA) testing and anti-extractable nuclear antigen (ant-ENA) form the mainstay of serologic testing for SLE (Agarwal et al. 2009). Clinically, the most widely used method is indirect immunofluorescence. The pattern of fluorescence suggests the type of antibody present in the patient's serum. ANA screening yields positive results in many connective tissue disorders and may occur in normal individuals. Subtypes of antinuclear antibodies include anti-Smith (Sm) and anti-double stranded DNA (dsDNA) antibodies (which are linked to SLE) and anti-histone antibodies (which are linked to drug-induced lupus). Anti-dsDNA antibodies are highly specific for SLE. They are present in 70% of cases, whereas they appear in only 0.5% of people without SLE. Other ANAs that may occur in SLE sufferers are anti-U1 RNP (also in systemic sclerosis), SS-A (or anti-Ro), and SS-B (or anti-La also in Sjögren's syndrome). The lupus erythematosus (LE) cell test was previously commonly employed for the diagnosis, but it is no longer in use because the LE cells are only found in 50–77% of SLE cases, and they are also found in other syndromes (Rahman and Isenberg 2008; Buyon and Clancy 2003).

Recent evidence indicates that neutrophils traps may play an important role in the induction of autoimmune responses and organ damage and in the pathogenesis of systemic lupus erythematosus (Villanueva et al. 2011). As above mentioned, the backbone of the neutrophil extracellular trap consists of double stranded DNA which is a prime target for auto-antibodies present in SLE. The possible mechanism includes the formation of NET-antibody complexes. The accumulation of these structures can provoke vascular endothelium damage and can lead to thrombosis or heart-failure (Oehmcke et al. 2009). Moreover, blockade of NETs degradation has been observed in some SLE cases. Specific antibodies bind to NET structures, where they can be recognized by DNAse enzymes. Preventing DNase1 access to NETs stops *in situ* clearance. A prolonged life time of neutrophil traps is devastating for the SLE patient because dangerous complexes are being created in enormous amounts. Villanueva et al. (2011) postulate that a distinct neutrophil fraction, called low density granulocytes (LDGs), is strongly involved in NETs formation. LDGs are found in peripheral blood of adult SLE patients. These specific cells are not characterized by any specific surface markers. They can differ from normal neutrophils only by their density, although LDGs nuclear morphology suggests that this population of cells is slightly immature. The mechanisms by which LDGs are more potent to make NETs are still unclear, but a crucial role for elastase, reactive oxygen species, and even the cyto-skeleton has been proposed (Villanueva et al. 2011; Denny et al. 2010). On the other hand, it is certain that immature neutrophils cannot create NESs due to their lack of specific receptors. Even though low density granulocytes are considered to have immature phenotype, they still have ability to create extracellular traps. This phenomenon can be contributed to a high level of expression of mRNA that encodes the neutrophil serine proteases; the process which is strongly associated with NETosis (Villanueva et al. 2011).

Since we have learned about neutrophil extracellular traps just about several years ago, we still have gaps in the basic knowledge. During recent years, we have discovered that these DNA-traps are not only related to one type of cells, but at least to three types of granulocytes. We know what basic agents induce NETosis, thus we can procure its creation *in vitro*. These unique structures seem destined to surprise us many more times.

Conflicts of interest: The authors declare no conflicts of interest in relation to this article.

References

Agarwal, S., Harper, J., & Kiely, P. D. (2009). Concentration of antibodies to extractable nuclear antigens and disease activity in systemic lupus erythematosus. *Lupus, 18*, 407–412.

Ara, J., Mirapeix, E., Arrizabalaga, P., Rodriguez, R., Ascaso, C., Abellana, R., Font, J., & Darnell, A. (2001). Circulating soluble adhesion molecules in ANCA-associated vasculitis. *Nephrology, Dialysis, Transplantation, 16*, 276–285.

Ballestar, E., Esteller, M., & Richardson, B. C. (2006). The epigenetic face of systemic lupus erythematosus. *Journal of Immunology, 176*, 7143–7147.

Beck, G., & Gail, S. H. (2007). Immunity and the invertebrates. *Scientific American, 275*, 60–66.

Bleyer, W. A. (1990). Acute lymphoblastic leukemia in children. Advances and prospectus. *Cancer, 65*, 689–695.

Brinkmann, V., Reichard, U., Goosmann, Ch, Fauler, B., Uhlemann, Y., Weiss, D. S., Weinrauch, Y., & Zychlinsky, A. (2004). Neutrophil extracellular traps kill bacteria. *Science, 303*, 1532–1535.

Buyon, J. P., & Clancy, R. M. (2003). Maternal autoantibodies and congenital heart block: Mediators, markers, and therapeutic approach. *Seminars in Arthritis and Rheumatism, 33*, 140–154.

Clark, S. R., Ma, A. C., Tavener, S. A., McDonald, B., Goodarzi, Z., Kelly, M. M., Patel, K. D., Chakrabarti, S., McAvoy, E., Sinclair, G. D., Keys, E. M., Allen-Vercoe, E., DeVinney, R., Doig, Ch. J., Green, F. H. Y., & Kubes, P. (2007). Platelet TLR4 activates neutrophil extracellular traps to ensnare bacteria in septic blood. *Nature Medicine, 13*, 463–469.

Denny, M. F., Yalavarthi, S., Zhao, W., Thacker, S. G., Anderson, M., Sandy, A. R., McCune, W. J., & Kaplan, M. J. (2010). A distinct subset of proinflammatory neutrophils isolated from patients with systemic lupus erythematosus induces vascular damage and synthesizes type I IFNs. *Journal of Immunology, 184*, 3284–3297.

Gomez-Puerta, J. A., Hernandez-Rodríguez, J., Lopez-Soto, A., & Bosch, X. (2009). Respiratory disease antibody-associated vasculitides and antineutrophil cytoplasmic. *Chest, 136*, 1101–1111.

Hirotsu, T., & Akatsuka, J. (1991). Infectious complications in childhood leukemia. *Acta Paediatrica Japanese, 33*, 564–572.

Hubel, K., Hegener, K., Schnell, R., Mansmann, G., Oberhause, F., Staib, P., Diehl, V., & Engert, A. (1999). Suppressed neutrophil function as a risk factor for severe infection after cytotoxic chemotherapy in patient with acute nonlymphocytic leukemia. *Annals of Hematology, 78*, 73–77.

Jennette, J. C., & Falk, R. J. (1998). Pathogenesis of the vascular and glomerular damage in ANCA-positive vasculitis. *Nephrology, Dialysis, Transplantation, 13*, 16–20.

Kallenberg, C. G. (2010). Pathophysiology of ANCA-associated small vessel vasculitis. *Current Rheumatology Reports, 12*, 399–405.

Kessenbrock, K., Krumbholz, M., Schonermarck, U., Back, W., Gross, W. L., Werb, Z., Grone, H. J., Brinkmann, V., & Jenne, D. E. (2009). Netting neutrophils in autoimmune small-vessel vasculitis. *Nature Medicine, 15*, 623–625.

Klaassen, R. J., Goodman, T. R., Pham, B., & Doyle, J. J. (2000). 'Low-risk' prediction rule for paediatric oncology patients presenting with fever and neutropenia. *Journal of Clinical Oncology, 18*, 1012–1019.

Kockritz-Blickwede, M., & Nizet, V. (2009). Innate immunity turned inside-out: Antimicrobial defense by phagocyte extracellular traps. *Journal of Molecular Medicine, 87*, 775–783.

Krishnan, E., & Hubert, H. B. (2006). Ethnicity and mortality from systemic lupus erythematosus in the US. *Annals of the Rheumatic Diseases, 65*, 1500–1505.

Li, P., Li, M., Lindberg, M. R., Kennett, M. J., Xiong, N., & Wang, Y. (2010). PAD4 is essential for antibacterial innate immunity mediated by neutrophil extracellular traps. *The Journal of Experimental Medicine, 207*(9), 1853–1862.

Maranda, L., Seweryn, M., Giebel, S., Holowiecki, J., Piatkowska-Jakubas, B., Wegrzyn, J., Skotnicki, A., Kielbinski, M., Kuliczkowski, K., Paluszewska, M., Jedrzejczak, W. W., Dutka, M., Hellmann, A., Flont, M., Zdziarska, B., Palynyczko, G., Konopka, L., Szpila, T., Gawronski, K., Sulek, K., Sokolowski, J., Kloczko, J., Warzocha, K., & Robak, T. (2010). Infectious complications in patients with acute myeloid leukemia treated according to the protocol with daunorubicin and cytarabine with or without addition of caladribine. A multicenter study by the Polish Adult Leukemia Group (PALG). *International Journal of Infectious Diseases, 14*, e132–e140.

Marcos, V., Zhou, Z., Yildirim, A. O., Bohla, A., Hector, A., Vitkov, L., Wiedenbauer, E. M., Krautgartner, W. D., Stoiber, W., Belohradsky, B. H., Rieber, N., Kormann, M., Koller, B., Roscher, A., Roos, D., Griese, M., Eickelberg, O., Doring, G., Mall, M. A., & Hartl, D. (2010). CXCR2 mediates NADPH oxidase-independent neutrophil extracellular trap formation in cystic fibrosis airway inflammation. *Nature Medicine, 16*, 1018–1023.

Martinelli, S., Urosevic, M., Daryadel, A., Oberholzer, P. A., Baumann, C., Fey, M. T., Dummer, R., Simon, H. U., & Yousefi, S. (2004). Induction of genes mediating interferon-dependent extracellular trap formation during neutrophil differentiation. *Journal of Biological Chemistry, 279*, 44123–44132.

Oehmcke, S., Morgelin, M., & Herwald, H. (2009). Activation of the human contact system on neutrophil extracellular traps. *Journal of Innate Immunity, 1*, 225–230.

Orozco, G., Eyre, S., Hinks, A., Bowes, J., Morgan, A. W., Wilson, A. G., Wordsworth, P., Steer, S., Hocking, L., Thomson, W., Worthington, J., & Barton, A. (2011). Study of the common genetic background for rheumatoid arthritis and systemic lupus erythematosus. *Annals of the Rheumatic Diseases, 70*, 463–468.

Ozaki, S. (2007). ANCA-associated vasculitis: Diagnostic and therapeutic strategy. *Allergology International, 56*, 87–96.

Papayannopoulos, V., & Zychlinsky, A. (2009). NETs: A new strategy for using old weapons. *Trends in Immunology, 30*, 513–521.

Papayannopoulos, V., Metzler, K. D., Hakkim, A., & Zychlinsky, A. (2010). Neutrophil elastase and myeloperoxidase regulate the formation of neutrophil extracellular traps. *The Journal of Cell Biology, 191*(3), 677–691.

Rada, B., & Leto, T. L. (2008). Oxidative innate immune defenses by Nox/Duox family NADPH oxidases. *Contributions to Microbiology, 15*, 164–187.

Rahman, A., & Isenberg, D. A. (2008). Systemic lupus erythematosus. *The New England Journal of Medicine, 358*, 929–939.

Ramos-Kichik, V., Mondragon-Flores, R., Mondragon-Castelan, M., Gonzalez-Pozos, S., Muniz-Hernandez, S., Rojas-Espinosa, O., Chacon-Salinas, R., Estrada-Parra, S., & Estrada-García, I. (2009). Neutrophil extracellular traps are induced by *Mycobacterium tuberculosis*. *Tuberculosis, 89*, 29–37.

Rarok, A. A., Limburg, P. C., & Kallenberg, C. G. (2003). Neutrophil-activating potential of antineutrophil cytoplasm autoantibodies. *Journal of Leukocyte Biology, 74*, 3–15.

Schmidt, W. H., Heesen, C., Csernok, E., Rautmann, A., & Gross, W. L. (1992). Elevated serum levels of soluble interleukin-2 receptor in patients with Wegener's granulomatosis. Association with disease activity. *Arthritis and Rheumatism, 35*, 1088–1096.

Sebastiani, G. D., & Galeazzi, M. (2009). Infection-genetics relationship in systemic lupus erythematosus. *Lupus, 18*, 1169–1175.

Soehnlein, O. (2009). An elegant defense: How neutrophils shape the immune response. *Trends in Immunology, 30*(11), 511–512.

Stegeman, C. A., Tervaert, J. W., Sluiter, W. J., Manson, W. L., de Jong, P. E., & Kallenberg, C. G. (1994). Association of chronic nasal carriage of *Staphylococcus Aureus* and higher relapse rates in Wegener granulomatosis. *Annals of Internal Medicine, 120*, 12–17.

Tadema, H., Abdulahad, W. H., Lepse, N., Stegeman, C. A., Kallenberg, C. G., & Heeringa, P. (2010). Bacterial DNA motifs trigger ANCA production in ANCA-associated vasculitis in remission. *Rheumatology, 50*, 689–696.

Tandon, A., Ibanez, D., Gladman, D. D., & Urowitz, M. B. (2004). The effect of pregnancy on lupus nephritis. *Arthritis and Rheumatism, 50*, 3941–3946.

Urban, C. F., Reichard, U., Brinkmann, V., & Zychlinsky, A. (2006). Neutrophil extracellular traps capture and kill *Candida albicans* yeast and hyphal forms. *Cellular Microbiology, 8*(4), 668–676.

van Rossum, A. P., Limburg, P. C., & Kallenberg, C. G. (2005). Activation, apoptosis, and clearance of neutrophils in Wegener's granulomatosis. *Annals of the New York Academy of Sciences, 1051*, 1–11.

Villanueva, E., Yalavarthi, S., Berthier, C. C., Hodgin, J. B., Khandpur, R., Lin, A. M., Rubin, C. J., Zhao, W., Olsen, S. H., Klinker, M., Shealy, D., Denny, M. F., Plumas, J., Chaperot, L., Kretzler, M., Bruce, A. T., & Kaplan, M. J. (2011). Netting neutrophils induce endothelial damage, infiltrate tissues, and expose immunostimulatory molecules in systemic lupus erythematosus. *Journal of Immunology, 187*, 538–552.

Wartha, F., Beiter, K., Normark, S., & Henriques-Normark, B. (2007). Neutrophil extracellular traps: Casting the NET over pathogenesis. *Current Opinion in Microbiology, 10*, 52–56.

Wilde, B., Thewissen, M., Damoiseaux, J., van Paassen, P., Witzke, O., & Tervaert, J. W. (2010). T cells in ANCA-associated vasculitis: What can we learn from lesional versus circulating T cells? *Arthritis Research & Therapy, 12*, 204.

Yousefi, S., Mihalache, C., Kozlowski, E., Schmidt, I., & Simon, H. U. (2009). Viable neutrophils release mitochondrial DNA to form neutrophil extracellular traps. *Cell Death and Differentiation, 16*, 1438–1444.

Chapter 2
Tiotropium Increases PPARγ and Decreases CREB in Cells Isolated from Induced Sputum of COPD Patients

A. Holownia, R.M. Mroz, T. Skopinski, A. Kolodziejczyk, E. Chyczewska, and J.J. Braszko

Abstract Chronic obstructive pulmonary disease (COPD) is characterized by progressive airflow limitation and chronic inflammation of airways and lung parenchyma. Our aim was to assess two important elements of intracellular signaling involved in regulation of inflammation in COPD in patients subjected to long-acting beta2-agonist or long-acting beta2-agonist plus long-acting anti-muscarinic: peroxisome proliferator-activated receptor gamma (PPARγ) protein, which has antiinflammatory and immunomodulatory properties and cAMP response element binding protein (CREB) and activated (CREB-P) protein which has histone acetyltransferase activity and increases histone acetylation and transcriptional activation of chromatin. Twenty one stable COPD patients (18 males and 3 females, mean age 65 years) receiving 12 μg B.I.D formoterol were assayed before and after 3 month add-on therapy, consisting of 18 μg Q.D. tiotropium. In all patients, sputum induction, spirometry, lung volumes, and DLCO were performed before and after therapy. Sputum cells were isolated and processed to isolate cytosolic and nuclear fractions. PPARγ, CREB, or CREB-P proteins were quantified in subcellular fractions using Western blot. Tiotropium add-on therapy improved respiratory parameters: FEV1 and lung volumes. After therapy mean expression of PPARγ in cell nuclei was significantly increased by about 180%, while CREB and phosphorylated CREB levels in cytosol and nuclei were decreased by about 30%. Our data show that the mechanism whereby tiotropium reduces exacerbations may be associated not only with persistent increase in airway functions and reduced hyperinflation mediated by muscarinic receptors, but also with possible anti-inflammatory effects of the drug, involving increased PPARγ and decreased CREB signaling.

Keywords COPD • CREB • Histone acetylation • PPARγ • Tiotropium

A. Holownia (✉) • T. Skopinski • A. Kolodziejczyk • E. Chyczewska • J.J. Braszko
Department of Clinical Pharmacology, Medical University of Bialystok,
Waszyngtona 15a, 15-279 Bialystok, Poland
e-mail: holow_sinai@hotmail.com

R.M. Mroz
Department of Chest Diseases and Tuberculosis, Medical University of Bialystok,
Waszyngtona 15a, 15-279 Bialystok, Poland

M. Pokorski (ed.), *Respiratory Regulation - The Molecular Approach*,
Advances in Experimental Medicine and Biology 756, DOI 10.1007/978-94-007-4549-0_2,

2.1 Introduction

Irreversible and progressive airflow limitation is a landmark of chronic obstructive pulmonary disease (COPD), the only major disease with an increasing death rate (Viegi et al. 2007). In COPD, airflow obstruction is caused by increased activity of parasympathetic system and chronic inflammation of the airways and lung parenchyma, very frequently associated with chronic tobacco smoking (Viegi et al. 2007). COPD is considered as a fatal disease, but it can be managed, controlled and slowed down, however a necessary step is smoking cessation. In pharmacotherapy of moderate to severe COPD long-acting bronchodilators are used (Global Strategy for the Diagnosis, Management and Prevention of COPD 2008). Currently approved drugs for the treatment of COPD are: long-acting beta2-agonists (LABA), i.e., formoterol, salmeterol, indacaterol, combined with long-acting antimuscarinic agents (LAMA) such as tiotropium bromide (Meyer et al. 2011). Formoterol, a selective LABA, increases adenylyl cyclase and cyclic adenosine monophosphate (cAMP) resulting in relaxation of bronchial smooth muscles (Kaur et al. 2008). Tiotropium acts as antagonist of M3 and M1 muscarinic receptors, modulating inositol 1,4,5-trisphosphate (IP3) and 1,2-diacyl-glycerol (DAG) signaling pathways (Casarosa et al. 2010). Drug binding produces prolonged improvement in clinical respiratory parameters and usually a single inhaled dose reverses compromised respiratory function (Kato et al. 2006). Our previous data indicate that tiotropium altered pharmacodynamic parameters of cholinergic M3 receptors and increased histone acetylation in chromatin of inflammatory cells migrating to the airways of COPD patients (Holownia et al. 2010). However, the possible anti-inflammatory mechanisms related to tiotropium are unknown. Our aim was to assess important elements of cytosolic and nuclear inflammatory signaling - expression and activation (Ser133 phosphorylation) of cAMP response element binding protein (CREB), and peroxisome proliferator-activated receptor gamma (PPARγ) in cells isolated from induced sputum of COPD patients before and after tiotropium therapy. CREB is an end-point and integration site of several signaling pathways, with histone acetyltransferase (HAT) activity (Lim et al. 2011), whether PPARγ acts as nuclear hormone receptor regulating glucose metabolism and the expression of inflammatory cytokines with possible histone deacetylase (HDAC) activity (Miard and Fajas 2005).

2.2 Methods

2.2.1 Subjects and Treatment

Twenty one (18 males and three females, mean age 65 years) COPD patients with stable disease, defined according to Global Initiative for Chronic Obstructive Lung Disease (GOLD) guidelines (Global Strategy for the Diagnosis, Management and Prevention of COPD 2008) were enrolled into the study. All patients with COPD had airflow limitation (FEV1 < 80% predicted, FEV1/FVC < 70%, GOLD stage 2–4) and received stable formoterol therapy for 4 weeks preceding inclusion. All subjects were characterized with respect to sex, age, smoking history, COPD symptoms, comorbidity, and current medical treatment. Exclusion criteria included the following: other systemic diseases, other lung diseases apart from COPD and lung tumors, pulmonary infection and antibiotic treatment 4 weeks before inclusion, no inhaled or oral glucocorticosteroids in the 3 months preceding inclusion. All patients gave their informed consent after a full discussion of the nature of the study, which had been approved by a local Ethics Committee. No patient in the study had symptoms nor was treated for COPD exacerbation during at least 2 months preceding the day of inclusion.

The lung function and DLCO tests were performed with body box (Elite DL, Medgraphics, USA). The measurement was performed using standard protocols according to American Thoracic Society guidelines. Twenty one patients underwent 4 week stable therapy with 12 μg B.I.D. formoterol and subsequently were subjected to sputum induction. Next patients were treated for 12 additional weeks with add-on 18 μg Q.D. tiotropium and their sputum was collected.

2.2.2 *Sputum Induction and Processing*

Sputum was induced by the inhalation of a 4.5% hypertonic aerosol saline solution, generated by an ultrasonic nebulizer (Voyager, Secura Nova; Warsaw, Poland) (Loh et al. 2005). Throughout the procedure, subjects were encouraged to cough and to expectorate into a plastic container. Three flow volume curves were performed before and after each inhalation, and the best FEV1 was recorded. Induction of sputum was stopped if the FEV1 value fell by at least 20% from baseline or if troublesome symptoms occurred. Samples were processed within 15 min after the termination of the induction.

Induced sputum samples were solubilized in equal volumes of 0.1% dithiothreitol (Sigma Chemicals Co, Poznan, Poland) in Hanks solution and incubated for 15 min in an ice bath. Cell suspension was then rinsed twice with Hanks solution, filtered by a nylon membrane and centrifuged (1,000 rpm) on Histopaque 1077. Isolated cells were further processed to obtain cytosolic and nuclear fractions.

To isolate subcellular fractions, sputum cells were centrifuged, resuspended in cold hypotonic buffer containing 10 mM HEPES, pH 7.9, 1.5 mM $MgCl_2$, 10 mM KCl, 50 mM dithiothreitol, 100 mM phenanthroline, 1 mg/ml pepstatin, 100 mM trans-epoxysuccinyl-L-leucylamido-(4-guanidino)butane, 100 mM 3,4-dichloroisocoumarin, 10 mM NaF, 100 mM sodium orthovanadate, 25 mM b-glycerophosphate and centrifuged at 14,000 × *g* for 5 min at 4°C (Mroz et al. 2007). Cells were then lysed in a solution of the same buffer containing 0.2% (v/v) Nonidet P- 40 for 10 min on ice and centrifuged at 14,000 × *g* for 10 min at 4°C. The supernatant was collected as a cytosolic extract. The remaining pellet was resuspended in extraction buffer (20 mM HEPES, pH 7.9, 420 mM NaCl, 1.5 mM MgCl2, 0.2 mM EDTA, 25% (v/v) glycerol, 100 mM 3,4-dichloroisocoumarin), incubated for 15 min at 4°C, and centrifuged at 14,000 × *g* for 10 min at 4°C. The supernatant including soluble nuclear protein was collected as a nuclear extract.

Cytosolic and nuclear fractions were evaluated for the expression of CREB and CREB-P proteins, while PPARγ was assessed only in nuclear fractions using sodium dodecyl sulfate polyacrylamide gel electrophoresis (SDS-PAGE) and Western blots. Sample proteins were separated in reducing conditions, transferred onto polyvinylidene difluoride (PVDF) membranes, and incubated with specific rabbit monoclonal antibodies against human CREB or PPARγ proteins (Abcam, Cambridge, USA). After washing, bound antibody was detected using appropriate secondary anti-rabbit antibody (Abcam, Cambridge, USA) linked to horseradish peroxidase. The bound complexes were detected using enhanced chemiluminescence (ECL, Amersham, GE Healthcare, Little Chalfont, UK) and quantified using Quantity One software (BioRad, Warsaw, Poland). The constitutively expressed protein – β-actin, served as a loading control and the data were quantified in respect to β-actin expression. For the negative control study, membranes were treated similarly but without the addition of primary antibody. Protein levels were measured using a BCA kit (Sigma-Aldrich, Poznan, Poland).

Statistical analysis was performed using statistical package – Statistica (Statsoft, Cracow, Poland) using nonparametric Wilcoxon test for paired data. The data were expressed as means ± SD. $P < 0.05$ was as considered statistically significant.

2.3 Results

Table 2.1 and Fig. 2.1 show respiratory parameters: forced expiratory volume in one second (FEV1), inspiratory capacity (IC), residual volume (RV) and residual volume divided by total lung capacity (RV/TLC) and biochemical data: cytosolic and nuclear CREB and phosphorylated CREB as well as nuclear PPARγ levels in cells isolated from induced sputum of COPD patients before and after tiotropium ad-on therapy. Representative Western blot pictures of CREB, CREB-P and PPARγ protein are shown (Fig. 2.1). Therapy improved lung function parameters. After therapy, mean FEV1 increased by 14% ($P < 0.05$), IC increased by 14% ($P < 0.05$), residual volume was reduced by 13% ($P < 0.05$), and RV/TLC decreased by 11% ($P < 0.05$) from baseline.

Table 2.1 Respiratory parameters: forced expiratory volume in 1 s (FEV1), inspiratory capacity (IC), residual volume (RV) and residual volume divided by total lung capacity (RV/TLC) and cytosolic and nuclear CREB and phosphorylated CREB as well as nuclear PPARγ levels (relative units) in cells isolated from induced sputum of COPD patients before and after tiotropium add-on therapy

	Formoterol(F)		Formoterol + Tiotropium (FT)	
FEV1 (L)	1.52 ± 0.18		1.73 ± 0.19*	
% predicted	52%		56%	
IC (L)	1.87 ± 0.13		2.14 ± 0.22*	
% predicted	62%		71%	
RV (L)	3.39 ± 0.21		2.92 ± 0.23*	
% predicted	152%		132%	
RV/TLC	53 ± 6%		47 ± 7%*	
	Cytosol	Nuclei	Cytosol	Nuclei
CREB	100.0 ± 21.3	100.0 ± 25.4	75.4 ± 18.4*	64.3 ± 26.2*
CREB-P	100.0 ± 37.2	100.0 ± 31.3	71.2 ± 19.3*	112.4 ± 7.5
PPARγ	100.0 ± 33.9	–	281.0 ± 45.7**	–

*P < 0.05; **P < 0.01 – comparing to corresponding data from F-monotherapy

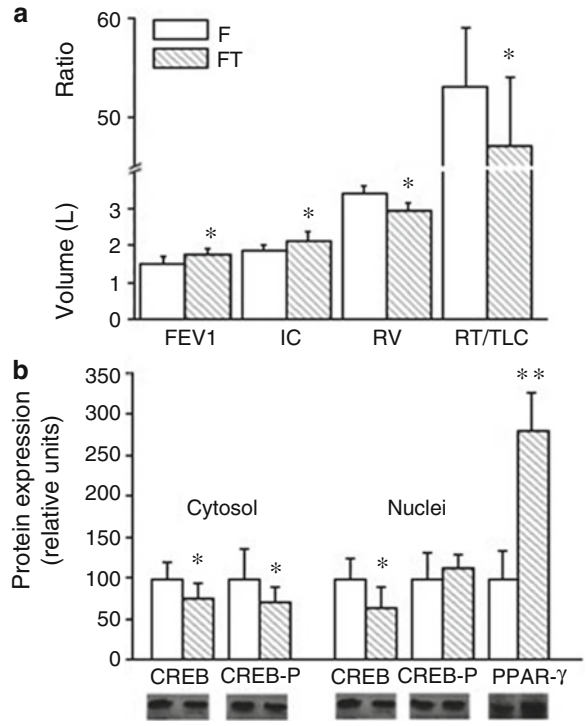

Fig. 2.1 **(a) Respiratory parameters:** forced expiratory volume in one second (*FEV1*), inspiratory capacity (*IC*), residual volume (*RV*) and residual volume divided by total lung capacity (*RV/TLC*); **(b) Cytosolic and nuclear CREB, phosphorylated CREB, and nuclear PPARγ** (relative units) in cells isolated from induced sputum of COPD patients before and after tiotropium add-on therapy. Representative Western blot pictures of cytosolic and nuclear CREB, CREB-P, and PPARγ protein are also shown. *F* formoterol, *FT* formoterol + tiotropium; *P < 0.05 and **P < 0.01 compared with the corresponding data from F-monotherapy

Tiotropium decreased expressions of CREB and phosphorylated CREB in cytosol by about 25% ($P<0.05$) and 29% ($P<0.05$) for cytosolic CREB and CREB-P, respectively. In cell nuclei CREB was also decreased after tiotropium therapy by about 36% ($P<0.05$), but CREB-P levels were not altered. Comparing to values from patients on formoterol monotherapy, tiotropium significantly increased PPARγ in cell nuclei (increase by about 180%, $P<0.01$).

2.4 Discussion

We have previously shown that in cells isolated from induced sputum of COPD patients treated with tiotropium, acetylated H3 histone levels are significantly higher (Holownia et al. 2010). This observation may be important to inflammatory signaling, because acetylated histones represent a type of epigenetic tag which is responsible for gene transcription within chromatin. Histone acetylation mediated by HAT neutralizes the positive charge on the histone molecules (Khan and Khan 2010). As a consequence, chromatin is transformed into a more relaxed structure, associated with greater levels of gene transcription which is relevant to inflammatory signaling. In asthma, bronchial tissue and alveolar macrophages have increased HAT and decreased HDAC1 expression (Grabiec et al. 2008). In COPD formoterol and glucocorticosteroids were found to increase HAT-active CREB, especially in the cytosol of sputum cells (Mroz et al. 2007). In our patients cytosolic CREB (both inactive and phosphorylated) was slightly reduced after antimuscarinic therapy. In cell nuclei, unphosphorylated CREB was also lowered but phosphorylated, active CREB was not decreased after LAMA treatment. Given the important role of CREB in adrenergic signaling (Kaur et al. 2008), it seems that described changes may reflect adaptation of adrenergic receptors to chronic stimulation of β_2 receptors by formoterol. It is interesting to note that the PPARγ agonist rosiglitazone can decrease adrenoceptor desensitization and increase salbutamol effects on airway smooth muscle (Fogli et al. 2011). On the other hand, it was shown, that downregulation of PPARγ increased airway inflammation (Belvisi and Mitchell 2009). We have found significant increase in PPARγ expression in sputum cells, not only after tiotropium therapy, but also after formoterol/inhaled corticosteroids treatment (Holownia et al. 2008). Although in the allergen challenge of asthmatic patients, rosiglitazone was associated with only modest reduction in the late asthmatic reaction (Richards et al. 2010), our data suggest that combined therapy of tiotropium and rosiglitazone in COPD may be more effective.

The role of tiotropium in regulation of histone signaling is not clear. However, interactions of anticholinergic drugs and immune system are well established. It is well known that chronic lung diseases are related to *in utero* nicotine exposure (Miller and Marty 2010). In COPD there is higher acetylcholine release, increased vagal tone, airway inflammation and increased mucus production, all efficiently blocked by tiotropium (Gosens et al. 2006). It has been shown that the bronchodilatory activity of tiotropium against acetylcholine-induced bronchoconstriction is in the same dose range as the anti-inflammatory activity (Wollin and Pieper 2010). In asthma, tiotropium bromide significantly reduced airway inflammation and the T helper cytokine production in bronchoalveolar lavage fluid (Ohta et al. 2010). Our earlier data showed that tiotropium therapy involved pharmacodynamic changes in cholinergic M3 receptors and alterations in histone acetylation (Holownia et al. 2010). The present data suggest that the latter effect is most probably not mediated by alterations in CREB signaling.

Our results show that the mechanism whereby tiotropium reduces COPD exacerbations and ameliorates respiratory parameters is not only a result of persistent increase in airway functions and reduced hyperinflation caused by the drug, but also of its anti-inflammatory effects, involving increased PPARγ and decreased CREB signaling.

Conflicts of interest: The authors declare no conflicts of interest in relation to this article.

References

Belvisi, M. G., & Mitchell, J. A. (2009). Targeting PPAR receptors in the airway for the treatment of inflammatory lung disease. *British Journal of Pharmacology, 158*, 994–1003.

Casarosa, P., Kiechle, T., Sieger, P., Pieper, M., & Gantner, F. (2010). The constitutive activity of the human muscarinic M3 receptor unmasks differences in the pharmacology of anticholinergics. *Journal of Pharmacology and Experimental Therapeutics, 333*, 201–209.

Fogli, S., Pellegrini, S., Adinolfi, B., Mariotti, V., Melissari, E., Betti, L., Fabbrini, L., Giannaccini, G., Lucacchini, A., Bardelli, C., Stefanelli, F., Brunelleschi, S., & Breschi, M. C. (2011). Rosiglitazone reverses salbutamol-induced β(2)-adrenoceptor tolerance in airway smooth muscle. *British Journal of Pharmacology, 162*, 378–391.

Global Strategy for the Diagnosis, Management and Prevention of COPD. (2008). *Global Initiative for Chronic Obstructive Lung Disease* (GOLD). Available from: http://www.goldcopd.org

Gosens, R., Zaagsma, J., Meurs, H., & Halayko, A. J. (2006). Muscarinic receptor signaling in the pathophysiology of asthma and COPD. *Respiratory Research, 7*, 73–88.

Grabiec, A. M., Tak, P. P., & Reedquist, K. A. (2008). Targeting histone deacetylase activity in rheumatoid arthritis and asthma as prototypes of inflammatory disease: Should we keep our HATs on? *Arthritis Research and Therapy, 10*, 226.

Holownia, A., Mroz, R. M., Noparlik, J., Chyczewska, E., & Braszko, J. J. (2008). Expression of CREB-binding protein and peroxisome proliferator-activated receptor gamma during formoterol or formoterol and corticosteroid therapy of chronic obstructive pulmonary disease. *Journal of Physiology and Pharmacology, 59*(Suppl. 6), 303–309.

Holownia, A., Mroz, R. M., Skopinski, T., Kielek, A., Kolodziejczyk, A., Chyczewska, E., & Braszko, J. J. (2010). Tiotropium increases cytosolic muscarinic M3 receptors and acetylated H3 histone proteins in induced sputum cells of COPD patients. *European Journal of Medical Research, 15*(Suppl. 2), 64–67.

Kato, M., Komamura, K., & Kitakaze, M. (2006). Tiotropium, a novel muscarinic M3 receptor antagonist, improved symptoms of chronic obstructive pulmonary disease complicated by chronic heart failure. *Circulation Journal, 70*, 1658–1660.

Kaur, M., Holden, N. S., Wilson, S. M., Sukkar, M. B., Chung, K. F., Barnes, P. J., Newton, R., & Giembycz, M. A. (2008). Effect of beta2-adrenoceptor agonists and other cAMP-elevating agents on inflammatory gene expression in human ASM cells: A role for protein kinase A. *American Journal of Physiology. Lung Cellular and Molecular Physiology, 295*, 505–514.

Khan, S. N., & Khan, A. U. (2010). Role of histone acetylation in cell physiology and diseases: An update. *Clinica Chimica Acta, 411*, 1401–1411.

Lim, E. J., Lu, T. X., Blanchard, C., & Rothenberg, M. E. (2011). Epigenetic regulation of the IL-13-induced human eotaxin-3 gene by CREB-binding protein-mediated histone 3 acetylation. *Journal of Biological Chemistry, 286*, 13193–13204.

Loh, L. C., Kanabar, V., D'Amato, M., Barnes, N. C., & O'Connor, B. J. (2005). Sputum induction in corticosteroid-dependant asthmatics: Risks and airway cellular profile. *Asian Pacific Journal of Allergy and Immunology, 23*, 189–196.

Meyer, T., Reitmeir, P., Brand, P., Herpich, C., Sommerer, K., Schulze, A., Scheuch, G., & Newman, S. (2011). Effects of formoterol and tiotropium bromide on mucus clearance in patients with COPD. *Respiratory Medicine, 105*, 900–906.

Miard, S., & Fajas, L. (2005). Atypical transcriptional regulators and cofactors of PPARγ. *International Journal of Obesity, 29*, 10–12.

Miller, M. D., & Marty, M. A. (2010). Impact of environmental chemicals on lung development. *Environmental Health Perspectives, 118*, 1155–1164.

Mroz, R. M., Holownia, A., Chyczewska, E., Drost, E. M., Braszko, J. J., Noparlik, J., Donaldson, K., & Macnee, W. (2007). Cytoplasm-nuclear trafficking of CREB and CREB phosphorylation at Ser133 during therapy of chronic obstructive pulmonary disease. *Journal of Physiology and Pharmacology, 58*, 437–444.

Ohta, S., Oda, N., Yokoe, T., Tanaka, A., Yamamoto, Y., Watanabe, Y., Minoguchi, K., Ohnishi, T., Hirose, T., Nagase, H., Ohta, K., & Adachi, M. (2010). Effect of tiotropium bromide on airway inflammation and remodelling in a mouse model of asthma. *Clinical and Experimental Allergy, 40*, 1266–1275.

Richards, D. B., Bareille, P., Lindo, E. L., Quinn, D., & Farrow, S. N. (2010). Treatment with a peroxisomal proliferator activated receptor gamma agonist has a modest effect in the allergen challenge model in asthma: A randomised controlled trial. *Respiratory Medicine, 104*, 668–674.

Viegi, G., Pistelli, F., Sherrill, D. L., Maio, S., Baldacci, S., & Carrozzi, L. (2007). Definition, epidemiology and natural history of COPD. *European Respiratory Journal, 30*, 993–1013.

Wollin, L., & Pieper, M. P. (2010). Tiotropium bromide exerts anti-inflammatory activity in a cigarette smoke mouse model of COPD. *Pulmonary Pharmacology & Therapeutics, 23*, 345–354.

Chapter 3
Expression of Ki-67, Bcl-2, Survivin and p53 Proteins in Patients with Pulmonary Carcinoma

E. Halasova, M. Adamkov, T. Matakova, D. Vybohova, M. Antosova, M. Janickova, A. Singliar, D. Dobrota, and V. Jakusova

Abstract Apoptosis is the fundamental process necessary for eliminating damaged or mutated cells. Alterations in the apoptotic pathway appear to be key events in cancer development and progression. Bcl-2 is the key member of the Bcl-2 family of apoptosis regulator proteins with anti-apoptotic effects. Survivin acts as an inhibitor of apoptosis as well and has been implicated in both inhibition of apoptosis and mitosis regulation. p53 is one of the tumor suppressor proteins, prevents tumor formation through cell cycle blocking and eliminates damaged cells *via* the activation of apoptosis. The Ki-67 protein is a cellular marker for proliferation. To investigate the possible interactions of the aforementioned proteins, we examined their expression in 76 patients with diagnosed lung cancer using immunohistochemical visualisation. Ki-67 protein was expressed in the cancer cells of all patients with small cell lung cancer (SCLC). We found a negative correlation

E. Halasova
Department of Medical Biology, Comenius University in Bratislava,
Jessenius Faculty of Medicine in Martin, Martin, Slovakia

M. Adamkov (✉) • D. Dobrota
Institute of Histology and Embryology, Comenius University in Bratislava,
Jessenius Faculty of Medicine in Martin, Mala hora 4, Martin SK-03754, Slovakia
e-mail: adamkov@jfmed.uniba.sk

T. Matakova
Department of Medical Biochemistry, Comenius University in Bratislava,
Jessenius Faculty of Medicine in Martin, Martin, Slovakia

D. Vybohova
Department of Anatomy, Comenius University in Bratislava,
Jessenius Faculty of Medicine in Martin, Martin, Slovakia

M. Antosova
Department of Pharmacology, Comenius University in Bratislava,
Jessenius Faculty of Medicine in Martin, Martin, Slovakia

M. Janickova
Clinics of Stomatology and Maxillofacial Surgery, Comenius University in Bratislava,
Jessenius Faculty of Medicine in Martin and Faculty Hospital in Martin, Martin, Slovakia

A. Singliar
Department of Pathology, Hospital in Dolny Kubin, Dolby Kubin, Slovakia

V. Jakusova
Department of Public Health, Jessenius Faculty of Medicine in Martin, Martin, Slovakia

M. Pokorski (ed.), *Respiratory Regulation - The Molecular Approach*,
Advances in Experimental Medicine and Biology 756, DOI 10.1007/978-94-007-4549-0_3,

between survivin and p53 expression. A decreased intensity of survivin expression and fewer cells positive for survivin (66.7%) in SCLC in comparison with other lung cancer types (98.0%) was detected. Reversely, expression of Bcl-2 was found in more than 90% of cases with SCLC. We hypothesize that high expression and intensity of Bcl-2 protein could be a factor behind a bad prognosis in SCLC.

Keywords Lung cancer • Ki-67 protein • Bcl-2 protein • Survivin • p53 protein • Immunohistochemistry

3.1 Introduction

Lung cancer has now become the leading cause of cancer deaths in both men and women worldwide (Ferlay et al. 2010; Krug et al. 2008). Small cell lung cancer (SCLC) is an aggressive and highly metastatic disease, and it accounts for about one-quarter of all lung cancer cases. Although SCLC tumors are initially responsive to chemotherapy, multidrug resistance tends to develop after relapse, and the majority of SCLC patients die of their disease within 2 years (Tsao and Glisson 2006).

Carcinogenesis is a multi step process involving changes in expression of many genes especially related to regulation of cell cycle, differentiation, and apoptosis. Apoptosis or programmed cell death is needed for maintenance of cell homeostasis and to destroy cells that represent a threat to the integrity of organism. Apoptosis can be induced by either specific extracellular or internal signals. The molecular mechanisms involved in apoptotic enzymatic pathways have been sufficiently reviewed (Jinz and El-Deiry 2005). Protein p53 plays an important role in apoptosis induction. It acts as a transcription factor which in humans is encoded by the TP53 gene (Matlashewski et al. 1984; Isobe et al. 1986). p53 is activated by various stress signals such as radiation (UV, gamma, or X), carcinogens (polycyclic aromatic carbohydrates, heavy metals), oxidative stress, hypoxia, oncogene activation, telomere shortening, and others (Pluquet and Hainaut 2001). Many genes are involved in p53-dependent apoptotic pathways (Moll and Zaika 2001; Schuler and Green 2001; Pietenpol and Stewardt 2002; Yu and Zhang 2005). Expression and activity of p53 is precisely regulated at several levels (Coutts and Thangue 2006). p53 prevents tumor formation through cell cycle blocking and eliminates damaged cells. Mutations or inactivation of p53 are the most frequent changes in tumor cells (Deng and Wu 2000).

On the other hand, cancer cells overexpress proteins which can block the apoptosis. Survivin is a member of the apoptosis inhibitors (IAP) gene family, which has been implicated in both apoptosis inhibition and mitosis regulation (Altieri 2003). Survivin upregulates genes in tumor tissues (Velculescu et al. 1999). High survivin expression is related to poor prognosis in many cancer types (Kawasaki et al. 1998; Yamashita et al. 2007). There are many studies showing that p53 leads to repression of survivin expression in non-small lung cancers (see e.g., Mirza et al. 2002). However, the studies on the expression of the aforementioned proteins in SCLC are sparse (Nakano et al. 2005; Akyürek et al. 2006; Jin et al. 2006). The Bcl-2 proto-oncogene functions as a suppressor of apoptotic death as well. The protein contributes to cell survival also by diminishing the rate of cell proliferation (Borner 1996). It has been estimated that up to 90% of SCLC overexpress Bcl-2 (Higashiyama et al. 1995). Ectopic expression of Bcl-2 in a SCLC cell line increases resistance to apoptosis induced by chemotherapy (Shert et al. 2008). The main characteristic of cancer cells is their ability to proliferate. The Ki-67 protein is used as a cellular marker of proliferation. Studies point to a prognostic value of Ki-67 in cancer, but the results are inconsistent (Soomro et al. 1998; Han et al. 2009; Skov et al. 2010).

In this study, we focused on the expression and correlation of selected pro- and anti-apoptotic proteins in different types of lung carcinoma.

3.2 Methods

A hundred operative samples from pulmonary carcinoma patients were evaluated for survivin, Bcl-2, Ki-67, and p53 expression. Seventy six of them were enrolled into this study. The remaining cases had to be excluded because of specimen damage. The hematoxylin and eosin stained slides from each case were independently reviewed by two pathologists to ascertain the diagnosis based on morphological and immunohistochemical parameters and correlated with clinical data. Three sections, 4 μm thick, from each paraffin block were stained for p53 and survivin proteins. To achieve greater adherence of the sections to the glass surface, silanized slides (DAKO, Denmark) were used, baked for 2 h at 56°C before use. Then, the sections were deparaffinized in xylene for 20 min, rehydrated in a series of descending ethanol concentrations and washed with phosphate-buffered saline (PBS). The endogenous peroxidase activity was blocked with 3% hydrogen peroxide for 30 min. Antigen unmasking was achieved by heating the sections immersed in a target solution (DAKO) in water bath at 96°C for 45 min. Immunohistochemical staining was performed using monoclonal mouse anti-p53 (Clone DO-7), anti-survivin (Clone12C4), anti-Ki-67 antibody (Clone MIB-1), and anti-Bcl2 (Clone 124) antibodies; all diluted 1:50, obtained from DAKO. After overnight incubation, the p53 and survivin antigens were visualized by means of the LSAB Visualization System (DAKO) using 3,3'-diaminobenzidine chromogen as substrate, according to the manufacturer's instructions. All sections were counterstained with Mayer's hematoxylin (DAKO). Negative controls were obtained by omitting the primary antibodies.

3.2.1 Evaluation of Immunochemical Staining

Survivin, p53, Bcl-2, and Ki-67 antibody stained sections were observed in a light microscope. In each case, the following features were assessed: (1) intensity of staining, (2) relative number of positively stained cells, and (3) subcellular localization of p53 and survivin antigens.

The positivity of cytoplasmic (C), nuclear (N), or a combination of both was determined. Survivin and p53 expressions were scored semi-quantitatively as follows:

1. The intensity of staining:
   a. negative
   b. weak (+)
   c. moderate (++)
   d. strong (+++)
2. Number of positively stained cells
   a. more than 10% (≥10%) per field of view
   b. less than 10% (≤10%) per field of view
3. Subcellular localization of staining
   a. nuclear (N) only
   b. cytoplasmic (C) only
   c. combined nuclear and cytoplasmic (NC)

3.2.2 Statistical Analysis

Chi-square (χ^2) test or Fischer's exact test was used for comparison between survivin and p53 immunoreactivity. Spearman's coefficient was used to estimate the correlation between parameters. All statistical calculations were performed using MedCalc v.5 software for Windows.

3.3 Results

The results of expression profiling are summarized in Table 3.1 and illustrated in Fig. 3.1a–d. Survivin was predominantly expressed in both nucleus and cytoplasm in 58 cases (96.7%) (Fig. 3.1a), whereas p53 was expressed in the nucleus only in 64 (90.1%) (Fig. 3.1b). Expression of Ki-67 was found in nucleus (Fig. 3.1c) and Bcl-2 was in the cytoplasm only (Fig. 3.1d). In the majority of cases (17; 100% in SCLC and 49; 92% in NSCLC), there was >10% of positively stained cells per field of view for p53. All cases of SCLC showed the expression of Ki-67, but only 13 (78%) had >10% of positively stained cells per field; in NSCLC it was 48 (88%); the difference was insignificant. Survivin was positively stained in 12 (66%) of cases in SCLC and in 48 (98%) cases in NSCLC. There was a negative correlation ($r=-0.72$) between survivin and p53 expression. It seems, therefore, that p53 down-regulated survivin expression.

Comparison of SCLC and NSCLC for survivin expression showed a significant decrease in intensity and number of positive stained cells in the former type (χ^2; 15.30, $P<0.001$ and 8.43, $P<0.05$, respectively). There were no significant differences in intensity and number of positive cells for p53 between SCLC and NSCLC. A different trend was found in Bcl-2 expression, where 13 cases (92%) in SCLC and only 44 cases (75%) in NSCLC expressed the protein, although the difference did not assume statistical significance (χ^2; 1.97, $P=0.15$) . No correlations between Bcl-2 and p53 or survivin were observed.

3.4 Discussion

Lung tumorigenesis proceeds in multiple steps and is due to interrelated genetic events. p53 is a multifunctional protein that regulates cell division and activates apoptosis. On the other hand, survivin can act as an apoptosis inhibitor which is overexpressed in malignancies, including lung carcinoma.

Table 3.1 Expression of survivin, p53, Bcl-2, and Ki-67 in biopsies from patients with lung cancer

		I				%		SL		
		Negative	+	++	+++	<10	>10	N	C	NC
Survivin	SCLC	6	2	8	2	1	11	0	0	12
	NSCLC	1	19	24	5	14	34	1	1	46
p53	SCLC	1	2	10	5	0	17	15	0	2
	NSCLC	4	15	20	19	5	49	49	1	4
Bcl-2	SCLC	1	1	5	7	1	12	0	13	0
	NSCLC	14	18	21	5	13	21	0	44	0
Ki-67	SCLC	0	1	6	7	3	11	12	0	0
	NSCLC	6	0	24	30	6	48	49	0	0

I intensity of immunoreactivity: + weak, ++ moderate, +++ strong, % of labeled cells; *SL*: subcellular localization of survivin and p53 positivity: *N* nuclear, *C* cytoplasmic, *NC* nuclear and cytoplasmic

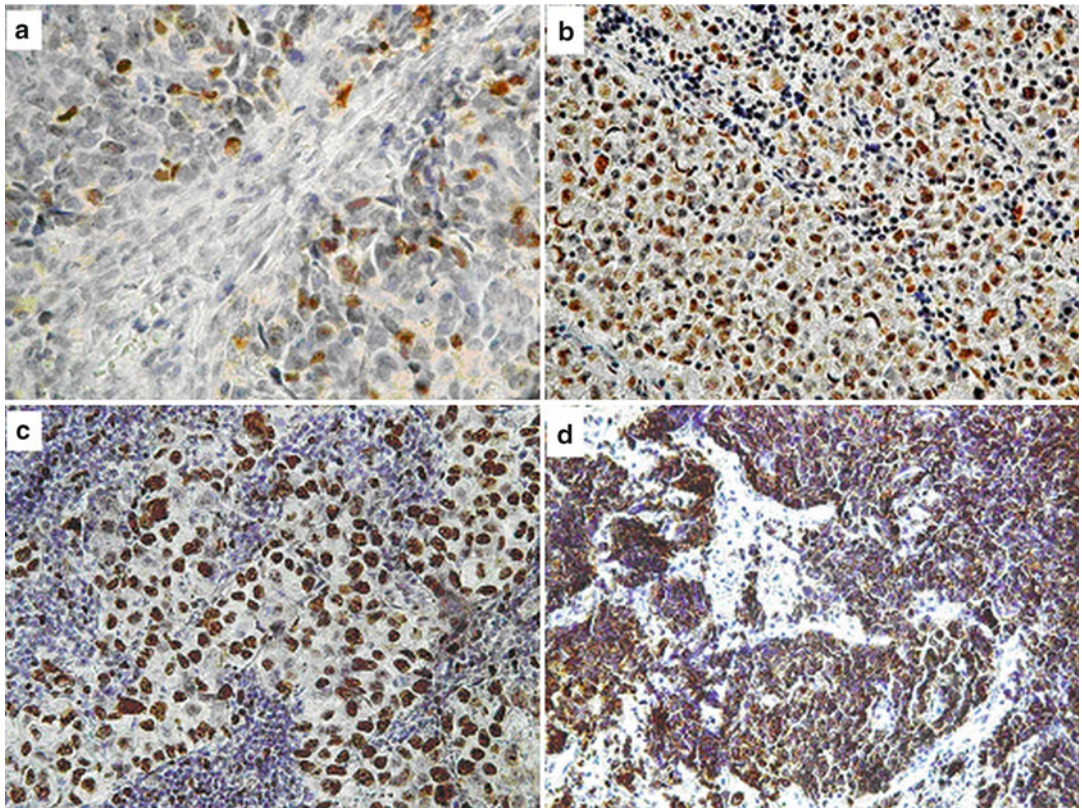

Fig. 3.1 Immunoreactions in tumor cells. (**a**) Combined cytoplasmic and nuclear survivin expression; (**b**) Nuclear p53 expression; (**c**) Ki-67 nuclear expression; (**d**) Bcl-2 cytoplasmic expression. Original magnifications: ×400 in panel (**a**) and ×200 in the remaining panels

A lot of studies have focused on the relationship between survivin and p53 expression, but the results have been quite controversial. Jin et al. (2006) suggested that survivin expression is negatively regulated by p53. Nakano et al. (2005) investigated survivin and p53 expression in specimens from 140 NSCLC patients. The authors found significant differences in survivin expression between squamous cell carcinomas and adenocarcinomas. Furthermore, survivin expression in tumors with mutant p53 was significantly higher than that in tumors with wild-type p53. They concluded that survivin gene expression is negatively regulated by p53 in NSCLC, and that survivin could inhibit apoptosis and accelerate tumor proliferation to produce more aggressive carcinomas. These findings are consistent with our results. We found a negative correlation between p53 and survivin expressions that possibly confirms a relationship between these two opposite acting proteins. The opposite results were published by Akyürek et al. (2006). The authors investigated the role of survivin in the early steps of lung carcinogenesis, in NSCLC, and its relationship to the expression of p53. They found no correlation between survivin and p53 expression; however, the patients with the expression of survivin had clearly worse prognosis.

Dysregulation of the apoptotic process has been implicated in both tumorigenesis and therapeutic resistance. Key regulators of this process, which are overexpressed in SCLC pathology, include Bcl-2 and TP53; the proteins which can synergize with classical oncogenes (Kitada et al. 1994; Higashiyama et al. 1995; Jiang et al. 1995; Schmitt et al. 2000; Wistuba et al. 2001). In the present study, a high incidence of Bcl-2 expression was noted in SCLC which is in accord with the literature outlined above, but surprisingly this expression also was highly elevated in NSCLC.

The molecular mechanisms of tumor progression and apoptosis are still unclear. Several predictors, such as nodal involvement, tumor stage, Ki-67, Bcl-2, survivin, and p53 expressions have been reported. Nevertheless, the relationships of Ki-67, Bcl-2, p53, or survivin to the prognosis of lung cancer patients are still subject to varying interpretations (Mitsudomi et al. 2000; Fan et al. 2008; Yamashita et al. 2009). To the best of our knowledge, our study is the first to show the expression of survivin in relation to p53 in small cell lung carcinomas, suggesting that survivin expression decreases in this type of cancer compared with other lung cancers. With regard to Bcl-2 protein, we can hypothesize that it is critical for inhibiting apoptosis, particularly in small cell lung cancer cells. Alternative study designs are required to further explore the exact determinants of the activation of the proteins studied in lung cancer cells.

Acknowledgments Supported by MZ 2007/48-UK-13 and VEGA 1/0050/11 Grants.

Conflicts of interest: The authors declare no conflicts of interest in relation to this article.

References

Akyürek, N., Memiş, L., Ekinci, O., Köktürk, N., & Oztürk, C. (2006). Survivin expression in pre-invasive lesions and non-small cell lung carcinoma. *Virchows Archiv, 449*(2), 164–170.

Altieri, D. C. (2003). Validating survivin as a cancer therapeutic target. *Nature Reviews. Cancer, 3*, 46–54.

Borner, Ch. (1996). Diminished cell proliferation associated with the deathprotective activity of Bcl-2. *Journal of Biological Chemistry, 271*(22), 12695–12698.

Coutts, A. S., & Thangue, N. (2006). The p53 response during DNA damage: Impact of transcriptional cofactors. *Biochemical Society Symposium, 73*, 181–189.

Deng, Y., & Wu, X. (2000). Peg3/Pw1 promotes p53-mediated apoptosis by inducing Bax translocation from cytosol to mitochondria. *Proceedings of the National Academy of Sciences of the USA, 97*, 12050–12055.

Fan, J., Wang, L., Jiang, G. N., He, W. X., & Ding, J. A. (2008). The role of survivin on overall survival of non-small cell lung cancer, a meta-analysis of published literatures. *Lung Cancer, 61*, 91–96.

Ferlay, J., Parkin, D. M., & Steliarova-Foucher, E. (2010). Estimates of cancer incidence and mortality in Europe in 2008. *European Journal of Cancer, 46*(4), 765–781.

Han, B., Lin, S., Yu, L. J., Wang, R. Z., & Wang, Y. Y. (2009). Correlation of 18F-FDG PET activity with expressions of survivin, Ki-67, and CD34 in non-small-cell lung cancer. *Nuclear Medicine Communications, 30*(11), 831–837.

Higashiyama, M., Doi, O., Kodama, K., Yokouchi, H., & Tateishi, R. (1995). High prevalence of Bcl-2 oncoprotein expression in small cell lung cancer. *Anticancer Research, 15*(2), 503–505.

Isobe, M., Emanuel, B. S., Givol, D., Oren, M., & Croce, C. M. (1986). Localization of gene for human p53 tumor antigen to band 17p13. *Nature, 320*(6057), 84–85.

Jiang, S. X., Sato, Y., Kuwao, S., & Kameya, T. (1995). Expression of Bcl-2 oncogene protein is prevalent in small cell lung carcinomas. *The Journal of Pathology, 177*(2), 135–138.

Jin, H. O., Yoon, S. I., Seo, S. K., Lee, H. C., Woo, S. H., Yoo, D. H., Lee, S. J., Choe, T. B., An, S., Kwon, T. J., Kim, J. I., Park, M. J., Hong, S. I., Park, I. C., & Rhee, C. H. (2006). Synergistic induction of apoptosis by sulindac and arsenic trioxide in human lung cancer A549 cells via reactive oxygen species-dependent down-regulation of survivin. *Biochemical Pharmacology, 72*(10), 1228–1236.

Jinz, Z., & El-Deiry, W. S. (2005). Overview of cell death signaling pathways. *Cancer Biology & Therapy, 4*, 139–163.

Kawasaki, H., Altieri, D. C., Lu, C. D., Toyoda, M., Tenjo, T., & Tanigawa, N. (1998). Inhibition of apoptosis by survivin predicts shorter survival rates in colorectal cancer. *Cancer Research, 58*, 179–185.

Kitada, S., Takayama, S., De Riel, K., Tanaka, S., & Reed, J. C. (1994). Reversal of chemoresistance of lymphoma cells by antisense-mediated reduction of Bcl-2 gene expression. *Antisense Research and Development, 4*(2), 71–79.

Krug, L. M., Kris, M. G., Rosenzweig, K., & Travis, W. D. (2008). Cancer of the lung. In V. T. DeVita Jr., S. Hellman, & S. A. Rosenberg (Eds.), *Cancer: Principles & practice of oncology* (8th ed., pp. 947–966). Philadelphia: Lippincott Williams Wilkins.

Matlashewski, G., Lamb, P., Pim, D., Peacock, J., Crawford, L., & Benchimol, S. (1984). Isolation and characterization of a human p53 cDNA clone: Expression of the human p53 gene. *EMBO Journal, 3*(13), 3257–3262.

Mirza, A., McGuirk, M., Hockenberry, T. N., Wu, Q., Ashar, H., Black, S., Wen, S. F., Wang, L., Kirschmeier, P., Bishop, W. R., Nielsen, L. L., Pickett, C. B., & Liu, S. (2002). Human survivin is negatively regulated by wild-type p53 and participates in p53-dependent apoptotic pathway. *Oncogene, 21*, 2613–2622.

Mitsudomi, T., Hamajima, N., Ogawa, M., & Takahashi, T. (2000). Prognostic significance of p53 alterations in patients with non-small cell lung cancer: A meta-analysis. *Clinical Cancer Research, 6*, 4055–4063.

Moll, U. M., & Zaika, A. (2001). Nuclear and mitochondrial apoptotic pathways of p53. *FEBS Letters, 493*, 65–69.

Nakano, J., Huang, C. L., Liu, D., Ueno, M., Sumitomo, S., & Yokomise, H. (2005). Survivin gene expression is negatively regulated by p53 tumor suppressor gene in non-small cell lung cancer. *International Journal of Oncology, 27*(5), 1215–1221.

Pietenpol, J. A., & Stewardt, Z. A. (2002). Cell cycle checkpoint signaling: Cell cycle arrest versus apoptosis. *Toxicology, 181*, 475–481.

Pluquet, O., & Hainaut, P. (2001). Genotoxic and non-genotoxic pathways of p53 induction. *Cancer Letters, 174*, 1–15.

Schmitt, C. A., Rosenthal, C. T., & Lowe, S. W. (2000). Genetic analysis of chemoresistance in primary murine lymphomas. *Nature Medicine, 6*(9), 1029–1035.

Schuler, M., & Green, D. (2001). Mechanisms of p53-dependent apoptosis. *Biochemical Society Transactions, 29*, 36–42.

Shert, T., Dy, G. K., & Adjei, A. (2008). Small cell lung cancer. *Mayo Clinic Proceedings, 83*(3), 355–367.

Skov, B. G., Holm, B., Erreboe, A., Skov, T., & Mellemgaard, A. (2010). ERCC1 and Ki-67 in small cell lung carcinoma and other neuroendocrine tumors of the lung: Distribution and impact on survival. *Journal of Thoracic Oncology, 5*(4), 453–459.

Soomro, I. N., Holmes, J., & Whimster, W. F. (1998). Predicting prognosis in lung cancer: Use of proliferation marker, Ki-67 monoclonal antibody. *The Journal of the Pakistan Medical Association, 48*(3), 66–69.

Tsao, A., & Glisson, B. (2006). Small cell lung cancer. In H. Kantarjian, R. Wolff, & C. Koller (Eds.), *Anderson manual of medical oncology* (pp. 233–256). New York: McGraw-Hill.

Velculescu, V. E., Madden, S. L., Zhang, L., Lash, A. E., Yu, J., Rago, C., Lal, A., Wang, C. J., Beaudry, G. A., Ciriello, K. M., Cook, B. P., Dufault, M. R., Ferguson, A. T., Gao, Y., He, T. C., Hermeking, H., Hiraldo, S. K., Hwang, P. M., Lopez, M. A., Luderer, H. F., Mathews, B., Petroziello, J. M., Polyak, K., Zawel, L., & Kinzler, K. W. (1999). Analysis of human transcriptomes. *Nature Genetics, 32*, 387–388.

Wistuba, L., Gadzar, A. F., & Minna, J. D. (2001). Molecular genetics of small cell lung carcinoma. *Seminars in Oncology, 28*(Suppl 4), 3–13.

Yamashita, S., Masuda, Y., Kurizaki, T., Haga, Y., Murayama, T., Ikei, S., Kamei, M., Takeno, S., & Kawahara, K. (2007). Survivin expression predicts early recurrence in early-stage breast cancer. *Anticancer Research, 27*, 2803–2808.

Yamashita, S., Chujo, M., Miyawaki, M., Tokuishi, K., Anami, K., Yamamoto, S., & Kawahar, K. (2009). Combination of p53AIP1 and survivin expression is a powerful prognostic marker in non-small cell lung cancer. *Journal of Experimental & Clinical Cancer Research, 28*(1), 22.

Yu, J., & Zhang, L. (2005). The transcriptional targets of p53 in apoptosis control. *Biochemical and Biophysical Research Communications, 331*, 851–858.

Chapter 4
Indacaterol Add-On Therapy Improves Lung Function, Exercise Capacity and Life Quality of COPD Patients

R.M. Mroz, L. Minarowski, and E. Chyczewska

Abstract Chronic obstructive pulmonary disease (COPD) is a progressive, inflammatory condition, involving airways and lung parenchyma. The disease leads to airflow limitation, and pulmonary hyperinflation, resulting in dyspnea, decreased exercise tolerance, and impaired quality of life. COPD pharmacotherapy guidelines are based on a combination of long-acting beta2-agonists (LABA), long-acting antimuscarinic agents (LAMA) and methyloxantins. Recently, indacaterol, ultralong acting beta2-agonist, has been introduced. The aim of our study was to assess the impact of indacaterol add-on therapy on lung function, exercise tolerance and quality of life of COPD patients. Thirty four COPD patients, receiving stable bronchodilator therapy were randomly allocated into two arms of add-on treatment (1:1 – indacaterol:placebo) for 3 months. Indacaterol replaced LABA in all patients receiving LABA. Spirometry, lung volumes, DLCO, St George's Respiratory Questionnaire (SGRQ) and 6 min Walk Distance (6MWD) were performed before and after therapy. We found that in the indacaterol group FEV1 did not changed significantly. However, there were significant improvements in ERV, 6MWD, and 6MWD-related dyspnea score. We also found that the degree of desaturation before and after 6MWD, and fatigue levels significantly improved in the indacaterol group. The patients' quality of life also changed favorably in the indacaterol treatment arm. We conclude that the add-on therapy with indacaterol exerts positive effects in COPD patients.

Keywords Antimuscarinic agents • COPD treatment • Dyspnea • Indacaterol • Inflammation • Airway • Quality of life • Six-minute walking distance • Spirometry • Pharmacotherapy

4.1 Introduction

Chronic obstructive pulmonary disease (COPD) is a major global health problem, as its mortality rate continues to climb steadily in most countries (Ford et al. 2011; Mannino and Buist 2007). This progressive, inflammatory condition lead to airflow limitation, and pulmonary hyperinflation, resulting in dyspnea, decreased exercise tolerance and impaired quality of life of COPD patients (Rabe et al. 2007).

R.M. Mroz (✉) • L. Minarowski • E. Chyczewska
Department of Lung Diseases, Medical University of Bialystok,
Zurawia 14, Bialystok, Poland
e-mail: robmroz@wp.pl

M. Pokorski (ed.), *Respiratory Regulation - The Molecular Approach*,
Advances in Experimental Medicine and Biology 756, DOI 10.1007/978-94-007-4549-0_4,

Effective bronchodilation is an important part of the management of patients with COPD and can improve breathlessness and ability to undertake physical activities (Jones et al. 2011). COPD pharmacotherapy guidelines recommend combination of long-acting beta2-agonists (LABA), long-acting antimuscarinic agents (LAMA), phosphodiesterase 4 (PDE-4) inhibitors and inhaled corticosteroids (ICS). Recently, indacaterol, a once-daily LABA indicated for maintenance treatment of moderate-to-severe COPD, has been introduced (Cazzola et al. 2005). Preliminary results from large clinical trials suggest that indacaterol improves lung function compared with placebo and other long-acting bronchodilators (Jones et al. 2011; Tashkin and Fabbri 2010). The aim of our study was to assess the impact of indacaterol add-on to usual care therapy on lung function, exercise tolerance and quality of life of COPD patients.

4.2 Methods

The study was performed in conformity with the Declaration of Helsinki for Human Experimentation and the protocol was approved by a local Ethics Committee. Study group consisted of 34 COPD patients (30 males/4 females, mean age 63.4, range 53–75 years), receiving stable bronchodilator therapy (usual care) for over 3 months. The patients were randomly allocated to an add-on 300 mg indacaterol Q.D. treatment (1:1 – indacaterol:placebo) for 3 months. Indacaterol replaced LABA, i.e., salmeterol or formoterol in all patients receiving these drugs. Spirometry, lung volumes, DLCO (Elite DL; MedGraphics, St Paul, MN, USA), St George's Respiratory Questionnaire (SGRQ) and 6 min Walk Distance test (6MWD) were performed before and after 1, 2, and 3 months (study group), or before and after 3 months of stable usual care (control) therapy. Additionally, 6MWD-related dyspnea and fatigue scores and arterial blood oxygen saturation were measured before and after the 6MWD test at each time point.

Statistical analysis was performed using Statistica 9.0 software (Stat Soft Inc., Tulsa, USA). K-S test was used for normality. All parametrical data was calculated by a *t*-test. Otherwise a non-parametrical Mann Whitney test was used. Results were presented as means ± SD. A value of $p < 0.05$ was considered to be the level of statistical significance.

4.3 Results

In the indacaterol group (IND), forced expiratory volume in 1 s (FEV1) did not change significantly before/after add-on therapy, respectively: 1.78 *vs.* 1.84 L. We did not find any significant FEV1 difference in the control group either: 1.22 *vs.* 1.21 L, $p > 0.05$ (Fig. 4.1a). There were, however, significant improvements in the IND group in inspiratory capacity (IC) (before/after add-on therapy, respectively): 2.04 *vs.* 2.28 L, $p < 0.05$, in expiratory reserve volume (ERV): 1.59 *vs.* 1.10 L, $p < 0.05$, and in the SGRQ score: 61.0 *vs.* 53.4, $p < 0.05$. The indices above outlined did not change appreciably in the control group before and after 3 months of usual care therapy (Fig. 4.1b, d).

Furthermore, we found that indacaterol improved physical efficiency of the patients. In the IND group, before and after add-on indacaterol treatment, the distance in the 6MWD test was: 540 *vs.* 559 m, respectively, $p < 0.05$; for comparison in the control group (CRTL) it was 473 *vs.* 469 m, pre and post 6MWD, respectively, $p > 0.05$ (Fig. 4.2a). The 6MWD-related dyspnea score, before and after add-on indacaterol treatment, was: 0.4–2.6 *vs.* 0.2–1.6, respectively, $p < 0.05$; CRTL: 0.8–2.0 *vs.* 0.8–2.2, pre and post 6MWD, respectively, $p > 0.05$ (Fig. 4.2b). The 6MWD-related fatigue score, before and after add-on indacaterol treatment, was: 1.6–4.0 *vs.* 1.6–3.0, pre- and post-6MWD, respectively, $p < 0.05$; CTRL: 1.5–3.7 *vs.* 1.7–4.3, pre and post 6MWD, respectively, $p > 0.05$ (Fig. 4.2d).

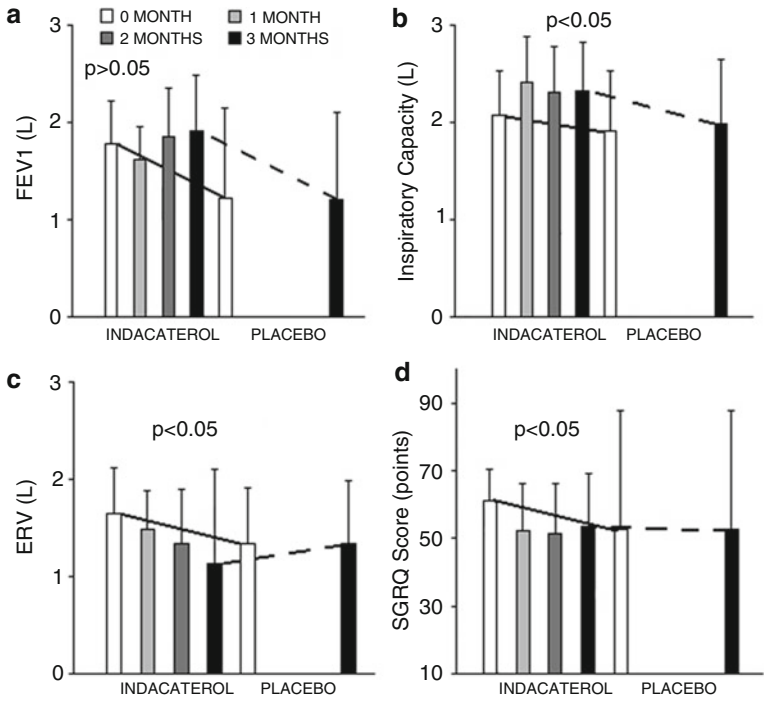

Fig. 4.1 Lung function and quality of life of COPD patients treated with add-on indacaterol therapy before and after treatment. **(a)** Forced expiratory volume in 1 s (*FEV1*), **(b)** inspiratory capacity, **(c)** expiratory reserve volume (*ERV*), and **(d)** Saint George respiratory questionnaire (*SGRQ*) score

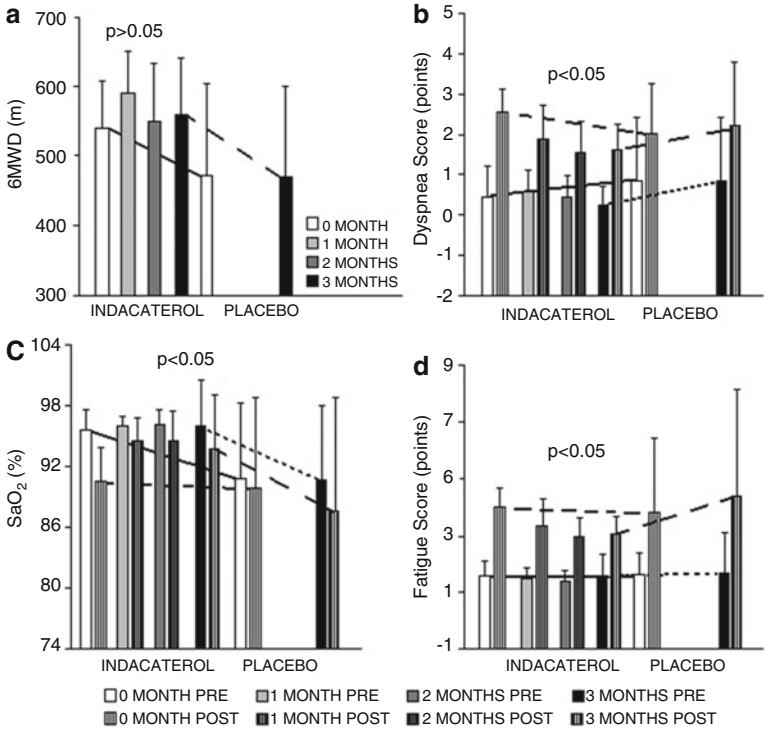

Fig. 4.2 Six minute walk distance (*6MWD*) of COPD patients treated with add-on indacaterol therapy. **(a)** 6MWD, **(b)** 6MWD-related dyspnea score, **(c)** 6MWD-related oxygen blood saturation, and **(d)** 6MWD-related fatigue score. The *bottom* legend concerns Panels b, c, and d

Arterial blood oxygen saturation significantly increased before and after 3 months of add-on indacaterol treatment: 95.4–90.6, pre and post 6MWD, respectively, *vs.* 96.0–93.5, pre and post 6MWD, respectively, $p<0.05$; CTRL: before usual care therapy – 90.6–89.6, pre and post 6MWD, respectively *vs.* 90.8–87.5, pre and post 6MWD, respectively, $p>0.05$ after 3 months of usual care therapy (Fig. 4.2c).

4.4 Discussion

The long-term goal of COPD therapy is to provide retardation of the accelerated loss of lung function during the course of disease. In the present study we found significant improvement in lung function measured by inspiratory capacity (IC) and expiratory residual volume (ERV), in the add-on indacaterol therapy (IND) in comparison with usual standard therapy (CTRL). We did not find significant difference in FEV1. Although an improvement in the mean trough FEV1 is associated with a proportional improvement in health status of COPD patients (Westwood et al. 2011), lung volumes such as IC and ERV are the key elements of detection of hyperinflation in COPD patients (Macklem 2010). Our findings are consistent with reports by Beeh et al. (2011) who found that 300 μg indacaterol administered once daily causes a clinically relevant increase in IC after 14 days of treatment. O'Donell et al. (2011) reported that indacaterol treatment improves the ability of COPD patients to exercise. In addition, the authors observed improvements in resting and end-exercise IC after a 3 week treatment.

The 6MWD with continuous pulse oximetry monitoring has widely been used to measure submaximal exercise performance of COPD patients, documenting the test-related oxygen desaturation, dyspnea, and fatigue (Sciurba et al. 2003). We found a significant increase in 6MWD achieved by indacaterol patients in comparison with control. The majority of 6MWD data are related to pulmonary rehabilitation programs. Eisner et al. (2008) analyzed the impact of respiratory impairment on the risk of physical functional limitations among adults with COPD using: lower extremity function (short physical performance battery), submaximal exercise performance (6MWD), standing balance (functional reach test), skeletal muscle strength (manual muscle testing with dynamometry), and self-reported functional limitation (standardized item battery). The authors conclude that pulmonary function impairment may be associated with multiple manifestations of physical functional limitation among COPD patients. Bailey et al. (2008) found that changes in 6MWD appear to have no relationship to changes in perceived quality of life. St. George's Respiratory Questionnaire (SGRQ) is well validated, disease-specific instrument available for health related quality of life (HRQL) status assessment in COPD, asthma and other lung diseases (Jones et al. 1991). We found that the indacaterol add-on treatment significantly improved HRQL measured by SGRQ. The impact of COPD pharmacotherapy on HRQL is one of its essential determinants in lung diseases. Moy et al. (2009) studying multivariate models of determinants of HRQL in severe COPD concluded that FEV1, 6MWD, and dyspnea significantly correlated with HRQL. They also found that a greater exercise capacity, prior participation in pulmonary rehabilitation, and the use of supplemental oxygen were all significantly associated with better HRQL; whereas self-perception of being disabled, depression, dyspnea, oral corticosteroid use, and daytime sleepiness were associated with worse HRQL. More recently, Celli et al. (2004) proposed the BODE index (body mass index – B, degree of airflow obstruction – O, dyspnea – D, and exercise capacity – E), measured by the 6MWD, as a simple multidimensional grading system for predicting the risk of death from any cause and from respiratory causes among patients with COPD. In the present study we found a significant increase in 6MWD-related pre- and post-test: dyspnea index, blood saturation, and the level of fatigue. Camargo and Pereira (2010), evaluating the correlations among various dyspnea scales, spirometric data, exercise tolerance data, and the BODE index in patients with COPD treated with formoterol, reported that the

MRC, BDI, and SOBQ correlated well with the 6MWD. Among the spirometric data, IC and FVC had the strongest correlations with 6MWD. The currently approved COPD pharmacotherapy includes combination of LABA, LAMA, PDE inhibitors, and ICS (Rabe et al. 2007). For the last two decades COPD treatment was based on inhaled and oral medicines with 12-h duration of action (Cazzola et al. 1994). Tiotropium bromide was the first, world-wide registered long-lasting anticholinergic drug providing 24-h duration of bronchodilation (Leckie et al. 2000; Maesen et al. 1993). Tashkin and Fabbri (2010) suggested that the introduction of once-daily LABAs provides the opportunity to develop combination inhalers of two or more classes of once-daily long-acting bronchodilators, which may be advantageous for COPD patients through simplification of treatment regimens as well as improvements in efficacy. Based on the present findings, we conclude that the indacaterol add-on to usual standard therapy improves lung function, exercise capacity, and quality of life of COPD patients.

Conflicts of interest: The authors declare no conflicts of interest in relation to this article.

References

Bailey, S. P., Brown, L., & Bailey, E. K. (2008). Lack of relationship between functional and perceived quality of life outcomes following pulmonary rehabilitation. *Cardiopulmonary Physical Therapy Journal, 19*(1), 3–10.

Beeh, K. M., Wagner, F., Khindri, S., & Drollmann, A. F. (2011). Effect of indacaterol on dynamic lung hyperinflation and breathlessness in hyperinflated patients with COPD. *COPD, 8*, 340–345.

Camargo, L. A., & Pereira, C. A. (2010). Dyspnea in COPD: Beyond the modified Medical Research Council scale. *Jornal Brasileiro de Pneumologia, 36*(5), 571–578.

Cazzola, M., Santangelo, G., Piccolo, A., Salzillo, A., Matera, M. G., D'Amato, G., & Rossi, F. (1994). Effect of salmeterol and formoterol in patients with chronic obstructive pulmonary disease. *Pulmonary Pharmacology, 7*(2), 103–107.

Cazzola, M., Matera, M. G., & Lotvall, J. (2005). Ultra long-acting beta2-agonists in development for asthma and chronic obstructive pulmonary disease. *Expert Opinion on Investigational Drugs, 14*(7), 775–783.

Celli, B. R., Cote, C. G., Marin, J. M., Casanova, C., de Montes, O. M., Mendez, R. A., Pinto, P. V., & Cabral, H. J. (2004). The body-mass index, airflow obstruction, dyspnea, and exercise capacity index in chronic obstructive pulmonary disease. *The New England Journal of Medicine, 350*(10), 1005–1012.

Eisner, M. D., Iribarren, C., Yelin, E. H., Sidney, S., Katz, P. P., Ackerson, L., Lathon, P., Tolstykh, I., Omachi, T., Byl, N., & Blanc, P. D. (2008). Pulmonary function and the risk of functional limitation in chronic obstructive pulmonary disease. *American Journal of Epidemiology, 167*(9), 1090–1101.

Ford, E. S., Mannino, D. M., Zhao, G., Li, C., & Croft, J. B. (2011). Changes in mortality among United States adults with chronic obstructive pulmonary disease in two national cohorts recruited during 1971 through 1975 and 1988 through 1994. *Chest, 141*, 101–110.

Jones, P. W., Quirk, F. H., & Baveystock, C. M. (1991). The St George's respiratory questionnaire. *Respiratory Medicine, 85*(Suppl B), 25–31.

Jones, P. W., Barnes, N., Vogelmeier, C., Lawrence, D., & Kramer, B. (2011). Efficacy of indacaterol in the treatment of patients with COPD. *Primary Care Respiratory Journal, 20*(4), 380–388.

Leckie, M. J., Bryan, S. A., Hansel, T. T., & Barnes, P. J. (2000). Novel therapy for COPD. *Expert Opinion on Investigational Drugs, 9*(1), 3–23.

Macklem, P. T. (2010). Therapeutic implications of the pathophysiology of COPD. *European Respiratory Journal, 35*(3), 676–680.

Maesen, F. P., Smeets, J. J., Costongs, M. A., Wald, F. D., & Cornelissen, P. J. (1993). Ba 679 Br, a new long-acting antimuscarinic bronchodilator: A pilot dose-escalation study in COPD. *European Respiratory Journal, 6*(7), 1031–1036.

Mannino, D. M., & Buist, A. S. (2007). Global burden of COPD: Risk factors, prevalence, and future trends. *Lancet, 370*(9589), 765–773.

Moy, M. L., Reilly, J. J., Ries, A. L., Mosenifar, Z., Kaplan, R. M., Lew, R., & Garshick, E. (2009). Multivariate models of determinants of health-related quality of life in severe chronic obstructive pulmonary disease. *Journal of Rehabilitation Research and Development, 46*(5), 643–654.

O'Donnell, D. E., Casaburi, R., Vincken, W., Puente-Maestu, L., Swales, J., Lawrence, D., & Kramer, B. (2011). Effect of indacaterol on exercise endurance and lung hyperinflation in COPD. *Respiratory Medicine, 105*(7), 1030–1036.

Rabe, K. F., Hurd, S., Anzueto, A., Barnes, P. J., Buist, S. A., Calverley, P., Fukuchi, Y., Jenkins, C., Rodriguez-Roisin, R., van Weel, C., & Zielinski, J. (2007). Global strategy for the diagnosis, management, and prevention of chronic

obstructive pulmonary disease: GOLD executive summary. *American Journal of Respiratory and Critical Care Medicine, 176*(6), 532–555.

Sciurba, F., Criner, G. J., Lee, S. M., Mohsenifar, Z., Shade, D., Slivka, W., & Wise, R. A. (2003). Six-minute walk distance in chronic obstructive pulmonary disease: Reproducibility and effect of walking course layout and length. *American Journal of Respiratory and Critical Care Medicine, 167*(11), 1522–1527.

Tashkin, D. P., & Fabbri, L. M. (2010). Long-acting beta-agonists in the management of chronic obstructive pulmonary disease: Current and future agents. *Respiratory Research, 11*, 149.

Westwood, M., Bourbeau, J., Jones, P. W., Cerulli, A., Capkun-Niggli, G., & Worthy, G. (2011). Relationship between FEV1 change and patient-reported outcomes in randomised trials of inhaled bronchodilators for stable COPD: A systematic review. *Respiratory Research, 12*, 40.

Chapter 5
Rapid DNA Extraction Protocol for Detection of Alpha-1 Antitrypsin Deficiency from Dried Blood Spots by Real-Time PCR

R. Struniawski, A. Szpechcinski, B. Poplawska, M. Skronski, and J. Chorostowska-Wynimko

Abstract The dried blood spot (DBS) specimens have been successfully employed for the large-scale diagnostics of α1-antitrypsin (AAT) deficiency as an easy to collect and transport alternative to plasma/serum. In the present study we propose a fast, efficient, and cost effective protocol of DNA extraction from dried blood spot (DBS) samples that provides sufficient quantity and quality of DNA and effectively eliminates any natural PCR inhibitors, allowing for successful AAT genotyping by real-time PCR and direct sequencing. DNA extracted from 84 DBS samples from chronic obstructive pulmonary disease patients was genotyped for AAT deficiency variants by real-time PCR. The results of DBS AAT genotyping were validated by serum IEF phenotyping and AAT concentration measurement. The proposed protocol allowed successful DNA extraction from all analyzed DBS samples. Both quantity and quality of DNA were sufficient for further real-time PCR and, if necessary, for genetic sequence analysis. A 100% concordance between AAT DBS genotypes and serum phenotypes in positive detection of two major deficiency S- and Z- alleles was achieved. Both assays, DBS AAT genotyping by real-time PCR and serum AAT phenotyping by IEF, positively identified PI*S and PI*Z allele in 8 out of the 84 (9.5%) and 16 out of 84 (19.0%) patients, respectively. In conclusion, the proposed protocol noticeably reduces the costs and the hand-on-time of DBS samples preparation providing genomic DNA of sufficient quantity and quality for further real-time PCR or genetic sequence analysis. Consequently, it is ideally suited for large-scale AAT deficiency screening programs and should be method of choice.

Keywords Alpha1-antitrypsin deficiency • Dried-blood spot • Genotyping • Real time PCR • Screening

5.1 Introduction

Alpha1-antitrypsin (AAT) deficiency (AATD) is a hereditary autosomal recessive disorder, one of the three most common genetic disorders in Caucasians. It considerably increases the risk of persistent pulmonary dysfunction, most often presented clinically as emphysema or chronic obstructive pulmonary disease (COPD) and chronic liver disorders such as neonatal liver disease, cholestasis or cirrhosis (Stolk et al. 2006).

R. Struniawski • A. Szpechcinski • B. Poplawska • M. Skronski • J. Chorostowska-Wynimko (✉)
Laboratory of Molecular Diagnostics and Immunology, National Institute of Tuberculosis and Lung Diseases, 26 Plocka St, 01-138 Warsaw, Poland
e-mail: j.chorostowska@igichp.edu.pl

M. Pokorski (ed.), *Respiratory Regulation - The Molecular Approach*,
Advances in Experimental Medicine and Biology 756, DOI 10.1007/978-94-007-4549-0_5,

The AAT protein is encoded by the protease inhibitor (Pi) locus located on chromosome 14q32.1 (SERPINA1-gene). AAT gene is 12.2 kb in length with 7 exons (4 coding and 3 non-coding) and 6 introns, while encoded protein includes 394 amino acids. The protease inhibitor locus is highly polymorphic with more than 120 single nucleotide polymorphisms (SNPs), resulting in numerous AAT isotypes effectively detected by isoelectric focusing (IEF). The wild type allele encodes the normal M-type protein. The most common mutations, E264V and E342K, result in the S-type (exon 3) and Z-type proteins (exon 5) respectively (DeMeo and Silverman 2004).

Nearly 97% of the population is homozygous for the normal PI*M allele, while Z allele is present in 1 out of 100 healthy individuals. Calculated value of PI ZZ prevalence in the European population is 1:4,727, whereas in Poland it is 1:9,110 (Blanco et al. 2006; Kaczor et al. 2007). Still, in the high risk group of patients with COPD Z allele is detected in up to 10%, ten times the frequency of the normal population.

Unfortunately, routine diagnostics for AAT deficiency is not freely available in number of European countries despite the fact that it is the major known genetic risk factor for COPD, the fourth leading cause of death (Brantly 2006). The joint guidelines of the American Thoracic Society/European Respiratory Society and the recent recommendations of the Polish Respiratory Society strongly recommend testing for AAT deficiency in individuals with fixed airway obstruction and some other respiratory and liver disorders (ATS/ERS 2003; Chorostowska-Wynimko et al. 2010).

The diagnosis of AAT deficiency is based exclusively on laboratory analyses involving combination of quantification, phenotyping, and genotyping. Although the assessment of AAT plasma/serum concentration is commonly performed by hospital laboratories, the isoelectric focusing, the gold standard for identification of deficiency alleles is technically challenging and requires a laboratory with highly qualified personnel. Meanwhile, genotyping allows only identification of the most common and clinically significant S and Z AAT deficiency alleles at the DNA level. The real-time PCR is considered the most robust and efficient method for fast AAT deficiency diagnostics, particularly useful for the population screening.

Similarly, dried blood spot (DBS) specimens have been successfully employed for large-scale diagnostics of AATD as an easy to collect and transport alternative to plasma/serum (Laurell and Sveger 1975). In 1998, the feasibility of PCR amplification of DBS-derived DNA was reported for the first time followed by the protocols allowing efficient AAT level determination and phenotyping (Caggana et al. 1998; Costa et al. 2000). The current algorithm for AATD screening suggests DBS samples analysis for AAT levels and subsequent genotyping for the two most common deficiency variants (S and Z) (Ferrarotti et al. 2007). Still, DNA isolation from DBS samples is quite challenging. It usually provides only minute amounts of DNA, often characterized by low quality, therefore affecting diagnostic procedure and results reliability.

Here, we propose the fast, efficient, and cost effective protocol of DNA extraction from DBS samples allowing effective AAT genotyping by hydrolysis probe-based real-time PCR and direct sequencing. It overcomes major technical obstacles affecting PCR reaction due to the purity of DBS DNA or interference of natural blood-derived PCR inhibitors. For the purpose of assay validation, the DBS AAT genotyping results were confirmed by 'gold-standard' IEF serum phenotyping and referred to serum AAT concentration assessed by immune nephelometry.

5.2 Methods

The study was in conformity with the Declaration of Helsinki of 1989 of the World Medical Association and was approved by a local Ethics Committee. Serum and DBS samples were collected simultaneously from 84 patients with chronic obstructive pulmonary disease diagnosed according to GOLD criteria referred to the Laboratory of Molecular Diagnostics and Immunology, National Institute of Tuberculosis and Lung Diseases in Warsaw for routine diagnostics (GOLD 2010).

5.2.1 Preparation of DBS Samples

The DBS samples were prepared for each patient by dropping of whole blood (ca. 50 μL per spot) from a finger prick onto the filter paper (Whatman #903), as described previously McDade et al. (2007). The samples were allowed to air-dry overnight prior to storage with desiccant in sealable plastic bags or mailing to the diagnostic laboratory.

5.2.2 DNA Extraction from DBS

Genomic DNA was extracted from DBS by use of the Extract-N-Amp Blood PCR Kit (Sigma-Aldrich, St. Louis, MO) according to the manufacturer's protocol. One 3-mm disc was punched from the blood card and placed into a microcentrifuge tube where the blood was lysed by incubation in 20 μL of the lysis solution at 55°C for 15 min. Next, 180 μL of neutralization solution was added to the blood and mixed thoroughly by vortexing. The neutralized blood extract was stored at 4°C (up to several months) or used immediately in PCR. In our protocol, 1 μL of neutralized blood extract provided 0.2–0.5 ng of genomic DNA, which was assessed by quantitative PCR with human β-actin gene as the amplifying target (99 bp).

5.2.3 Genotyping of PI*S and PI*Z AAT Alleles by Real-Time PCR

AAT genotyping was performed in the LightCycler 480 II instrument (Roche Diagnostics Ltd., Switzerland) using a set of specific oligonucleotide primers and 3′-minor groove binding (MGB) hydrolysis probes for PI*S and PI*Z alleles (sequences available upon request). All primers and MGB probes were synthesized by Applied Biosystems. Each 20-μL reaction contained: 3 μL of neutralized blood extract, 10 μL of 2×ready-to-use PCR supermix (FastStart Universal Probe Master, Roche Applied Science, Mannheim, Germany), primers (0.75 μM each) and MGB probes (0.25 μM each), PCR water. Each assay included an S/Z heterozygote, Z/Z homozygote and M/M homozygote (non-Z, non-S) controls, and no-template control. Two duplex real-time PCR reactions were performed simultaneously using fluorescent hydrolysis probes for detection of both wild-type and variant alleles.

The assembled reaction mixtures were amplified in 96-well microplates (Roche Applied Science) using the following cycling conditions: 10 min incubation at 95°C followed by 40 cycles at 95°C for 20 s, and at 60°C for 60 s. Fluorescence emissions of PI*S and PI*Z probes were detected in FAM channel and VIC channel respectively during the 60°C annealing step of each PCR cycle. The amplification results were interpreted according to the conventional endpoint genotyping principles using the LightCycler 480 Software, version 1.5 (Roche Applied Science).

It should be noted that the Extract-N-Amp Blood PCR Kit contains all the reagents needed to rapidly extract and amplify human genomic DNA from DBS; however, it is not originally dedicated for MGB-probe-based real-time PCR and as such the assay may require more stringent reaction conditions and additional optimization. Therefore, in the described protocol we propose to combine the Extract-N-Amp Blood PCR Kit for DNA extraction with any of TaqMan probe supermixes for efficient real-time PCR analysis.

5.2.4 AAT Sequence Analysis

DNA extracted from DBS was amplified by conventional PCR prior to direct sequence analysis. Each 20-μL reaction contained: 2 μL of neutralized blood extract (containing template DNA), 10 μL of Extract-N-Amp Blood PCR Ready Mix (Extract-N-Amp Blood PCR Kit, Sigma-Aldrich, St. Louis,

Table 5.1 Primers used for PCR amplification and sequence reactions

AAT Exon	Primer	Sequence
II	2exF	5′-ACGTGGTGTCAATCCCTGATCACTG-3′
	2exR	5′-GAGTTCAAGAACTGATGGTTTGAG-3′
III	3exF	5′-GCTACACTCTTCCAAACCT-3′
	3exR	5′-GTTCTCCTCATGGAGCAT-3′
IV	4exF	5′-CACTTGCACTGTGGTGGGTCCCAG-3′
	4exR	5′-TTCTTCCCTACAGATACCATGG-3′
V	5exF	5′-GAGCCTTGCTCGAGGCCTGGGATC-3′
	5exR	5′-CAGAGAAAACATGGGAGGGATTTACA-3′

MO), 0,4 μM of each primer and PCR water. Primers used for amplification and sequence reactions are listed in Table 5.1, as described previously (Ferrarotti et al. 2007; Zorzetto et al. 2008). Sequence reactions were performed as indicated by the manufacturer. ExoSAP-IT (USB, Cleveland) was used for PCR clean-up according to the manufacturer's protocol. Briefly: 2 μL of PCR product was mixed with 7 μL of ExoSAP-IT and incubated at 37°C for 15 min in thermalcycler (enzymatic removal of dNTP and single-stranded primer residuals) followed by 80°C for 15 min (ExoSAP-IT enzyme inactivation). Sequence analysis of AAT exons 2–4 was performed in 16-capillary 3130xl Genetic Analyzer (Applied Biosystems, USA) by Genomed (Warsaw, Poland).

5.2.5 Quantitative Determination of Serum AAT Concentration by Immune Nephelometry

The AAT measurement was performed in serum samples using a rate immune nephelometric method (Immage 800 Immunochemistry System, Beckman-Coulter, USA) with a commercially available reagents containing goat anti-human AAT antibody (Beckman-Coulter, USA). The immune nephelometer automatically dilutes samples 1:216 to achieve optimum antigen-antibody equilibrium in the assay. The normal range for AAT in serum samples was 88–174 mg/dL with cutoff value of 120 mg/dL.

5.2.6 Phenotyping of Serum AAT by Isoelectrofocusing (IEF)

Phenotype analysis of serum AAT was performed by IEF on polyacrylamide gel with pH of 4.2–4.9 using Multiphor II Electrophoresis System (GE Healthcare Bio-Sciences AB, Uppsala, Sweden) as described previously (Jeppsson and Franzén 1982). Each assay included control samples of individuals with known phenotypes (M1M2, MS, MZ and ZZ) established as standards by sequencing. Phenotypes of serum AAT samples were determined by comparing their migration patterns with control material.

5.3 Results

The one-step protocol of rapid DNA extraction allowed successful DNA isolation from all analyzed DBS samples collected in 84 COPD patients. Both quantity and quality of DNA was sufficient for further real-time PCR analysis of all samples. The 100% concordance between AAT DBS genotypes

Table 5.2 Results of DBS AAT genotyping, serum AAT phenotyping, and concentration measurement (mg/dL)

Serum AAT Phenotyping	Serum AAT Concentration	DBS AAT Genotyping
Phenotype (n)	Means ± SD (range)	Genotype (n)
MM (60)	148 ± 35 (88–310)	non-S, non-Z (61)
FM (1)	146 (–)	
MS (8)	127 ± 35 (86–249)	[non-S, non-Z]S (8)
MZ (13)	95 ± 28 (60–189)	[non-S, non-Z]Z (13)
ZZ (3)	34 ± 16 (17–52)	ZZ (3)

AAT genotype was determined by real-time PCR amplification of DNA extracted from DBS. Serum AAT phenotype was assessed by isoelectric focusing and concentration was measured by immune nephelometry

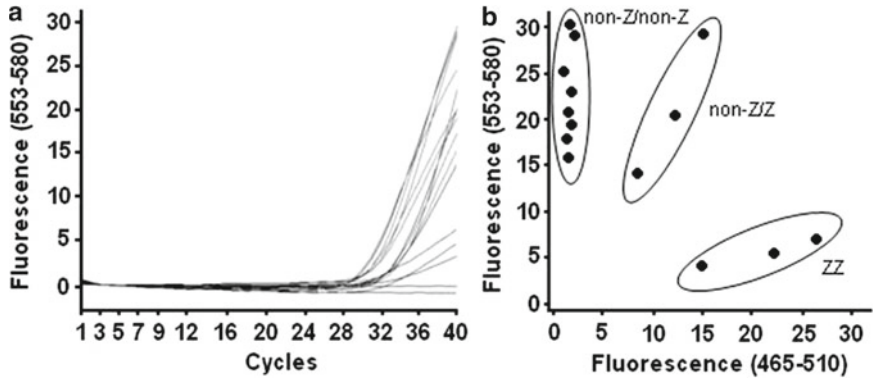

Fig. 5.1 DNA amplification curves (**a**) and allelic discrimination plot (**b**) for real-time PCR genotyping of AAT. The real-time PCR reaction was performed as duplex using the pair of dual-labeled fluorescent probes for detection of both wild-type and PI*Z variant alleles (similarly for PI*S). PCR amplification plots were baseline-subtracted and fitted automatically by the software of LightCycler 480. Genotypes were automatically scored using the endpoint genotyping graph for FAM *vs.* VIC fluorescence

and serum phenotypes in the positive detection of two major deficiency alleles was achieved. Both assays, the real-time PCR genotyping of AAT from DBS samples and serum AAT phenotyping by IEF positively identified PI*S and PI*Z alleles in 8 (9.5%) and 16 out of the 84 (19%) patients, respectively (Table 5.2).

In the allelic discrimination assay, two duplex real-time PCR reactions were performed using a set of fluorescent hydrolysis probes recognizing specifically the wild-type, S, and Z variation. It allowed determining the homozygous (3 out of the 16 patients had ZZ genotype) or heterozygous AAT genotype for each deficiency allele (Fig. 5.1). Thus, if single Z allele was detected, an individual was recognized as the Z heterozygote with Z/non-Z genotype, consistent with the carrier status. In individuals referred as (non-S, non-Z)Z genotype, the Z variation at codon 288 was present and the wild-type allele at the codon associated with the S allele. An analogous interpretation was accepted for the patient with a single S allele detected, referred further to (non-S, non-Z)S genotype. If neither Z nor S alleles were revealed by genotyping, the patient was described as the wild-type homozygote (two wild-type alleles). In genotype analysis, 61 out of the 84 (72.5%) DBS samples were negative for either S or Z allele, consistent with the non-S, non-Z genotype.

The results of DBS AAT genotyping were related to the serum AAT concentration. All patients identified as MM homozygote presented the mean serum AAT level of 148 mg/dL (normal range 88–174 mg/dL,

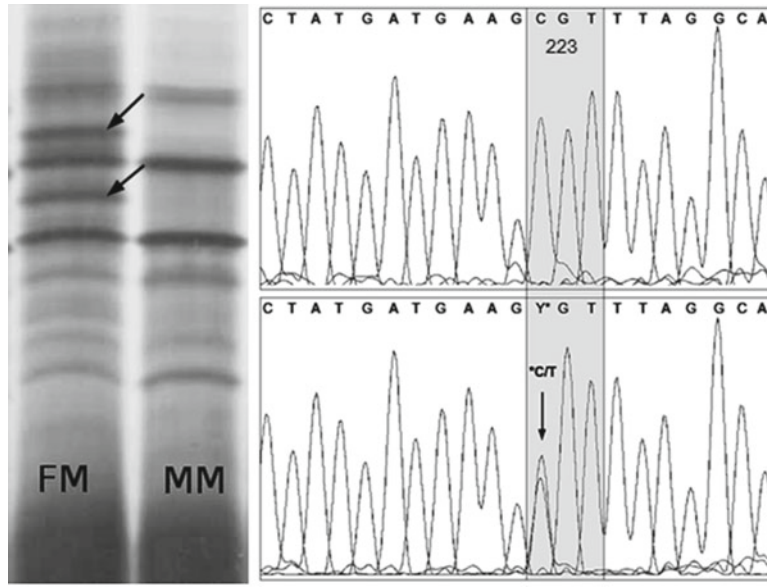

Fig. 5.2 Results of serum phenotyping and direct sequencing of DBS-extracted AAT gene DNA from the patient subsequently diagnosed with FM mutation variant. The exchange from CGT to TGT at codon 223 in exon III of AAT is demonstrated on the sequencing histogram. The additional AAT migration bands in the stained IEF gel are characteristic for the PI*F variant of AAT. The 'gold standard' phenotyping was performed by isoelectric focusing (IEF)

cut-off value of 120 mg/dL). The presence of PI*S deficiency allele in heterozygous genotype was not accompanied by a marked decrease in AAT serum concentration (mean 127 mg/dL). In most patients with MS genotype, the quantitative results were within normal limits (range 86–249 mg/dL). On the contrary, the presence of PI*Z allele in either heterozygous or homozygous genotype contributed to lower levels of serum AAT concentration (mean 95 and 34 mg/dL for MZ and ZZ, respectively).

In one sample recognized by genotyping as consistent with non-S, non-Z genotype, IEF analysis revealed an FM rare phenotype (Fig. 5.2). The AAT serum level was within normal limits (146 mg/dL) as it is usually observed for this phenotype. Subsequently, direct sequencing demonstrated the exchange from CGT to TGT at codon 223 in exon III – characteristic for the PI*F AAT variant. The DNA extracted from DBS by our rapid protocol provided excellent genotyping results by means of the real-time PCR efficiency and sequencing peak quality.

5.4 Discussion

We propose the simple, fast and efficient protocol of DNA extraction from DBS specimens for AAT genotype analysis by real-time PCR. We demonstrated that DNA extraction from DBS using neutralized blood in a very short time provides genetic material of sufficient quality and quantity for reliable AAT S- and Z- alleles genotyping. Diagnostic reliability of this protocol was confirmed by 100% concordance in positive detection of the two major deficiency alleles PI*S and Pi*Z by the DBS genotyping and 'gold-standard' IEF serum phenotyping. Genotyping results were also consistent with the nephelometric quantification of serum AAT.

Though IEF is still considered the 'gold standard' in AAT diagnostics, it is also more costly and time-consuming. According to current guidelines, it is still irreplaceable for detection of rare AAT variants. However, in the routine diagnostics of the most common and clinically relevant S- and

Z- deficiency variants and particularly in large-scale screening, genotyping supplemented with AAT serum quantification is recommended as an equivalent method (Costa et al. 2000).

Several assays have been developed for AAT PI*S and PI*Z genotyping, including PCR-mediated sited-directed mutagenesis (Tazelaar et al. 1992), single-strand conformation polymorphism analysis (SSCP) (Ortiz-Pallardo et al. 2000), PCR restriction fragment length polymorphism analysis (Ferrarotti et al. 2004) and DNA sequencing (Ferrarotti et al. 2007). All of them are rather cost and labor consuming, and require relatively large amounts of DNA usually obtained from peripheral-blood mononuclear cells.

As mentioned before, the importance of DBS sampling for AAT screening programs is due to an easy and cheap collecting and delivery to the central laboratory. Still, DBS samples provide only minute amounts of DNA that are often characterized by low purity and contain natural PCR inhibitors interfering DNA amplification (Caggana et al. 1998). Consequently, only few PCR-based protocols proved adequate for efficient AAT genotyping of DBS-derived material.

Costa et al. (2000) described the AAT deficiency screening algorithm using DBS specimens and a fast and cheap procedure of DNA extraction. The PCR-inhibiting components were eliminated by heating of water-washed DBS sample for 10 min at 99°C. Subsequently, four exons of the AAT gene were amplified by PCR and directly sequenced. Two years later protocol was modified and overnight incubation of DBS disc at 60°C was included, followed by 80°C for 30 min and 30-min centrifugation. That allowed more efficient elimination of contaminants and DNA elution, although considerably extended the procedure (Rodriguez et al. 2002). Though extremely cheap and effective in providing sufficient quantity and quality DNA, this protocol has one important limitation. The procedure highly relies on the manual skills of the laboratory personnel, thus hampering the proper quality control and result reproducibility. In our experience, the extremely high sensitivity of real-time PCR assay in detecting even trace amounts of DNA is also the main cause of its considerable vulnerability to sample contamination and inhibitors amplification that might result in AAT genotype misclassification.

As an alternative, large-scale extraction of DNA from DBS samples using paramagnetic resin or minicolumns was proposed (Ferrarotti et al. 2007; Snyder et al. 2006). Though very efficient, is both time-consuming and labor-intensive when performed manually, otherwise requires expensive automated systems. Meanwhile, we propose a simple, fast and reliable method of DNA extraction from DBS samples that requires only 15-min lysis of blood resin and mixture neutralization by the use of commercially available reagents. In our experience, optimized real-time PCR-ready supermix and only 3 μL of neutralized DNA extract provide sufficient amount of template material for AAT genotyping. The included *Taq* polymerase allows for specific hot start amplification, still the direct addition of specific primers and probes for real-time PCR might require additional optimization. In order to amplify the DNA template prior to direct sequencing, the neutralized DNA extract is to be simply mixed with the other component containing buffer, salts, dNTPs and *Taq* polymerase. It is also worth mentioning that the presented protocol might be optimized for rapid extraction of human genomic DNA from whole blood.

As emphasized, genotyping is not a method of choice for non-S, non-Z AAT mutations detection. The FM variant of AATD was not identified by real-time genotyping and with AAT serum concentration far within normal limits would be undetected by any routine screening implementing those two methods. As presented in our study, only IEF phenotyping or DNA sequencing provides sufficient diagnostic reliability for that purpose. Hence, routine AAT deficiency diagnostic algorithm combines AAT serum quantification and AAT phenotyping. In case of discordance between AAT concentration and phenotype or rare/unknown variant detection the diagnosis of hereditary AATD is established by AAT gene sequencing.

Still, large-scale screening programs, as a rule, target the most common and clinically relevant types of AAT deficiency, all of them due to the S-, or Z-allele mutations. Fast AATD screening by genotyping for PI*S and PI*Z variants simplifies the laboratory assessment of AAT deficiency

allowing for correct identification of ~96% of AATD individuals (Snyder et al. 2006). Interestingly, the combination of AAT concentration assessment and AAT genotyping, followed by IEF phenotyping if necessary, provides a sensitivity ~98% (Bornhorst et al. 2007).

The presented one-step protocol implementing DNA extraction by blood neutralization allows for the efficient use of dried blood spots (DBS) for diagnostic genotyping and sequencing. As shown in present study, it provides a good quality material sufficient for a reliable sample evaluation by fast and a highly sensitive real-time PCR method producing data concordant with the 'gold standard' IEF phenotyping. The method also is considerably more cost and time effective.

Acknowledgments Supported by National Institute of Tuberculosis and Lung Diseases in Warsaw (project 5/8) and by Ministry of Science and Higher Education, Republic of Poland (grant N404081539).

Conflicts of interest: The authors declare no conflicts of interest in relation to this article.

References

American Thoracic Society/European Respiratory Society Statement. (2003). Standards for the diagnosis and management of individuals with alpha-1 antitrypsin deficiency. *American Journal of Respiratory and Critical Care Medicine, 168*, 818–900.

Blanco, I., de Serres, F. J., Fernandez-Bustillo, E., Lara, B., & Miravitlles, M. (2006). Estimated numbers and prevalence of PI*S and PI*Z alleles of alpha-1 antitrypsin deficiency in European countries. *European Respiratory Journal, 27*, 77–84.

Bornhorst, J. A., Procter, M., Meadows, C., Ashwood, E. R., & Mao, R. (2007). Evaluation of an integrative diagnostic algorithm for the identification of people at risk for alpha-1 antitrypsin deficiency. *American Journal of Clinical Pathology, 128*, 482–490.

Brantly, M. (2006). Efficient and accurate approaches to the laboratory diagnosis of alpha1-antitrypsin deficiency: The promise of early diagnosis and intervention. *Clinical Chemistry, 52*, 2180–2181.

Caggana, M., Conroy, J. M., & Pass, K. A. (1998). Rapid, efficient method for multiplex amplification from filter paper. *Human Mutation, 11*, 404–409.

Chorostowska-Wynimko, J., Nizankowska-Mogilnicka, E., & The Working Group of the Polish Respiratory Society. (2010). Diagnosis and treatment of patients with alpha-1 antitrypsin (alpha-1 AT) deficiency. *Pneumonologia i Alergologia Polska, 78*, 348–355.

Costa, X., Jardi, R., Rodriguez, F., Miravitlles, M., Cotrina, M., Gonzalez, C., Pascual, C., & Vidal, R. (2000). Simple method for alpha1-antitrypsin deficiency screening by use of dried blood spot specimens. *European Respiratory Journal, 15*, 1111–1115.

DeMeo, D. L., & Silverman, E. K. (2004). Alpha-1 antitrypsin deficiency 2: Genetic aspects of alpha-1 antitrypsin deficiency: Phenotypes and genetic modifiers of emphysema risk. *Thorax, 59*, 259–264.

Ferrarotti, I., Zorzetto, M., Scabini, R., Mazzola, P., Campo, I., & Luisetti, M. A. (2004). Novel method for rapid genotypic identification of alpha-1 antitrypsin variants. *Diagnostic Molecular Pathology, 13*, 160–163.

Ferrarotti, I., Scabini, R., Campo, I., Ottaviani, S., Zorzetto, M., Gorrini, M., & Luisetti, M. (2007). Laboratory diagnosis of alpha-1 antitrypsin deficiency. *Translational Research, 150*, 267–274.

Global Initiative for Chronic Obstructive Lung Disease (GOLD). (2010). Global strategy for diagnosis, management, and prevention of COPD (update), http://www.goldcopd.org/guidelines-global-strategy-for-diagnosis-management.html

Jeppsson, J. O., & Franzén, B. (1982). Typing of genetic variants of alpha-1 antitrypsin by electrofocusing. *Clinical Chemistry, 28*, 219–225.

Kaczor, M. P., Sanak, M., Libura-Twardowska, M., & Szczeklik, A. (2007). The prevalence of alpha-1-antitrypsin deficiency in a representative population sample from Poland. *Respiratory Medicine, 101*, 2520–2525.

Laurell, C. B., & Sveger, T. (1975). Mass screening of newborn Swedish infants for alpha-1 antitrypsin deficiency. *American Journal of Human Genetics, 27*, 213–217.

McDade, T. W., Williams, S., & Snodgrass, J. J. (2007). What a drop can do: Dried blood spots as a minimally invasive method for integrating biomarkers into population-based research. *Demography, 44*, 899–925.

Ortiz-Pallardo, M. E., Ko, Y., Sachinidis, A., Vetter, H., Fischer, H. P., & Zhou, H. (2000). Detection of alpha-1 antitrypsin PiZ individuals by SSCP and DNA sequencing in formalin-fixed and paraffin-embedded tissue: A comparison with immunohistochemical analysis. *Journal of Hepatology, 32*, 406–411.

Rodriguez, F., Jardí, R., Costa, X., Cotrina, M., Galimany, R., Vidal, R., & Miravitlles, M. (2002). Rapid screening for alpha-1 antitrypsin deficiency in patients with chronic obstructive pulmonary disease using dried blood specimens. *American Journal of Respiratory and Critical Care Medicine, 166*, 814–817.

Snyder, M. R., Katzmann, J. A., Butz, M. L., Wiley, C., Yang, P., Dawson, D. B., Halling, K. C., Highsmith, W. E., & Thibodeau, S. N. (2006). Diagnosis of alpha-1 antitrypsin deficiency: An algorithm of quantification, genotyping, and phenotyping. *Clinical Chemistry, 52*, 2236–2242.

Stolk, J., Seersholm, N., & Kalsheker, N. (2006). Alpha-1 antitrypsin deficiency: Current perspective on research, diagnosis, and management. *International Journal of COPD, 1*, 151–160.

Tazelaar, J. P., Friedman, K. J., Kline, R. S., Guthrie, M. L., & Farber, R. A. (1992). Detection of alpha-1 antitrypsin Z and S mutations by polymerase chain reaction-mediated site-directed mutagenesis. *Clinical Chemistry, 38*, 1486–1488.

Zorzetto, M., Russi, E., Senn, O., Imboden, M., Ferrarotti, I., Tinelli, C., Campo, I., Ottaviani, S., Scabini, R., von Eckardstein, A., Berger, W., Brändli, O., Rochat, T., Luisetti, M., Probst-Hensch, N., & SAPALDIA Team. (2008). SERPINA1 gene variants in individuals from the general population with reduced alpha-1 antitrypsin concentrations. *Clinical Chemistry, 54*, 1331–1338.

Chapter 6
CRAC Ion Channels and Airway Defense Reflexes in Experimental Allergic Inflammation

M. Sutovska, M. Adamkov, M. Kocmalova, L. Mesarosova, M. Oravec, and S. Franova

Abstract Calcium release-activated calcium channels (CRAC) play unambiguous role in secretory functions of mast cells, T cells, and eosinophils. Less knowledge exists about the role of CRAC, widely distributed in airway smooth muscle (ASM) cells, in airway contractility. The presented study seeks to determine the possible participation of CRAC in ASM-based inflammatory airway disorders in guinea pigs. The acute and long-term administration (14 days) of the CRAC antagonist 3-fluoropyridine-4-carboxylic acid was used to examine the ASM contractility and associated reflexes in the guinea pig model of allergic airway inflammation by the following methods: (i) evaluation of specific airway resistance *in vivo*; (ii) evaluation of the contractile response of isolated ASM strips *in vitro*; and (iii) citric acid-induced cough reflex; (iv) measurement of exhaled NO levels (E_{NO}). Allergic airway inflammation was induced by repetitive exposure of guinea pigs to ovalbumin (10^{-6} M). The CRAC antagonist administered in a single dose to guinea pigs with confirmed allergic inflammation significantly reduced the cough response and the airway resistance, which corresponded with the findings *in vitro*. Long-term application of the CRAC antagonist had more strongly expressed effects. The results confirm the role of CRAC in the pathophysiology of experimental animal asthma and have a potential meaning for anti-asthma therapy.

Keywords Allergic inflammation • Airway • CRAC channels • Cough • Mast cells

6.1 Introduction

The intracellular free calcium (Ca^{2+}) is a ubiquitous second messenger that regulates rapid cellular responses ranging of secretion and cytoskeletal remodelling to long-term events such as cell proliferation and differentiation (Berridge et al. 2000). Cytosolic Ca^{2+} is adjusted through an influx of Ca^{2+} by voltage-, sensory-, or ligand-gated opening of plasma membrane channels and signal-mediated opening of calcium channels in the endoplasmic reticulum (ER) (Berridge et al. 2003). The molecular mechanisms and consequences of Ca^{2+} signaling are especially well characterized in cells of the

M. Sutovska (✉) • M. Kocmalova • L. Mesarosova • M. Oravec • S. Franova
Department of Pharmacology, Jessenius Faculty of Medicine, Comenius University,
Sklabinska 26 St., 03753 Martin, Slovakia
e-mail: sutovska@jfmed.uniba.sk

M. Adamkov
Institute of histology and Embryology, Jessenius Faculty of Medicine, Comenius University,
Sklabinska St, 03753 Martin, Slovakia

M. Pokorski (ed.), *Respiratory Regulation - The Molecular Approach*,
Advances in Experimental Medicine and Biology 756, DOI 10.1007/978-94-007-4549-0_6,

immune system. The primary mechanism of Ca^{2+} influx into cells of the peripheral immune system is a process known as store-operated Ca^{2+} entry. Previously, Putney (1986) suggested that depletion of ER Ca^{2+} stores could evoke sustained Ca^{2+} influx across the plasma membrane of non-excitable cells independently of receptor engagement or generation of second messengers. Parallel biophysical experiments established that lymphocytes and mast cells indeed express store-operated Ca^{2+} channels (SOC) that can be opened in response to store depletion by various agents (Lewis 2001; Parekh and Putney 2005). These channels termed CRAC (calcium release–activated calcium) channels contain as their pore subunits a class of four-pass transmembrane proteins Orai (a member of transient receptor potential proteins, TRP), gated by ER transmembrane proteins known as STIM. STIM proteins, the sensor of stored calcium, sense the depletion of Ca^{2+} from the ER, oligomerize, translocate to junctions adjacent to the plasma membrane, organize Orai (the pore-forming subunit) into clusters and open these channel (Hogan and Rao 2007). Increasing intracellular calcemia leads to dissociation of subunits and inhibits CRAC channel function. CRAC channel activity represents a chief mechanism of Ca^{2+} entry triggered when the endoplasmic reticulum (ER) Ca^{2+} store is depleted in mast cells and T cells (Ishikawa et al. 2003). These channels, along with eosinophils, are believed to be key cellular effectors which release mediators, granule proteins, and cytokines, resulting in the main clinical symptoms of asthma and other allergic diseases (Feske 2007). Mast cells have key functions as effectors of IgE-mediated allergic inflammation. Allergen stimulation induces Ca^{2+} influx and elicits the secretion of inflammatory mediators from mast cells. However, resting lymphocytes maintain a low concentration of Ca^{2+} and engagement of antigen receptors induces calcium influx from the extracellular space (Hogan et al. 2010).

CRAC channels are also widely distributed within airway smooth muscle cells and up-regulated in asthma. The contractile response of airway smooth muscle cells is dependent on both release from intracellular stores and influx through non-voltage-dependent pathways. The mechanisms of SOC entry in smooth muscle remain still incompletely understood. Recently, Peel et al. (2008) demonstrated expression and roles for ORAI homologues in store-operated calcium influx in primary cultured HASM cells, using the RNA interference approach. Since both the mechanisms underlying the activation of airway smooth muscle contraction and the immunological base are of fundamental importance to asthma, in the present study we set out to determine the role of CRAC channels in an experimental asthma model.

6.2 Methods

6.2.1 Animals

The experiments were approved by a local Ethics Committee of the Jessenius Faculty of Medicine in Martin, Slovakia, were performed in accordance with the revised Declaration of Helsinki from 1983 and followed the EU criteria of experimental animals' well fare. The animals used in the study – adult male Trik strain guinea pigs, weighing 150–350 g – were obtained from the Department of Experimental Pharmacology, Slovak Academy of Sciences, Dobra Voda, Slovakia and from a breeding facility of Velaz in Prague, Czech Republic and were housed in approved animal holding facility. A total of 64 animals were used in experiments. The guinea pigs were divided into the following groups, each consisting of eight animals:

1. Negative controls – one group of sensitized animals was used only for histological studies on Day 7 of sensitization, a second group received solvent used in the study (water for injection) in a dose 1 ml kg^{-1}, i.p.
2. Positive controls – two groups of sensitized guinea pigs received salbutamol (10 mg kg^{-1}, i.p.) or codeine (10 mg kg^{-1}, i.p.). Salbutamol was used as a control drug in tests of ASM reactivity and codeine in the measurement of cough response.

3. Experimental groups – four groups of animals underwent acute (single dose: 1.3, 1.5, and 1.7 mg kg^{-1}, i.p.) or long-term therapy (dose 1.5 mg kg^{-1}, i.p.) by the CRAC channels antagonist 3-fluoropyridine-4-carboxylic acid ($C_6H_4FNO_2$). The dose for long-term administration was selected from the doses used in acute therapy according to their influence on the defense airway reflexes.

6.2.2 Antigen-Induced Airway Hyperresponsiveness

Sensitization of animals by the antigen ovalbumin, which causes airway reactivity changes on immunological basis, was performed during 21 days. The allergen (ovalbumin – 10^{-5} mol l^{-1}) adsorbed on $Al(OH)_3$ was administered on Day 1 of sensitization (0.5 ml, i.p. and 0.5 ml, s.c.) and on Day 3 (1 ml, i.p.). Inhalation of the ovalbumin aerosol (PARI Jet Nebuliser, Paul Ritzau, Pari-Werk, Germany; output 5 $l s^{-1}$, particles mass median diameter 1.2 μm) during 1–2 min intervals was performed on Days 9, 12, 15, 18, and 20 using a double-chamber whole body plethysmograph (HSE type 855, Hugo Sachs Elektronik, Germany). Aerosol was delivered to the head chamber of the plethysmograph. All tests with sensitized animals were accomplished 24 h after the last allergen provocation on Day 21.

6.2.3 Chemicals

3-fluoropyridine-4-carboxylic acid was obtained from Alfa Aesar (Germany), citric acid, salbutamol, codeine and acetylcholine and histamine were purchased from Sigma-Aldrich (Lambda, Slovakia). The CRAC channel blocker, salbutamol, and codeine were dissolved in water for injection and all other drugs in 0.9% saline.

6.2.4 Evaluation of Airway Smooth Muscle (ASM) Reactivity In Vivo

ASM reactivity was evaluated using the double-chamber plethysmograph. The values of specific airway resistance (RV) calculated after Pennock et al. (1979) and their changes were regarded as an indicator of *in vivo* airways reactivity. RV is proportional to the phase difference between nasal and thoracic respiratory airflow. This non-invasive plethysmographic technique is commonly used for the evaluation of the effects of bronchoactive substances (Tohda et al. 2000).

RV was measured during 1 min after exposure to citric acid and recording the cough response. The intensities cough and RV prior to administration of salbutamol, solvent, and the CRAC channel antagonist were taken as baseline (N value in graphs). The next measurements were taken at 1, 2, and 5 h time intervals. Between the recording of the cough response and the measurements of RV there was a 2-min time lapse, during which fresh air was insufflated into the nasal chamber.

6.2.5 Cough Reflex Assessment

We used citric acid aerosol in concentration of 0.3 M in saline for cough provocation (Sutovska et al. 2007). The following two methods for detection of cough were used to distinguish the cough efforts from sneezing and movements:

- Changes in expiratory airflow interrupting the basic respiratory pattern during cough effort were measured by a pneumotachograph connected to the head chamber of the plethysmograph.
- Typical cough reflex movements and sounds were recognized by a trained observer.

Inhalation of citric acid in the plethysmograph lasted for 3 min. During this time, the number of cough efforts was counted on the basis of sudden enhancement of expiratory flow accompanied by a typical cough movement and sound. The cough response was measured prior to administration of any agent (baseline measurement; N value in graphs) and then after application of codeine, solvent, and the CRAC channel antagonist in the time intervals of 1, 2, and 5 h. These time intervals were chosen to prevent cough receptors adaptation to the irritant.

6.2.6 Evaluation of Airway Smooth Muscle (ASM) Reactivity In Vivo

Changes in ASM reactivity in response to cumulative doses of acetylcholine and histamine after administration of the above-mentioned drugs were assessed in an organ bath according to the method of Nosalova et al. (2006). Briefly, sensitized guinea pigs were sacrificed by interruption of the spinal cord in the neck, 1 h after i.p. administration of 3-fluoropyridine-4-carboxylic acid or saline (control group), and the respiratory organs were removed. Four strips (two of tracheal and two of pulmonary smooth muscle) obtained from each animal were placed in an organ bath chambers filled with Krebs-Henseleit's buffer (in mM: NaCl 112.9, KCl 4.7, $CaCl_2$ 2.8, $MgSO_4$ 0.5, $NaHCO_3$ 24.9, glucose 11.1) saturated with carbogen (95% O_2 + 5% CO_2) and maintained at 36°C ± 0.5°C and pH 7.5 ± 0.1. Single strips were fixed onto the sliding arm and the other end was bound with a thin thread to a hook of a transducer (TSR 10 G, Vyvoj, Slovakia) and amplifier (M1101, SUPR, Microtechna, Slovakia). The tension was transmitted to a linear recorder (Line Recorder TZ 4620, Laboratorni pristroje, Czech Republic) to monitor the intensity of contractile responses. The amplitude of isometric contraction (mN) of tracheal and pulmonary smooth muscles to cumulative doses of acetylcholine and histamine at concentrations 10^{-8}–10^{-3} mol l^{-1} was used for the evaluation of ASM reactivity.

6.2.7 Measurement of Exhaled NO (E_{NO})

Exhaled NO (E_{NO}) is considered a non-invasive, although indirect, means of detecting inflammation in the respiratory tract. During the E_{NO} measurements, the animals were placed into a separate chamber, connected with NIOX Flex Offline Start Kit 04-1210-F (Aerocrine AB, Sweden), and breathed NO-free air for 5 min. Subsequently, the exhaled gas (flow rate 5 ml s^{-1}) was analyzed during 7 s. NIOX system is equipped with a chemiluminescence gas analyzer of high sensitivity and specificity, along with integrated software, to measure NO molecules at the particle per billion concentrations, ppb. E_{NO} values were measured in the experimental groups before and after the sensitization procedure, 1 h after a single dose of 1.5 mg kg^{-1} of the CRAC antagonist 3-fluoropyridine-4-carboxylic acid, and on Days 7 and 14 of the long-term treatment with it.

6.2.8 Histological Evaluation

All specimens were fixed in 10% formaldehyde solution at least for 24 h. After fixation, the samples were dehydrated in alcohol-xylen mixtures and embedded into paraffin blocks. Tissue sections (4–6 μm thick) were cut in a slide microtome and stained with hematoxylin-eosin. For the assessment of mast cells, slides were stained with anti-mast cell tryptase (DAKO, Bio-serv, Slovakia, IS 640 clone AA1 mast cell tryptase, KIT K 0609 LSAB system- HRP for use in rat specimens).

All microscopic slides were assessed by two independent observers. Any possible discrepancies between the two were resolved by a repeated common assessment of a specimen under a

dual-head microscope. The evaluation focused particularly on eosinophilia and mast cells infiltration which were assessed semi quantitatively by a 4-level grading system (0: absence of infiltrate, 1: slight increase in both cell populations, 2: moderate increase in both cell populations, and 3: distinct cellular infiltrate).

6.2.9 Statistical Analysis

Except for histological results, which are expressed in the percentage terms, all data were given as means ± SE. For statistical analysis, a *t*-test was used. A $p<0.05$ was considered statistically significant.

6.3 Results

6.3.1 Airways Smooth Muscle Reactivity In Vivo

Acute administration of the CRAC channel antagonist 3-fluoropyridine-4-carboxylic acid to sensitized animals resulted in a significant and dose-dependent decrease of RV values. The highest dose used suppressed RV comparably with the effect of the bronchodilator salbutamol, used as the reference, regardless of the kind of bronchoprovocation, citric acid or histamine (Fig. 6.1a, b, respectively). Histamine-induced airway irritation was suppressed longer by all tested doses of the CRAC channel antagonist. The long-term treatment with 3-fluoropyridine-4-carboxylic acid resulted in prolonged and increased effectiveness, seen in the measurement 1 h after its i.p. administration (data not shown).

6.3.2 Airway Smooth Muscle Reactivity In Vitro

Acute administration of the CRAC channel antagonist in a dose of 1.5 mg kg^{-1} significantly reduced the contractile response of both tracheal and pulmonary smooth muscle strips to cumulative doses of acetylcholine and histamine (Table 6.1). The long-term treatment with the CRAC antagonist further

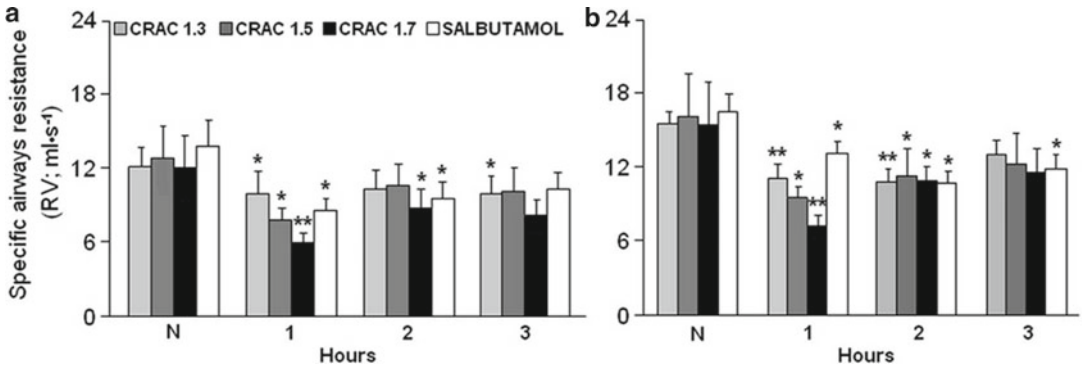

Fig. 6.1 Acute influence of 3-fluoropyridine-4-carboxylic acid, an antagonist of calcium release-activated calcium channels (CRAC), tested at different doses (1.3, 1.5, and 1.7 mg kg^{-1}) on specific airway resistance (RV). **(a)** Airway hyperreactivity induced by citric acid and **(b)** by histamine. The results were referenced to the effect of salbutamol at 1, 2, and 3 h. 'N' stands for normal values at baseline before application of any agents. *$p<0.05$; **$p<0.01$ *vs.* 'N'

Table 6.1 Contraction amplitude (mN) of isolated airway smooth muscle strips (tracheal and pulmonary) in response to cumulative doses of histamine and acetylcholine in sensitized control group (control OVA$^+$) and changes after acute (CRAC A) and long-term (CRAC LT) administration of CRAC channel antagonist

	Control OVA$^+$		CRAC A		CRAC LT	
Mediator	Trachea	Lungs	Trachea	Lungs	Trachea	Lungs
Histamine (log M)						
−8	0.15 ± 0.08	0.09 ± 0.04	0.09 ± 0.03	0.03 ± 0.01	0.07 ± 0.02**	0.05 ± 0.01
−7	0.37 ± 0.04	0.14 ± 0.04	0.22 ± 0.03*	0.16 ± 0.03	0.12 ± 0.04**	0.1 ± 0.01
−6	0.64 ± 0.08	0.24 ± 0.04	0.45 ± 0.06*	0.19 ± 0.04*	0.28 ± 0.05***	0.16 ± 0.03*
−5	1.06 ± 0.11	0.45 ± 0.03	0.71 ± 0.04*	0.28 ± 0.05*	0.65 ± 0.13*	0.27 ± 0.05**
−4	1.19 ± 0.10	0.60 ± 0.05	0.97 ± 0.07	0.39 ± 0.05**	0.85 ± 0.15*	0.38 ± 0.07***
−3	1.26 ± 0.09	0.73 ± 0.05	1.02 ± 0.07	0.49 ± 0.09**	0.92 ± 0.17*	0.44 ± 0.08**
Acetylcholine (log M)						
−8	0.09 ± 0.06	0.11 ± 0.04	0.05 ± 0.02	0.05 ± 0.03	0.11 ± 0.04	0.03 ± 0.01
−7	0.12 ± 0.06	0.17 ± 0.04	0.10 ± 0.03	0.09 ± 0.03*	0.18 ± 0.04	0.06 ± 0.02*
−6	0.15 ± 0.07	0.24 ± 0.10	0.24 ± 0.04	0.10 ± 0.01**	0.38 ± 0.07*	0.08 ± 0.02***
−5	0.23 ± 0.07	0.34 ± 0.09	0.49 ± 0.08	0.14 ± 0.04**	0.68 ± 0.06**	0.13 ± 0.02***
−4	0.31 ± 0.08	0.44 ± 0.09	0.68 ± 0.09*	0.22 ± 0.03**	0.91 ± 0.04***	0.21 ± 0.02***
−3	0.38 ± 0.08	0.53 ± 0.10	0.75 ± 0.09*	0.34 ± 0.04**	1.05 ± 0.03***	0.33 ± 0.03**

*p < 0.05; **p < 0.01; ***p < 0.001 *vs.* respective control tissues

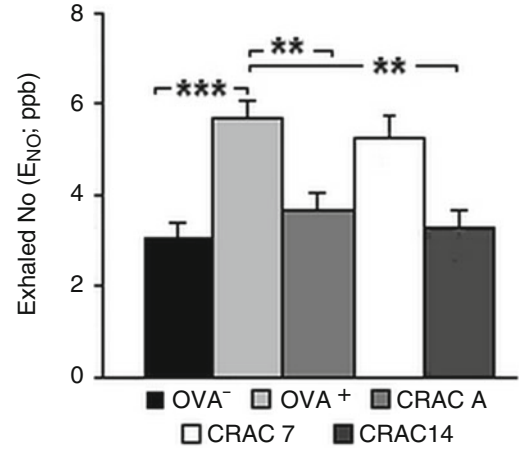

Fig. 6.2 Exhaled NO in non-sensitized (OVA$^-$) compared with sensitized (OVA$^+$) guinea pigs. Influence of acute (CRAC A) and long-term, for 7 and 14 days (CRAC 7 and CRAC 14), treatment with 3-fluoropyridine-4-carboxylic acid, an antagonist of calcium release-activated calcium channels (CRAC), on sensitization-enhanced E_{NO}. **p < 0.01; ***p < 0.001

augmented its relaxing effect on isolated tracheal strips in response to the two mediators, while the response of pulmonary strips remained similar to that observed during the acute response.

6.3.3 Exhaled NO Changes

The allergic inflammatory reaction which developed in the airways increased E_{NO} twofold. Subsequently, both acute and long-term administration of the CRAC channel antagonist 3-fluoropyridine-4-carboxylic acid reduced the increased E_{NO} down to the level present before sensitization (Fig. 6.2).

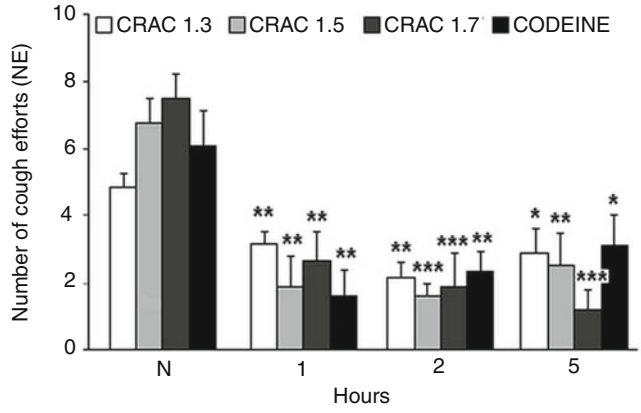

Fig. 6.3 (a) Acute influence of 3-fluoropyridine-4-carboxylic acid, an antagonist of calcium release-activated calcium channels (*CRAC*), tested at different doses (1.3, 1.5, and 1.7 mg kg^{-1}) on the number of citric acid-induced cough efforts (NE). The antitussive effects were referenced to the effects of codeine (10 mg kg^{-1}) at 1, 2, and 5 h. 'N' stands for normal values at baseline before application of any agents. *p<0.05; **p<0.01; ***p<0.001 *vs.* 'N'

Table 6.2 The number of tracheal and lung sections with positive (Pos) – grades 2 and 3 – and negative (Neg) – grades 0 and 1 – inflammatory changes seen as eosinophilia and mast cells infiltration in the ovalbumin (OVA)-sensitized control group of guinea pigs on Day 7 and Day 21 of sensitization and in the group which underwent acute treatment with the CRAC channel antagonist

	Trachea				Lungs			
Group	Mast cells		Eosinophils		Mast cells		Eosinophils	
	Neg	Pos	Neg	Pos	Neg	Pos	Neg	Pos
OVA 7 (n=6)	4	2	2	4	4	2	1	5
OVA 21 (n=8)	1	7	1	7	0	8	1	7
CRAC A (n=8)	2	6	5	3	4	4	1	7

6.3.4 Citric Acid-Induced Cough Reflex

Acute administration of the CRAC channel antagonist 3-fluoropyridine-4-carboxylic acid showed an unambiguous dose-dependent cough suppressive effect, which exceeded the action of the control antitussive drug codeine at 2 and 5 h after its administration (Fig. 6.3). The long-term pretreatment with the CRAC channel antagonist further augmented the antitussive effects; e.g., 1 h after its administration in a dose of 1.5 mg kg^{-1} citric acid-induced cough was nearly entirely suppressed (data not shown).

6.3.5 Histological Results

The tryptase positivity in the mast cells infiltrating the airways became apparent in epithelium/submucosa of the trachea and parenchyma/bronchioles of the lungs in specimens stained on the 21st day of sensitization with ovalbumin. Eosinophilia in the tracheal epithelium and bronchioles also appeared during the third week of sensitization, while it developed in the lungs earlier. A single dose of the CRAC channel antagonist 3-fluoropyridine-4-carboxylic acid evidently decreased pulmonary mast cells infiltration in the bronchioles and the eosinophilia in the trachea suggesting an anti-inflammatory potency of the agent (Table 6.2).

6.4 Discussion

Calcium ions represent a key second messenger controlling airway smooth muscle (ASM) contractility. Because Ca^{2+} itself is a function of cell activity and an expression of a variety of ion channels in both plasma membrane and sarcoplasmic reticulum, understanding the mechanisms underlying ASM contraction is of essential importance to asthma (Perez-Zoghbi et al. 2009). Over the last years, many ion channel mechanisms have been proposed, including the release of diffusion messengers and vesicle fusion, many of which have remained controversial (Clapham 2003). Recently, Peel et al. (2006) reported the expression of the STIM and Orai protein homologues and pointed to their key role in the activation of SOC influx in human ASM cells. Both proteins are the essential structural components of CRAC channels. In the present study, we demonstrated the role of CRAC channels in ASM reactivity in an animal model of allergic inflammation. A selective antagonist of CRAC channels, 3-fluoropyridine-4-carboxylic acid, dose-dependently decreased specific airway resistance regarded as a predictor of ASM reactivity *in vivo*. Moreover, long-term administration of the inhibitor enhanced and prolonged its bronchodilatory effects. According to Fomina et al. (2000), the number and function of CRAC channels is upregulated in asthma. Perez-Zoghbi et al. (2009) argue that airway hyperreactivity (AHR) may be explained by an abnormal increase in Ca^{2+} sensitivity and airway contractile response has to do with the number and size of ASM cells. Consequently, increased ASM cells proliferation and airway wall remodelling are believed to significantly contribute to AHR.

Augmented inhibition of ASM reactivity observed in the present experiments after long-term administration of 3-fluoropyridine-4-carboxylic acid may be partially conditioned by inhibition of inflammatory cell activity. Airway hyperactivity in asthma usually correlates with the severity of airway inflammation; a process that most likely involves a complex interaction among mast cells, lymphocytes, and eosinophils. In this study, preliminary results of histological investigation show that the CRAC antagonist distinctly decreased mast cell infiltration in the lungs and eosinophilic infiltration of the trachea; a suggested anti-inflammatory capability of CRAC channel antagonists. CRAC channels seem essential for mast cells secretory functions. Preponderance of mediators, playing a role in the asthma pathogenesis, is accompanied by CRAC channel activity. Many mediators, such as histamine, tryptase, IL-4, IL-13, PGD_2, and LTC_4 induce contraction of ASM cells (Brown et al. 2008). Previously, Ng et al. (2008) demonstrated that CRAC channel inhibition attenuates the response of mast cells to IgE stimulation; a triggering factor in allergic inflammation. Our data also are in line with those of Yoshino et al. (2007), who tested the pyrazole derivative YM-58483, known as a selective inhibitor of CRAC channels in T cells, and found that the agent prevents antigen inhalation-induced airway eosinophilia in actively sensitized Brown Norway rats. All taken together, confirms that the inhibition of Ca^{2+} influx through CRAC channels may counteract the antigen-induced airway inflammation, probably *via* inhibition of mast cells, Th2 cytokine formation, and release of inflammatory mediators. Eosinophils and mast cells are generally regarded as typical cells of allergic inflammation (Bochner and Hamid 2003). In the guinea pig, distribution, proportion, and function of airway receptors are similar to those in human airways and hence it is the preferred animal for experiments concerning the airways (Muccitelli et al. 1987). The present study demonstrates eosinophilic and mast cells infiltrations which developed on the 21st day of allergen sensitization, confirming the usefulness of this animal model for studying allergic airway inflammation.

The level of exhaled NO recorded in the present study corresponded well with the results above outlined. On the 21st day of sensitization, we recorded a twofold increase in E_{NO}, eosinophilia, mast cells infiltration of airways, and enhanced ASM reactivity, but then administration of the CRAC antagonist caused decreases in E_{NO} and cellular airway infiltrates, which was followed by reduced airway hyperactivity. Numerous studies have shown that E_{NO} is elevated in patients suffering from untreated asthma. Several of these reports have found correlations between E_{NO} and other variables including airway and induced sputum eosinophilia (Redington 2006). Upregulation of inducible

NO-synthase (iNOS) in inflamed airways is thought to underlie the increase in E_{NO}. Expression of iNOS by airway epithelial cells is regulated by exposure to proinflammatory cytokines released mainly from mast cells and eosinophils. Secretion of cytokines, mediators, and granule proteins by these cells is strongly associated with activated CRAC channels. Therefore, inhibition of CRAC channels in immune cells should be a rational explanation of the present findings. However, expression of NOS isoforms in airways should be studied to confirm the proposed notion.

Suppression of cough by the CRAC channel antagonist was observed in the present study after its acute and long-term administration; the effect was on par with that of codeine. The close relationship between bronchoconstriction and cough is well known. Cough suppressive activity of drugs with bronchodilatory properties (Chung 2005) or cough enhancing activity of those with bronchocontrictive properties, e.g., histamine (Belvisi 2003) have been demonstrated. Hence, presently observed antitussive activity could likely be a result of CRAC antagonistic influence on immune and ASM cells. Studies using various animal models of inflammation showed that allergic inflammation of airways is represented by their physical alterations, such as epithelial damage, mucosal swelling, and remodelling of the airway wall, which all contributes to changed cough response (Mazzone and McGovern 2007). Cough accompanying airway inflammation constitutes a serious medical problem and current antitussive agents, except of centrally acting antitussives with generally known side effects, provide only moderate relief (Morice 2004). Therefore, antitussive activity of a CRAC channel antagonist represents an interesting and promising result.

In conclusion, a selective CRAC channel antagonist caused reductions in airway smooth muscle reactivity in both *in vivo* and *in vitro* conditions, experimentally induced cough, exhaled NO, and airway eosinophilic and mast cells infiltrations. All these findings point to the CRAC ion channels as a rational target for novel antiasthmatic drugs.

Acknowledgments Supported by the project 'Centre of Experimental and Clinical Respirology II' co-financed from EC sources and a grant from the Agency for Science (VEGA) No. 1/0020/11, 1/0062/11.

Conflicts of interest: The authors declare no conflicts of interest in relation to this article.

References

Belvisi, M. G. (2003). Airway sensory innervation as a target for novel therapies: An outdated concept? *Current Opinion in Pharmacology, 3*, 239–243.

Berridge, M. J., Lipp, P., & Bootman, M. D. (2000). The versatility and universality of calcium signalling. *Nature Reviews Molecular Cell Biology, 1*(1), 11–21.

Berridge, M. J., Bootman, M. D., & Roderick, H. L. (2003). Calcium signalling: Dynamics, homeostasis and remodelling. *Nature Reviews Molecular Cell Biology, 4*(7), 517–529.

Bochner, B. S., & Hamid, Q. (2003). Advances in mechanisms of allergy. *The Journal of Allergy and Clinical Immunology, 111*, S819–S823.

Brown, J. M., Wilson, T. M., & Metcalf, D. D. (2008). The mast cell and allergic diseases: Role in pathogenesis and implications for therapy. *Clinical and Experimental Allergy, 38*(1), 4–18.

Chung, K. F. (2005). Drugs to suppress cough. *Expert Opinion on Investigational Drugs, 14*(1), 19–27.

Clapham, D. E. (2003). TRP channels as cellular sensors. *Nature, 426*, 517–524.

Feske, S. (2007). Calcium signalling in lymphocyte activation and disease. *Nature Reviews Immunology, 7*(9), 690–702.

Fomina, A. F., Fanger, C. M., Kozak, J. A., & Cahalan, M. D. (2000). Single channel properties and regulated expression of Ca^{2+} release-activated Ca^{2+} (CRAC) channels in human T cells. *The Journal of Cell Biology, 150*(6), 1435–1444.

Hogan, P. G., & Rao, A. (2007). Dissecting I_{CRAC}, a store-operated calcium current. *Trends in Biochemical Sciences, 32*(5), 235–245.

Hogan, P. G., Lewis, R. S., & Rao, A. (2010). Molecular basis of calcium signalling in lymphocytes: STIM and ORAI. *Annual Review of Immunology, 28*, 491–533.

Ishikawa, J., Ohga, K., Yoshino, T., Takezawa, R., Ichikawa, A., Kubota, H., & Yamada, T. (2003). A pyrazole derivative, YM-58483, potently inhibits store-operated sustained Ca^{2+} influx and IL-2 production in T lymphocytes. *The Journal of Immunology, 170*(9), 4441–4449.

Lewis, R. S. (2001). Calcium signalling mechanisms in T lymphocytes. *Annual Review of Immunology, 19*, 497–521.

Mazzone, S. B., & McGovern, A. E. (2007). Sensory neural targets for the treatment of cough. *Clinical and Experimental Pharmacology and Physiology, 34*(10), 955–962.

Morice, A. H. (2004). The diagnosis and management of chronic cough. *European Respiratory Journal, 24*(3), 481–492.

Muccitelli, R. M., Tucker, S. S., Hay, D. W. P., Torphy, T. J., & Wasserman, M. A. (1987). Is the guinea pig trachea a good in vitro model of human large and central airways? Comparison on leukotriene- methacholine-, histamine-, and antigen-induced contractions. *Journal of Pharmacology and Experimental Therapeutics, 243*(2), 467–473.

Ng, S. W., Capite, J., Singaravelu, K., & Parekh, A. B. (2008). Sustained activation of the tyrosine kinase Syk by antigen in mast cells requires local Ca^{2+} influx through Ca^{2+} release-activated Ca^{2+} channels. *Journal of Biological Chemistry, 283*(46), 31348–31355.

Nosalova, G., Franova, S., Mokry, J., & Sutovska, M. (2006). Pharmacotherapy of the cough. In J. Korpas, S. Paintal, & A. Anand (Eds.), *Cough from lab to clinic*. Delhi: Ane Books.

Parekh, A. B., & Putney, J. W., Jr. (2005). Store-operated calcium channels. *Physiological Reviews, 85*, 757–810.

Peel, S. E., Liu, B., & Hall, I. P. (2006). A key role for STIM1 in store operated calcium channel activation in airway smooth muscle. *Respiratory Research, 7*, 119.

Peel, S. E., Liu, B., & Hall, I. P. (2008). ORAI and store-operated calcium influx in human airway smooth muscle cells. *American Journal of Respiratory Cell and Molecular Biology, 38*(6), 744–749.

Pennock, B. E., Cox, C. P., Rogers, R. M., Cain, W. A., & Wells, J. H. (1979). A noninvasive technique for measurement of changes in specific airway resistance. *Journal of Applied Physiology, 46*(2), 399–406.

Perez-Zoghbi, J. F., Karner, C., Ito, S., Shepherd, M., Alrashdan, Y. A., & Sanderson, M. J. (2009). Ion channel regulation of intracellular calcium and airway smooth muscle function. *Pulmonary Pharmacology and Therapeutics, 22*, 388–397.

Putney, J. W. (1986). A model for receptor-regulated calcium entry. *Cell Calcium, 7*(1), 1–12.

Redington, A. E. (2006). Modulation of nitric oxide pathways: Therapeutic potential in asthma and chronic obstructive pulmonary disease. *European Journal of Pharmacology, 533*(1–3), 263–276.

Sutovska, M., Nosalova, G., & Franova, S. (2007). The role of potassium ion channels in cough and other reflexes of the airways. *Journal of Physiology and Pharmacology, 58*(Suppl 5), 673–683.

Tohda, Y., Muraki, M., Ywanaga, T., Haraguchi, R., Fukuoka, M., & Nakajima, S. (2000). Dual-phase response model for bronchial asthma. *Allergy and Asthma Proceedings, 21*(2), 79–84.

Yoshino, T., Ishikawa, J., Ogha, K., Morokata, T., Takewaza, R., Morio, H., Okada, A., Honda, K., & Yamada, T. (2007). YM-58483, a selective CRAC channel inhibitor, prevents antigen-induced airway eosinophilia and late phase asthmatic responses via Th2 cytokine inhibition in animal models. *European Journal of Pharmacology, 56*(2–3), 225–233.

Chapter 7
Experimental Model of Allergic Asthma

S. Franova, M. Joskova, V. Sadlonova, D. Pavelcikova, L. Mesarosova, E. Novakova, and M. Sutovska

Abstract The aim of the study was to prepare and evaluate the experimental model of allergic asthma. Changes in chough reflex, bronchoconstriction and the degree of inflammation were studied in ovalbumin (OVA) sensitized guinea pigs after 0, 7, 14, 21 days of exposure. The cough reflex was induced by citric acid inhalation in conscious animals in a double chamber body plethysmograph. Tracheal smooth muscle reactivity was assessed by examining the *in vitro* response to histamine (H) (10^{-8}–10^{-3} mol/l) and *in vivo* to H nebulization (10^{-6} mol/l). BALF levels of IL-4, IL-5 and the eosinophil count were used as parameters of airway inflammation. After 7 days of OVA sensitization, there was an increase in tracheal smooth muscle contractility *in vitro* to cumulative concentration of H and an increase in cough parameters. After 14 days of OVA sensitization, there was a further increase in tracheal smooth muscle contractility to H, an increase in airway resistance, and a small increase in cough parameters. After 21 day of OVA sensitization, cough parameters were significantly reduced, airway resistance after H inhalation was increased, and there were significant increases in IL-4, IL-5, and eosinophils in BALF. In conclusion, progress in asthmatic inflammation during 21-day OVA sensitization caused a gradual increase in inflammatory mediators, a decline in cough reflex, and enhanced bronchoconstriction. This experimental model of allergic asthma can be used for pharmacological modulations of defense reflexes and inflammation.

Keywords Airway hyperreactivity • Allergic asthma • Guinea pigs • Cough reflex • Ovalbumin • Sensitization • Citric acid

7.1 Introduction

Allergic asthma is a chronic inflammatory disorder of the airways. Characteristic features of this disease are allergen-induced early and late bronchial obstructive reactions, airway inflammation, structural changes of the airway wall associated with progressive decline in lung function, and airway

S. Franova (✉) • M. Joskova • V. Sadlonova • D. Pavelcikova • L. Mesarosova • M. Sutovska
Department of Pharmacology, Jessenius Faculty of Medicine, Comenius University,
Sklabinska 26, 037 05 Martin, Slovakia
e-mail: franova@jfmed.uniba.sk

E. Novakova
Department of Microbiology and Immunology, Jessenius Faculty of Medicine,
Comenius University, Sklabinska 26, 037 05 Martin, Slovakia

M. Pokorski (ed.), *Respiratory Regulation - The Molecular Approach*,
Advances in Experimental Medicine and Biology 756, DOI 10.1007/978-94-007-4549-0_7,

hyperresponsiveness. Airway hyperresponsiveness is a clinical hallmark of asthma and it is defined by an exaggerated obstructive response of the airways to a variety of pharmacological, chemical, and physical stimuli (Postma and Kerstjens 1998). Allergic asthma continues to be clinically important, since bronchoconstriction and airway hyperresponsiveness remain beyond our complete pharmacological control (Janssen 2009).

A major problem in experimental studies on the pharmacological approach to allergic asthma is lack of valid animal models which would mimic airway hyperreactivity, early and late allergen reaction, and inflammation all seen in human conditions. Different animal models of allergic asthma have been applied for the investigation of the mechanisms of acute and chronic airway hyperresponsiveness (Meurs et al. 2008). Currently, the most widely used experimental animal for modelling the allergic responses in the airways is the mouse, due likely to the availability of transgenic and gene targeted mice. The mouse also is easily sensitized to a number of antigens, including ovalbumin and human allergens. However, murine models appear to be less suited for the investigation of the mechanisms of airway hyperresponsiveness in relation to early and late asthmatic responses. Thus, airway hyperresponsiveness and early asthmatic reactions are usually observed only after repeated allergen challenges, and a late asthmatic reaction is rarely observed (Zosky and Sly 2007; Zosky et al. 2008). Difficulties in measuring these responses could be related to the anatomical structure of the mouse lung (Irvin and Bates 2003) and the unresponsiveness of airway smooth muscles to various bronchoconstrictors implicated in the pathophysiology of asthma (histamine, cysteinyl leukotrienes, neurokinins, bradykinin, and prostanoids) (Canning 2003).

The aim of the present study was to prepare and evaluate a model of late allergic asthmatic response in guinea pigs. Our experiments were focused on the assessment of airway reactivity and the degree of inflammation during 21-day allergen (ovalbumin) administration. The assessment consisted of tracheal smooth muscle reactivity *in vitro*, changes in specific airway resistance in response to histamine *in vivo*, the degree of inflammation evaluated by eosinophil count, and the estimation of the inflammatory cytokines IL-4 and IL-5 in bronchoalveolar lavage fluid (BALF).

7.2 Methods

The protocol of this experimental study was approved by the Ethics Committee of the Jessenius Faculty of Medicine in Martin, Slovakia. Ovalbumin (OVA, egg albumin grade V), histamine (histamine × 2 HCl), citric acid and other chemicals were purchased from Sigma Chemicals (Germany). Mouse IL-5, IL-4 ELISA Kits for protein array systems were purchased from RayBiotech, Inc. (Norcross, GA).

7.2.1 Sensitization of Guinea Pigs

Guinea pigs (200–250 g) were randomly divided into 2 experimental groups: Group 1 (Control) treated 21 days with saline only and Group 2 sensitized for 21 days with ovalbumin (OVA). There were 12 animals in each group.

Male Trik guinea pigs (200–250 g) were actively sensitized by administration of OVA (Grade V; Sigma Chemicals, Germany). Five milligrams of OVA (with 1 mg of aluminium hydroxide) were injected intraperitoneally together with 5 mg OVA in 1 ml of saline, subcutaneously, on Day 1. Subsequently, the guinea pigs were treated for 21 days with repeated i.p. OVA injections every 3 days. Additionally, the guinea pigs were exposed to nebulized OVA (1% in 0.9% sterile sodium chloride

solution) in an aerosol chamber for the last 5 days. This scheme of allergen sensitization has previously been found to evoke a sufficient degree of chronic inflammation in the airways of guinea pigs (Franova et al. 2009)

7.2.2 Tracheal Smooth Muscle Contraction in vitro

Reactivity of tracheal smooth muscle was assessed before OVA sensitization and then after 7, 14, 21 days of sensitization. Tracheal strips were placed in a 20 ml organ chamber containing Krebs-Henseleit buffer of the following composition in mM: NaCl 110.0, KCl 4.8, $CaCl_2$ 2.35, $MgSO_4$ 1.20, K_2PO_4 1.20, and $NaHCO_3$ 25.0 in glass-distilled water. The chamber was maintained at 36.5°C ± 0.5°C and was aerated continuously with a mixture of 95% O_2 and 5% CO_2 to maintain pH 7.5 ± 0.1. The tracheal tissue strips were initially set to 4 g of tension (30-min loading phase). Afterward, tension was readjusted to the baseline of 2 g (30-min adaptation phase). The amplitude of muscle contraction (mN) to the cumulative doses of histamine (H) of 10^{-8}–10^{-3} mol/l was used as a parameter of tracheal smooth muscle reactivity.

7.2.3 Evaluation of Airway Reactivity in vivo

Airway reactivity was evaluated *in vivo* using a rodent double chamber body plethysmograph (HSE type 855; Hugo Sachs Electronic-Harvard, with HSE Pulmodyn Pennock W software, Germany) before and after OVA sensitization according to the time schedule above outlined for the in vitro studies. Changes in specific airway resistance (RxW) after a 2-min inhalation of H (10^{-6} mol/l in saline) were considered an indicator of airways reactivity. There was an interval of 5 min between histamine exposure and airway resistance measurement. During this interval, fresh air was insufflated into the breathing chamber.

7.2.4 Chemically Induced Cough

Conscious guinea pigs, both control and OVA sensitized, were placed in a body plethysmograph box and was exposed to 0.3 M citric acid aerosol for 3 min. Cough detection and distinguishing of cough efforts from sneezing was based on expiratory airflow traces, recorded by a pneumotachograph connected to the head chamber of the plethysmograph, and typical cough movements and sounds recognized by a trained observer. The number of coughs was measured at 30 min intervals up to 120 min at a given day of sensitization above outlined.

7.2.5 Measurement of Inflammatory Cytokines

The left lung was lavaged with 0.9% NaCl (37°C) 2×10 ml/kg and BALF was centrifuged at 1,500 rpm for 10 min. The supernatant was used for subsequent biological analysis. Concentrations of IL-4 and IL-5 were determined by ELISA method in BALF, using commercially available kits (RayBiotech, Inc., Norcross, GA). The minimum detectable level of cytokines was 0.1 pg/ml.

7.2.6 Histological Examination

The trachea was fixed in 10% buffered formaldehyde. Sections of 10 μm were made and stained with haematoxylin and eosin for light microscopy at a magnification 240x. On the basis of eosinophils counted, the degree of inflammation was divided into mild – up to 50, medium – up to 100, and strong – over 100 eosinophils.

7.2.7 Data Analysis

All results were expressed as means ± SE. Statistical analysis was performed using one-way ANOVA. Differences were considered statistically significant when p value was below 0.05.

7.3 Results

The effects of allergen sensitization on guinea pig tracheal smooth muscle reactivity were evaluated before OVA application and after 7, 14, 21 days OVA sensitization by *in vitro* responses to cumulative H. The results show progressive significant increases in contraction amplitude of tracheal strips to cumulative doses of H after 7 days of OVA sensitization, with a clear plateauing of the increase at the highest concentration of H (Fig. 7.1a). After another week of OVA sensitization, there was an enhancement of this progressive increase in contraction amplitude along all increasing H concentrations employed; the plateauing of the effect at the highest H concentration was no more observed (Fig. 7.1b). The contraction amplitude of tracheal strips remained at the same enhanced level after the 3rd week of OVA sensitization (Fig. 7.1c).

OVA sensitization caused gradual increases in specific airway resistance (RxW) after H nebulization (10^{-6} mol/l); the increase assumed significance as of the 14th day and was further appreciably augmented after 3 weeks of sensitization (Fig. 7.2a–c).

Concerning the cough reflex, the results were different. The number of chemically induced cough efforts was the greatest already after 7 days of OVA sensitization. From that point on, cough gradually

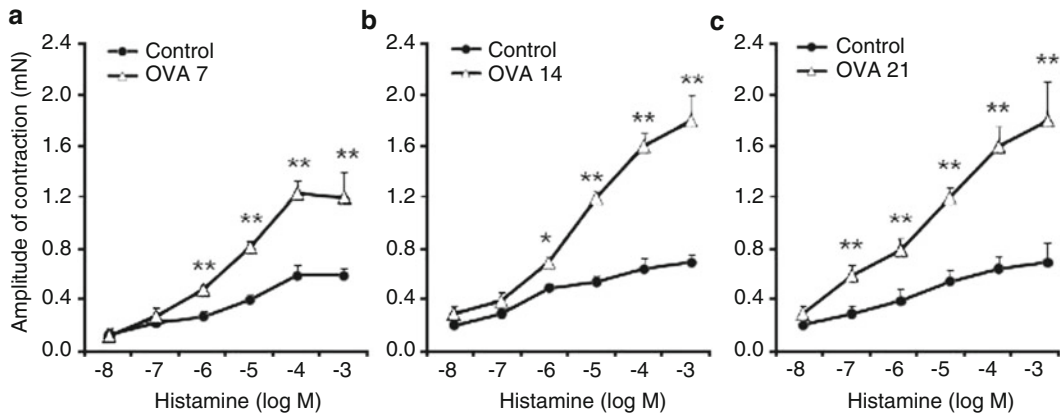

Fig. 7.1 Changes in amplitude of tracheal smooth muscle contraction in response to cumulative doses of histamine after (**a**) 7, (**b**) 14, and (**c**) 21-day of OVA sensitization; *p<0.05 and **p<0.01 for control *vs.* OVA

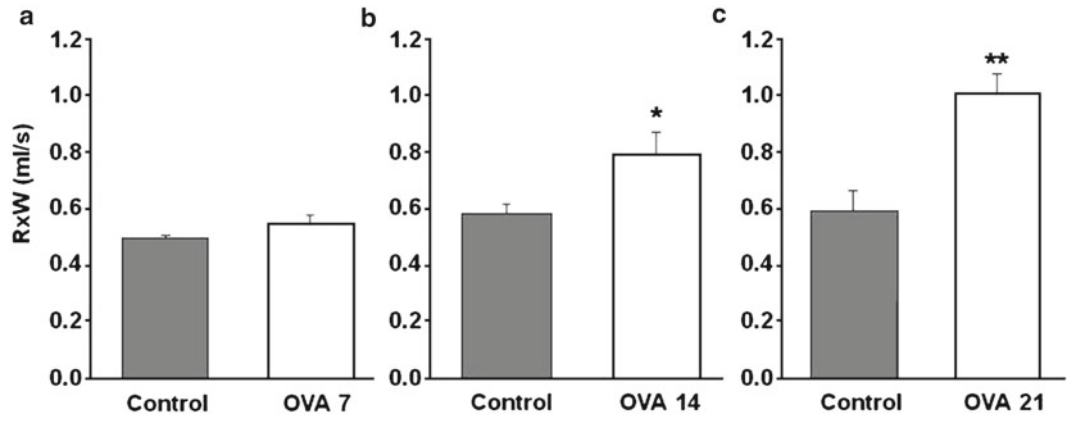

Fig. 7.2 Changes in specific airway resistance after inhalation of histamine (10^{-6} mol/l) between control healthy guinea pigs and then after (**a**) 7, (**b**) 14, (**c**) 21 days of OVA sensitization; *p<0.05 and **p<0.01 for control *vs.* OVA

Fig. 7.3 Comparison of the number of citric-acid-induced coughs in control healthy guinea pigs and then after 7, 14, 21 days of OVA sensitization; **p<0.01 for control *vs.* OVA 7 days

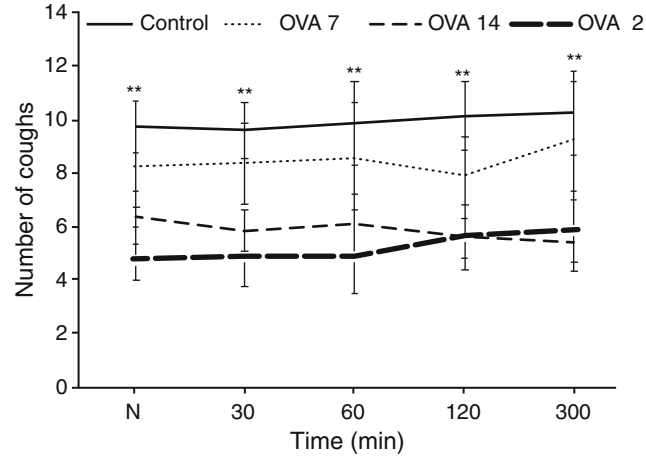

Fig. 7.4 Changes in the inflammatory cytokines IL-4, IL-5 in BALF between control healthy guinea pigs and after 21 days of OVA sensitization (OVA 21); *p<0.05 and **p<0.01 for control *vs.* OVA 21

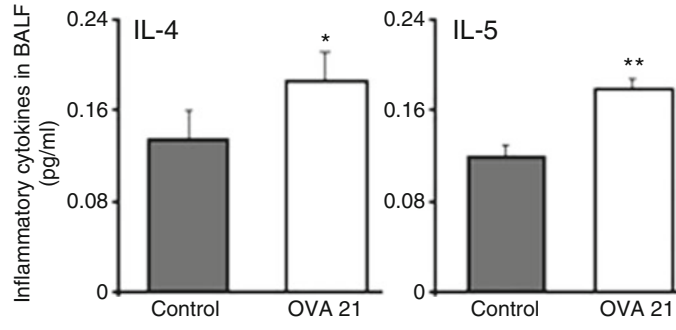

decreased with the extension of OVA sensitization time and actually dropped below the control level recorded before commencement of sensitization after 21 days (Fig. 7.3).

OVA sensitization also influenced the levels of airway inflammatory cytokines measured in BALF, as typified by IL-4 and IL-5. Both cytokines significantly increased; the increases were however noted not until the 21st day of sensitization (Fig. 7.4).

Histological examinations of tracheal mucosa of guinea pigs after OVA sensitization revealed, in general, eosinophilic infiltrations of the epithelium and submucosa. The intensity of inflammation in 12 animals after 21 days of sensitization was as follows: mild – 3, medium – 4, and strong – 3 cases. Eosinophils were organized into microabscess-like entities in the epithelium.

7.4 Discussion

In the present study we evaluated a model of the late allergic asthmatic response in guinea pigs, based on OVA sensitization. The results confirm the progression of airway inflammation after sensitization. The inflammatory cytokines IL-4 and IL-5 in BALF were gradually increasing throughout the period of sensitization, from the 7th up to the 21st day, reaching a significantly higher level at the end of that period. Sensitization also enhanced airway readiness for bronchoconstrictive responses. The cough reflex, on the other hand, after an early strong enhancement, clearly declined in the later part of the sensitization process.

Allergic asthma is defined in as a chronic inflammatory disorder characterized by reversible airways obstruction and airway hyperresponsiveness (AHR). Inflammation is thought to cause symptoms of asthma directly and indirectly by inducing contraction of airway smooth muscles, enhancing airway responsiveness to various stimuli and by inducing changes in structural components of the airway wall, including ASM cells, leading to airway remodeling (Zuyderduyn et al. 2008). Airway smooth muscle cells contribute to airway hyperresponsiveness, remodelling, and inflammation by virtue of their increased sensitivity to bronchoconstrictive stimuli (e.g., histamine, prostaglandins, kinins, or tachykinis) and increased proliferation (Meurs et al. 2008).

In this study we confirmed the development of an increase in tracheal smooth muscle reactivity during a 21-day period of OVA sensitization. Allergen application increased the amplitude of contraction of the tracheal smooth muscle strips, prepared from OVA sensitized guinea pigs, to cumulative doses of histamine. Concerning the *in vivo* airway reactivity, we observed a gradual increase in specific airway resistance measured in a double-chamber body plethysmograph over the sensitization period.

Another reflex which is modulated during inflammatory conditions is cough. The cough response is thought to be regulated by a neuronal network in the brainstem which receives signals from sensory receptors in the larynx and lower respiratory tract. Inflammation is a powerful stimulus for coughing. It has recently been determined that tachykinins, substance P, and the neurokinins A and B are released from non-myelinated C-fiber endings and have a role in airway inflammatory responses such as cough (Widdicombe 1995). It follows that depletion of tachykinins due to destruction of airway C-fibre receptors during inflammation might weaken the cough reflex. Karlsson (1996) has indeed reported a decrease in cough induced by capsaicin and citric acid due to inflammation. The results of the present study also confirm that inflammatory changes in the airways decrease cough reflex sensitivity.

In allergic asthma, it is assumed that the early-phase reaction is due to antigen cross-linking of immunoglobulin IgE molecules bound to specific cell-surface receptors on mast cells (Fc epsilon RI receptors). Subsequent activation of IgE leads to the release of bronchoconstricting mediators, notably leukotrienes and histamine. The allergic late-phase reaction is, in addition to the effects above outlined, linked with the infiltration of the airway wall by inflammatory cells (eosinophils, lymphocytes, and, particularly, CD4-positive T-cells). The immunological processes involved are characterized by proliferation and activation of Th2 lymphocytes (Van Oosterhout and Bloksma 2005). Th2-derived cytokines play a key role in orchestrating the eosinophilic inflammatory response in asthma. The Th2-mediated allergic inflammation is accomplished with cytokines, such as IL-4 and IL-13 the role of which is to make B lymphocytes synthesize IgE, IL-5 which has a role in maturation and activation of eosinophils, and IL-13 which has a role in mast cell genesis (Kips 2001). The estimation of inflammatory cytokines is thus a good marker of the advancement of asthmatic inflammation.

In conclusion, we can summarized that progress in asthmatic inflammation after 21 days sensitization of guinea pigs with OVA is associated with increase in inflammatory cytokines in BALF and amount of eosinophils in tracheal tissue, with the decline of cough reflex and strengthen of bronchoconstriction. From pharmacological point of view sensitised guinea pigs may be preferable as an animal model for investigating of late asthmatic reactions and AHR in asthma.

Acknowledgments This work was supported by the Center of Experimental and Clinical Respirology II. The project was co-financed from EU sources and VEGA 1/0020/10.

Conflicts of interest: The authors declare no conflicts of interest in relation to this article.

References

Canning, B. J. (2003). Modeling asthma and COPD in animals: A pointless exercise? *Current Opinion in Pharmacology, 3*, 244–250.

Franova, S., Joskova, M., Novakova, E., Adamicova, K., Sutovska, M., & Nosal, S. (2009). Effects of flavin7 on allergen induced hyperreactivity of airways. *European Journal of Medical Research, 14*(Suppl 4), 78–81.

Irvin, C. G., & Bates, J. H. (2003). Measuring the lung function in the mouse: The challenge of size. *Respiratory Research, 4*, 4.

Janssen, L. J. (2009). Asthma therapy: How far have we come, why did we fail and where should we go next? *European Respiratory Journal, 33*, 11–20.

Karlsson, J. (1996). The role of capsaicin-sensitive C-fibre afferent nerves in the cough reflex. *Pulmonary Pharmacology, 9*, 315–321.

Kips, J. C. (2001). Cytokines in asthma. *European Respiratory Journal, 18*, 24–33.

Meurs, H., Gosens, R., & Zaagsma, J. (2008). Airway hyperresponsiveness in asthma: Lessons from in vitro model systems and animal models. *European Respiratory Journal, 32*, 487–502.

Postma, D. S., & Kerstjens, H. A. (1998). Characteristics of airway hyperresponsiveness in asthma and chronic obstructive pulmonary disease. *American Journal of Respiratory and Critical Care Medicine, 158*, S187–S192.

Van Oosterhout, J. M., & Bloksma, N. (2005). Regulatory T-lymphocytes in asthma. *European Respiratory Journal, 26*, 918–932.

Widdicombe, J. G. (1995). Neurophysiology of the cough reflex. *European Respiratory Journal, 8*, 1193–1202.

Zosky, G. R., & Sly, P. D. (2007). Animal models of asthma. *Clinical and Experimental Allergy, 37*, 973–988.

Zosky, G. R., Larcombe, A. N., & White, O. J. (2008). Ovalbumin sensitized mice are good models for airway hyperresponsiveness but not acute physiological responses to allergen inhalation. *Clinical and Experimental Allergy, 38*, 829–838.

Zuyderduyn, S., Sukkar, M. B., Fust, A., Dhaliwal, S., & Burgess, J. K. (2008). Treating asthma means treating airway smooth muscle cells. *European Respiratory Journal, 32*, 265–274.

Chapter 8
Effects of Selective Inhibition of PDE4 and PDE7 on Airway Reactivity and Cough in Healthy and Ovalbumin-Sensitized Guinea Pigs

Juraj Mokry, Marta Joskova, Daniela Mokra, Ingrid Christensen, and Gabriela Nosalova

Abstract Phosphodiesterases (PDEs) are enzymes responsible for degradation of cAMP and cGMP in cells. Thus, PDE inhibitors may have significant clinical benefit in respiratory diseases associated with inflammation. The aim of the present study was to evaluate the effects of selective PDE4 (rolipram, ROL) and PDE7 inhibitors (BRL50481, BRL) on citric acid-induced cough, *in vivo* and *in vitro* airway smooth muscle reactivity in both healthy and ovalbumin sensitized guinea pigs. The drugs tested were administered intraperitoneally to male guinea pigs once daily for 7 days – ROL 1 mg/kg, BRL 1 mg/kg, and ROL+BRL 0.5 mg/kg. Double chamber whole body plethysmography was used for the evaluation of citric acid (0.6 M)-induced cough and specific airway resistance. An organ bath method was used for the measurement of tracheal and lung tissue strip contractions evoked by cumulative doses (10^{-8}–10^{-3} mol/L) of acetylcholine (ACH) and histamine (HIS). In healthy guinea pigs, the only significant relaxation was observed after ROL in ACH-induced contractions *in vitro* and the effect on cough was negligible. In ovalbumin-sensitized animals, more pronounced *in vitro* relaxing effects of BRL in HIS-induced contractions and of combination (ROL+BRL) in ACH-induced contractions were observed, with similar results *in vivo*, and no significant change in the number of cough efforts was observed in any of the groups tested. The results suggest that PDE4 and PDE7 inhibitors have stronger anti-inflammatory effects compared with direct effects on smooth muscle and cough, with a potential benefit of their concomitant administration.

Keywords Cough • Airway resistance • Ovalbumin • Inflammation • Acetylcholine • Histamine • Phosphodiesterase inhibitors • Rolipram

J. Mokry (✉) • M. Joskova • I. Christensen • G. Nosalova
Department of Pharmacology, Jessenius Faculty of Medicine, Comenius University,
Sklabinska 26 St, 036 01 Martin, Slovakia
e-mail: mokry@jfmed.uniba.sk

D. Mokra
Department of Physiology, Jessenius Faculty of Medicine, Comenius University,
Mala Hora 4 St, 036 01 Martin, Slovakia

M. Pokorski (ed.), *Respiratory Regulation - The Molecular Approach*,
Advances in Experimental Medicine and Biology 756, DOI 10.1007/978-94-007-4549-0_8,

8.1 Introduction

Chronic inflammation, cough, and bronchoconstriction are key symptoms of bronchial asthma and chronic obstructive pulmonary disease (COPD). Historically, several agents from a group of xanthine derivatives are used in therapy of these airway diseases (Mokry et al. 2009). The mechanism of action of these agents includes a non-selective inhibition of phosphodiesterase (PDE). However, in therapeutically relevant plasma concentrations several other mechanisms also are involved (Mokra and Mokry 2010). In previous studies, the antitussive effects of xanthine derivatives have been confirmed, with no particular discussion about the underlying mechanism (Nosalova and Mokry 2001; Usmani et al. 2005; Mokry et al. 2009).

Xanthine derivatives, due to their mixed and little specific mechanisms, interactions with other drugs, and a narrow therapeutic range are often associated with the occurrence of adverse effects which can limit their use as antitussive drugs (Antoniu 2006; Lipworth 2005). Thus, the selective PDE3, PDE4, or PDE7 inhibitors, or the dual PDE3/4 and PDE4/7 inhibitors could be of greater benefit in therapy of diseases associated with cough (Spina et al. 1998; Chung 2006). The notion has been strengthened by the findings that PDE isoenzymes play a role in the regulation of airway diameter and smooth muscle function. PDE3 and PDE4, both hydrolyzing cAMP, are described as the major PDE isoforms in airways. However, airway smooth muscle and inflammatory cells present in respiratory system also contain PDE1, PDE3, PDE4, PDE5, and PDE7.

PDEs represent 11 superfamilies of metalophosphohydrolases, hydrolyzing cAMP and cGMP to their inactive metabolites (Bender and Beavo 2006). PDE3 is expressed in airway smooth muscle, myocardium, vessels, and the gastrointestinal tract and thus its inhibition would seem a suitable target in affecting airway reactivity and cough. However, inhibitors of PDE4 are considered as the most important therapeutic tools. The first generation inhibitor of PDE4 is rolipram, which was not yet introduced into clinical practice due to its adverse effects at higher doses (nausea, vomiting). Second generation of PDE4 inhibitors (roflumilast, cilomilast) have better perspectives, as they maintained anti-inflammatory and immunomodulating effects with a lower incidence of adverse effects (Karish and Gagnon 2006). Nowadays, there are no relevant data about their antitussive effects, but roflumilast has recently been approved for clinical use in adult patients with severe COPD (Fabbri et al. 2010; Giembycz and Field 2010). BRL50481, a selective PDE7 inhibitor, has been found to be effective in *in vitro* suppression of inflammatory cells, like human monocytes, lung macrophages, and CD8+ T-lymphocytes (Smith et al. 2004). Thus, therapeutic potential of these drugs in airway inflammatory diseases should be evaluated

In the present study we examined the effects of selective inhibitors of PDE4 (rolipram) and PDE7 (BRL50481), and their co-administration on cough and airway reactivity were assessed in healthy and ovalbumin-sensitized guinea pigs.

8.2 Methods

The study protocol was approved by a local Ethics Committee at Jessenius Faculty of Medicine, Comenius University in Martin, Slovakia. Sixty four healthy, male guinea pigs (250–350 g) were used for the study. They were kept in an animal house and had food and water *ad libitum*. In four groups of animals (n = 8 in each), airway hyperresponsiveness was induced with an antigen (ovalbumin) and the other four groups were used as naïve controls without sensitization (n = 8 in each). In each set of the four groups, the first group was left without treatment – only solvent, 10% dimethylsulfoxide (DMSO) at the dose of 3.0 ml/kg was used. All animals in the second group were treated with the PDE4 inhibitor rolipram (Sigma Aldrich, Germany, 1.0 mg/kg), in the third group with the PDE7 inhibitor BRL

50481 (Sigma Aldrich, Germany, 1.0 mg/kg), and in the fourth group with their combination, both at a dose of 0.5 mg/kg. All tested drugs were dissolved in 10% DMSO (3.0 ml/kg). Exactly same dosing schema was applied in the healthy and the in ovalbumin-sensitized guinea pigs.

8.2.1 Antigen-Induced Airway Hyperresponsiveness

Sensitization of the animals with ovalbumin, which causes airway reactivity changes on immunological basis, was performed during 14 days (Franova et al. 2007; Mokry et al. 2009). The allergen (1.0% ovalbumin) was administered on Day 1 of sensitization intraperitoneally (0.5 ml) and subcutaneously (0.5 ml), on Day 3 intraperitoneally (1 ml), and on Day 14 only by inhalation (30 sec). The airway reactivity to mediators of bronchospasm was studied *in vivo* immediately after the ovalbumin inhalation and *in vitro* after sacrificing the animal. The tested drugs were administered 30 min before nebulization.

8.2.2 Cough Reflex Assessment

The method of chemically-induced cough was used for assessing the cough reflex (Mokry and Nosalova 2007; Sutovska et al. 2009). We used citric acid aerosol in concentration of 0.6 M in saline for cough provocation. The inhalation of citric acid in a double chamber plethysmograph lasted 2 min. During this time and during the following 2 min, two well trained observers evaluated visually the number of cough efforts. To distinguish cough from sneezing or movement artifacts, subsequent evaluation of the computer records of air flow in nasal chamber was performed.

8.2.3 Evaluation of Airway Reactivity In Vivo

In vivo airway reactivity was evaluated using a double chamber whole body plethysmograph immediately after administration of bronchoconstrictors (Mokry et al. 2008). Specific airway resistance and its changes after a short-term inhalation (2 min) of bronchoconstricting agents (histamine at a concentration of 10^{-6} mol/L in saline) were considered as an indicator of the *in vivo* reactivity changes. For comparison, reactivity after nebulization of saline was used. Between the two exposures, there was an interval of minimum 5 min. During intervals, fresh air was insufflated into the nasal chamber.

8.2.4 Evaluation of Airway Reactivity In Vitro

After sacrificing the animals, trachea and lungs were immediately excised. Tracheal strips (approximately 15 mm) were cut on the opposite side of a smooth muscle. Lung tissue strips (2 × 2 × 15 mm) were cut from the margin of upper lobe of right and left lungs. The strips were mounted between two hooks and placed in a 30 ml organ chambers with Krebs-Henseleit's buffer (containing in mmol/L: NaCl 110.0, KCl 4.8, $CaCl_2$ 2.4, $MgSO_4$ 1.2, K_2HPO_4 1.2, $NaHCO_3$ 25.0, and glucose 10.0 in glass-distilled water). The chambers were maintained at 36.5°C ± 0.5°C and aerated continuously with a mixture of 95% O_2 and 5% CO_2 to maintain pH 7.5 ± 0.1. One of the hooks was connected to a force transducer (TENSIL10, RES Martin, Slovakia) and an amplifier (TEMES 1052, RES Martin, Slovakia), and tension changes

were recorded online using computer software (TEMES 1, RES Martin, Slovakia). Tissue strips were initially set to 4 g of tension for 30 min (loading phase). Then, in each strip the tension was readjusted to a baseline value of 2 g for another 30 min (adaptation phase). During both periods, tissue strips were washed at 10 min intervals. Cumulative doses of histamine or acetylcholine (10^{-8}–10^{-3} mol/L, Sigma-Aldrich, Germany) were added after the adaptation phase had been finished and a continuous recording of contractions was made (Strapkova et al. 1995; Mokry et al. 2009). Data of the tracheal and lung tissue reactivity are shown in grams (g) of the smooth muscle tension.

8.2.5 Statistical Analysis

Data are shown as means ± SE. For statistical analysis, a *t*-test was used. A $p < 0.05$ was considered statistically significant

8.3 Results

Intraperitoneal administration of the PDE4 inhibitor rolipram, or the PDE7 inhibitor BRL50481, or their combination led to no appreciable changes in the number of cough efforts in either healthy or ovalbumin-sensitized guinea pigs. Nevertheless, a tendency to decrease of cough was observed after rolipram (Fig. 8.1a).

Specific airway resistance measured in a whole body double chamber plethysmograph was used as a marker of *in vivo* airway responsiveness. Administration of either rolipram or BRL50481 at a dose of 1.0 mg/kg each caused a significant decrease of specific airway resistance after histamine nebulization only in ovalbumin-sensitized guinea pigs. The pre-treatment with both PDE inhibitors together at a dose of 0.5 mg/kg each showed a significant suppressant effect on specific airways resistance, which was stronger than that observed after rolipram alone and weaker than that observed after BRL50481 alone (Fig. 8.1b).

In vitro testing of contractility of lung smooth muscle tissue strips in the healthy guinea pigs in response to cumulative doses of acetylcholine demonstrated a significant suppression of strips

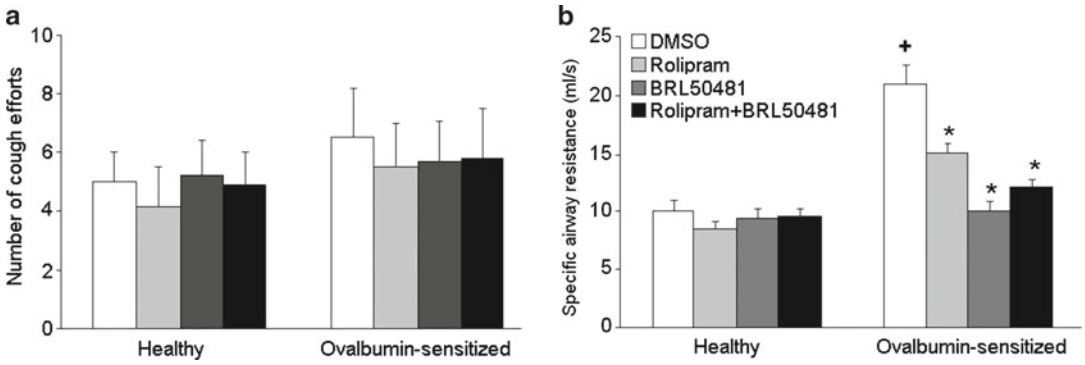

Fig. 8.1 **(a) Number of cough efforts** during (2 min) and after (2 min) inhalation of citric acid aerosol and **(b) specific airway resistance** after inhalation of histamine (10^{-6} mol/L) in healthy and ovalbumin-sensitized guinea pigs after 7-day pre-treatment with vehicle (10% DMSO, 3.0 ml/kg), rolipram (1.0 mg/kg), BRL50481 (1.0 mg/kg), and their combination (each 0.5 mg/kg); $^{+}p < 0.05$ *vs.* healthy, $^{*}p < 0.05$ *vs.* DMSO in the ovalbumin-sensitized group

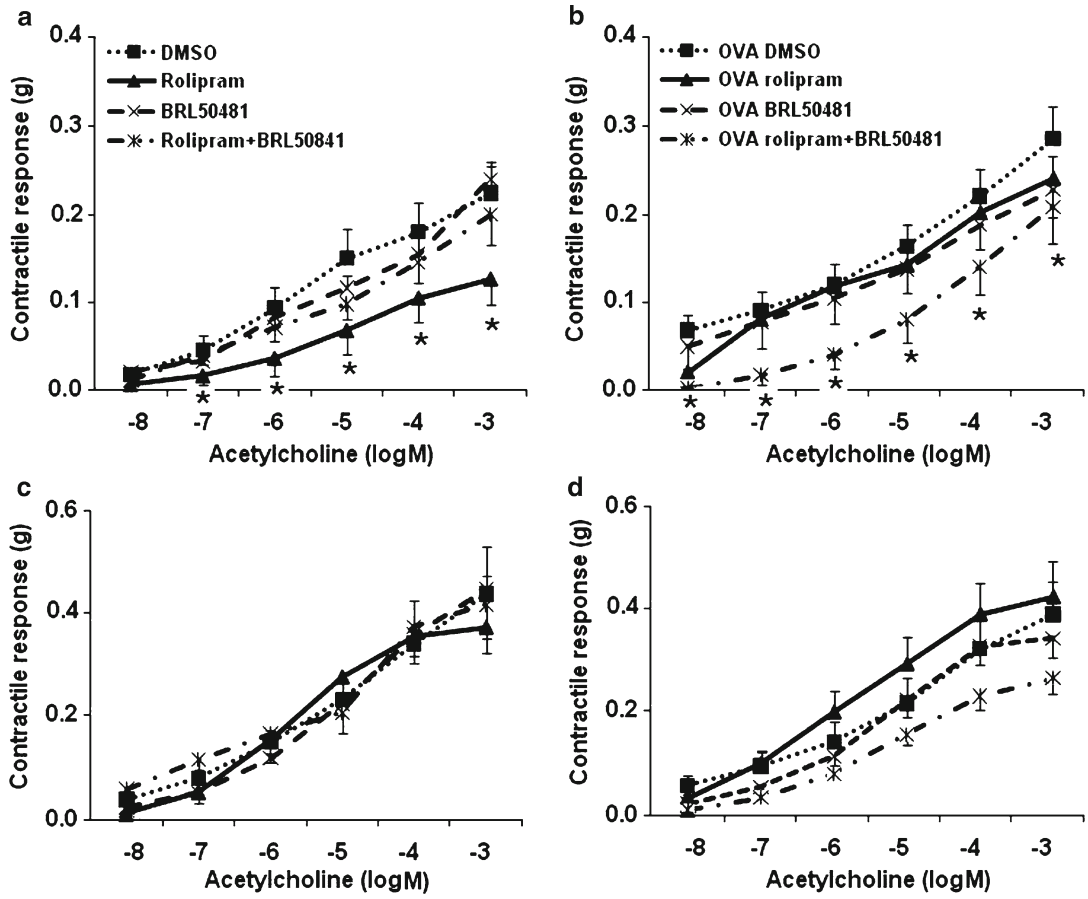

Fig. 8.2 ***In vitro*** **airway reactivity to acetylcholine** (lung strips – *top*, tracheal strips – *bottom*) in healthy (*left*) and ovalbumin-sensitized guinea pigs (*right*) after 7-day pre-treatment with vehicle (10.0% DMSO, 3.0 ml/kg), rolipram (1.0 mg/kg), BRL50481 (1.0 mg/kg), and their combination (each 0.5 mg/kg); *$p < 0.05$ *vs.* DMSO or OVA DMSO

reactivity only after rolipram pretreatment. BRL50481 did not influence here the *in vitro* airway reactivity (Fig. 8.2a). In tracheal smooth muscles, no significant changes of its reactivity after pre-treatment with the PDE4 and 7 inhibitors tested were observed (Fig. 8.2c). In the ovalbumin-sensitized guinea pigs, only combined administration of both rolipram and BRL50481 showed a significant decrease in *in vitro* airway reactivity (lung and trachea) to acetylcholine-induced contraction (Fig. 8.2b, d). Contractions evoked by histamine were significantly decreased in tracheal strips by pretreatment with BRL50481 and by co-administration of both inhibitors; rolipram did not influence these contractions significantly (Fig. 8.3).

8.4 Discussion

Selective inhibitors of PDE, particularly of PDE3 and PDE4, have been extensively studied for their anti-inflammatory action and their inhibition was previously confirmed as a suitable target for influencing the airway inflammation and the contractility of airway smooth muscles (Chung 2006). Several clinical studies testing second generation of PDE4 inhibitors (piclamilast, cilomilast,

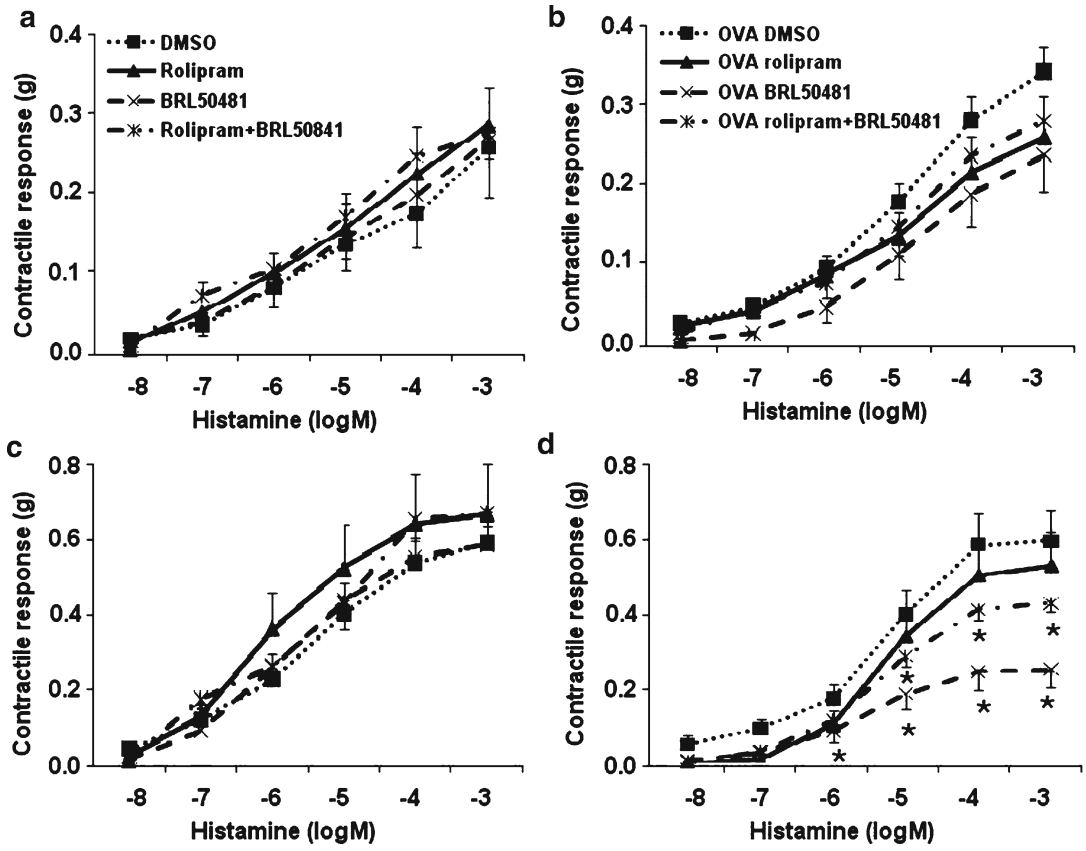

Fig. 8.3 ***In vitro*** **airway reactivity to histamine** (lung strips – *top*, tracheal strips – *bottom*) in healthy (*left*) and ovalbumin-sensitized guinea pigs (*right*) after 7-day pre-treatment with vehicle (10% DMSO, 3.0 ml/kg), rolipram (1.0 mg/kg), BRL50481 (1.0 mg/kg), and their combination (each 0.5 mg/kg); *p < 0.05 *vs.* DMSO or OVA DMSO

roflumilast) have confirmed their bronchodilating, anti-inflammatory, and antitussive effects previously demonstrated in experimental conditions. Furthermore, the emphasis has been put on the necessity of testing other PDE isoforms (Beeh et al. 2004; Giembycz 2005a; Rabe et al. 2005).

In our present experiments, the selective inhibitor of PDE4 rolipram did not show any significant antitussive effects either in healthy (*naïve*) or in ovalbumin-sensitized guinea pigs. These results are at variance with our previous experiments, where significant antitussive effect of PDE4 inhibition was demonstrated (Mokry et al. 2008). However, a different PDE4 inhibitor (citalopram) and a different dosing regimen were used in those experiments.

Despite the negligible antitussive effects we confirmed that the inhibition of PDE4 by rolipram seems to be a highly perspective choice in therapy of chronic inflammatory diseases associated with airway hyperresponsiveness. Inhibitors of PDE4 (rolipram, citalopram, cilomilast, roflumilast, piclamilast) have predominantly anti-inflammatory and immunomodulating effects with markedly reduced adverse effects compared with non-selective PDE inhibitors (Karish and Gagnon 2006). In our present experiments we found a significant decrease of specific airway resistance (a marker of *in vivo* airway reactivity) after rolipram in ovalbumin-sensitized guinea pigs but not in healthy animals, suggesting its major role in inflammation. However, in *in vitro* experiments a significant effect of rolipram on the contractile responses evoked by cumulative doses of acetylcholine was found only in healthy animals and in co-administration with BRL50481 in sensitized guinea pigs. In histamine-evoked smooth muscle strip contractions we did not find any effect of rolipram. On the contrary, the

previously tested PDE4 inhibitor citalopram showed a significantly suppressing effect only in *in vitro* conditions and not *in vivo* (Mokry et al. 2008).

PDE7 inhibition by BRL50481 alone and in combination with rolipram led to significant decreases in both *in vivo* airway reactivity and in *in vitro* contractility. The most significant suppression of the contractile responses to acetylcholine was observed in ovalbumin-sensitized animals after co-administration of both inhibitors. This suggests that both these agents can be used in clinical states associated with allergic inflammation, which was mimicked by ovalbumin sensitization. Furthermore, patients may benefit from their synergistic effects, as only half a dose of each was used during their combined administration; thus the potential adverse effects of PDE4 inhibitors can be minimized. This concept has been described in the literature and a new dual PDE inhibitors are studied (e.g., PDE3/4 and PDE4/7) for their anti-inflammatory action (Giembycz 2005b).

As there have so far been no relevant data on the antitussive effects of PDE7 inhibitors, our results indicate their alternative efficiency in influencing the cough. However, in our experiments we did not reach the level of significance. Nevertheless, the model we used is considered as a model of asthma, with the predominance of eosinophils (Mokry et al. 2008). Other models, e.g., COPD models, with the prevailing neutrophils, should also be tested to exclude or confirm the efficacy of these groups of drugs in regard to cough.

In conclusion, we did not observe any antitussive effects of the PDE4 and PDE7 inhibitors tested. Nevertheless, a significant suppression of airway hyperresponsiveness by the PDE4 and PDE7 inhibitors indicates stronger anti-inflammatory effects than the direct ones on smooth muscle and cough, with a potential benefit of their combined administration.

Acknowledgments Authors thank to M. Duchonova, M. Kocmalova, and M. Repcakova for technical assistance. Supported by VEGA grant 1/0030/11 and by the Center of Experimental and Clinical Respirology II – 'Project co-financed from EU sources'.

Conflicts of interest: The authors declare no conflicts of interest in relation to this article.

References

Antoniu, S. A. (2006). Roflumilast for the treatment of chronic obstructive pulmonary disease. *Current Opinion in Investigational Drugs, 7*, 412–417.

Beeh, K. M., Beier, J., Lerch, C., Schulz, A. K., & Buhl, R. (2004). Effects of piclamilast, a selective phosphodiesterase-4 inhibitor, on oxidative burst of sputum cells from mild asthmatics and stable COPD patients. *Lung, 182*, 369–377.

Bender, A. T., & Beavo, J. A. (2006). Cyclic nucleotide phosphodiesterases: Molecular regulation to clinical use. *Pharmacological Reviews, 58*, 488–520.

Chung, K. F. (2006). Phosphodiesterase inhibitors in airways disease. *European Journal of Pharmacology, 533*, 110–117.

Fabbri, L. M., Beghe, B., Yasothan, U., & Kirkpatrick, P. (2010). Roflumilast. *Nature Reviews. Drug Discovery, 9*, 761–762.

Franova, S., Nosalova, G., Pechanova, O., & Sutovska, M. (2007). Red wine polyphenolic compounds inhibit tracheal smooth muscle contraction during allergen-induced hyperreactivity of the airways. *Journal of Pharmacy and Pharmacology, 59*, 727–732.

Giembycz, M. A. (2005a). Life after PDE4: Overcoming adverse events with dual-specificity phosphodiesterase inhibitors. *Current Opinion in Pharmacology, 5*, 238–244.

Giembycz, M. A. (2005b). Phosphodiesterase-4: Selective and dual-specificity inhibitors for the therapy of chronic obstructive pulmonary disease. *Proceedings of the American Thoracic Society, 2*, 326–333.

Giembycz, M. A., & Field, S. K. (2010). Roflumilast: First phosphodiesterase 4 inhibitor approved for treatment of COPD. *Drug Design, Development and Therapy, 4*, 147–158.

Karish, S. B., & Gagnon, J. M. (2006). The potential role of roflumilast: The new phosphodiesterase-4 inhibitor. *The Annals of Pharmacotherapy, 40*, 1096–1104.

Lipworth, B. J. (2005). Phosphodiesterase-4 inhibitors for asthma and chronic obstructive pulmonary disease. *Lancet, 365*, 167–175.

Mokra, D., & Mokry, J. (2010). *Meconium aspiration syndrome. From pathomechanisms to treatment* (1st ed., p. 130). New York: Nova Science Publishers.

Mokry, J., & Nosalova, G. (2007). Evaluation of the cough reflex and airway reactivity in toluene- and ovalbumin-induced airway hyperresponsiveness. *Journal of Physiology and Pharmacology, 58*(Suppl 5), 419–426.

Mokry, J., Mokra, D., Nosalova, G., Beharkova, M., & Feherova, Z. (2008). Influence of selective inhibitors of phosphodiesterase 3 and 4 on cough and airway reactivity. *Journal of Physiology and Pharmacology, 59*(Suppl. 6), 473–482.

Mokry, J., Nosalova, G., & Mokra, D. (2009). Influence of xanthine derivatives on cough and airway reactivity in guinea pigs. *Journal of Physiology and Pharmacology, 60*(Suppl 5), 87–91.

Nosalova, G., & Mokry, J. (2001). The mechanism of action of xanthine derivatives and suppression of cough. *Acta Medica Martiniana, 1*, 14–18.

Rabe, K. F., Bateman, E. D., O'Donnel, D., Witte, S., Bredenbroker, D., & Bethke, T. D. (2005). Roflumilast: An oral anti-inflammatory treatment for chronic obstructive pulmonary disease: A randomised controlled trial. *Lancet, 366*, 563–571.

Smith, S. J., Cieslinski, L. B., Newton, R., Donnelly, L. E., Fenwick, P. S., Nicholson, A. G., Barnes, P. J., Barnette, M. S., & Giembycz, M. A. (2004). Discovery of BRL 50481 [3-(N, N-dimethylsulfonamido)-4-methyl-nitrobenzene], a selective inhibitor of phosphodiesterase 7: In vitro studies in human monocytes, lung macrophages, and CD8+ T-lymphocytes. *Molecular Pharmacology, 66*, 1679–1689.

Spina, D., Landells, L. J., & Page, C. P. (1998). The role of theophylline and phosphodiesterase4 isoenzyme inhibitors as antiinflammatory drugs. *Clinical and Experimental Allergy, 28*(Suppl 3), 24–34.

Strapkova, A., Nosalova, G., Banovcin, P., & Giacova, D. (1995). Changes in airway smooth muscle reactivity after exposure to toluene. *Studia Pneumologica et Phthiseologica, 55*, 263–271.

Sutovska, M., Franova, S., & Sutovsky, J. (2009). The influence of animal species on the relationship between ATP-sensitive potassium ion channels and defense reflexes of the airways. *Bratislava Medical Journal, 110*(5), 269–275.

Usmani, O. S., Belvisi, M. G., Patel, H. J., Crispino, N., Birrell, M. A., Korbonits, M., Korbonits, D., & Barnes, P. J. (2005). Theobromine inhibits sensory nerve activation and cough. *The FASEB Journal, 19*, 231–233.

Chapter 9
Naloxone Blocks Suppression of Cough by Codeine in Anesthetized Rabbits

M. Simera, M. Veternik, and I. Poliacek

Abstract Opioid receptors which are involved in cough generation are abundantly expressed in the brainstem. Codeine is a potent μ-opioid receptor agonist. In the present study we examined the effects of naloxone, a μ-opioid receptor antagonist, on mechanically-induced tracheobronchial cough and on the cough suppressing effect of codeine in six pentobarbitone anesthetized spontaneously breathing rabbits. A single dose of naloxone (0.4 mg/kg) followed by a single dose of codeine (7 mg/kg) were administered intravenously. The number and amplitude of cough and sneeze reflexes were examined sequentially; before and after naloxone, and then after codeine. We found that neither did naloxone alone nor codeine given after prior naloxone pretreatment appreciably affect coughing or sneezing. Likewise, there were no significant differences in the diaphragm and abdominal muscles electromyographic moving averages, or the inspiratory and expiratory esophageal pressure amplitudes. However, we detected a tendency for the rise in expiratory motor drive during coughing and sneezing after injection of naloxone. The respiratory rate was significantly higher after naloxone in comparison with control ($P < 0.001$). No significant differences in arterial blood pressure were observed. We conclude that the failure of codeine to suppress the cough reflex on the background of naloxone pretreatment confirms the involvement of μ-opioid mechanism in the central antitussive effect of codeine.

Keywords Codeine • Naloxone • Sneezing • Tracheobronchial cough • Opioid receptor

9.1 Introduction

Narcotic antitussives such as codeine affect cough primarily *via* μ-opioid receptors in the central nervous system (Kotzer et al. 2000; Takahama and Shirasaki 2007). These receptors are expressed the ambiguus nucleus, the solitary tract nucleus, the dorsal motor nucleus of the vagus, the medial parabrachial nucleus, the periaqueductal gray, and the raphe nuclei. κ-opioid receptors also are expressed with similar or lower density in these regions. δ-opioid receptors are generally less abundant in the brainstem, with the exception of the parabrachial nuclei area (Takahama and Shirasaki 2007). Naloxone, a competitive antagonist, has a high affinity for μ-opioid receptors (Waldhoer et al. 2004;

M. Simera (✉) • M. Veternik • I. Poliacek
Department of Medical Biophysics, Jessenius Faculty of Medicine in Martin,
Comenius University in Bratislava, Mala Hora 4, 037 54 Martin, Slovakia
e-mail: simera@jfmed.uniba.sk

M. Pokorski (ed.), *Respiratory Regulation - The Molecular Approach*,
Advances in Experimental Medicine and Biology 756, DOI 10.1007/978-94-007-4549-0_9,

Goodman et al. 2007), but has a lower affinity for other types of opioid receptors (Takahama and Shirasaki 2007).

A previous study has shown that naloxone given intraperitoneally 5 min before the application of codeine did not prevent its cough suppressant effect in unanesthetized cats (Nosalova et al. 1991). This finding suggests a possible role of a non-opioid mechanism in codeine-induced cough suppression. However, intramuscular administration of naloxone eliminated the antitussive effect of codeine in guinea pigs (Kotzer et al. 2000), indicating a dominant role of μ-opioid receptors in codeine cough suppression in this species.

In the present study we seek to determine whether codeine would suppress tracheo-bronchial cough through the μ-opioid receptor mechanism in the rabbit.

9.2 Methods

All procedures were performed in accordance with the rules of the EU for animal experiments. The Ethics Committee of Jessenius Faculty of Medicine in Martin, Slovakia approved the protocol.

The experiments were performed in six male rabbits (New Zealand white, line P91; weight 2.8 ± 0.1SE kg) anesthetized with sodium pentobarbital (Biowet, Pulawy, Poland; 35 mg/kg, i.p.). Supplementary doses of the anesthetic were administered (1–3 mg/kg, i.v.) as needed. Atropine (Biotika; 0.15 mg/kg, i.v.) was given at the beginning of the experiment to reduce bronchial secretions. The trachea, femoral artery, and vein were cannulated. The animals were allowed to breathe spontaneously with a gas mixture of 30–60% oxygen balanced with nitrogen. Arterial blood pressure (BP), end-tidal CO_2 concentration ($ETCO_2$), respiratory rate (RR) and body temperature were monitored continuously. Body temperature was maintained at 39.0°C ± 0.5°C. Samples of arterial blood were removed periodically for blood gases and pH analysis.

Bipolar fine wire hook electrodes were placed in the crural diaphragm (DIA) and bilaterally in the transversal abdominal or the external oblique abdominal muscle (ABD) for electromyogram (EMG) recordings. A soft balloon was inserted into the esophagus for the measurement of intrathoracic pressure changes (esophageal pressure – EP).

Tracheobronchial cough was induced by mechanical stimulation of the trachea and the carina with a soft nylon fiber or catheter which were moved fore-and backward around the carina four times during a stimulation trial. Sneeze was induced by mechanical touch of the nasal septum with a nylon fiber (∅ 0.25 mm), which was repeated five times. Cough and sneeze were defined as a large augmenting burst of diaphragm (DIA) EMG activity immediately followed (and partially overlapped) by a burst of expiratory ABD EMG activity (Jakus et al. 1987), corresponding to the related inspiratory-expiratory wave of EP.

A single dose of naloxone (0.4 mg/kg; Naloxone hydrochloride, WZF Polfa, Warszawa, Poland) followed by a single dose of codeine (7 mg/kg, Codeinum dihydrogenphosphate; Interpharm, Bratislava, Slovakia) were injected. Stimulation of tracheobronchial airways and nasal mucosa were performed at 1 min intervals; two tracheobronchial stimulations were performed at baseline and then after naloxone and codeine injections. The experiment was terminated by an overdose of pentobarbitone, followed by a saturated solution of KCl.

All EMGs were amplified, filtered (300–3,000 Hz; Grass, USA), digitalized (12-bit multi-function plug-in ISA card, Dataq Instruments, USA, sampling frequency of 20,000 Hz), and recorded (WinDaq, Dataq Instruments-Akron, USA) along with the waveforms of BP and EP.

The mean numbers of cough efforts (CN), per four penetrations of carina, and of sneeze efforts (SN), per five touches of nasal mucosa, were analyzed in each sequence of trials. Differences in amplitudes of DIA and ABD moving averages and those of inspiratory and expiratory components of the EP recording in response to naloxone and codeine were measured. The results were expressed as

means ± SE. For statistical analysis, a *t*-test, Mann-Whitney-U test, and repeated measures of ANOVA with a Student-Newman-Keuls *post-hoc* test were applied. $P < 0.05$ were considered significant.

9.3 Results

Mechanical tracheobronchial stimulation produced coughing and that of the nasal septum resulted in vigorous sneezing. Naloxone alone and also codeine administered on the background of naloxone did not significantly modify coughing or sneezing. A representative illustration of the raw recordings during cough induction at the sequential experimental steps is shown in Fig. 9.1. The number of cough and sneeze reflexes, DIA and ABD EMG moving average amplitudes, and peak inspiratory and expiratory EP during the reflexes were not significantly altered (Table 9.1). There was just a trend for increases in cough and sneeze ABD EMG amplitudes after both naloxone and codeine injections (Fig. 9.2, Table 9.1).

We found no differences in BP during our protocol. There were, however, increases in RR after naloxone (54.0 ± 3.6 breaths/min; $P < 0.05$; 3 min post-naloxone) and following codeine (56.3 ± 3.0 breaths/min; $P < 0.001$; 1.5 min post-codeine, 6 min post-naloxone) compared with the control pre-injection value (40.2 ± 1.8 breaths/min).

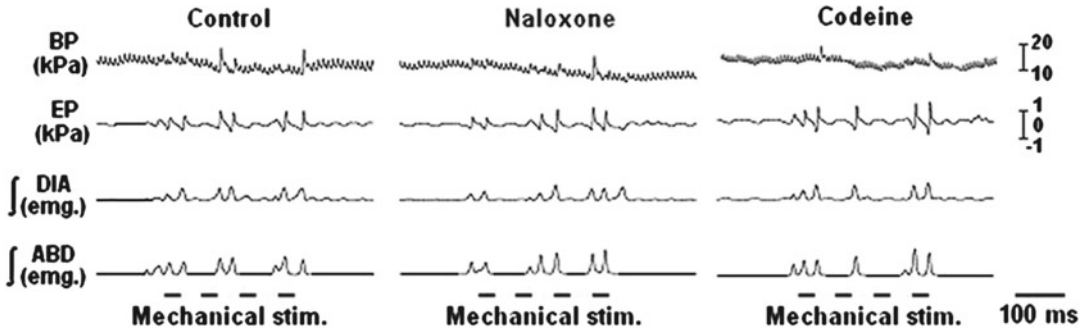

Fig. 9.1 Representative experimental recordings. Codeine administered after prior naloxone failed to reduce the tracheobronchial cough. *BP* blood pressure, *EP* esophageal pressure, *∫DIA* integrated EMG of the diaphragm, *∫ABD* integrated EMG of abdominal muscles, *stim* tracheobronchial stimulation

Table 9.1 Effects on coughing and sneezing of codeine administered on the background of naloxone

Cough	CN	%dif DIA	%dif ABD	%dif EPI	%dif EPE
Control	4.07 ± 0.62	100	100	100	100
Naloxone	3.58 ± 0.81	89 ± 11	122 ± 19	98 ± 27	104 ± 8
Codeine	3.17 ± 0.78	99 ± 9	144 ± 47	110 ± 29	103 ± 11
ANOVA	P > 0.05	P > 0.05	P > 0.05	P > 0.05	P > 0.05
Sneeze	SN	% dif DIA	% dif ABD	% dif EP I	% dif EP E
Control	5.50 ± 0.43	100	100	100	100
Naloxone	5.67 ± 0.67	95 ± 14	109 ± 14	79 ± 25	83 ± 14
Codeine	5.77 ± 1.09	103 ± 7	146 ± 24	107 ± 31	119 ± 18
ANOVA	P > 0.05	P > 0.05	P > 0.05	P > 0.05	P > 0.05

CN cough number, *SN* sneeze number, *%dif DIA* and *%difABD* peak diaphragm and abdominal EMG activities normalized to control responses, *EP* peak esophageal pressure, *I* and *E* inspiratory and expiratory components of esophageal pressure trace

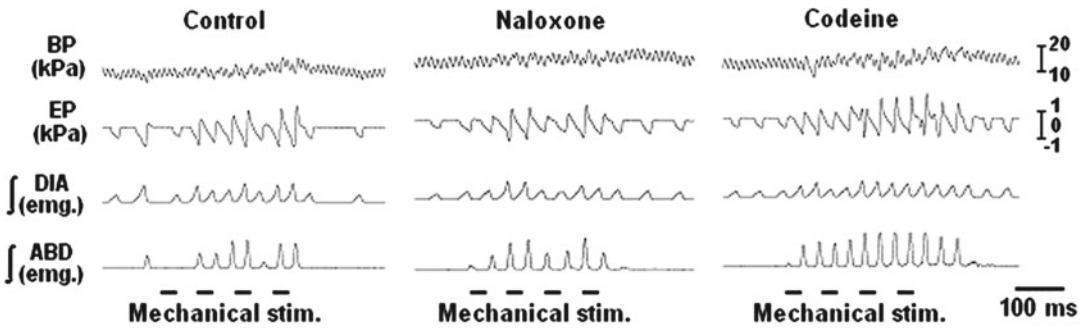

Fig. 9.2 Representative experimental recordings. Codeine administered after prior naloxone failed to affect sneezing. *BP* blood pressure, *EP* esophageal pressure, *∫DIA* integrated EMG of the diaphragm, *∫ADB* integrated EMG of abdominal muscles, *stim* nasal stimulation

9.4 Discussion

The major finding of this study was that codeine failed to appreciably inhibit the cough reflex after prior pretreatment with an antagonist of μ-opioid receptors in the rabbit. The inference thus is that the antitussive activity of codeine is mediated predominantly by μ-opioid receptors. These results are in accord with those of our previous study in which we reported a significant about 50% reductions in CN (from 2.6 ± 0.7 to 1.2 ± 0.4) and ABD EMG amplitudes (51 ± 12% of control) after a cumulative dose of 5 mg/kg of codeine given without pretreatment with naloxone (Simera et al. 2010).

Cough triggered by stimulation of 'cough receptors' is responsive to mechanical and acidic stimuli (Canning 2009) within the tracheo-bronchial airways and is attenuated by narcotic antitussives such as codeine (Adcock et al. 1988; Dhuley 1999; Chattopadhyay et al. 2011). The data presented by Cox et al. (1984) have demonstrated a reduction of intensity of citric acid induced cough by codeine also in humans. Higher doses of codeine are required to inhibit capsaicin induced cough supposedly triggered *via* C-fibers (Canning 2009), even in allergic guinea pigs (Bolser et al. 1995a), compared with the doses inhibiting mechanical or citric acid cough (Adcock et al. 1988; Karlsson et al. 1990). This fact is consistent with the existence of two separate pathways mediating the cough response ('cough receptors' *vs.* C-fibers) (Canning 2009) and with different sensitivities of these two types of coughs to opioids. Similarly, there is an uneven threshold for codeine suppression for coughs induced mechanically from the larynx and from the tracheobronchial airways (particularly from the tracheal bifurcation; Bolser et al. 1995a; Gestreau et al. 1997). Korpas and Tomori (1979) found in cats that codeine (16 mg/kg, i.v.) abolishes cough from the tracheal bifurcation but not from the larynx. Even higher doses of codeine (30 mg/kg, i.p.) do not eliminate expiration reflex from the vocal folds (Korpas and Jakus 2000). The expiration reflex-like short expirations induced mechanically from the trachea appear to be less sensitive to codeine than cough (Poliacek et al. 2008).

Central antitussive effects mechanically-induced tracheobronchial cough in rabbits of codeine have been confirmed in other studies (Eddy et al. 1969; Bolser et al. 1995a; Jakus et al. 2010; Simera et al. 2010; Gao et al. 2010). To-date, two effective sites for the action of antitussive drugs such as codeine have been found in the brainstem: the solitary tract nucleus (Ohi et al. 2005; Mutolo et al. 2008) and the caudal ventral respiratory group (Mutolo et al. 2010; Poliacek et al. 2010). In these and possibly other cough-related brainstem areas (Jakus et al. 2008), opioid sensitive neurons may contribute to reduced excitability of cough and attenuate expiratory motor output.

Binding studies concerning guinea-pig and human opioid receptors have demonstrated that codeine and dihydrocodeine are more selective to μ- than κ- or δ-opioid receptors (Mignat et al. 1995; Kotzer et al. 2000). Morphine, a selective μ-opioid receptor agonist, also has potent antitussive activity in the

cat (Chau et al. 1983; Takahama and Shirasaki 2007). Therefore, primarily μ- and κ-opioid receptors have been considered as being involved in opioid. Furthermore, pharmacological studies carried out in rats, mice, and μ_1-opioid receptor deficient mice suggest that μ_2- rather than μ_1-subtype of these receptors contributes to the antitussive activity of opioids.

The issue of cough mediation by μ-opioid receptors is, however, more complex and contentious. Drugs acting at non-μ-opioid receptors also seem involved in cough regulation (Nosalova 1998). In a study by Nosalova et al. (1991) naloxone given intraperitoneally 5 min before application of codeine did not prevent the cough suppressing effect of codeine in unanesthetized cats. Other studies showed that the antitussive effects of both isomers of codeine (*d* and *l*) were not inhibited by naloxone in anesthetized cats (Chau and Harris 1980). Similarly, Chau et al. (1983) reported no effect of intravenous naloxone on antitussive effects of codeine in lightly anesthetized cats. However, in another study, intramuscular administration of naloxone eliminated the antitussive effect of codeine on citric acid-induced cough in guinea pigs (Karlsson et al. 1990; Kotzer et al. 2000).

Our present results showed suppression of the antitussive effect of codeine by naloxone on mechanically-induced tracheobronchial cough in anesthetized rabbits. Effective doses of codeine for cough suppression codeine are higher in the guinea pig (Dhuley 1999) and rabbit (Simera et al. 2010) compared with those in the cat (Bolser et al. 1995b). Furthermore, the ineffectiveness of naloxone to block the antitussive activity of codeine in the cat (Nosalova et al. 1991; Chau et al. 1983) suggests the existence of a non-opioid mechanism in cough suppression by codeine in this species. GABAergic, serotoninergic, and NMDA receptor mechanisms could participate in the antitussive activity of opioid drugs. The cough-suppressant effect of codeine also can be modified by decreases in brain monoamine content (Nosalova 1998). Codeine and similar drugs inhibit excitatory transmission from the primary afferent fibers to the second-order NTS neurons *via* opioid receptors (Ohi et al. 2007) or by postsynaptic inhibition of NTS relay neuron excitability (Canning 2009).

Previous studies confirmed that opiates play an important role in the central regulation of respiration (Pokorski and Lahiri 1981; Faden and Feuerstein 1983; Nosalova et al. 1991). However, doses of codeine effectively depressing cough usually do not alter breathing (Bolser et al. 1995b; Simera et al. 2010). Opioids can have a number of side effects such as physical dependence, sedation, respiratory depression, and gastrointestinal symptoms in humans (Bianchi and Barillot 1975; Afshari et al. 2007; Belvisi and Hele 2009). In suppression of pathological coughing, herbal medicine and plant extracts may be very effective (Chattopadhyay et al. 2011), avoiding unwanted side effects of opiate drugs. Naloxone increases respiratory frequency (Lawson et al. 1979; Pokorski and Lahiri 1981); the effect confirmed in the present study in the rabbit. Naloxone likely competes at opioid receptors with endogenous opioids, known to be involved in the regulation of respiration, resulting in a higher excitability of brainstem respiratory network.

Acknowledgments We gratefully acknowledge the technical assistance of Assoc. Prof. Helena Barani, Mgr. Nadezda Visnovcova, Iveta Najslova, Ing. Peter Machac, Roman Kubizna, and Mgr. Ivana Lamosova. This work was supported by the Center of Experimental and Clinical Respirology (CECR II). The project was co-financed by the European Regional Developmental Fund (ERDF).

Conflicts of interests: The authors declare no conflicts of interest in relation to this article.

References

Adcock, J. J., Schneider, C., & Smith, T. W. (1988). Effects of codeine, morphine and a novel opioid pentapeptide BW443C, on cough, nociception and ventilation in the unanaesthetized guinea-pig. *British Journal of Pharmacology, 93*, 93–100.

Afshari, R., Maxwell, S. R., & Bateman, D. N. (2007). Hemodynamic effects of methadone and dihydrocodeine in overdose. *Clinical Toxicology (Philadelphia, Pa.), 45*(7), 763–772.

Belvisi, M. G., & Hele, D. J. (2009). Cough sensors III. Opioid and cannabinoid receptors on vagal sensory nerves. *Handbook of Experimental Pharmacology, 187*, 63–76.

Bianchi, A. L., & Barillot, J. C. (1975). Activity of medullary respiratory neurones during reflexes from the lungs in cats. *Respiration Physiology, 25*(3), 335–352.

Bolser, D. C., Degennaro, F. C., O'Reilly, S., Hey, J. A., & Chapman, R. W. (1995a). Pharmacological studies of alergic cough in the guinea pig. *European Journal of Pharmacology, 277*(2–3), 159–164.

Bolser, D. C., DeGennaro, F. C., Chapman, R. W., & Hey, J. A. (1995b). Central and peripheral sites of action of antitussive drugs in the cat. In C. O. Trouth & R. M. Millis (Eds.), *Ventral brainstem mechanisms and control of respiration and blood pressure* (pp. 95–102). New York: Marcel Dekker.

Canning, B. J. (2009). Central regulation of the cough reflex: Therapeutic implications. *Pulmonary Pharmacology & Therapeutics, 22*(2), 75–81.

Chattopadhyay, N., Nosalova, G., Saha, S., Bandyopadhyay, S. S., Fleskova, D., & Ray, B. (2011). Structural features and antitussive activity of water extracted polysaccharide from *Adhatoda vasica*. *Carbohydrate Polymers, 83*, 1970–1974.

Chau, T. T., & Harris L. S. (1980). Comperative studies of the pharmacological effects of the d- and l- isomers of codeine. *Journal of Pharmacology and Experimental Therapeutics, 215*, 668–672.

Chau, T. T., Carter, F. E., & Harris, L. S. (1983). Antitussive effects of the optical isomers of mu, kappa and sigma opiate agonists/antagonists in the cat. *Journal of Pharmacology and Experimental Therapeutics, 226*, 108–112.

Cox, I. D., Wallis, P. J., Apps, M. C., Hughes, D. T., Empey, D. W., Osman, R. C., & Burke, C. A. (1984). An electromyographic method of objectively assessing cough intensity and use of the method to assess effects of codeine on the dose-response curve to citric acid. *British Journal of Clinical Pharmacology, 18*(3), 377–382.

Dhuley, J. N. (1999). Antitussive effect of *Adhatoda vasica* extract on mechanical or chemical stimulation-induced coughing in animals. *Journal of Ethnopharmacology, 67*, 361–365.

Eddy, N. B., Friebel, H., Hahn, K. J., & Halbach, H. (1969). Codeine and its alternates for pain and cough relief. 3. The antitussive action of codeine-mechanisms, methodology and evaluation. *Bulletin of the World Health Organization, 40*(3), 425–454.

Faden, A. I., & Feuerstein, G. (1983). Hypothalamic regulation of the cardiovascular and respiratory systems: Role of specific opiate receptors. *British Journal of Pharmacology, 79*(4), 997–1002.

Gao, S., Li, P., Yang, H., Fang, S., & Su, W. (2010). Antitussive effect of naringin on experimentally induced cough in Guinea pigs. *Planta Medica, 77*(1), 16–21.

Gestreau, C., Bianchi, A. L., & Grelot, L. (1997). Differential brainstem Fos like immunoreactivity after laryngeal-induced coughing and its reduction by codeine. *Journal of Neuroscience, 17*(23), 9340–9352.

Goodman, A. J., LeBourdonnec, B., & Dolle, R. E. (2007). Mu opioid receptor antagonists: Recent developments. *ChemMedChem, 2*(11), 1552–1570.

Jakus, J., Tomori, Z., Stransky, A., & Boselova, L. (1987). Bulbar respiratory activity during defensive airways reflexes in cat. *Acta Physiologica Hungarica, 70*, 245–254.

Jakus, J., Poliacek, I., Halasova, E., Murin, P., Knocikova, J., Tomori, Z., & Bolser, D. C. (2008). Brainstem circuitry of tracheal-bronchial cough: C-Fos study in anesthetized cats. *Respiratory Physiology & Neurobiology, 160*(3), 289–300.

Jakus, J., Stransky, A., & Jakusova, V. (2010). Central cough reflex mechanisms. *Folia Medica Cassoviensia, 65*(2), 3–9. Article in Slovak.

Karlsson, J. A., Lanner, A. S., & Persson, C. G. (1990). Airway opioid receptors mediate inhibition of cough and reflex bronchoconstriction in guinea pigs. *Journal of Pharmacology and Experimental Therapeutics, 252*(2), 863–868.

Korpas, J., & Jakus, J. (2000). The expiration reflex from the vocal folds. *Acta Physiologica Hungarica, 87*(3), 201–215.

Korpas, J., & Tomori, Z. (1979). *Cough and other respiratory reflexes*. Basel: Karger.

Kotzer, C. J., Hay, D. W., Dondio, G., Giardina, G., Petrillo, P., & Underwood, D. C. (2000). The antitussive activity of delta-opioid receptor stimulation in guinea pigs. *Journal of Pharmacology and Experimental Therapeutics, 292*, 803–809.

Lawson, E. E., Waldrop, T. G., & Eldridge, F. L. (1979). Naloxone enhances respiratory output in cats. *Journal of Applied Physiology, 47*(5), 1105–1111.

Mignat, C., Wille, U., & Ziegler, A. (1995). Affinity profiles of morphine, codeine, dihydrocodeine and their glucuronides at opioidreceptor subtypes. *Life Sciences, 56*, 793–799.

Mutolo, D., Bongianni, F., Cinelli, E., Fontana, G. A., & Pantaleo, T. (2008). Modulation of the cough reflex by antitussive agents within the caudal aspect of the nucleus tractus solitarii in the rabbit. *American Journal of Physiology. Regulatory, Integrative and Comparative Physiology, 295*, R243–R251.

Mutolo, D., Bongianni, F., Cinelli, E., & Pantaleo, T. (2010). Depression of cough reflex by microinjections of antitussive agents into caudal ventral respiratory group of the rabbit. *Journal of Applied Physiology, 109*(4), 1002–1010.

Nosalova, G. (1998). Actions of drugs affecting the cough reflex. *Bratislavske Lekarske Listy, 99*(10), 531–535. Article in Slovak.

Nosalova, G., Strapkova, A., & Korpas, J. (1991). Relationship between the antitussic and analgesic activity of substances. *Acta Physiologica Hungarica, 77*(2), 173–178.

Ohi, Y., Yamazaki, H., Takeda, R., & Haji, A. (2005). Functional and morphological organization of the nucleus tractus solitarius in the fictive cough reflex of guinea pigs. *Neuroscience Research, 53*(2), 201–209.

Ohi, Y., Kato, F., & Haji, A. (2007). Codeine presynaptically inhibits the glutamatergic synaptic transmission in the nucleus tractus solitarius of the guinea pig. *Neuroscience, 146*(3), 1425–1433.

Pokorski, M., & Lahiri, S. (1981). Effects of naloxone on carotid body chemoreception and ventilation in the cat. *Journal of Applied Physiology, 51*, 1533–1538.

Poliacek, I., Halasova, E., & Bolser, D. C. (2008). Short reflex expirations (expiration reflexes) induced by mechanical stimulation of the trachea in anesthetized cats. *Cough, 4*, 1.

Poliacek, I., Wang, C., Corrie, L. W., Rose, M. J., & Bolser, D. C. (2010). Microinjection of codeine into the region of the caudal ventral respiratory column suppresses cough in anesthetized cats. *Journal of Applied Physiology, 108*(4), 858–865.

Simera, M., Poliacek, I., & Jakus, J. (2010). Central antitussive effect of codeine in the anesthetized rabbit. *European Journal of Medical Research, 15*(Suppl 2), 184–188.

Takahama, K., & Shirasaki, T. (2007). Central and peripheral mechenisms of narcotic antitussives: codein-sensitive and -resistant coughs. *Cough, 3*, 8.

Waldhoer, M., Bartlett, S. E., & Whistler, J. L. (2004). Opioid receptors. *Annual Review of Biochemistry, 73*, 953–990.

Chapter 10
Influence of Sublingual Immunotherapy on the Expression of Mac-1 Integrin in Neutrophils from Asthmatic Children

Olga Ciepiela, Anna Zawadzka-Krajewska, Iwona Kotula, Beata Pyrzak, and Urszula Demkow

Abstract Asthma can be effectively treated with sublingual immunotherapy. The influence of sublingual immunotherapy on the function of granulocytes in asthmatic patients is largely unknown. Mac-1 integrin is a transmembrane protein containing α (CD11b) and β (CD18) chains. High expression of the complex is found on the surface of neutrophils, NK cells, and macrophages. CD11b/CD18 may bind to CD23, ICAM-1, ICAM-2, and ICAM-4. It plays a crucial role in diapedesis of neutrophils. The aim of the present study was to assess Mac-1 expression on neutrophils from asthmatic children before and after sublingual immunotherapy. Twenty five children aged of 8.1 ± 3.1 suffering from atopic asthma and allergic rhinitis, shortlisted for specific immunotherapy, served as the study group. Fifteen healthy individuals, aged 9.8 ± 3.4, served as a control group. The assessment of CD11b and CD18 expression on cells from peripheral blood was performed with a flow cytometer. The tests were performed before and after 12 months of sublingual immunotherapy. In the asthmatic children, 98.08 (90.79–99.12)% of Mac-1 positive neutrophils were detected. The group was divided into two subgroups: of more than 98% and less than 95% of neutrophils with CD11b/CD18 expression in the sample. After immunotherapy, the percentage of Mac-1 positive granulocytes increased to 99.60 (99.29–99.68)%, $p = 0.01$. In the control group, 90.56 (87.08–88.86)% granulocytes were Mac-1 positive, $p = 0.002$. We conclude that sublingual immunotherapy strongly influences the function of the immunological system, including Mac-1 expression on neutrophils.

Keywords Asthma • CD11b/CD18 chains • Mac-1 integrin • Neutrophils • Sublingual immunotherapy

O. Ciepiela (✉) • I. Kotula • U. Demkow
Department of Laboratory Diagnostics and Clinical Immunology of Developmental Age, Warsaw Medical University, Marszalkowska 24 St, 00-576 Warsaw, Poland
e-mail: olga.ciepiela@wum.edu.pl

A. Zawadzka-Krajewska
Department of Pediatric Pneumology and Allergology, Warsaw Medical University, Dzialdowska 1 St, 01-184 Warsaw, Poland

B. Pyrzak
Department of Pediatric Endocrinology, Warsaw Medical University, Marszalkowska 24 St, 00-576 Warsaw, Poland

M. Pokorski (ed.), *Respiratory Regulation - The Molecular Approach*,
Advances in Experimental Medicine and Biology 756, DOI 10.1007/978-94-007-4549-0_10,

10.1 Introduction

The role of neutrophils in the pathogenesis of asthma is still unclear (Foley and Hamid 2007). An increased number of these cells are found in the peripheral blood and airways of asthmatic patients, especially during exacerbations. It is not clear whether neutrophils are mobilized naturally in the course of disease or their migration is secondary to steroids treatment (Monteseirín 2009).

It is postulated that the accumulation of neutrophils in airways is mediated by IL-8 and TNF-α, as neutrophils' chemotactic factors released from macrophages and epithelial cells in the respiratory tract (MacDowell and Peters 2007). IL-8 triggers degranulation of neutrophils and release of myeloperoxidase, β-glucuronidase, elastase, gelatinase, leukotriene B4, and oxygen radicals. Neutrophils play important role in asthma due to their ability to release IL-9, TNF-α and TGF-β. Noteworthy, IL-9 regulates the function of Th2 cells, eosinophils, mast cells, as well as airway epithelial cells (Foley and Hamid 2007).

Mac-1 integrin is a transmembrane protein containing α (CD11b) and β (CD18) chains. High expression of this complex is found on the surface of neutrophils, NK cells, monocytes, and macrophages. CD11b/CD18 may bind to CD23, the inter-cellular adhesion molecules ICAM-1, ICAM-2, and ICAM-4, iC3b, to fibrinogen and LPS/LBP complex. It plays a crucial role in diapedesis of neutrophils (Hogg 1997a, b).

Sublingual immunotherapy (SLIT) is found to be an effective and well tolerated treatment. Its influence on the function of granulocytes from children suffering from bronchial asthma is largely unknown. It is postulated that SLIT inhibits the inflammatory process in airways. Synthesis of ICAM particles from epithelial cells is decreased under the influence of sublingual immunotherapy (Silvestri et al. 2002). A decreased expression of adhesion molecules inhibits the influx of eosinophils and neutrophils to the inflamed tissue. This observation has been indirectly confirmed by monitoring the concentration of eosinophil cationic protein (ECP) in bronchoalveolar fluid (BALF) (Leatherman et al. 2007).

The goal of the present study was to assess Mac-1 expression on neutrophils from asthmatic children before and after SLIT as compared with non-atopic children.

10.2 Methods

10.2.1 Subjects

The experiments were approved by the Ethics Committee of Warsaw Medical University in Warsaw, Poland. Blood was collected with parents' approval.

Twenty five individuals aged 8.1 ± 3.1, 21 boys and four girls, suffering from atopic asthma and allergic rhinitis, sensitized to grass pollen and/or *Dermatophagoides pteronyssinus* allergens, confirmed by skin prick test, shortlisted for specific immunotherapy, served as the study group. The analysis was performed before and after 12 months of specific sublingual immunotherapy. Nineteen children (76%), 18 boys and one girl, were reexamined after 1 year of SLIT. None of the subjects was treated with corticosteroids for 4 weeks before tests. The patients were treated with Staloral 300 (Stallergens) according to the manufacturer's instructions. One child did not obtain the maximum dose of the vaccine due to low tolerability. Fifteen healthy individuals, aged 9.8 ± 3.4, seven boys and eight girls, served as a control group. Inclusion criteria for the control group were low quantitative IgE level, a negative history of atopy and asthma or any systemic diseases and no recent infections. The characteristic of included children were presented in Table 10.1.

Table 10.1 Characteristics of children enrolled into the study

Parameter	Asthmatic children	Healthy children
Age (year)	8.1 ± 3.1 (5–15)	9.8 ± 3.4 (5.5–14.5)
Gender (F/M)	4/21	8/7
Bronchial asthma (%)	100%	0%
Allergic rhinitis (%)	100%	0%
Allergen-specific IgE (>0.7 kU/l)		
Grass pollen	88%	0%
Artemisia vulgaris (Wormwood pollen)	20%	0%
Betula verrucosa (Birch pollen)	56%	0%
D. pteronyssinus	28%	0%
D. farinae	28%	0%
Family history of atopic diseases	52%	0%

10.2.2 Flow Cytometry

Fifty microliters of peripheral blood collected to tubes containing EDTA were transferred to cytometric tubes to which 10 μl of a suitable monoclonal antibody were added. Antigens CD11b and CD18 were identified on the cells, after staining with monoclonal (Beckman Coulter) antiCD11b-PC5 and antiCD18-FITC antibodies. An appropriate isotypic control with monoclonal antiIgG1-FITC and antiIgG1-PC5 antibodies was performed for each sample before the proper test. Additional staining with CD23-PE monoclonal antibody was performed to exclude from analysis CD23 positive cells (eosinophils).

The tubes containing blood mixed with monoclonal antibodies were incubated for 30 min in the dark at room temperature. After incubation, erythrocytes were lysed with a lysing solution (BD Pharm Lyse-Becton Dickinson), the sample was dissolved in distilled water and mixed. Then, the tubes were washed twice with 3 ml 0.9% NaCl and centrifuged after each washing. The cells stained with monoclonal antibodies were resuspended in 1 ml of saline. The sample was analyzed in a flow cytometer (Cytomics FC500; Beckman Coulter). The first cytogram divided the peripheral blood leukocytes into three main populations on the basis of size and granularity of cells (FS – forward scatter, SS – side scatter). Further analysis was performed on cells from B gate (granulocytes). The cytograms of cells expressing the antigens were presented in Fig. 10.1.

10.2.3 Statistical Analysis

Results were presented as median (Q1, Q3). Statistical analysis was performed using the Mann-Whitey U and Wilcoxon matched-pair tests. A $p < 0.05$ was considered significant.

10.3 Results

10.3.1 Percentage of CD11b/CD18+ Neutrophils in Asthmatic and Healthy Children

98.08 (90.79–99.12)% of Mac-1 positive neutrophils were detected in the peripheral blood of children suffering from atopic asthma *vs.* 99.69 (99.5–99.8)% in the group of healthy children, $p = 0.002$ (Fig. 10.2). Interestingly, in the asthma group we could distinguish two subgroups: the patients with more than

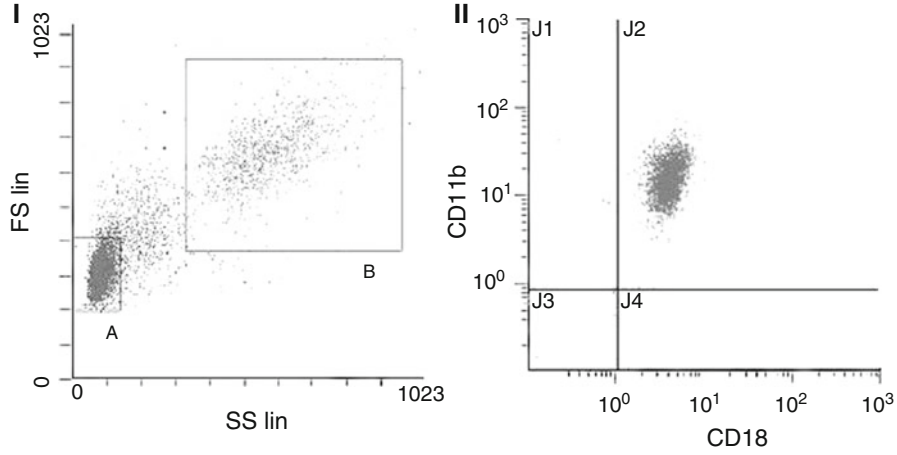

Fig. 10.1 Flow cytometric protocols presenting CD11b/CD18 positive granulocytes; (I) FS/SS cytogram; Gate A contains mononuclear cells (lymphocytes) and gate B contains polynuclear cells (granulocytes) (**II**) analysis of the cells from Gate B

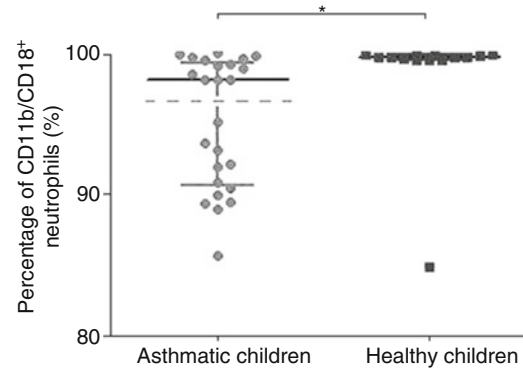

Fig. 10.2 Percentage of CD11b/CD18+ neutrophils in asthmatic and healthy children. *Dashed line* separates the two population subgroups, with >98% and <95% of Mac-1 positive cells, *$p < 0.05$

98% of Mac-1 positive neutrophils and those with less than 95% of CD11b/CD18+ neutrophils. In the former subgroup, 99.60 (99.29–99.68)% Mac-1 positive granulocytes were detected compared with 90.56 (87.08–88.86)% in the latter subgroup, $p = 0.0003$. No significant differences between the percentages of Mac-1 positive neutrophils was found when comparing the former subgroup of asthmatics and healthy children, $p = 0.26$.

10.3.2 Percentage of CD11b/CD18+ Neutrophils in Asthmatic Children Before and After 1 Year of Sublingual Immunotherapy

As mentioned above, 98.08 (90.79–99.12)% of Mac-1 positive neutrophils were detected in the asthmatic children before treatment. After 1 year of SLIT, the relative number of CD11b/CD18 positive neutrophils increased to 99.62 (99.17–99.92)%; the difference between both time-points was significant, $p = 0.01$ (Fig. 10.3).

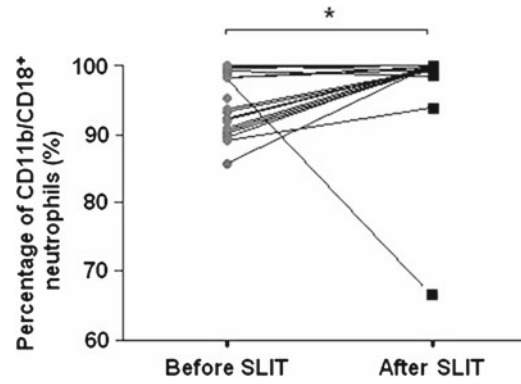

Fig. 10.3 Percentage of CD11b/CD18+ neutrophils before and after 1 year of SLIT; *p < 0.05

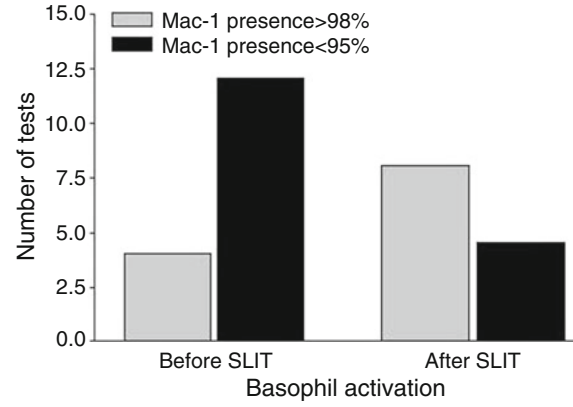

Fig. 10.4 Association between the initial percentage of Mac-1 positive neutrophils and the change of basophil activation in response to specific allergens after 1 year of SLIT

We also observed that in the subgroup with more than 98% neutrophils expressing Mac-1 integrin, SLIT did not cause any appreciable effect in the relative number of cells; 99.42 (98.11–99.81)% before *vs.* 99.64 (99.07–99.90)% after 1 year of SLIT, p = 0.91. On the other side, in the subgroup with less than 95% of CD11b/CD18+ neutrophils, a significant increase in their relative number was observed; 90.56 (89.39–92.04)% before *vs.* 99.62 (99.28–99.89)% after SLIT, p = 0.002.

10.3.3 Association Between the Percentage of Mac-1 Positive Neutrophils and the Response of Basophils to Immunotherapy

Additionally, we evaluated the activation of basophils by specific allergens before and after one year of sublingual immunotherapy in relation to the Mac-1 expression. As a measure of basophil activation, the expression of CD203c antigen on cell surface was evaluated according to the methodology described elsewhere (Potapinska et al. 2009). Before SLIT, the response of basophils to specific allergens was weaker in the subgroup of asthmatic children with the high >98% expression than in those with the lower <95% expression of Mac-1; basophils became desensitized just in 33% children (4 out of the 12). The situation was the reverse after SLIT. Here, the response was weaker in 75% children (12 out of the 16) in the subgroup with the lower <95% expression of Mac-1 positive neutrophils (Fig. 10.4). These changes reached borderline significance (p = 0.053).

10.4 Discussion

The role of neutrophils in the pathogenesis of asthma is still unclear. In the present study we examined the expression of Mac-1 integrin on neutrophils from the peripheral blood of asthmatic children before and after one year of sublingual immunotherapy. We found that two subgroups of patients suffering from atopic asthma could be distinguished: one with high and the other with a significantly lower expression of Mac-1 integrin. The percentage of CD11b/CD18 positive cells was not associated with the stage of asthma control, polysensitization or monosensitization, or with the presence of any other atopic disease.

Mac-1 integrin is formed by a complex of CD11b and CD18 antigens. The role of CD11b/CD18 is to interact with ICAM-1, ICAM-2, ICAM-3 adhesion molecules on the epithelial cell surface. Furthermore, it binds fibrinogen, complement system proteins and coagulation factor X (Hermanowicz-Salamon et al. 2006). Mac-1 integrin plays a crucial role in granulocyte migration and in intracellular signaling of neutrophils. It determines the ability of neutrophils to diapedesis and enables their migration to the place of an inflammatory process.

It has been observed that BALF from asthmatic subjects contains more CD11b positive macrophages that BALF from healthy individuals. The presence of Mac-1 positive cells in bronchi confirms the occurrence of an inflammatory process (Hermanowicz-Salamon et al. 2006). A higher number of CD11b+ neutrophils have been found in sputum than in peripheral blood in asthmatic subjects. In contrast, Maestrelli et al. (1999) have found no difference in the number of Mac-1 positive neutrophils between blood and sputum in healthy individuals.

In the present study, a significant difference was observed in the percentage of CD11b positive granulocytes in the peripheral blood between the asthmatic and healthy children. The finding is discrepant to that of Maestrelli et al. (1999) who have reported no such difference. One explanation of the discrepancy may lie in a small number of just eight patients in the mentioned study.

It has been suggested that a low percentage of CD11b+ granulocytes in the peripheral blood of asthmatic individuals may result from steroid therapy. Sale et al. (2004) have found that mometasone furoate and dexamethasone may decrease the expression of integrins on neutrophils and eosinophils; an effect also attributed to theophyline (Spoelstra et al. 1998). However, Mann and Chung (2006) failed to confirm this observation for prednisolone. Children enrolled in the present study were only occasionally treated with inhalant glucocorticosteroids and the treatment was not used at least 4 weeks before the blood analysis. Thus, glucocorticosteroid use should not confound the present results.

In this study we found that the relative number of Mac-1 positive neutrophils increased after one year of SLIT, particularly in the asthmatic children who had had less than 95% of CD11b+ granulocytes before immunotherapy. The surface expression of integrins enables the cell to migrate after its activation; the results are however contentious. Drost and MacNee (2002) found that density of Mac-1 particles on neutrophils from asthmatic subjects rises after fMLP (N-formyl-methionine-leucine-phenylalanine), PAF (platelet activation factor), or IL-8 stimulation, but Gabrijelcic et al. (2003) observed a decrease in CD11b+ on expression of neutrophils under the influence of PAF, whereas Catalli et al. (2008) reported no change in CD11b on neutrophils after allergen provocation. An increase in the number of Th1 cells after sublingual immunotherapy was repeatedly reported (Cosmi et al. 2006; Kim et al. 2011). That also may influence CD11b expression on neutrophils as Klebanoff et al. (1992) reported that Th1 cells release interferon γ (IFN-γ).

An increase in migration ability of neutrophils in asthma may promote airway remodeling. However, such hypothesis cannot be advanced without the evaluation of the number of neutrophils in bronchial walls. Only would the presence of inflammatory infiltration with a high percentage of neutrophils confirm that an increase in Mac-1 positive granulocytes may potentially contribute to airway remodeling. On the other hand, granulocytes, capable of diapedesis, migrate effectively to the place of pathogens invasion and can eliminate them efficiently. Our preliminary clinical observations show

that children after 1 year of SLIT suffer from seasonal viral rhinitis and bronchitis less frequently than before treatment. Increased antiviral immunity may result from the rise of Th1 cell number and increased release of interferon γ, while augmented antibacterial immunity may also refer to increased number of Th1 cells, since cytokines from the Th1 profile triggers macrophage activation and IgM and IgG synthesis in B cells. The immunoglobulins determine the opsonization process and activation of the complement system (Romagnani 2000). Additionally, increased migration ability of neutrophils may also improve antibacterial resistance.

In the present study we also found a trend for the association between the response of basophils to stimulation with specific allergens and the percentage of Mac-1 positive cells after SLIT. In the subgroup of asthmatic children with less than 95% of CD11b/CD18+ neutrophils, desensitization of basophils after SLIT was stronger than in the subgroup with a higher percentage of Mac-1 positive granulocytes. Further studies, including Mac-1 expression on basophils, will be continued on a larger group of patients. Noteworthy, the observation mentioned above is original in view of the fact that no other reports point to a relationship between the expression of integrins on granulocytes and the response of the immunological system to the allergen-specific immunotherapy.

In conclusion, sublingual immunotherapy is an effective treatment in atopic diseases, strongly influencing the function of the immunological system. Neutrophil activation and their ability to migrate seem one of sublingual immunotherapy targets, although further investigations in this area are necessary.

Acknowledgments This work was supported by a Ph.D. Scholarship 1WW/NK1D/09 funded by the Medical University of Warsaw and by Mazovia Voivodeship.

Conflicts of interest: The authors declare no conflicts of interest in relation to this article.

References

Catalli, A. E., Thomson, J. V., Babirad, I. M., Duong, M., Doyle, T. M., Howie, K. J., Newbold, P., Craggs, R. I., Foster, M., Gauvreau, G. M., O'Byrne, P. M., & Sehmi, R. (2008). Modulation of beta1-integrins on hemopoietic progenitor cells after allergen challenge in asthmatic subjects. *The Journal of Allergy and Clinical Immunology, 122*(4), 803–810.

Cosmi, L., Santarlasci, V., Angeli, R., Liotta, F., Maggi, L., Frosali, F., Rossi, O., Falagiani, P., Riva, G., Romagnani, S., Annunziato, F., & Maggi, E. (2006). Sublingual immunotherapy with *Dermatophagoides* monomeric allergoid down-regulates allergen-specific immunoglobulin E and increases both interferon gamma and interleukin-10-production. *Clinical and Experimental Allergy, 36*, 261–272.

Drost, E. M., & MacNee, W. (2002). Potential role of IL-8, platelet-activating factor and TNF-alpha in the sequestration of neutrophils in the lung: Effects on neutrophil deformability, adhesion receptor expression, and chemotaxis. *European Journal of Immunology, 32*(2), 393–403.

Foley, S. C., & Hamid, Q. (2007). Images in allergy and immunology: Neutrophils in asthma. *The Journal of Allergy and Clinical Immunology, 119*(5), 1282–1286.

Gabrijelcic, J., Acuña, A., Profita, M., Paternò, A., Chung, K. F., Vignola, A. M., & Rodríguez-Roisin, R. (2003). Neutrophil airway influx by platelet-activating factor in asthma: Role of adhesion molecules and LTB4 expression. *European Respiratory Journal, 22*(2), 290–297.

Hermanowicz-Salamon, J., Domagala-Kulawik, J., Maskey-Warzechowska, M., & Chazan, R. (2006). Macrophage phenotype in induced sputum in asthma subjects. *Pneumonologia i Alergologia Polska, 74*, 101–105.

Hogg, N. (1997a). Leukocyte typing VI; white cell differentiation antigens. In T. Kishimoto, et al. (Eds.), *CD11b workshop panel report* (pp. 345–347). New York: Garland Publishing Inc.

Hogg, N. (1997b). Leukocyte typing VI; white cell differentiation antigens. In T. Kishimoto, et al. (Eds.), *CD18 workshop panel report* (pp. 347–348). New York: Garland Publishing Inc.

Kim, E. H., Bird, J. A., Kulis, M., Laubach, S., Pons, L., Shreffler, W., Steele, P., Kamilaris, J., Vickery, B., & Burks, A. W. (2011). Sublingual immunotherapy for peanut allergy: Clinical and immunologic evidence of desensitization. *The Journal of Allergy and Clinical Immunology, 127*, 640–646.e1.

Klebanoff, S. J., Olszowski, S., Van Voorhis, W. C., Ledbetter, J. A., Waltersdorph, A. M., & Schlechte, K. G. (1992). Effects of gamma-interferon on human neutrophils: Protection from deterioration on storage. *Blood, 80*(1), 225–234.

Leatherman, B. D., Owen, S., Parker, M., Chadwick, S., Fornadley, J. A., Colson, D., & Fass, P. (2007). Sublingual immunotherapy: Past, present, paradigm for the future? A review of the literature. *Otolaryngology – Head and Neck Surgery, 136*(Suppl 3), S1–20.

MacDowell, A. L., & Peters, S. P. (2007). Neutrophils in asthma. *Current Allergy and Asthma Reports, 7*(6), 464–468.

Maestrelli, P., De Fina, O., Bertin, T., Papiris, S., Ruggieri, M. P., Saetta, M., Mapp, C. E., & Fabbri, L. M. (1999). Integrin expression on neutrophils and mononuclear cells in blood and induced sputum in stable asthma. *Allergy, 54*(12), 1303–1308.

Mann, B. S., & Chung, K. F. (2006). Blood neutrophil activation markers in severe asthma: Lack of inhibition by prednisolone therapy. *Respiratory Research, 7*, 59–69.

Monteseirín, J. (2009). Neutrophils and asthma. *Journal of Investigational Allergology and Clinical Immunology, 19*(5), 340–354.

Potapinska, O., Gorska, E., Demkow, U., Zawadzka-Krajewska, A., Kulus, M., & Wasik, M. (2009). The usefulness of CD203c expression measurement on basophils after activation with grass pollen and *Dermatophagoides pteronyssinus* antigens. Preliminary study. *Pneumonologia i Alergologia Polska, 77*(2), 138–144.

Romagnani, S. (2000). The role of lymphocytes in allergic response. *The Journal of Allergy and Clinical Immunology, 105*, 399–408.

Sale, R., Sabatini, F., Silvestri, M., Serpero, L., Petecchia, L., & Rossi, G. A. (2004). Concentration-dependent activity of mometasone furoate and dexamethasone on blood eosinophils isolated from atopic children: Modulation of Mac-1 expression and chemotaxis. *International Immunopharmacology, 4*(13), 1687–1696.

Silvestri, M., Spallarossa, D., Battistini, E., Sabatini, F., Pecora, S., Parmiani, S., & Rossi, G. A. (2002). Changes in inflammatory and clinical parameters and in bronchial hyperreactivity asthmatic children sensitized to house dust mites following sublingual immunotherapy. *Journal of Investigational Allergology and Clinical Immunology, 12*(1), 52–59.

Spoelstra, F. M., Berends, C., Dijkhuizen, B., de Monchy, J. G., & Kauffman, H. F. (1998). Effect of theophylline on CD11b and L-selectin expression and density of eosinophils and neutrophils in vitro. *European Respiratory Journal, 12*(3), 585–591.

Chapter 11
L-Arginine Supplementation and Experimental Airway Hyperreactivity

M. Antosova and A. Strapkova

Abstract The interest in L-arginine metabolism was triggered primarily by the discovery of nitric oxide (NO) synthesis in mammals and its remarkable biological roles. The real role of L-arginine in the airway hyperreactivity (AHR) has not been established yet. Therefore, we studied whether supplementation of L-arginine can influence the experimental AHR evoked by two different triggers – allergen and exogenous irritant (toluene vapours). Male TRIK strain guinea pigs were used in the study. We used two patterns of pretreatment with L-arginine *in vivo*, short- and long-term, in a dose of 300 mg/kg administered i.p., after which we studied reactivity of airway smooth muscles *in vitro*. Pretreatment with L-arginine for 3 days decreased the airway smooth muscle reactivity induced by toluene vapour, whereas pretreatment for 17 days was without any additional effect on smooth muscle reactivity. The short-term pretreatment in ovalbumin-induced hyperreactivity caused an increase in airway smooth muscle reactivity to lower concentrations of both bronchoconstrictors. On the other side, this pretreatment significantly decreased smooth muscle reactivity to high concentrations of both bronchoconstrictors. Supplementation of L-arginine resulted in a modification of the airway smooth muscle response. The effect of supplementation was different depending on the AHR trigger, airway region and pretreatment duration. The results also underscore the importance of an optimal L-arginine level for the control of bronchial tone.

Keywords Airway hyperreactivity • Arginase • L-arginine • Nitric oxide • NO synthase

11.1 Introduction

L-arginine is the basic substrate for nitric oxide biosynthesis. This semi-essential amino acid is also a precursor for the synthesis of various proteins, urea, polyamines, proline, glutamate, creatine and agmatine. The synthesis and catabolism of L-arginine is influenced by several enzymes such as arginine succinate synthase, two isoenzymes of arginase, four NO synthases and arginine decarboxylase. Changes in the activity of these enzymes play an important role in the determination of L-arginine metabolic pathway under physiological and pathological conditions (Wu and Morris 1998).

M. Antosova (✉) • A. Strapkova
Department of Pharmacology, Jessenius Faculty of Medicine, Comenius University,
Sklabinska 26 St., 036 01 Martin, Slovakia
e-mail: antosova@jfmed.uniba.sk

M. Pokorski (ed.), *Respiratory Regulation - The Molecular Approach*,
Advances in Experimental Medicine and Biology 756, DOI 10.1007/978-94-007-4549-0_11,

Intracellular concentration of L-arginine is higher than 100 μmol/l. Its utilization depends not only on the presence of enzymes, but also on their catalytic effect. The optimal level of L-arginine in humans is sufficient for continuous production of NO (Chandran et al. 1998). Although the catalytic activity of NO synthase is relatively low (K_m (L-Arg) 1.4–32.2 μmol/l – depending on the isoform type), exogenous L-arginine can increase the bioavailability of nitric oxide (Su et al. 1997). Therapy with L-arginine is associated with increased concentrations of NO in exhaled air and with increased concentration of L-arginine and nitrate in plasma. This confirms that an increased amount of the substrate can increase endogenous NO production (Kharitonov et al. 1995). NO synthesis is dependent not only on the bioavailability of L-arginine, but also on different cofactors.

Another important enzyme using L-arginine is arginase. In humans it is constitutively expressed in two forms: arginase I and arginase II. Both enzymes have different properties, they are unevenly distributed in tissues and cells and have also different regulation of gene expression (Jenkinson et al. 1996; Li et al. 2001). Induction of arginase of any type may reduce the bioavailability of L-arginine for NO synthesis and subsequently attenuate the effects mediated by NO (Gobert et al. 2000). It is assumed that arginase II is involved in the regulation of bioavailability of L-arginine for NO synthesis, although it is not confirmed which type of arginase competes for substrate (Boucher et al. 1999). The imbalance between the activity of NO synthase and arginase is induced, e.g., by the action of inflammatory mediators (Cook et al. 1994). The maximal activity of arginase at physiological conditions significantly exceeds that activity of NO synthase. While arginase activity in rat liver is about 1,400 μmol/l/min/mg, NO synthase activity is approximately 1 μmol/l/min/mg (Reczkowski and Ash 1994; Griffith and Stuehr 1995). In terms of inflammation, this rate may even increase, therefore L-arginine can be considered as a major limiting factor for NO production, the lack of which may contribute to the development of airway hyperreactivity (AHR).

The metabolic pathway of L-arginine and balance between arginase and NO synthase are important factors preventing the onset and development of AHR (North et al. 2009). Endogenous NO is involved in the regulation of airway responsiveness to bronchoconstrictive stimuli, including the muscarinic receptor agonists, histamine and bradykinin (Meurs et al. 2003). A number of studies have shown that deficiency of endogenous NO promotes AHR in response to various stimuli (de Boer et al. 2001).

Deficiency of NO is the main stimulus for the development of AHR after the late asthmatic response. This deficiency is due to reduced availability of L-arginine in the airways, which may be caused by two different mechanisms: increased activity of arginase competing with iNOS for the common substrate, or increased release of eosinophilic substances, which inhibits the transport of L-arginine to NO-producing cells (Maarsingh et al. 2009).

A decrease in bioavailability of the basic substrate for NO synthesis – L-arginine can influence bronchial tone and can be one of the factors contributing to AHR. Therefore, we studied whether supplementation of L-arginine can influence the experimental AHR or whether it has beneficial effects on airway reactivity evoked by two different triggers – allergen or exogenous irritant.

11.2 Methods

Experimental protocols had been approved by a local Ethics Committee of the Jessenius Faculty of Medicine in Martin, Slovakia, in accordance with internationally accepted recommendations regarding the experimental animal care and use. Outbreed male TRIK strain guinea pigs (250–300 g) were used in the experiments. The animals were housed individually in climate-controlled commercial animal cages. The guinea pigs were weighed before and during the study and had *ad libitum* access to water and food.

11.2.1 Study Design

We recorded changes in airway smooth muscle reactivity after L-arginine pretreatment in response to toluene or allergen exposure. We divided the animals into seven groups, each made up of eight animals: four experimental and three control ones. All animals from the experimental groups received L-arginine (Sigma Aldrich, St. Louis, MA), dissolved in water, in a dose of 300 mg/kg daily, i.p. as short-, for 3 days, and long-, for 17 days, pretreatment. The animals in the control groups received 'water for injection' alone – 1 ml/kg.

The first experimental group received L-arginine 30 min before toluene exposure during 3 consecutive days (short-term pretreatment).

The second experimental group received L-arginine for 17 days (long-term pretreatment); during the last 3 days 30 min before toluene exposure.

The third experimental group received L-arginine 30 min before each allergen exposure (short-term pretreatment: three times).

The fourth experimental group received L-arginine during over the whole period of sensitization – 14 days – once a day (long-term pretreatment).

All animals in the control groups received 'water for injection' as above outlined under otherwise the same experimental and hyperreactivity paradigms.

11.2.2 Airway Hyperreactivity Induction

Toluene exposure. The method of *in vivo* exposure to toluene vapours described by Strapkova et al. (1996) was used in this study. The guinea pigs were spontaneously breathing toluene vapors in a Plexiglas exposure chamber which consisted of the compressor, flow-meter, vaporizer and exposure cage. The device was situated in the fume-cupboard at 22°C. Toluene vapours were delivered into the cage at a constant flow of 4 l/min. The average concentration of toluene was 6 mg/l (1,600 ppm). The duration of each exposure was 2 h for 3 consecutive days.

Allergen sensitization. Guinea pigs were sensitized with ovalbumin (OVA, Sigma Aldrich). The animals received OVA during 14 days: the 1st day – 100 μg OVA dissolved in 1 ml saline (0.5 ml – subcutaneously in the neck and 0.5 ml i.p.), the 3rd day – OVA in the same dose i.p. only. The guinea pigs inhaled 0.1% OVA solution for 3 min on the 14th day.

11.2.3 Airway Smooth Muscle Reactivity

Airway smooth muscle reactivity was recorded in response to cumulative doses (10^{-8}–10^{-3} mol/l) of histamine and acetylcholine (Sigma Aldrich, St. Louis, MA) after 1 h of tissue incubation *in vitro*. The animals were killed 24 h after last toluene or allergen exposure. The trachea and lungs were removed and thin organ strips were prepared and placed into a bath with Krebs-Henseleit solution containing 110.0 mmol/l NaCl, 4.8 mmol/l KCl, 2.35 mmol/l $CaCl_2$, 1.20 mmol/l $MgSO_4$, 1.20 mmol/l KH_2PO_4, 25.0 mmol/l $NaHCO_3$ and 4 g glucose in glass-distilled water. The solution was continuously aerated with a mixture of 95% O_2 and 5% CO_2 at pH 7.5 ± 0.1 and temperature 36.0°C ± 0.5°C. The strip endings were connected to a force transducer and an amplifier (RES s.r.o, Martin, Slovakia). Changes in tension were recorded on PC with specific software (RES s.r.o, Martin, Slovakia). The tissue strips were exposed initially to the tension of 4 g (30 min – loading phase). Thereafter, the tension was reduced to the baseline of 2 g (30 min – adaptation phase). The Krebs-Henseleit solution was exchanged every

10 min. A cumulative concentration-response curve to 10^{-8}–10^{-3} mol/l histamine or acetylcholine was determined for every strip.

All results were expressed as means ± SE. Statistical analysis was performed using one-way analysis of variance ANOVA. Comparisons of baseline values between groups were analyzed with a two-sided *t*-test. All statistical analyses were done with Microsoft Excel and Microcal Origin 7.0 (OriginLab, Data analysis and Graphing Software). Differences were considered statistically significant with $p < 0.05$.

11.3 Results

11.3.1 Pretreatment with L-Arginine in Toluene-Induced Airway Hyperreactivity

Short-term pretreatment with L-arginine caused significant changes in *in vitro* reactivity of trachea and lung tissues obtained from the animals exposed to toluene *in vivo*. There were increases in tracheal smooth muscle reactivity in response to the lowest concentrations of both mediators (10^{-8}–10^{-7} mol/l of histamine and 10^{-8} mol/l of acetylcholine) in comparison with the control group. However, we further recorded a significant decrease in tracheal smooth muscle reactivity with gradually increasing concentrations of the mediators (10^{-4}–10^{-3} mol/l of histamine (Fig. 11.1a) and 10^{-5}–10^{-3} mol/l of acetylcholine) (Fig. 11.1b). In contrast, lung smooth muscles responded to histamine with an insignificant decrease in reactivity (Fig. 11.1c), but with a dedicated decrease in reactivity in response to acetylcholine at all concentrations used after short-term administration of L-arginine (Fig. 11.1d).

Long-term pretreatment with L-arginine resulted in insignificant decreases in both tracheal and lung smooth muscle reactivity (data not shown).

11.3.2 Pretreatment with L-Arginine in Allergen-Induced Airway Hyperreactivity

The effects of short-term pretreatment with L-arginine in the ovalbumin sensitized guinea pigs followed by the allergen exposure *in vivo* on the *in vitro* reactivity of tracheal smooth muscles to histamine and acetylcholine were in general similar to those observed for the toluene-exposed animals above outlined. The tracheal smooth muscles responded with increases in reactivity at the lowest concentrations of both mediators, followed by decreases at higher concentrations after short-term pretreatment with L-arginine (Fig. 11.2a, b).

With regard to the long-term pretreatment with L-arginine, the response of the tracheal smooth muscle, taken from the allergen-sensitized guinea pigs, to histamine was similar to that observed after the short-term pretreatment; increases in reactivity at low concentrations and decreases at higher concentrations of histamine (Fig. 11.2a). Concerning acetylcholine, the effects were more variable. Compared with control reactivity, there was first an increase at the lowest 10^{-8} mol/l acetylcholine concentration, but at higher acetylcholine concentrations no appreciable changes in the amplitude of muscle contraction were observed (Fig. 11.2b).

Lung smooth muscle, taken from the allergen-sensitized guinea pigs, responded with marked increases in reactivity due both to histamine (10^{-8}–10^{-7} mol/l) (Fig. 11.2c) and acetylcholine (10^{-8}–10^{-7} mol/l) (Fig. 11.2d) after both short- and long-term L-arginine pretreatment. The increases were however apparent only at low concentrations of the mediators and were stronger after the short-term pretreatment with L-arginine compared with the long-term pretreatment (Fig. 11.2c, d).

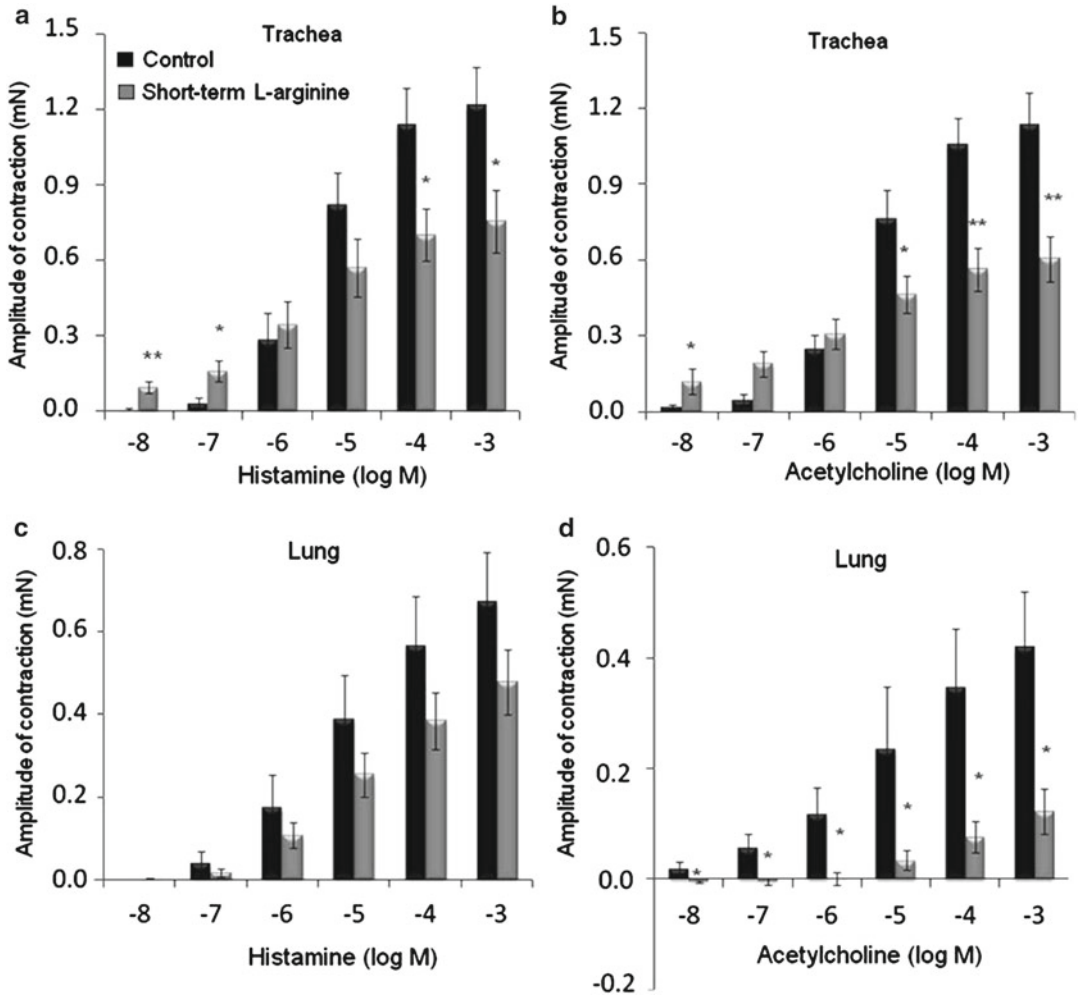

Fig. 11.1 Tracheal (Panels a–b) and lung (Panels c–d) tissues reactivity to histamine and acetylcholine *in vitro* after short-term pretreatment with L-arginine in guinea pigs exposed to toluene *in vivo*; *p < 0.05; **p < 0.01

11.4 Discussion

We focused in our work on changes in airway hyperreactivity induced by toluene and ovalbumin after application of L-arginine, the main precursor for NO synthesis. Many experimental studies have demonstrated that a deficit rather than an increase of NO (mainly iNOS-derived) is a major cause of airway hyperreactivity after the late asthmatic response. NO deficiency caused by reduced availability of L-arginine in the airways may be a consequence of two different mechanisms. First, increased activity of arginase that competes with NOS for a common substrate, and second, increased release of eosinophil-derived substances (e.g., peroxidase, polycation proteins) that inhibit the transport of L-arginine to NO-producing cells (Maarsingh et al. 2009).

We found that short-term application of L-arginine caused substantial reductions in tracheal smooth muscle reactivity to both mediators and a reduction in lung tissue reactivity to acetylcholine in toluene-induced hyperreactivity. We can suppose that the ultimate effect of L-arginine depends

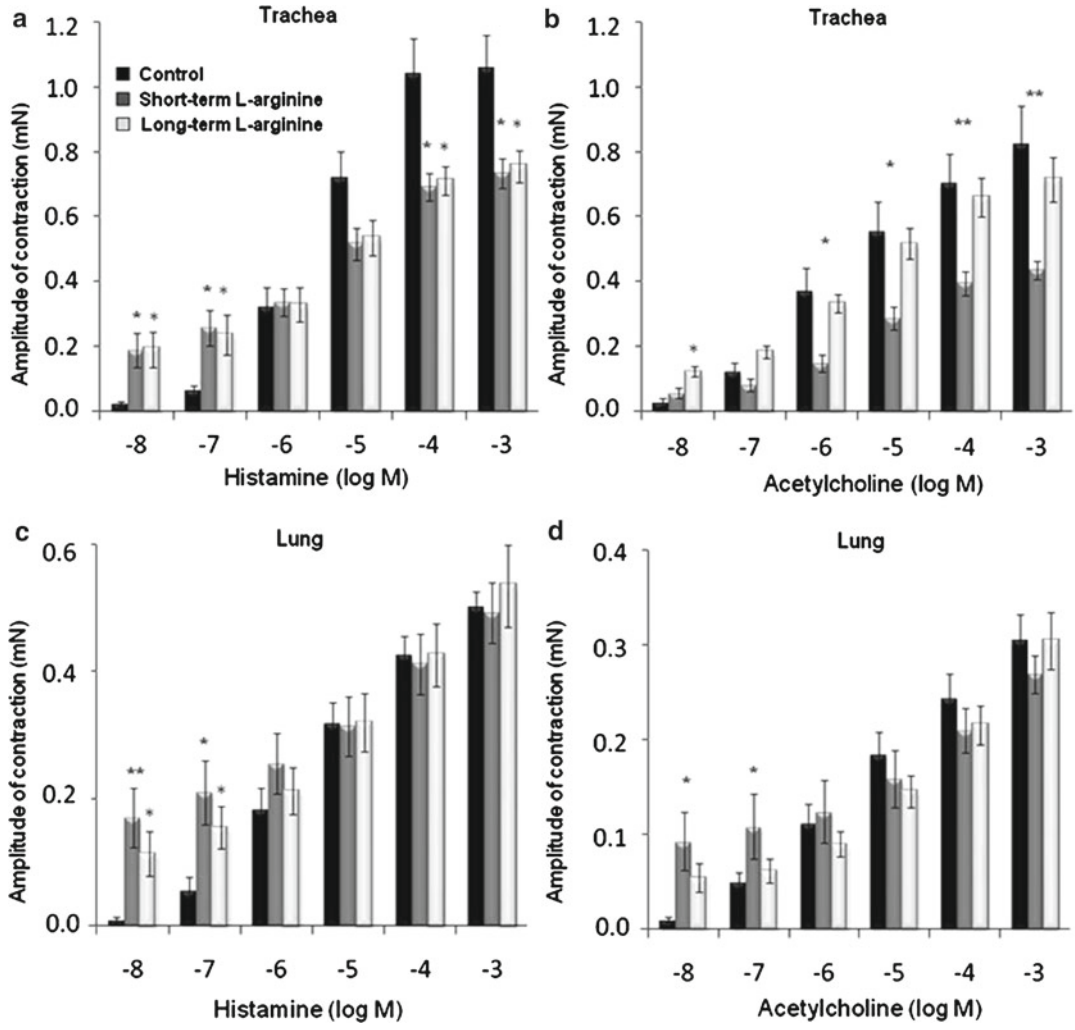

Fig. 11.2 Tracheal (Panels a–b) and lung (Panels c–d) tissue reactivity to histamine and acetylcholine *in vitro* after short- and long-term pretreatment with L-arginine in guinea pigs sensitized with ovalbumin and subsequently exposed to the allergen *in vivo*; *p<0.05; **p<0.01

on the type of enzyme which is dominant in its synthesis and on the way of its administration. The question therefore arises which enzymes are important in the pathogenesis of airway hyperreactivity. Substitution of L-arginine and its utilization with constitutive NO synthase isoforms have predominantly beneficial effects. Increased of iNOS activity or activity of other enzymes (especially arginase) may induce the opposite situation. The literature shows an effort to clarify these hypotheses. Inhalation of L-arginine does not worsen symptoms or lung function in patients with mild asthma (Sapienza et al. 1998). Oral administration (Kharitonov et al. 1995) or inhalation of L-arginine in patients with primary ciliary dyskinesia improves cilia dysfunction and respiratory antibacterial protection (Loukides et al. 1998). L-arginine modifies the endothelial dysfunction in patients with COPD (Hutchinson et al. 2001). L-arginine pretreatment also improves airway hyperreactivity induced by viruses, which also correlates with increased NO in exhaled air (de Gouw et al. 1999). In reducing symptoms of asthma or COPD, L-arginine could also work, in addition to NO

modulation, by its antioxidant properties due to the presence of guanidine group in its molecule (Lass et al. 2002). It is possible that some of these mechanisms could be involved in the protective effects of L-arginine in toluene-induced hyperreactivity in the present study.

In the experiments concerning allergen-induced hyperreactivity of airway smooth muscles, short-term pretreatment with L-arginine decreased the tracheal reactivity to both histamine and acetylcholine, with the exception of the lowest histamine concentrations. In the case of lung tissue, short-term application of L-arginine caused an increase in reactivity in response to the lowest concentrations of both mediators.

In *in vivo* studies in experimental models of guinea pigs with allergic asthma, iNOS-derived NO has a beneficial effect on allergen-induced airway hyperreactivity after the late asthmatic response, and a partial weakening of bronchial hyperreactivity in relation to its bronchodilator effect (Maarsingh et al. 2009). On the other side, disruption of the delicate balance between NO synthase and arginase may lead to reduced availability of L-arginine for constitutive isoforms of NOS and thus increased oxidative stress and airway hyperreactivity. Mabalirajan et al. (2009) observed the effect of high doses of L-arginine metabolizing enzymes and the subsequent biological response, such as cGMP production, lipid peroxidation, peroxynitrite formation, hyperreactivity and airway inflammation in ovalbumin-sensitized mice models of asthma. L-arginine significantly reduced AHR and airway inflammation. In addition, L-arginine increased NO levels in exhaled air and nitro-markers of oxidative stress, e.g., nitrotyrosine. This was associated with reduced activity and expression of arginase-1, increased expression of eNOS and reduction of iNOS in bronchial epithelium.

The reason why we did not observe a beneficial effect of long-term L-arginine pretreatment in the airway hyperreactivity conditions is not readily explicable, but that phenomenon has been observed by others as well. De Gouw et al. (1999) described that orally administered L-arginine had no effect on airway responsiveness to histamine in patients with asthma. Takano et al. (1998) found that oral administration of L-arginine increased airway inflammation. Therefore, we can assume that long-term application of L-arginine inhibit its short-term beneficial effects on airway hyperreactivity. An increase in the substrate for NO production probably inhibits cNOS, resulting in amplification of bronchoconstriction. L-arginine may increase NO production by iNOS or, conversely, may increase production of free radicals, which is associated with increased readiness of airway smooth muscle to bronchoconstriction. The differences in the action of L-arginine in different regions of the respiratory system may be caused by different localization of enzymes that utilize L-arginine and by diverse locations of antioxidant mechanisms in the upper and lower airways (Strapkova et al. 2008). The proximal airways also have a higher number of L-arginine utilizing NOS neurons than the distal parts. Therefore, NO works as a bronchodilator mainly in the proximal part of the airways (Prado et al. 2005). Another explanation is that the respiratory system responds to ovalbumin with adaptive responses in larger airways in which it regulates the concentration of L-arginine in the epithelial cell layer (Kenyon et al. 2008).

Some authors report a different respiratory response to histamine and acetylcholine, while reactivity to histamine is more pronounced (Matsumoto et al. 1997; Strapkova et al. 2008). This can be caused by differences in the proportion of neuronal reflex mechanisms. Histamine induces bronchoconstriction directly and indirectly. Direct contraction of airway smooth muscle is mediated through a receptor and indirect one is through neuronal reflexes and the excitation of cholinergic neural pathways. Acetylcholine is less effective for neural reflex mediated bronchoconstriction (Matsumoto et al. 1997). In our experiments, the response to both mediators did not differ significantly. The disagreement with other authors may be caused by using a different stimulus to induce airway hyperreactivity. In our case, the stimuli were an exogenous irritant and ovalbumin sensitization.

In summary, pretreatment with L-arginine resulted in a modification of the response of airway smooth muscles. The effects of supplementation depended on the airway hyperreactivity trigger, airway region and pretreatment duration. The results show a protective effect of short-term pretreatment with L-arginine mainly in irritant-induced experimental airway hyperreactivity. The study underscores the importance of L-arginine for the control of bronchomotoric tone.

Acknowledgments This work was supported by Grant MZ SR 2007/46-UK-11, VEGA and by the Center of Experimental and Clinical Respirology.

Conflicts of interest: The authors declare no conflicts of interest in relation to this article.

References

Boucher, J. L., Moali, C., & Tenu, J. P. (1999). Nitric oxide biosynthesis, nitric oxide synthase inhibitors and arginase competition for L-arginine utilization. *Cellular and Molecular Life Sciences, 55*, 1015–1028.

Chandran, S., Sridhar, N., & Veeranjaneyulu, A. (1998). Nitric oxide: Concepts, current perspectives and future therapeutic implications. *Indian Journal of Pharmacology, 30*, 351–366.

Cook, H. T., Jansen, A., Lewis, S., Largen, P., O'Donnell, M., Reaveley, D., & Cattell, V. (1994). Arginine metabolism in experimental glomerulonephritis: Interaction between nitric oxide synthase and arginase. *American Journal of Physiology. Renal Physiology, 267*, 646–653.

de Boer, J., Meurs, H., Flendrig, L., Koopal, M., & Zaagsma, J. (2001). Role of nitric oxide and superoxide in allergen-induced airway hyperreactivity after the late asthmatic reaction in guinea-pigs. *British Journal of Pharmacology, 133*, 1235–1241.

de Gouw, H. W. F. M., Verbruggen, M. B., Twiss, I. M., & Sterk, P. J. (1999). Effect of oral L-arginine on airway hyperresponsiveness to histamine in asthma. *Thorax, 54*, 1033–1035.

Gobert, A. P., Daulouede, S., Lepoivre, M., Boucher, J. L., Bouteille, B., Buguet, A., Cespuglio, R., Veyret, B., & Vincendau, P. (2000). L-arginine availability modulates local nitric oxide production and parasite killing in experimental trypanosomiasis. *Infection and Immunity, 68*, 4653–4657.

Griffith, O. W., & Stuehr, D. J. (1995). Nitric oxide synthases: Properties and catalytic mechanism. *Annual Review of Physiology, 57*, 707–736.

Hutchinson, S. J., Sievers, R. E., Zhu, B. Q., Sun, Y. P., Stewart, D. J., Parmley, W. W., & Chateerjee, K. (2001). Secondhand tobacco smoke impairs rabbit pulmonary artery endothelium-dependent relaxation. *Chest, 120*, 2004–2012.

Jenkinson, C. P., Grody, W. W., & Cederbaum, S. D. (1996). Comparative properties of arginases. *Comparative Biochemistry and Physiology, 114B*, 107–132.

Kenyon, N. J., Bratt, J. M., Linderholm, A. L., Last, M. S., & Last, J. A. (2008). Arginase I and II in lungs of ovalbumin-sensitized mice exposed to ovalbumin: Sources and consequences. *Toxicology and Applied Pharmacology, 230*, 269–275.

Kharitonov, S. A., Lubec, G., Lubec, B., Hjelm, M., & Barnes, P. J. (1995). L-arginine increases exhaled nitric oxide in normal human subject. *Clinical Science, 88*, 135–139.

Lass, A., Suessenbacher, A., Wolkart, G., Mayer, B., & Brunner, F. (2002). Functional and analytical evidence for scavenging of oxygen radicals by L-arginine. *Molecular Pharmacology, 61*, 1081–1088.

Li, H., Meininger, C. J., Hawker, J. R., Jr., Haynes, T. E., Kepka-Lenhart, D., Mistry, S. K., Morris, S. M., Jr., & Wu, G. (2001). Regulatory role of arginase I and II in nitric oxide, polyamine and proline syntheses in endothelial cells. *American Journal of Physiology, Endocrinology and Metabolism, 280*, E75–E82.

Loukides, S., Kharitonov, S. A., Wodenhouse, T., Cole, P. J., & Barnes, P. J. (1998). Effect of L-arginine on mucociliary function in primary ciliary dyskinesia. *Lancet, 352*, 371–372.

Maarshing, H., Bossenga, B. E., Bos, I. S. T., Volders, H. H., Zaagsma, J., & Meurs, H. (2009). L-Arginine deficiency causes airway hyperresponsiveness after the late asthmatic reaction. *European Respiratory Journal, 34*, 191–199.

Mabalirajan, U., Ahmad, T., Leishangtem, G. D., Joseph, D. A., Dinda, A. K., Agrawal, A., & Ghosh, B. (2009). Beneficial effects of high dose of L-arginine on airway hyperresponsiveness and airway inflammation in a murine model of asthma. *The Journal of Allergy and Clinical Immunology, 125*, 626–635.

Matsumoto, K., Aizawa, H., Takata, S., Inoue, H., Takahashi, N., & Hara, N. (1997). Nitric oxide derived from sympathetic nerves regulates airway responsiveness to histamine in guinea pigs. *Journal of Applied Physiology, 83*, 1432–1437.

Meurs, H., Maarsingh, H., & Zaagsma, J. (2003). Arginase and asthma: Novel insights into nitric oxide homeostasis and airway hyperresponsiveness. *Trends in Pharmacological Sciences, 24*, 450–455.

North, M. L., Khanna, N., Marsden, P. A., Grasemann, H., & Scott, J. A. (2009). Functionally important role for arginase-1 in the airways hyperresponsiveness of asthma. *American Journal of Physiology. Lung Cellular and Molecular Physiology, 289*, L677–L683.

Prado, C. M., Leick-Maldonado, E. A., Kasahara, D. I., Capelozzi, V. L., Martins, M. A., & Tibério, I. F. (2005). Effects of acute and chronic nitric oxide inhibition in an experimental model of chronic pulmonary allergic inflammation in guinea pigs. *American Journal of Physiology. Lung Cellular and Molecular Physiology, 289*, L677–L683.

Reczkowski, R. S., & Ash, D. E. (1994). Rat liver arginase: Kinetic mechanism, alternate substrates, and inhibitors. *Archives of Biochemistry and Biophysics, 312*, 31–37.

Sapienza, M. A., Kharitonov, S. A., Horvath, I., Chung, K. F., & Barnes, P. J. (1998). Effect of inhaled L-arginine on exhaled nitric oxide in normal and asthmatic subjects. *Thorax, 53*, 172–175.

Strapkova, A., Nosalova, G., & Hanacek, J. (1996). Effect of irritants on airways reactivity. *Central European Journal of Public Health, 4*, 54–56.

Strapkova, A., Antosova, M., & Nosalova, G. (2008). Relation of L-arginine to airway hyperreactivity. *General Physiology and Biophysics, 27*, 85–91.

Su, Y., Couch, M., & Block, E. R. (1997). Substrate inhibition of nitric oxide synthase in pulmonary artery endothelial cells in culture. *Nitric Oxide, 1*, 469–475.

Takano, H., Lim, H. B., Miyabara, Y., Ichinose, T., Yoshikawa, T., & Sagai, M. (1998). Oral administration of L-arginine potentiates allergen-induced airway inflammation and expression of interleukin-5 in mice. *Journal of Pharmacology and Experimental Therapeutics, 286*, 767–771.

Wu, G., & Morris, S. M. (1998). Arginine metabolism: Nitric oxide and beyond. *Biochemical Journal, 336*, 1–17.

Chapter 12
Polyphenols and Their Components in Experimental Allergic Asthma

M. Joskova, V. Sadlonova, G. Nosalova, E. Novakova, and S. Franova

Abstract The aim of the study was to investigate the potential anti-inflammatory effects in experimental allergic asthma of natural polyphenolic compounds or their single major components. The experiment was performed after 21-days sensitization of guinea pigs with ovalbumin suspension. Changes in airway reactivity after the long-term treatment with the polyphenolic compounds Provinol and Flavin-7 and their single major components quercetin and resveratrol during were assessed using a whole body plethysmography. Reactivity of tracheal smooth muscle was studied *in vitro* in response to cumulative doses of the bronchoconstrictive mediators histamine and acetylcholine. Furthermore, concentrations of the inflammatory cytokines IL-4 and IL-5 were measured in bronchoalveolar lavage fluid. The results demonstrate significant anti-inflammatory effects of Provinol and Flavin-7 exerted in the airways. In contrast, chronic treatment with quercetin and resveratrol, single components of the two polyphenols, did not show such activity. We conclude that polyphenolic compounds are more effective in the anti-inflammatory effects in the airways than their separate components.

Keywords Allergic inflammation • Airway hyperreactivity • Asthma • Polyphenols • Quercetin • Resveratrol • Inflammatory cytokines

12.1 Introduction

Allergic asthma is a chronic inflammatory disorder of airways in which many inflammatory cells, airways structural cellular elements, and inflammatory mediators play a role in the induction of airways hyperreactivity and bronchoconstriction. The early allergic response occurring within seconds to minutes of allergen exposure is manifested with bronchoconstriction, edema in the airways and mucin hypersecretion induced by inflammatory mediators of mast cells (histamine, prostaglandin D2,

M. Joskova (✉) • V. Sadlonova • G. Nosalova • S. Franova
Department of Pharmacology, Jessenius Faculty of Medicine, Comenius University,
Sklabinska 26 St, SK-037 53 Martin, Slovakia
e-mail: joskova@jfmed.uniba.sk

E. Novakova
Department of Microbiology and Immunology, Jessenius Faculty of Medicine, Comenius University,
Sklabinska 26 St, SK-037 53, Martin, Slovakia

M. Pokorski (ed.), *Respiratory Regulation - The Molecular Approach*,
Advances in Experimental Medicine and Biology 756, DOI 10.1007/978-94-007-4549-0_12,

and leukotriene C4). The late-phase allergic reaction related to activation of inflammatory cells (mast cells, T cells, eosinophils, and neutrophils), inflammatory cell recruitment in the lungs, airway hyperreactivity, and production of IgE might occurs a few hours later (Galli et al. 2008). Th1/Th2 imbalance with a predominance of Th2 inflammatory cytokines such as IL-4, IL-5, IL-9, and IL-13 is a consequence of allergen challenge. In the presence of IL-4 and IL-13, and co-stimulatory molecules (CD40 and CD80 or CD86) B lymphocytes undergo a class switch to produce IgE antibodies (Lebman and Coffman 1988; Van der Pouw Kraan et al. 1998). Higher expression of IL-5 is associated with eosinophil-mediated inflammation in the airways (Shi et al. 1998). IL-9 enhances proliferation of mast cells (Temann et al. 1998).

Recently, there has been a great deal of interest in polyphenols due to their beneficial pulmonary actions both in animals and humans. These natural substances are present in all plants. They are generally divided into two main categories: flavonoids (anthocyanins and anthoxanthins) and non-flavonoids like stilbenes, phenolic acids, and tannins. Polyphenolic natural products exhibit a wide range of biological and pharmacological properties. On the basis of many experimental studies, it has been accepted that polyphenols have anti-inflammatory, bronchodilator, antioxidant, and expectorant effects in the airways (Lee et al. 2009; Gilani et al. 2006; Brozmanova et al. 2007; Moon et al. 2008; Park et al. 2009). They are able to suppress allergen-induced inflammatory cell infiltration during the late-phase of allergic reaction, to reduce levels of inflammatory cytokines IL-4, IL-5 and IL-13 in plasma and bronchoalveolar lavage fluid (BALF), to decrease serum IgE levels, and to inhibit histamine release from mast cells during both early and late phase of allergic reaction, which all results in their anti-inflammatory effects in airways (Jung et al. 2007; Hurst et al. 2010; Iwamura et al. 2010).

The aim of our study was to assess changes in respiratory defence reflexes during experimental allergic inflammation in the airways in response to treatment with selected polyphenols. The study was designed to evaluate the potential anti-inflammatory effects of polyphenols by the use of *in vivo* and *in vitro* methods; the latter analyzing the inflammatory cytokines IL-4 and IL-5 in BALF. In the study we used the phenolic compounds Provinol and Flavin-7, as well as their separable major components quercetin and resveratrol.

Provinol as an alcohol-free red wine extract which contains more than 95% of polyphenols. We took interest in this compound due to its reported vasorelaxant effect on arterial smooth muscle (Andriambeloson et al. 1997). Flavin-7, in turn, is able to relax the tracheal smooth muscle of healthy animals and possesses antioxidant properties in airways (Brozmanova et al. 2007; Szentmiklósi 2003). We were also interested in the antiasthmatic effects of the flavonol quercetin and the stilbene resveratrol which belong to the main polyphenolic components of Provinol and Flavin-7.

12.2 Methods

12.2.1 Experimental Protocol

The study protocol was approved by a local Ethics Committee of Jessenius Faculty of Medicine, Comenius University in Martin, Slovakia. Male Trik guinea pigs were used in our experiment (250–300 g). They were randomly divided into three main groups each consisting of ten animals: control (n = 10) – treated for 21 days only with saline, sensitized with the allergen ovalbumin (OVA) for 21 days, and POVA, FOVA, KOVA or ROVA – groups of guinea pigs sensitized for 21 days with OVA and simultaneously treated with Provinol (20 mg kg^{-1} per day); Flavin-7 (2 ml kg^{-1} per day); quercetin (20 mg kg^{-1} per day), or resveratrol (10 mg kg^{-1} per day), respectively. Polyphenols were administered for 21 days daily orally simultaneously with sensitization of guinea pigs. Evaluating the chronic anti-inflammatory effect of polyphenols was performed on the 21st day of animal sensitization.

12.2.2 Materials

Provinol (dry powder of red wine polyphenolic compounds) was provided by D. Ageron (Société Francaise de Distillerie, Vallont Pont d'Arc, France). Provinol is a mixture of proanthocyanidins, total anthocyanins, free anthocyanins, catechins, phenolic acids and flavonols. Flavin-7 is a concentrated fruit extract (red grape, blackberry, black cherry, black currant, elderberry, blackthorn, and plum) riched on bioflavonoids and stilbene resveratrol. Flavin-7 was a gift from Vita Crystal Slovakia (Slovakia). Quercetin, resveratrol, ovalbumin (egg albumin grade V), histamine hydrochloride, acetylcholine and other chemicals were purchased from Sigma Aldrich (Taufkirchen, Germany) and aluminium hydroxide from AFT (Bratislava, Slovakia). RayBio® mouse IL-4 and IL-5 ELISA kits were purchased from BioTech X-ray (St.Louis, MO).

The composition of Provinol was (in mg g^{-1} dry powder): proanthocyanins 480, total anthocyanins 61, free anthocyanins 19, catechin 38, hydroxycinnamic acid 18, and flavonols 14. The composition of Flavin-7 was: total polyphenols 220 mg of which 170 mg flavonoids (myricetin, quercetin, kaempferol, isorhamnetine, (+)-catechin, (−)-epicatechin, malvidin-3-glucoside, chrysin, galangin, apigenin, fizetin and luteolin) and resveratrol 0.17 mg in 10 ml of this product.

12.2.3 Sensitization of Guinea Pigs

The intermittent exposure to allergen (suspension of 5 mg ovalbumin and 100 mg aluminium hydroxide) took 21 days. The suspension (0.5 ml) was injected both subcutaneously and intraperitonealy on the 1st day, subsequently either subcutaneosuly or intraperitonealy again during 2 weeks. 1% ovalbumin was nebulizated by guinea pigs for 1–3 min last week.

12.2.4 Assessment of Airways Reactivity

Changes in specific airway resistance of sensitized guinea pigs were induced by inhaling histamine (10^{-4} mol l^{-1}) for 2 min during *in vivo* conditions. A non-invasive technique for the measurement of these changes was conducted in a whole-body plethysmography after the long-term administration of polyphenols (Provinol, Flavin-7, quercetin, and resveratrol).

Changes in force of tracheal smooth muscle contraction evoked by cumulative doses (10^{-8}–10^{-3} mol l^{-1}) of histamine and acetylcholine were analyzed during *in vitro* conditions. These bronchoconstrictor mediators were added into the organ bath with Krebs-Henseleit solution (in mmol l^{-1}: NaCl 110.0; KCl 4.80; $CaCl_2$ 2.35; $MgSO_4$ 1.20; KH_2PO_4 1.20; $NaHCO_3$ 25.0; glucose 10.0). The amplitude of tracheal smooth muscle contraction (mN) after the long-term administration of polyphenols to sensitized animals was monitored.

12.2.5 Assessment of Airways Inflammation

Levels of inflammatory cytokines IL-4 and IL-5 were analyzed in BALF of the left lung. The lavage was performed twice with sterile isotonic saline solution (37°C; 10 ml kg^{-1}) using a tracheal cannula. The supernatant of BALF after centrifugation (1,500 rpm for 10 min) was used for immunological analysis of cytokine concentrations using commercially available ELISA kits (RayBiotech, Inc). The minimum detection levels for each cytokine was <5 pg ml^{-1}.

12.2.6 Statistical Data Analysis

The values for bronchial hyperreactivity and inflammatory cytokines in BALF were expressed as means±SE. ANOVA was performed to test for any differences in the mean values between groups. $p < 0.05$ was considered to be statistically significant.

12.3 Results

On the 21st day of animal sensitization, the experiments focused on the assessment of airway reactivity and allergic inflammation and the effects on them of the long-term administration of the antioxidants. Allergen-induced bronchial hyperreactivity resulted in an increase in specific airways resistance in response to histamine *in vivo* and in amplitude of tracheal smooth muscle contraction in response to both histamine and acetylcholine *in vitro*. There were also significant elevations in the inflammatory cytokines IL-4 and IL-5 in BALF.

The polyphenolic compounds Provinol and Flavin-7 significantly reduced both airway reactivity (Fig. 12.1a) and tracheal smooth muscle contraction evoked by both histamine and acetylcholine (Fig. 12.2a). The single components of these compounds quercetin and resveratrol had only mild, insignificant bronchodilator effects (Fig. 12.1b). Incubation of tracheal smooth muscle with quercetin reduced the amplitude of contraction in response to histamine and to higher concentrations of acetylcholine (10^{-5}–10^{-3} mol l^{-1}). Resveratrol failed to reduce contraction of tracheal smooth muscle provoked by both histamine and acetylcholine in sensitized guinea pigs (Fig. 12.2b).

Likewise, the polyphenolic Provinol and Flavin-7 effectively reduced the levels of IL-4 and IL-5 in BALF of sensitized animals, while quercetin and resveratrol failed to cause appreciable changes in these inflammatory cytokines (Fig. 12.3).

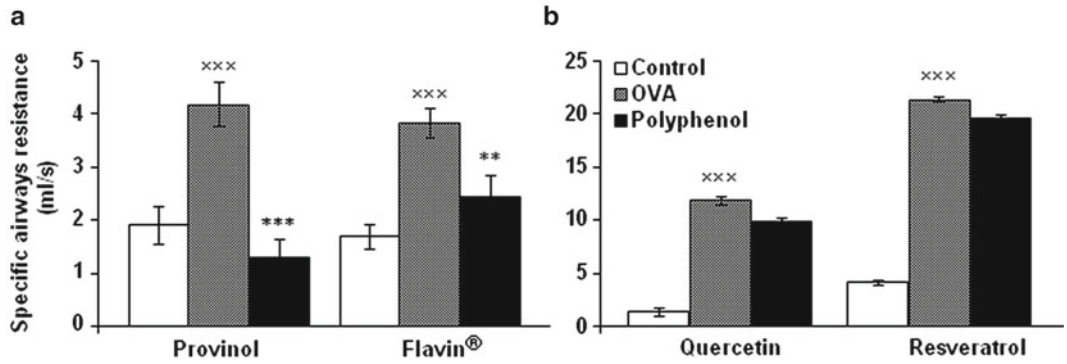

Fig. 12.1 Specific airway resistance after chronic administration of polyphenols in guinea pigs. (**a**) Provinol and Flavin-7 and (**b**) quercetin and resveratrol. Control – non-sensitized guinea pigs treated for 21 days with saline; OVA – guinea pigs sensitized for 21 days with ovalbumin (OVA); Polyphenol – guinea pigs sensitized with OVA for 21 days and simultaneously treated with Provinol (20 mg kg^{-1} per day) and Flavin-7 (2 ml kg^{-1} per day) or quercetin (20 mg kg^{-1} per day) and resveratrol (10 mg kg^{-1} per day). Data are means±SE, n = 10; $^{\times\times\times}p < 0.001$ compared with the control group; $^{**}p < 0.01$ and $^{***}p < 0.001$ compared with the OVA group

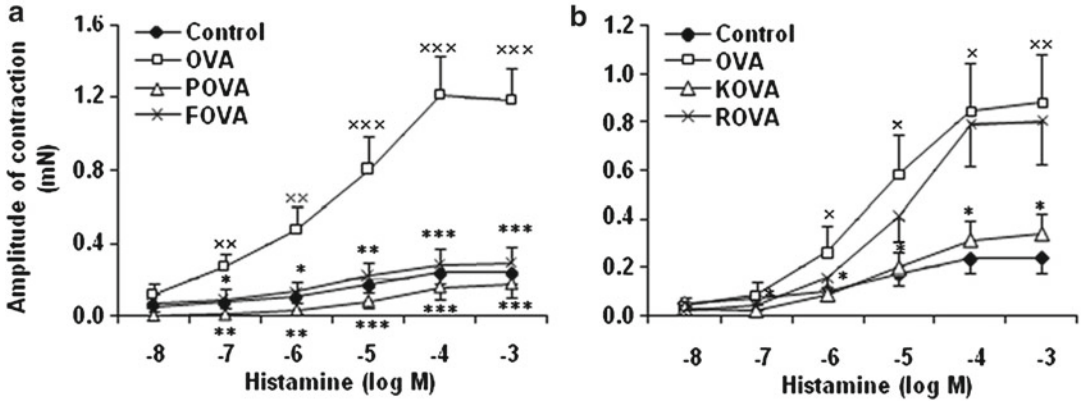

Fig. 12.2 Amplitude of tracheal smooth muscle contraction evoked by histamine 10^{-8}–10^{-3} mol l^{-1} after chronic administration of (**a**) Provinol and Flavin-7 and (**b**) quercetin and resveratrol. Control – non-sensitizated guinea pigs treated for 21 days with saline; OVA –guinea pigs sensitized for 21 days with ovalbumin (OVA); POVA – guinea pigs sensitized with OVA for 21 days and simultaneously treated with Provinol (20 mg kg^{-1} per day); FOVA – guinea pigs sensitized OVA for 21 days and simultaneously treated with Flavin-7 (2 ml kg^{-1} per day); KOVA – guinea pigs sensitized with OVA for 21 days and simultaneously treated with quercetin (20 mg kg^{-1} per day), and ROVA – guinea pigs sensitized with OVA for 21 days and simultaneously treated with resveratrol (10 mg kg^{-1} per day). Data are means±SE; n = 10; $^{\times}p<0.05$, $^{\times\times}p<0.01$, and $^{\times\times\times}p<0.001$ compared with the control group; $^{*}p<0.05$, $^{**}p<0.01$, $^{***}p<0.001$ compared with the OVA group

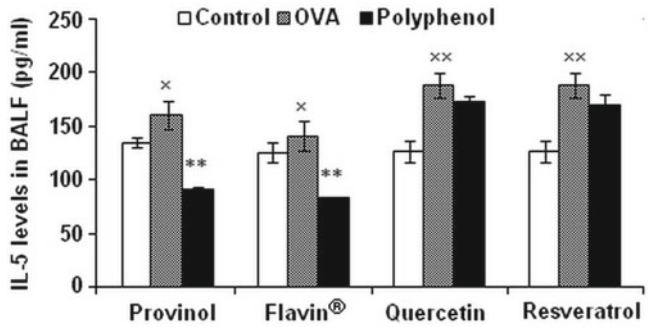

Fig. 12.3 Inflammatory cytokine IL-5 in bronchoalveolar lavage fluid (*BALF*) after chronic administration of polyphenols: Provinol, Flavin-7, quercetin, and resveratrol. Control – guinea pigs treated for 21 days with saline; OVA – guinea pigs sensitized for 21 days with ovalbumin; polyphenol – guinea pigs sensitized for 21 days with OVA and simultaneously treated with Provinol (20 mg kg^{-1} per day), Flavin-7 (2 ml kg^{-1} per day), quercetin (20 mg kg^{-1} per day), or resveratrol (10 mg kg^{-1} per day). Data are means±SE; n = 10; $^{\times}p<0.05$ and $^{\times\times}p<0.01$ compared with the control group; $^{**}p<0.01$ compared with the OVA group

12.4 Discussion

Treatment strategy of bronchial asthma is aimed at reducing airways hyperresponsiveness and allergic inflammation, the main features of asthma. Natural substances are less harmful to human health and have fewer unwanted effects compared with bronchodilators or corticosteroids. Recently, such compounds have become research objects in inflammatory disorders.

In the present study we assessed the effects of selected polyphenols on airway hyperresponsiveness and inflammation in experimentally evoked allergic asthma. The polyphenolic compounds Provinol and Flavin-7 effectively reduced bronchial hyperreactivity and contractile responses of tracheal smooth muscle to bronchoconstrictive mediators. Zenebe et al. (2003) have found similar biological effects of Provinol on vascular smooth muscle. This polyphenolic compound of red wine produces endothelium-dependent relaxation as a result of enhanced nitric oxide (NO) synthesis. In our previous study, we have also shown that the relaxant effect of Provinol in the airways is partially mediated through NO metabolism (Joskova et al. 2009). With regard to Flavin-7, Szentmiklósi (2003) has reported the compound's bronchodilator activity in healthy animals. On the other hand, the bronchodilating and anti-inflammatory effects of quercetin and resveratrol, single components of the two polyphenols outlined above were not confirmed in the present study. The latter negative result is divergent with a number of experimental studies which have shown potential benefits of quercetin in regard to the limitation of allergic inflammation in the airways. In those studies, however, quercetin was administered for a much shorter time or in much higher doses (Nanua et al. 2006; Jung et al. 2007; Moon et al. 2008; Park et al. 2009; Rogerio et al. 2010). Quercetin and its metabolites preferentially accumulate in the rat lungs (de Boer et al. 2005), which is in accord with its local protective action against experimentally-induced lung fibrosis in rats (El-Sayed and Rizk 2009). The present study failed to confirm the beneficial effect of quercetin in the bronchial allergic condition. One reason of the negative finding could be difficult or reduced solubility of quercetin (Ferry et al. 1996; Kim et al. 2009). Concerning resveratol, the lack of an effect could be due to too small a dose we employed, as doses three times higher apparently are able to exert an effect on the airways (Lee et al. 2009). In the present study we chose to use a moderate dose of resveratrol, although higher doses might be justified in view of its oxidative degradation *in vitro* in the presence of bicarbonate ions (Yang et al. 2010).

Allergen administration induces early and late allergic reactions in which many inflammatory cytokines play a role. IL-4 mediates induction of the IgE isotype switch and its secretion by B-lymphocytes (Lebman and Coffman 1988), expression of vascular cell adhesion molecule-1 (VCAM-1) on vascular endothelium (Iademarco et al. 1995), migration of eosinophils through endothelium, mucus induction, and differentiation of T helper type 2 lymphocytes and their recruitment to the lungs (Cohn et al. 1997). IL-5 promotes activation of B-lymphocytes resulting in enhanced serum antibody levels and eosinophil number in the blood and their infiltration into the lungs (Shi et al. 1998). In the present study we confirmed that both polyphenols Provinol and Flavin-7, but not their separable components quercetin and resveratrol, reduced the levels of inflammatory cytokines IL-4 and IL-5 in BALF of sensitized guinea pigs. In contrast, some other studies have found that the separable components of polyphenols may suppress allergic inflammation in airways due to a reduction in proinflammatory cytokines (Park et al. 2007, 2009). It is therefore a reasonable assumption that the final effect of polyphenolic compounds is a result of mutual interactions among their separable components. The latter components if applied alone may require much higher doses for the biological effect to show up. That assumption is in line with the studies in which the antioxidant effects of a mixture of flavonoids were produced (Kühnau 1976), while flavonoid monomers did not induce the biological response (Fitzpatrick et al. 1993).

In conclusion, the results of our experiments point to the appreciable anti-inflammatory effects of the polyphenolic compounds Provinol and Flavin-7 in experimental asthma. Such compounds are more effective than their separable components. Natural polyphenols may become useful ancillary therapy in the management of asthma.

Acknowledgement This work was supported by the projects 'Center of Experimental and Clinical Respirology II' and 'Support of human resources development using the most modern methods and forms of education at JLF UK in Martin' co-financed from EU sources and the European Social Fund and by VEGA grant 1/0020/11.

Conflicts of interest: The authors declare no conflicts of interest in relation to this article.

References

Andriambeloson, E., Kleschyov, A. L., Muller, B., Beretz, A., Stoclet, J. C., & Andriantsitohaina, R. (1997). Nitric oxide production and endothelium-dependent vasorelaxation induced by wine polyphenols in rat thoracic aorta. *British Journal of Pharmacology, 120*(6), 1053–1058.

Brozmanova, M., Bartos, V., Plank, L., Plevkova, J., & Tatar, M. (2007). Dietary intake of flavonoids and hyperoxia-induced oxidative stress related cough in guinea pigs. *Bratislavské Lekárske Listy, 108*(12), 489–494.

Cohn, L., Homer, R. J., Marinov, A., Rankin, J., & Bottomly, K. (1997). Induction of airway mucus production by T helper 2 (Th2) cells: A critical role for IL-4 in cell recruitment but not mucus production. *The Journal of Experimental Medicine, 186*(10), 1737–1747.

De Boer, V. C., Dihal, A. A., van der Woude, H., Arts, I. C., Wolffram, S., Alink, G. M., Rietjens, I. M., Keijer, J., & Hollman, P. C. (2005). Tissue distribution of quercetin in rats and pigs. *Journal of Nutrition, 135*(7), 1718–1725.

El-Sayed, N. S., & Rizk, Sh. M. (2009). The protective effect of quercetin, green tea or malt extracts against experimentally-induced lung fibrosis in rats. *African Journal of Pharmacy and Pharmacology, 3*(5), 191–201.

Ferry, D. R., Smith, A., Malkhandi, J., Fyfe, D. W., deTakats, P. G., Anderson, D., Baker, J., & Kerr, D. J. (1996). Phase I clinical trial of the flavonoid quercetin: Pharmacokinetics and evidence for *in vivo* tyrosine kinase inhibition. *Clinical Cancer Research, 2*(4), 659–668.

Fitzpatrick, D., Hirschfield, S. L., & Coffey, R. G. (1993). Endothelium-dependent relaxing activity of wine and other grape products. *American Journal of Physiology, 265*, 774–778.

Galli, S. J., Tsai, M., & Piliponsky, A. M. (2008). The development of allergic inflammation. *Nature, 454*(7203), 445–454.

Gilani, A. H., Khan, A. U., Ghayur, M. N., Ali, S. F., & Herzig, J. W. (2006). Antispasmodic effects of Rooibos tea (Aspalathus linearis) is mediated predominantly through K^+- channel activation. *Basic & Clinical Pharmacology & Toxicology, 99*(5), 365–373.

Hurst, S. M., McGhie, T. K., Cooney, J. M., Jensen, D. J., Gould, E. M., Lyall, K. A., & Hurst, R. D. (2010). Blackcurrant proanthocyanidins augment IFN-γ induced suppression of IL-4 stimulated CCL26 secretion in alveolar epithelial cells. *Molecular Nutrition & Food Research, 54*, 159–170.

Iademarco, M. F., Barks, J. L., & Dean, D. C. (1995). Regulation of vascular cell adhesion molecule-1 expression by IL-4 and TNF-α in cultured endothelial cells. *Journal of Clinical Investigation, 95*(1), 264–271.

Iwamura, Ch, Shinoda, K., Yoshimura, M., Watanabe, Y., Obata, A., & Nakayama, T. (2010). Naringenin chalcone suppresses allergic asthma by inhibiting the type-2 function of CD4 T cells. *Allergology International, 59*(1), 67–73.

Joskova, M., Franova, S., Nosalova, G., Pechanova, O., Prisenznakova, L., & Sutovska, M. (2009). A beneficial influence of provinol on the reduction of allergen induced hyperreactivity in guinea pigs. *Bratislavské Lekárske Listy, 110*(8), 454–458.

Jung, Ch. H., Lee, J. Y., Cho, C. H., & Kim, C. J. (2007). Anti-asthmatic action of quercetin and rutin in conscious guinea-pigs challenged with aerosolized ovalbumin. *Archives of Pharmacal Research, 30*(12), 1599–1607.

Kim, M. K., Park, K. S., Yeo, W. S., Choo, H., & Chong, Y. (2009). In vitro solubility, stability and permeability of novel quercetin-amino acid conjugates. *Bioorganic & Medicinal Chemistry, 17*(3), 1164–1171.

Kühnau, J. (1976). The flavonoids: A class of semi-essential food components: Their role in human nutrition. *World Review of Nutrition and Dietetics, 24*, 117–191.

Lebman, D. A., & Coffman, R. L. (1988). Interleukin-4 causes isotype switching to IgE in T cell-stimulated clonal B cell cultures. *The Journal of Experimental Medicine, 168*(3), 853–862.

Lee, M., Kim, S., Kwon, O. K., Oh, S. R., Lee, H. K., & Ahn, K. (2009). Anti-inflammatory and anti-asthmatic effects of resveratrol, a polyphenolic stilbene, in a mouse model of allergic asthma. *International Immunopharmacology, 9*(4), 418–424.

Moon, H., Choi, H. H., Lee, J. Y., Moon, H. J., Sim, S. S., & Kim, C. J. (2008). Quercetin inhalation inhibits the asthmatic responses by exposure to aerosolized-ovalbumin in conscious guinea-pigs. *Archives of Pharmacal Research, 31*(6), 771–778.

Nanua, S., Zick, S. M., Andrade, J. E., Sajjan, U. S., Burgess, J. R., Lukacs, N. W., & Hershenson, M. B. (2006). Quercetin blocks airway epithelial cell chemokine expression. *American Journal of Respiratory Cell and Molecular Biology, 35*(5), 602–610.

Park, S. J., Shin, W. H., Seo, J. W., & Kim, E. J. (2007). Anthocyanins inhibit airway inflammation and hyperresponsiveness in a murine asthma model. *Food and Chemical Toxicology, 45*(8), 1459–1467.

Park, H. J., Lee, C. M., Jung, I. D., Lee, J. S., Jeong, Y. I., Chang, J. H., Chun, S. H., Kim, M. J., Choi, I. W., Ahn, S. C., Shin, Y. K., Yeom, S. R., & Park, Y. M. (2009). Quercetin regulates Th1/Th2 balance in a murine model of asthma. *International Immunopharmacology, 9*(3), 261–267.

Rogerio, A. P., Dora, C. L., Andrade, E. L., Chaves, J. S., Silva, L. F., Lemos-Senna, E., & Calixto, J. B. (2010). Anti-inflammatory effect of quercetin-loaded microemulsion in the airways allergic inflammatory model in mice. *Pharmacological Research, 61*(4), 288–297.

Shi, H. Z., Xiao, C. Q., Zhong, D., Qin, S. M., Liu, Y., Liang, G. R., Xu, H., Chen, Y. Q., Long, X. M., & Xie, Z. F. (1998). Effect of inhaled interleukin-5 on airway hyperreactivity and eosinophilia in asthmatics. *American Journal of Respiratory and Critical Care Medicine, 157*(1), 204–209.

Szentmiklósi, A. J. (2003). Study on cardiovascular and bronchial effects of Flavin-7 in isolated tissue. *Internal Issue of Crystal Institute Ltd.*, pp. 1–79.

Temann, U. A., Geba, G. P., Rankin, J. A., & Flavell, R. A. (1998). Expression of interleukin-9 in the lungs of transgenic mice causes airway inflammation, mast cell hyperplasia, and bronchial hyperresponsiveness. *The Journal of Experimental Medicine, 188*(7), 1307–1320.

Van der Pouw Kraan, T. C., Van der Zee, J. S., Boeije, L. C., De Groot, E. R., Stapel, S. O., & Aarden, L. A. (1998). The role of IL-13 in IgE synthesis by allergic asthma patients. *Clinical and Experimental Immunology, 111*(1), 129–135.

Yang, N. Ch., Lee, C. H., & Song, T. Y. (2010). Evaluation of resveratrol oxidation *in vitro* and the crucial role of bicarbonate ions. *Bioscience, Biotechnology, and Biochemistry, 74*(1), 63–68.

Zenebe, W., Pechánová, O., & Andriantsitohaina, R. (2003). Red wine polyphenols induce vasorelaxation by increased nitric oxide bioactivity. *Physiological Research, 52*(4), 425–432.

Chapter 13
Green Tea and Its Major Polyphenol EGCG Increase the Activity of Oral Peroxidases

Baruch Narotzki, Yishai Levy, Dror Aizenbud, and Abraham Z. Reznick

Abstract Oral peroxidases (OPO) consist mainly of salivary peroxidase and myeloperoxidase and are involved in oral defense mechanisms. Salivary peroxidase is synthesized and secreted by salivary glands, whereas myeloperoxidase is found in polymorphonuclear leukocytes, which migrate into the oral cavity at gingival crevices. Green tea is the world's second most popular drink after water. Polyphenols are the most biologically active group of tea components. The purpose of our study was to elucidate the interaction between green tea & EGCG (Epigallocatechin 3-gallate), its main polyphenol and OPO. In previous studies we have shown that elderly trained people who drink green tea for 3 months, have a higher level of OPO activity compared to non-drinkers. Thus, we decided to extend our project in order to understand the above observations by studying the interaction of green tea and OPO both *in vitro* and *in vivo*. Addition of green tea and black tea infusions (50 μl/ml) and EGCG (50 μM) to saliva, resulted in a sharp rise of OPO activity +280% ($p=0.009$), 54% ($p=0.04$) and 42% ($p=0.009$), respectively. The elevation of OPO activity due to addition of green tea and EGCG was in a dose dependent manner: $r=0.91$ ($p=0.001$) and $r=0.637$ ($p=0.019$), respectively. Also, following green tea infusion mouth rinsing, a rise of OPO activity was observed: +268% ($p=0.159$). These results may be of great clinical importance, as tea consumer's oral epithelium may have better protection against the deleterious effects of hydroxyl radicals, produced by not removed

B. Narotzki • A.Z. Reznick (✉)
Department of Anatomy and Cell Biology, The Bruce Rappaport Faculty of Medicine,
Technion-Israel Institute of Technology, P.O. Box 9649, 31096 Haifa, Israel
e-mail: reznick@tx.technion.ac.il

Y. Levy
The Bruce Rappaport Faculty of Medicine, Technion-Israel Institute of Technology,
P.O. Box 9649, 31096 Haifa, Israel

Department of Medicine D, Rambam Health Care Campus, Haifa, Israel

D. Aizenbud
The Bruce Rappaport Faculty of Medicine, Technion-Israel Institute of Technology,
P.O. Box 9649, 31096 Haifa, Israel

Orthodontic and Craniofacial Center, Graduate School of Dentistry,
Rambam Health Care Campus, Haifa, Israel

M. Pokorski (ed.), *Respiratory Regulation - The Molecular Approach*,
Advances in Experimental Medicine and Biology 756, DOI 10.1007/978-94-007-4549-0_13,

hydrogen peroxides in the presence of metal ions. Higher OPO activity upon green tea drinking may provide an extra protection against oxidative stress in the oral cavity.

Keywords Oral peroxidases • Salivary peroxidase • Myeloperoxidase • Green tea • Epigallocatechin 3-gallate • Polymorphonuclear leukocytes • Saliva

13.1 Introduction

Oral peroxidases (OPO) consist mainly of salivary peroxidase (SPO) and myeloperoxidase (MPO). SPO is secreted from salivary glands, mainly from the parotid gland. MPO is secreted from leukocytes that migrate to inflammatory regions of the oral cavity (Reznick et al. 2003). The OPO has a pivotal role in microorganism's defense; they use hydrogen peroxide (H_2O_2) as an oxidant and use mainly thiocyanate (SCN^-) and Cl^- to produce antimicrobials that are generally more effective than H_2O_2 itself (Ashby 2008). MPO is able to use both SCN^- and Cl^- as substrates, but in saliva SCN^- is used more readily. In contrast, SPO is able to use SCN^- but not Cl^- (Ihalin et al. 2006).

Other then direct peroxidation of H_2O_2 by OPO, $OSCN^-$ the oxidation product of SCN^-, causes an indirect decrease in H_2O_2 by preventing the growth of H_2O_2 producing bacteria. H_2O_2 is harmful to human since it can be converted to OH^- in the presence of transition metals such as Fe & Cu and cause an irreversible damage to DNA, proteins and membrane lipids (Ihalin et al. 2006). On the other hand, $OSCN^-$ is less cytotoxic to human cells but it can oxidize sulphydryl (SH) groups of microbial enzymes and other proteins, which results in leakage of potassium ions, amino acids and peptides, and damage the synthesis of proteins, RNA and DNA (Kussendrager and van Hooijdonk 2000).

Tea (*Camellia sinensis*) is the most popular beverage in the world after water (Wu and Wei 2002). Tea is classified to few categories that differ one from another. Green tea is polyphenols rich tea, while in black tea most of the polyphenols are oxidized to dark polyphenolic components. The main polyphenols that present in the green tea are catechins. The four main catechins are: epigallocatechin 3-gallate (EGCG) that constitutes about 59% from total catechins, epigallocatechin (EGC), epicatechin 3 gallate (ECG) and epicatechin (EC) (McKay and Blumberg 2002).

During our ongoing work on the subject, we have shown that a group of elderly that performed physical exercise, and consumed three cups of green tea and one capsule of vitamin E (400 IU) daily, increased their OPO enzymatic activity more then the control exercising group who did not receive any nutritional intervention. Because of the known green tea polyphenols interaction with Fe that is present in SPO & MPO enzymes active sites (Cabrera et al. 2006), we hypothesized that adding green tea infusion and EGCG to saliva would lead to an increase in OPO enzymatic activity. Therefore, we have initiated *in vitro* and *in vivo* investigations to try to ascertain this increase.

13.2 Methods

The project was approved by an institutional Ethics Committee. Green tea infusion was prepared from tea bags (1.5 g per pack) purchased from Wissotzky Tea Company (Israel). For the preparation of the infusion, tea bags brewed in 100 ml DDW and stirred for 1 h in 85°C. EGCG was purchased from Sigma-Aldrich (St. Louis, USA).

Whole saliva was collected from healthy volunteers under non-stimulatory conditions, as described previously (Nagler et al. 2001). The collected saliva was centrifuged in 2,000 rpm for 10 min to

remove squamous cells and cell debris. Then, the supernatant fluid was collected and analyzed for OPO enzymatic activity.

In the *in vitro* study, the OPO activity of the volunteers was measured before and after the addition of tea infusions or EGCG. In the *in vivo* study, saliva samples were taken after 1 min of mouth rinse with 20 ml DDW. Twenty minutes after producing the saliva sample, each volunteer rinsed his mouth with 20 ml green tea infusion for 1 min and provided another saliva sample.

OPO enzymatic activity was measured according to the NBS-SCN^- method described by Pruitt (Pruitt et al. 1990). In this assay DTNB was reduced to NBS by the addition of β-mercaptoethanol. The disappearance of NBS while reacting with OSCN, the product of OPO, was monitored at 412 nm at pH 5.6. One unit of enzyme activity was defined as the level of enzyme activity needed to cleave one μmol of NBS/min at 22°C, using a molar extinction coefficient of 12,800.

All data are given as means ± SD. One sample *t*-test was used for *in vitro* statistical analysis comparing between treatments (tea or EGCG) and control (PBS). Pearson's bivariate correlation was used to establish green tea and EGCG dose dependent manner. A two sample *t*-test was used for *in vivo* experiments to compare between OPO enzymatic activity after rinsing the mouth with DDW and green tea. Statistical significant was set at $p < 0.005$.

13.3 Results

Saliva was freshly obtained from healthy volunteers and was exposed *in vitro* to different volumes of green tea infusion. The immediate effects of green tea infusions on saliva were considerable increases of OPO enzymatic activity; the increase was 280% with 50 μl/ml green tea infusion compared with control; $p = 0.009$ (Fig. 13.1a). These increases of OPO enzymatic activity were dose-dependent manner; $r = 0.91$, $p = 0.001$ (Fig. 13.1b). An *in vivo* experiment in which healthy volunteers rinsed their mouth with green tea infusion showed similar effects to green tea addition to saliva *in vitro*. Mouth rinsing with tea increased OPO enzymatic activity (268%), but this increase was not statistically significant compared with DDW rinse; $p = 0.159$ (Fig. 13.2a).

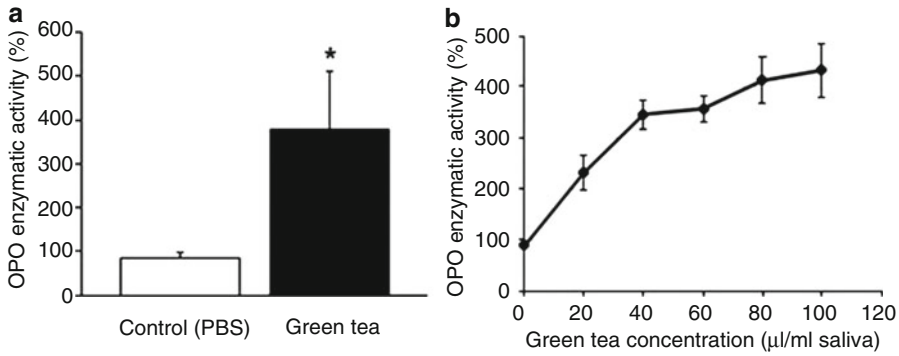

Fig. 13.1 (a) Effect of green tea (*GT*, 50 μl/ml) on oral peroxidases (*OPO*) enzymatic activity. One milliliter of saliva was added with 50 μl GT infusion and OPO enzymatic activity was measured. Data of five different saliva donors are represented as percent of OPO enzymatic activity after GT/PBS addition, compared with before. *Different from control; $p = 0.009$. **(b) Dose dependent effect of GT on OPO enzymatic activity**. Saliva was added with GT (20, 40, 60, 80 and 100 μl/ml saliva) infusion and OPO enzymatic activity was measured. Data of three independent experiments of different saliva donors are represented as percent of OPO enzymatic activity, where PBS added saliva represents concentration zero

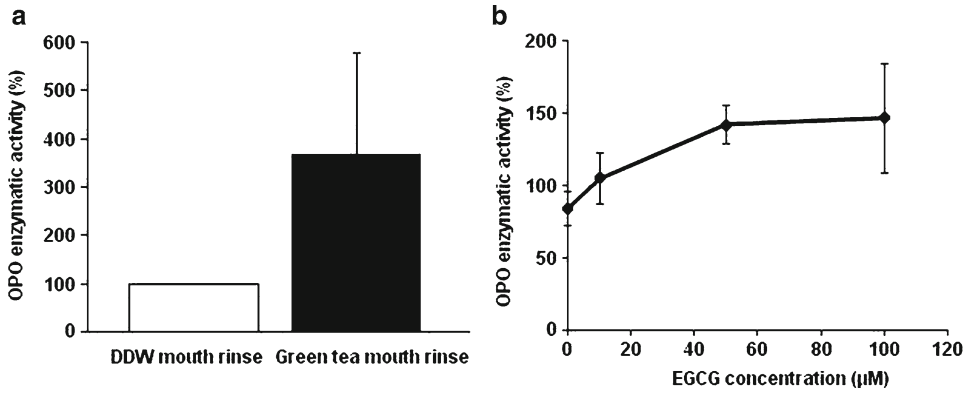

Fig. 13.2 (a) Effect of mouth rinsing with green tea (*GT*) on oral peroxidases (*OPO*) enzymatic activity. OPO enzymatic activity was measured in saliva sample obtained after 1 min of 20 ml DDW mouth rinse and compared with saliva sample from the same donor after 1 min of 20 ml GT infusion mouth rinsing. Data of three different saliva donors are represented as percent of OPO enzymatic activity after GT mouth rinsing, where DDW mouth rinsing represents 100%. **(b) Dose dependent effect of epigallocatechin 3-gallate (*EGCG*) on oral peroxidases (*OPO*) enzymatic activity.** Saliva was added with EGCG (10, 50 and 100 μM saliva) and OPO enzymatic activity was measured. Data are represented as percent of OPO enzymatic activity of four independent experiments of different saliva donors, where PBS added saliva represent concentration zero

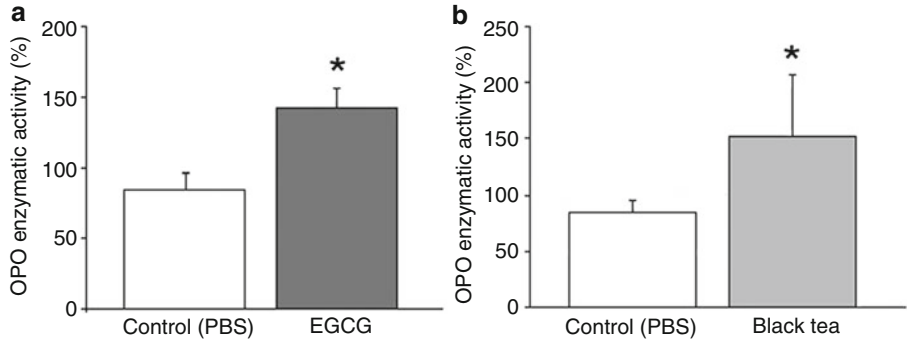

Fig. 13.3 (a) Effect of epigallocatechin 3-gallate (*EGCG*) on oral peroxidases (*OPO*) enzymatic activity. Saliva was added with 50 μM EGCG and OPO enzymatic activity was measured. Data of four different saliva donors are represented as percent of OPO enzymatic activity after EGCG/PBS addition, compared with before. *Difference from control; $p = 0.009$. **(b) Effect of black tea (*BT*, 50 μl/ml) on oral peroxidases (*OPO*) enzymatic activity.** One milliliter of saliva was added with 50 μl BT infusion and OPO enzymatic activity was measured. Data of seven different saliva donors are represented as percent of OPO enzymatic activity after BT/PBS addition, compared with before. *Difference from control; $p = 0.04$

Addition of 20–100 μM EGCG to saliva *in vitro* resulted in dose-dependent increases in OPO enzymatic activity; $r = 0.637$, $p = 0.019$, which were similar to green tea but less expressed (Fig. 13.2b). The increased OPO enzymatic activity with the addition of 50 μM EGCG was modest (42%) compared with green tea but significant compared with control, $p = 0.009$ (Fig. 13.3a). Similar to EGCG, 50 μl/ml black tea infusion had a modest influence in increasing OPO enzymatic activity (54%); this elevation was also significant compared with control; $p = 0.04$ (Fig. 13.3b).

13.4 Discussion

There is increasing evidence that green tea is beneficial to oral health. Tea is effective in decreasing plaque score, preventing dentin wear, as an anti-cariogenic and in prevention of oral cancers (Ooshima et al. 1994; Hamilton-Miller 2001; Chandra Mohan et al. 2005; Magalhaes et al. 2009). The results of this study show that green tea and black tea infusion and EGCG were able to increase the enzymatic activity of OPO. Studies show that SPO is able to degrade mutagenic compounds such as pyrolysates of tryptophan and N-hydroxy-2-acetylaminofluorene and others (Ihalin et al. 2006). The increased OPO enzymatic activity due to tea infusion may account for some of the green tea benefits in oral cancer prevention.

The mechanism by which tea increases OPO enzymatic activity is unclear. We surmised that tea polyphenols have an evident role in that increase. Addition of various concentrations of green tea infusion to saliva resulted in a dose dependent increase in OPO enzymatic activity. This increase was linear in the range of 0–40 μl/ml. Further increase in green tea concentration (60–100 μl/ml) resulted in a more moderate increase in OPO enzymatic activity. This biphasic increase hints on allosteric activation of the enzymes due to saturation of the allosteric sites of SPO or MPO.

Green tea had an outstanding affect in increasing OPO enzymatic activity, both *in vitro* and *in vivo* (almost threefold increase). Thus, we expected that EGCG, the green tea most abundant polyphenol, will have a similar affect. Indeed, addition of EGCG to saliva caused to a dose-dependent increase in OPO enzymatic activity, but the magnitude of the effect was limited compared with green tea, only 42% increase with 50 μM EGCG.

Green and black teas differ from each other mainly in the content of polyphenols or their oxidized derivatives. Therefore, we examined whether a polyphenol poor black tea will be able to amplify OPO enzymatic activity. We discovered that black tea had a reduced influence on OPO, which was about fivefold less than that of green tea. The *in vitro* effects of the different treatments are presented in (Fig. 13.4) Those findings support the notion that tea polyphenols are responsible for the increased enzymatic activity. However, it seems that EGCG is not the only polyphenol that increase OPO enzymatic activity. Further research is needed in order to determine which of the tea polyphenols has the predominant effect on OPO enzymes.

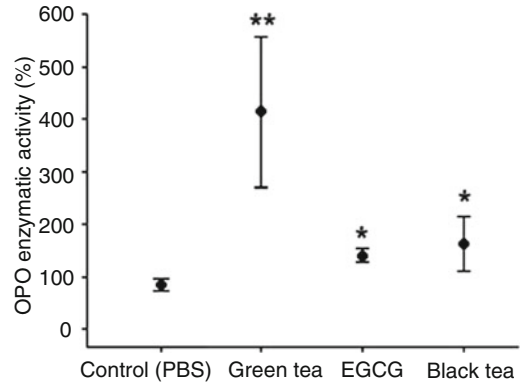

Fig. 13.4 Effects of green tea (GT, 50 μl/ml), black tea (BT, 50 μl/ml) and EGCG (50 μM) on oral peroxidases (OPO) enzymatic activity. One milliliter of saliva was added with tea infusion or EGCG and OPO enzymatic activity was measured. Data of three (PBS), five (GT), four (EGCG), and seven (BT) different saliva donors are represented as percent of OPO enzymatic activity after Tea/EGCG/PBS addition, compared with before. *Difference from control, $p<0.05$ and **difference from EGCG and BT, $p<0.01$

Acknowledgments Supported by the Krol foundation of Barnegat NJ, USA, Rappaport Institute for Research and Myers-JDC-Brookdale Institute of Gerontology and Human Development and Eshel-the Association for the Planning and Development of Services for the Aged in Israel.

Conflicts of interest: The authors declare no conflicts of interest in relation to this article.

References

Ashby, M. T. (2008). Inorganic chemistry of defensive peroxidases in the human oral cavity. *Journal of Dental Research, 87*, 900–914.

Cabrera, C., Artacho, R., & Gimenez, R. (2006). Beneficial effects of green tea-a review. *Journal of the American College of Nutrition, 25*, 79–99.

Chandra Mohan, K. V., Hara, Y., Abraham, S. K., & Nagini, S. (2005). Comparative evaluation of the chemopreventive efficacy of green and black tea polyphenols in the hamster buccal pouch carcinogenesis model. *Clinical Biochemistry, 38*, 879–886.

Hamilton-Miller, J. M. (2001). Anti-cariogenic properties of tea (*Camellia sinensis*). *Journal of Medical Microbiology, 50*, 299–302.

Ihalin, R., Loimaranta, V., & Tenovuo, J. (2006). Origin, structure, and biological activities of peroxidases in human saliva. *Archives of Biochemistry and Biophysics, 445*, 261–268.

Kussendrager, K. D., & Van Hooijdonk, A. C. (2000). Lactoperoxidase: Physico-chemical properties, occurrence, mechanism of action and applications. *British Journal of Nutrition, 84*(Suppl 1), S19–25.

Magalhaes, A. C., Wiegand, A., Rios, D., Hannas, A., Attin, T., & Buzalaf, M. A. (2009). Chlorhexidine and green tea extract reduce dentin erosion and abrasion in situ. *Journal of Dentistry, 37*, 994–998.

Mckay, D. L., & Blumberg, J. B. (2002). The role of tea in human health: An update. *Journal of the American College of Nutrition, 21*, 1–13.

Nagler, R. M., Klein, I., & Reznick, A. Z. (2001). The interaction between saliva and cigarette smoke and its devastating biological effects as related to oral cancer. *Harefuah, 140*, 614–618.

Ooshima, T., Minami, T., Aono, W., Tamura, Y., & Hamada, S. (1994). Reduction of dental plaque deposition in humans by oolong tea extract. *Caries Research, 28*, 146–149.

Pruitt, K. M., Kamau, D. N., Miller, K., Mansson-Rahemtulla, B., & Rahemtulla, F. (1990). Quantitative, standardized assays for determining the concentrations of bovine lactoperoxidase, human salivary peroxidase, and human myeloperoxidase. *Analytical Biochemistry, 191*, 278–286.

Reznick, A. Z., Klein, I., Eiserich, J. P., Cross, C. E., & Nagler, R. M. (2003). Inhibition of oral peroxidase activity by cigarette smoke: In vivo and in vitro studies. *Free Radical Biology & Medicine, 34*, 377–384.

Wu, C. D., & Wei, G. X. (2002). Tea as a functional food for oral health. *Nutrition, 18*, 443–444.

Chapter 14
Mangiferin and Its Traversal into the Brain

Dominika Zajac, Agnieszka Stasinska, Rene Delgado, and Mieczyslaw Pokorski

Abstract Mangiferin, the main active substance of the mango tree bark (*Mangifera indica* L.), is known for its use in natural medicine, not only as a health enhancing panacea or adjunct therapeutic, but also for brain functions improvement. In this context, we deemed it worthwhile to establish whether mangiferin could traverse into the brain after systemic administration; an essential piece of information for the rational use of a compound as a neurotherapeutic, remaining so far inconclusive regarding mangiferin. We addressed this issue by studying recoverability of mangiferin in membrane and cytosolic fractions of rat brain homogenates after its intraperitoneal administration in a dose of 300 mg/kg. We used three preparations of mangiferin of decreasing purity to find out whether its penetration to the brain could have to do with the possible presence of contaminants. The qualitative methods of thin-layered-chromatography and UV/VIS spectrophotometry were employed in this study. The results were clearly negative, as we failed to trace mangiferin in the brain fractions with either method, which makes it unlikely that the compound traverse the blood-brain barrier after being systemically administered. We conclude that it is improbable that mangiferin could act *via* direct interaction with central neural components, but rather has peripheral, target specific functions which could be secondarily reflected in brain metabolism.

Keywords Blood-brain barrier • Brain homogenate • Mangiferin • Polyphenols • Natural medicine

14.1 Introduction

Recently, there is a remarkable interest in compounds extracted from medicinal plants, particularly those that demonstrate antioxidant properties, which are increasingly used in complimentary medicine. Mangiferin, a glucosyl xanthone, extracted from the mango tree (*Mangifera indica* L.) is one

D. Zajac • A. Stasinska • M. Pokorski (✉)
Department of Respiratory Research, Medical Research Center, Polish Academy of Sciences,
Pawinskiego 5, 02-106 Warsaw, Poland
e-mail: m_pokorski@hotmail.com

R. Delgado
Laboratory of Molecular Pharmacology, Drug Research and Development Center (CIDEM),
Havana, Cuba

M. Pokorski (ed.), *Respiratory Regulation - The Molecular Approach*,
Advances in Experimental Medicine and Biology 756, DOI 10.1007/978-94-007-4549-0_14,

such bioactive compound that attracts attention due to a spate of antioxidant (Leiro et al. 2004; Muruganandan et al. 2005a; Pardo-Andreu et al. 2006a, b), antiinflammatory (Garrido et al. 2004), neuroprotective (Martinez Sánchez et al. 2001; Gottlieb et al. 2006), and antidiabetic (Miura et al. 2001; Muruganandan et al. 2005b) actions, reported in both *in vivo* and *in vitro* experimental studies. In addition, the mango plant has been used in the traditional Indian medicine for mood and cognition improvement (Chopra et al. 1956). The latter is suggestive of a central effect of systemically administered mangiferin. However, only one study to-date has directly addressed the issue of whether mangiferin can penetrate into the brain after systemic administration (Lai et al. 2003). This study demonstrates that mangiferin is undetectable in brain dialysates after intravenous administration. The authors of a couple of other studies surmise on indirect evidence that mangiferin may be available for brain tissue after its chronic oral or intraperitoneal administration, as it protected against neuronal cell death induced by transient ischemic insults or by glutamate in neuronal cortical cultures (Martinez Sánchez et al. 2001; Gottlieb et al. 2006); the effects attributed to mangiferin's antioxidant properties. Mangiferin, administered intraperitoneally, also inhibits monoamino oxidase activity (MAO), which has been observed at the functional level as potentiation of analgesia or reversal of reserpine-induced sedation in the rat (Bhattacharya et al. 1972). Such central-like effects may, however, be a reflection of mangiferin's peripheral, e.g., vascular or neurotransmitter action (Beltrán et al. 2004) or be mediated by mangiferin's O-methylated metabolites peripherally formed (Lai et al. 2003).

The present study was designed on the premise that further advances in mangiferin neuropharmacology require the essential piece of information on the ability of mangiferin to cross the blood-brain barrier, which has not yet been tested adequately. Therefore, we set out to determine whether mangiferin could be recovered from the brain after its systemic administration in the rat. A second aim was to determine whether the equivocal results on mangiferin penetration into the brain above outlined could have to do with the varying purity of mangiferin preparations employed. To this end we investigated the three most commonly studied mangiferin preparations of decreasing purity, from absolute to crude (see details below). The qualitative techniques of thin-layered chromatography and spectrophotometry were used in this study. Overall, the study failed to provide evidence for the mangiferin passage into the brain. Part of this work has been reported in the abstract form elsewhere (Pokorski et al. 2010).

14.2 Methods

14.2.1 Animals

The study was performed in accord with the Polish Animal Protection Bill of August 21, 1997 and with the NIH Guide for Care and Use of Laboratory Animals and was approved by a local Ethics Committee. Eight adult, male Wistar rats weighing 260–320 g were used for the study. The animals were kept in a ventilated room on an artificial 12/12 h light/dark cycle at 21°C, with free access to food and water until use.

14.2.2 Mangiferin Preparations and Protocol

The following three preparations of mangiferin, all aqueous extracts from the stem bark of Mango tree, were used: commercially available mangiferin compound of 100% analytical grade purity obtained from Sigma-Aldrich (St. Louis, MO) used in three animals, mangiferin extract of ~90% purity (three animals), and a preparation under the brand name Vimang®, a mixture of polyphenols,

flavonoids, terpenoids, steroids, fatty acids, and microelements, clinically used in the Caribbean region as a panacean medicine in which mangiferin makes up a major about 20% fraction of ingredients (Capote et al. 1998; Sánchez et al. 2000b; Núñez-Sellés et al. 2002) (two animals). Vimang® is a preparation which has been an extensively tested, found nontoxic, and showing a significant free radical scavenging activity (Pardo-Andreu et al. 2006a, b), particularly for hydroxyl radicals (Sánchez et al. 2000a), and a protective effect against rat brain phospholipid peroxidation (Cholbi et al. 1991). The latter two compounds were a generous gift from the Center of Pharmaceutical Chemistry in Havana, Cuba, where they were extracted and prepared.

Each preparation of mangiferin was administered to respective animals intraperitoneally in a single dose of 300 mg/kg dissolved in 300 µl of DMSO. In one case, the 90% mangiferin extract was administered in a dose of 100 mg/kg dissolved and injected as above outlined. One hour after injection, the animals were anesthetized with 50 mg/kg sodium pentobarbital and sacrificed by perfusion with ice-cold 0.9% NaCl through the left heart. Then, the brain was rapidly enucleated from the skull, homogenized, and membrane and cytosolic fractions were prepared according to the method of Xu et al. (1993).

14.2.3 Brain Homogenates

Brain tissue was homogenized in the isolation buffer containing 2.5 mM $MgCl_2 \times 6\ H_2O$, 1 mM $KHCO_3$, 2 mM Tris × HCl pH 7.4, 3 mM EDTA, 100 µM benzamidine, and 100 µM PMSF. All reagents were of analytical grade and were purchased from Sigma-Aldrich (St. Louis, MO). The sample was centrifuged at 2,000×*g* for 10 min at 4°C. The supernatant was collected and re-centrifuged at 40,000×*g* at 10°C for 18 min (L7 Ultracentrifuge; Beckman Instruments, Palo Alto, CA). The pellet, representing the membrane fraction, was washed two times with the isolation buffer, whereas the supernatant representing the cytosolic fraction was collected. The isolation buffer was added to membrane fraction to bring its volume up to 1 ml. Then, the extraction solution, consisting of chloroform:methanol:water (4:3:2 v/v) in a volume of 1.125 ml, was added to either fraction to extract mangiferin. Following centrifugation at 4,000×*g* for 10 min at 4°C, the upper aqueous and lower organic phases were collected and dried under nitrogen. The residues were dissolved in 0.5 ml methanol and were then analyzed with both thin-layered chromatography (TLC) and spectrophotometry (Cintra 10e UV/VIS Spectrophotometer equipped with Spectral 1.70 software; GBC Scientific Equipment Pty Ltd., Victoria, Australia). For TLC, samples of either phase from both cytosolic and membrane extracts from each brain specimen were plated in duplicate in the volumes of 10 and 20 µl on standard silica gel plates (Merck, KGaA, Darmstadt, Germany). Mangiferin standard was plated as 5 µg in 10 µl. As an additional control, crude, uncentrifuged brain homogenate was also chromatographed. The mobile phase consisted of a mixture of n-butanol:acetic acid:water 4:1:2 (v/v). The detection was performed visually under visible and ultraviolet lights. The bands were developed with iodine vapors, photographed, and digitalized. Solutions of cytosolic and membrane extracts, as outlined above, also were used for the spectrophotometric analyses, with methanol as a control solution. Here all individual samples were studied in triplicate.

14.3 Results

Figure 14.1 demonstrates the results of TLC screening and verification by standards of mangiferin compounds in rat brain homogenates. The homogenates were analyzed 1 h after i.p. injection of mango tree bark extracts of the 90% purity mangiferin and the less-purity Vimang®, either in a dose of 300 mg/kg.

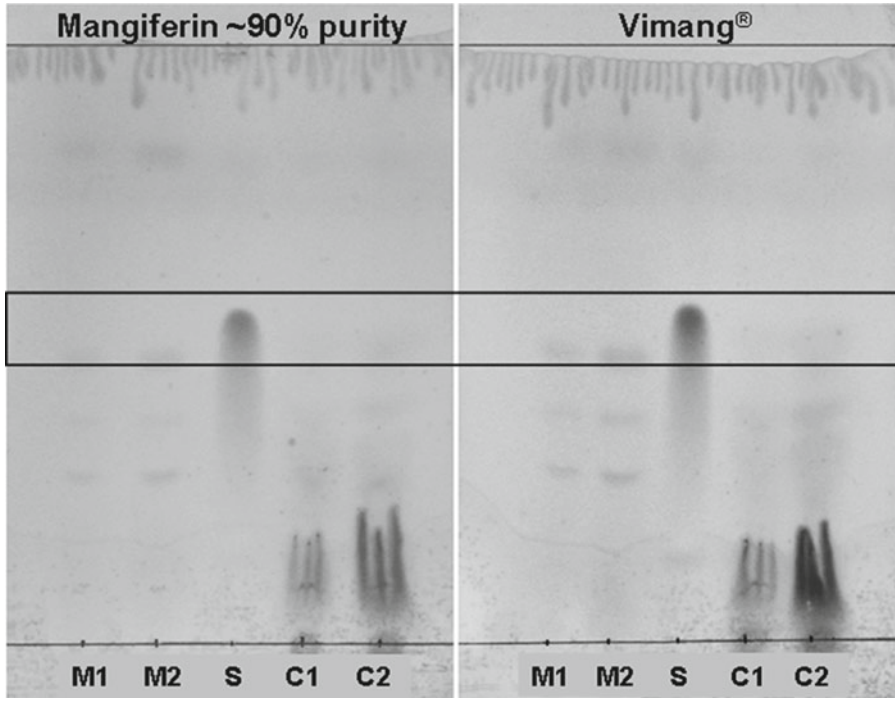

Fig. 14.1 TLC plates of rat brain homogenates 1 h after administration of two mangiferin preparations: 90% purity and crude ~20% purity (Vimang®) in a dose 300 mg/kg. i.p. M – membrane and C – cytosolic fractions in double concentrations marked as 1 = 10 μl and 2 = 20 μl taken from 0.5 ml methanol solution (see Methods for details), S – mangiferin standard (100% purity) – 10 μl from 0.5 mg/ml methanol solution. Chromatographic conditions: stationary phase – silica gel 60; mobile phase – n-butanol:acetic acid:water 4:1:2 (v/v); detection – iodine vapors. At the level of the mangiferin standard outlined by the rectangular frames no traceable spots of mangiferin presence in biological samples could be visible

The aqueous phases of brain membrane (M) and cytosolic (C) fractions were plated in double volumes alongside the mangiferin standard (S). The R_f factor corresponding to the standard band was 0.54. There were no traceable bands at the level of the mangiferin standard at either concentration of brain samples from mangiferin-treated rats in both cytosolic and membrane fractions. Likewise, a negative result concerning the visible presence of mangiferin-related TLC bands also was obtained in regard to the third preparation studied, mangiferin of analytical grade purity. Furthermore, mangiferin could not be recovered from the organic phases obtained from both fractions nor could it be traced in the crude, uncentrifuged brain homogenate taken as an additional basic control (data not shown).

We also sought to determine spectrophotometrically mangiferin's presence in the brain after its intraperitoneal administration. The results of this analysis for the 90% purity mangiferin extract are displayed in Fig. 14.2. Mangiferin standard shows a characteristic spectrum consisting of four peaks at 241, 258, 316, and 363 nm, which is the same in both membrane and cytosolic fractions. The spectra obtained from brain samples of the mangiferin-treated rats were identical to those obtained from the background brain samples of the untreated rats in either membrane (Fig. 14.2a) or cytosolic (Fig. 14.2b) fraction; the latter fraction showing a single peak at 252 nm in both treated and untreated rats and both fractions' spectra bore no resemblance to those of the standard. Likewise, there were no differences noted in the shape of spectra between the brain samples from mangiferin-treated and untreated rats regarding the other two preparations of mangiferin investigated (100 and 20% purity – Vimang®); with either type of spectrum being strikingly different from that of mangiferin standard (data not shown).

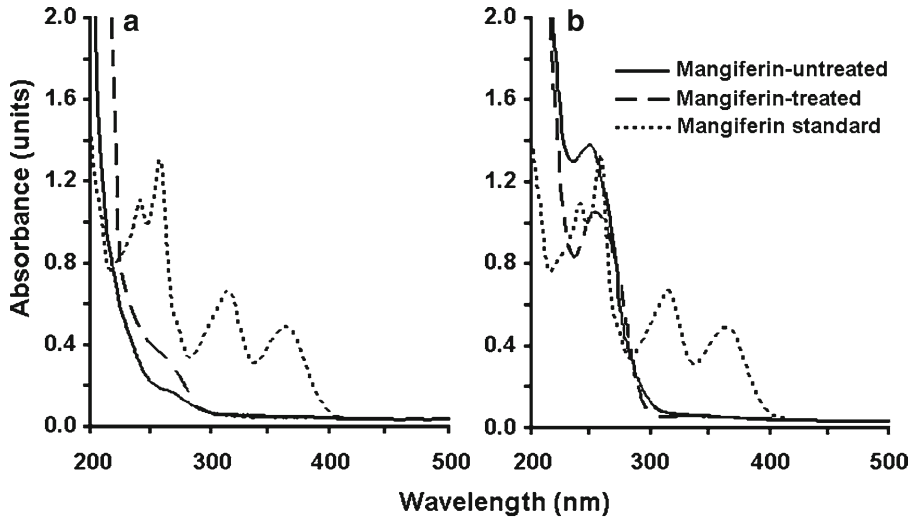

Fig. 14.2 Experimental absorption UV/VIS spectra obtained from brain homogenates of untreated and mangiferin (90% purity – 300 mg/kg. i.p)-treated rats. (**a**) – membrane and (**b**) – cytosolic fractions

14.4 Discussion

Medicinal interest in mangiferin, a compound derived from the mango tree bark, has increased appreciably of late. This interest is reflected in the increasing number of studies being recently performed on aspects of therapeutic and health-associated advantages of mangiferin a diverse range of diseases (Martinez Sánchez et al. 2001; Miura et al. 2001; Garrido et al. 2004; Leiro et al. 2004, Muruganandan et al. 2005a, b; Gottlieb et al. 2006; Pardo-Andreu et al. 2006a, b). Some of the mangiferin's health ameliorative properties also involve the pathological conditions of the central nervous system (Bhattacharya et al. 1972), suggesting that mangiferin could be a potential neurotherapeutic. To this end, in the present study, we deemed it worthwhile to investigate whether mangiferin could traverse into the brain after systemic administration; an issue which has been unresolved as of yet. The results of the study were clearly negative. We failed to demonstrate the recoverability of mangiferin in brain homogenates after its systemic administration in the rat. Therefore, it seems improbable that mangiferin could act *via* direct interaction with central neural components. We also demonstrate that the failure of mangiferin passage into the brain is independent of the substance purity, but is likely due to structural impediment of the molecule, as even the total freedom of contaminants did not make it penetrable.

In this study we used the qualitative methods of TLC and UV/VIS spectrophotometry to screen for mangiferin in membrane and cytosolic fractions of brain homogenates. Although we did not detect the presence of mangiferin in brain tissue, we cannot preclude its passage into the brain in subthreshold amounts for detection. It seems dubious, however, that minute amounts of mangiferin could exert dedicated central effects as reported in some studies (Bhattacharya et al. 1972). The detection methods, as gross as they may be judged, seem sound since the wavelengths of the four-peak mangiferin absorption spectra we obtained are close to those reported by Gómez-Zaleta et al. (2006) at a slightly different pH of 8.0. Also, similar methodological procedures are sufficient to detect neuroactive substances in brain tissue homogenates of even larger than mangiferin's molecular mass, administered in like manner (Zajac et al. 2006). Thus, we reckon mangiferin truly fails to pass into the brain in biologically relevant amounts.

The blood-brain barrier frequently obstructs the passage of neurotherapeutics into the brain, in particular when the molecule is relatively big, of high polarity, and has a highly asymmetric structure,

all of which regard mangiferin, which is one of the most polar xanthones of a molecular weight of 422 Da. In addition, mangiferin is not lipid soluble and is a glucosylated compound, which may further impact its permeability through the barrier. Although the mangiferin molecule is still below the upper limit of diffusible size, it is known that the larger the molecule the more difficult diffusion would be, regardless of other characteristics. Sugars also, for instance glucose (Simpson et al. 1999), require their own highly specific transport proteins expressed at the barrier for the carrier-mediated transport into the brain. Such a carrier may not be available for mangiferin which is foreign to the brain tissue. The reason why mangiferin molecule is turned away at the blood-brain barrier is thus not readily explainable and should be investigated with alternative study designs.

That mangiferin does not penetrate into the brain does not necessarily undervalues its potential clinical usefulness. The proven functions of mangiferin are those relating it to antioxidant capacity in serum, stymieing lipid peroxidation in vascular endothelial cells, immunomodulation of white blood cells, and pancreatic homeostasis as target tissues (Miura et al. 2001; Leiro et al. 2004; Muruganandan et al. 2005a, b; Pardo-Andreu et al. 2006a, b). These peripheral functions, along with MAO inhibition (Bhattacharya et al. 1972), which should lead to enhanced availability of catecholamines in the periphery, may cogently be reflected in secondary modifications in brain metabolism and function.

In conclusion, we believe we have shown that mangiferin, a bioactive compound derived from the mango tree bark, having a good medical record, particularly in natural medicine, does not traverse the blood-brain barrier after being systemically administered. Nevertheless the compound has got the known peripheral, target specific functions. Despite recent advances in the study of mangiferin pharmacology, the central neural correlates of its action remain largely unknown.

Acknowledgments This research was supported by the statutory budget of the Medical Research Center, Polish Academy of Sciences in Warsaw.

Conflicts of interest: The authors report no conflicts of interest in relation to this article.

References

Beltrán, A. E., Alvarez, Y., Xavier, F. E., Hernanz, R., Rodriguez, J., Núñez, A. J., Alonso, M. J., & Salaices, M. (2004). Vascular effects of the *Mangifera indica L.* extract (Vimang®). *European Journal of Pharmacology, 499*, 297–305.

Bhattacharya, S. K., Sanyal, A. K., & Ghosal, S. (1972). Monoamine oxidase-inhibiting activity of mangiferin isolated from *Canscora decussata*. *Naturwissenschaften, 59*, 651.

Capote, R., Guardado, I., Novoa, H., Agüero, J., Paneque, A., & Sordo, L. (1998). Chemical-analytical characterization of aqueous extract of *Mangifera indica* L. *Revista Cubana de Química, 10*, 111–112.

Cholbi, M. R., Paya, M., & Alcaraz, M. J. (1991). Inhibitory effect of phenolic compounds on CCL4-induced microsomal lipid peroxidation. *Experientia, 472*, 195–199.

Chopra, R. N., Nayar, S. L., & Chopra, I. C. (1956). *Glossary of Indian medicinal plants* (p. 49). New Delhi: CSIR.

Garrido, G., González, D., Lemus, Y., Garcia, D., Lodeiro, L., Quintero, G., Delporte, C., Alberto, J., Núñez-Sellés, A. J., & Delgado, R. (2004). In vivo and in vitro anti-inflammatory activity of *Mangifera indica* L. extract (Vimang®). *Pharmacological Research, 50*, 143–149.

Gómez-Zaleta, B., Ramírez-Silva, M. T., Gutierréz, A., González-Vergara, E., Güizado-Rodríguez, M., & Rojas-Hernández, A. (2006). UV/VIS, 1H, and 13C NMR spectroscopic studies to determine mangiferin p*K*a values. *Spectrochimica Acta Part A: Molecular and Biomolecular Spectroscopy, 64*, 1002–1009.

Gottlieb, M., Leal-Campanario, R., Campos-Esparza, M. R., Sánchez-Gómez, M. V., Alberdi, E., Arranz, A., Delgado-Garcıa, J. M., Gruart, A., & Matute, C. (2006). Neuroprotection by two polyphenols following excitotoxicity and experimental ischemia. *Neurobiology of Disease, 23*, 374–386.

Lai, L., Lin, L.-C., Lin, J.-H., & Tsai, T.-H. (2003). Pharmacokinetic study of free mangiferin in rats by microdialysis coupled with microbore high-performance liquid chromatography and tandem mass spectrometry. *Journal of Chromatography. A, 987*, 367–374.

Leiro, J., Arranz, J. A., Yanez, M., Ubeira, F. M., Sanmartin, M. L., & Orallo, F. (2004). Expression profiles of genes involved in the mouse nuclear factor-kappa B signal transduction pathway are modulated by mangiferin. *International Journal of Immunopharmacology, 4*, 763–778.

Martinez Sánchez, G., Candelario-Jalil, E., Giuliani, A., León, O. S., Sam, S., Delgado, R., & Núñez-Sellés, A. J. (2001). *Mangifera indica* L. (QF808) reduces ischaemia induced neuronal loss and oxidative damage in the gerbil brain. *Free Radical Research, 35*, 465–473.

Miura, T., Ichiki, H., Hashimoto, I., Iwamoto, N., Kato, M., Kubo, M., Ishihara, E., Komatsu, Y., Okada, M., Ishida, T., & Tanigawa, K. (2001). Antidiabetic activity of a xanthone compound, mangiferin. *Phytomedicine, 8*, 85–87.

Muruganandan, S., Lal, J., & Gupta, P. K. (2005a). Immunotherapeutic effects of mangiferin mediated by the inhibition of oxidative stress to activated lymphocytes, neutrophils and macrophages. *Toxicology, 215*, 57–68.

Muruganandan, S., Srinivasan, K., Gupta, S., Gupta, P. K., & Lal, J. (2005b). Effect of mangiferin on hyperglycemia and atherogenicity in streptozotocin diabetic rats. *Journal of Ethnopharmacology, 97*, 497–501.

Núñez-Sellés, A., Vélez-Castro, H., Agüero-Agüero, J., González-González, J., Naddeo, F., De Simone, F., & Rastrelli, L. (2002). Isolation and quantitative analysis of phenolic antioxidants, free sugars, fatty acids and polyols from mango (*Mangifera indica* L.) stem bark aqueous decoction used in Cuba as nutritional supplement. *Journal of Agricultural and Food Chemistry, 50*, 762–766.

Pardo-Andreu, G. L., Delgado, R., Núñez-Sellés, A. J., & Vercesi, A. E. (2006a). Vimang® seems to act as an antioxidant by complexing iron ions, rendering them inactive or poorly active in the Fenton reaction. *Phytotherapy Research, 20*, 120–124.

Pardo-Andreu, G., Philip, S., Riaño, A., Sánchez, C., Viada, C., Núñez-Sellés, A. J., & Delgado, R. (2006b). *Mangifera indica* L. Vimang® protection against serum oxidative stress in elderly humans. *Archives of Medical Research, 37*, 158–164.

Pokorski, M., Delgado Hernandez, R., & Rekawek, A. (2010). Mangiferin: A neuroactive polyphenol. 4th International Congress of Pharmacology and Therapeutics; Havana, Cuba. *Vaccine vial Monitors,* 19(Suppl 2):161.

Sánchez, G. M., Delgado, R., Núñez-Sellés, A. J., Davison, G. P., Garrido, G., & León, O. S. (2000a). Evaluation of the in vitro antioxidant activity of *Mangifera indica* L. extract (Vimang®). *Phytotherapy Research, 14*, 424–427.

Sánchez, G. M., Re, L., Giuliani, A., Núñez-Sellés, A. J., Davison, G. P., & León-Fernández, O. S. (2000b). Protective effects of *Mangifera indica* L. extract, mangiferin and selected antioxidants against TPA-induced biomolecules oxidation and peritoneal macrophage activation in mice. *Pharmacological Research, 42*, 565–573.

Simpson, I. A., Appel, N. M., Hokari, M., Oki, J., Holman, G. D., Maher, F., Koehler-Stec, E. M., Vannucci, S. J., & Smith, Q. R. (1999). Blood-brain barrier glucose transporter: Effects of hypo- and hyperglycemia revisited. *Journal of Neurochemistry, 72*, 238–247.

Xu, X., De Pergola, G., Eriksson, P. S., Fu, L., Carlsson, B., Yang, S., Edén, S., & Björntorp, P. (1993). Postreceptor events involved in the up-regulation of beta-adrenergic receptor mediated lipolysis by testosterone in rat white adipocytes. *Endocrinology, 132*, 1651–1657.

Zajac, D., Matysiak, Z., Czarnocki, Z., & Pokorski, M. (2006). Membrane association of *N*-oleoyl-dopamine in rat brain. *Journal of Physiology and Pharmacology, 57*(Suppl 4), 403–408.

Chapter 15
Plasma Selectins in Patients with Obstructive Sleep Apnea

S. Cofta, E. Wysocka, S. Dziegielewska-Gesiak, S. Michalak, T. Piorunek, H. Batura-Gabryel, and L. Torlinski

Abstract Obstructive sleep apnea (OSA) is an independent risk factor in the pathogenesis of cardiovascular diseases. The aim of the study was to analyze three specific adhesion molecules involved in the development of an atherosclerotic plaque: E-selectin (endothelium), L-selectin (leukocyte surface), and P-selectin (from platelet), circulating in plasma in patients at different OSA severity. Eighty non-smoking male Caucasians aged 30–64 were enrolled into the study after clinical, biochemical, and polysomnographic examinations. The patients were divided into four groups based on the results of apnea/hypopnea index (AHI): OSA-0 with AHI 0–4.9 (n = 20), OSA-1 with AHI 5–15 (n = 21), OSA-2 with AHI 16–30 (n = 18), OSA-3 with AHI ≥ 31 (n = 21). Complete blood count, oral glucose tolerance test, fasting lipid profile, C-reactive protein and insulin, and plasma concentrations of soluble E-selectin, P-selectin and L-selectin were measured. We found a progressive increase in the concentrations of all three selectins with the severity of OSA. In conclusion, the level of plasma adhesion molecules may be indicative of OSA severity and may contribute to cardiovascular sequelae.

Keywords Adhesive molecules • Atherosclerosis • Cardiovascular disease • Selectins • Sleep apnea syndrome

15.1 Introduction

Obstructive sleep apnea (OSA) is a common disorder characterized by the presence of recurrent episodes of upper airway obstruction during a sleep, followed by blood oxygen desaturations and sleep fragmentation. It affects approximately 2–4% of adults, particularly middle-aged obese men,

S. Cofta (✉) • T. Piorunek • H. Batura-Gabryel
Department of Pulmonology, Allergology and Respiratory Oncology, Poznan University of Medical Sciences, 84 Szamarzewskiego St, 60-569 Poznan, Poland
e-mail: s.cofta@gmail.com

E. Wysocka • S. Dziegielewska-Gesiak • L. Torlinski
Department of Clinical Biochemistry and Laboratory Medicine, Poznan University of Medical Sciences, 84 Szamarzewskiego St, 60-569 Poznan, Poland

S. Michalak
Department of Neurochemistry and Neuropathology, Poznan University of Medical Sciences, 84 Szamarzewskiego St, 60-569 Poznan, Poland

M. Pokorski (ed.), *Respiratory Regulation - The Molecular Approach*,
Advances in Experimental Medicine and Biology 756, DOI 10.1007/978-94-007-4549-0_15,

although its presence in women is also recognized. The prevalence of OSA in patients with the cardiovascular diseases is high. It is diagnosed in about 50% of patients with hypertension, 30% of those with acute coronary syndrome, 25% of patients with congestive heart failure, and around 60% of patients with stroke (Parati et al. 2002; Peker et al. 1999).

In the past decade, the relationship between OSA and cardiovascular risk factors has been a subject of many scientific discussions (Peker et al. 2002; Dyugovskaya et al. 2005; Gjørup et al. 2007). Endothelial dysfunction is an important factor in the pathogenesis of atherosclerosis and it is one of the linking mechanisms between OSA and cardiovascular diseases. Systemic inflammation, oxidative stress, and sympathetic activation may all contribute to the development of endothelial dysfunction. One of the earliest stages in the development of an atherosclerotic plaque is the migration of leukocytes into the subendothelial layer (Bobryshev 2006). Specific adhesion molecules, like selectins (L, P, E) and their ligands, are involved in the development of an atherosclerotic plaque (Blankerberg et al. 2003). L-selectin, found on the surface of leukocytes, is a major contributor to leukocyte rolling along the endothelium and, together with P-selectin and E-selectin, is responsible for leukocyte adhesion and migration (Eriksson et al. 2001). P-selectin is expressed on activated platelets and endothelium and is involved in leukocyte rolling and attachment as well. This molecule may initiate and increase an atherosclerosis (Ridker et al. 2001). The plasma concentrations of P-selectin rise in patients with hypertension, dyslipidemia, and dysglycemia (Lim et al. 2004). E-selectin, which is specific for the endothelium, is considered to facilitate rolling and activation of leukocytes (Biondi-Zoccai et al. 2003).

The aim of this study was to analyze plasma levels of the three soluble selectins: E-selectin, L-selectin and P-selectin, in patients at different stages of OSA.

15.2 Methods

15.2.1 Study Groups

The study protocol was approved by the Bioethical Committee of the University of Medical Sciences in Poznan, Poland and the participants of the study gave informed consent.

Non-smoking Caucasian males aged 30–64 suspected of OSA, without any acute or chronic disease and using no medication, were screened by The Epworth Sleepiness Scale. After physical examination, and biochemical and somnographic procedures, patients with a body mass index (BMI) 25.0–40.0 kg/m^2 were included into the study. A 75.0 g-oral glucose tolerance test (OGTT) was performed according to WHO recommendations and newly diagnosed type 2 diabetics (t2DM) were excluded from the study.

The patients were divided into four groups based on the results of the apnea/hypopnea index (AHI): OSA-0 (n = 20) with AHI<5 (without evident breathing disorder); OSA-1 (n = 21) with AHI = 5–15 (with mild obstructive disorder); OSA-2 (n = 18) with AHI = 16–30 (with moderate obstructive disorder); OSA-3 (n = 21) with AHI ≥ 31 (with severe obstructive disorder), including subjects with comparable metabolic characteristics.

15.2.2 Measurements

The OSA-suspected subjects were evaluated in a sleep laboratory of the Department of Pulmonology, Allergology and Respiratory Oncology of the University of Medical Sciences in Poznan, Poland, and they underwent a full-night monitoring by a polysomnographic system EMBLA S4000 (Remlogic,

EMBLA Co., Denver, CO). Airflow was monitored by a nasal flow canula. Abdominal and thoracic movements were assessed by respiratory inductive plethysmography. Night recordings of hemoglobin oxygen saturation were obtained by finger pulsoximetry. Snoring sounds, heart rate, and sleep positions were also recorded. Apnea was defined as a cessation of airflow lasting more than 10 s, and hypopnea was defined as a discrete reduction (two thirds) of airflow and/or abdominal ribcage movements lasting more than 10 s and associated with a decrease of more than 4% in oxygen saturation.

All subjects underwent complete physical examination, including the measurement of systolic (SBP) and diastolic (DBP) blood pressures, and the calculation of BMI in kg/m^2. Blood samples were collected from ulnar vein twice: fasting (0 min) and at 120 min of OGTT. Fasting blood samples were used to determine complete blood count (Cell-Dyn Ruby, Abbott Laboratories, Abbott Park, IL). The concentrations of plasma glucose during OGTT, fasting lipid profile: total cholesterol (TC), triglycerides (TG), HDL-cholesterol, LDL-cholesterol, and serum high sensitivity C-reactive protein (hsCRP) were measured (Dimension Xpand Plus Systems, Siemens Healthcare Diagnostics, Deerfield, IL).

Fasting serum samples were stored at −25°C until the concentration of insulin was determined by ELISA method (BioSource, Nivelles, Belgium) on microplater reader Sunrise™ (Tecan Group Ltd, Männedorf, Switzerland), with a sensitivity of 0.15 mIU/l. The 3.8% intra-assay and 4.5% inter-assay coefficients of variation were calculated. The Homeostatic Model Assessment for Insulin Resistance, HOMA={[G0] * [Ins]/22.5} was assessed.

Fasting plasma samples were frozen at −80°C until the measurement of soluble E-selectin, P-selectin, and L-selectin were performed using an ELISA method (R&D Systems, Minneapolis, MN) and a microplater reader BioTek Elx800 (Bio Tek Instruments, Inc., Winooski, VT). The minimal detectable levels of E, P, and L-selectins were 0.009, 0.5, and 0.3 ng/ml, respectively. The respective intra-assay and inter-assay coefficients of variation were: for E-selectin 6.5% and 7.4%, for P-selectin 3.6% and 4.1%, and for L-selectin 5.0% and 6.5%.

15.2.3 Statistical Analysis

All results are shown as median and quartiles, lower and upper (in parentheses). Shapiro-Wilk's test was used to check the normality of distributions. Differences among OSA-0, OSA-1, OSA-2, and OSA-3 groups were evaluated with a nonparametric Kruskal-Wallis ANOVA & median test. Differences between two groups were evaluated with a Mann-Whitney U test. Spearman's correlation coefficient was used to describe relationships. $p<0.05$ was taken as an indicator of statistical significance. Statistical calculations were performed using Statistica 6.0 for Windows program.

15.3 Results

The study groups did not differ in respect to age, BMI, glucose, insulin, lipid parameters, hsCRP, and white blood cell count (WBC). The detailed baseline characteristics are presented in Table 15.1.

We found a progressive increase in the concentrations of all three selectins which correlated with the severity of OSA. A nonparametric analysis of the data, using Kruskal-Wallis and median test (Figs. 15.1, 15.2, and 15.3), revealed significant differences in the concentration of a given selectin at sequential stages of OSA. A subsequent Mann–Whitney U test showed the following differences in adhesive molecules:

E-selectin: OSA-0 *vs*. OSA-1 ($p<0.001$), OSA-0 *vs*. OSA-2 ($p<0.001$), OSA-0 *vs*. OSA-3 ($p<0.001$), OSA-1 *vs*. OSA-3 ($p=0.050$);
P-selectin: OSA-0 *vs*. OSA-3 ($p<0.001$), OSA-1 *vs*. OSA-3 ($p=0.050$);
L-selectin: OSA-0 *vs*. OSA-3 ($p=0.003$), OSA-1 *vs*. OSA-3 ($p=0.030$).

Table 15.1 Characteristics of the study groups

	OSA-0 (n=20)	OSA-1 (n=21)	OSA-2 (n=18)	OSA-3 (n=21)
Age (year)	55 (39; 61)	53 (43; 60)	55 (48; 61)	55 (46; 60)
AHI (events/h)	2.9 (1.7; 4.3)	8.2 (7.1; 12.2)	19.2 (16.8; 22.5)	45.5 (36.3; 61.7)
BMI (kg/m^2)	30.1 (28.0; 33.6)	28.7 (27.1; 30.3)	30.4 (27.8; 32.4)	31.6 (27.5; 36.1)
SBP (mmHg)	130 (120; 130)	130 (125; 140)	130 (130; 130)	130 (130; 140)
DBP (mmHg)	80 (73; 90)	80 (80; 90)	80 (80; 85)	80 (80; 90)
G 0' (mmol/l)	5.20 (5.02; 5.74)	5.32 (5.02; 5.72)	5.45 (5.19; 5.73)	5.57 (5.31; 5.91)
G 120' (mmol/l)	6.57 (5.58; 7.97)	7.06 (6.12; 7.95)	5.93 (4.50; 7.43)	5.61 (4.80; 7.64)
Ins 0' (mU/l)	22.8 (20.5; 31.8)	21.9 (18.1; 24.4)	19.2 (17.0; 26.0)	21.4 (20.5; 27.7)
HOMA	5.8 (4.9; 7.4)	5.6 (4.4; 6.2)	4.8 (4.1; 6.1)	6.1 (5.0; 7.8)
TC (mmol/l)	5.49 (4.87; 5.95)	5.39 (4.17; 5.97)	5.23 (4.66; 6.17)	5.36 (4.72; 6.28)
TG (mmol/l)	1.77 (1.27; 2.22)	1.49 (1.01; 1.80)	1.65 (1.12; 1.93)	1.65 (1.08; 2.38)
HDL (mmol/l)	1.17 (0.98; 1.44)	1.28 (1.14; 1.48)	1.20 (1.07; 1.29)	1.09 (0.97; 1.16)
LDL (mmol/l)	3.44 (3.05; 4.09)	3.39 (2.40; 3.97)	3.74 (3.04; 4.56)	3.56 (2.67; 4.04)
hsCRP (mg/l)	2.00 (1.02; 2.74)	2.42 (1.65; 3.96)	2.12 (1.66; 2.78)	2.75 (1.66; 3.90)
WBC (10^9/l)	6.5 (6.0; 7.3)	7.3 (6.1; 8.2)	6.8 (5.8; 8.0)	7.3 (5.9; 8.5)
E-selectin (ng/ml)	16.3 (8.1; 19.9)	22.7 (21.2; 25.3)	26.0 (20.9; 34.4)	31.8 (23.6; 35.6)
P-selectin (ng/ml)	45.0 (36.5; 54.6)	47.2 (35.9;80.2)	64.7 (44.5; 79.5)	75.3 (55.1; 84.1)
L-selectin (ng/ml)	1476 (1274; 1649)	1848 (1630; 2308)	1965 (1464; 2654)	2471 (1838; 3180)

Data are presented as median and quartiles, lower and upper (*in parentheses*). See Sect. 15.2 for the stratification of study groups and the acronyms of the indices examined

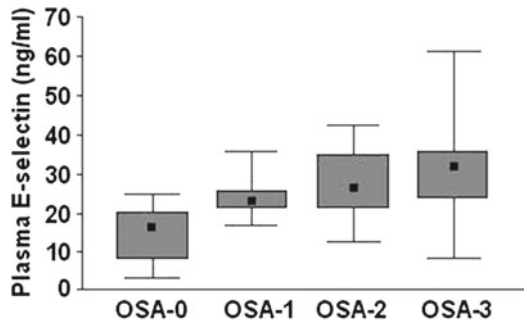

Fig. 15.1 Comparison of E-selectin concentration among the study groups by Kruskal-Wallis test and median test ($p<0.001$). Data are shown as median (•) with interquartile ranges and minimal (⊥) to maximal (⊤) values. See Sect. 15.2.1 for the stratification of study groups

A number of metabolic relationships involving E-, P-, and L-selectins were found in the whole study population (n=80) and in the different OSA-stage subjects. Positive relationships were present between AHI and adhesive molecules in the whole study population: AHI & E-selectin ($r=0.50$, $p<0.001$), AHI & P-selectin ($r=0.33$, $p=0.005$), and AHI & L-selectin ($r=0.35$, $p=0.003$). There were the following positive relationships in the OSA-0 group: E-selectin & DBP ($r=0.47$, $p=0.030$) and E-selectin & TG ($r=0.50$, $p=0.036$). The OSA-1 subjects displayed a negative relationship of P-selectin & HDL ($r=-0.52$, $p=0.015$). The OSA-2 subjects displayed the following positive relationships: P-selectin & TC ($r=0.50$, $p=0.030$), L-selectin & TC ($r=0.64$, $p=0.003$), L-selectin & LDL ($r=0.68$, $p=0.002$). Finally, the OSA-3 subjects displayed these positive relationships: E-selectin & BMI ($r=0.48$, $p=0.049$) and E-selectin & DBP ($r=0.49$, $p=0.045$).

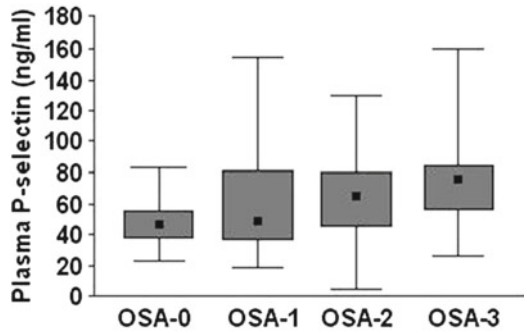

Fig. 15.2 Comparison of P-selectin concentration among the study groups by Kruskal-Wallis test and median test ($p=0.012$). Data are shown as median (▪) with interquartile ranges and minimal ($\perp$) to maximal ($\top$) values. See Sect. 15.2.1 for the stratification of study groups

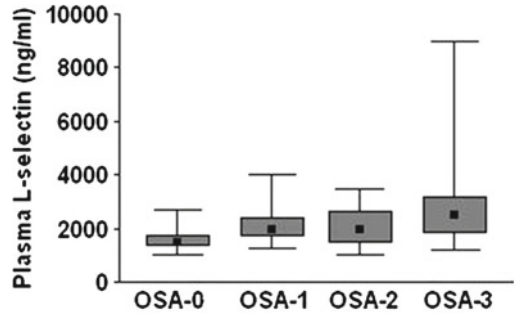

Fig. 15.3 Comparison of L-selectin concentration among the study groups by Kruskal-Wallis test and median test ($p=0.012$). Data are shown as median (▪) with interquartile ranges and minimal ($\perp$) to maximal ($\top$) values. See Sect. 15.2.1 for the stratification of study groups

15.4 Discussion

Obstructive sleep apnea patients have been shown to have increased cardiovascular morbidity and mortality. It is not clear whether and to what extent the increased cardiovascular risk is associated with OSA pathology itself and what the effects of other obesity-related disorders would be, including arterial hypertension, t2DM, dyslipidemia, and smoking habits or alcohol abuse. From the clinical standpoint, the knowledge about early markers of atherosclerosis could improve the management of OSA. A study of E, L, and P selectins in relation to OSA severity and cardiovascular risk factors has not yet been performed.

In the present study, we found a progressive increase in the concentrations of all three selectins that correlated with the severity of obstructive sleep apnea. However, different cardiovascular risk factors were related to individual selectins at sequential stages of OSA severity. At the mild stage of OSA-1, we noted a potentially beneficial relationship between HDL and P-selectin, while at the moderate stage of OSA-2, TC and LDL may contribute to elevated either P or L-selectin. At the most severe stage of OSA-3, there was an evident influence of BMI and DBP on E-selectin increase.

Robinson et al. (2004) found higher P-selectin levels, as compared with unmatched controls, which correlated only with BMI. The increased level of P-selectin did not decline after 1 month of continuous positive airway pressure (CPAP) therapy. The authors concluded that platelet activation

was not related to OSA severity. Other researchers report that elevated P-selectin concentration might result from obesity and high leptin levels, which activates platelets, rather than from a direct consequence of OSA (Phillips et al. 2000; Corsonello et al. 2002). Minoguchi et al. (2007) found significantly higher serum levels of soluble P-selectin in patients with moderate-to-severe OSA than in either mild-OSA patients or obese control subjects without comorbidities. In addition, a higher prevalence of silent brain infarction (SBI) was documented in patients with moderate-to-severe OSA (25.0%) than in patients with mild OSA (7.7%), or in controls (6.7%) in brain magnetic resonance images. Consequently, OSA patients with SBI displayed increased P-selectin, as compared with non-SBI-OSA subjects. Moreover, 3 months treatment with nasal CPAP significantly decreases P-selectin in subjects with moderate-to-severe OSA (Minoguchi et al. 2007).

In our earlier study, we found higher concentrations of plasma soluble E-selectin in patients with more severe OSA. However, there were no correlations found between the level of this adhesion molecule and AHI or other studied metabolic parameters (Cofta et al. 2009). Yun et al. (2010), who in addition measured carotid intima-media thickness (IMT), described similar findings. In their study, increased P-selectin in OSA patients did not correlate with either AHI or IMT. The authors also noted that 4–6 weeks of CPAP therapy decreased the concentrations of soluble E-selectin in OSA patients. A beneficial influence of CPAP therapy on the plasma levels of soluble selectins (Chin et al. 2000), even if a direct linking mechanism is not definitely recognized, does suggest the OSA contribution to the development of atherosclerosis.

El-Solh et al. (2002) verified the hypothesis that different adhesion molecules, including E- and L-selectins, are associated with OSA, although with no relation to coexisting coronary artery disease. In that study, E-selectin was increased in the OSA group compared with control subjects and correlated with the AHI and the oxygen desaturation index, but L-selectin was not. L-selectin was not changed before and after sleep in both OSA and control subjects in another study as well (Ohga et al. 1999).

The patients of the present study were free of any inflammatory processes, which was verified by serum hsCRP and WBC account (see Table 15.1). Therefore, it is a reasonable assumption that the changes in plasma selectins observed were due mostly to the underlying OSA. The patients at the severe stage of OSA displayed evidently higher P- and L-selectin levels. In contrast, E-selectin was increasing continuously from the mild-to-severe stages of OSA.

15.5 Conclusions

Our study documents that E-, P- and L-selectins may be related to cardiovascular complications at more severe stages of OSA and that soluble E-selectin is the most sensitive indicator of cardiovascular risk among the adhesive molecules investigated, as it increases progressively with the growing severity of OSA.

Conflicts of interest: The authors declare no conflicts of interest in relation to this article.

References

Biondi-Zoccai, G. G., Abbate, A., Liuzzo, G., & Biasucci, L. M. (2003). Atherothrombosis, inflammation, and diabetes. *Journal of the American College of Cardiology, 41*, 1071–1077.

Blankerberg, S., Barbaux, S., & Tiret, L. (2003). Adhesion molecules and atherosclerosis. *Atherosclerosis, 170*, 191–203.

Bobryshev, Y. V. (2006). Monocyte recruitment and foam cell formation in atherosclerosis. *Micron, 37*, 208–222.

Chin, K., Nakamura, T., Shimizu, K., Mishima, M., Nakamura, T., Miyasaka, M., & Ohi, M. (2000). Effects of nasal continuous positive airway pressure on soluble cell adhesion molecules in patients with obstructive sleep apnea syndrome. *American Journal of Medicine, 109*, 562–567.

Cofta, S., Wysocka, E., Michalak, S., Piorunek, T., Batura-Gabryel, H., & Torlinski, L. (2009). Endothelium-derived markers and antioxidant status in the blood of obstructive sleep apnea males. *European Journal of Medical Research, 14*(Suppl 4), 49–52.

Corsonello, A., Malara, A., Ientile, R., & Corica, F. (2002). Leptin enhances adenosine diphosphate-induced platelet aggregation in healthy subjects. *Obesity Research, 10*, 306.

Dyugovskaya, L., Lavie, P., & Lavie, L. (2005). Lymphocyte activation as a possible measure of atherosclerotic risk in patients with sleep apnea. *Annals of the New York Academy of Sciences, 1051*, 340–350.

El-Solh, A. A., Mador, M. J., Sikka, P., Dhillon, R. S., Amsterdam, D., & Grant, B. J. (2002). Adhesion molecules in patients with coronary artery disease and moderate- to-severe obstructive sleep apnea. *Chest, 121*, 1541–1547.

Eriksson, E. E., Xie, X., Werr, J., Thoren, P., & Lindbom, L. (2001). Importance of primary capture and l-selectin–dependent secondary capture in leukocyte accumulation in inflammation and atherosclerosis in vivo. *The Journal of Experimental Medicine, 194*, 205–218.

Gjørup, P. H., Sadauskiene, L., Wessels, J., Nyvad, O., Strunge, B., & Pedersen, E. B. (2007). Abnormally increased endothelin-1 in plasma during the night in obstructive sleep apnea: Relation to blood pressure and severity of disease. *American Journal of Hypertension, 20*, 44–52.

Lim, H. S., Blann, A. D., & Lip, G. Y. (2004). Soluble CD40 ligand, soluble P-selectin, interleukin-6, and tissue factor in diabetes mellitus: Relationships to cardiovascular disease and risk factor intervention. *Circulation, 109*, 2524–2528.

Minoguchi, K., Yokoe, T., Tazaki, T., Minoguchi, H., Oda, N., Tanaka, A., Yamamoto, M., Ohta, S., O'Donnell, C. P., & Adachi, M. (2007). Silent brain infarction and platelet activation in obstructive sleep apnea. *American Journal of Respiratory and Critical Care Medicine, 175*, 612–617.

Ohga, E., Nagase, T., Tomita, T., Teramoto, S., Matsuse, T., Katayama, H., & Ouchi, Y. (1999). Increased levels of circulating ICAM-1, VCAM-1, and L-selectin in obstructive sleep apnea syndrome. *Journal of Applied Physiology, 87*, 10–14.

Parati, G., Ongaro, G., Bonsignore, M. R., Glavina, F., Di Rienzo, M., & Mancia, G. (2002). Sleep apnoea and hypertension. *Current Opinion in Nephrology and Hypertension, 11*, 201–214.

Peker, Y., Kraiczi, H., Hedner, J., Löth, S., Johansson, A., & Bende, M. (1999). An independent association between obstructive sleep apnoea and coronary artery disease. *European Respiratory Journal, 14*, 179–184.

Peker, Y., Hedner, J., Norum, J., Kraiczi, H., & Carlson, J. (2002). Increased incidence of cardiovascular disease in middle-aged men with obstructive sleep apnea: A 7-year follow up. *American Journal of Respiratory and Critical Care Medicine, 166*, 159–165.

Phillips, B. G., Kato, M., Narkiewicz, K., Choe, I., & Somers, V. K. (2000). Increases in leptin levels, sympathetic drive and weight gain in obstructive sleep apnea. *American Journal of Physiology. Heart and Circulatory Physiology, 279*, 234–237.

Ridker, P. M., Buring, J. E., & Rifai, N. (2001). Soluble P-selectin and the risk of future cardiovascular events. *Circulation, 103*, 491–495.

Robinson, G. V., Pepperell, J. C., Segal, H. C., Davies, R. J., & Stradling, J. R. (2004). Circulating cardiovascular risk factors in obstructive sleep apnoea: Data from randomized controlled trials. *Thorax, 59*, 777–782.

Yun, C. H., Jung, K. H., Chu, K., Kim, S. H., Ji, K. H., Park, H. K., Kim, H. C., Lee, S. T., Lee, S. K., & Roh, J. K. (2010). Increased circulating endothelial microparticles and carotid atherosclerosis in obstructive sleep apnea. *Journal of Clinical Neurology, 6*, 89–98.

Chapter 16
Blood Antioxidant Status, Dysglycemia and Obstructive Sleep Apnea

Ewa Wysocka, Szczepan Cofta, Tomasz Piorunek, Sylwia Dziegielewska-Gesiak, Wieslaw Bryl, and Lech Torlinski

Abstract Obstructive sleep apnea (OSA) patients present increased cardiovascular morbidity and mortality. Oxidative stress is involved in OSA and cardiovascular pathology. The aim of the study was to assess oxidative stress markers in the blood of OSA males during oral glucose tolerance test (OGTT). The study involved OSA-suspected obese males (BMI ≥ 25 kg/m^2) aged 35–64, with no acute or chronic disorders, appointed for polysomnography to diagnose OSA (AHI ≥ 5). The results of OGTT allowed to select prediabetic (Pre) subjects and normal glucose tolerance (N), excluding newly diagnosed diabetes. Blood was collected at 0 min (fasting) and 120 min of the test. Plasma glucose, total antioxidant status (TAS), thiobarbituric acid-reacting substances (TBARS), and activity of superoxide dismutase-1 (SOD) in erythrocytes, were determined at the two time points and the difference (D) between the 120 and 0 min time points was calculated for either oxidative stress variable (D-TAS, D-SOD and D-TBARS). Fasting serum insulin and lipids also were measured fasting. There were four groups of subjects, each consisting of 22 individuals N-OSA-neg(ative), N-OSA-pos(itive), Pre-OSA-neg and Pre-OSA-pos. The N-OSA-pos and Pre-OSA-pos subjects demonstrated decreased SOD-0 compared with OSA-negative groups. In N-OSA-neg and N-OSA-pos groups, the positive differences D-SOD and D-TAS were observed, while Pre-OSA subjects presented negative differences. In conclusion, prediabetic OSA patients may consume blood antioxidant factors to counter the effects of oxidative stress, more than individuals with normal glucose tolerance.

Keywords Cardiovascular morbidity • Obstructive sleep apnea • Oxidative stress • Prediabetes • Oral glucose tolerance • Obesity • Antioxidant status

E. Wysocka (✉) • S. Dziegielewska-Gesiak • L. Torlinski
Department of Clinical Biochemistry and Laboratory Medicine, Poznan University of Medical Sciences, Grunwaldzka 6 St, 60-780 Poznan, Poland
e-mail: ewysocka@ump.edu.pl

S. Cofta • T. Piorunek
Department of Pneumology, Allergology and Respiratory Oncology, Poznan University of Medical Sciences, Szamarzewskiego 84 St, 60-569 Poznan, Poland

W. Bryl
Department of Internal Medicine, Hypertension and Metabolic Disorders, Poznan University of Medical Sciences, Szamarzewskiego 84 St, 60-569 Poznan, Poland

M. Pokorski (ed.), *Respiratory Regulation - The Molecular Approach*,
Advances in Experimental Medicine and Biology 756, DOI 10.1007/978-94-007-4549-0_16,

16.1 Introduction

Obstructive sleep apnea (OSA) affects 3–7% of adult men in the developed countries and is considered to be the second most common chronic respiratory disorder in adults (Punjabi 2008). The OSA population is recognized with increased cardiovascular morbidity and mortality, with combined stroke and coronary event risk at about 3% per year (Peker et al. 2002). However, it is still debatable whether this situation is related to OSA pathology or to the conventional cardiovascular risk factors associated incidentally present in OSA patients (Peppard et al. 2000; Shahar et al. 2001).

OSA patients often present with obesity (60–70%), hypertension (60–68%), dyslipidemia (50–63%), and type 2 diabetes mellitus (t2DM) (16%) (Kiely and McNicholas 2000; Peker et al. 2002; Yaggi et al. 2005). In particular, disordered glucose metabolism seems sharply on the rise in OSA patients. In a Japanese study, 30% of OSA patients had t2DM and another 30% had impaired glucose tolerance (IGT) (Tamura et al. 2008). OSA is proposed to be an independent risk factor for cardiovascular disease (CVD) (McNicholas et al. 2007); however, a cumulative effect of different metabolic abnormalities in one individual is debatable (Dorkova et al. 2008).

Data from both epidemiological and clinical studies (Shaw et al. 2008; Tasali et al. 2008) show that OSA is independently associated with dysglycemia and raises the risk for the development of t2DM. The pathomechanism of dysglycemia would be decreased insulin sensitivity and glucose intolerance (Theorell-Haglöw et al. 2008) which are independent of age, gender, or anthropometric findings such as BMI and waist circumference (Punjabi et al. 2004). Oxidative stress is at play in OSA pathology (Lavie 2003) and also underlies metabolic abnormalities in t2DM and cardiovascular disease (CVD) (Ceriello and Motz 2004; Rabbani et al. 2010). Therefore, the aim of the present study was to assess markers of oxidative stress in the blood of OSA patients during oral glucose tolerance test and to compare them with those in control subjects without OSA. To this end we used the accepted methods of determining the blood antioxidant status. We measured the erythrocyte superoxide dismutase-1 (SOD), an intracellular antioxidant enzyme, and the plasma total antioxidant status (TAS), which reflects the extracellular compartment, both described as reflecting the antioxidant blood capacity (Habdous et al. 2003), while thiobarbituric acid-reacting substances (TBARS) reflect plasma lipid peroxidation (Okhawa et al. 1979).

16.2 Methods

16.2.1 Subjects

The study was performed in accordance with the Declaration of Helsinki for Human Research and the study protocol was approved by the Bioethical Committee of University of Medical Sciences in Poznan, Poland. The subjects gave informed consent to the study procedure.

Eighty eight male non-smoking subjects, aged 35–64, with body mass index (BMI) ≥25 kg/m^2, suspected of obstructive sleep apnea participated in the study. Otherwise, the subjects had no acute or chronic disorders. They were qualified for a 75 g oral glucose tolerance test (OGTT) according to WHO recommendations (1994). The results of OGTT allowed selecting the subjects with normal glucose tolerance (N) and prediabetes (Pre); while those with newly diagnosed t2DM were excluded from further evaluation. The interpretation of OGTT, based on the American Diabetes Association guidelines (2011) was presented in Table 16.1. The subjects qualifying for further evaluation (N and Pre subjects) were submitted to polysomnography and the apnea/hypopnea index (AHI) was calculated to select OSA-pos(itive) (AHI ≥ 5) and OSA-neg(ative) (AHI < 5) individuals. As a result of the

Table 16.1 Interpretation of oral glucose tolerance test (OGTT)

Categories of glycemia		Plasma glucose concentration	
		Fasting (at 0 min)	at 120 min
Normal glucose tolerance (N)		<5.60 mmol/l	<7.80 mmol/l
High risk of diabetes (Prediabetes)	Impaired fasting glycemia (IFG)	5.60–6.99 mmol/l	<7.80 mmol/l
	Impaired glucose tolerance (IGT)	<7.00 mmol/l	7.80–11.09 mmol/l
Diabetes mellitus (DM)		<7.00 mmol/l	≥11.10 mmol/l

selection process we had four groups of subjects: normal glucose tolerance without obstructive sleep apnea (N-OSA-neg), normal glucose tolerance with obstructive sleep apnea (N-OSA-pos), prediabetes without obstructive sleep apnea (Pre-OSA-neg) and prediabetes with obstructive sleep apnea (Pre-OSA-pos); each consisted of 22 subjects.

16.2.2 Measurements

Complete physical examination, including the measurement of systolic (SBP) and diastolic arterial blood pressure (DBP), and the calculation of body mass index (BMI, kg/m^2) was performed.

OSA-suspected persons were evaluated in the Sleep Laboratory of the Department of Pulmonology, Allergology and Respiratory Oncology by full-night polysomnography (Remlogic, EMBLA S4000 system, Denver, CO). Airflow was monitored by a nasal flow canula. Abdominal and thoracic movements were assessed by respiratory inductive plethysmography. Night recordings of hemoglobin oxygen saturation were obtained by finger pulsoximetry. Snoring sounds, heart rate, and sleep position were recorded. Apnea was defined as a cessation of airflow lasting more than 10 s and hypopnea was defined as a two-third reduction of airflow and/or abdominal ribcage movements lasting more than 10 s associated with a decrease of ≥4 % of SaO_2.

Blood was sampled from the ulnar vein at baseline (time 0′) and at 120 min (120′) of the OGTT. Glucose (G), total antioxidant status (TAS), thiobarbituric acid-reacting substances (TBARS) in plasma, and the activity of superoxide dismutase-1 EC.1.15.1.1. (SOD) in erythrocytes were determined at the time intervals outlined above. The difference in the values of the markers obtained between the 120 min and 0 min (baseline level) of the OGTT (D = 120′–0′) was calculated. In addition, fasting plasma lipids and insulin (INS) also were measured.

Glucose, total cholesterol (TC), high-density lipoprotein cholesterol (HDL) and triglycerides (TG) were determined by enzymatic methods (BioMérieux, Marcy-l'Etoile, France) in a UV-160A Shimadzu spectrophotometer (Shimadzu, Kyoto, Japan). Low-density lipoprotein cholesterol (LDL) was calculated due to Friedewald's formula: LDL = TC-HDL-0.45TG. The reference sera level 1 and level 2 (Randox) were used for monitoring the accuracy of the determinations.

Insulin was measured by an ELISA method (BioSource, Nivelles, Belgium) in a microplater reader Sunrise (Tecan Group, Männedorf, Switzerland), with sensitivity of 0.15 mU/l. The intra- and inter-assay coefficients of variation (CV) were 3.8% and 4.5%, respectively. Homeostatic model assessment for insulin resistance: HOMA-IR = G 0′·INS/22.5, was calculated.

TAS and SOD were measured spectrophotometrically (Randox Laboratories, Crumlin, Antrim, UK) on Statfax 1904 Plus (Awareness Technology, Palm City, FL) and TBARS (Okhawa et al. 1979) using Sigma reagents (Germany) and Specord M40 (Germany). The intra- and inter-assay CV for SOD (1.6% and 2.7%), TAS (1.5% and 3.8%), and TBARS (1.8% and 3.7%) were calculated.

16.2.3 Statistical Analysis

All results were shown as median and quartiles, lower and upper (in parentheses). Normality of data distributions was checked with the Shapiro-Wilk test. Significance of differences among the four groups studied was verified with a nonparametric Kruskal-Wallis ANOVA and median test and between two groups by Mann-Whitney U test. Correlations were described by Spearman's coefficient (r). A $p<0.05$ was taken as indicative of significant differences. Statistical calculations were performed using Statistica 6.0 package for Windows.

16.3 Results

Clinical and biochemical characteristics of the subjects studied are shown in Table 16.2. All subjects were similar in age, SBP, DBP, INS, TC, HDL, and LDL. Understandably, prediabetic (Pre-OSA-neg and Pre-OSA-pos) subjects had higher levels of BMI, HOMA-IR, and glucose than those in the subjects with normal glucose tolerance (N-OSA-neg and N-OSA-pos). However, there were no differences between the N-OSA-neg and N-OSA-pos subjects regarding the parameters outlined above. Likewise, there were no differences between the prediabetic subjects (Pre-OSA-neg and Pre-OSA-pos) irrespective of the presence of OSA, except for the higher HOMA-IR ($p=0.04$) and TG ($p=0.03$) in Pre-OSA-neg group.

In general, the subjects with OSA had significant decreases in blood antioxidant status, compared with the non-OSA subjects. TAS 0′ and TAS 120′ were lower in both normal glucose tolerance and prediabetic OSA subjects, while SOD 0′ and SOD 120′ declined in the normal glucose tolerance OSA subjects only. On the other hand, the prediabetic subjects, both OSA-neg and OSA-pos, had higher SOD 0′ compared with the respective groups of the normal glucose tolerance subjects. The Pre-OSA-neg subjects had lower SOD 120′ compared with N-OSA-neg and the Pre-OSA-pos subjects had lower TAS 120′ compared with N-OSA-pos. Both TBARS 0′ and TBARS 120′ were increased in the Pre-OSA-neg subjects. These differences and their significance are presented in detail in Table 16.2.

Changes in the markers of oxidative stress in the groups studied are presented in Figs. 16.1, 16.2, and 16.3. In the normal glucose tolerance groups, N-OSA-neg and N-OSA-pos, the differences (D) between the values at 120 min and 0 min (baseline) of the OGTT were positive for SOD and TAS, while they were negative in the prediabetic groups of subjects, Pre-OSA-neg and Pre-OSA-pos. A progressive decrease of this difference for TAS (DTAS) was observed from N-OSA-neg through N-OSA-pos and Pre-OSA-neg to Pre-OSA-pos. Different correlations between oxidative stress markers determined during the OGTT and metabolic parameters are presented in Table 16.3.

16.4 Discussion

OSA increases the risk of insulin resistance and glucose intolerance, although the syndrome does not actually predict the development of t2DM in a significant way (Lévy et al. 2009). Nevertheless, OSA is linked to increased oxidative stress (Lavie and Lavie 2009) which, in turn, in experimental animal studies modeling chronic intermittent hypoxia, corresponding to OSA syndrome in humans, appreciably contributes to respiratory control (Edge et al. 2010). That study also points to gender differences in the control of breathing in rats, which might be in line with a higher prevalence of OSA in the male gender.

Table 16.2 Clinical and biochemical characteristics of the subjects studied (n = 22 in each group)

	N-OSA-neg	N-OSA-pos	Pre-OSA-neg	Pre-OSA-pos	p
Age (years)	52 (46–58)	53 (51–61)	53.5 (49–59)	54 (49–62)	
AHI (events/h)	2.4 (1.0–3.5)	20.7 (9.9–35.8)	2.9 (1.6–3.0)	31.3 (15.4–52.6)	
BMI (kg/m^2)	29.7 (27.1–32.2)	28 (26.2–30.4)	33.0 (29.8–36.1)	32.3 (28.4–34.9)	
SBP (mmHg)	120 (115–130)	130 (120–130)	135 (128–140)	130 (130–140)	
DBP (mmHg)	80 (70–80)	80 (75–85)	80 (78–83)	80 (80–85)	
G 0′ (mmol/l)	5.04 (4.93–5.24)	5.31 (4.85–5.50)	5.94 (5.69–6.70)	5.70 (5.39–5.91)	
G 120′ (mmol/l)	5.20 (4.57–6.71)	5.58 (4.82–6.24)	7.85 (6.66–8.95)	7.95 (5.61–8.62)	
INS 0′ (mU/l)	21.3 (17.4–28.2)	20.6 (15.8–24.4)	25.9 (19.8–33.7)	21.4 (17.7–25.3)	
HOMA-IR	4.68 (3.75–6.04)	4.89 (3.45–5.75)	6.86 (5.56–8.88)	5.37 (4.67–6.27)	
TC (mmol/l)	5.00 (4.44–5.91)	5.49 (4.24–6.39)	5.81 (5.29–6.55)	5.08 (4.50–5.99)[a]	[a]0.04
TG (mmol/l)	1.65 (1.06–1.89)	1.54 (0.97–1.96)	2.25 (1.64–3.29)	1.51 (1.14–2.14)[a]	[a]0.02
HDL (mmol/l)	1.32 (1.03–1.47)	1.16 (1.02–1.29)	1.35 (1.07–1.58)	1.13 (1.03–1.36)	
LDL (mmol/l)	3.21 (2.29–3.85)	3.79 (2.62–4.22)	3.54 (3.00–4.53)	3.47 (2.65–4.02)	
SOD 0′ (U/gHGB)	1332 (1245–1425)	1064 (996–1234)[b]	1456 (1341–1650)[c]	1433 (1092–1485)[d]	[b]0.0002, [c]0.02, [d]0.01
SOD 120′ (U/gHGB)	1425 (1336–1562)	1171 (981–1419)[b]	1289 (1180–1483)[c]	1241 (1005–1365)[e]	[b]0.01, [c]0.02, [e]0.0001
TAS 0′ (μmol/l)	1405 (1270–1541)	1264 (1134–1,359)[b]	1446 (1273–1483)	1257 (1224–1364)[a]	[b]0.04, [a]0.003
TAS 120′ (μmol/l)	1520 (1293–1690)	1320 (1225–1,499)[b]	1385 (1241–1493)	1147 (1080–1271)[a,d,e]	[b]0.04, [a]0.0001, [d]0.001, [e]0.0001
TBARS 0′ (μmol/l)	5.86 (4.91–6.24)	5.89 (4.95–7.22)	6.88 (6.08–8.53)[c]	6.20 (5.36–7.35)	[c]0.01
TBARS 120′ (μmol/l)	5.55 (4.43–6.09)	5.24 (4.19–8.08)	6.45 (4.65–8.67)[c]	6.32 (5.21–8.83)	[c]0.05

Data are median and quartiles, lower and upper (*in parentheses*)

N-OSA-neg normal glucose tolerance without obstructive sleep apnea, *N-OSA-pos* normal glucose tolerance with obstructive sleep apnea, *Pre-OSA-neg* prediabetes without obstructive sleep apnea, *Pre-OSA-pos* prediabetes with obstructive sleep apnea

[a]Pre-OSA-neg *vs,* Pre-OSA-pos

[b]N-OSA-neg *vs.* N-OSA-pos

[c]N-OSA-neg *vs.* Pre-OSA-neg

[d]N-OSA-pos *vs.* Pre-OSA-pos

[e]N-OSA-neg *vs.* Pre-OSA-pos

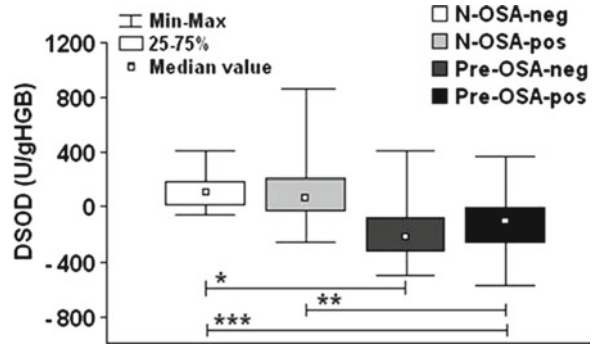

Fig. 16.1 Difference (D) in the erythrocyte superoxide dismutase (SOD) activity between the values measured at 120 min and 0 min (baseline) of oral glucose tolerance test in the groups studied. *p<0.01, **p=0.01, ***p=0.0001. *N-OSA-neg* normal glucose tolerance without obstructive sleep apnea, *N-OSA-pos* normal glucose tolerance with obstructive sleep apnea, *Pre-OSA-neg:* prediabetes without obstructive sleep apnea, *Pre-OSA-pos* prediabetes with obstructive sleep apnea

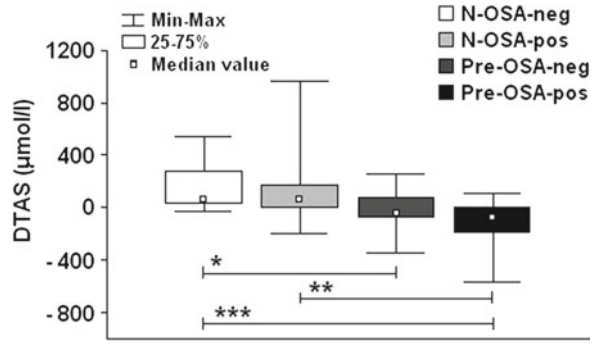

Fig. 16.2 Difference (D) in the plasma total antioxidant status (TAS) between the values measured at 120 min and 0 min (*baseline*) of oral glucose tolerance test in the groups studied. *p=0.0002, **p=0.0003, ***p=0.00001. *N-OSA-neg* normal glucose tolerance without obstructive sleep apnea, *N-OSA-pos* normal glucose tolerance with obstructive sleep apnea, *Pre-OSA-neg* prediabetes without obstructive sleep apnea, *Pre-OSA-pos* prediabetes with obstructive sleep apnea

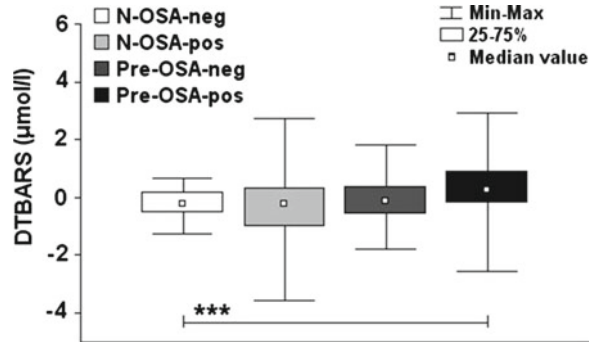

Fig. 16.3 Difference (D) in the plasma thiobarbituric acid-reacting substances (TBARS) between the values measured at 120 min and 0 min (baseline) of oral glucose tolerance test in the groups studied. ***p=0.05. *N-OSA-neg* normal glucose tolerance without obstructive sleep apnea, *N-OSA-pos* normal glucose tolerance with obstructive sleep apnea, *Pre-OSA-neg* prediabetes without obstructive sleep apnea, *Pre-OSA-pos* prediabetes with obstructive sleep apnea

Table 16.3 Correlations between oxidative stress markers and metabolic parameters in the groups studied

	N-OSA-neg	N-OSA-pos	Pre-OSA-neg	Pre-OSA-pos
TAS 0′ and HDL	r = −0.46; p = 0.04	r = −0.45; p = 0.04	r = −0.46; p = 0.04	–
DTAS and AHI	–	r = −0.54; p = 0.01	–	–
DTAS and TC	–	r = −0.53; p = 0.01	–	–
DTAS and LDL	–	r = −0.56; p = 0.01	–	–
DTAS and G120′	–	–	r = 0.45; p = 0.04	–
DTBARS and HDL	r = −0.53; p = 0.01	–	–	–
DTBARS and G 120′	–	–	r = 0.48; p = 0.03	–

See text for acronyms

The literature does not show any data concerning the blood antioxidant capacity during the oral glucose tolerance test in obstructive sleep apnea patients. Therefore, we deemed interesting to evaluate the changeability of oxidative stress markers in connection with the risk of diabetes, in relation to the results of the glucose tolerance test, and with sleep apnea. We addressed the issue by examining the blood levels of TAS, SOD, and TBARS, the basic markers of the oxidant/antioxidant blood capacity, fasting and at 120 min of oral glucose tolerance test, in two clinical situations, normal glucose tolerance and dysglycemia, taken as a prediabetic state, in individuals with and without obstructive sleep apnea diagnosis. The results demonstrate differences in the TAS and SOD responses to glucose load between normal glucose tolerance and dysglycemia and that OSA worsened the antioxidant defenses; particularly it decreased the plasma total antioxidant status.

An increased of the prooxidant superoxide anion (Schulz et al. 2000) and decreased plasma TAS (Barceló et al. 2006) have been documented in the blood of OSA patients compared with healthy individuals. We have previously reported that OSA decreases the antioxidant blood capacity, including fasting erythrocyte SOD and plasma TAS of overweight and obese patients (Wysocka et al. 2008). Realizing the coexistence of OSA and dysglycaemia, even if the pathogenetic scenario is still not quite clear (Rasche et al. 2010), the present study indicates the role of the antioxidant balance in protection against t2DM in OSA patients.

It seems unclear whether OSA changes the picture of carbohydrate metabolism or dysglycemia influences the pathogenesis of OSA. In this investigation, increased fasting activity of erythrocyte SOD in prediabetic, mainly OSA-negative, subjects might reflect some metabolic mobilization. A decrease in blood antioxidants at 120 min of OGTT, particularly regarding the plasma TAS in prediabetic OSA-positive subjects, might indicate an elevated turnover of the marker. All those changes are likely to keep lipid peroxidation products at a stable level, as TBARS did not differ among the groups studied. The studies on oxidative stress in prediabetes are rather sparse. Song et al. (2007) investigated Chinese subjects with normal glucose tolerance (n = 92), impaired glucose regulation (n = 78), and with newly diagnosed t2DM (n = 113) subjects. They found a progressively lower SOD in impaired glucose regulation and t2DM subjects compared with those having normal glucose tolerance, while lipid peroxides and total antioxidant capacity (TAC) were not decreased unless in t2DM. However, the mixed-gender population of that study presented a definitely lower BMI, normal or overweight, than the subjects of the present study. Some ethnic differences also may exist in the context of abdominal obesity and the development of t2DM (Alberti et al. 2009).

It seems difficult to separate metabolic influences from oxidative stress markers in OSA as judged from the correlation we found in this study. In the OSA-positive subjects with normal glucose tolerance, increased AHI, but also TC and LDL were associated with decreased DTAS, suggesting the plasma antioxidant capacity run short. In the OSA-negative prediabetic subjects, both DTAS and DTBARS were positively associated with G 120′; therefore, keeping the oxidative stress down might be important to prevent or delay the development of t2DM; the appearance of which is facilitated by an accumulation of oxidative stress-provoking changes.

In conclusion, the study suggests that prediabetic OSA patients consume blood antioxidant factors to a greater extent than OSA-negative individuals with normal glucose tolerance for want of avoiding oxidative stress. The metabolic contributions of obstructive sleep apnea should be considered in clinical practice.

Conflicts of interest: No conflict of interests were declared by the authors in relation to this work.

References

Alberti, K. G. M. M., Eckel, R. H., Grundy, S. M., Zimmet, P. Z., Cleeman, J. I., Donato, K. A., Fruchart, J.-C., James, W. P. T., Loria, C. M., & Smith, S. C., Jr. (2009). Harmonizing the metabolic syndrome: A join interim statement of the International Diabetes Federation Task Force on Epidemiology and Prevention; National Heart, Lung, and Blood Institute; American Heart Association; World Heart Federation; International Atherosclerosis Society; and International Association for the Study of Obesity. *Circulation, 120*, 1640–1645.

American Diabetes Association. (2011). The expert committee on the diagnosis and classification of diabetes: Diagnosis and classification of diabetes mellitus. *Diabetes Care, 34*, S62–S69.

Barceló, A., Barbé, F., de la Peña, M., Vila, M., Pérez, G., Piérola, J., Durán, J., & Agustí, A. G. (2006). Antioxidant status in patients with sleep apnoea and impact of continuous positive airway pressure treatment. *European Respiratory Journal, 27*, 756–760.

Ceriello, A., & Motz, E. (2004). Is oxidative stress the pathogenic mechanism underlying insulin resistance, diabetes, and cardiovascular disease? The common soil hypothesis revisited. *Arteriosclerosis, Thrombosis, and Vascular Biology, 24*, 816–823.

Dorkova, Z., Petrasova, D., Molcanyiova, A., Popovnakova, M., & Tkacova, R. (2008). Effects of continuous positive airway pressure on cardiovascular risk profile in patients with severe obstructive sleep apnea and metabolic syndrome. *Chest, 134*, 686–692.

Edge, D., Skelly, J. R., Bradford, A., & O'Halloran, K. D. (2010). Respiratory plasticity in the behaving rat following chronic intermittent hypoxia. *Advances in Experimental Medicine and Biology, 669*, 267–270.

Habdous, M., Herbeth, B., Vincent-Viry, M., Lamont, J. V., Fitzgerald, P. S., Visvikis, S., & Siest, G. (2003). Serum total antioxidant status, erythrocyte superoxide dismutase and whole-blood glutathione peroxidase activities in the Stanislas cohort: Influencing factors and reference intervals. *Clinical Chemistry and Laboratory Medicine, 41*, 209–215.

Kiely, J. L., & McNicholas, W. T. (2000). Cardiovascular risk factors in patients with obstructive sleep apnoea syndrome. *European Respiratory Journal, 16*, 128–133.

Lavie, L. (2003). Obstructive sleep apnoea syndrome–an oxidative stress disorder. *Sleep Medicine Reviews, 7*, 35–51.

Lavie, L., & Lavie, P. (2009). Molecular mechanisms of cardiovascular disease in OSAHS: The oxidative stress link. *European Respiratory Journal, 33*, 1467–1484.

Lévy, P., Bonsignore, M. R., & Eckel, J. (2009). Sleep, sleep-disordered breathing and metabolic consequences. *European Respiratory Journal, 34*, 243–260.

McNicholas, W. T., Bonsignore, M. R., & The Management Committee of the COST Action B26. (2007). Sleep apnoea as an independent risk factor for cardiovascular disease: Current evidence, basic mechanisms and research priorities. *European Respiratory Journal, 29*, 156–178.

Okhawa, H., Ohishi, N., & Yagi, K. (1979). Assay for lipid peroxides in animal tissues by thiobarbituric acid reaction. *Analytical Biochemistry, 95*, 351–358.

Peker, Y., Hedner, J., Norum, J., Kraiczi, H., & Carlson, J. (2002). Increased incidence of cardiovascular disease in middle-aged men with obstructive sleep apnea: A 7-year follow up. *American Journal of Respiratory and Critical Care Medicine, 166*, 159–165.

Peppard, P. E., Young, T., Palta, M., & Skatrud, J. (2000). Prospective study of the association between sleep-disordered breathing and hypertension. *The New England Journal of Medicine, 342*, 1378–1384.

Punjabi, N. M. (2008). The epidemiology of adult obstructive sleep apnea. *Proceedings of the American Thoracic Society, 5*, 136–143.

Punjabi, N. M., Shahar, E., Redline, S., Gottlieb, D. J., Givelber, R., Resnick, H. E., & Sleep Heart Health Study Investigators. (2004). Sleep-disordered breathing, glucose intolerance, and insulin resistance: The Sleep Heart Health Study. *American Journal of Epidemiology, 160*, 521–530.

Rabbani, N., Chittari, M. V., Bodmer, C. W., Zehnder, D., Ceriello, A., & Thornalley, P. J. (2010). Increased glycation and oxidative damage to apolipoprotein B100 of LDL cholesterol in patients with type 2 diabetes and effect of metformin. *Diabetes, 59*, 1038–1045.

Raport of a WHO Study Group. (1994). *Prevention of diabetes mellitus*. WHO Technical Report Series, Vol. 844. Geneva: World Health Organization.

Rasche, K., Keller, T., Tautz, B., Hader, C., Hergenc, G., Antosiewicz, J., Di Giulio, C., & Pokorski, M. (2010). Obstructive sleep apnea and type 2 diabetes. *European Journal of Medical Research, 15*(Suppl. II), 152–156.

Schulz, R., Mahmoudi, S., Hattar, K., Sibelius, U., Olschewski, H., Mayer, K., Seeger, W., & Grimminger, F. (2000). Enhanced release of superoxide from polymorphonuclear neutrophils in obstructive sleep apnea. *American Journal of Respiratory and Critical Care Medicine, 162*, 566–570.

Shahar, E., Whitney, C. W., Redline, S., Lee, E. T., Newman, A. B., Javier Nieto, F., O'Connor, G. T., Boland, L. L., Schwartz, J. E., & Samet, J. M. (2001). Sleep-disordered breathing and cardiovascular disease: Cross sectional results of the Sleep Heart Health Study. *American Journal of Respiratory and Critical Care Medicine, 163*, 19–25.

Shaw, J. E., Punjabi, N. M., Wilding, J. P., Alberti, K. G., Zimmet, P. Z., & International Diabetes Federation Taskforce on Epidemiology and Prevention. (2008). Sleep-disordered breathing and type 2 diabetes: A report from the International Diabetes Federation Taskforce on Epidemiology and Prevention. *Diabetes Research and Clinical Practice, 81*, 2–12.

Song, F., Jia, W., Yao, Y., Hu, Y., Lei, L., Lin, J., Sun, X., & Liu, L. (2007). Oxidative stress, antioxidant status and DNA damage in patients with impaired glucose regulation and newly diagnosed type 2 diabetes. *Clinical Science, 112*, 599–606.

Tamura, A., Kawano, Y., Watanabe, T., & Kadota, J. (2008). Relationship between the severity of obstructive sleep apnea and impaired glucose metabolism in patients with obstructive sleep apnea. *Respiratory Medicine, 102*, 1412–1416.

Tasali, E., Mokhlesi, B., & Van Cauter, E. (2008). Obstructive sleep apnea and type 2 diabetes: Interacting epidemics. *Chest, 133*, 496–506.

Theorell-Haglöw, J., Berne, C., Janson, C., & Lindberg, E. (2008). Obstructive sleep apnoea is associated with decreased insulin sensitivity in females. *European Respiratory Journal, 31*, 1054–1060.

Wysocka, E., Cofta, S., Cymerys, M., Gozdzik, J., Torlinski, L., & Batura-Gabryel, H. (2008). The impact of the sleep apnea syndrome on oxidant-antioxidant balance in the blood of overweight and obese patients. *Journal of Physiology and Pharmacology, 59*(Suppl 6), 761–769.

Yaggi, H. K., Concato, J., Kernan, W. N., Lichtman, J. H., Brass, L. M., & Mohsenin, V. (2005). Obstructive sleep apnea as a risk factor for stroke and death. *The New England Journal of Medicine, 353*, 2034–2041.

Chapter 17
Anti-natrium/Iodide Symporter Antibodies and Other Anti-thyroid Antibodies in Children with Turner's Syndrome

Anna M. Kucharska, Barbara Czarnocka, and Urszula Demkow

Abstract Antibodies against the Na/I symporter (anti-NIS ab) have been found in adult patients with autoimmune thyroid diseases. As easily available for the immune system, NIS can play a role in the initial stage of autoimmune thyroid diseases. Children with Turner's syndrome (TS) being at high risk of autoimmune thyroid disease development seem a valuable group for the investigation of the early autoimmune process. The aim of the study was to investigate the presence of anti-NIS ab and its potential clinical significance in TS children. Fifty four girls with TS were examined (age 11.9 ± 2.46 years), and 23 healthy girls with normal thyroid function, free of autoimmune diseases. Anti-NIS antibodies were measured by the in-house ELISA method and the Western blotting. Sera considered positive for anti-NIS ab were used for the iodide uptake bioassay using COS7 cells stably transfected with hNIS. In all patients the thyroid function, antithyroid antibodies presence and thyroid ultrasonography were evaluated. In 20% of the patients a subclinical hypothyroidism was diagnosed and 70.4% had antithyroid antibodies (anti-TPO – 64.8% and Anti-Tg – 24%). Anti-NISab were present in 14.8% girls with TS and in none of the control group. Their presence was unrelated to other antithyroid antibodies titre or patients' age. A positive correlation between the anti-NIS ab presence and the hypothyroidism was found ($p < 0.04$). Anti-NIS ab-positive sera did not suppress iodine uptake. In conclusion, anti-NIS antibodies were present in 14.8% of children with TS and they were related to the presence of hypothyroidism.

Keywords Autoantibodies • Autoimmune thyroiditis • Children • Na/I symporter • Turner's syndrome

A.M. Kucharska (✉)
Department of Paediatrics and Endocrinology, Medical University of Warsaw,
Marszalkowska 24 St, 00-756 Warsaw, Poland
e-mail: anna.kucharska@litewska.edu.pl

B. Czarnocka
Department of Biochemistry, Medical Center of Postgraduate Education, Warsaw, Poland

U. Demkow
Department of Laboratory Diagnostics and Clinical Immunology of the Developmental Age,
Medical University of Warsaw, Marszalkowska 24 St, 00-756 Warsaw, Poland

M. Pokorski (ed.), *Respiratory Regulation - The Molecular Approach*,
Advances in Experimental Medicine and Biology 756, DOI 10.1007/978-94-007-4549-0_17,

17.1 Introduction

Natrium/Iodide symporter (NIS) is a transmembrane protein responsible for the iodide transport into thyrocytes. Since its first description (Dai et al. 1996; Smanik et al. 1996), NIS is considered to be an antigen involved in autoimmune thyroid diseases (Raspe et al. 1995). As NIS is localized in the basal membrane of the thyroid follicular cells, it is potentially easily available for T cells and seems to be a potential autoantigen. Anti-NIS antibodies have been found in some patients with autoimmune thyroid diseases including Graves' disease and Hashimoto's thyroiditis (Ajjan et al. 2000; Endo et al. 1996a, b; Morris et al. 1997; Raspe et al. 1995). However, Ho Su Chin et al. (2000) and Seissler et al. (2000) reported, that the frequency of anti-NIS antibodies in adult patients with autoimmune thyroid diseases is rather low. Clinical implications of the anti-NIS antibodies remain still unclear (Dohan et al. 2003; Riesco-Eizaguirre and Santisteban 2006).

Hashimoto's thyroiditis is diagnosed in the majority of cases at the developed stage, when the goiter or hypothyroidism is present. The process is age-related and the latent period prior to the clinical manifestation of autoimmune thyroiditis could be very long. The observations of the natural course of autoimmune thyroid diseases in children show that autoimmune markers are not directly related to the severity of the immune process (Radetti et al. 2006). The investigation of the natural course of the disease from the initial phase in human is not possible due to an obscure time of disease onset. Children at high risk of autoimmune thyroid disease seem a valuable group for the investigation of early stages of the autoimmune process. A high prevalence of autoimmune thyroid diseases in adult and children with Turner's syndrome (TS) is well known (Germain and Plotnick 1986; Gruñeiro de Papendieck et al. 1987; Chiovato et al. 1996; Elsheikh et al. 2001; Radetti et al. 1995; Saenger et al. 2001). Between 10% and 30% of TS patients develop primary hypothyroidism in association with the presence antithyroid antibodies (Radetti et al. 1995; Saenger et al. 2001). One can expect that there are individuals in the initial phase of autoimmune thyroiditis among TS children. The aim of the present study was to evaluate whether anti-NIS antibodies are present in TS children and whether these antibodies would interfere with thyroid function.

17.2 Methods

The study was approved by the Bioethics Committee of Medical University of Warsaw, Poland. Parents and patients signed informed consent for the participation in the study.

Sera were obtained from 54 girls with TS (the mean age: 11.9 ± 2.5 years, range 1–18 years). Karyotypes distribution within the group was as follows: 55.5% (n = 30) with 45,X, 16.7% (n = 9) with Xq isochromosome (mosaicism and homologous line), and 27.8% (n = 15) with mosaicism (45X/46XX; 45X/47XXX; 45X/46Xr; 45X/46XY).

The control group consisted of 23 healthy age-matched girls with normal thyroid function, free of autoimmune diseases. The girls in the control group were negative for anti-thyroglobulin (anti-Tg ab) and anti-thyroid peroxidase antibodies (anti-TPO ab). The thyroid gland echogenicity and volume was evaluated by ATL 3,000 HDI, with linear sound 7.5–12.0 MHz. TSH was measured by IRMA-III generation test (Bio Source Europe S.A., Belgium), normal range: 0.5–4.5 mIU/L. Thyroid hormones were measured by RIA method (CIS Bio International Filiale de Schering S.A., France): free thyroxine (normal range: 7.0–18 pg/ml) and free triiodothyronine (normal range 2.0–4.25 pg/ml). Antithyroglobulin antibodies (anti-Tg ab), and anti-thyroid peroxidase antibodies (anti-TPO ab) were measured by an ELISA method (BRAHMS), a cut-off level discriminating between positive and negative results was set at 60 IU/L.

The anti-NIS autoantibodies (anti-NIS ab) were detected by in-house ELISA method and confirmed with a Western blot analysis. Additionally, in sera considered positive for anti-NISab were used for iodide uptake bioassay on stable transfected Chinese hamster ovary cell line 7 (COS-7) with hNIS expression.

17.2.1 Iodide Uptake Bioassay

COS-7 cells were grown until they reached approximately 75% confluence. They were then transfected by a lipofectamine technique (Gibco BRL) with pcDNA 3.1 plasmid containing the gene for the full-length hNIS (provided by Dr N. Carrasco, Department of Molecular Pharmacology, Albert Einstein College of Medicine, Bronx, New York) or with a pcDNA3.1 vector only. Forty eight hours after transfection, the COS-7 cells were used for membrane preparation. The membrane from COS-7 cells was prepared by a modification of a previously described procedure (Levy et al. 1997). In brief, COS-7 cells, plated on 100 mm dishes, were washed with ice-cold PBS, harvested, resuspended in ice-cold SBE buffer (250 mM sucrose, 1 mM EDTA, 10 mM HEPES pH 7.4, containing cocktail of proteases inhibitors). The homogenate was centrifuged twice at 500 × *g* for 15 min at 4°C. Following centrifugation, 100 μl of 1 M Na_2CO_3/ml was added to the supernatant and incubated at 4°C for 45 min with continuous shaking. Then, a further centrifugation at 100,000 × *g* was performed for 15 min. The pellet was resuspended in an appropriate volume of the above mentioned buffer and stored at −80°C until use. The presence of hNIS protein in the membrane preparation was always confirmed by SDS-Western blot analysis with site-directed anti-hNIS antibodies. Protein concentration was determined by a BCA micro-method (Pierce Chemical Co., USA).

17.2.2 Synthesis of Human NIS Peptides

Peptides corresponding to the sequences: aa 560–579 (peptide 4th) and aa 629–643 (peptide 5th) were synthesized by a conventional solid phase method and after purity verification they were used for the ELISA method. Affinity chromatography with protein A agarose (Pharmacia, Sweden) was used for IgG purification from all tested sera.

17.2.3 Anti-NIS Antibody Detection by ELISA Method

Maxisorb microtiter plates (Nunc, Denmark) were coated with 100 μl of the membrane protein prepared from transfected COS-7 cells or synthetic hNIS peptides diluted to 10 μg/ml in 0.1 M carbonate buffer pH 9.6, overnight at 4°C, then blocked with 1% bovine serum albumin (BSA) in the same buffer.

Sera diluted at the proportion 1:1,000 or IgGs preparation (1 mg/ml) from the sera in phosphate-buffered saline (PBS), pH 7.4 containing 0.01% Tween 20 and 0.1% BSA was added to each well and incubated overnight at 4°C. The plates were washed three times with PBS-Tween 20 and incubated with affinity-purified anti-human IgG/HRP conjugate diluted 1:10,000 (Jackson Immuno Research, USA) for 2 h at room temperature. After washing, substrate was added (TMB, Sigma, USA) and optical density at 450 nm (OD_{450}) was estimated. Values above the sum of the mean OD_{450} ($\bar{E}$) plus 2SD of the control group were considered the positive result.

The iodide uptake bioassay was performed by a modification of a previously described procedure (Ho Su Chin et al. 2000). In brief, COS-NIS-7 cells stably expressing hNIS have been used.

5,000 COS-NIS-7 cells were seeded in wells of a 96-well flat bottom Polystyrene Microplate (Cultur Plate™, Packard Instrument Company, USA) and grown in DMEM with 10% fetal calf serum for 24 h. Fifty microlitres of diluted serum were added and incubated for an hour at 37°C. Then, 50 μl of Hank's buffer containing 0.05 μCi carrier free Na ^{125}I and 3 μM KI were added and incubated for 30 min at 37°C. After that the cells were rapidly washed with the ice cold Hank's buffer. After the wash 100 μl of MICROSCINT 20 were dispensed into each well and shaken after sealing the top of the microplate with a layer of adhesive plastic. The samples were counted on TopCount (Packard Instrument, USA) for β emission. Non-specific trapping was corrected by 10 μM sodium perchlorate addition and incubation with Hank's buffer instead of the serum. All sera were evaluated in triplicates.

17.2.4 Statistical Analysis

Statistical calculations were performed using a *t*-test, Mann-Withney U-Test, and Pearson's test with the use of statistic software Statistica 7.0. $P<0.05$ was considered statistically significant.

17.3 Results

In 20% of the TS patients hypothyroidism was diagnosed, but only of minimal (subclinical) form (TSH <10 mIU/L and normal or slightly decreased thyroid hormone concentration). The anti-TPO and/or anti-Tg antibodies were present in 38 out of the 54 (70.4%) TS patients. Thirty five TS patients (65%) were positive for anti-TPO ab and 13 (24%) for anti-Tg ab. The mean anti-NIS ab level in sera from the TS patients was significantly higher than that in the control group ($p<0.05$). The anti-NISab were considered as positive, when the OD_{450} value was higher than the mean value in the control group ($\bar{E}_S$) plus 2SD ($\bar{E}_S + 2SD$). In the control subjects, none of the sera reached the OD_{450} above $\bar{E}_S + 2SD$. In the TS patients, the OD_{450} value was higher than $\bar{E}_S + 2SD$ in nine sera and in three of them this value was higher than $\bar{E}_S + 3SD$. Comparable results were found after IgG purification. Among IgG samples, eight were positive, with the OD_{450} values higher than $\bar{E}_{igG} + 2SD$ (Fig. 17.1). Summarizing, increased OD_{450} values were found in both sera and immunoglobulin preparations (Table 17.1) in eight of the TS patients (14.8%).

For the immunoglobulins with increased OD_{450} in the ELISA method for anti-NIS ab, the Western blot analysis was performed (data not shown). The results also suggest the presence of immunoglobulins bound to the NIS protein.

A weak positive correlation was found between high OD_{450} in the ELISA method for anti-NIS ab, and anti-Tg antibodies and the presence of anti-TPO antibodies, but the results were not statistically significant ($r=0.3$; $p>0.05$). Hypothyroidism in the group of TS patients positive for anti-NIS antibodies was more frequent than in the whole group of TS patients: 3/8 (38%) *vs.* 11/54 (20%), $p<0.04$. The iodide uptake in COS7 culture with stable expression of human NIS (hNIS) was not inhibited after the incubation with patients' sera. I-uptake was increased in both TS patients and controls and did not differ between the two groups (Fig. 17.2).

17.4 Discussion

The first report describing NIS as a potential thyroid autoantigen was published by Raspe et al. (1995). Since then many papers considering this issue have been published. Some authors reported the presence of NIS-binding immunoglobulins in patients with autoimmune thyroid diseases, others evaluated

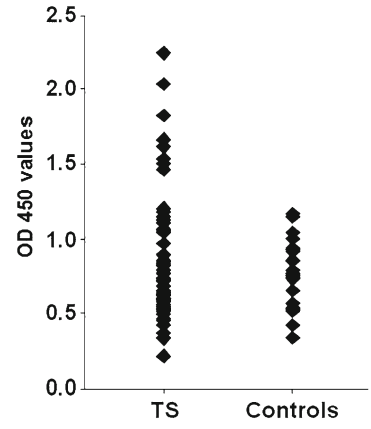

Fig. 17.1 OD_{450} values of IgG samples received in anti-NISab ELISA in Turner's syndrome (TS) girls and controls

Table 17.1 Characteristics of patients positive for anti hNIS ab

Extinction value in sera (OD_{450})	Extinction value in IgG (OD_{450})	Anti-TPOab (IU/L)	Anti-TGab (IU/L)	Subclinical hypothyroidism	Karyotype	Age (years)
2.26[a]	2.04[a]	–	–	+	45,X	14.9
2.25[a]	2.24[a]	201.0	–	+	i(Xq)	11.8
2.20[a]	1.62[b]	570.0	–	+	46,X iX(q)	13.4
2.10[b]	1.83 [b]	36.0	–	–	45,X	12.6
2.01[b]	1.13	615.0	–	–	46,X iX(q)	13.6
2.04[b]	1.61[b]	560.0	–	+	45,X	10.6
1.98[b]	1.54[b]	192.0	–	–	45X/47XXX	4.5
1.91[b]	1.67[b]	670.0	–	–	45,X	9.1
1.87[b]	1.47[b]	420.0	292.0	–	45,X	15.3

[a]OD_{450} higher than the mean value in the control group *+3SD*
[b]OD_{450} higher than the mean value in the control group *+2SD*

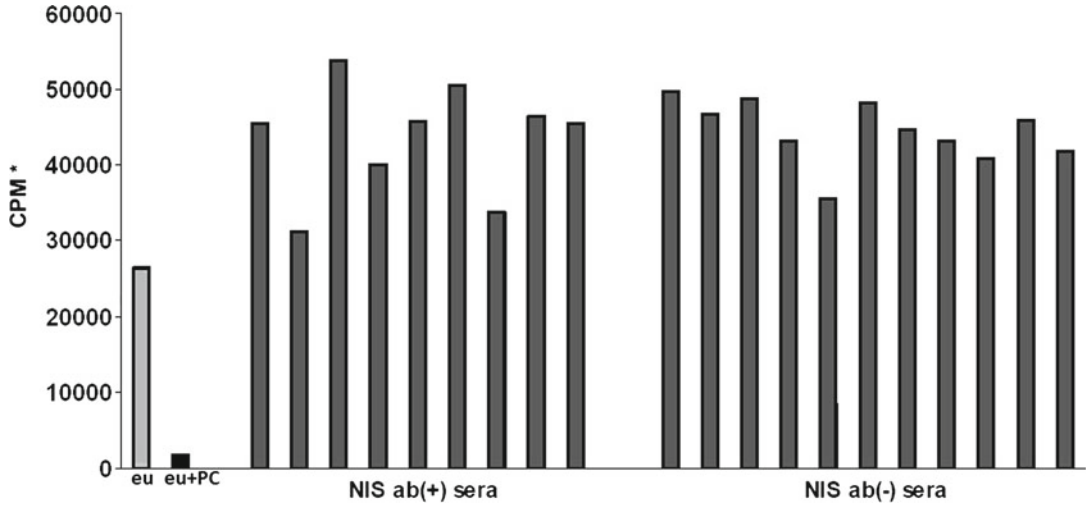

Fig. 17.2 Influence of patients' sera on the iodide uptake in the COS-hNIS7cells. *CPM** the mean value of triplicates, *eu* euthyroid control sample, *eu + PC* euthyroid control with perchlorate addition

also its biological activity. These two effects of the presence of anti-NIS antibodies should be distinguished. The presence of antibodies recognizing NIS protein in patients with autoimmune thyroid diseases confirms that NIS could be an important antigen in autoimmune process, but their biological activity may have variable functional effects, like in case of anti-TSH-receptor antibodies.

In our study, girls with Turner's syndrome were investigated as a group of patients at high risk of autoimmune thyroid diseases development. In serum samples from the majority of them we found antithyroid antibodies. These results confirmed our hypothesis that among out patients there were some in the early stages of autoimmune thyroiditis. Increased OD_{450} values were found by the anti-NIS ELISA method in sera and also in immunoglobulin preparations in 14.8% of TS patients. This result suggests that anti-NIS antibodies belong to the IgG immunoglobulins. Similar results were described by Endo et al. (1996b). They reported that 15% of sera from patients with Hashimoto's thyroiditis and 84% of sera from patients with Graves' disease recognized rat NIS (rNIS) protein in Western blot analysis. Similar results were obtained in purified IgG fractions (Endo et al. 1996b). Morris et al. (1997) also found that autoantibodies against NIS are frequently present in sera of patients with autoimmune thyroid diseases.

Biological activity of anti-NIS antibodies could be measured by their effect on iodide uptake. Different laboratory approaches were used for anti-NIS antibodies activity evaluation. The majority of authors used transfected cell cultures with human or rat NIS expression (Ajjan et al. 1998, 2000; Endo et al. 1996a; Raspe et al. 1995). Inhibition of ^{125}I uptake by anti-NIS antibodies was observed in the studies of Endo et al. (1996a), and Ajjan et al. (1998, 2000). However, both authors suggested that blocking activity of sera from patients with autoimmune thyroid disease is rather rare. Endo et al. (1996a) found only 4 out of the 34 sera of patients with Hashimoto's thyroiditis showing NIS binding IgGs, which suppressed I-uptake in CHO cells with rNIS expression. In another study, Ajjan et al. (2000) found that almost one third of serum samples from patients with Graves' disease and Hashimoto's thyroiditis were positive for anti-NIS antibodies. However, none of them modulated NIS transporting activity. Similarly, Ho Su Chin et al. (2000), Seissler et al. (2000), and Tonacchera et al. (2001) observed that in the sera of patients with autoimmune thyroid diseases the IgGs recognizing NIS protein are rather rare. Ho Su Chin et al. (2000) found that only 14 out of the 299 analyzed sera of patients with autoimmune thyroid diseases inhibited iodide uptake in stably transfected COS7 cell with hNIS expression. Moreover, this inhibitory activity disappeared when fractionated IgGs were examined. These results suggested that the inhibitory effect was not antibody-mediated. Similar data were obtained by Tonacchera et al. (2001). The authors evaluated the effects of sera and purified IgGs from both Graves' disease and Hashimoto's thyroiditis on biological activity of the NIS protein. They showed that several serum samples inhibited I-uptake *in vitro*, but none of the purified preparation of IgG had an inhibitory activity. In the present study we used the bioassay with stably transfected COS7 cells with hNIS expression to detect the inhibition of ^{125}I uptake. However, we did not detect an inhibition of I-uptake by sera containing anti-NIS antibodies. Surprisingly, an increase in the I-uptake was observed in the presence of both patients and control sera. We cannot explain this finding. Nevertheless, taking into account that the present study was performed during the first years of mandatory salt iodination in Poland, one can speculate that the increase of I-uptake might depend on the process of elimination of iodine deficiency. However, it is difficult to elucidate the mechanism of this stimulatory effect of sera we observed. Seissler et al. (2000) analyzed anti-NIS antibodies frequency and their activity, using recombinant hNIS expressed by *in vitro* transcription and translation method, in a large group of patients with autoimmune thyroid diseases. In that study, the prevalence of anti-NIS antibodies was higher in patients with Hashimoto's thyroiditis than in those with Graves' disease: 20.8% *vs.* 10.7% respectively, although it was rather low in the both groups. Little is known about the clinical consequences and associations of anti-NIS antibodies in patients with autoimmune thyroiditis. Seissler et al. (2000) found a weak positive correlation between anti-hNIS and anti-TPO antibodies ($r = 0.35$, $p < 0.05$). We also found a weak positive, but not significant, correlation between the anti-NIS antibodies and anti-Tg or anti-TPO antibodies. Furthermore, we observed an appreciable

correlation between subclinical hypothyroidism and the presence of anti-NIS ab. Since the antibodies did not suppress I-uptake, we presume that hypothyroidism might be a result of some other mechanisms of their activity or unrelated to their presence. The anti-NIS antibodies might be only an additional marker of autoimmune disease. However, a positive correlation with hypothyroidism in our study and with other antithyroid antibodies in other works (Seissler et al. 2000) suggests that injury of thyroid cells is somehow related to the presence of anti-NIS antibodies at the beginning of an autoimmune process. The clinical and pathogenic role of anti-NIS antibodies in autoimmune thyroid diseases remains to be elucidated in further studies.

Acknowledgement We wish to thank Prof. Nancy Carrasco of the Department of Molecular Pharmacology, Albert Einstein College of Medicine, Bronx, New York for the gift of the plasmid containing full length human NIS cDNA. The authors also thank Dr Cornelia Rinderle of the BRAHMS Diagnostica GmbH Henningsdorf in Berlin for the evaluation of iodide uptake in bioassay.

Conflicts of interest: The authors declare no conflicts of interest in relation to this article.

References

Ajjan, R. A., Findlay, C., Metcalfe, R. A., Watson, P. F., Crisp, M., Ludgaten, M., & Weetman, A. P. (1998). The modulation of the human sodium iodide symporter activity by Graves' disease sera. *Journal of Clinical Endocrinology and Metabolism, 83*, 1217–1221.

Ajjan, R. A., Kemp, E. H., Waterman, E. A., Watson, P. F., Endo, T., Onaya, T., & Weetman, A. P. (2000). Detection of binding and blocking autoantibodies to the human sodium-iodide symporter in patients with autoimmune thyroid disease. *Journal of Clinical Endocrinology and Metabolism, 85*, 2020–2027.

Chin, H. S., Chin, D. K., Morgenthaler, N. G., Vassart, G., & Costagliola, S. (2000). Rarity of anti-Na/I symporter (NIS) antibody with iodide uptake inhibiting activity in autoimmune thyroid diseases (AITD). *Journal of Clinical Endocrinology and Metabolism, 85*, 3937–3940.

Chiovato, L., Larizza, D., Bendinelli, G., Tonacchera, M., Marino, M., Mammoli, C., Lorini, R., Severi, F., & Pinchera, A. (1996). Autoimmune hypothyroidism and hyperthyroidism in patients with Turner's syndrome. *European Journal of Endocrinology, 134*, 568–575.

Dai, G., Levy, O., & Carrasco, N. (1996). Cloning and characterization of the thyroid iodide transporter. *Nature, 379*, 458–460.

Dohan, O., De la Vieja, A., Paroder, V., Riedel, C., Artani, M., Reed, M., Ginter, Ch. S., & Carrasco, N. (2003). The sodium/iodide symporter (NIS): Characterisation, regulation, and medical significance. *Endocrine Reviews, 24*, 48–77.

Elsheikh, M., Wass, J. A. H., & Conway, G. S. (2001). Autoimmune thyroid syndrome in women with Turner's syndrome-the association with karyotype. *Clinical Endocrinology, 55*, 223–226.

Endo, T., Kaneshige, M., Nakazato, M., Kogai, T., Saito, T., & Onaya, T. (1996a). Autoantibody against thyroid iodide transporter in the sera from patients with Hashimoto's thyroiditis possesses iodide transport inhibitory activity. *Biochemical and Biophysical Research Communications, 228*, 199–202.

Endo, T., Kogai, T., Nakazato, M., Saito, T., Kaneshige, M., & Onaya, T. (1996b). Autoantibody against Na/I symporter in the sera of patients with autoimmune thyroid disease. *Biochemical and Biophysical Research Communications, 224*, 92–95.

Germain, E. L., & Plotnick, L. P. (1986). Age-related anti-thyroid antibodies and thyroid abnormalities in Turner's syndrome. *Acta Paediatrica Scandinavica, 75*, 750–755.

Gruñeiro de Papendieck, L., Iorkansky, S., Coco, R., Rivarola, M. A., & Bergada, C. (1987). High incidence of thyroid disturbances in 49 children with Turner's syndrome. *The Journal of Pediatrics, 111*, 258–261.

Levy, O., Dai, G., Riedel, C. X., Ginter, C. S., Paul, E. M., Lebowitz, A. N., & Carrasco, N. (1997). Characterisation of the thyroid Na^+/I symporter with an anti-COOH terminus antibody. *Proceedings of the National Academy of Sciences of the United States of America, 94*, 5568–5573.

Morris, J. C., Bergert, E. R., & Bryant, W. P. (1997). Binding of immunoglobulin G from patients with autoimmune thyroid disease to rat sodium-iodide symporter peptides: Evidence for the iodide transporter as an autoantigen. *Thyroid, 7*, 527–534.

Radetti, G., Mazzanti, L., Paganini, C., Bernasconi, S., Russo, G., Rigon, F., & Cacciari, E. (1995). Frequency, clinical and laboratory features of thyroiditis in girls with Turner's syndrome. *Acta Paediatrica, 84*, 909–912.

Radetti, G., Gottardi, E., Bona, G., Corrias, A., Salardi, S., Loche, S., & Study Group for Thyroid Diseases of the Italian Society for Pediatric Endocrinology and Diabetes (SIEDP/ISPED). (2006). The natural history of euthyroid Hashimoto's thyroiditis in children. *The Journal of Pediatrics, 149*, 827–832.

Raspe, E., Costagliola, S., Ruf, J., Mariotti, S., Dumont, J. E., & Ludgate, M. (1995). Identification of the thyroid Na/I cotransporter as a potential autoantigen in thyroid autoimmune disease. *European Journal of Endocrinology, 132*, 399–405.

Riesco-Eizaguirre, G., & Santisteban, P. (2006). A perspective view of sodium iodide symporter research and its clinical implications. *European Journal of Endocrinology, 155*, 495–512.

Saenger, P., Albertsson Wikland, K., Conway, G. S., Davenport, M., Gravholt, C. H., Hintz, R., Hovatta, O., Hultcrantz, M., Landin-Wilhelmsen, K., Lin, A., Lippe, B., Pasquino, A. M., Ranke, M. B., Rosenfeld, R., & Silberbach, M. (2001). Recommendations for the diagnosis and management of Turner's syndrome. *Journal of Clinical Endocrinology and Metabolism, 86*, 3061–3069.

Seissler, J., Wagner, S., Schott, M., Lettmann, M., Feldkamp, J., Scherbaum, W. A., & Morgenthaler, N. G. (2000). Low frequency of autoantibodies to the human Na/I symporter in patients with autoimmune thyroid disease. *Journal of Clinical Endocrinology and Metabolism, 85*, 4630–4634.

Smanik, P. A., Liu, Q., Furminger, T. L., Ryu, K., Xing, S., Mazzaferri, E. L., & Jhiang, S. M. (1996). Cloning of the human sodium iodide symporter. *Biochemical and Biophysical Research Communications, 226*, 339–345.

Tonacchera, M., Agretti, P., Ceccarini, G., Lenza, R., Refetoff, S., Santini, F., Pinchera, A., Chiovato, L., & Vitti, P. (2001). Autoantibodies from patients with autoimmune thyroid disease do not interfere with the activity of the human iodide symporter gene stably transfected in CHO cells. *European Journal of Endocrinology, 144*, 611–618.

Chapter 18
Influence of Sera from Interstitial Lung Disease Patients on Angiogenic Activity of Mononuclear Cells

T.M. Zielonka, K. Zycinska, E. Radzikowska, M. Filewska, B. Bialas, M.H. Obrowski, E. Skopinska-Rozewska, and U. Demkow

Abstract Chronic inflammation stimulates of neovascularization. The aim of this study was to evaluate the effect of sera from interstitial lung diseases (ILD) patients on angiogenic capabilities of different subsets of mononuclear cells. Serum samples were obtained from 22 patients with sarcoidosis, 20 with hypersensitivity pneumonitis, 20 with idiopathic pulmonary fibrosis, 9 with systemic sclerosis, 6 with pulmonary Langerhans cells histiocytosis, and from 20 healthy volunteers. Animal model of leukocyte induced angiogenesis assay was used as an angiogenic test. The pattern of angiogenic reaction was different in different diseases. Sera from systemic sclerosis and pulmonary Langerhans cells histiocytosis patients exerted inhibitory effects on angiogenesis, but sera from sarcoidosis, hypersensitivity pneumonitis, and idiopathic pulmonary fibrosis patients stimulated angiogenesis. Sera from sarcoidosis and pulmonary Langerhans cells histiocytosis primed monocytes for the production of angiogenic factors. The number of microvessels created after incubation of mononuclear cells depleted of monocytes with sera from systemic sclerosis patients significantly decreased. We conclude that the role of monocytes in the modulation of angiogenesis varies depending on the type of ILD. Sera from sarcoidosis stimulate and from pulmonary Langerhans cells histiocytosis patients inhibit neovascularization induced by monocyte mediators. Sera from systemic sclerosis inhibit angiogenesis induced by lymphocyte products.

Keywords Angiogenesis • Chronic inflammation • Interstitial lung disease • Lymphocytes • Monocytes

T.M. Zielonka (✉) • K. Zycinska • M.H. Obrowski
Department of Family Medicine, Medical University of Warsaw, Banacha 1a St,
02-097 Warsaw, Poland
e-mail: tmzielonka@wp.pl

E. Radzikowska
Department of Lung Diseases, Institute of Tuberculosis and Lung Diseases,
Plocka 26 St, 01-138 Warsaw, Poland

M. Filewska • B. Bialas
Department of Laboratory Diagnostics and Immunology, Institute of Tuberculosis and Lung Diseases,
Plocka 26 St, 01-138 Warsaw, Poland

E. Skopinska-Rozewska
Department of Pathology, Biostructure Center, Medical University of Warsaw,
Chalubinskiego 5 St, 02-004 Warsaw, Poland

U. Demkow
Department of Laboratory Diagnostics and Clinical Immunology of the Developmental Age,
Medical University of Warsaw, Marszalkowska 24 St, 00-576 Warsaw, Poland

M. Pokorski (ed.), *Respiratory Regulation - The Molecular Approach*,
Advances in Experimental Medicine and Biology 756, DOI 10.1007/978-94-007-4549-0_18,

18.1 Introduction

The growth of new blood vessels is possible through vasculogenesis (the mobilization of bone marrow-derived endothelial stem cells) or angiogenesis (direct proliferation of endothelial cells) (Carmeliet and Jain 2000; Semenza 2007; Hirshoren et al. 2010). A difference between physiological and pathological angiogenesis is that the latter is often induced by inflammation (Lingen 2001). Interstitial lung diseases (ILD) are characterized by inflammation, cell proliferation, and excessive extracellular matrix deposition (Keane and Strieter 2002). An increase in angiogenic activity has been demonstrated in the lung tissue of idiopathic pulmonary fibrosis (IPF) (Keane et al. 1997; Renzoni et al. 2003). Pro- and anti-angiogenic factors are produced by tumor cells, fibroblasts, endothelial or immunological cells, and also extracellular matrix (Carmeliet and Jain 2000; Griffioen and Molema 2000). Many stimulators of inflammation such as interleukin-1 (IL-1), IL-6, IL-8, basic fibroblast growth factor, vascular endothelial growth factor (VEGF), platelet derived growth factor, tumor necrosis factor alpha (TNFα) also demonstrate pro-angiogenic properties. On the other side, inhibitors of inflammation such as IL-10, IL-12, interferon gamma (INFγ), and transforming growth factor beta (TGFß) affect adult blood vessel formation (Pepper et al. 1996). Increased expression of VEGF (fundamental regulator of angiogenesis) has been demonstrated in sarcoid granulomas and alveolar macrophages (Tolnay et al. 1998). Recently, we have described that sera from extrinsic allergic alveolitis (Zielonka et al. 2010) and other ILD patients (Zielonka et al. 2007) constitute a source of mediators participating in angiogenesis. The role of angiogenesis in the pathogenesis of ILD is unclear. Yet, the understanding of this role could lead to the development of new target drugs. The aim of the present study was to evaluate the effect of sera from ILD patients on the angiogenic capability of different subsets of human peripheral blood mononuclear cells.

18.2 Methods

18.2.1 Patients

The study was approved by a local Ethics Committee and informed consent was obtained from all participants of the study. The examined group consisted of 77 patients with ILD (Table 18.1). The diagnosis of sarcoidosis (SAR) was made according to ATS/ERS/WASOG standards (Hunninghake et al. 1999). On the basis of chest X-rays, 3 patients were classified in Stage I; 12 in Stage II, and 7 in Stage III. The diagnosis of idiopathic pulmonary fibrosis (IPF) was based on American Thoracic

Table 18.1 Characteristics of examined groups

	n	Age Means ± SD	Female/Male (n)	Smokers/ Nonsmokers (n)
PLH	6	35.4 ± 8.3	2/4	6/0
SSC	9	50.0 ± 11.3	8/1	0/9
HP	20	47.0 ± 14.5	7/13	5/15
IPF	20	61.6 ± 12.4	8/12	5/15
SAR	22	41.9 ± 11.9	8/14	6/16
Healthy volunteers	20	38.7 ± 11.4	8/12	2/18

PLH pulmonary Langerhans cells histiocytosis, *SSC* systemic sclerosis, *HP* hypersensitivity pneumonitis, *IPF* idiopathic pulmonary fibrosis, *SAR* sarcoidosis

Society and European Respiratory Society standards (ATS/ERS 2002). The diagnosis of hypersensitivity pneumonitis (HP) – bird fancier's lung, was based on clinical, radiological and serological criteria, bronchoalveolar lavage fluid (BALF), and histopathological findings. Systemic sclerosis (SSC) with pulmonary manifestations was diagnosed according to the American Rheumatism Association criteria (ARA 1980). The diagnosis of pulmonary Langerhans cells histiocytosis (PLH) in all cases was based on a lung biopsy. Blood samples were drawn before any treatment was started. Sera from 20 healthy volunteers were used as control.

18.2.2 Mononuclear Cell (MNC) Preparation

Peripheral blood MNC derived from the buffy-coat cells of healthy blood donors (Central Warsaw Blood Bank) were prepared using the gradient technique. Mononuclear cells viability was assessed by trypan blue exclusion (≥98%). This method yielded MNC preparation containing 10–15% monocytes and 85–90% lymphocytes, based on morphologic criteria and MPO staining. MNC were depleted in monocytes by glass adherence and the phagocytosis of iron particles using 15 mg of iron particles per 10×10^6 cells.

18.2.3 Angiogenic Test

As an angiogenic test, we used a leukocyte induced angiogenesis assay in an animal model (Sidky and Auerbach 1975) with some modifications (Zielonka et al. 2010). Animal handling in all the experiments conformed to the Polish legal requirements for the protection of animals and to NIH standards. Lymphocytes or MNC were incubated under identical conditions in PBS supplemented with 25% of the same serum from ILD patients. As control, we used MNC or lymphocytes incubated in PBS supplemented with 25% of serum from health donors or PBS only. After 1 h of incubation, MNC and or lymphocytes were washed and suspended in Parker medium (5×10^6 cells/ml). Inbred 8–10-weeks old female BALB/c anesthetized mice were injected intradermally with these cells. After 72 h, newly formed blood vessels localized to the inner surface of the skin of each mouse were counted using a microscope (Nikon, Japan) at 6x magnification. The result was evaluated blindly by the same person based on the previously described criteria (Sidky and Auerbach 1975).

18.2.4 Statistical Analysis

Results were expressed as means ± SD of microvessels. A *t*-test for independent samples was used to determine differences between groups. $P < 0.05$ was used to indicate statistical significance. Analysis was performed using the Statistica 6 for Windows package.

18.3 Results

The effects on angiogenesis of sera obtained from the patients with different ILD are presented in Fig. 18.1. The HP, SAR, and IPF patients' sera stimulated angiogenesis compared with the sera from healthy volunteers. However, normal sera also exerted a stimulatory effect on angiogenesis compared

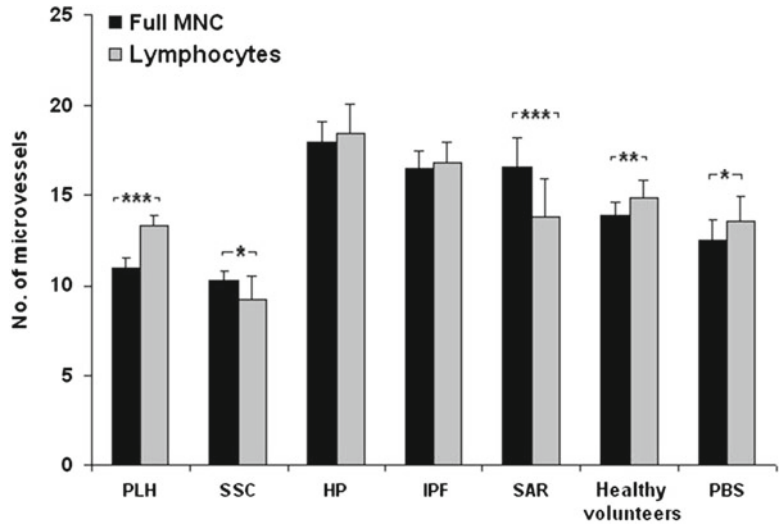

Fig. 18.1 Number of microvessels after injection of full mononuclear cell suspension or lymphocytes incubated with sera from patients with various interstitial lung diseases. *PLH* pulmonary Langerhans cells histiocytosis, *SSC* systemic sclerosis, *HP* hypersensitivity pneumonitis, *IPF* idiopathic pulmonary fibrosis, *SAR* sarcoidosis, *PBS* phosphate buffer solution; *$p<0.05$, **$p<0.01$, ***$p<0.001$

with PBS. The PLH and SSC patients' sera strongly decreased the angiogenic capability of MNC compared with PBS. The number of microvessels created after incubation of lymphocytes with the PLH patients' sera was higher compared with that found with the full MNC suspension incubation. However, the situation was the reverse when lymphocytes were incubated with the SSC patients' sera; here the number of microvessels was significantly higher with the full MNC suspension. The angiogenic effects of the HP and IPF patients' sera were similar for both MNC and lymphocytes. The number of microvessels created after injection of lymphocytes incubated with the SAR patients' sera was significantly lower compared with that after injection of full MNC suspension incubated with the same sera. Finally, the number of microvessels created after injection of lymphocytes incubated with the healthy volunteers' sera or just in PBS was higher compared with that after injection of full MNC suspension (Fig. 18.1).

18.4 Discussion

Recently, we have more evidence of the role that angiogenesis plays in the pathogenesis of ILD (Renzoni et al. 2003; Zielonka et al. 2010; Antoniou et al. 2006; Navarro et al. 2003). The possible role of alveolar neovascularization in the regeneration of alveolar septa in IPF is discussed as a significant increase in alveolar capillaries in non-fibrotic lesions, and a decrease in fibrotic lesions (Ebina et al. 2004). Although angiogenesis is not mentioned in the pathogenesis of disease by the ATS/ERS/WASOG statement on sarcoidosis, many observations suggest the important role of angiogenesis (Tolnay et al. 1998; Antoniou et al. 2006; Meyer et al. 1989).

Particular attention is paid to the mediators of angiogenesis and their receptors in both pathological changes and in the blood. (Keane et al. 1997; Pepper et al. 1996; Zielonka et al. 2007; Navarro et al. 2003; Simler et al. 2004). Increased angiogenic activity in lung tissue of IPF provoked by pro- and anti-angiogenic CXC chemokine imbalance has been demonstrated (Keane et al. 1997). Simler et al. (2004) have shown that patients with IPF have significantly higher baseline plasma

concentrations of IL-8 and endothelin-1, but not of VEGF, compared with healthy controls. Navarro et al. (2003) have demonstrated a significant increase in the VEGF in HP patients' serum and in BAL fluid in relation to healthy subjects. Previously, we have demonstrated a correlation between the angiogenic activity of ILD patients' sera and TNFα serum concentration, but we did not observe the relationship with IL-6, IL-8, or IL-12 (Zielonka et al. 2007).

Much less is known about the role of cells involved in angiogenesis of ILD patients. Interstitial lung diseases are a heterogeneous group of disorders dependant on different mechanisms, cells, and mediators. In sarcoidosis and hypersensitivity pneumonitis, lymphocytes play a central role (Hunninghake et al. 1999). However in IPF, neutrophils are more important (ATS/ERS 2002). Previously, we have demonstrated that sera from ILD patients constitute a source of mediators modulating angiogenesis (Zielonka et al. 2007, 2010). The present study demonstrated different roles of monocytes and lymphocytes in the modulation of angiogenesis under the influence of mediators in the serum of patients with various forms of ILD. Removal of monocytes from MNC resulted in significant changes, especially in patients with sarcoidosis and histiocytosis. MNC strongly stimulated vascularization under the influence of mediators in the serum of patients with sarcoidosis, in comparison with sera from healthy individuals or with PBS. The sera of patients with PLH significantly inhibited this process. Sera of patients with sarcoidosis and PHL, with MNC depleted of monocytes, influenced the process of neovascularization in the same manner as incubation with PBS. That indicates a crucial role of monocytes in angiogenesis in sarcoidosis and in PLH.

Proangiogenic factors in sera from sarcoidosis patients modulate neovascularization evidently through monocytes. This has been confirmed by previous studies of Meyer et al. (1989), who demonstrated an increase in the angiogenesis-inducing ability of the activated alveolar macrophages in BALF specimens obtained from sarcoidosis patients. Okabe and Takaku (1986) identified in a culture of macrophages from sarcoidosis patients, a factor stimulating the proliferation of vascular endothelial cells. Tests using the *in situ* hybridisation and immunohistochemistry of lung cross-sections in sarcoidosis patients provided evidence of increased expression of mRNA for VEGF in lung macrophages (Tolnay et al. 1998). We demonstrated that there are angiogenesis inhibitory factors in the sera of adult patients with PLH, which monocyte-related.

The role of angiogenesis in PLH has not yet been determined. The pathological picture in PLH confirms only vasculitis, with no excessive vascularization, and destructive lesions of a cystic type, accompanied by poorer vascularization (Kambouchner et al. 2002). Interestingly, sera exerted an inhibitory effect when macrophages were present. A high macrophage count in BALF patients with PLH is a common, but nonspecific finding, which merely reflects exposure to tobacco (Uebelhoer et al. 1995). An increase in oxygen radical release and fibronectin production leads to tissue injury and increased fibrosing capacity of alveolar macrophages in PLH (Uebelhoer et al. 1995).

Contrary to sera of patients with sarcoidosis, sera of healthy individuals stimulated angiogenesis mainly through lymphocytes. Removal of monocytes from MNC resulted in a significant increase in the number of newly formed vessels under the influence of lymphocytes incubated either with control sera, or with PBS. Lymphocytes incubated with the serum of patients with IPF or HP stimulated angiogenesis to a similar extent as the MNC incubated with the same sera. Although sera of patients with sarcoidosis, IPF, and HP exhibited proangiogenic activity, the effects were mediated by different cells. Unlike in sarcoidosis, IPF patient's sera exerted its angiogenic effect not only through monocytes, which may be linked to a distinct profile of cytokines and cells participating in this process in IPF patients (Antoniou et al. 2006). Whereas in the pathogenesis of sarcoidosis macrophages play a key role, in IPF the most significant role is attributed to neutrophils and fibroblasts (Lynch et al. 1992). Keane et al. (1997, 2001) have demonstrated that angiogenic members of the CXC chemokine family, such as IL-8 and epithelial neutrophil activating protein ENA-78, increase the expression in fibrotic lung tissue compared with the angiostatic chemokines. In HP, the pathogenesis is more complex and depends upon the disease activity and exposure to an allergen leading to the formation of granulomas within the lung (Girard et al. 2004). Granulomatous inflammation also is

observed in sarcoidosis (Hunninghake et al. 1999). However, the clinical course of both diseases varies. In the presented model, sera of HP patients showed the strongest proangiogenic effect. Navarro et al. (2003) have demonstrated a significant increase in the VEGF in HP patients' serum and in BALF in relation to healthy subjects. Although the sera of patients with sarcoidosis and HP stimulate angiogenesis, different cells participate in the process.

In contrast to all other groups, lymphocytes of healthy donors incubated with sera from patients with SSC strongly inhibited vascular angiogenesis compared with MNC incubated with sera from the same patients. Functional and structural vascular disorders constitute an important element in the course of progressive SSC (Herrick 2000). Previous works have demonstrated increased serum angiogenic activity in a limited form of the disease. In systemic forms, however, serum angiogenic activity was weaker than in healthy controls (Majewski et al. 1985). The imbalanced expression of VEGF and its vascular receptors is in part due to insufficient local production of VEGF; too low compared with VEGF receptor expression and is responsible for angiogenesis failure in SSC (Mackiewicz et al. 2002). The angiogenic effects of VEGF also may be inhibited by a concomitant increase of angiostatic factors. Endostatin has been characterized as a potent inhibitor of VEGF-induced angiogenesis (Yamaguchi et al. 1999). The angioinhibitory effect is more pronounced following depletion of monocytes from MNC, which suggests that lymphocytes incubated with sera from SSC patients are responsible for the inhibition, contrary to the situation observed in other ILD.

Interstitial lung diseases represent a diverse group of diseases with different etiology and pathogenesis. Growing evidence indicates the role of angiogenesis in the pathogenesis of these diseases both in inflammatory and fibrotic changes in the lungs. The role of neovascularization in ILD seems variable. This may depend on both type and severity of disease. Angiogenesis in ILD is a complex process that depends on many factors, both inhibitory and stimulatory. The presented results demonstrate that the serum factors affect angiogenesis by various cells, which underscores the diversity of angiogenesis modulating mechanisms and a limited understanding of the process. Normalization of angiogenesis in ILD could provide a future therapeutic target.

Acknowledgments Supported by an internal grant of the Institute of Tuberculosis and Lung Diseases in Warsaw.

Conflicts of interest: No conflict of interest was declared with relation to this work.

References

Antoniou, K. M., Tzouvelekis, A., Alexandrakis, M. G., Sfiridaki, K., Tsiligianni, I., Rachiotis, G., Tzanakis, N., Bouros, D., Milic-Emili, J., & Siafakas, N. M. (2006). Different angiogenic activity in pulmonary sarcoidosis and idiopathic pulmonary fibrosis. *Chest, 130*(4), 982–988.

ARA. Subcommittee for scleroderma criteria of the American Rheumatism Association Diagnostic and Therapeutic Criteria Committee. (1980). Preliminary criteria for the classification of systemic sclerosis (scleroderma). *Arthritis and Rheumatism, 23*(5), 581–590.

ATS/ERS. (2002). International multidisciplinary consensus classification of the idiopathic interstitial pneumonias. *American Journal of Respiratory and Critical Care Medicine, 165*(3), 277–304.

Carmeliet, P., & Jain, R. K. (2000). Angiogenesis in cancer and other diseases. *Nature, 407*(6801), 249–257.

Ebina, M., Shimizukawa, M., Shibata, N., Kimura, Y., Suzuki, T., Endo, M., Sasano, H., Kondo, T., & Nukiwa, T. (2004). Heterogeneous increase in CD34-positive alveolar capillaries in idiopathic pulmonary fibrosis. *American Journal of Respiratory and Critical Care Medicine, 169*(11), 1203–1208.

Girard, M., Israël-Assayag, E., & Cormier, Y. (2004). Pathogenesis of hypersensitivity pneumonitis. *Current Opinion in Allergy and Clinical Immunology, 4*(2), 93–98.

Griffioen, A. W., & Molema, G. (2000). Angiogenesis: Potentials for pharmacologic intervention in the treatment of cancer, cardiovascular diseases, and chronic inflammation. *Pharmacological Reviews, 52*(2), 237–268.

Herrick, A. L. (2000). Vascular function in systemic sclerosis. *Current Opinion in Rheumatology, 12*(6), 527–533.

Hirshoren, N., Neuman, T., Gross, M., & Eliashar, R. (2010). Angiogenesis in chronic rhinosinusitis with nasal polyps and in antrochoanal polyps. *Inflammation Research, 60*(4), 321–327.

Hunninghake, G. W., Costabel, U., Ando, M., Baughman, R., Cordier, J. F., du Bois, R., Eklund, A., Kitaichi, M., Lynch, J., Rizzato, G., Rose, C., Selroos, O., Semenzato, G., & Sharma, O. P. (1999). ATS/ERS/WASOG statement on sarcoidosis. *Sarcoidosis, Vasculitis, and Diffuse Lung Diseases, 16*(2), 149–173.

Kambouchner, M., Basset, F., Marchal, J., Uhl, J. F., Hance, A. J., & Soler, P. (2002). Three-dimensional characterization of pathologic lesions in pulmonary Langerhans cell histiocytosis. *American Journal of Respiratory and Critical Care Medicine, 166*(11), 1483–1490.

Keane, M. P., & Strieter, R. M. (2002). The importance of balanced pro-inflammatory and anti-inflammatory mechanisms in diffuse lung disease. *Respiratory Research, 3*(1), 5–11.

Keane, M. P., Arenberg, D. A., Lynch, J. P., 3rd, Whyte, R. I., Iannettoni, M. D., Burdick, M. D., Wilke, C. A., Morris, S. B., Glass, M. C., DiGiovine, B., Kunkel, S. L., & Strieter, R. M. (1997). The CXC chemokines, IL-8 and IP-10, regulate angiogenic activity in idiopathic pulmonary fibrosis. *The Journal of Immunology, 159*(3), 1437–1443.

Keane, M. P., Belperio, J. A., Burdick, M. D., Lynch, J. P., Fishbein, M. C., & Strieter, R. M. (2001). ENA-78 is an important angiogenic factor in idiopathic pulmonary fibrosis. *American Journal of Respiratory and Critical Care Medicine, 164*(12), 2239–2242.

Lingen, M. W. (2001). Role of leukocytes and endothelial cells in the development of angiogenesis in inflammation and wound healing. *Archives of Pathology & Laboratory Medicine, 125*(1), 67–71.

Lynch, J. P., 3rd, Standiford, T. J., Rolfe, M. W., Kunkel, S. L., & Strieter, R. M. (1992). Neutrophilic alveolitis in idiopathic pulmonary fibrosis. The role of interleukin-8. *The American Review of Respiratory Disease, 145*(6), 1433–1439.

Mackiewicz, Z., Sukura, A., Povilenaité, D., Ceponis, A., Virtanen, I., Hukkanen, M., & Konttinen, Y. T. (2002). Increased but imbalanced expression of VEGF and its receptors has no positive effect on angiogenesis in systemic sclerosis skin. *Clinical and Experimental Rheumatology, 20*(5), 641–646.

Majewski, S., Skopinska-Rozewska, E., Jablonska, S., Polakowski, I., Pawinska, M., Marczak, M., & Szmurlo, A. (1985). Modulatory effect of sera from scleroderma patients on lymphocyte-induced angiogenesis. *Arthritis and Rheumatism, 28*(10), 1133–1139.

Meyer, K. C., Kaminski, M. J., Calhoun, W. J., & Auerbach, R. (1989). Studies of bronchoalveolar lavage cells and fluids in pulmonary sarcoidosis. I Enhanced capacity of bronchoalveolar lavage cells from patients with pulmonary sarcoidosis to induce angiogenesis in vivo. *The American Review of Respiratory Disease, 140*(5), 1446–1449.

Navarro, C., Ruiz, V., Gaxiola, M., Carrillo, G., & Selman, M. (2003). Angiogenesis in hypersensitivity pneumonitis. *Archives of Physiology and Biochemistry, 111*(4), 365–368.

Okabe, T., & Takaku, F. (1986). A macrophage factor that stimulates the proliferation of vascular endothelial cells. *Biochemical and Biophysical Research Communications, 134*(1), 344–350.

Pepper, M. S., Mandriota, S. J., Vassalli, J. D., Orci, L., & Montesano, R. (1996). Angiogenesis-regulating cytokines: Activities and interactions. *Current Topics in Microbiology and Immunology, 213*(Pt 2), 31–67.

Renzoni, E. A., Walsh, D. A., Salmon, M., Wells, A. U., Sestini, P., Nicholson, A. G., Veeraraghavan, S., Bishop, A. E., Romanska, H. M., Pantelidis, P., Black, C. M., & Du Bois, R. M. (2003). Interstitial vascularity in fibrosing alveolitis. *American Journal of Respiratory and Critical Care Medicine, 167*(3), 438–443.

Semenza, G. L. (2007). Vasculogenesis, angiogenesis, and arteriogenesis: Mechanisms of blood vessel formation and remodeling. *Journal of Cellular Biochemistry, 102*(4), 840–847.

Sidky, Y. A., & Auerbach, R. (1975). Lymphocyte-induced angiogenesis: A quantitative and sensitive assay for the graft-versus-host reaction. *The Journal of Experimental Medicine, 141*(5), 1084–1101.

Simler, N. R., Brenchley, P. E., & Horrocks, A. W. (2004). Angiogenic cytokines in patients with idiopathic interstitial pneumonia. *Thorax, 59*(7), 581–585.

Tolnay, E., Kuhnen, C., Voss, B., Wiethege, T., & Müller, K. M. (1998). Expression and localization of vascular endothelial growth factor and its receptor fit in pulmonary sarcoidosis. *Virchows Archiv, 432*(1), 61–65.

Uebelhoer, M., Bewig, B., Sternberg, K., Rabe, K., Nowak, D., Magnussen, H., & Barth, J. (1995). Alveolar macrophages from bronchoalveolar lavage of patients with pulmonary histiocytosis X: Determination of phenotypic and functional changes. *Lung, 173*(3), 187–195.

Yamaguchi, N., Anand-Apte, B., Lee, M., Sasaki, T., Fukai, N., Shapiro, R., Que, I., Lowik, C., Timpl, R., & Olsen, B. R. (1999). Endostatin inhibits VEGF-induced endothelial cell migration and tumor growth independently of zinc binding. *The EMBO Journal, 18*(16), 4414–4423.

Zielonka, T. M., Demkow, U., Filewska, M., Radzikowska, E., Bialas, B., Korczynski, P., Szopiński, J., Soszka, A., & Skopinska-Rozewska, E. (2007). Angiogenic activity of sera from interstitial lung diseases patients to IL-6, IL-8, IL-12 and TNFα serum level. *Central European Journal of Immunology, 32*(1), 53–60.

Zielonka, T. M., Demkow, U., Filewska, M., Bialas, B., Zycinska, K., Radzikowska, E., Wardyn, A. K., & Skopinska-Rozewska, E. (2010). Angiogenic activity of sera from extrinsic allergic alveolitis patients in relation to clinical, radiological, and functional pulmonary changes. *Lung, 188*(5), 375–380.

Chapter 19
Antiendothelial Cells Antibodies in Patients with Systemic Sclerosis in Relation to Pulmonary Hypertension and Lung Fibrosis

K. Lewandowska, M. Ciurzynski, E. Gorska, P. Bienias, K. Irzyk, M. Siwicka, K. Zycinska, P. Pruszczyk, and U. Demkow

Abstract Although scleroderma is generally considered a fibrosing disease, it is now recognized that the underlying vascular pathology is playing a fundamental role in its pathogenesis. The present study was aimed at testing the prevalence of anti-endothelial cell antibodies (AECA) in systemic scleroderma (SSc) patients with and without pulmonary hypertension (PH) and in relation to the presence of pulmonary fibrosis. Fifty four SSc patients (50 females and 4 male, mean age 55.7 ± 16.3 years) were prospectively screened. All patients underwent transthoracic echocardiography with the estimation of pulmonary artery pressure (PAP) and tricuspid regurgitant peak gradient (TRPG). All patients suspected to have pulmonary hypertension were referred for right heart catheterization. Restrictive lung disease was confirmed by HRCT. A healthy control group included (n = 27; 7 men and 20 women, mean age 49.8 ± 12.1 years). The study of AECA was performed using the indirect immunofluorescence method on commercially available human umbilical vein endothelial cells. The HRCT scans in patients with suspected interstitial lung disease revealed signs of lung fibrosis in 15 (out of the 36 examined patients). TRPG at rest of 31 mmHg was demonstrated in 14 (21%) patients. During cardiac catheterization, arterial PH was found in two patients. Resting venous PH was found in one patient and an excessive post capillary PAP elevation at rest was demonstrated in 11 patients. At the baseline, 14/54 patients (26%) were positive for AECA. In the control group, the frequency of the antibodies was 3/27 (11%). No statistical correlation between antibody titter and the presentation of the disease existed. AECA were highly prevalent in a subgroup of patients suffering from interstitial pulmonary fibrosis. Out of the 15 patients suffering from lung fibrosis, 7 were AECA positive. The presence of AECA correlated very well with antinuclear antibodies (ANA), but was not related to the profile of

K. Lewandowska • E. Gorska • U. Demkow (✉)
Department of Laboratory Diagnostics and Clinical Immunology of Developmental Age, Medical University of Warsaw, Marszałkowska 24 St, 00-576 Warsaw, Poland
e-mail: urszula.demkow@litewska.edu.pl

M. Ciurzynski • P. Bienias • K. Irzyk • P. Pruszczyk
Department of Internal Medicine and Cardiology, Medical University of Warsaw, Marszałkowska 24 St, 00-576 Warsaw, Poland

M. Siwicka
Department of Dermatology, Medical University of Warsaw, Marszałkowska 24 St, 00-576 Warsaw, Poland

K. Zycinska
Department of Familial Medicine, Medical University of Warsaw, Marszałkowska 24 St, 00-576 Warsaw, Poland

M. Pokorski (ed.), *Respiratory Regulation - The Molecular Approach*,
Advances in Experimental Medicine and Biology 756, DOI 10.1007/978-94-007-4549-0_19,

ANA. Our findings support evidence that endothelial cell damage is involved in SSc, as there was increased prevalence of circulating AECA of the IgG isotype in SSc patients. AECA may also be related to the complications of SSc, like pulmonary fibrosis.

Keywords Anti-endothelial cell antibodies • Interstitial lung disease • Pulmonary fibrosis • Pulmonary hypertension • Systemic scleroderma

19.1 Introduction

Systemic sclerosis (scleroderma – SSc) is characterized by prominent fibrosis in the affected organs. Concomitant vascular involvement also plays a role in the course of the disease (Wigley 2009). The pathogenesis of scleroderma vasculopathy is largely unknown, although endothelial cell (EC) injuries induced by infections, cytotoxicity, antiendothelial antibodies, and ischemia-reperfusion have been implicated (Müller-Ladner et al. 2009). SSc patients have significantly fewer and functionally impaired endothelial progenitor cells in peripheral blood and bone marrow. In addition, endothelial apoptosis seems to play a primary role in the pathogenesis of vascular damage (Del Papa et al. 2010; Zielonka et al. 2010). Injured EC from SSc patients produce a large array of biomarkers of vascular damage that reflect disease activity and may predict clinical outcome, including von Willebrand factor, endothelin-1, soluble adhesion molecules, thrombomodulin, circulating endothelial cells, anti-endothelial cell antibodies (AECA), serum vascular endothelial growth factor, endostatin, prostacyclin and thromboxane metabolites (Wigley 2009). A complex interaction between endothelial cells, smooth muscle cells, extracellular matrix, and circulating factors is now recognized to contribute to the vascular reactivity, remodelling and occlusive disease of SSc and may lead to severe complications including nailfold capillaries, telangiectases, Raynaud phenomenon, scleroderma renal crisis and pulmonary hypertension (Wigley 2009; Nagai et al. 2007; Maricq et al. 1976). The clinical consequences of the scleroderma vascular disease are associated with severe organ dysfunction, significant morbidity and mortality (Wigley 2009). Understanding the mechanisms underlying these processes may provide a rationale of novel prophylactic and therapeutic strategies and targeted therapy.

Circulating AECA have been defined as autoantibodies targeting EC and have been implicated in the pathogenesis of endothelial injury. AECA have been described in autoimmune and inflammatory conditions and play a pathogenic role in the development of these diseases (Servettaz et al. 2008; Katritsis et al. 2010; Mihai and Tervaert 2010; Wigley 2009). AECA have also been described in systemic vasculitis – a heterogeneous group of diseases characterized by the presence of inflammatory lesions within the vessel wall (Guilpain and Mouthon 2008). EACA may be also responsible for acute rejection of transplanted organs due to rapid vascular obliteration in the graft (Grandtnerova et al. 2008).

Endothelial cells express several clinically relevant non-HLA antigenic determinants. AECA target antigens include a wide range of extracellular matrix proteins and molecules that adhere to EC, such as DNA in systemic lupus erythematosus beta2-glycoprotein I, or phospholipids in anti-phospholipid syndrome (Wigley 2009). AECA target antigens may also correspond to the wide-spread proteins known to be targets of common disease-associated autoantibodies. For example, IgG EACA from patients with diffuse SSc is bound to a 100-kDa protein band in extracts of human umbilical vein EC (HUVEC) identified as DNA topoisomerase-1, whereas IgG AECA from patients with limited cutaneous SSc is bound to centromeric protein-B (Wigley 2009).

AECA have also been detected in healthy individuals (Servettaz et al. 2008). By using a proteomic approach combining two-dimensional electrophoresis and immunoblotting using HUVEC as a source of self antigens, it has recently been reported that IgG from healthy individuals recognized a restricted

set of highly conserved ubiquitous proteins playing key roles in cell biology and maintenance of homeostasis including cytoskeletal proteins (β actin, α tubulin and vimentin), glycolytic enzymes and other (Papadopoulos et al. 2006). Thus, the repertoire of AECA is heterogeneous and may also depend on the disease entity.

AECA has also been described in sera from SSc patients, but the AECA role in the pathogenesis of SSc and its vascular complications remains largely unknown (Del Papa et al. 2010; Servettaz et al. 2008; Norton and Nardo 1970). The present study was aimed at testing the prevalence of AECA in patients with diffuse and limited SSc, with and without pulmonary hypertension and in relation to the presence of pulmonary fibrosis.

19.2 Methods

19.2.1 Patients

The study was approved by the Ethics Committee of Warsaw Medical University, Warsaw, Poland, and all patients and volunteers gave written informed consent. We prospectively screened 54 SSc patients (50 females and 4 males, mean age 55.7 ± 16.3 years) referred from the Dermatology Clinic at Medical University of Warsaw, Poland, in order to determine if they had evidence of pulmonary hypertension (PH) or restrictive lung disease. All patients were diagnosed with SSc according to the guidelines given by the Subcommittee for Scleroderma Criteria of the American Rheumatism Association Diagnostic and Therapeutic Criteria Committee (1980). Subjects received standard medical care for SSc. All patients underwent transthoracic echocardiography with estimation of pulmonary artery pressure (PAP) and tricuspid regurgitant peak gradient (TRPG). The PH was suspected when TRPG at rest was >31 mmHg. All patients suspected to have pulmonary hypertension were referred for right heart catheterization at rest and during exercise.

Restrictive lung disease was assessed by a combination of resting pulmonary function tests (PFT) by chest X-ray (CXR), and by high-resolution computed tomography (HRCT). An HRCT was performed if there were abnormalities in PFTs or CXR.

19.2.2 Screening of AECA Antibodies

Blood samples were collected by venipuncture. Sera were kept frozen at −80°C until use. The study of AECA was performed using the indirect immunofluorescence method on commercially available human umbilical vein endothelial cells (HUVEC; Euroimmun, Lübeck, Germany). This test detects autoantibodies against cytoskeletal fibers on HUVEC. Bound antibodies were detected with a secondary fluoresceinated antibody against human immunoglobulin G. After being washed, slides were read on fluorescence microscope. A cut-off was set at 1/10 dilution. The presence of AECA was performed at baseline and reassessed after 1 year of follow-up. Antinuclear antibodies (ANA) were detected using indirect immunofluorescence. Anticardiolipin antibodies were detected using ELISA assay. To establish the frequency of AECA in normal individuals, a healthy control group was also included (n = 27; 7 men and 20 women, mean age 49.8 ± 12.1 years). Both SSc and control groups included subjects with mild primary hypertension.

To compare distributions, the χ^2 test and Mann–Whitney *U* test were performed for qualitative and quantitative variables, respectively. Statistica 6.0 was used as software. $p < 0.05$ was considered significant.

19.3 Results

The examined group included 30 (55%) patients with diffuse SSc and 24 (45%) patients with limited SSc. The available HRCT scans in patients with suspected interstitial lung disease revealed signs of lung fibrosis in 15 out of the 36 examined patients. TRPG at rest >31 mmHg was demonstrated in 14 (21%) patients. During cardiac catheterization arterial PH was found in two patients and an excessive precapillary PAP was elevation in two patients. Resting venous PH was found in one patient and an excessive postcapillary PAP elevation at rest was demonstrated in 11 patients.

At baseline, 14/54 patients (26%) and 3/27 (11%) control subjects were positive for AECA; the difference between the two groups was significant ($p < 001$). The presence of AECA in SSc patients was very stable. None of the negative patients at the baseline was positive after 1-year observation time and only in two cases the antibodies disappeared. The frequency of AECA in the subgroups of SSc patients is presented in Table 19.1. No statistical correlation between antibody titter and the presentation of the disease existed. Positive and negative AECA groups did not differ in terms of age, gender, primary hypertension and immunosupression treatment.

The presence of AECA correlated well with the antinuclear antibodies (ANA). None of the sera negative for ANA gave a positive staining with different cytoskeletal fibers on HUVEC. The relation between the frequency of AECA and the auto-antibodies characteristic for SSc is presented in Table 19.1. The differences in the prevalence of AECA between the patients positive for any SSc related antibodies were not statistically significant.

Table 19.1 Prevalence of anti-endothelial cell antibodies (AECA) in control subjects and SSc patients

	AECA (%)	Statistical significance
Control group (n = 27)	3 (11%)	
SSc all patients (n = 54)	14 (26%)	Control group *vs.* all SSc patients; $p < 0.01$
SSc limited (n = 24)	4 (17%)	
SSc diffuse (n = 30)	10 (33%)	Limited *vs.* diffuse SSc; $p < 0.05$
SSc70 antibodies – DNA-topoisomerase I antibodies positive (n = 25)	8 (32%)	
SSc70 antibodies – DNA-topoisomerase I antibodies negative (n = 15)	6 (40%)	SSc 70 positive *vs.* SSc 70 negative; NS
ACA – anti-centromere antibodies positive (n = 18)	4 (22%)	
ACA – anti-centromere antibodies negative (n = 26)	10 (38%)	ACA positive *vs.* ACA negative; NS

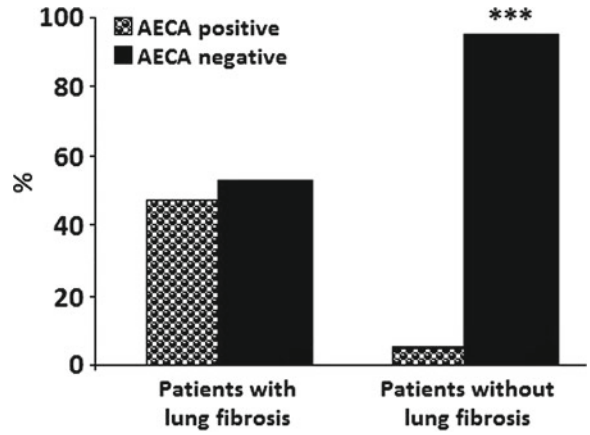

Fig. 19.1 Frequency of antiendothelial cell antibodies (*AECA*) in systemic sclerodermia (*SSc*) patients with and without pulmonary fibrosis confirmed by HRCT examination

Interestingly, only one of the patients with TRPG above 31 mmHg was positive for AECA. This was a patient with pulmonary arterial hypertension confirmed by the right heart catheterization. AECA were highly prevalent in patients suffering from interstitial pulmonary fibrosis confirmed by HRCT. Out of the 15 patients suffering from lung fibrosis, 7 were AECA positive. In contrast, only 1 out of the 21 patients without radiographic signs of fibrosis was AECA positive (Fig. 19.1).

19.4 Discussion

It is known that the EC layer of microvessels is activated early in the course of SSc, leading to EC dysfunction, overexpression of adhesion molecules, and activation of coagulation system and influx of a perivascular infiltrate (Norton and Nardo 1970; Guiducci et al. 2007; Hummers 2008; Konttinen et al. 2003). Moreover EC in SSc patients undergo premature apoptosis. These events are accompanied by oxidative stress and increased production of proinflammatory mediators and growth factors stimulating the appearance of myofibroblast in the vessel wall that synthesize a thickened intima layer. All these events contribute to luminal narrowing and extravascular fibrosis (Wigley 2009). Circulating progenitor cells fail to restore normal vasculogenesis. The mechanism of the endothelial injury is unknown, but there is evidence that apoptosis induced by antiendothelial antibodies may play a role in scleroderma vascular disease (Del Papa et al. 2010; Wigley 2009). In the present study we showed a high prevalence of the circulating AECA antibodies of IgG isotype detected by indirect immunofluorescence on HUVEC cells in different clinical forms of SSc. On the other hand, around three fourth of our SSc patients did not produce antibodies against different cytoskeletal fibers of HUVEC. This observation is consistent with the reports of other authors, suggesting that IgG antibodies reacting with endothelial cells may be important in the pathogenesis of the disease (Del Papa et al. 2010; Wigley 2009). The identity of the antigens targeted by AECA is unknown, however they may react with actin, vimentin, tubulin, calreticulin and other structural proteins of the cell. Moreover, target antigens of AECA include heparan sulfate or even non-constitutive proteins like DNA/histone complexes in SLE, and proteinase 3 in Wegener's granulomatosis (Belizna and Tervaert 1997). The binding of various plasma components to the EC membrane has also been suggested. Once attached to EC, these plasma components might focus the related autoantibodies to the cell membrane (Revélen et al. 2002). Western blotting techniques, however, have revealed considerable discrepancies. Incubation of AECA-positive sera from SLE patients with HUVEC precipitated 19 proteins ranging from 15 to 200 kD (Révélen et al. 2002). In the present study we concentrated on autoantibodies directed against EC structural proteins but not proteins attached to EC. There is a wide variation in the results obtained by other authors likely stemming from different detection methods. It is therefore worthwhile to establish a reliable assay for the detection of AECA. Indirect IF is a sensitive technique. However, it is not suitable to detect autoantibodies against non-constitutive proteins of EC. The problem of the target autoantigens remains also an open issue. In fact, given the impressive diversity of conditions associated with AECA, they represent a heterogenous family and raise a number of questions. Based on the use of new technologies, such as proteomic approach and two-dimensional electrophoresis, accurate data should be generated in the near future (Servettaz et al. 2008).

It is not clear whether AECA antibodies represent a primary mechanism inducing endothelial cell damage or if they are a consequence of cell injury and death. The specific pathogenic role of these antiendothelial cell antibodies in scleroderma remains unclear; they can be seen in other diseases with vascular involvement and sometimes in healthy individuals (Del Papa et al. 2010; Servettaz et al. 2008; Katritsis et al. 2010). We were able to detect AECA in three subjects out of our control group. This observation confirms that the role of AECA in the pathogenesis of SSc or other autoimmune diseases is not straightforward. On the other hand AECA in sera of examined patients highly correlated with other autoantibodies, especially ANA of different specificity, but the prevalence of AECA

was not related to any particular autoantibody profile. Other authors have found association between AECA and autoantibodies in a number of connective tissue diseases. For example antiendothelial antibodies together with C1q-binding immune complexes and anticardiolipin antibodies were found in 18 of 28 scleroderma patients (Wigley 2009). However, as for AECA, for most of these antibodies, their role in pathogenesis is not established. Anti-centromere antibodies are associated with limited cutaneous involvement and risk for pulmonary hypertension, whereas anti-topoisomerase I is associated with diffuse progressive disease and severe interstitial lung disease but their clear role in the pathogenesis of the disease is rather obscure (Wigley 2009).

Several studies found a correlation between the presence of AECA in SSc and clinical vascular disease, including severe digital ischemia, pulmonary arterial hypertension, abnormal nailfold capillaries, and microvascular disease associated with pulmonary fibrosis (Del Papa et al. 2010; Wigley 2009; Salerni et al. 1977). We were able to confirm only the last mentioned association. Surprisingly, we observed a very low prevalence (only in one patient) of these antibodies in pulmonary hypertension. On the other hand, we found only two cases of pulmonary arterial hypertension and in the remaining cases venous pulmonary hypertension was diagnosed. Vasculopathy in the course of SSc is usually limited to small arteries and microcirculation, less is known about possible involvement of venous part of the circulation (Ciurzynski et al. 2011). We can conclude that the pathogenesis of venous pulmonary hypertension is probably unrelated to AECA-mediated endothelial damage. We were able to find a correlation between the presence of AECA and the occurrence of pulmonary fibrosis. Pulmonary fibrosis represents a severe complication of the disease. AECA may trigger an inflammatory process *via* complement- or antibody-dependent cellular cytotoxicity (Magro et al. 2006; Yoshio 2001), but also by the induction of EC apoptosis and necrosis (Wigley 2009).

Apoptosis of endothelial cells induced by AECA is reported to trigger the release of fibrogenic mediators (Wigley 2009); thus linking antibody-induced apoptosis and tissue fibrosis. This hypothesis is consistent with our observations. Ahmed et al. (2006) have demonstrated that human sera from patients with SSc contain AECA able to induce apoptosis of EC. Pulmonary fibrosis is likely to be secondary to the associated small-vessel disease (Orfanos et al. 2001). Despite having distinct etiological and clinical manifestations, most chronic fibrotic disorders are characterized by substantial vascular remodelling which often occurs prior to the development of fibrosis (Abraham and Varga 2005). Apoptosis of endothelial cells induced by AECA is reported to trigger the release of fibrogenic mediators (Wigley 2009).

Although scleroderma is generally considered a fibrosing disease of tissues, it is now recognized that the underlying vascular disease is playing a fundamental role in its pathogenesis. Both processes are closely connected. Our findings support the evidence that an autoimmune component associated with endothelial cell damage is involved in SSc, as there is an increased prevalence of circulating AECA of the IgG isotype in SSc patients. AECA represent a heterogenous group of antibodies directed against a variety of antigenic determinants on EC. Induction of EC apoptosis is one of the mechanisms by which AECA may be pathogenic. The detection of these antibodies may be valuable tool to monitor disease activity. Further characterization of putative antigens is needed to better understand their pathophysiological role.

Conflicts of interest: The authors declare no conflicts of interest in relation to this article.

References

Abraham, D. J., & Varga, J. (2005). Scleroderma: From cell and molecular mechanisms to disease models. *Trends in Immunology, 26*(11), 587–595.

Ahmed, S. S., Tan, F. K., Arnett, F. C., Jin, L., & Geng, Y. J. (2006). Induction of apoptosis and fibrillin 1 expression in human dermal endothelial cells by scleroderma sera containing anti-endothelial cell antibodies. *Arthritis and Rheumatism, 54*(7), 2250–2262.

Belizna, C., & Tervaert, J. W. (1997). Specificity, pathogenicity, and clinical value of antiendothelial cell antibodies. *Seminars in Arthritis and Rheumatism, 27*(2), 98–109.

Ciurzynski, M., Bienias, P., Irzyk, K., Rymarczyk, Z., Kostrubiec, M., Szewczyk, A., Glinska-Wielochowska, M., Zylkowska, J., Kurzyna, M., & Pruszczyk, P. (2011). Usefulness of echocardiography in the identification of an excessive increase in pulmonary arterial pressure in patients with systemic sclerosis. *Kardiologia Polska, 69*(1), 9–15.

Del Papa, N., Quirici, N., Scavullo, C., Gianelli, U., Corti, L., Vitali, C., Ferri, C., Giuggioli, D., Manfredi, A., Maglione, W., Onida, F., Colaci, M., Bosari, S., & Lambertenghi Deliliers, G. (2010). Antiendothelial cell antibodies induce apoptosis of bone marrow endothelial progenitors in systemic sclerosis. *The Journal of Rheumatology, 37*(10), 2053–2063.

Grandtnerova, B., Mackova, N., Hovoricova, B., & Jahnova, E. (2008). Hyperacute rejection of living related kidney grafts caused by endothelial cell-specific antibodies: Case reports. *Transplantation Proceedings, 40*(7), 2422–2424.

Guiducci, S., Giacomelli, R., & Cerinic, M. M. (2007). Vascular complications of scleroderma. *Autoimmunity Reviews, 6*, 520–523.

Guilpain, P., & Mouthon, L. (2008). Antiendothelial cells autoantibodies in vasculitis-associated systemic diseases. *Clinical Reviews in Allergy & Immunology, 35*(1–2), 59–65.

Hummers, L. K. (2008). Biomarkers of vascular disease in scleroderma. *Rheumatology (Oxford, England), 47*(Suppl 5), v21–v22.

Katritsis, D. G., Zografos, T., Korovesis, S., Giazitzoglou, E., Youinou, P., Skopouli, F. N., & Moutsopoulos, H. M. (2010). Antiendothelial cell antibodies in patients with coronary artery ectasia. *Coronary Artery Disease, 21*(6), 352–356.

Konttinen, Y. T., Mackiewicz, Z., Ruuttila, P., Ceponis, A., Sukura, A., Povilenaite, D., Hukkanen, M., & Virtanen, I. (2003). Vascular damage and lack of angiogenesis in systemic sclerosis skin. *Clinical Rheumatology, 22*, 196–202.

Magro, C. M., Waldman, W. J., Knight, D. A., Allen, J. N., Nadasdy, T., Frambach, G. E., Ross, P., & Marsh, C. B. (2006). Idiopathic pulmonary fibrosis related to endothelial injury and antiendothelial cell antibodies. *Human Immunology, 67*(4–5), 284–297.

Maricq, H. R., Downey, J. A., & LeRoy, E. C. (1976). Standstill of nailfold capillary blood flow during cooling in scleroderma and Raynaud's syndrome. *Blood Vessels, 13*, 338–349.

Mihai, C., & Tervaert, J. W. (2010). Anti-endothelial cell antibodies in systemic sclerosis. *Annals of the Rheumatic Diseases, 69*(2), 319–324.

Müller-Ladner, U., Distler, O., Ibba-Manneschi, L., Neumann, E., & Gay, S. (2009). Mechanisms of vascular damage in systemic sclerosis. *Autoimmunity, 42*(7), 587–595.

Nagai, Y., Yamanaka, M., Hashimoto, C., Nakano, A., Hasegawa, A., Tanaka, Y., Yokoo, H., Nakazato, Y., & Ishikava, O. (2007). Autopsy case of systemic sclerosis with severe pulmonary hypertension. *The Journal of Dermatology, 34*, 769–772.

Norton, W. L., & Nardo, J. M. (1970). Vascular disease in progressive systemic sclerosis (scleroderma). *Annals of Internal Medicine, 73*, 317–324.

Orfanos, S. E., Psevdi, E., Stratigis, N., Langleben, D., Catravas, J. D., Kyriakidis, M., Moutsopoulos, H. M., Roussos, C., & Vlachoyiannopoulos, P. G. (2001). Pulmonary capillary endothelial dysfunction in early systemic sclerosis. *Arthritis and Rheumatism, 44*, 902–911.

Papadopoulos, D. P., Makris, T. K., Krespi, P., Papazachou, U., Stavroulakis, G., Hatzizacharias, A., & Votteas, V. (2006). Antiendothelial cell antibody levels in healthy normotensives with high normal blood pressure. *Clinical and Experimental Hypertension, 28*(8), 663–667.

Revelen, R., D'Arbonneau, F., Guillevin, L., Bordron, A., Youinou, P., & Dueymes, M. (2002). Comparison of cell-ELISA, flow cytometry and Western blotting for the detection of antiendothelial cell antibodies. *Clinical and Experimental Rheumatology, 20*(1), 19–26.

Salerni, R., Rodnan, G. P., Leon, D. F., & Shaver, J. A. (1977). Pulmonary hypertension in the CREST syndrome variant of progressive systemic sclerosis (scleroderma). *Annals of Internal Medicine, 86*, 394–399.

Servettaz, A., Guilpain, P., Camoin, L., Mayeux, P., Broussard, C., Tamby, M. C., Tamas, N., Kaveri, S. V., Guillevin, L., & Mouthon, L. (2008). Identification of target antigens of antiendothelial cell antibodies in healthy individuals: A proteomic approach. *Proteomics, 8*(5), 1000–1008.

Subcommittee for Scleroderma Criteria of the American Rheumatism Association Diagnostic and Therapeutic Criteria Committee. (1980). Preliminary criteria for the classification of systemic sclerosis. *Arthritis and Rheumatism, 23*, 581–590.

Wigley, F. M. (2009). Vascular diseases in scleroderma. *Clinical Reviews in Allergy & Immunology, 36*(2–3), 150–175.

Yoshio, T. (2001). Antiendothelial cell antibodies and their relation to pulmonary hypertension in connective tissue diseases. *Nihon Rinshō Men'eki Gakkai Kaishi, 24*(4), 133–141.

Zielonka, T. M., Demkow, U., Radzikowska, E., Bialas, B., Filewska, M., Zycinska, K., Obrowski, M. H., Kowalski, J., Wardyn, K. A., & Skopinska-Rozewska, E. (2010). Angiogenic activity of sera from interstitial lung disease patients in relation to pulmonary function. *European Journal of Medical Research, 15*(Suppl 2), 229–234.

Chapter 20
Leptin Receptor in Childhood Acute Leukemias

E. Gorska, K. Popko, and M. Wasik

Abstract Ob-R receptor is encoded by *db* gene and belongs to class I cytokine receptors family. Its expression was observed in hematopoietic CD34+ stem cells, erythropoietic, myeloid and lymphoblastic lineages cell lines and in human leukemic blast cells in lymphomas, acute myeloid leukemia (AML), acute lymphoblastic leukemia (ALL), and chronic myeloid leukemia (CML). The studies on human bone marrow cells show that JAK/STAT pathway plays a substantial role in signal transduction in young bone marrow cells. The aim of the study was to examine the relationship between leptin receptor expression and the proliferation of neoplastic hematopoietic cells in bone marrow. The study was performed in a total of 57 children of both sexes aged 3 months to 16 years. A group of 46 patients with acute leukemia involved 25 children with ALLB, 11 children with ALLT and 10 children with ANNL. The control group consisted of 11 non-obese children with non-malignant hematological disturbances. The tests were performed on bone marrow samples. The assessments of membrane expression of Ob-R and the antigens determining the phenotype of bone marrow cells were performed using a flow cytometry method. In acute lymphoblastic leukemia, a significant decrease of Ob-R expression on leukemic blasts was observed in comparison with respective populations of normal bone marrow cells. Also in progenitor cells populations a significant decrease of CD34+Ob-R+w ALLT and ALLB was observed in comparison with the cells from normal bone marrow. No statistically significant differences in the percentage of Ob-R+ cells in ANNL bone marrow and in control bone marrow were observed.

Keywords Leptin receptor • Bone marrow • Children • Lymphoblastic leukemia • Myeloid leukemia • Neoplastic hematopoietic cells

20.1 Introduction

Leptin biological activity strongly depends on its proper interactions with specific Ob-R receptor (Sweeney 2002). Ob-R receptor is encoded by *db* gene and belongs to class I cytokine receptors family. The products of alternative RNA splicing of *db* gene are expressed in six isoforms (Ahima and

E. Gorska (✉) • K. Popko • M. Wasik
Department of Laboratory Diagnostics and Clinical Immunology of Developmental Age,
Medical University of Warsaw, 24 Marszalkowska St, 00-576 Warsaw, Poland
e-mail: elgorska@litewska.edu.pl

M. Pokorski (ed.), *Respiratory Regulation - The Molecular Approach*,
Advances in Experimental Medicine and Biology 756, DOI 10.1007/978-94-007-4549-0_20,

Osei 2004). Because of some structure differences, the receptors' isoforms were divided into three classes: long, short and soluble isoform.

The major leptin signal transduction pathway through membrane receptors is mediated through JAK/STAT pathway. Among all Ob-R isoforms, only full-length isoform, Ob-Rb, exerts the ability to fully transduce an activator signal into the cell. A long, fully active isoform Ob-Rb is expressed mainly in hypothalamus, where it takes part in energy homeostasis and regulation of secretory organs function. It is also present in all types of immune cells, involved in both innate and adaptive immunity (Li et al. 2007; Martin-Romero et al. 2000; Gao et al. 2009).

The studies on human bone marrow cells showed that JAK/STAT pathway plays substantial role in mediating leptin activity on immune system cells and signal transduction in young bone marrow cells expressing Ob-R receptor. The experiments performed in neoplastic cells of acute and chronic leukemias involved the assessment of RNA expression, but not the membrane receptor level. The presence of RNA for long and short isoforms of Ob-R has been observed in leukemic myeloblasts, whereas in lymphoblasts a low level of RNA for the short isoform has been described. The expression of RNA for long isoform of the receptor is much more often observed in primary ANLL than in secondary ANLL or CML (Konopleva et al. 1999). In CML cells the receptor expression depends on clinical stage of the disease and is much higher in immature blasts during blast crisis. It has been shown in ANLL that leptin through its receptor stimulates cell proliferation in concert with other hematopoietic growth factors, such as IL-1β, IL-3, IL-6, TNFα, GM-CSF, and SCF (Bruserud et al. 2002; Konopleva et al. 1999).

The aim of the study was to examine the Ob-R receptor expression on malignant blast cells in comparison with respective normal cells. The expression of membrane Ob-R receptor on bone marrow cells in children with B-cell or T-cell acute lymphoblastic leukemia and with non-lymphoblastic leukemia has not been studied before. There are also no observations on changes of Ob-R expression in other, not-transformed bone marrow cells.

20.2 Methods

The protocol of the study was approved by the Ethics Committee of Medical University of Warsaw, Poland. The study was performed in a total of 57 children (16 girls and 46 boys) aged 3 months to 16 years. The control group (age and sex matched) consisted of children referred, due to unexplained anemia or thrombocytopenia, to the Department of Pediatrics, Hematology and Oncology, of the Medical University of Warsaw, Poland,. This group involved 11 children (three girls and eight boys), aged 5 months to 15 years, BMI of 10.5–22.1 kg/m^2.

The group of affected children consisted of patients with acute leukemia. The group involved: 25 children with ALLB, aged 3 months to 15 years, BMI of 11.7–20.8 kg/m^2, 11 children with ALLT, aged 3–16 years, BMI of 14.1–21.4 kg/m^2, and 10 children with ANNL aged 2.5–16 years, BMI of 11.78–22.03 kg/m^2. There was no difference in BMI between the acute leukemia and control groups. The tests were performed in bone marrow collected on heparin. All tests were performed on the day of diagnosis.

The assessments of membrane expression of Ob-R and determination of bone marrow cells phenotype were performed using flow cytometry method (Cytometer FC 500, Beckman Coulter, USA). Nucleated bone marrow cells were isolated on density gradient using Histopaque with relative density $d = 1.077 \pm 0.001$ g/cm^3 and $d = 1.115 \pm 0.002$ g/cm^3 (Sigma Aldrich, CO, USA).

Membrane expression of Ob-R antigen was analyzed simultaneously with determination of phenotype using monoclonal antibodies anti CD2, CD5, CD7, CD4 and CD8 for T cells and anti CD19 and CD22 for B-cells. Monocytic cells lineage was recognized using anti CD4 and CD14 antibodies, while

granulocytic lineage was identified with anti CD33 antibody. The assessment of bone marrow cells phenotype was performed according to the standard method using monoclonal antibodies manufactured by Beckman Coulter. Ob-R receptor was stained according to the indirect immunofluorescence method using murine monoclonal IgG2A antibody against human leptin receptor manufactured by R&D Systems and secondary FITC-conjugated affinipure goat anti-mouse IgG manufactured by Jackson ImmunoResearch Laboratories, Inc. All tests were accompanied with suitable isotype controls.

Statistical analysis was performed using Statistica v. 7.1 and Excel 2007 (Microsoft) software. As the distributions of the parameters studied were not normal, nonparametric tests for independent samples were performed. The results were shown for median values (Q_1- first quartile, Q_3- third quartile). The Mann-Whitney U test was used for the intergroup differences. A value of $p < 0.05$ was considered statistically significant.

20.3 Results

The percentage of bone marrow subpopulations of cells expressing Ob-R receptor in children with acute leukemia and in the control group are shown in Table 20.1. In the bone marrow from children with ALLT and ALLB a significantly smaller number of T and B blasts expressed Ob-R in comparison with T and B-cells in the normal bone marrow. A significant difference in Ob-R expression was observed mainly in the T CD8+ subpopulation. The percentages of T CD4+Ob-R+ normal bone marrow cells and CD4+Ob-R+ blasts from ALLT were comparable (Fig. 20.1). No significant differences between the control bone marrow and CD14+CD4+Ob-R+ and CD33+Ob-R+ blasts expression were observed.

Analysis of the populations of progenitor cells has shown a significant decrease in CD34+Ob-R+ in children with ALLB and ALLT in comparison with the cells from the control bone marrow. No statistically significant differences between the number of CD34+Ob-R+ blasts in ANLL and the number of respective cells in the normal bone marrow expressing Ob-R+ were observed (Fig. 20.2).

Table 20.1 Comparison of the percentage of Ob-R expressing cells in acute leukemias – ALLT, ALLB, ANLL with that in control bone marrow cells

Population of cells	Antigen	Control cells (%) median (Q_1, Q_3) (n = 11)	ALLB (%) median (Q_1, Q_3) (n = 25)	ALLT (%) median (Q_1, Q_3) (n = 11)	ANNL (%) median (Q_1, Q_3) (n = 10)
Whole population Ob-R+		43.9 (38.8–51.7)	2.8 (2.3–4.8)	4.8 (3.5–8.0)	64.2 (27.4–98.0)
		Ob-R (%)	**Ob-R (%)**	**Ob-R (%)**	**Ob-R (%)**
T lymphocytes	CD2+ CD5+ CD7+	8.0 (3.7–12.7)		2.05 (0.1–3.5)	
	CD2+ CD4+	11.9 (7.6–19.4)		5.1 (1.8–16.6)	
	CD2+ CD8+	37.7 (30.3–59.8)		11.2 (3.5–21.6)	
B lymphocytes	CD19+ CD22+	9.5 (5.7–13.8)	2.7 (1.4–4.0)		
Monocytes	CD14+ CD4+	90.3 (84.9–94.5)			79.9 (66.9–91.3)
Granulocytes	CD33+	75.8 (62.8–86.4)			72.6 (60.2–98.9)
Progenitor cells	CD34+	51.5 (46.5–65.1)	2.8 (1.2–4.4)	9.3 (4.3–32.9)	79.6 (13.3–85.3)

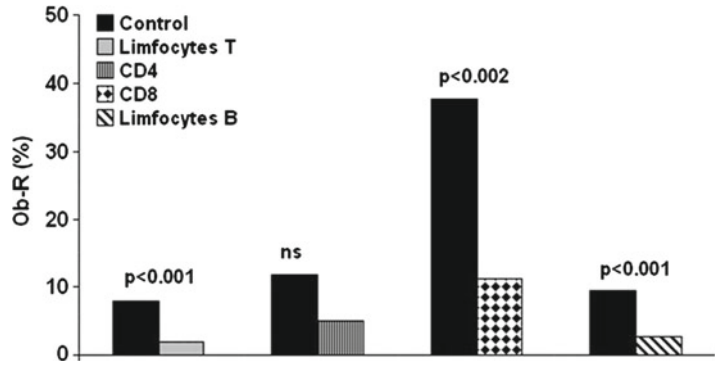

Fig. 20.1 Percentages of Ob-R expressing cells in B and T lineage in control bone marrow and in ALLT and ALLB leukemias

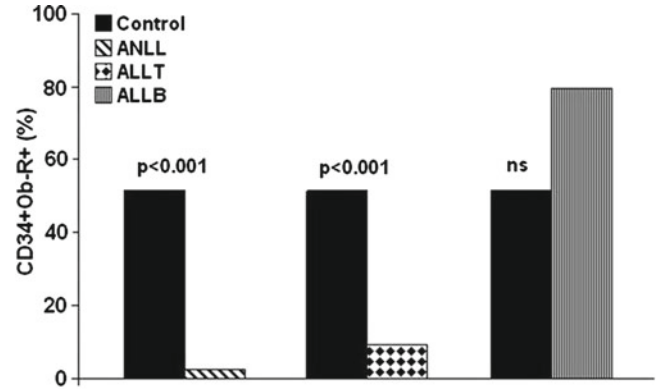

Fig. 20.2 Percentage of CD34 + Ob-Rb + blasts in control bone marrow and in ANLL, ALLT, and ALLB leukemias

20.4 Discussion

The understanding of the relationship between the expression of leptin receptor and malignant proliferation of hematopoietic cells may shed light on the role of leptin and its receptor in the development of leukemic processes in children. Numerous authors have observed the expression of leptin receptors in hematopoietic CD34+ stem cells, erythropoietic, myeloid and lymphoblastic lineages of cell lines and in human leukemic blast cells in lymphomas, AML, ALL and CML (Blanco-Diaz et al. 2007; Konopleva et al. 1999; Mouzaki et al. 2010; Shahab et al. 2010).

In the present study the number of cells expressing leptin receptor was assessed using flow cytometry with monoclonal anti-ObR antibody. Since till now no publication has described the expression of the receptor on cancer and normal cells in children using flow cytometry, our results were compared with the data obtained using RT-PCR to test the mRNA expression in respective bone marrow cells populations.

In acute lymphoblastic B-cell leukemia, a significant decrease of the percentage of leptin receptor expressing CD19+CD22+ cells in comparison with normal bone marrow cells was observed. Moreover, in children with acute lymphoblastic T-cell leukemia a substantial decrease of Ob-R T CD2+ and T CD8+ blasts was observed in comparison with the respective control bone marrow cells. In the Ob-R+CD4+ cell population, there also was a decrease in Ob-R+lymphoblasts in comparison with normal CD4+ lymphocytes, although in this case the difference failed to reach a statistical significance. In both types of lymphoblastic leukemias, there was a significant decrease in CD34+ cells expressing leptin receptor in comparison with the number of CD34+Ob-R+ from the control group (Table 20.1).

Wex et al. (2002) have identified RNA for the leptin receptor in lymphoblasts of 33% of children with acute ALLB and ALLT leukemias at the onset of disease. During remission, RNA expression

strongly increased and was detected in 71% of these children. Konopleva et al. (1999) have observed the presence of mRNA for the short Ob-R isoform only in lymphoblastic lineage cells in very low concentration. The presence of mRNA for the long isoform of the receptor in lymphoblasts was not observed. The results described above confirm the results presented in our study.

The expression of Ob-R short isoform may indicate the impairment in signal transduction in lymphoblastic leukemia cells, even if bone marrow leptin levels are normal. It is possible that anti-Ob-R monoclonal antibody used in our experiments binds an extracellular domain of the short isoform of the receptor. Low leptin concentration may be caused by hypoxia which is responsible for HIF-1α activation that inhibits Ob gene promoter (Wex et al. 2002). The circulating leptin level can also be regulated by binding of the hormone to its soluble receptor (Chan et al. 2002; Lammert et al. 2001). Increased concentration of proinflammatory cytokines, especially TNFα, also decreases the level of leptin (Kurzrock 2001; Laharrague et al. 2000a, b). Low leptin concentration along with low Ob-R expression in lymphoblasts may suggest that leptin and Ob-R do not influence the rate of lymphoblast proliferation.

In the present study we found a high percentage of CD14+ CD33+ myeloblastic cells expressing Ob-R in ANLL samples. However, the percentage of these cells was comparable with the number of respective cells in the normal bone marrow (Table 20.1). These results are consistent with those on mRNA Ob-R expression reported by others. Nakao et al. (1998) have identified the presence of mRNA for leptin receptor, without differentiating between isoforms, in leukemic cells obtained from patients with ANLL. Konopleva et al. (1999) have shown a high expression of mRNA for both leptin receptor isoforms not only in several leukemic cell lines, but also in the majority of samples from patients with ANLL. Other authors have confirmed these observations (Tsiotra et al. 2005), finding a high expression of both isoforms on cells from ANLL patients. The analysis of Ob-R isoforms expression in patients with ANLL suggests that Ob-R may play a role in the pathogenesis of some myeloid leukemia, because both isoforms are present on leukemic blasts from the majority of ANLL patients.

The results showed a tendency for an increase in the percentage of CD34+ cells expressing Ob-R in ANLL in comparison with normal cells (Fig. 20.2). High leptin concentration in bone marrow of patients with ANLL may, along with hematopoietic growth factor, stimulate the development of leukemic myeloid lineage. It has been shown that leptin, depending on the concentration, stimulates proliferation of human myeloid bone marrow cells and human leukemic OCI/AMl2 and MO7e cell lines (Gainsford et al. 1996; Konopleva et al. 1999; Laharrague et al. 2000a, b). Through the autocrine activation of its receptor, leptin may influence proliferation of myeloblasts and decrease their apoptosis (Konopleva et al. 1999).

The literature shows that expression of a short isoform of Ob-R_S is more common than that of a long isoform, both in healthy volunteers and in patients with hematologic diseases. However, in the majority of myeloblastic cell lines the expression of a long rather than short isoform is observed (Konopleva et al. 1999; Tsiotra et al. 2005). The longest Ob-R_L isoform has long, intracellular domain containing conservative sequences with motifs necessary to bind signal transduction factors such as JAK and STAT family, which are needed for proper signal transduction, whereas short isoforms have shortened cytoplasmic domains. The latter, however, have motifs that actively bind JAK on their carboxyl-terminus the isoforms and may also take part in transduction of leptin signal, which differs from the effects of long isoform activation. Some authors suggest that short isoforms of the receptor may modulate the activity of long ones (White et al. 1997; Burguera et al. 2000; Frűhbeck 2006), which may play a significant role in expression of the receptor in various types of leukemias.

Not only do normal hematopoietic but also leukemic cells express functional receptors for various cytokines including IL-3, IL-6, GM-CSF, G-CSF, M-CSF, SCF, and thrombopoietin. These cytokines are also able to regulate leukemia cell survival, proliferation, and differentiation (Hino et al. 2000; Mouzaki et al. 2010). Abnormal cytokine and their receptors expression can disturb signal transduction in leukemic cells. It has been shown that leptin alone is not able to increase the expression of other cytokines receptors (Konopleva et al. 1999). Possibly, pro-inflammatory cytokines or growth factors, through the interaction with their receptors, modulate leptin receptor expression in various types of leukemic cells.

20.5 Conclusions

- In children with ALLT or ALLB bone marrow lymphoblasts are characterized by lower expression of leptin receptors.
- Myeloblasts obtained from children with ANLL show slightly higher expression of leptin receptors in comparison with cells of normal myeloid lineage.
- Changes observed in leptin receptor expression in malignant cells do not allow excluding or explicitly determining the role of leptin receptor in the development of acute leukemia in children.

Conflicts of interest: The authors declare no conflicts of interest in relation to this article.

References

Ahima, R. S., & Osei, S. Y. (2004). Leptin signaling. *Physiology & Behavior, 81*, 223–241.

Blanco-Diaz, E., Bruns, I., Neumann, F., Fischer, J. C., Graef, T., Rosskopf, M., Brors, B., Pechtel, S., Bork, S., Koch, A., Baer, A., Rohr, U. P., Kobbe, G., Haeseler, A., Gattermann, N., Haas, R., & Kronenwett, R. (2007). Molecular signature of CD34+ hematopoietic stem and progenitor cells of patients with CML in chronic phase. *Leukemia, 21*, 494–504.

Bruserud, O., Huang, T. S., Glenjen, N., Tore, B., & Foss, B. (2002). Leptin in human acute myelogenous leukemia: Studies of in vivo levels and in vitro effects on native functional leukemic blasts. *Haematologica, 87*, 584–595.

Burguera, B., Couce, M. E., Long, J., Lamsam, J., Laakso, K., Jensen, M. D., Parisi, J. E., & Lloyd, R. V. (2000). The long form of the leptin receptor (OB-Rb) is widely expressed in the human brain. *Neuroendocrinology, 71*, 187–195.

Chan, J. L., Blüher, S., Yannakouris, N., Suchard, M. A., Kratzsch, J., & Mantzoros, C. S. (2002). Regulation of circulating soluble leptin receptor levels by gender, adiposity, sex steroids, and leptin: Observational and interventional studies in humans. *Diabetes, 51*, 2105–2112.

Frűhbeck, G. (2006). Intracellular signaling pathways activated by leptin. *The Biochemical Journal, 393*, 7–20.

Gainsford, T., Willson, T., Metcalf, D., Handman, D., McFarlane, C., Ng, A., Nicola, N. A., Alexander, W. S., & Hilton, D. J. (1996). Leptin can induce proliferation, differentiation, and functional activation of hemopoietic cells. *Proceedings of the National Academy of Sciences of the United States of America, 93*, 14564–14568.

Gao, J., Tian, J., Lv, Y., Shi, F., Kong, F., Shi, H., & Zhao, L. (2009). Leptin induces functional activation of cyclooxygenase-2 through JAK2/STAT3, MAPK/ERK, and PI3K/AKT pathways in human endometrial cancer cells. *Cancer Science, 100*, 389–395.

Hino, M., Nakao, T., Yamane, T., Ohta, K., Takubo, T., & Tatsumi, N. (2000). Leptin receptor and leukemia. *Leukemia & Lymphoma, 36*, 457–461.

Konopleva, M., Mikhail, A., Estrov, Z., Zhao, S., Harris, D., Sanchez-Williams, G., Kornblau, S. M., Dong, J., Kliche, K. O., Jiang, S., Snodgrass, H. R., Estey, E. H., & Andreeff, M. (1999). Expression a function of leptin receptor isoforms in myeloid leukemia and myelodysplastic syndromes: Proliferative and anti-apoptotic activities. *Blood, 5*, 1668–1676.

Kurzrock, R. (2001). The role of cytokines in cancer-related fatigue. *Cancer, 92*, 1684–1688.

Laharrague, P., Oppert, J. M., Brousset, P., Charlet, J. P., Campfield, A., Fontanilles, A. M., Guy-Brand, B., Corberand, J. X., Penicaud, L., & Casteilla, L. (2000a). High concentration of leptin stimulates myeloid differentiation from human bone marrow CD34+ progenitors: Potential involvement in leukocytosis of obese subjects. *International Journal of Obesity, 9*, 1212–1216.

Laharrague, P., Truel, N., Fontanilles, A. M., Corberand, J. X., Penicaud, L., & Casteilla, L. (2000b). Regulation by cytokines of leptin expression in human bone marrow adipocytes. *Hormone and Metabolic Research, 32*, 381–385.

Lammert, A., Kiess, W., Bottner, A., Glasow, A., & Kratzsch, J. (2001). Soluble leptin receptor represents the main leptin binding activity in human blood. *Biochemical and Biophysical Research Communications, 283*, 982–988.

Li, Q., Li, J. Y., Li, Y., & Zhang, J. C. (2007). Expression of long isoform leptin receptor and shortest membrane bound variant in peripheral blood mononuclear cells from the obese and normal individuals. *Zhonghua Yi Xue Za Zhi, 87*, 3288–3299.

Martin-Romero, C., Santoz-Alvarez, J., Goberna, R., & Sanchez-Margalet, V. (2000). Human leptin enhances activation and proliferation of human circulating T lymphocytes. *Cellular Immunology, 199*, 15–24.

Mouzaki, A., Panagoulias, I., Dervilli, Z., Zolota, V., Spadidea, P., Rodi, M., Panitsas, F. P., Lagadinou, E., de Lastic, A. L., & Georgakopoulos, T. (2010). Expression patterns of leptin receptor (OB-R) isoforms and direct in vitro effects of

recombinant leptin on OB-R, leptin expression and cytokine secretion by human hematopoietic malignant cells. *Cytokine, 48*, 203–211.

Nakao, T., Hino, M., Yamane, T., Nishizawa, Y., Morii, H., & Tatsumi, N. (1998). Expression of the leptin receptor in human leukaemic blast cell. *British Journal of Haematology, 102*, 740–745.

Shahab, U., Rong, B., Maqbool, A., Azhar, R. H., Dahish, A., Fouad, A.-D., Prashant, B., & Hawla, S. A. (2010). Leptin receptor expression and its association with PI3K/AKT signaling pathway in diffuse large B-cell lymphoma. *Leukemia & Lymphoma, 51*, 1305–1314.

Sweeney, G. (2002). Leptin signaling. *Cellular Signaling, 14*, 655–663.

Tsiotra, P. C., Pappa, V., Koukourava, A., Economopoulos, T., Tsigos, C., & Raptis, S. A. (2005). Expression of leptin receptors in mononuclear cells from myelodysplastic syndromes and acute myeloid leukemias. *Acta Haematologica, 114*, 1–77.

Wex, H., Ponelis, E., Wex, T., Dressendörfer, R., Mittler, U., & Vorwerk, P. (2002). Plasma leptin and leptin receptor expression in childhood acute lymphoblastic leukemia. *International Journal of Hematology, 76*, 446–452.

White, D., Kuropatwinski, K. K., Devos, R., Baumann, H., & Tartaglia, L. A. (1997). Leptin receptor (OB-R) signaling. *The Journal of Biological Chemistry, 272*, 4065–4071.

Chapter 21
Expression of Cytotoxic T Lymphocyte Antigen-4 in T Cells from Children with Hashimoto's Thyroiditis

Anna M. Kucharska, Elzbieta Gorska, Maria Wasik, and Urszula Demkow

Abstract The cytotoxic T lymphocyte antigen-4 (CTLA-4) (CD152) is a basic negative regulatory molecule of T cell activation and its hypo-function is associated with severe lymphoproliferative syndrome. The aim of the present study was to evaluate the intracellular and surface expression of CTLA-4 on peripheral T cells before and after T cell activation in children with Hashimoto's thyroiditis (HT). Blood samples were obtained from 46 children: 25 with Hashimoto's thyroiditis and 21 controls free of autoimmune disease or thyroid disorders. T cell phenotype was evaluated by flow cytometry with the use of monoclonal antibodies combination: CD4- FITC/ CD28 -PC5/ CD152 -PE and CD8 -FITC/ CD28 -PC5/ CD152 -PE on T cell surface and intracellularly at baseline and after 48 h of T cell culture with the mitogen 48-PHA. We found that the number of T cells with intracellular CD152 expression was comparable in HT patients and controls at baseline and increased after 48-PHA, in CD4 subset only, in both patients and controls. However, the increase was more evident in the HT patients. The number of T cells with the surface expression of CD152 at baseline was significantly lower in the HT patients than in controls ($p < 0.0002$) in non-stimulated CD4+ and CD8+ T cells. After 48-PHA, surface CD152 expression in CD4+T cells increased in both groups; the increase was greater in controls. In conclusion, impaired function of CTLA-4 in HT patients may depend on the imbalance of intracellular/surface expression of CD152 in T cells.

Keywords Children • CTLA-4 • Hashimoto's thyroiditis • Lymphocytes • T cell activation

21.1 Introduction

The cytotoxic T lymphocyte antigen-4 (CTLA-4) (CD152) is a basic negative regulatory molecule of T cell activation (Chambers et al. 1996). It is one of the key molecules which provide co-stimulatory signal during T cell activation. CD28, another co-stimulatory molecule, and CD152 are homological

A.M. Kucharska (✉)
Department of Pediatrics and Endocrinology, Medical University of Warsaw,
Marszalkowska 24 St, 00-756 Warsaw, Poland
e-mail: anna.kucharska@litewska.edu.pl

E. Gorska • M. Wasik • U. Demkow
Department of Laboratory Diagnostics and Clinical Immunology of the Developmental Age,
Medical University of Warsaw, Marszalkowska 24 St, 00-756 Warsaw, Poland

M. Pokorski (ed.), *Respiratory Regulation - The Molecular Approach*,
Advances in Experimental Medicine and Biology 756, DOI 10.1007/978-94-007-4549-0_21,

in about 30% and bind to the same ligands on antigen presenting cells (APC). CD28 is constitutively present on naive CD4+ T cells. In contrast, CD152 is rarely expressed on naive CD4+ T cells, but its expression increases after T cell receptor (TCR) activation. The mRNA of CTLA-4 is detectable as soon as 1 h after TCR activation (Lindsten et al. 1993). The CTLA-4 protein is stored intracellularly and appears in detectable amounts 24 h after activation and is still present on the surface of a T cell 48–72 later (Maszyna et al. 2003). The regulation of the surface expression of CD152 is dependent on the reaction between the clathrin-coated pit adaptor protein (AP-2) and the intracellular thyrosine motif of CTLA-4 (Chuang et al. 1997; Shiratori et al. 1997). The majority of CTLA-4 is stored in clathrin-associated complexes and after activation it is relocalized to the surface of a T cell, where it becomes an integral part of an immunological synapse (Linsley et al. 1996; Darlington et al. 2002; Egen and Allison 2002). Surface expression of CTLA-4 is dynamically regulated by the process of its passing trough the cell membrane into cytoplasm. Alegre et al. (1996) revealed that the surface CTLA-4 after the activation constitutes only 10% of the whole number of the molecules in a T cell and the ratio between the surface and intracellular expression is constant. A direct down-regulation of TCR activation by CTLA-4 is dependent on the surface located molecules, but in the light of recent findings, CTLA-4 plays also an important role as a modulator of function and maturation of T regulatory cells (Treg). In knock-out mice, the loss of CTLA-4 leads to a massive lymphoproliferative syndrome (Tivol et al. 1995; Waterhouse et al. 1995). Impaired function of CTLA-4 is associated with disorders of peripheral autotolerance and autoimmunity in experimental animals and also in humans. One of the most frequent organ specific autoimmune diseases in humans is the autoimmune Hashimoto's thyroiditis (HT). Therefore, HT patients constitute an attractive group for the investigation of T cell function in humans. The aim of the present study was to assess the surface and intracellular expressions of CTLA-4 in T cells isolated from peripheral blood of children with HT at baseline and after *in vitro* T cells activation and to compare it with those in healthy controls.

21.2 Methods

The protocol of the study was approved by the Bioethics Committee of Medical University of Warsaw, Poland. Parents of the patients signed informed consent for the participation in the study.

Blood samples were obtained from 46 children: 25 with HT of the mean age of 14.9 ± 2.3 years and 21 age-matched controls. HT was diagnosed on the basis of the presence of high levels of anti-thyroid antibodies: anti-thyroid peroxidase and/or anti-thyroglobulin antibodies together with disseminated hypoechogenicity of thyroid gland in an ultrasound examination. Children in the control group were free from any infection, autoimmune disease, or thyroid disorders.

The cell preparation before cytometric analysis has been described previously (Kucharska et al. 2009). Briefly, heparinized blood samples obtained from patients and controls were diluted three times with saline, and centrifuged for 30 min at $400 \times g$ on Histopaque 1077-1 density gradient from SIGMA Diagnostics (St. Louis, MO). Isolated PBMCs were incubated with monoclonal antibodies for 30 min at 25°C in darkness. Analysis was performed with the use of monoclonal antibodies combination: CD4- FITC/ CD28 -PC5/ CD152 -PE and CD8 -FITC/ CD28 -PC5/ CD152 -PE from Immunotech Beckman Coulter Company (Beckman Coulter Company, Paris Nord, France). After incubation, samples were fixed and lysed by the reagent set Uti-Lyse (Dako Cytomation, Gdynia, Poland). The T cell phenotype was evaluated using the flow cytometer Beckman Coulter EPICS XL 4C (EPICS XL/XL-MCL, version 2.0, Beckman Coulter Company, Paris Nord, France). T cell phenotype was evaluated at baseline and after 48 h of T cell culture with phytohemagglutinine (48-PHA) as the mitogen activating the T cell.

Results were statistically analyzed by a *t*-test or Mann- Whitney U-test as required. $P < 0.05$ was considered to indicate statistical significance.

21.3 Results

21.3.1 Intracellular Expression of CD152 on T Cells

The number of T cells with intracellular CD152 expression was comparable at baseline in both HT patients and control children: 3.4% *vs.* 2.7%, respectively ($p > 0.05$). The CD4+ subset of T cells positive for CD152 reached 2.2% and 2.1% in the HT and control children, respectively; the difference being insignificant. Likewise, CD8+ cells expressing CD152+ intracellularly did not differ significantly between the patients and controls (Table 21.1).

After stimulation with 48-PHA, the intracellular CD152 increased to comparable values in both HT and control children; from 3.4% to 8.8% and from 2.7 to 6.3, respectively. The CD4+ subset of T cells positive for CD152 reached 6.5% and 4.8% in the HT and control children, respectively. In the CD8+ subset, intracellular CD152 was present in 3.0% and 3.6% of T cells in the HT and control children, respectively. These differences between the patients and controls were not significant (Table 21.1). The alterations of the intracellular phenotype of T cells are illustrated in Fig. 21.1a and b.

21.3.2 The Surface Expression of CD152 on T Cells

At baseline, the number of T cells with surface expression of CD152 was significantly lower in the HT than that in the control children: 2.6% ± 1.8% *vs.* 4.5% ± 1.5%, respectively ($p < 0.001$); the difference remained significant when T cells were divided into CD4+ ($p < 0.001$) and CD8+ subsets ($p < 0.001$) (Table 21.2).

After 48-PHA stimulation, the number of CD152+ T cells increased in both HT and control children, but the increase was higher in CD4+ than in CD8+ subset. In the CD8+ T cells, the difference

Table 21.1 Intracellular CD profile of T cells in Hashimoto's thyroditis (HT) and healthy control children at baseline and after 48 h activation by 48-PHA

		CD4+152+ (%)	CD8+152+ (%)	CD152+ (%)	CD4+ (%)	CD8+ (%)
Baseline	**HT**	2.2 ± 1.5	2.6 ± 3.7	3.4 ± 1.4	37.0 ± 11.1	18.3 ± 4.9
	Control	2.1 ± 1.1	1.8 ± 1.4	2.7 ± 1.4	29.4 ± 10.9	22.9 ± 9.3
48-PHA	**HT**	6.5 ± 3.1	3.0 ± 1.9	8.8 ± 3.8	33.1 ± 10.9	13.8 ± 4.9
	Control	4.8 ± 3.5	3.6 ± 1.6	6.3 ± 3.1	21.9 ± 9.1	15.3 ± 6.1

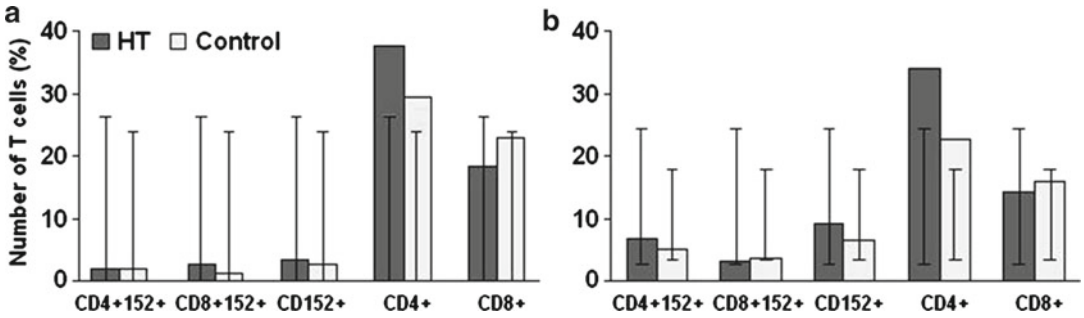

Fig. 21.1 Alterations of the intracellular CD phenotype of T cells before (**a**) and after (**b**) PHA stimulation in Hashimoto's thyroditis children and controls

Table 21.2 Surface CD profile of T cells in Hashimoto's thyroditis (HT) and healthy control children at baseline and after 48 h activation by 48-PHA

		CD4+152+ (%)	CD8+152+ (%)	CD152+ (%)	CD4+ (%)	CD8+ (%)
Baseline	**HT**	1.0 ± 0.8	1.2 ± 1.6	2.6 ± 1.8	23.7 ± 10.1	16.6 ± 8.0
	Control	2.5 ± 1.6	2.5 ± 1.6	4.5 ± 1.5	23.9 ± 9.6	17.0 ± 5.9
48-PHA	**HT**	2.9 ± 1.8	2.0 ± 1.5	4.1 ± 2.2	21.8 ± 11.4	12.2 ± 5.7
	Control	3.4 ± 1.4	4.0 ± 1.5	6.1 ± 0.9	15.6 ± 5.1	14.2 ± 4.4

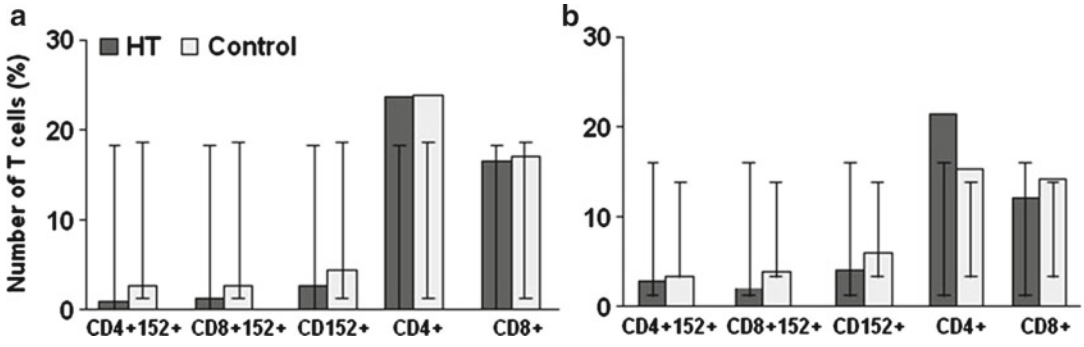

Fig. 21.2 Alterations of the surface CD phenotype of T cells before (**a**) and after (**b**) PHA stimulation

between the number of CD152+ T cells at baseline and after 48-PHA was not statistically significant in either group of children (Table 21.2). Figure 21.2a and b illustrate the alterations of the surface CD phenotype of T cells.

21.4 Discussion

In the present study, the number of CD4+ T cells with the intracellular expression of CD152 was similar in HT and healthy children, but only a part of T cells showed the surface expression of CD152 antigen. This suggests that in HT patients T cells are able to produce the CD152 molecule, but its transport from cytoplasm to cell membrane is hampered. It is unclear why CD152 molecule can not reach the surface of a cell in the course of HT. Anjos et al. (2002) formed an interesting hypothesis that one of the polymorphisms of the CTLA-4 gene associated with autoimmune diseases changes the signal peptide of CTLA-4, alters the early endoplasmic reticulum trafficking or processing of CTLA-4 (CD152), and leads to its differential expression on the cell surface. Thus, a change in a signal peptide can lead to incomplete glycosylation of the protein and results in impaired transit between clathrin-coated vesicles and the cell membrane, resulting in a lower expression of CD152 on the cell surface. Our present data confirm that in HT patients the CD152 molecule lacks the ability of being expressed on T cell surface, even though its intracellular resources are similar to healthy controls. It is unresolved why the basic subsets, CD4+ and CD8+ T cells, have a different pattern of the CD152 antigen response to cell stimulation: an increase in the CD152 on CD4+ T cell subset and no response of CD8+ T cells. This observation was noted only in HT patients. The CD152 antigen in T cells behaved differently in healthy individuals in whom the number of CD152+ T cells increased both intracellularly and on cell surface after stimulation. A dissimilar response of CD8+ CD152+ T cells in HT patients and controls might reflect impaired function of CD152 on regulatory cells (Tregs) and suggests that the alterations are specific for this disease. In HT, the autoimmune process is mainly modulated

by CD8+ effector cells and their cytotoxicity (Weetman 2003; Weetman and McGregor 1994). Nevertheless, it has been recently found that in autoimmune thyroid diseases the naturally occurring regulatory T cells CD4+CD25+ and also CD8+CD122+ play an important role (Marazuela et al. 2006; McLachlan et al. 2007). According to the study of McLachlan et al. (2007), Tregs are a major factor in the intermolecular spreading of the immune response to thyroid antigens and in a shift from Graves' disease and Hashimoto's thyroiditis. Saitoh et al. (2007) supported this idea in excellent animal study. Our present observation on the CD8+ subset can reflect their importance in the pathogenesis of HT in humans. The difference between the CD152 regulation in CD4+ and CD8+ is in concert with the observation of several authors, confirming that induction of CD152 restricts clonal expansion of helper T cells (Doyle et al. 2001) and plays a role in the differentiation and action of Th1 and Th2 cells (Alegre et al. 1998; Bour-Jordan et al. 2003). Under normal conditions, CD152 is constitutively expressed on Tregs (Eggena et al. 2004) and is necessary for their proper function (Takahashi et al. 2000) and generation (Tang et al. 2004; Zheng et al. 2006). On the other hand, hypo-function of CD152 can impair the regulation of the T cell response to a mitogen. Stephens et al. (2001) have found that the CD4+ CD25+ Treg proliferate poorly in response to mitogenic stimulation and suppress the proliferation of $CD4^{+}CD25^{-}$ cells in co-culture. Therefore, impaired function of these cells can explain an increase in the number of CD4+ after mitogen stimulation in our HT patients.

21.5 Conclusions

Hashimoto's thyroiditis is characterized by impaired inhibitory function of CD152. The impairment may depend on imbalance of intracellular/surface CD152 expression on T cells.

Conflicts of interest: The authors declare no conflicts of interest in relation to this article.

References

Alegre, M. L., Noel, P. J., Eisfelder, B. J., Chuang, E., Clark, M. R., Reiner, S. L., & Thompson, C. B. (1996). Regulation of surface and intracellular expression of CTLA-4 on mouse T cells. *The Journal of Immunology, 157*, 4762–4770.

Alegre, M. L., Shiels, H., Thompson, C. B., & Gajewski, T. F. (1998). Expression and function of CTLA-4 in Th1 and Th2 cells. *The Journal of Immunology, 161*, 3347–3356.

Anjos, S., Nguyen, H., Ounissi-Benkalha, H., Tessier, M. C., & Polychronakos, C. (2002). A common autoimmunity predisposing signal peptide variant of the cytotoxic T-lymphocyte antigen 4 results in inefficient glycosylation of the susceptibility allele. *The Journal of Biological Chemistry, 277*, 46478–46486.

Bour-Jordan, H., Grogan, J. L., Tang, Q., Auger, J. A., Locksley, R. M., & Bluestone, J. A. (2003). CTLA-4 regulates the requirement for cytokine -induced signals in Th2 lineage commitment. *Nature Immunology, 4*, 182–188.

Chambers, C. A., Krummel, M. F., Boitel, B., Hurwitz, A., Sullivan, T. J., Fournier, S., Cassel, D., Brunner, D., & Allison, J. P. (1996). The role of CTLA-4 in the regulation and initiation of T-cell responses. *Immunology Reviews, 153*, 27–46.

Chuang, E., Alegre, M. L., Duckett, C. S., Noel, P. J., Van der Heiden, M. G., & Thompson, C. B. (1997). Interaction of CTLA-4 with the clathrin- associated protein AP50 results in ligand-independent endocytosis that limits cell surface expression. *The Journal of Immunology, 159*, 144–151.

Darlington, P. J., Baroja, M. L., Chau, T. A., Siu, E., Ling, V., Carreno, B. M., & Madrenas, J. (2002). Surface cytotoxic T-lymphocyte-associated antigen 4 partitions within lipid rafts and relocates to the immunological synapse under conditions of inhibition of T cell activation. *The Journal of Experimental Medicine, 195*, 1337–1347.

Doyle, A. M., Mullen, A. C., Villarino, A. V., Hutchins, A. S., High, F. A., Lee, H. W., Thompson, C. B., & Reiner, S. L. (2001). Induction of cytotoxic T lymphocyte antigen 4 (CTLA-4) restricts clonal expansion of helper T cells. *The Journal of Experimental Medicine, 194*, 893–902.

Egen, J. G., & Allison, J. P. (2002). Cytotoxic T lymphocyte antigen-4 accumulation in the immunological accumulation in the immunological synapse is regulated by TCR signal strength. *Immunity, 16*, 23–35.

Eggena, M. P., Walker, L. S., Nagabhushanam, V., Barron, L., Chodos, A., & Abbas, A. K. J. (2004). Cooperative roles of CTLA-4 and regulatory T cells in tolerance to an islet cell antigen. *The Journal of Experimental Medicine, 21*, 1725–1730.

Kucharska, A. M., Gorska, E., Wasik, M., Pyrzak, B., & Demkow, U. (2009). Expression of CD152 (CTLA-4) in children with autoimmune thyroiditis and +49 A/G polymorphism of exon 1 of the CTLA-4 gene. *Journal of Physiology and Pharmacology, 60*(Suppl 5), 77–80.

Lindsten, T. K. P., Lee, S., Harris, B., Petryniak, N., Craighead, N., Reynolds, P. J., Lombard, D. B., Freeman, G. J., Nadler, L. M., Gray, G. S., Thompson, C. B., & June, C. H. (1993). Characterisation of CTLA-4 structure and expression on human T cells. *The Journal of Immunology, 151*, 3489–3499.

Linsley, P. S., Bradshaw, J., Greene, J., Peach, R., Bennett, K. L., & Mittler, R. S. (1996). Intracellular trafficking of CTLA-4 and focal localisation towards sites of TCR engagement. *Immunity, 4*, 535–543.

Marazuela, M., Garcia-Lopez, M. A., Figueroa-Vega, N., de la Fuente, H., Alvarado-Sanches, B., Monsivais-Urenda, A., Sanches-Madrid, F., & Gonzalez-Amaro, R. (2006). Regulatory T cells in human autoimmune thyroid disease. *The Journal of Clinical Endocrinology and Metabolism, 91*, 3639–3646.

Maszyna, F., Hoff, H., Kunkel, D., Radbruch, A., & Brunner-Weinzierl, M. C. (2003). Diversity of clonal T cell proliferation is mediated by differential expression of CD152 (CTLA-4) on the cell surface of activated individual T lymphocytes. *The Journal of Immunology, 171*, 3459–3466.

McLachlan, S. M., Nagayama, Y., Pichurin, P. N., Mizutori, Y., Chen, C. R., Misharin, A., Aliesky, H. A., & Rapoport, B. (2007). The link between Graves' disease and Hashimoto's thyroiditis: A role for regulatory T cells. *Endocrinology, 148*, 5724–5733.

Saitoh, O., Abiru, N., Nakahara, M., & Nagayama, Y. (2007). CD8+CD122+ T cells, a newly identified regulatory T subset, negatively regulate Graves' hyperthyroidism in a murine model. *Endocrinology, 148*, 6040–6046.

Shiratori, T., Miyatake, S., Ohno, H., Nakaseko, C., Isono, K., Bonifacino, J. S., & Saito, T. (1997). Tyrosine phosphorylation controls internalization of CTLA-4 by regulating its interaction with clathrin-associated adaptor complex AP-2. *Immunity, 6*, 583–589.

Stephens, L. A., Mottet, C., Mason, D., & Powrie, F. (2001). Human CD4(+)CD25(+) thymocytes and peripheral T cells have immune suppressive activity in vitro. *European Journal of Immunology, 31*, 1247–1254.

Takahashi, T., Tagami, T., Yamazaki, S., Uede, T., Shimizu, J., Sakaguchi, N., Mak, T. W., & Sakaguchi, S. (2000). Immunologic self-tolerance maintained by CD25(+)CD4(+) regulatory T cells constitutively expressing cytotoxic T lymphocyte-associated antigen 4. *The Journal of Experimental Medicine, 17*, 303–310.

Tang, Q., Boden, E. K., Henriksen, K. J., Bour-Jordan, H., Bi, M., & Bluestone, J. A. (2004). Distinct roles of CTLA-4 and TGF-beta in CD4+CD25+ regulatory T cell function. *European Journal of Immunology, 34*, 2996–3005.

Tivol, E. A., Borriello, F., Schweitzer, A. N., Lynch, W. P., Bluestone, J. A., & Sharpe, A. H. (1995). Loss of CTLA-4 leads to massive lymphoproliferation and fatal multiorgan tissue destruction, revealing a critical negative regulatory role of CTLA-4. *Immunity, 3*, 541–547.

Waterhouse, P., Penninger, J. M., Timms, E., Wakcham, A., Shahinian, A., Lee, K. P., Thompson, C. B., Griesser, H., & Mak, T. W. (1995). Lymphoproliferative disorders with early lethality in mice deficient in CTLA-4. *Science, 270*, 985–988.

Weetman, A. P. (2003). Autoimmune thyroid disease: Propagation and progression. *European Journal of Endocrinology, 148*, 1–9.

Weetman, A. P., & McGregor, A. M. (1994). Autoimmune thyroid disease: Further developments in our understanding. *Endocrine Reviews, 15*, 788–830.

Zheng, S. G., Wang, J. H., Stohl, W., Kim, K. S., Gray, J. D., & Horwitz, D. A. (2006). TGF-beta requires CTLA-4 early after T cell activation to induce FoxP3 and generate adaptive CD4+CD25+ regulatory cells. *The Journal of Immunology, 176*, 3321–3329.

Chapter 22
Exercise in Cold Air and Hydrogen Peroxide Release in Exhaled Breath Condensate

E. Marek, J. Volke, K. Mückenhoff, P. Platen, and W. Marek

Abstract Athletes have changes in the lung epithelial cells caused by inhalation of cold and dry air. The exhaled breath condensate contains a number of mediators from the respiratory system and H_2O_2 is described as a marker of airways inflammation. The aim of this study was to determine the influence of exercise combined with cold air on the H_2O_2 release in the exhaled breath. Twelve males (23.1 ± 1.5 years) were randomly assigned at 2 different days (1 day rest) to perform a 50 min run (75–80% of their max. heart rate) under normal (N) laboratory (18.1 ± 1.1°C) or cold (C) field condition (−15.2 ± 3.1°C). Before and immediately after each run, the EBC was collected under laboratory conditions and was analyzed amperometrically. Prior to the two runs, H_2O_2 concentrations were 145.0 ± 31.0 (N) and 160.0 ± 49.1 nmol/L (C) and theoretical release was 70.3 ± 37.1 (N) and 82.6 ± 27.1 pmol/min (C) ($p > 0.05$). After each run, H_2O_2 concentration increased significantly to 388.0 ± 22.8 nmol/L (N) and 622.1 ± 44.2 nmol/L (C) ($p < 0.05$), along with an increase in the theoretical release: 249.2 ± 35.7 pmol/min (N) and 400.9 ± 35.7 pmol/min (C) ($p < 0.05$). We conclude that release of H_2O_2 into the EBC takes place under both resting conditions and after exercise. The concentration and release of H_2O_2 increased after exercise in cold air compared to resting and laboratory conditions, which points to an increase in inflammatory and oxidative stress.

Keywords Hydrogen peroxide • Oxygen • Exhaled breath condensate • Oxidative stress • Airway inflammation

22.1 Introduction

It has been reported that endurance athletes of winter (Karjalainen et al. 2000; Sue-Chu et al. 1999) and summer sports show increased airway neutrophil counts (Koskela 2007) at both rest and after exercise. Furthermore, many publications indicate that especially winter athletes have bronchial hyperresponsiveness (BHR) and symptoms like bronchoconstriction and changes in the epithelial cells caused by the inhalation of cold and dry air (Bougault et al. 2009).

E. Marek (✉) • J. Volke • P. Platen
Department of Sports Medicine and Sports Nutrition, Ruhr University Bochum,
Overbergstraße 19, D-44780 Bochum, Germany
e-mail: eike.marek@rub.de

K. Mückenhoff • W. Marek
Institute of Occupational Physiology, Augusta-Kranken-Anstalt, Bochum, Germany

M. Pokorski (ed.), *Respiratory Regulation - The Molecular Approach*,
Advances in Experimental Medicine and Biology 756, DOI 10.1007/978-94-007-4549-0_22,

Carlsen (2009) pointed out that an increased ventilation during repeated heavy exercise causes stress to the airway epithelium and increases airway mucosal inflammation. Environmental agents, like cold air, will probably increase this stress by an increase in bronchial responsiveness. These findings were supported by several studies. Bougault et al. (2009) demonstrate the effect of heavy endurance training upon the respiratory tract (Larsson et al. 1998). This study shows an increase in the bronchial epithelial cells and an increased number of neutrophils among the athletes, as well as a rise in the number of eosinophils in athletes with BHR. The reason for this increase is described as the wear and tear effect that may be caused by increased ventilation during endurance training and by increased airways inflammation due to training. Taking bronchial biopsies from skiers Helenius et al. (2005) and Karjalainen et al. (2000) reported increased levels of eosinophils and neutrophils and increased concentrations of sputum eosinophil peroxidase and human neutrophil lipocalin in induced sputum from endurance athletes. Davis et al. (2002) performed bronchoscopy and bronchoalveolar lavage in elite racing sled dogs 24–48 h after the completion of a 1,100-mile endurance race in Alaska. Nearly 80% of the dogs showed abnormal accumulations of intraluminal debris, and bronchalveolar lavage obtained after the race showed significantly higher nucleated macrophage and eosinophil counts as compared with sedentary control dogs.

Exhaled breath condensate (EBC) contains a large number of mediators which are influenced by airway infections and other lung diseases and modulated by therapeutic intervention. Among others there is hydrogen peroxide (H_2O_2), which can be measured by currently developed micro enzyme detectors of high sensitivity (Horvath et al. 2005). Hydrogen peroxide is suggested to be a parameter of oxidative stress or inflammatory processes. It is released by neutrophilic and eosinophilic lymphocytes, macrophages, and epithelial airway cells. It provides one line of immune defense, should infection occur, and is the most important marker of airway infection. H_2O_2 is synthesised by superoxide dismutase induced reaction of O^- radicals and H^+-ions. A peroxidase is secreted by airway epithelial cells, which converts hydrogen peroxide into hypothiocyanous acid, a toxic compound that kills pathogens (Horvath et al. 2005).

The aim of the present investigation was to determine the influence of endurance exercise combined with cold air on the H_2O_2 release as a marker of airway inflammation in exhaled breath. Therefore, H_2O_2 was determined in the EBC before and after the same exercise intensity in two different environmental situations. Furthermore, the correlation between the theoretical H_2O_2 release and ventilation was determined to distinguish the exercise effect and the cold air effect on the release of H_2O_2 EBC.

22.2 Methods

The study was performed in conformity with the Declaration of Helsinki (1989) for Human Experimentation and the protocol was approved by a local Ethics Committee.

22.2.1 Anthropometric Data

The investigation was carried out on 12 healthy male subjects, age 23.1 ± 1.5 years, height 178.2 ± 2.4 cm, and normal BMI 23.3 ± 1.2 kg/m^2 (range 22.1–24.1 kg/m^2). The subjects were free from acute airway infections and had, according to the ECCS references (Quanjer et al. 1993), normal values for the forced vital capacity (113.1 ± 11.4%pred). The mean values for FEV_1 were normal, 105.7 ± 8.8%pred. Tiffeneau Index, another marker for airway obstruction, was also normal in all subjects (107.1 ± 4.5%pred).

22.2.2 Study Protocol

The subjects were randomly assigned to 2 different days (with 1 day rest) to perform one 50 min run (75–80% of their maximum heart rate) under normal laboratory (18.1 ± 1.1°C,) and one under cold field conditions (−15.2 ± 3.1°C). Humidity in the laboratory was 44.5 ± 1.2% and under cold field conditions 77.2 ± 10.7%. Five days before the two runs at different environmental conditions each subject performed a treadmill ramp tests until exhaustion (RQ > 1.1) with a warm-up at 2.4 m/s and 2.8 m/s at 1% uphill grade and exertion of 5% uphill grade with increments of 0.2 m/s every 30 s, to determine the individual maximum heart rate, which amounted to 174 beats/min. The mean heart rate was set at 80% of the maximum rate. Exercise duration was similar in both exercise tests (40.2–41.2 min).

22.2.3 EBC Collection

During rest and immediately after the exercise 100 L of exhaled air were collected. The EBC was obtained by cooling the expired air to −20°C (ECoScreen I, FILT, Berlin, Germany). From the EBC sample, three aliquots were taken each. One sample was immediately analyzed; the two other samples were stored on ice and frozen to −20°C.

The subjects were instructed to breathe normally and to avoid contamination with saliva. During quiet breathing, 99% of the condensate is derived from water vapor. The trap inlay in which the exhaled breath was cooled down was Teflon coated and the condenser cooled the expired air in a counter-flow principle. At rest, 100 L of exhaled air was collected in nearly 8.0 ± 1.1 min and 1.3 ± 0.3 mL EBC was obtained with the ventilation of 10.3 ± 1.3 L/min (average of the two collection time points) (Table 22.1). After exercise, 100 L of exhaled air was collected in 6.5 ± 0.9 min and 1.2 ± 0.3 mL EBC was obtained with the ventilation of 16.7 ± 2.3 L/min. 100 L of exhaled air at 37°C saturated with water vapor at standard atmospheric pressure (101 kPa) should contain 4.4 mL water (Marek et al. 2010). The collected EBC volumes represent nearly 27–29% of the theoretical water vapor content of 100 L of exhaled air. No significant differences in the EBC volume were found before and after the exercise. In the recovery period after exercise, the EBC volume was slightly decreased and represented 27.6% of the theoretical water content (Table 22.1).

22.2.4 Hydrogen Peroxide Analysis

Hydrogen peroxide concentration was analyzed using an EcoCheck amperometer (FILT, Berlin, Germany). H_2O_2 analysis was performed after conversion of H_2O_2 by peroxidase ($H_2O_2 \rightarrow 2H^+ + O_2 + 2e^-$) using miniaturized enzyme detectors (ECoCheck, FILT, Berlin, Germany). Measurements can be performed in an effective range between 30–3,000 nmol/L. Calibrations were performed daily. The method was described in detail in previous papers (Marek et al. 2010). Acid-base parameters were measured in crude EBC samples. H_2O_2 was measured in 0.3 mL EBC diluted in 0.3 mL buffer solution. The rate of release from the lung (pmol/min) is calculated from the concentration of hydrogen peroxide and the collection time of EBC.

22.2.5 Statistical Analysis

Data were compiled in tables (Microsoft, Excel 2003). The final statistical analysis was performed using the SPSS 11.5 statistic program. After testing the data for homogeneity and normal distribution, means ± SD were calculated. By using a paired *t*-test, respiratory, cardiovascular, and EBC data were tested for significant differences ($p < 0.05$).

Table 22.1 Results of EBC collection

	Laboratory exercise		Cold air exercise	
Parameter	Pre exercise	Post exercise	Pre exercise	Post exercise
Ventilation (L)	12.1 ± 1.5 (9.9–14.4)	17.2 ± 2.5 (12.5–20.1)	8.4 ± 1.0 (6.9–10.1)	16.3 ± 2.1 (10.0–16.6)
Collection time (min)	8.4 ± 1.0 (6.9–10.1)	6.8 ± 0.9 (5.0–8.0)	7.6 ± 1.3 (6.2–10.5)	6.2 ± 0.8 (5.1–8.3)
EBC volume (mL)	1.3 ± 0.2 (0.9–1.2)	1.2 ± 0.2 (0.9–1.5)	1.3 ± 0.3 (0.9–1.2)	1.2 ± 0.3 (0.9–1.9)
% of theoretical volume[a]	29.5 ± 3.5 (20.9–27.9)	27.3 ± 5.8 (20.9–34.4)	29.5 ± 3.6 (20.7–27.8)	27.1 ± 7.3 (20.9–44.3)
H_2O_2 concentration (nmol/L)	145.0 ± 31.1 (100.9–200.0)	388.0 ± 22.8* (280.0–370.0)	160.1 ± 49.1 (95.9–185.0)	622.1 ± 44.2* (550.0–690.0)
Theoretical H_2O_2 release (pmol/min)	70.3 ± 37.1 (51.6–107.3)	249.2 ± 35.7* (193.0–317.3)	82.6 ± 27.1 (49.6–111.3)	400.9 ± 35.7* (332.4–503.8)

*$p < 0.05$

[a]Derived from 100 L exhaled air statured with water vapor

22.3 Results

22.3.1 H_2O_2 Concentration and H_2O_2 Release in EBC

At rest before the laboratory exercise, the H_2O_2 concentration and theoretical release in EBC were 145.0 ± 31.1 nmol/L and 70.3 ± 37.1 pmol/min, respectively. In the recovery phase after exercise, the H_2O_2 concentration and its release in EBC significantly increased to 388.0 ± 22.8 nmol/L and 249.2 ± 35.7 pmol/min, respectively, compared with the resting situation ($p < 0.05$) (Table 22.1).

At rest before the cold air exercise, the H_2O_2 concentration and its release in the collected EBC were 160.1 ± 49.1 nmol/L and 82.6 ± 27.1 pmol/min, respectively. In the recovery phase after exercise, the respective values amounted to 622.1 ± 44.2 nmol/L and 400.9 ± 35.7 pmol/min; being significantly greater compared to rest ($p < 0.05$) (Table 22.1).

Comparing the resting situations before the laboratory and cold air exercise, the H_2O_2 concentration and its release in EBC were not significantly different. In contrast, comparing the recovery phase after the laboratory and cold air exercise, there were significant differences regarding both H_2O_2 concentration and its release in EBC (Table 22.1).

22.3.2 Correlation Between the Theoretical H_2O_2 Release in EBC and Ventilation

The theoretical H_2O_2 release in EBC significantly correlated with the ventilation for resting situations ($r = 0.77$, $p < 0.05$) (Fig. 22.1), and in the recovery phase after exercise in both laboratory condition ($r = 0.85$, $p < 0.05$) and cold air ($r = 0.81$, $p < 0.05$). Furthermore, H_2O_2 release increased significantly more after cold air exercise, with nearly the same ventilation.

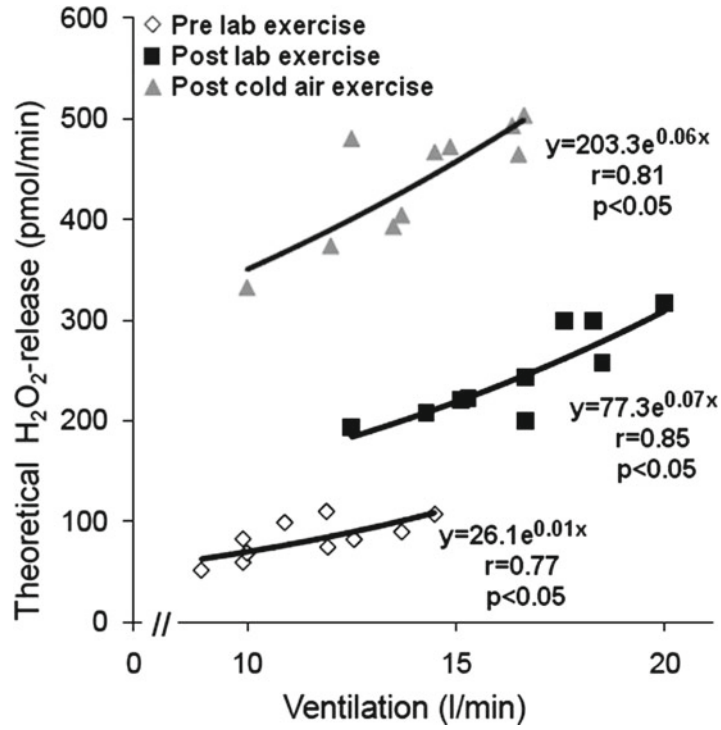

Fig. 22.1 Correlation of H_2O_2 release and ventilation in resting situation, after exercise in the laboratory, and after exercise in cold air

22.4 Discussion

The release of H_2O_2 into the EBC has been shown under resting conditions and after exercise. Concentration and release significantly increased after exercise in cold air compared to resting and laboratory conditions and indicate an increase of inflammatory and oxidative stress.

22.4.1 Airway Inflammation in Athletes

The prevalence of asthma and bronchial hyperresponsiveness is greater among elite athletes than in the general population and even higher among certain groups of athletes (long distance runners, cyclists, skiers, and swimmers) than among athletes in general. Belda et al. (2008) mention that the underlying inflammation in such athletes is quite similar to the pattern seen in other persons with asthma. Inflammation has been related in some athletes to the presence of asthma, atopy, and type of sport, season, and duration of training. The reason for the inflammation is still not fully understood. Koskela (2007) suggested cold air as a possible reason for respiratory symptoms. At rest and during light exercise, athletes often breathe through the nose. Even subfreezing air is almost completely saturated and warmed to near body temperature when it passes the nasal cavity (Koskela 2007). Therefore, at rest and during light exercise, the possible trigger sites for cold air-provoked respiratory symptoms include the facial skin and nasal mucosa but not lower airways. Exercise is associated with hyperpnea. A shift from nose to combined nose-and-mouth breathing takes place when the ventilation level exceeds approximately 30 L/min. When the ventilation level further increases, incompletely conditioned air can reach lower airways (Koskela 2007). Therefore, during heavy exercise the trigger sites for cold air-provoked respiratory symptoms also include oral mucosa, pharynx, larynx and the lower airways. Furthermore, animal studies have shown that repeated cooling and desiccation of peripheral airways lead to a loss of ciliated epithelium, thickening of the lamina propria with increased concentrations of inflammatory cells, hyperresponsiveness and airway obstruction (Koskela 2007). Thus, experimental studies suggest that cooling and drying can damage the airway epithelium and, if repeated, can lead to changes in the airway wall structure and function.

22.4.2 Factors Which Influence the Exhaled Breath Condensate/Mediators

A number of studies have reported a highly variable concentration of H_2O_2 in healthy adults, ranging from ≤50 nmol/L (Gerritsen et al. 2005) through 250–300 nmol/L (Loukides et al. 2002; Nowak et al. 2001) to 480 nmol/L (Svensson et al. 2004) in EBC. One reason for these wide differences could be that the collection time is different from subject to subject. The higher the ventilation the greater is the dilution of the exhaled breath. So it is necessary to calculate the release of H_2O_2 in the exhaled breath and the EBC. This hypothesis is support by Schleiss et al. (2000) who found lower exhaled H_2O_2 concentrations at higher flow rates. Another reason could be that there is an intraindividual release of markers like H_2O_2 in EBC (Knobloch et al. 2008). H_2O_2 in EBC is unstable and has to be analyzed directly after collection or should be frozen for later analysis (Horvath et al. 2005). In the present investigation three aliquots were taken. One sample was immediately analyzed; the two other samples were frozen to −20°C, so no major loss of H_2O_2 should be considered.

In young and healthy non-smokers, Nowak et al. (2001) reported H_2O_2 concentrations from 0.0 to 0.9 µmol/L. The H_2O_2 values were significantly increased in older healthy subjects and smokers. The authors also found a circadian rhythm in H_2O_2 concentration, with the highest values at 12:00 and 24:00 h. The results from this investigation (152 ± 80 nmol/L) are in accord with those from the literature (150–340 nmol/L) (Loukides et al. 2002).

22.4.3 H_2O_2 as Oxidative Stress and Inflammatory Marker

Physical exercise is characterized by an increase in reactive oxygen species (ROS) production (Riediker and Danuser 2007). The main sources of ROS during exercise are the mitochondrial respiratory chain, xanthine oxidase-catalysed reaction and neutrophil activation (Sen 2001). H_2O_2 correlates with oxygen consumption at rest, and under moderate and exhausting exercise (Heinicke et al. 2009; Marek et al. 2009, 2010). The higher the oxygen consumption the greater is the H_2O_2 release in EBC, because H_2O_2 is produced after converting superoxide anions O_2^- to H_2O_2. The present results after exercise in laboratory condition showed a nearly 2.5-fold increase in H_2O_2 concentration and a 3.5-fold increase in H_2O_2 release. These increases could be associated with a higher oxygen consumption during and immediately after exercise. The results can be interpreted as a higher level of oxidative stress.

In the respiratory tract, H_2O_2 is released from neutrophile and eosinophile lymphocytes as well as from macrophages and epithelial cells (Conner et al. 2002) in inflammatory processes. Compared with healthy subjects, increased levels of H_2O_2 are found in the EBC from smokers (Nowak et al. 1996), patients with bronchial asthma (Antczak et al. 1997; van Beurden et al. 2002), COPD (Dekhuijzen et al. 1996; Nowak et al. 1998), and bronchiectases (Loukides et al. 2002). In induced sputum H_2O_2 correlates with the amount of eosinophiles and airway responsiveness (Horvath et al. 1998) in subjects with moderate asthma. H_2O_2 as an inflammatory marker is of special interest for the time course of disease and therapy control. Exacerbations of COPD enhance the level of H_2O_2 compared with stable phases (Dekhuijzen et al. 1996). Antioxidative therapy with N-acetylcystein results in a decrease in H_2O_2 in the EBC (Kasielski and Nowak 2001). The present results after exercise in the cold air environment show a nearly 3-fold increase in H_2O_2 concentration and a 5-fold increase in H_2O_2 release.

In the present study, H_2O_2 concentration and H_2O_2 release increased nearly 1.6-fold when athletes performed exercise of the same intensity in cold air, compared with a laboratory condition. This increase could have to do with the hypothesis put forward by Koskela (2007) which suggests that cold air hyperpnea leads to hyperosmolarity of airway surface fluid, which in turn induces a mediator release from cells along airway mucosa. The cells that respond to hyperosmolarity could be the neutrophils, eosinophils, or the mast cell releasing leukotrienes, prostaglandins, or histamine (Koskela 2007) or H_2O_2 (Marek et al. 2009). It seems possible that an increased number of inflammatory cells and higher release of H_2O_2 in the lungs following a short exposure to cold air is a normal response in healthy subjects.

In conclusion, release of H_2O_2 in exhaled breath conspicuously increased after exercise in cold air, which may be due to inflammatory and oxidative stress developing during exhausting exercise in cold air.

Conflicts of interest: No conflicts of interest were reported in relation to this article.

References

Antczak, A., Nowak, D., Shariati, B., Krol, M., Piasecka, G., & Kurmanowska, Z. (1997). Increased hydrogen peroxide and thiobarbituric acid-reactive products in expired breath condensate of asthmatic patients. *The European Respiratory Journal, 10*, 1235–1241.

Belda, J., Ricart, S., Casan, P., Giner, J., Bellido-Casado, J., Torrejon, M., Margarit, G., & Drobnic, F. (2008). Airway inflammation in the elite athlete and type of sport. *British Journal of Sports Medicine, 42*, 244–249.

Bougault, V., Turmel, J., St-Laurent, J., Bertrand, M., & Boulet, L. P. (2009). Asthma, airway inflammation and epithelial damage in swimmers and cold-air athletes. *The European Respiratory Journal, 33*, 740–746.

Carlsen, K. H. (2009). Asthma, airway inflammation and epithelial damage in elite athletes. *The European Respiratory Journal, 33*, 713–714.

Conner, G. E., Salathe, M., & Forteza, R. (2002). Lactoperoxidase and hydrogen peroxide metabolism in the airway. *American Journal of Respiratory and Critical Care Medicine, 166*, S57–S61.

Davis, M. S., Mckiernan, B., Mccullough, S., Nelson, S., Jr., Mandsager, R. E., Willard, M., & Dorsey, K. (2002). Racing Alaskan sled dogs as a model of "ski asthma". *American Journal of Respiratory and Critical Care Medicine, 166*, 878–882.

Dekhuijzen, P. N., Aben, K. K., Dekker, I., Aarts, L. P., Wielders, P. L., Van Herwaarden, C. L., & Bast, A. (1996). Increased exhalation of hydrogen peroxide in patients with stable and unstable chronic obstructive pulmonary disease. *American Journal of Respiratory and Critical Care Medicine, 154*, 813–816.

Gerritsen, W. B., Zanen, P., Bauwens, A. A., Van den Bosch, J. M., & Haas, F. J. (2005). Validation of a new method to measure hydrogen peroxide in exhaled breath condensate. *Respiratory Medicine, 99*, 1132–1137.

Heinicke, I., Boehler, A., Rechsteiner, T., Bogdanova, A., Jelkmann, W., Hofer, M., Rawlings, P., Araneda, O. F., Behn, C., Gassmann, M., & Heinicke, K. (2009). Moderate altitude but not additional endurance training increases markers of oxidative stress in exhaled breath condensate. *European Journal of Applied Physiology, 106*, 599–604.

Helenius, I., Lumme, A., & Haahtela, T. (2005). Asthma, airway inflammation and treatment in elite athletes. *Sports Medicine, 35*, 565–574.

Horvath, I., Donnelly, L. E., Kiss, A., Kharitonov, S. A., Lim, S., Chung, K. F., & Barnes, P. J. (1998). Combined use of exhaled hydrogen peroxide and nitric oxide in monitoring asthma. *American Journal of Respiratory and Critical Care Medicine, 158*, 1042–1046.

Horvath, I., Hunt, J., Barnes, P. J., Alving, K., Antczak, A., Baraldi, E., Becher, G., Van Beurden, W. J., Corradi, M., Dekhuijzen, R., Dweik, R. A., Dwyer, T., Effros, R., Erzurum, S., Gaston, B., Gessner, C., Greening, A., Ho, L. P., Hohlfeld, J., Jobsis, Q., Laskowski, D., Loukides, S., Marlin, D., Montuschi, P., Olin, A. C., Redington, A. E., Reinhold, P., Van Rensen, E. L., Rubinstein, I., Silkoff, P., Toren, K., Vass, G., Vogelberg, C., & Wirtz, H. (2005). Exhaled breath condensate: Methodological recommendations and unresolved questions. *The European Respiratory Journal, 26*, 523–548.

Karjalainen, E. M., Laitinen, A., Sue-Chu, M., Altraja, A., Bjermer, L., & Laitinen, L. A. (2000). Evidence of airway inflammation and remodeling in ski athletes with and without bronchial hyperresponsiveness to methacholine. *American Journal of Respiratory and Critical Care Medicine, 161*, 2086–2091.

Kasielski, M., & Nowak, D. (2001). Long-term administration of N-acetylcysteine decreases hydrogen peroxide exhalation in subjects with chronic obstructive pulmonary disease. *Respiratory Medicine, 95*, 448–456.

Knobloch, H., Becher, G., Decker, M., & Reinhold, P. (2008). Evaluation of H_2O_2 and pH in exhaled breath condensate samples: Methodical and physiological aspects. *Biomarkers, 13*, 319–341.

Koskela, H. O. (2007). Cold air-provoked respiratory symptoms: The mechanisms and management. *International Journal of Circumpolar Health, 66*, 91–100.

Larsson, K., Tornling, G., Gavhed, D., Muller-Suur, C., & Palmberg, L. (1998). Inhalation of cold air increases the number of inflammatory cells in the lungs in healthy subjects. *The European Respiratory Journal, 12*, 825–830.

Loukides, S., Bouros, D., Papatheodorou, G., Lachanis, S., Panagou, P., & Siafakas, N. M. (2002). Exhaled H_2O_2 in steady-state bronchiectasis: Relationship with cellular composition in induced sputum, spirometry, and extent and severity of disease. *Chest, 121*, 81–87.

Marek, E., Platen, P., Volke, J., Muckenhoff, K., & Marek, W. (2009). Hydrogen peroxide release and acid-base status in exhaled breath condensate at rest and after maximal exercise in young, healthy subjects. *European Journal of Medical Research, 14*(Suppl 4), 134–139.

Marek, E. M., Volke, J., Hawener, I., Platen, P., Muckenhoff, K., & Marek, W. (2010). Measurements of lactate in exhaled breath condensate at rest and after maximal exercise in young and healthy subjects. *Journal of Breath Research, 4*, 017105.

Nowak, D., Antczak, A., Krol, M., Pietras, T., Shariati, B., Bialasiewicz, P., Jeczkowski, K., & Kula, P. (1996). Increased content of hydrogen peroxide in the expired breath of cigarette smokers. *The European Respiratory Journal, 9*, 652–657.

Nowak, D., Kasielski, M., Pietras, T., Bialasiewicz, P., & Antczak, A. (1998). Cigarette smoking does not increase hydrogen peroxide levels in expired breath condensate of patients with stable COPD. *Monaldi Archives for Chest Disease, 53*, 268–273.

Nowak, D., Kalucka, S., Bialasiewicz, P., & Krol, M. (2001). Exhalation of H_2O_2 and thiobarbituric acid reactive substances (TBARs) by healthy subjects. *Free Radical Biology & Medicine, 30*, 178–186.

Quanjer, P. H., Tammeling, G. J., Cotes, J. E., Pedersen, O. F., Peslin, R., & Yernault, J. C. (1993). Lung volumes and forced ventilatory flows. Report Working Party Standardization of Lung Function Tests, European Community for Steel and Coal. Official Statement of the European Respiratory Society. *The European Respiratory Journal. Supplement, 16*, 5–40.

Riediker, M., & Danuser, B. (2007). Exhaled breath condensate pH is increased after moderate exercise. *Journal of Aerosol Medicine, 20*, 13–18.

Schleiss, M. B., Holz, O., Behnke, M., Richter, K., Magnussen, H., & Jorres, R. A. (2000). The concentration of hydrogen peroxide in exhaled air depends on expiratory flow rate. *The European Respiratory Journal, 16*, 1115–1118.

Sen, C. K. (2001). Antioxidant and redox regulation of cellular signaling: Introduction. *Medicine and Science in Sports and Exercise, 33*, 368–370.

Sue-Chu, M., Henriksen, A. H., & Bjermer, L. (1999). Non-invasive evaluation of lower airway inflammation in hyper-responsive elite cross-country skiers and asthmatics. *Respiratory Medicine, 93*, 719–725.

Svensson, S., Olin, A. C., Larstad, M., Ljungkvist, G., & Toren, K. (2004). Determination of hydrogen peroxide in exhaled breath condensate by flow injection analysis with fluorescence detection. *Journal of Chromatography. B, Analytical Technologies in the Biomedical and Life Sciences, 809*, 199–203.

Van Beurden, W. J., Harff, G. A., Dekhuijzen, P. N., Van den Bosch, M. J., Creemers, J. P., & Smeenk, F. W. (2002). An efficient and reproducible method for measuring hydrogen peroxide in exhaled breath condensate. *Respiratory Medicine, 96*, 197–203.

Chapter 23
Non-invasive Assessment of Exhaled Breath Pattern in Patients with Multiple Chemical Sensibility Disorder

Andrea Mazzatenta, Mieczyslaw Pokorski, Sergio Cozzutto, Pierluigi Barbieri, Vittore Veratti, and Camillo Di Giulio

Abstract Multiple chemical sensitivity (MCS) is a complex disorder initiated by chemical exposure, particularly through the airways. MCS patients report sensitivity or intolerance to low levels of a wide spectrum of chemicals. Symptoms could include asthma-like signs, rhinitis, fatigue, cognitive dysfunction, psycho-physiological alteration, and other specific tissue reactions resembling hypoxic and oxidative stress effects. To recognize physiological signs that would allow the diagnosis of MCS in a non-invasive way we investigated the potential application of a new sensor system. In healthy volunteers, we measured exhaled breath content in the control condition and under exposure to olfactory stressors that mimic hypoxic or pollutant stressors playing a potential role in the generation of the MCS disorder. The recording system used is based on metal oxide semiconductor (MOS) sensor having a sensing range of 450–2,000 ppm CO_2 equivalents, which is able to detect a broad range of compounds playing a potential role in the generation of the MCS disorder, while correlating directly with the CO_2 levels. The results indicate that the recording system employed was suitable for the analysis of exhaled breath content in humans. Interestingly, the system was able to detect and discriminate between the exhaled breath content taken from the control condition and those from conditions under stress that mimicked exposures to pollutant or hypoxia. The results suggest that chronic hypoxia could be involved in the MCS disorder.

Keywords Breath analysis • Exhaled breath content • Multiple chemical sensitivity syndrome • Smell • Volatile organic compounds

A. Mazzatenta (✉) • V. Veratti • C. Di Giulio
Sensorial Physiology Unit, Department of Neuroscience and Imaging,
University of Chieti-Pescara 'G. d'Annunzio', Via dei Vestini 31, 66100 Chieti, Italy
e-mail: amazzatenta@yahoo.com

M. Pokorski
Department of Respiratory Research, Medical Research Center, Polish Academy of Sciences,
Warsaw, Poland

S. Cozzutto
ARCO Solutions srl, Spin off Trieste University, Trieste, Italy

P. Barbieri
Department of Chemical and Pharmaceutical Science, University of Trieste, Trieste, Italy

M. Pokorski (ed.), *Respiratory Regulation - The Molecular Approach*,
Advances in Experimental Medicine and Biology 756, DOI 10.1007/978-94-007-4549-0_23,

23.1 Introduction

The recognition of exhaled breath in order to achieve a diagnosis has a long history. Ancient Greek physicians already knew that the smell of human breath could provide clues of pathology. Characteristically, the sweet and fruity odor of acetone is a sign of diabetes, the musty, fishy reek is the evidence of advancement of a liver disease, the urine-like smell accompanies failing kidneys, while the putrid stench is that of lung abscess (Phillips 1992). Nowadays, breath markers are known to be released in broad range of diseases, e.g., lung diseases, metabolic disorder, and exposure to volatile organic compounds (VOCs), which could be used for the monitoring of the respiratory CO_2/O_2 ratio and the detection of drug abuse or pollutant exposure (Folke et al. 2003; Cao and Duan 2006). In oxidative stress diseases, like asthma, COPD, bronchiectasis, or during lipid peroxidation the following compound are released: methylated alkane (Moretti et al. 2004), H_2O_2 (Kostikas et al. 2003), pentane and ethane (Aghdassl et al. 2003). In lung cancer, pulmonary allograft dysfunction, lung transplant recipient with acute rejection, and in cystic fibrosis the exhaled compounds are: NO, CO, H_2O_2, isoprostanes, nitrite/nitrate, eicosanoids (leukotrienes, prostanoids, isoprostanes), and exhaled carbonyl sulfide (Fisher et al. 1998; Phillips et al. 2003a; Studer et al. 2001; Montuschi et al. 2000). In diabetes, acetone is exhaled (Phillips et al. 2004), while exposure to VOCs provokes a blow-out of the vinyl chloride and cis-1,2-dichloroethene, chloroform, bromodichloromethane, and trichloroethene (Miekisch et al. 2004).

Breath micro-assays give the possibility to detect markers of pathologies linked to oxidative stress, because reactive oxygen species (ROS) oxidize polyunsaturated fatty acids in membranes to alkanes, such as ethane and pentane, which are excreted in the breath as VOCs (Phillips et al. 1999, 2000). This breath test demonstrates that the intensity of oxidative stress varies with age (Phillips et al. 2003a) and it is significantly increased by breathing oxygen (Phillips et al. 2003b), normal pregnancy and preeclampsia of pregnancy (Moretti et al. 2004). Oxidative stress, originated by a cascade of ROS leaking from mitochondria, plays a central role in onset of a number of diseases (Knight 1998). A biological concentration of oxygen keeps the cell enzymatic machinery functional. However, when oxidative stress and hypoxia are established, physiological reactions induce multiple changes in ventilation and in the cardiocirculatory and psychophysiological systems (Schumacker 2003). A cumulative result of oxidative damage induced in cells by ROS derives from aerobic metabolism (Finkel and Holbrook 2000). Physiological antioxidant defenses maintain ROS at harmless levels preventing damage; the balance is strictly related to a constant oxygen concentration (Cataldi and Di Giulio 2009). When this balance falters, for instance in aging or chronic exposure to pollutants, a reduction in homeostatic adaptation to metabolic requirements occurs through the activity of such enzymes as endothelial nitric oxide synthase (eNOS) (Drew and Leeuwenburgh 2002). Chronic hypoxia, *per se*, promotes a remodeling of the structure and function of the bodily systems (Cataldi and Di Giulio 2009).

Anyone or all of the elements above outlined may be involved in the generation of the symptoms of multiple chemical sensitivity (MCS) disorder. Before Randolph Theron, an allergologist who scientifically described in 1945 the first cases of MCS disorder, its depiction existed only in the non-scientific literature, "The Fall of the House of Usher", written by Edgar Allan Poe (1839). Today, MCS disorder is also known as chemical sensitivity or intolerance, toxic, or chemical injury syndrome, environmental illness, sick building syndrome, toxicant-induced loss of tolerance, or idiopathic environmental intolerance emphasizing the role of chemicals in initiating the disease. Epidemiological studies report a discrepant MCS prevalence, ranging from less than 5% up to 20% of the population, revealing a pandemic distribution with a potentially strong inference on public health (Kreutzer et al. 1999; Caress and Steinemann 2004; Joffres et al. 2001). The discrepancy could be explained by the fact that MCS is of a controversial diagnosis because of the debate between those who contend that it is a psychogenic disorder (Gots 1996) and those who believe it is a chemical-caused illness (Pall 2009).

From the point of view of the somatic-psychiatric origin, the phenomenon of MCS is defined as a peculiar manifestation of a technophobic and chemophobic lifestyle. MCS is an ailment in which

the patient defines both the cause and the manifestations of his own condition (Gots 1996). It has been rejected as an established organic disease due to the arguing that chemicals are not involved in generating MCS disorders, because of the lack of a mechanism explaining the puzzling characteristics of it, and the lack of diagnostic physiological tests for scientific validation (Davidoff et al. 2000; Das-Munshi et al. 2007). From the standpoint of a chemically induced illness, MCS is defined as a multi-complex syndrome ascribable to chronic low level exposure to chemicals (Pall 2009). MCS patients are affected by sensitivity or intolerance to low levels of a wide range of chemicals. They report qualitative and quantitative variable symptoms ranging in number from 41 to 74 and affecting nervous, neuromuscular, musculoskeletal, gastrointestinal, cardiac, and airway systems (Miller 2001). Three categories, depending on the site of chemical contact, are distinguished: ingestion, dermal contact, and breathing, all able to produce several levels of irritation, pain, fatigue, sensorial magnification, and anxiety.

Chemoreception is involved at different levels in this syndrome. In MCS patients, there has been shown chemoreceptor activation of sensory nerve C-fibres leading to the release of inflammatory mediators and to alterations in the odor processing as an expression of the lower brain responses to odorants (Hillert et al. 2007; Orriols et al. 2009). MCS sufferer exhibit changes in brain function seen in brain-imaging studies with positron emission tomography (PET), single photon emission computed tomography (SPECT), and electroencephalography (EEG) (Heuser and Wu 2001; Hillert et al. 2007; Simon et al. 1994; Heuser et al. 1994; Bell et al. 1999; Lorig et al. 1991). Genetic studies demonstrate a role of genetic polymorphisms influencing MCS susceptibility. These studies suggest that the interaction between the genetic pool and the environment gives the probability that a person will become ill. Therefore, genetic evidence reinforces the position that MCS is a toxicological phenomenon (Schnakenberg et al. 2007).

Six consensus criteria were identified for the MCS diagnosis (Pall 2009): symptoms are reproducible with repeated chemical exposures; the condition has persisted for a significant period of time; low levels of exposure lower than previously or commonly tolerated result in manifestations of the syndrome, i.e., in increased sensitivity; the symptoms improve, or resolve completely, when the triggering chemicals are removed; responses often occur to multiple, chemically unrelated substances; symptoms involve multiple-organ symptoms.

The MCS begins in response to exposure to one or more chemicals of seven classes. These include three groups of pesticides (organophosphorus, pyrethroid and organochlorine), a large assortment of volatile organic compounds (VOCs) and related compounds. In addition, mercury and its compounds, e.g., dental amalgams, hydrogen sulphide, and carbon monoxide are implicated as initiators. All these classes of chemicals produce a common response, such as excessive activity of the NMDA receptor. Organophosphorus and carbamate are acetyl cholinesterase inhibitors producing an increase in acetylcholine, which stimulates the muscarinic receptors, which in turn increases glutamate release leading to an increase in NMDA receptor stimulation. Organochlorine, chlordane, lindane, dieldrin, and aldrin lower GABAA receptor activity, which produces elevated NMDA activity. Pyrethroid acts on sodium channel opening probability, which increases NMDA stimulation and similarly acts on GABAA as do other pesticides. Organic solvents and VOCs act on the transfer receptor potential (TRP) family, leading to an increase in NMDA activity. Mercury and its compounds, hydrogen sulphide and carbon monoxide produce increased NMDA activity (Pall 2009). Furthermore, animal studies have demonstrated that toxic responses to chemicals belonging to each of these seven classes are greatly decreased by using drugs that inhibit the NMDA response. Enhanced NMDA activity also produces an increases in NO and its oxidant $ONOO^-$ realizing a vicious cycle. These compounds act to generate local sensitivity in regions of the brain and in peripheral tissues, including the lungs, the skin and the upper respiratory and the gastrointestinal tracts (Pall 2009). Apart from the above outlined factors, we hypothesized the existence of a linkage between the MCS syndrome and the oxidative stress induced by inhaled VOCs stressors which could be detected by a new metal oxide semiconductor (MOS)-sensor based system.

23.2 Methods

Healthy volunteers (n = 10), who provided written informed consent, were enrolled into the study. The procedures were performed in agreement with the Ethical Standards of the Helsinki Declaration and were accepted by a local Ethics Committee. We measured the exhaled breath content in the control condition and under exposure to the olfactory stressor n-propanol which mimics the hypoxic or pollutant stressors. The recording system used in this experiments was an iAQ-2000 (AppliedSensor, Warren, NJ) equipped with a metal oxide semiconductor (MOS) having a sensing range of 450–2,000 ppm CO_2 equivalents which is able to detect a broad range of volatile compounds (both organic and inorganic, e.g., alcohols, aldehydes, aliphatic hydrocarbons, amines, aromatic hydrocarbons, ketones, organic acids and CO), while correlating directly with the CO_2 levels. The MOS sensor is based on chemical reaction which occurs between the surface of the sensor and the volatile compounds. This reaction cause closure of an electrical circuit, which sends a raw electrical signal in Ohm to the acquisition system. The signal is recorded, saved, and elaborated by the system algorithm, which expresses the VOCs concentration. A Wohler A600 gas analyzer (Wohler USA Inc. Danvers, MA) was used to verify the O_2 and CO_2 measurements done by the iAQ-2000. The exhaled breath was collected into a tight-sealed mask that completely covered the nose, which leaved free inspiration through the mouth, and was directly measured by the iAQ-2000 system. Data treatment and statistical analysis was done by Excel and Origin software.

23.3 Results

In order to recognize physiological characteristics which would allow to diagnose the MCS or exposure to VOCs in a non-invasive procedure we recorded breath exhale using an MOS-sensor system. The normalized breathing raw recordings in a representative subject, presented as a comparison of the control *vs.* n-propanol stressor conditions are superimposed in the consecutive panels of Fig. 23.1. In this and the following figures there are normalized data on the vertical axis according to the formula: N = (x−min)/(max−min).

The recordings from the Wohler A600 gas analyzer, serving as a reference for verification are shown in Fig. 23.1a and c, while those obtained from the MOS-sensor system are shown in Fig. 23.1b and d. Statistical comparisons of the corresponding grand averages of the raw data obtained in the control *vs.* n-propanol stressor conditions are presented in Fig. 23.2; panels a and c concern the data from the Wohler A600 gas analyzer and panels b & d concern those obtained from the MOS-sensor system. In response to the olfactory stressor, the mean fraction of CO_2 increased and that of O_2 decreased in the exhaled breath, which was accompanied by an increase in VOCs ($p < 0.05$, *t*-test for all comparisons).

Figure 23.3a and b demonstrate comparison of breathing frequency traces between the control *vs.* n-propanol stressor conditions. As is convincingly seen, breathing frequency increased in response to the olfactory stressor. In Fig. 23.4, in turn, the grand averages of breath frequency are presented as a power spectrum analysis. For comparison, the frequency spectra obtained in the control condition are superimposed on those from the n-propanol stressor condition; Fig. 23.4a and c shows the spectra pertaining to the Wohler A600 gas analysis, while the remaining panels (Fig. 23.4b, d) pertain to the recordings based on the MOS-sensor system ($p < 0.05$, *t*-test for all comparisons).

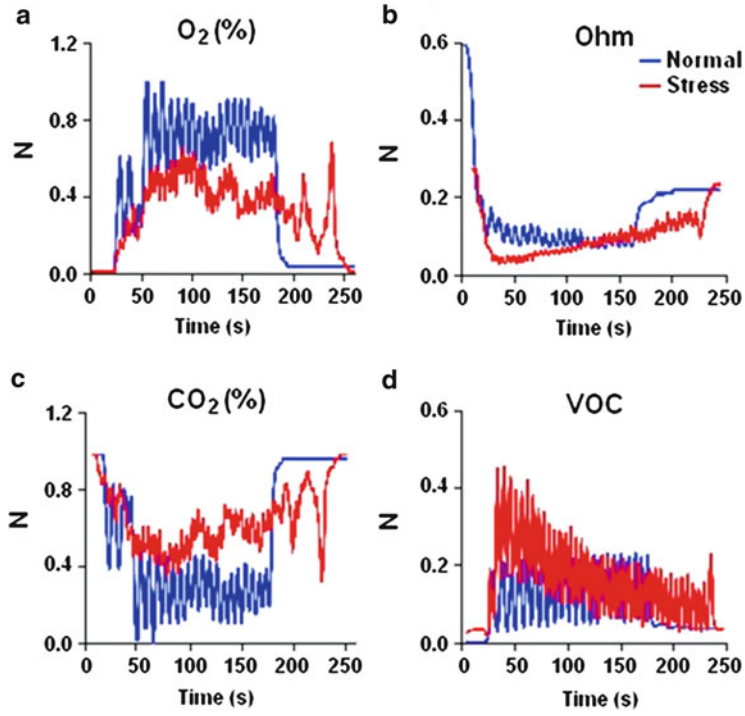

Fig. 23.1 Representative breathing raw data comparison in control *vs.* stressor (n-propanol): (**a**) O_2 from Wohler A600 analyzer; (**b**) Ohm is the electrical signal recorded by the MOS-sensor as a direct measure of the volatile compounds reacting with the sensing surface of it; (**c**) CO_2 from Wohler A600 analyzer; (**d**) VOC is the signal elaborated by the MOS-sensor algorithm which express the VOCs concentration. 'N' stands for normalized data: N = (x−min)/(max−min). Note different scales in Y axes

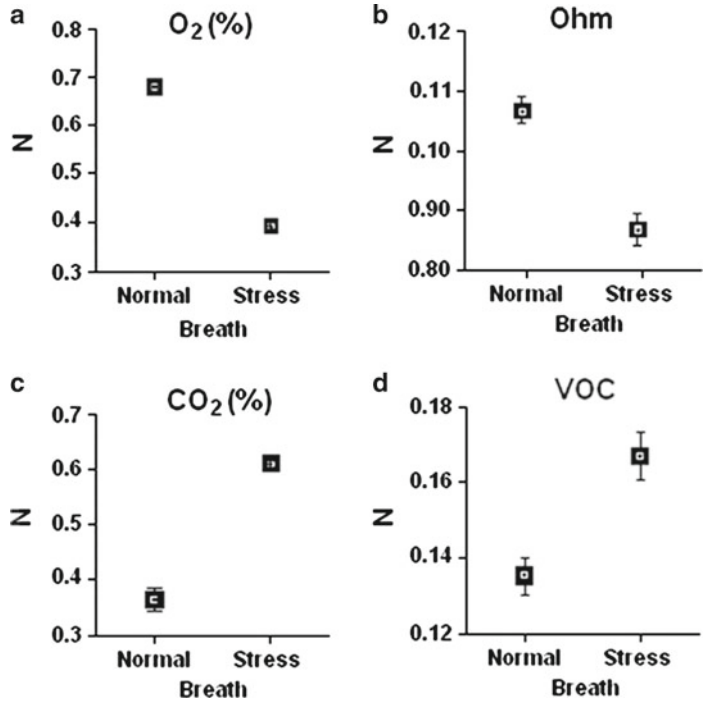

Fig. 23.2 Comparisons of the grand averages of raw breathing data in control *vs.* stressor (n-propanol): (**a**) O_2 from Wohler A600 analyzer; (**b**) Ohm from MOS-sensor; (**c**) CO_2 from Wohler A600 analyzer; (**d**) VOC from MOS-sensor. 'N' stands for normalized data, note different scale in Y axis ($p < 0.05$ for all comparisons)

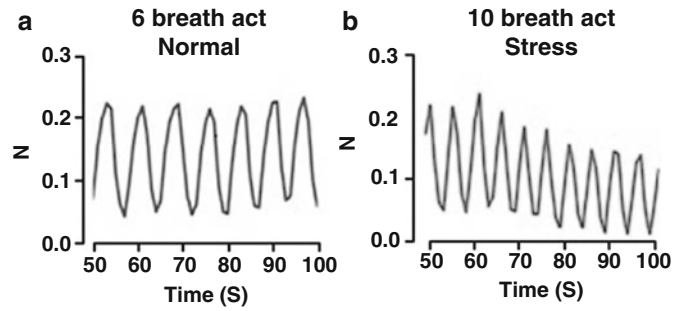

Fig. 23.3 Representative comparison of the breath traces in control (**a**) *vs.* stressor (n-propanol) (**b**) from MOS-sensor system in a subject freely breathing through a nose mask. 'N' stands for normalized data

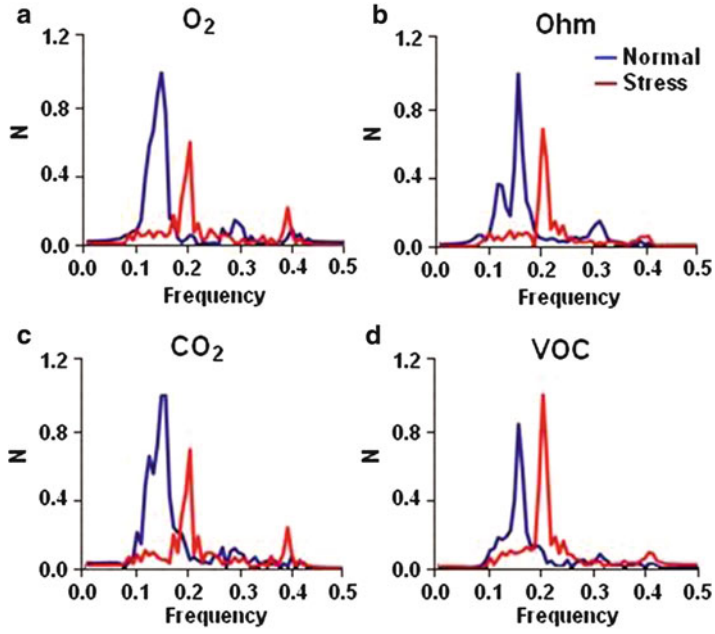

Fig. 23.4 Power spectrum analysis of grand averages of breath frequency in control *vs.* stressor (n-propanol): (**a**) O_2 from Wohler A600 analyzer; (**b**) Ohm from MOS-sensor; (**c**) CO_2 from Wohler A600 analyzer; (**d**) VOC from MOS-sensor

On the other hand, the volume component of ventilation, represented by breath amplitude, decreased in response to the olfactory stressor. The decrease can be seen in the recordings based on the MOS-sensor system comparing the breath amplitude in the control *vs.* n-propanol stressor conditions (Fig. 23.5) ($p<0.05$ for all, except the VOCs). The opposing alterations in breathing frequency and amplitude were confirmed by the Ohm signals recorded with the MOS sensor (Figs. 23.4 and 23.5).

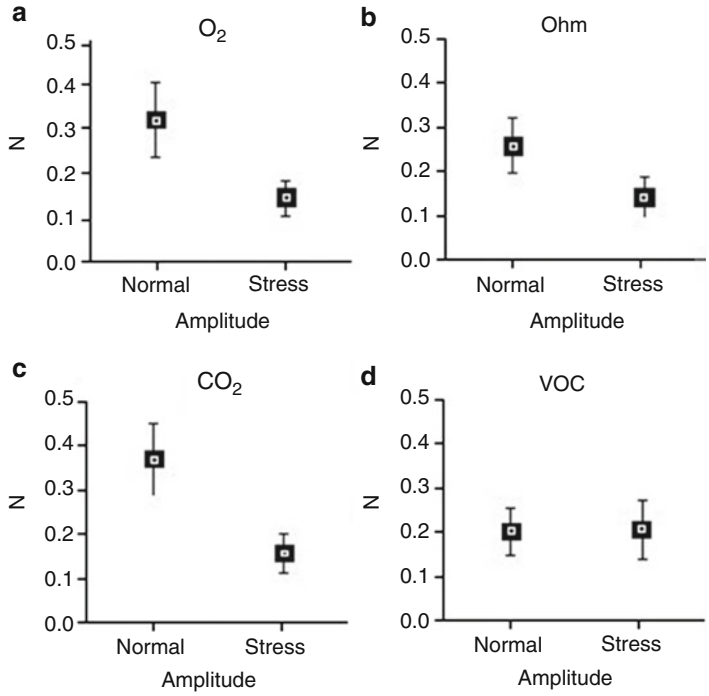

Fig. 23.5 Comparison of breath amplitude in control *vs.* stressor (n-propanol): (**a**) O_2 from Wohler A600 analyzer; (**b**) Ohm from MOS-sensor; (**c**) CO_2 Wohler A600 analyzer ($p<0.05$); (**d**) VOC from MOS-sensor ($p>0.05$)

23.4 Discussion

Our findings indicate that the recording system employed in this study was suitable for the analysis of the breath exhale content in humans. Interestingly, the system was able to detect and discriminate between the exhaled breath content taken from the control condition and that from the stressful condition which mimicked exposures to pollutants or hypoxia known to lay a groundwork for the development of multiple chemical sensitivity disorder (MCS). Figure 23.6 demonstrates the hypothetical links between the oxygen supply cascade and NO/NOO^- vicious cycle. The key steps are the formation of NO and ROS, both of which increase directly or indirectly NMDA receptor activity as results of oxidative stress, which could create the basis for the subsequent effects of pollutant exposures or hypoxia resulting in MCS symptoms.

The bulk matrix of exhale breath is a combination of nitrogen, oxygen, CO_2, H_2O, and inert gases. The remaining fraction consists of numerous VOCs with concentrations in a range of parts per million (ppm) to parts per trillion (ppt) by volume (Miekisch et al. 2004; Phillips et al. 1999; Mukhopadhyay 2004). The VOCs are generated in the body (endogenous) or may be absorbed as contaminants from the environment (exogenous). The composition of VOCs in breath varies widely from person to person and alters in pathological conditions, both qualitatively and quantitatively. Although the number of VOCs found to-date in human breath is more than 1,000, only a few VOCs are common to all humans or characteristic of a given disease. These markers, which include isoprene, pentane, acetone, ethane and methanol, etc., are products of core metabolic processes and are especially informative for clinical diagnostics (Mukhopadhyay 2004). Notable exception is NO, which is released into the airway in case of airway inflammation. Testing for variation in the quantity of the endogenous mix

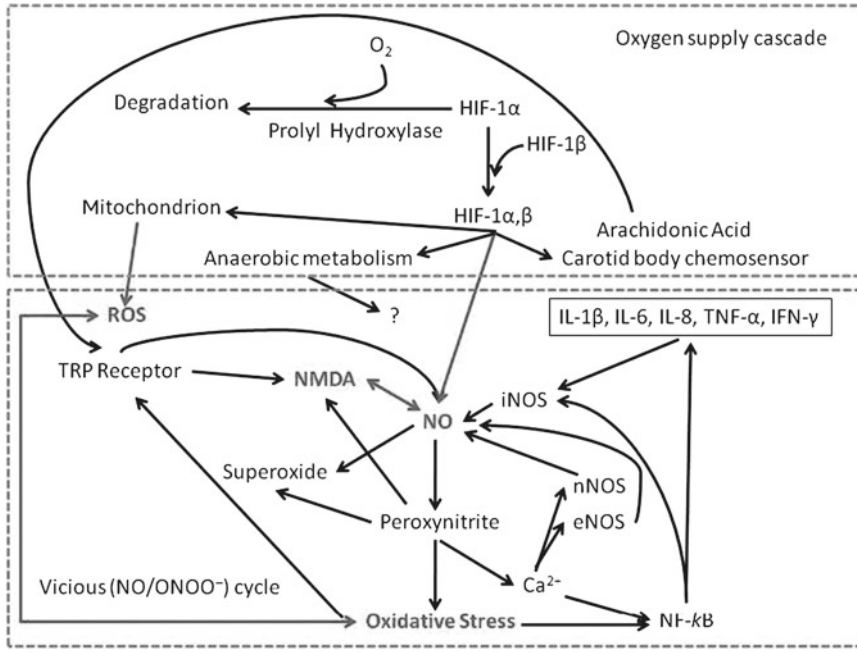

Fig. 23.6 Physiological link between oxygen supply cascade and NO/NOO⁻ vicious cycle. Key steps are the formation of NO and ROS, both increase NMDA receptor activity as a result of oxidative stress which could be a trigger for the multiple chemical sensitivity symptoms due to pollutant exposure or hypoxia

and the presence of new compounds can provide valuable information concerning a possible disease state. Furthermore, exogenous molecules, such as halogenated organic compounds, can indicate recent exposure to drugs or environmental pollutants (Miekisch et al. 2004).

The advantages of breath analysis over hitherto existing serum or urine analysis include noninvasiveness, ease of repetition, no discomfort associated with blood and urine tests; let alone the samples closely reflect the arterial concentrations of biological substances. Breath analysis could be particularly advantageous when a number of arterial blood samples are required, e.g., in monitoring a patient. Breath exhalation also is a much less complicated mixture than serum or urine and is amenable to complete analysis of all compounds present, and no work-up of a breath sample is required, in contrast to many analyses performed on serum or urine samples. Breath analysis can dynamically in real-time monitor the decay of volatile toxic substances in the body (Mukhopadhyay 2004; Phillips 1992). However, breath testing has its limitations. A considerable problem hampering the use of breath tests in clinical practice is the lack of standardization of analytical methods and the wide variation in results obtained in different studies and sample collection and pre-concentration are usually necessary because most substance concentrations in exhaled breath fall in the nmol/l to pmol/l (ppb to ppt by volume) range. Pre-concentration can be achieved by adsorption on sorbent traps, coated fibers (solid-phase microextraction), or by direct cryofocusation. Standardization of breath sample collection and pre-concentration is more difficult than that for serum. Different analytical methods may give very different results. Another critical issue is a high water content of breath samples, which may affect pre-concentration, separation, and detection of single compounds. This is especially true for mechanically ventilated patients if active humidifiers are used in the respiratory circuit. Compared with the simple chemical tests widely used in serum and urine analysis, instruments for breath analysis are expensive. At present, the most commonly used method, GC-MS, requires bulky instrumentation, is time-consuming, and needs skilled operators. The lack of established links between breath substances and disease is also a problem. Therefore, in some case, the breath test is not a conclusive

diagnostic tool, but can be used as a part of a range of diagnostics. However, new MOS-sensor based systems could solve part of these problem and are helpful in diagnosis of diseases and the assessment of exposure to VOCs. These sensors are activated at ppm concentration by several classes of VOCs (both organic and inorganic, e.g.: alcohols, aldehydes, aliphatic hydrocarbons, amines, aromatic hydrocarbons, ketones, organic acids, and CO), while correlating directly with the CO_2 levels (Mazzatenta et al. 2011). As our data show, an iAQ-2000 sensor identifies breath characteristics as Ohm resistance signal and transduces them into VOCs equivalents. These values are directly comparable to the measurements obtained with the laboratory control system such as a gas analyzer. Furthermore, the signal includes physiological parameters such as breath frequency and amplitude. In addition, the test may be self performed by the patient. Thus such test seems advantageous compared with other exhale breath tests.

The present study demonstrates that the MOS-sensor can discriminate qualitative and quantitative variables in the breath concentrations of VOCs and physiological variables. We showed that by comparing the variables recorded in healthy subjects in the control non-stimulated condition with those obtained from the same subjects exposed to the olfactory n-propanol stressor. The MOS-sensor was able to discriminate between the two conditions and showed an increase in VOCs in body response to a bad quality of the inhaled air and impending hypoxic condition. The results also help advance a biological hypothesis based on the cross interaction between the $NO/ONOO^-$ vicious cycle (Pall 2009) and the oxygen supply cascade linked by two possible pathways, a direct one *via* NO and an indirect one trough the oxidative stress-mediated release of ROS resulting in neural sensitization *via* NMDA over activation and MCS induction.

In conclusion, we submit that the MOS sensor recordings may be useful in as diagnostic, non-invasive tests able to detect physiological variables which can validate the existence of an MCS disorder as well as for the measurement of VOCs concentrations in threatened environmental conditions.

Conflicts of interest: The authors declare no conflicts of interest in relation to this article.

References

Aghdassl, E., Wendland, B. E., Steinhart, A. H., Wolman, S. L., Jeejeebhoy, K., & Allard, J. P. (2003). Antioxidant vitamin supplementation in Crohn's disease decreases oxidative stress: A randomized controlled trial. *The American Journal of Gastroenterology, 98*, 348–353.

Bell, I. R., Szarek, M. J., Dicenso, D. R., Baldwin, C. M., Schwartz, G. E., & Bootzin, R. R. (1999). Patterns of waking EEG spectral power in chemically intolerant individuals during repeated chemical exposures. *The International Journal of Neuroscience, 97*, 41–59.

Cao, W., & Duan, Y. (2006). Breath analysis: Potential for clinical diagnosis and exposure assessment. *Clinical Chemistry, 52*, 800–811.

Caress, S. M., & Steinemann, A. C. (2004). A national population study of the prevalence of multiple chemical sensitivity. *Archives of Environmental Health, 59*, 300–305.

Cataldi, A., & Di Giulio, C. (2009). 'Oxygen Supply' as modulator of aging processes: Hypoxia and hyperoxia models for aging studies. *Current Aging Science, 2*, 95–102.

Das-Munshi, J., Rubin, G. J., & Wessely, S. (2007). Multiple chemical sensitivities: Review. *Current Opinion in Otolaryngology & Head and Neck Surgery, 15*, 274–280.

Davidoff, A. L., Fogarty, L., & Keyl, P. M. (2000). Psychiatric inferences from data on psychologic/psychiatric symptoms in multiple chemical sensitivities syndrome. *Archives of Environmental Health, 55*, 165–175.

Drew, B., & Leeuwenburgh, C. (2002). Aging and the role of reactive nitrogen species. *Annals of the New York Academy of Sciences, 959*, 66–81.

Finkel, T., & Holbrook, N. J. (2000). Oxidants, oxidative stress and the biology of ageing. *Nature, 408*, 239–247.

Fisher, A. J., Gabbay, E., Small, T., Doig, S., Dark, J. H., & Corris, P. A. (1998). Cross sectional study of exhaled nitric oxide levels following lung transplantation. *Thorax, 53*, 454–458.

Folke, M., Cernerud, L., Ekstrom, M., & Hok, B. (2003). Critical review of non-invasive respiratory monitoring in medical care. *Medical & Biological Engineering & Computing, 41*, 377–383.

Gots, R. E. (1996). Multiple chemical sensitivities: Distinguishing between psychogenic and toxicodynamic. *Regulatory Toxicology and Pharmacology, 24*, 8–15.

Heuser, G., & Wu, J. C. (2001). Deep subcortical (including limbic) hypermetabolism in patients with chemical intolerance: Human PET studies. *Annals of the New York Academy of Sciences, 933*, 319–322.

Heuser, G., Mena, I., & Alamos, F. (1994). NeuroSpect findings in patients exposed to neurotoxic chemicals. *Toxicology and Industrial Health, 10*, 561–571.

Hillert, L., Musabasic, V., Berglund, H., Ciumas, C., & Savic, I. (2007). Odor processing in multiple chemical sensitivity. *Human Brain Mapping, 28*, 172–182.

Joffres, M. R., Williams, T., Sabo, B., & Fox, R. A. (2001). Environmental sensitivities: Prevalence of major symptoms in a referral center: The Nova Scotia Environmental Sensitivities Research Center Study. *Environmental Health Perspectives, 109*, 161–165.

Knight, J. A. (1998). Free radicals: Their history and current status in aging and disease. *Annals of Clinical and Laboratory Science, 28*, 331–346.

Kostikas, K., Papatheodorou, G., Psathakis, K., Panagou, P., & Loukides, S. (2003). Oxidative stress in expired breath condensate of patients with COPD. *Chest, 124*, 1373–1380.

Kreutzer, R., Neutra, R. R., & Lashuay, N. (1999). Prevalence of people reporting sensitivities to chemicals in a population-based survey. *American Journal of Epidemiology, 150*, 13–16.

Lorig, T. S., Huffman, E., DeMartino, A., & DeMarco, J. (1991). The effects of low concentration odors on EEG activity and behavior. *Journal of Psychophysiology, 5*, 69–77.

Mazzatenta, A., Cozzutto, S., Barbieri, P., Di Giulio, C., & d'Alessandro, N. (2011). *A MOS-sensor based system to asses respiratory physiology* (p. 15). Teramo: Sensor Workshop.

Miekisch, W., Schubert, J. K., & Noeldge-Schomburg, G. F. (2004). Diagnostic potential of breath analysis: Focus on volatile organic compounds. *Clinica Chimica Acta, 347*, 25–39.

Miller, C. S. (2001). The compelling anomaly of chemical intolerance. *Annals of the New York Academy of Sciences, 933*, 1–19.

Montuschi, P., Kharitonov, S. A., Ciabattoni, G., Corradi, M., van Rensen, L., Geddes, D. M., Hodson, M. E., & Barnes, P. J. (2000). Exhaled 8-isoprostane as a new non-invasive biomarker of oxidative stress in cystic fibrosis. *Thorax, 55*, 205–209.

Moretti, M., Phillips, M., Abouzeid, A., Cataneo, R. N., & Greenberg, J. (2004). Increased breath markers of oxidative stress in normal pregnancy and in preeclampsia. *American Journal of Obstetrics and Gynecology, 190*, 1184–1190.

Mukhopadhyay, R. (2004). Don't waste your breath. Researchers are developing breath tests for diagnosing diseases, but how well do they work? *Analytical Chemistry, 76*, 273A–276A.

Orriols, R., Costa, R., Cuberas, G., Jacas, C., Castell, J., & Sunyer, J. (2009). Brain dysfunction in multiple chemical sensitivity. *Journal of the Neurological Sciences, 287*, 72–78.

Pall, M. L. (2009). Multiple chemical sensitivity: Toxicological questions and mechanisms. In B. Ballantyne, T. ŁC. Marrs & T. Syversen (Eds.), *General and applied toxicology* (pp. 2303–2352). John Wiley & Sons, London.

Phillips, M. (1992). Breath tests in medicine. *Scientific American, 267*, 74–79.

Phillips, M., Herrera, J., Krishnan, S., Zain, M., Greenberg, J., & Cataneo, R. N. (1999). Variation in volatile organic compounds in the breath of normal humans. *Journal of Chromatography. B, Biomedical Sciences and Applications, 729*, 75–88.

Phillips, M., Cataneo, R. N., Greenberg, J., Gunawardena, R., Naidu, A., & Rahbari-Oskoui, F. (2000). Effect of age on the breath methylated alkane contour, a display of apparent new markers of oxidative stress. *The Journal of Laboratory and Clinical Medicine, 136*, 243–249.

Phillips, M., Cataneo, R. N., Greenberg, J., Grodman, R., Gunawardena, R., & Naidu, A. (2003a). Effect of oxygen on breath markers of oxidative stress. *The European Respiratory Journal, 21*, 48–51.

Phillips, M., Cataneo, R. N., Cummin, A. R. C., Gagliardi, A. J., Gleeson, K., Greenberg, J., Maxfield, R. A., & Rom, W. N. (2003b). Detection of lung cancer with volatile markers in the breath. *Chest, 123*, 2115–2123.

Phillips, M., Cataneo, R. N., Cheema, T., & Greenberg, J. (2004). Increased breath biomarkers of oxidative stress in diabetes mellitus. *Clinica Chimica Acta, 344*, 189–194.

Schnakenberg, E., Fabig, K. R., Stanulla, M., Strobl, N., Lustig, M., Fabig, N., & Schloot, W. (2007). A cross-sectional study of self-reported chemical-related sensitivity is associated with gene variants of drug-metabolizing enzymes. *Environmental Health, 6*, 6–16.

Schumacker, P. T. (2003). Current paradigms in cellular oxygen sensing. *Advances in Experimental Medicine and Biology, 543*, 57–71.

Simon, T. R., Hickey, D. C., Fincher, C. E., Johnson, A. R., Ross, G. H., & Rea, W. J. (1994). Single photon emission computed tomography of the brain in patients with chemical sensitivities. *Toxicology and Industrial Health, 10*, 573–577.

Studer, S. M., Orens, J. B., Rosas, I., Krishnan, J. A., Cope, K. A., Yang, S., Conte, J. V., Becker, P. B., & Risby, T. H. (2001). Patterns and significance of exhaled-breath biomarkers in lung transplant recipients with acute allograft rejection. *The Journal of Heart and Lung Transplantation, 20*, 1158–1166.

Chapter 24
Anti-inflammatory Treatment in Dysfunction of Pulmonary Surfactant in Meconium-Induced Acute Lung Injury

D. Mokra, A. Drgova, J. Kopincova, R. Pullmann, and A. Calkovska

Abstract Inflammation, oxidation, lung edema, and other factors participate in surfactant dysfunction in meconium aspiration syndrome (MAS). Therefore, we hypothesized that anti-inflammatory treatment may reverse surfactant dysfunction in the MAS model. Oxygen-ventilated rabbits were given meconium intratracheally (25 mg/ml, 4 ml/kg; Mec) or saline (Sal). Thirty minutes later, meconium-instilled animals were treated by glucocorticoids budesonide (0.25 mg/kg, i.t.) and dexamethasone (0.5 mg/kg, i.v.), or phosphodiesterase inhibitors aminophylline (2 mg/kg, i.v.) and olprinone (0.2 mg/kg, i.v.), or the antioxidant N-acetylcysteine (10 mg/kg, i.v.). Healthy, non-ventilated animals served as controls (Con). At the end of experiments, left lung was lavaged and a differential leukocyte count in sediment was estimated. The supernatant of lavage fluid was adjusted to a concentration of 0.5 mg phospholipids/ml. Surfactant quality was evaluated by capillary surfactometer and expressed by initial pressure and the time of capillary patency. The right lung was used to determine lung edema by wet/dry (W/D) weight ratio. Total antioxidant status (TAS) in blood plasma was evaluated. W/D ratio increased and capillary patency time shortened significantly, whereas the initial pressure increased and TAS decreased insignificantly in Sal *vs*. Con groups. Meconium instillation potentiated edema formation and neutrophil influx into the lungs, reduced capillary patency and TAS, and decreased the surfactant quality compared with both Sal and Con groups ($p>0.05$). Each of the anti-inflammatory agents reduced lung edema and neutrophil influx into the lung and partly reversed surfactant dysfunction in the MAS model, with a superior effect observed after glucocorticoids and the antioxidant N-acetylcysteine.

Keywords Antiinflammatory treatment • Inflammation • Lung • Meconium aspiration • Surfactant • Antioxidant status • Lung edema

D. Mokra (✉) • J. Kopincova • A. Calkovska
Department of Physiology, Jessenius Faculty of Medicine, Comenius University,
Mala Hora 4, SK-03601 Martin, Slovakia
e-mail: mokra@jfmed.uniba.sk

A. Drgova
Department of Medical Biochemistry, Jessenius Faculty of Medicine, Comenius University,
Mala Hora 4, SK-03601 Martin, Slovakia

R. Pullmann
Department of Clinical Biochemistry, Jessenius Faculty of Medicine, Comenius University
and the University Hospital, Kollarova 2, SK-03601 Martin, Slovakia

M. Pokorski (ed.), *Respiratory Regulation - The Molecular Approach*,
Advances in Experimental Medicine and Biology 756, DOI 10.1007/978-94-007-4549-0_24,

24.1 Introduction

Pulmonary surfactant is a mixture of phospholipids, neutral lipids, proteins, and saccharides coating the conducting airways down to terminal airspaces. Surfactant phospholipids reduce the surface tension of air/liquid interphase in alveoli and terminal bronchioles and keep it at low values at the end of expiration preventing their collapse. Other components of surfactant – specific proteins – regulate the metabolism and secretion of surfactant compounds, enhance the properties of phospholipids and participate in immune responses. Forming a barrier between the environment and the body, surfactant plays a role also in the fluid balance and gas exchange (Robertson and Halliday 1998).

Primary surfactant deficiency is an underlying cause of the respiratory distress syndrome (RDS) in premature newborns, where the surfactant production by alveolar type II cells is insufficient due to immaturity of the lungs (Hallman et al. 2001). However, dysfunction of pulmonary surfactant has been described also in patients with mature lungs in various forms of respiratory distress caused by aspiration of meconium, infections, etc. (Robertson and Halliday 1998; Finer 2004). In the meconium aspiration syndrome (MAS), function of surfactant may be inhibited by components of meconium, plasma proteins leaking through injured alveolo-capillary membrane, or substances released in lung inflammation (mediators, reactive oxygen species, proteolytic enzymes, etc.; Finer 2004; Lopez-Rodriguez et al. 2011). The situation is worsened by hypoxia from respiratory insufficiency (Jain and Sznajder 2005) or hyperoxia due to artificial ventilation with high oxygen concentrations (Dombrowsky et al. 2006).

Acknowledging that dysfunction of alveolar surfactant in MAS is multifaceted; the aim of this study was to ascertain the relationship between surfactant properties and inflammation, lung edema, and hypoxia/hyperoxia in the condition of experimental meconium aspiration. Furthermore, this study evaluated to what extent surfactant dysfunction could be reversed by anti-inflammatory treatment. To the latter end we used the glucocorticoids budesonide and dexamethasone, and the phosphodiesterase (PDE) inhibitors aminophylline and olprinone, and finally the antioxidant N-acetylcysteine.

24.2 Methods

24.2.1 Experimental Design

The design of experiments was approved by a local Ethics Committee of Jessenius Faculty of Medicine in Martin, Slovakia. Rabbits, mean weight 2.5 ± 0.3 kg, were anesthetized with intramuscular ketamine (20 mg/kg; Narketan, Vétoquinol, UK) and xylazine (5 mg/kg; Xylariem, Riemser, Germany) followed by infusion of ketamine (20 mg/kg/h). Tracheotomy was performed and catheters were inserted into the femoral artery and right atrium for sampling the blood, and into the femoral vein to administer supplemental doses of anesthetics as required. The animals were paralyzed with pipecuronium bromide (0.3 mg/kg/30 min; Arduan, Gedeon Richter, Hungary) and subjected to pressure-controlled ventilation (Beat-2, Chirana, Slovakia). All animals were ventilated with frequency of 30/min, fraction of inspired oxygen (FiO_2) of 0.21, peak inspiratory pressure (PIP) to keep a tidal volume (V_T) between 7–9 ml/kg, with no positive end-expiratory pressure (PEEP) at this stage of the experiment. After stabilization, ventilatory parameters were recorded and blood samples were taken for blood gas analysis (Rapidlab™348, Bayer Diagnostics, Germany). Controls, untreated and non-ventilated animals (Con, n = 7) were sacrificed by an overdose of anesthetics. In additional animals, 4 ml/kg of saline (Sal, n = 7) or meconium suspension (25 mg/ml) was instilled into the tracheal tube. From this moment on, animals were ventilated with 100% oxygen.

Within 30 min after meconium instillation, respiratory failure developed, defined as >30% decrease in dynamic lung-thorax compliance and $PaO_2 < 10$ kPa at FiO_2 1.0. Meconium-instilled animals were treated by budesonide (Pulmicort inh. susp., Astra Zeneca, 0.25 mg/kg intratracheally, Mec + Bud, n = 8), dexamethasone (Dexamed, Medochemie, 0.5 mg/kg i.v., Mec + Dex, n = 8), aminophylline (Syntophyllin, Hoechst Biotika, 2 mg/kg i.v., Mec + Amin, n = 7), all three given 0.5 and 2.5 h after meconium; and by olprinone (Olprinone Hydrochloride, Sigma Aldrich, 0.2 mg/kg i.v., Mec + Olp, n = 7) or N-acetylcysteine (ACC Injekt, Sandoz Pharmaceuticals, 10 mg/kg i.v., Mec + Acc, n = 7), both given in a single dose 0.5 h after meconium; or animals were left untreated (Mec, n = 8). Animals were oxygen-ventilated (FiO_2 1.0, PEEP 0.3 kPa, V_T 7–9 ml/kg) for additional 5 h after administration of the first dose of treatment. At the end of experiments, blood samples were taken, centrifuged and plasma stored at −70°C for biochemical analyses. Then, animals were killed by an overdose of anesthetics and lungs were excised.

24.2.2 Bronchoalveolar Lavage, Lung Edema, and Total Antioxidant Status

After ligation of the right bronchus, left lungs were lavaged by saline (3 × 10 ml/kg, 37°C). Bronchoalveolar lavage (BAL) fluid was firstly centrifuged at 1,500 rpm for 10 min to separate cells. Samples of BAL showing macroscopic presence of blood were excluded from data analysis.

Differential white blood cell (WBC) count in the sediment of BAL fluid was evaluated microscopically after panchromatic Pappenheim staining (May-Grünwald and Giemsa-Romanowsky staining).

Supernatant of BAL fluid was further centrifuged at 40,000 rpm for 1 h at 4°C to separate large surfactant aggregates. The surfactant pellet was then lyophilized and dry mass was resuspended in 10 µl of standard buffer (3.5 mM $CaCl_2$, 10 mM HEPES, and 0.5 mM EDTA, pH = 7) (Braun et al. 2004) to a final concentration of PL of 0.5 mg PL/ml. Surface activity of BAL fluid samples was evaluated by capillary surfactometer CS 2005 (Calmia Medical, Canada). Surface properties of the fluid containing surfactant are assessed indirectly considering a transportability of material through the capillary that simulates the terminal conducting airways. During the assessment, the initial pressure necessary to transport the sample through the narrow part of the capillary and the percentage of the total time (120 s) for which the capillary is open (capillary patency) are measured (Fig. 24.1). Each sample was measured three times and the mean value was used for final data analysis.

To assess lung edema, the right lung was cut out; strips of the tissue were weighed and dried at 60°C for 24 h to determine the wet/dry (W/D) lung weight ratio expressing lung edema formation.

The quantification of total antioxidant status (TAS) in blood plasma at the end of experiments was carried out using ABTS (2,2'-azino-di-[3-ethylbenzthiazoline sulphonate]) radical formation kinetics (Randox TAS kit, Randox Laboratories Ltd., UK).

24.2.3 Statistical Elaboration

Data were expressed as means ± SE. Because of non-parametric distribution of some data, the Kruskal-Wallis test for between-group comparisons was used. The strength of the associations between the surface properties of BAL fluid *vs.* the number of neutrophils in BAL, lung edema, and plasma TAS concentration were expressed by Pearson's correlation coefficient (r) and Bonferroni probability (p). A $p < 0.05$ was considered statistically significant. Statistical analysis was made using a commercial Systat for Windows package.

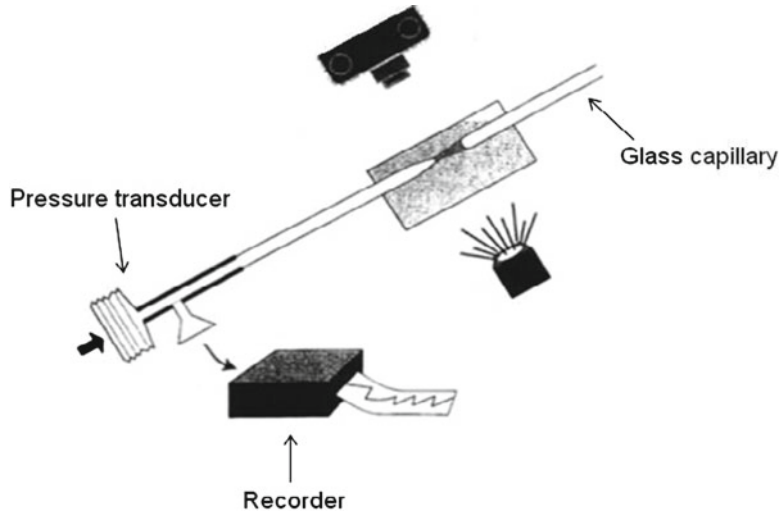

Fig. 24.1 Scheme of measurements by capillary surfactometer. A small volume of the liquid (0.5 μl) is sucked by a micropipette and placed in the upper part of a capillary (ID 0.25 mm) simulating terminal airways (Enhorning 2001). The other end of the capillary is connected to a bellow and a pressure transducer. Automatically generated initial pressure extrudes the sample from the narrow part of the capillary. If the sample contains well functioning surfactant, the liquid will not return to the narrow part, pressure is abruptly lowered to zero and capillary will be open till the end of the measurement. If surfactant is defunct, the liquid returns repeatedly, initial pressure repeatedly increases, and the time of capillary patency is reduced

24.3 Results

24.3.1 Surface Properties of BAL Samples

Capillary patency decreased ($p<0.05$) and initial pressure showed a trend to increase ($p>0.05$) in saline-instilled and oxygen-ventilated animals (Sal group) in comparison with non-ventilated controls (Con group). More pronounced changes in surface properties of BAL were observed after meconium instillation; capillary patency decreased and initial pressure increased in the Mec *vs.* both Con and Sal groups ($p<0.001$ and $p<0.01$, respectively). Administration of anti-inflammatory drugs used enhanced capillary patency (all $p<0.001$) compared with the non-treated Mec group. Moreover, dexamethasone ($p<0.01$) and aminophylline ($p<0.05$) reduced the initial pressure compared with the Mec group (Table 24.1).

24.3.2 Wet/Dry (W/D) Lung Weight Ratio

Ventilation with oxygen slightly increased accumulation of edema fluid in the lungs in the Sal group compared with non-ventilated controls ($p<0.01$). A further increase in fluid accumulation was observed after meconium instillation ($p<0.001$ for Mec *vs.* both Sal and Con groups). All the tested anti-inflammatory drugs showed some anti-edematous effect; the superior action was observed after both glucocorticoids and N-acetylcysteine ($p<0.01$ *vs.* Mec), lower efficacy was after aminophylline ($p<0.05$ *vs.* Mec), and insignificant anti-edematous action was observed after olprinone ($p>0.05$ *vs.* Mec) (Table 24.1).

Table 24.1 Parameters expressing surface activity and inflammatory and oxidation markers

	Capillary patency (%)	Initial pressure (cmH_2O)	W/D ratio	Neu in BAL (%)	Plasma TAS (mmol/l)
Con	94.4 ± 2.5	5.8 ± 1.0	4.7 ± 0.2	2.7 ± 1.0	0.88 ± 0.03
Sal	50.2 ± 13.4[a]	6.5 ± 0.9	5.7 ± 0.2[b]	5.1 ± 1.3	0.80 ± 0.05
Mec	0.1 ± 0.0[cf]	10.0 ± 0.2[ce]	7.4 ± 0.2[cf]	79.2 ± 4.6[cf]	0.70 ± 0.02[bd]
Mec + Bud	2.2 ± 1.0[i]	9.5 ± 0.2	6.0 ± 0.2[h]	63.8 ± 5.8[g]	0.79 ± 0.03[g]
Mec + Dex	8.2 ± 3.1[i]	7.9 ± 0.5[h]	6.1 ± 0.2[h]	61.0 ± 5.9[h]	0.80 ± 0.02[h]
Mec + Amin	1.8 ± 0.5[i]	9.3 ± 0.2[g]	6.5 ± 0.3[g]	64.8 ± 9.4	0.74 ± 0.03
Mec + Olp	0.9 ± 0.2[i]	9.8 ± 0.4	6.7 ± 0.4	69.2 ± 7.9	0.79 ± 0.03[g]
Mec + Acc	3.7 ± 1.1[i]	10.2 ± 0.5	6.0 ± 0.3[h]	58.6 ± 8.9[h]	0.80 ± 0.03[h]

Between-group comparisons: for Sal and Mec groups *vs.* Con: [a]$p<0.05$; [b]$p<0.01$; [c]$p<0.001$; for Mec *vs.* Sal group: [d]$p<0.05$; [e]$p<0.01$; [f]$p<0.001$; for treated groups *vs.* Mec: [g]$p<0.05$; [h]$p<0.01$; [i]$p<0.001$

Table 24.2 Strength of association between surface properties of BALF *vs.* the number of neutrophils in BALF, lung edema, and plasma TAS evaluated by Pearson's correlations (r) and Bonferroni probability (p)

	Capillary patenc y	Initial pressure	Neutrophils in BAL	WD ratio	TAS in plasma
Capillary patency	–	r = −0.77, p < 0.001	r = −0.75, p<0.001	r = −0.63, p < 0.001	r = 0.31, p = 0.027
Initial pressure	r = −0.77, p < 0.001	–	r = 0.61, p < 0.001	r = 0.50, p < 0.001	r = −0.13, p = 0.381

24.3.3 Neutrophils in BAL Fluid

Oxygen ventilation did not increase significantly the number of BAL neutrophils in the Sal group compared with the non-ventilated controls ($p>0.05$). However, a significantly higher count of neutrophils in BAL fluid was found in the Mec group compared with both Sal and Con groups ($p<0.001$). Anti-inflammatory treatment partially reduced the count of neutrophils in BAL fluid in comparison with the Mec group, with a superior effect observed after both glucocorticoids ($p<0.01$ for dexamethasone and $p<0.05$ for budesonide) and the antioxidant N-acetylcysteine ($p<0.01$), while the effects of olprinone and aminophylline were insignificant ($p>0.05$) (Table 24.1).

24.3.4 Total Antioxidant Status (TAS) of Blood Plasma

TAS decreased slightly in the Sal *vs.* Con group ($p>0.05$). However, instillation of meconium decreased TAS significantly in the Mec group *vs.* both Sal ($p<0.05$) and Con groups ($p<0.01$). The decrease in TAS was prevented by treatment, with the strongest effect after dexamethasone and N-acetylcysteine (both $p<0.01$ *vs.* Mec), weaker effect after budesonide and olprinone (both $p<0.05$ *vs.* Mec), and no significant effect after aminophylline ($p>0.05$ *vs.* Mec) (Table 24.1).

24.3.5 Associations Between Surface Properties of BAL and BAL Neutrophils and Lung Edema

Pearson's evaluation of the associations between the variables showed negative correlations between capillary patency and initial pressure ($r=-0.77$, $p<0.001$), capillary patency and the number of neutrophils in BAL fluid ($r=-0.75$, $p<0.001$), and capillary patency and wet/dry ratio ($r=-0.63$, $p<0.001$). Positive correlations were found between capillary patency and TAS ($r=0.31$, $p=0.027$), the initial pressure and the number of neutrophils in BAL fluid ($r=0.61$, $p<0.001$), and the initial pressure and the WD ratio ($r=0.50$, $p<0.001$) (Table 24.2).

24.4 Discussion

Dysfunction of pulmonary surfactant in MAS is attributed to several factors: components of meconium, proteinaceous edema fluid, bioactive substances including ROS released during inflammation, hypoxia due to respiratory insufficiency, and hyperoxia due ventilation with oxygen. In the present study, surface properties of BAL fluid, lung edema formation, inflammation, and oxidative injury were compared in meconium-instilled *vs.* saline-instilled animals, and *vs.* non-ventilated healthy controls. We found that the extent of lung edema, the number of neutrophils in BAL fluid and total antioxidant status clearly correlated with changes in the surface properties of BAL fluid. Furthermore, our study demonstrate that anti-inflammatory treatment had a potential to prevent worsening of the surfactant properties after meconium instillation, with differences in efficacy depending on the kind of pharmacological agent used.

Surfactant function may be impaired due to exposure to meconium alone - by hydrophilic fraction containing mucopolysaccharides, bile acids, and gastrointestinal enzymes including pancreatic phospholipase A_2, and by hydrophobic fraction consisting of cholesterol, free fatty acids, triglycerides, and others (Moses et al. 1991; Lopez-Rodriguez et al. 2011). The effects of both fractions of meconium are additive, whereas the hydrophobic fraction has a stronger impairing effect than the hydrophilic one (Moses et al. 1991). As expected, intratracheal administration of meconium led to the development of pulmonary edema, neutrophil migration from systematic circulation into the lung, and to a significant decrease of plasma antioxidant status, an indicator of excessive oxidative load. These changes correlated well with surfactant dysfunction, expressed by a marked decrease in capillary patency requiring a higher initial pressure, which is suggestive of the role of lung edema, inflammation, and oxidation in the process of surfactant dysfunction in MAS.

In the treatment of MAS, several anti-inflammatory drugs have been tested with intent to mitigate surfactant inactivation secondary to the inflammatory and oxidative lung injury; the effects of these drugs have not yet been clarified. However, we should also consider the contribution of direct surfactant stimulating action of some agents, e.g., glucocorticoids (Brownfoot et al. 2008) or aminophylline (Barnes 2005).

In the present study, treatment with glucocorticoids – intravenous dexamethasone and intratracheal budesonide – significantly suppressed pulmonary edema formation, neutrophil migration, and oxidative load, showing an efficient influence of glucocorticoids at various levels of the inflammatory cascade. However, the effects of the glucocorticoids on surfactant inactivation differed from each other. While dexamethasone succeeded in decreasing the initial pressure necessary to open the capillary and also heighten capillary patency, budesonide did not affect the initial pressure. There are several plausible explanations of such difference. The first one results from lipophilicity of glucocorticoids (Fernandes et al. 2005). Considering aqueous basis of meconium, the meconium layer could form a mechanical barrier between intratracheally administered remedy and injured tissue. Moreover, budesonide was administered in a dose half smaller than that of dexamethasone, which could provide just a partial preventing effect. A second explanation of lower efficacy of the intratracheally administered glucocorticoid may be related to a high number of activated neutrophils in the lungs and airways. Excessive production of reactive species may cause characteristic resistance of glucocorticoids to the anti-inflammatory effects, particularly after their local administration, as it has verified in other respiratory disease with neutrophil-induced inflammation – chronic obstructive pulmonary disease (COPD) (Barnes 2005).

Another agent used in this study which effectively ameliorated oxidation, lung edema, and decreased the neutrophil count was N-acetylcysteine. It is known that the presence of oxidative stress may induce chemotactic reactions (Petrone et al. 1980) due probably to activation of toll-like receptors and by stimulating interleukins (Yanagisawa et al. 2009). Thus, prevention of ROS formation should mitigate the inflammatory processes such as neutrophil migration and edema. Nevertheless, we observed just a partial improvement of surfactant properties after N-acetylcysteine, as the capillary patency increased but the initial pressure was not reduced after the treatment.

The other anti-inflammatory agents olprinone and aminophylline, phosphodiesterase (PDE) inhibitors, used in the present study are known to have bronchodilator and spasmolytic effects *via* preventing the degradation of cyclic adenosine and guanosine monophosphate (Hirota et al. 2001; Barnes 2005). However, their effects differed regarding MAS. The non-selective PDE inhibitor aminophylline improved surfactant surface activity, resulting in a higher capillary patency, lower initial pressure, and a reduced W/D ratio, but its effects on neutrophils and ROS formation was weaker than those of glucocorticoids or N-acetylcysteine. On the other hand, the selective PDE3 inhibitor olprinone was capable of lowering the oxidative load, and hence partially improved surfactant activity, but it did not affect the initial pressure and other inflammatory parameters. The differences between the two PDE inhibitors are probably caused by the capability of olprinone to produce a more potent pulmonary vasodilation and to reduce oxidative stress through inhibition of PDE3, whereas the action of aminophylline is equipotent *via* inhibition of all phosphodiesterases, antagonism of adenosine receptors, or the effects on inflammatory genes (Hashimoto et al. 2000; Barnes 2005).

In conclusion, changes in surface properties of BAL fluid after meconium instillation clearly correlated with lung edema formation, the number of neutrophils in BAL, and TAS in plasma. Anti-inflammatory treatment demonstrated some potential to prevent worsening of the surfactant properties after meconium instillation into the trachea, with differences present among individual pharmacological agents.

Acknowledgments Supported by project 'Center of Excellence for Perinatology Research (CEPV II)' No. 26220120036 co-financed from EU sources. Authors thank J. Neuschlova, D. Kuliskova, D. Durcova, Ing. M. Petraskova, and Ing. M. Hutko for technical assistance.

Conflicts of interest: The authors declare no conflicts of interest in relation to this article.

References

Barnes, P. J. (2005). Theophylline in chronic obstructive pulmonary disease. New horizons. *Proceedings of the American Thoracic Society, 2*, 334–339.

Braun, A., Steinecker, M., Schumacher, S., & Griese, M. (2004). Surfactant function in children with chronic airway inflammation. *Journal of Applied Physiology, 97*, 2160–2165.

Brownfoot, F. C., Crowther, C. A., & Middleton, P. (2008). Different corticosteroids and regimens for accelerating fetal lung maturation for women at risk of preterm birth. *Cochrane Database of Systematic Reviews, 8*, CD006764.

Dombrowsky, H., Tschernig, T., Vieten, G., Rau, G. A., Ohler, F., Acevedo, C., Behrens, C., Poets, C. F., von der Hardt, H., & Bernhard, W. (2006). Molecular and functional changes of pulmonary surfactant in response to hyperoxia. *Pediatric Pulmonology, 41*, 1025–1039.

Enhorning, G. (2001). Pulmonary surfactant function studied with the pulsating bubble surfactometer (PBS) and the capillary surfactometer (CS). *Comparative Biochemistry and Physiology. Part A, Molecular & Integrative Physiology, 129*, 221–226.

Fernandes, A. B. S., Zin, W. A., & Rocco, P. R. M. (2005). Corticosteroids in acute respiratory distress syndrome. *Brazilian Journal of Medical and Biological Research, 38*, 147–159.

Finer, N. N. (2004). Surfactant use for neonatal lung injury: Beyond respiratory distress syndrome. *Paediatric Respiratory Reviews, 5*(Suppl A), S289–S297.

Hallman, M., Glumoff, V., & Ramet, M. (2001). Surfactant in respiratory distress syndrome and lung injury. *Comparative Biochemistry and Physiology. Part A, Molecular & Integrative Physiology, 129*, 287–294.

Hashimoto, Y., Hirota, K., Yoshioka, H., Kudo, T., Ishihara, H., & Matsuki, A. (2000). A comparison of the spasmolytic effects of olprinone and aminophylline on serotonin-induced pulmonary hypertension and bronchoconstriction with or without β-blockade in dogs. *Anesthesia and Analgesia, 91*, 1345–1350.

Hirota, K., Yoshioka, H., Kabara, S., Kudo, T., Ishihara, H., & Matsuki, A. (2001). A comparison of the relaxant effects of olprinone and aminophylline on methacholine-induced bronchoconstriction in dogs. *Anesthesia and Analgesia, 93*, 230–233.

Jain, M., & Sznajder, J. I. (2005). Effects of hypoxia on the alveolar epithelium. *Proceedings of the American Thoracic Society, 2*, 202–220.

Lopez-Rodriguez, E., Echaide, M., Cruz, A., Taeusch, H. W., & Perez-Gil, J. (2011). Meconium impairs pulmonary surfactant by a combined action of cholesterol and bile acids. *Biophysical Journal, 100*, 646–655.

Moses, D., Holm, B. A., Spitale, P., Liu, M. Y., & Enhorning, G. (1991). Inhibition of pulmonary surfactant function by meconium. *American Journal of Obstetrics and Gynecology, 164*, 477–481.

Petrone, W. F., English, D. K., Wong, K., & McCord, J. M. (1980). Free radicals and inflammation: Superoxide-dependent activation of a neutrophil chemotactic factor in plasma. *Proceedings of the National Academy of Sciences of the United States of America, 77*, 1159–1163.

Robertson, B., & Halliday, H. L. (1998). Principles of surfactant replacement. *Biochimica et Biophysica Acta, 1408*, 346–361.

Yanagisawa, S., Koarai, A., Sugiura, H., Ichikawa, T., Kanda, M., Tanaka, R., Akamatsu, K., Hirano, T., Matsunaga, K., Minakata, Y., & Ichinose, M. (2009). Oxidative stress augments toll-like receptor 8 mediated neutrophilic responses in healthy subjects. *Respiratory Research, 10*, 50.

Chapter 25
Microcirculation in the Lungs: Special Features of Construction and Dynamics

K.P. Ivanov, I.L. Potekhina, Yu.S. Alyukhin, and N.N. Melnikova

Abstract In this study we investigated microcirculation in the lungs in their *in situ* physiological location inside the thorax. The study was performed with the use of a system of contact optics. A 'window', 4×4 mm in size, was made in thorax tissues and pleura of an anaesthetized rat. The lung collapsed and then was filled with oxygen or hypoxic gas mixture under the pressure of 10–15 cm H_2O through a tracheostomic canula. This almost excluded the respiratory movements of the lung. Then, the lung was brought in contact with a lens (1.7 mm aperture). We showed that there is a whole system of wide microvessels (20–30 μm in diameter) which run between the alveoli; the finding contradicting the hitherto notion that each alveolus is supplied with blood *via* the thinnest (5–10 μm in diameter) lung arterioles. The microvessels we visualized surround each alveolus almost from all sides. In this way, each alveolus receives a maximum amount of blood. Such a structure of lung circulation accounts for a substantial blood flow through the lungs (up to 6 l per min in humans) and for a rapid saturation of the blood with oxygen (about 100 ml per second). The alveoli saturate the blood with oxygen and subsequently the microvessels form the lung veins entering the left auricle. The photographs and video films of the alveoli at a high magnification were presented, demonstrate the special features of the structure and circulation in the alveoli. The plausible mechanisms of rapid saturation of the blood with oxygen are discussed.

Keywords Lung • Microcirculation • Alveoli • Blood flow • Oxygen saturation

25.1 Introduction

Microcirculation is the most important component of circulation. The study of microcirculation is hampered by a substantial variability of its physiological parameters. For example, according to our data the rate of capillary blood flow in various capillaries of the brain and muscles may differ by a factor of almost 20; from 0.1 to 1.8–2.0 mm/s. To determine the average rate of microcirculation in various physiological states it is necessary to plot a histogram of the rates in a certain, rather large number of capillaries. It is interesting that the blood flow even in the same capillary occurs by peculiar

K.P. Ivanov (✉) • I.L. Potekhina • Y.S. Alyukhin • N.N. Melnikova
The I.P. Pavlov Institute of Physiology, Russian Academy of Sciences, Nab. Makarova 6,
Sankt Petersburg 199034, Russia
e-mail: kpivanov@nc2490.spb.edu

M. Pokorski (ed.), *Respiratory Regulation - The Molecular Approach*,
Advances in Experimental Medicine and Biology 756, DOI 10.1007/978-94-007-4549-0_25,

impulses, i.e., with momentary changes in the rate. This appeared to be associated with leukocytes passing through the capillaries, since they have a greater volume than erythrocytes by a factor of 2.0–2.5. Hence, a leukocyte passing through a capillary slows down the capillary blood flow for a time (Dvoretskii 1980; Ivanov et al. 1981, 1985). Since the leukocytes entering capillaries are an unpredictable process, changes in the blood flow rate in the capillaries in time are also unpredictable. In a detailed study of the microcirculation processes we have been able to show that, contrary to almost 100 years old Krog's paradigm stating that the gas exchange between the blood and tissues occurs only in the capillaries, the brain receives almost 30% of oxygen through the walls of the brain arterioles 25–15 μm in diameter (Dvoretskii 1980). The special features of the physiology of microcirculation in the brain, muscles, and liver are given in the published works and in our numerous studies (Ivanov et al. 1979, 1981, 1985; Ivanov 1993, 2001; Komkov 2004; Duling et al. 1979; Hornsfeld 1989; Renkin 1984; Zweifach and Lipowsky 1984).

Microcirculation in the lungs is very complicated to investigate and at the same time is of great interest, since it deals with the most important process of life – the blood saturation with oxygen. The lung structure (Komkov 2004; Hornsfeld 1989; Weibel 1984, 1989) and its hemodynamics (Komkov 2004; Dvoretskii and Tkachenko 1987; West 1988) are described in a number of monographs and reviews. Nevertheless, up to now we have no generally accepted scheme of the structure of the microcirculation system in the lungs. There are only rather old ideas about the blood supply of alveoli. According to these ideas, the alveoli are hanging like grapes on thin pulmonary arterioles. These ideas advanced as long ago as in 1947 by Miller (1947) have been retained till today. The same structure of the lung microcirculation is given in a modern text book on fundamental physiology (Komkov 2004). There is a series of problems waiting to be solved. First, whether all the alveoli receive the blood only *via* individual lung arterioles or several alveoli or the multitude of alveoli is supplied from the same source, and the blood saturation with oxygen occurs successively. This problem was put forward by Weibel (1984, 1989), Dvoretskii and Tkachenko (1987), and others. It is of special significance, since it deals with the features of the general construction of microcirculation in the lungs. The second problem is of more complicated nature. The matter is that the lungs are the organs with comparatively small mass. In humans, they weigh only 600 g. However, under physiological conditions they let pass up to 6 l of blood per min, i.e., the minute volume of the heart. This is a very large volume of the blood. Let us compare the circulation in the brain, 15% of the blood output passing it, i.e., 900 ml of blood, although the brain weighs 1,500 g on average, which means greater by a factor of 2.5 than the lungs. In other words, the amount of blood passing through the lungs is seven times as large as that passing through the brain (West 1988). The question arises: what must be the construction of the lung microcirculation, if it is able of transmitting such a large amount of blood per minute. The third problem is concerned with the blood oxygenation. How can such a large amount of blood be oxygenated completely during 1 min? This is even a more difficult problem, since it is concerned with a large number of important problems of oxygen diffusion, blood physiology, and lung circulation.

In this experimental work we tried to elucidate these problems to the extent possible.

25.2 Methods

The study was approved by a local Ethics Committee and was performed according to the international guidance concerning Care and Welfare of Experimental Animals.

The work was carried out in anesthetized rats (Nembutal 40 mg/kg). Altogether, ten rats weighing from 200 to 230 g were used. We made a 'window' in the thorax of the animals 4×4 mm in size with a rib resected. A fraction of pleura above the 'window' was removed. The lung was filled with oxygen through a catheter inserted into the tracheostomic canula up to the trachea brunching. A special objective of a contact microscope was fitted through the 'window' into the thorax. It touched the lung

surface, the latter remaining in the thorax in a physiological position. The photographs were made at a small magnification, when 10–15 alveoli were photographed at once. The photographs of one or two alveoli were made at greater magnification.

25.3 Results

We were able to take a series of panoramic photographs of the lung surface (the panoramic photographs are those made from above the subject). We managed to imprint several (from 10 to 15) alveoli at once and wide blood flows between them. The blood flows between the alveoli had the width of about 20–40 μm. Given a good oxygen supply of the lungs, the bright red blood moved along these ducts. In separate parts of these ducts between the alveoli there were rare sites with the blood of darker venous color. The apexes of alveoli had dark red or grayish brown color. Moreover, at a greater magnification we made separate photographs of one or two alveoli. These photographs showed that each alveolus is surrounded with powerful blood flows. Each flow was 20–40 μm in width. Corresponding patterns are given in Fig. 25.1a and b. The direction of the blood flows along the ducts between the alveoli could be observed in video films. Along all the ducts, the blood moved in one direction – from one visual angle to the opposite visual angle. The motion was very quick; hence it appeared impossible to estimate its rate in separate experiments.

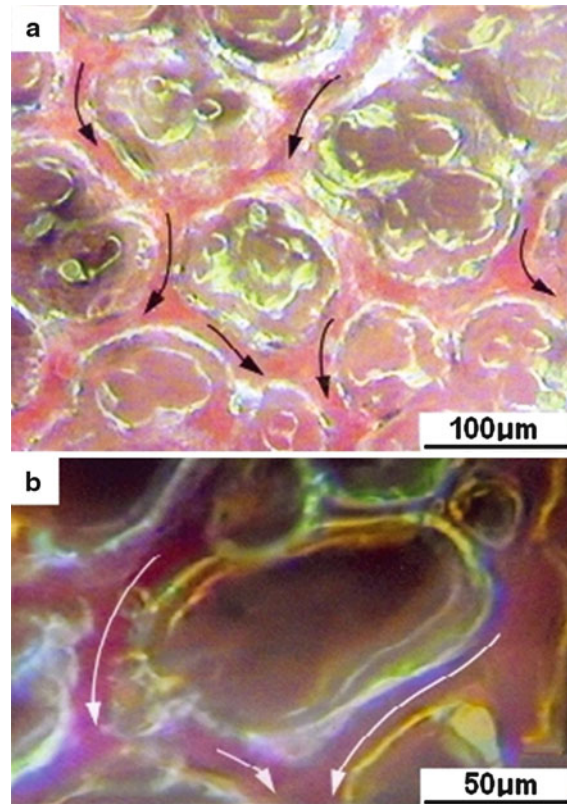

Fig. 25.1 Panoramic photographs of microvessels in-between rat lung alveoli. **(a)** Several alveoli at once and the blood flows between them. The width of the blood flows between the alveoli is 20–40 μm; **(b)** A large alveolus from the middle fraction of the rat lung. The alveolus is surrounded with powerful blood flows, their width is 20–40 μm. The *arrows* show the direction of the blood flow

25.4 Discussion

Photographs of the lung surface under physiological conditions (inside the thorax) show that the alveoli are located in parallel rows on the lung surface. Separate alveoli seem to have no individual blood supply. We suggest that the wide blood flows (which we call 'rivers of blood') lying between the alveoli are microvessels starting from the lung arterioles filled with venous blood. As the blood flows between the alveoli, a fraction of the blood from these microvessels pours to the alveoli. The blood gets saturated with oxygen there and again, as we suppose, enters the duct (the 'river of blood'). In the following alveoli, the blood is additionally saturated with oxygen. The area of the blood flows between the alveoli comprises about 30% of the total area of the alveoli. This suggests that the volumes of these large microvessels and alveoli are almost in the same ratio. The capability of the lungs to let pass a very large volume of the blood (up to 6 l per min) is accounted for by a great amount of very wide and capacious microvessels lying between the alveoli. In the capillaries of the brain, the average rate of the blood flow is about 1 cm/s (Ivanov et al. 1981, 1985; Ivanov 1993). Since the rate of the total blood flow in the lungs is by a factor of 7 greater than that in the brain, we can say with a fair degree of confidence that the volume blood flowing through the wide ducts between the alveoli is also greater by a factor of about 7 than that in the brain capillaries. All these numerical relationships are essentially approximate. However, they allow us to understand why the lungs having a very small mass are capable of letting pass such a large amount of the blood through them.

About a high rate of saturating a very large volume of the blood in the lungs we can say the following. First, the rate of oxygenating the blood is well known to exceed the rate of deoxygenating the blood by a factor of 2–3. This is the first explanation of a high rate of oxygenating the blood in the lungs. But the matter is not only in this. The second reason consists in the fact that oxygenating the blood in the alveoli occurs very intensively because the alveolus wall is about 0.2 μm thick at 60% of its surface (Weibel 1984). This accelerates manyfold the diffusion of oxygen from the air of the alveoli into the blood.

It is interesting that we never saw any separate capillaries in the alveoli walls, though our means for magnification are sufficient enough to see the capillaries only 4–5 μm thick. Consequently, the blood seems to form lacunas at the walls of alveoli as a continuous thinnest layer of the blood without barriers, which facilitates the gas exchange. There is one more reason. In 1980, Dvoretskii (1980) and Conhaim (1980) found the capability of the lungs to saturate the venous blood in the pulmonary arterioles, i.e., even before the alveoli. This property might contribute to the acceleration of the blood saturation with oxygen.

We answered the questions raised in this work only partially, making some proposals based on the obtained facts. The panoramic photographs of many alveoli at once and of separate alveoli bear much information, which still needs to be deciphered. A lot of interesting material is given also by the video films representing the special features of the blood motion in the wide capillaries and on the alveoli walls. This is a completely special demonstration material. Unfortunately, video films are impossible to be given in a journal. We hope that in the nearest future a possibility will appear to supply each paper with the disks describing the blood motion. Then, it will be possible to determine the direction and rate of the blood flow.

Conflicts of interest: The authors declare no conflicts of interest in relation to this article.

References

Conhaim, R. L. (1980). Reflection spectrophotometric measurement of O_2 uptake in pulmonary arterioles of cats. *Journal of Applied Physiology, 48*, 848–856.

Duling, B. R., Kushinsky, W., & Wahl, M. (1979). Measurements of the perivascular PO_2 in the vicinity of pial vessels. *Pflügers Archiv, 383*, 29–34.

Dvoretskii, D. P. (1980). Extracapillary oxygenation of the blood. *Fiziol J SSSR, 66*, 1522–1529.
Dvoretskii, D. P., & Tkachenko, B. I. (1987). *Hemodynamics in the lungs*. Moscow: Medicine.
Hornsfeld, K. (1989). Functional morphology of the pulmonary vasculature. *Respiration Physiology, 40*, 499–532.
Ivanov, K. P. (1993). *Principles of energetics of an organism* (Vol. 2). Sankt-Petersburg: Nauka.
Ivanov, K. P. (2001). *Principles of energetics of an organism* (Vol. 3). Sankt-Petersburg: Nauka.
Ivanov, K. P., Derii, M. O., & Samoilov, M. O. (1979). Oxygen diffusion from arterioles. *Doklady Akademia Nauk SSSR, 244*, 1509–1513.
Ivanov, K. P., Kalinina, M. K., & Levkovich, Yu. I. (1981). Blood flow velocity in capillaries. *Microvascular Research, 22*, 143–155.
Ivanov, K. P., Kalinina, M. K., & Levkovich, Yu. I. (1985). Microcirculation velocity. *Microvascular Research, 30*, 10–18.
Komkov, A. V. (Ed.). (2004). *Fundamental and clinical Physiology*. Textbook. Moscow: Akademiya.
Miller, W. S. (1947). *The lung* (p. 210). Springfield/Baltimore: Thomas.
Renkin, E. M. (1984). Control of microcirculation. In E. M. Renkin, C. C. Michel, & S. R. Geiger (Eds.), Handbook of physiology, Sect. 2: The cardiovascular system (Vol. 4, Part 2, pp. 627–688). Bethesda: American Physiological Society.
Weibel, E. R. (1984). *The pathway for oxygen*. Cambridge: Harvard University Press.
Weibel, E. R. (1989). Lung morphometry. *Respiration Physiology, 40*, 1–56.
West, J. (1988). *Respiration physiology*. Moscow: Mir.
Zweifach, B.W., & Lipowsky, H.H. (1984). Pressure-flow relation in blood and lymph microcirculation. In E. M. Renkin, C. C. Michel (Eds.), Handbook of physiology, Sect. 2: The cardiovascular system (Vol. 4, Part 1, pp. 217–250). Bethesda: American Physiological Society.

Chapter 26
Immunotargeting of the Pulmonary Endothelium *via* Angiotensin-Converting-Enzyme in Isolated Ventilated and Perfused Human Lung

Kai Nowak, Hans C. Kölbel, Roman P. Metzger, Christine Hanusch, Marc Frohnmeyer, Peter Hohenberger, and Siergiej M. Danilov

Abstract Vascular immunotargeting of catalase *via* angiotensin-converting-enzyme (ACE) attenuated lung ischemia reperfusion injury in the rat. As this might be a promising modality for extension of the viability of human lung grafts for transplantation we tested the hypothesis whether anti-ACE antibodies are suitable for human lung protection within the model of isolated perfused and ventilated human lung resections. Right after surgery for lung cancer, human lung specimens were isolated, ventilated and perfused under physiological conditions with 500 μg of either mouse monoclonal antibodies (mAb) to human ACE (9B9, I2H5, 3G8) or non-immune mouse IgG (as a negative control) followed by wash-out perfusion. Perfusion pressure, pH and lung weight gain were measured before and during perfusion. After mAb perfusion and wash-out perfusion period lung tissue was tested for the uptake of mAbs by immunohistochemistry and by enzyme-capture technique. Furthermore, antibody concentration and ACE shedding were measured within the perfusate. We found that ACE activity in tumor and normal lung tissue did not differ between the groups perfused with different mAbs. However, ACE activity in normal lung tissue (17.0 ± 6.0 U/g) was significantly higher compared to tumor tissue (6.0 ± 3.0; $p < 0.01$). Absolute retaining of mAbs was with $1.3 \pm 1.1\%$ of injected dose per gram of tissue in normal lung tissue, $0.7 \pm 0.7\%$ of injected dose per gram of tumor tissue and was

K. Nowak (✉)
Division of Thoracic Surgery, Department of Surgery, Mannheim University Medical Center, University of Heidelberg, Theodor-Kutzer-Ufer 1-3, 68135 Mannheim, Germany
e-mail: kai.nowak@umm.de

Department of Thoracic Surgery, Royal Brompton Hospital, London, UK

H.C. Kölbel • M. Frohnmeyer • P. Hohenberger
Division of Thoracic Surgery, Department of Surgery, Mannheim University Medical Center, University of Heidelberg, Theodor-Kutzer-Ufer 1-3, 68135 Mannheim, Germany

R.P. Metzger
Department of Pediatric Surgery, University of Leipzig, Leipzig, Germany

C. Hanusch
Department of Anesthesia and Critical Care, Mannheim University Medical Center, University of Heidelberg, Theodor-Kutzer-Ufer 1-3, 68135 Mannheim, Germany

S.M. Danilov
Department of Anesthesiology, University of Illinois, Chicago, IL, USA

M. Pokorski (ed.), *Respiratory Regulation - The Molecular Approach*,
Advances in Experimental Medicine and Biology 756, DOI 10.1007/978-94-007-4549-0_26,

significantly higher compared to non-immune mouse IgG (0.1 ± 0.1%/g; $p < 0.01$). Anti-ACE mAbs concentration in the perfusate dropped significantly to 47 ± 11% ($p < 0.001$) at 40 min of perfusion. No significant difference between different anti-ACE mAbs in the depletion from perfusate has been observed. mAb 9B9 showed the most intense immunostaining (i.e., most significant lung uptake) after each experiment in normal and tumor lung tissue compared to mAbs i2H5 and 3G8 ($p < 0.01$). These results validate the possibility of immunotargeting of pulmonary endothelium in the human lung tissue by anti-ACE mAbs under *in vivo* conditions. Furthermore, the model might be useful to investigate targeted therapies in lung cancer without side effects for the patient.

Keywords Angiotensin converting enzyme • Pulmonary endothelium • Lung cancer • Lung transplantation • Lung perfusion

26.1 Introduction

The concept of immunotargeting of antioxidative enzymes into pulmonary endothelium for alleviation of lung oxidative injury, including ischemia-reperfusion (I/R) injury in lung transplantation, has been successfully demonstrated with monoclonal antibodies to several endothelial antigens: angiotensin-converting enzyme-ACE (Atochina et al. 1998; Muzykantov et al. 1996a; Danilov et al. 2001; Nowak et al. 2007b, 2010), inter-cellular adhesion molecule (ICAM-I) (Christofidou-Solomidou et al. 2002, 2003) or platelet/endothelial cell adhesion molecule (PECAM) (Kozower et al. 2003).

However, the preferential expression of ACE in pulmonary capillaries (Morell et al. 1995; Danilov et al. 2001) makes it the most optimal target for therapy directed toward the pulmonary endothelium (Danilov et al. 1991, 2001; Balyasnikova et al. 2002b). We demonstrated that anti-ACE mAbs could serve as specific carriers for the delivery of therapeutic substances and therapeutic genes to the lung vasculature (Danilov et al. 1991, 2001; Atochina et al. 1997, 1998; Reynolds et al. 2000, 2001). By targeting catalase to the pulmonary endothelium *via* conjugation with anti-ACE antibodies we were able to limit I/R injury of the lung in rat models *in vivo* (Nowak et al. 2007b, 2010). Nevertheless it remains unclear, whether anti-ACE mAbs are suitable for targeting human lung endothelial cells. Therefore, in the present study we investigated the specific uptake of several anti-human ACE mAbs in isolated ventilated and perfused lung resections of lung cancer patients.

26.2 Methods

26.2.1 Selection of Specimens and Tissue Procurement

All experiments have been approved by the Ethics Committee of the Mannheim University Medical Center and written informed consent from the patient was obtained.

Operative specimen of eight males (63.4 ± 8.5 years) and five females (59.6 ± 7.2 years) undergoing elective lobectomy for lung cancer were obtained for isolated ventilation and perfusion. Patient details including sex, age, and type of surgery and histological subtyping of lung cancer are shown in Table 26.1.

Surgery of lung resections was performed and time points of cross-clamping of the vessels and bronchus were documented. After resection, the specimen was taken directly to the laboratory to be connected to the perfusion/ventilation system as described (Nowak et al. 2007a). Histological assessment of the resection specimen followed after perfusion consented by the pathologist.

Table 26.1 Patient characteristics

Antibody	Age	Sex	UICC	TNM	Histology	Therapy
Mouse **gG**	73	m	IA	pT1 pN0 G2	Bronchial carcinoid	Right UL
	61	f	IIIB	pT2 pN2 G2	Adenocarcinoma	Left UL
	69	f	IB	pT2 pN0 G2	Adenocarcinoma	Right LL
ACE **9B9**	60	m	n.a.	n.a.	Calcificating pneumonia	Left UL
	65	m	IIIA	pT2 pN1 G3	Squamous carcinoma	Left LL
	73	m	IB	pT2 pN0 G2	Adenocarcinoma	Right UL
ACE **i2H5**	57	m	IB	pT2 pN0 G2	Adenocarcinoma	Right UL
	49	f	IB	pT2 pN0 G3	Adenocarcinoma	Left UL
	58	f	IA	pT1 pN0 G2	Squamous carcinoma	Right UL
ACE **3G8**	66	m	IB	pT2 pN0 G2	Adenocarcinoma	Right UL
	62	m	IA	pT1 pN0 G3	Squamous carcinoma	Left LL
	1	m	IA	pT2 pN1 G2	Squamous carcinoma	Left pneumectomy

Patient characteristics including age, sex, therapy: resection type (*UL* upper lobe, *LL* lower lobe) and neoadjuvant treatment (NA), UICC and TNM classification and histology are presented for each type of antibody. In a 60 year old male perfused with ACE 9B9 mAb, histology turned out to be a calcificating pneumonia instead of a primarily supposed lung cancer with pneumonia. TNM and UICC where therefore not applicable (n.a.) in that very case

26.2.2 Ventilation-Perfusion System

Isolated lung ventilation and perfusion has been performed as described earlier in a recirculating manner under standardized physiologic conditions (Nowak et al. 2007a).

Total volume of the perfusate was 1.5 l. A physiological salt solution supplemented with albumin was used throughout the experiments as described (Nowak et al. 2007a). The perfusate was divided into solution A (1.3 l) and solution B (200 ml). Different specific anti-ACE mAbs or non-immune mouse IgG (as a negative control) was added to solution B at a dose of 500 μg.

Ventilatory parameters, inspiratory peak pressure and inspiratory tidal volume were documented throughout the experiments. Perfusion pressures were kept below 20 mmHg systolic PAP.

Stable temperatures of perfusate and specimen were ensured by continuous monitoring within the water-warmed perfusion reservoir and within the incubator. The pH value was continuously monitored in the perfusion reservoir. Values of pH, PCO_2, PO_2 and base excess (BE) were monitored during each experiment by an ABL 50 blood gas analyzer (Radiometer, Copenhagen, Denmark).

26.2.3 Antibody Perfusion and Study Groups

Three different mouse anti-human ACE mAbs recognizing different epitopes on the N domain of human ACE were compared in this study for their ability to accumulate in the human lung during warm lung perfusion -9B9 (Danilov et al. 1994, 2001; Balyasnikova et al. 2002b; Gordon et al. 2010), i2H5 (Balyasnikova et al. 2002b; Danilov et al. 1994; Skirgello et al. 2006) and 3G8 (Danilov et al. 1994; Gordon et al. 2010).

After an equilibration phase of 10 min with perfusion solution A, lung perfusion was performed with solution B, where 500 μg of mouse anti-human ACE mAbs i2H5, 3G8 or 9B9 (each n = 3) or non-immune mouse IgG (n = 3) were added. Lung perfusion with mAbs was performed in a recirculating manner over a period of 40 min. Thereafter a washout period with solution A followed over 20 min.

26.2.4 Detection and Quantification of Lung Accumulation of mAbs to ACE

Qualitatively lung uptake of anti-ACE mAbs was detected immunohistochemically. The primary antibodies used are listed in Table 26.1. After perfusion, all tissues were snap frozen and stored in liquid nitrogen. Tissues were sectioned at 5 μm by a cryostat microtome (Modell HM 560, FA Microm, Germany). The slides were air-dried at room temperature for 12–24 h and stored at −30°C. Immunohistochemistry was performed using the anti-mouse alkaline-phosphatase-anti-alkaline-phosphatase (APAAP) technique with standardized protocol (Dako Cytomation). Sections were incubated by the secondary rabbit anti-mouse immunoglobulin (1:40, Dako Cytomation) and the mouse APAAP complex (1:50, Dako Cytomation) twice. Each step lasted 30 min at RT. Alkaline phosphatase substrate reaction with new fuchsin (100 μg/ml) and levamisole (400 μg/ml) was performed for 20 min at RT. Sections were counterstained with hematoxylin and mounted in gelatin. The levels of immunoreactivity in different renal cells and compartments were scored into four subgroups as follows: 0 = no expression detectable, 1 = slight expression, 2 = moderate expression and 3 = strong expression.

Quantitatively lung uptake of these mAbs was detected and quantified using a variant of enzyme-capture immunoassay. Piece of normal lung or cancer tissue (0.5–1 g) was homogenized in 5 ml volume of PBS buffer, containing 0.5% of Triton-X-100 (for solubilization of membrane-bound form of tissue ACE and mAbs bind to this form). Then the supernatants (after centrifugation at 10000 *g* for 15 min) were added to the wells of 96-well plate, coated (50 μl, 10 μg/ml, overnight at 4°C) with affinity purified goat polyclonal anti-mouse IgG antibodies (Danilov et al. 1994). Specific mouse anti-human ACE mAbs, which accumulated in the lung tissue during perfusion, were captured to the bottom of the wells of 96-well plates by goat-anti-mouse IgG, adsorbed to the bottom of these wells. Part of the membrane-bound ACE, solubilized from the lung tissue, bind to specific mAbs to ACE, that were present in this piece of lung tissue, and thus was precipitated (captured) by goat-anti-mouse IgG adsorbed on the bottom of the wells. After washing out of the unbound mouse IgG (specific or non-specific) a substrate for ACE (Hip-His-Leu, 5 mM) was added directly into the well, and precipitated ACE activity was quantified. Therefore, the amount of mAbs to ACE uptake during perfusion of lung tissues was measured *via* quantification of ACE, bound by these mAbs accumulating in the lung and precipitated by goat antibodies to mouse IgG.

Disappearance of mouse-anti-human ACE mAbs from perfusate during long perfusion was quantified by another variant of this immune-capture assay. Aliquots of the perfusates, containing decreasing (with time) concentrations of antibodies (mouse IgG) were incubated with microtiter plates coated with goat-anti-mouse IgG. Then, fixed amount of human ACE (supernatants of human lung homogenate-10 mU/ml) was added to each well. The depletion of mAbs to ACE from perfusate during perfusion of lung tissues was measured *via* quantification of ACE, bound by these mAbs precipitated by goat antibodies to mouse IgG.

26.2.5 Statistical Analysis

Statistical differences in the studied parameters between groups were determined with a double sided U-Test (SPSS scientific software, Version 14.1, USA). Results are given in mean ± SD in the text and are displayed in mean ± SE. Tests with $p < 0.05$ were considered as statistical significant.

26.3 Results

26.3.1 Immunohistochemical Detection of mAbs to ACE Accumulating in the Lung

Lung uptake of anti-ACE mAbs was detected by immunohistochemistry. In perfused lung and tumor tissues monoclonal anti-human ACE antibodies (mAbs 9B9, i2H5, 3G8) accumulated in endothelial cells of capillaries, arterioles and small muscle arteries (Fig. 26.1a–d). ACE containing alveolar macrophages remained negative, serving as an internal control (Fig. 26.1a, c).

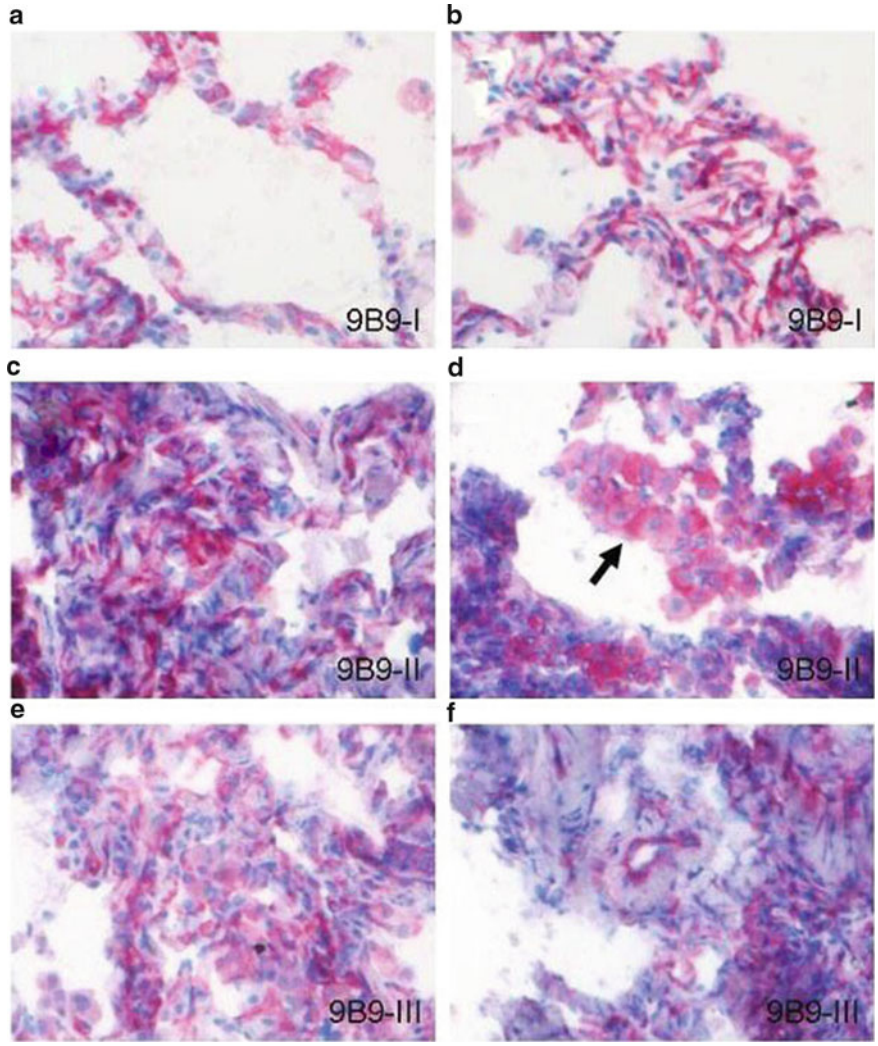

Fig. 26.1 Lung uptake of anti-ACE mAbs detected by immunohistochemistry. In the perfused lungs anti-ACE mAbs accumulate grossly in endothelial cells of alveolar capillaries of lung tissue (a and c) and in endothelial cells of the tumor vascularization (b and d)-*red* color. ACE containing alveolar macrophages are negative (*arrow* in d) as they are localized in the depth of lung tissue and did not get in contact with anti-ACE mAbs during the perfusion period. Lung perfusion with non-immune mouse IgG showed no specific mouse IgG binding to lung endothelium (e and f). A/B, anti ACE mAb 9B9; C/D, anti ACE mAb i2H5; E/F, mouse IgG. Original magnification A to F ×20, APAAP

Table 26.2 Intensity of immunostaining in lung tissues after perfusion with anti-ACE mAbs

mAbs	Lung	Tumor
IgG	0	0
3G8	1.5	1.3
i2H5	1.7	0.7
9B9	2.7	2.0

Immunostaining of lung and tumor tissue was not positive for lungs perfused with non-immune mouse IgG (negative control). Anti-ACE mAb 9B9 showed strongest staining in the lung and tumor tissue compared to other applied anti-ACE antibodies- i2H5 and 3G8. Semi-quantification of the intensity of immunostaining was performed as described in Material and Methods

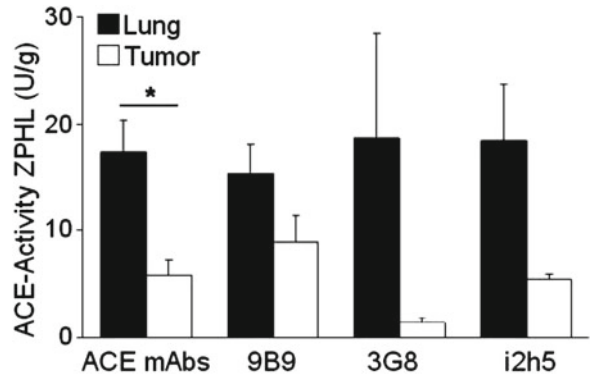

Fig. 26.2 ACE activity in the perfused lung tissues. ACE activity was measured in lung tissue (*filled bars*) and tumor tissue (*open bars*) at the end of each perfusion experiment fluorimetrically with ZPHL as substrate. Lowest ACE activity was found in tumor tissue of 3G8 perfused specimen. The differences between lung tissue and tumor tissue were greater in 3G8 and i2H5. The differences did not reached statistical significance due to the limited numbers of lung specimens (n = 3). Overall in mean of all three ACE mAbs (ACE mAbs) perfused lungs (9B9, 3G8, i2H5) ACE activity was significantly higher in lung tissue compared to tumor tissue ($p < 0.01$)

In contrast, lung and tumor tissues perfused by the non-specific mouse IgG were negative for both endothelial cells and macrophages (Fig. 26.1e, f). In general, the mAb 9B9 showed the most intense binding after each experiment in normal and tumor lung tissue compared to i2H5 and 3G8 (Fig. 26.1, Table 26.2).

26.3.2 Quantification of Lung Uptake of Mouse Anti-human ACE mAbs

As we described in the methods section, the amount of mAbs bound to ACE in the human lung during perfusion of lung tissues was measured *via* quantification of ACE, bound by these mAbs after uptake within the lung and precipitated by goat antibodies to mouse IgG.

ACE activity solubilized from tumor and normal lung tissue by detergent (Triton X-100) did not differ between the groups with different anti-ACE mAbs. However, ACE activity in normal lung tissue (17.0 ± 6.0 U/g) was significantly higher compared to tumor tissue (6.0 ± 3.0; $p < 0.01$, Fig. 26.2).

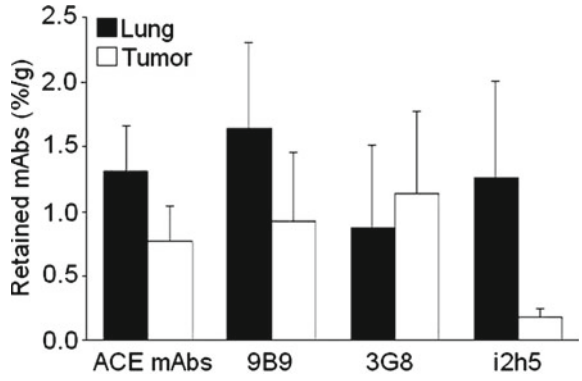

Fig. 26.3 Uptake of anti-ACE mAbs by the lung tissue during lung perfusion. In lung tissue (*filled bar*) 1.3%/g of the dose was retained compared to 0.7%/g in tumor tissue (*open bar*). Lung tissues perfused with mAb 9B9 showed the highest mAb uptake. Specimen perfused with mAb i2H5 showed the lowest mAb uptake within tumor tissue. Mean of different ACE mAbs (ACE mAbs; n = 9) did not show statistically significant differences between tumor and lung tissue

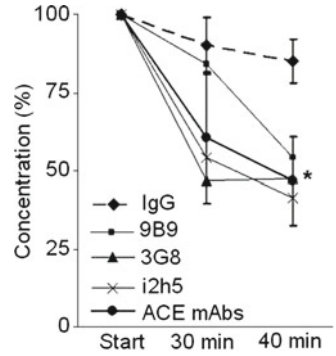

Fig. 26.4 Depletion of anti-ACE mAbs from perfusate during lung perfusion. After equilibration lung perfusion with mAbs was started over a period of 40 min. ACE-mAbs (all experiments with antibodies 9B9, 3G8 and i2H5 (n = 9)) dropped in the perfusate significantly by 54% compared with 15% in IgG-mouse during this period (*$p < 0.05$). No significant differences could be found between iso-antibody concentrations of 9B9, 3G8 and i2H5 in the perfusate during perfusion

Absolute retaining of anti-ACE mAbs was 1.3 ± 1% of the injected dose per gram of tissue in normal lung and 0.7 ± 0.7% of injected dose/g in tumor tissue. Both in tumor and healthy lung tissue anti-ACE mAbs retaining was significantly higher compared with negative control (non-immune mouse IgG) (0.1 ± 0.1%/g; $p < 0.01$; Fig. 26.3). Therefore, all three tested mouse mAbs to human ACE specifically accumulate in the human lung after perfusion of lung lobes.

We also quantified the disappearance of anti-ACE mAbs from the perfusate during long (40 min) recirculating perfusion. In the perfusate, concentration of anti-ACE mAbs dropped significantly from the initial 100% to 47 ± 11% ($p < 0.001$) after 40 min of lung lobe perfusion with these mAbs. Concentration of mouse IgG in the perfusate after 40 min of perfusion was significantly higher in the case of lung lobe perfusion with non-specific mouse IgG (85 ± 7%) compared to specific anti-ACE mAbs (47 ± 11%; $p < 0.05$; Fig. 26.4). This is another indication that depletion of anti-ACE mAbs from perfusate to lung tissues was active and due to specific uptake by lung tissue.

26.4 Discussion

Pulmonary endothelium plays a major role in lung ischemia reperfusion injury during lung transplantation. Reperfusion induces an important inflammatory response, characterized by a massive production of free radicals and by the activation of the complement and leukocyte neutrophils (De Perrot et al. 2003). Oxidative stress, the production of cytokines and the secondary mitochondrial lesions that occur with reperfusion will induce apoptosis on the level of the parenchyma and the vascular structures. The proinflammatory state induced by reperfusion continues for several days and can affect the patient's prognosis (Gourdin et al. 2009). Specific targeting of the pulmonary vasculature with antioxidant enzymes (Catalase, superoxide dismutase) could offer alternative treatment options to increase efficacy of donor lung preservation for lung transplantation.

It has been proposed that vascular immunotargeting of anti-oxidant enzymes to endothelial antigens (e.g., PECAM, ICAM-1, ACE) *via* mAbs to these antigens improve the therapeutic effect of these enzymes (Muzykantov et al. 1996a; Atochina et al. 1998; Christofidou-Solomidou et al. 2002). Attenuation of *in vivo* lung injury has been achieved by anti-PECAM conjugates with catalase in a rodent model of vascular oxidative stress (Christofidou-Solomidou et al. 2003; Atochina et al. 1998). The same group effectively demonstrated a strong protective effect of vascular immunotargeting of catalase in an *in vivo* model of lung transplantation in rats (Kozower et al. 2003).

Despite this effective protection of lung endothelium by catalase, conjugated with anti-PECAM antibodies, we believe that the conjugates of antioxidant enzymes with anti-ACE mAbs, should be even more effective, and at least, more selective. In contrast to PECAM, which is significantly expressed in other organs beside the lung (Danilov et al. 2001), ACE is expressed in 100% of the pulmonary capillaries compared to 10–20% of capillaries in other organs (Morell et al. 1995; Danilov et al. 2001). Therefore, we reasoned that conjugates of catalase with anti-ACE mAbs should offer even more specific pulmonary endothelial immunotargeting. We used anti-ACE mAb 9B9 conjugated with catalase (9B9-CAT), which have been shown to accumulate selectively in the rat lung endothelium compared to biotinylated catalase (Muzykantov et al. 1996a; Atochina et al. 1998). Recently we have reported, that conjugates of mAb 9B9 to catalase protected from lung ischemia reperfusion injury in warm and cold rat models *in vivo* without major side effects (Nowak et al. 2007b, 2010).

The series of our papers on the rat model using anti-human ACE mAb 9B9, which cross-react with rat ACE, clearly demonstrated that the lung endothelial immunotargeting of catalase conjugated with anti-ACE antibodies provide a real opportunity for possible translation of laboratory studies on animals into clinical settings.

Beside mAb 9B9, which accumulates specifically in the lung of rat, hamster, cat, monkeys and human after systemic injection (Danilov et al. 1991, 2001; Muzykantov et al. 1996b; Balyasnikova et al. 2002b), we have another mAbs which could be even better candidates for translation of this approach into clinic. mAb i2H5 bind even stronger to human ACE than mAb 9B9, at least on the surface of human ACE expressing cells (Balyasnikova et al. 2002b). Besides, this mAb, in contrast to mAb 9B9, does not induce ACE shedding, which could compromise, to some extent, the efficacy of catalase targeting (Balyasnikova et al. 2002b). Also, this mAb demonstrates the highest binding to monkey ACE, which can provide a convenient large animal model, before translation of this approach into clinic. mAb 3G8 has another advantage as it binds well to ACE on the surface of cells and also inhibits ACE shedding, which could theoretically even increase the efficacy of ACE targeting in the human lung (Balyasnikova et al. 2002a).

Recently we developed a method for isolation and perfusion of human lung resections (Nowak et al. 2007a). The human isolated lung resection perfusion model offers a unique possibility to study the effects of endobronchial or intravascular administered substances on lung and tumor tissue under physiologic conditions without possible harm for the patient. The availability of this method and a set of mAbs to human ACE, that could be used for human lung endothelial targeting allowed us to investigate

whether these mAbs really accumulates specifically into human lung endothelial cells after perfusion of human lung lobes (tissue).

The results presented in this paper clearly show that the mouse anti-human ACE mAbs 9B9, i2H5 and 3G8 specifically accumulate in the human lung endothelial cells after perfusion of human lung lobes and theoretically can deliver anti-oxidant enzymes (catalase, superoxide dismutase) or other substances to the pulmonary endothelium for protection of donor lungs. Nevertheless, the following steps need to be done, to translate this approach to the clinic:

- Genes for these mAbs should be isolated and cDNA coding for single-chain.
- Fv fragments (scFv) of these mAbs should be cloned. Recently, we successfully isolated scFv for mAb 9B9.
- These fragments should be humanized.
- A fusion protein of scFv of humanized version of anti-human mAb to ACE with cDNA for human catalase or superoxide dismutase should be prepared.

The knowledge of therapy tolerance of the human lung tissue acquired with this model ex-vivo might also get of importance for neoadjuvant therapeutic strategies aiming at *in vivo* and *in situ* perfusion of lungs to treat pulmonary metastases or for downstaging of lung carcinoma (Hendriks and Van Schil 1998).

Conflicts of interest: The authors declare no conflicts of interest in relation to this article.

References

Atochina, E. N., Muzykantov, V. R., Al, M. A., Danilov, S. M., & Fisher, A. B. (1997). Normoxic lung ischemia/reperfusion accelerates shedding of angiotensin converting enzyme from the pulmonary endothelium. *American Journal of Respiratory and Critical Care Medicine, 156*, 1114–1119.

Atochina, E. N., Balyasnikova, I. V., Danilov, S. M., Granger, D. N., Fisher, A. B., & Muzykantov, V. R. (1998). Immunotargeting of catalase to ACE or ICAM-1 protects perfused rat lungs against oxidative stress. *The American Journal of Physiology, 275*, L806–L817.

Balyasnikova, I. V., Karran, E. C., Albrecht, R. F., & Danilov, S. M. (2002a). Epitope-specific antibody-induced cleavage of angiotensin-converting enzyme from the cell surface. *The Biochemical Journal, 362*, 585–595.

Balyasnikova, I. V., Yeomans, D. C., Mcdonald, T. B., & Danilov, S. M. (2002b). Antibody-mediated lung endothelium targeting: In vivo model on primates. *Gene Therapy, 9*, 282–290.

Christofidou-Solomidou, M., Kozover, S., Scherpereel, A., Wiewrodt, R., Solomides, C. C., Pietra, G. G., Murciano, J. C., Shah, S. A., Ischiropoulos, H., Albelda, S. M., & Muzykantov, V. R. (2002). Vascular immunotargeting of glucose oxidase to the endothelial antigens induces distinct forms of oxidant acute lung injury. *The American Journal of Pathology, 160*, 1155–1169.

Christofidou-Solomidou, M., Scherpereel, A., Wiewrodt, R., Ng, K., Sweitzer, T., Arguiri, E., Shuvaev, V., Solomides, C. C., Albelda, S. M., & Muzykantov, V. R. (2003). PECAM directed delivery of catalase to endothelium protects against pulmonary vascular oxidative stress. *American Journal of Physiology. Lung Cellular and Molecular Physiology, 285*, L283–L292.

Danilov, S. M., Muzykantov, V. R., Martynov, A. V., Atochina, E. N., Sakharov, I., Trakht, I. N., & Smirnov, V. N. (1991). Lung is the target organ for a monoclonal antibody to angiotensin-converting enzyme. *Laboratory Investigation, 64*, 118–124.

Danilov, S. M., Atochina, E. N., Hiemisch, H., Churakova, T., Moldobaeva, A., Ryan, U., & Muzykantov, V. R. (1994). Interaction of mAb to angiotensin-converting enzyme (ACE) with antigen in vitro and in vivo: Antibody targeting to the lung induces ACE antigenic modulation. *International Immunology, 6*, 5213–5218.

Danilov, S. M., Gavryliuk, V. D., Franke, V. E., Pauls, K., Harshaw, D. W., Mcdonald, T. D., Miletich, D. J., & Muzykantow, V. R. (2001). Lung uptake of antibodies to endothelial antigens: Key determinants of vascular immunotargeting. *American Journal of Physiology. Lung Cellular and Molecular Physiology, 280*, L1335–L1347.

De Perrot, M., Liu, M., Waddell, T. K., & Keshavjee, S. (2003). Ischemia-reperfusion-induced lung injury. *American Journal of Respiratory and Critical Care Medicine, 167*, 490–511.

Gordon, K., Balyasnikova, I. V., Nesterovitch, A. B., Schwartz, D. E., Sturrock, E. D., & Danilov, S. M. (2010). Fine epitope mapping of monoclonal antibodies 9B9 and 3G8 to the N domain of angiotensin-converting enzyme (CD143) defines a region involved in regulating angiotensin-converting enzyme dimerization and shedding. *Tissue Antigens, 75*, 136–150.

Gourdin, M. J., Bree, B., & De Kock, M. (2009). The impact of ischaemia-reperfusion on the blood vessel. *European Journal of Anaesthesiology, 26*, 537–547.

Hendriks, J. M., & Van Schil, P. E. (1998). Isolated lung perfusion for the treatment of pulmonary metastases. *Surgical Oncology, 7*, 59–63.

Kozower, B. D., Christofidou-Solomidou, M., Sweitzer, T. D., Muro, S., Buerk, D. G., Solomides, C. C., Albelda, S. M., Patterson, G. A., & Muzykantov, V. R. (2003). Immunotargeting of catalase to the pulmonary endothelium alleviates oxidative stress and reduces acute lung transplantation injury. *Nature Biotechnology, 21*, 392–398.

Morell, N. W., Atochina, E. N., Morris, K. G., Danilov, S. M., & Stenmark, K. R. (1995). Angiotensin converting enzyme expression is increased in small pulmonary arteries of rats with hypoxia induced pulmonary hypertension. *The Journal of Clinical Investigation, 96*, 1823–1833.

Muzykantov, V. R., Atochina, E. N., Ischiropoulos, H., Danilov, S. M., & Fisher, A. B. (1996a). Immunotargeting of antioxidant enzyme to the pulmonary endothelium. *Proceedings of the National Academy of Sciences of the United States of America, 93*, 5213–5218.

Muzykantov, V. R., Atochina, E. N., Kuo, A., Barnathan, E. S., Notarfrancesco, K., Shuman, H., Dodia, C., & Fisher, A. B. (1996b). Endothelial cells internalize monoclonal antibody to angiotensin-converting enzyme. *The American Journal of Physiology, 270*, L704–L713.

Nowak, K., Hanusch, C., Kolbel, H. C., Schwarzbach, M., Post, S., Beck, G., Gebhard, M. M., Metzger, R., & Hohenberger, P. (2007a). Alterations of tumor and normal tissue of human lung cancer resection specimens after isolation perfusion. *Journal of Physiology and Pharmacology, 58*(Suppl 5), 501–511.

Nowak, K., Weih, S., Metzger, R., Albrecht, R. F., 2nd, Post, S., Hohenberger, P., Gebhard, M. M., & Danilov, S. M. (2007b). Immunotargeting of catalase to lung endothelium via anti-angiotensin-converting enzyme antibodies attenuates ischemia-reperfusion injury of the lung in vivo. *American Journal of Physiology. Lung Cellular and Molecular Physiology, 293*, L162–L169.

Nowak, K., Hanusch, C., Nicksch, K., Metzger, R. P., Beck, G., Gebhard, M. M., Hohenberger, P., & Danilov, S. M. (2010). Pre-ischaemic conditioning of the pulmonary endothelium by immunotargeting of catalase via angiotensin-converting-enzyme antibodies. *European Journal of Cardio-Thoracic Surgery, 37*, 859–863.

Reynolds, P. N., Zinn, K. R., Gavrilyuk, V. D., Balyasnikova, I. V., Rogers, B. E., Buchsbaum, D. J., Wang, M. H., Miletich, D. J., Grizzle, W. E., Douglas, J. T., Danilov, S. M., & Curiel, D. T. (2000). A targetable, injectable adenoviral vector for selective gene delivery to pulmonary endothelium in vivo. *Molecular Therapy, 2*, 562–578.

Reynolds, P. N., Nicklin, S. A., Kaliberova, L., Boatman, B. G., Grizzle, W. E., Balyasnikova, I. V., Baker, A. H., Danilov, S. M., & Curiel, D. T. (2001). Combined transductional and transcriptional targeting improves the specificity of transgene expression in vivo. *Nature Biotechnology, 19*, 838–842.

Skirgello, O. E., Balyasnikova, I. V., Binevski, P. V., Sun, Z. L., Baskin, I. I., Palyulin, V. A., Nesterovitch, A. B., Albrecht, R. F., 2nd, Kost, O. A., & Danilov, S. M. (2006). Inhibitory antibodies to human angiotensin-converting enzyme: Fine epitope mapping and mechanism of action. *Biochemistry, 45*, 4831–4847.

Chapter 27
Angiogenic Activity of Sera from Interstitial Lung Disease Patients in Relation to Angiotensin-Converting Enzyme Activity

T.M. Zielonka, K. Zycinska, J. Chorostowska-Wynimko, M. Filewska, B. Bialas, M.H. Obrowski, E. Radzikowska, E. Skopinska-Rozewska, and U. Demkow

Abstract The role of angiogenesis in the pathogenesis of interstitial lung diseases (ILD) is unknown. Angiotensin-converting enzyme (ACE) is a marker of sarcoidosis activity and may modulate angiogenesis. The aim of this study was to examine the relationship between ACE activity in ILD patients' sera and their effect on microvessels formation in an *in vivo* model of leukocyte-induced angiogenesis. The study population consisted of 77 sarcoidosis patients, 22 idiopathic pulmonary fibrosis patients, 16 bird fanciers lung patients, eight silicosis patients and 14 healthy donors. Serum ACE activity was assayed by spectrophotometric method. As an angiogenic test, a leukocyte-induced angiogenesis assay in an animal model was used. Sera from interstitial lung disease patients significantly stimulated angiogenic activity of mononuclear cells compared with healthy donors ($p < 0.001$). The highest ACE serum activity was measured in sera from the silicosis patients, and lowest in sera from the sarcoidosis and IPF patients. A significantly lower serum ACE activity was detected in the bird fanciers lung patients. Serum angiogenic activity of ILD patients measured by angiogenesis index negatively correlated with ACE serum activity ($r = -0.52$; $p < 0.01$). This correlation was highest in the sarcoidosis group ($r = -0.6$; $p < 0.001$). Sera from ILD patient constitute the source of factors modulating angiogenesis.

T.M. Zielonka (✉) • K. Zycinska • M.H. Obrowski
Department of Family Medicine, Medical University of Warsaw, Banacha 1a St, 02-097 Warsaw, Poland
e-mail: tmzielonka@wp.pl

M. Filewska • B. Bialas
Department of Laboratory Diagnostics and Immunology, Institute of Tuberculosis and Lung Diseases, Plocka 26 St, 01-138 Warsaw, Poland

J. Chorostowska-Wynimko
Laboratory of Molecular Diagnostics, Institute of Tuberculosis and Lung Diseases, Plocka 26 St, 01-138 Warsaw, Poland

E. Radzikowska
Department of Lung Diseases, Institute of Tuberculosis and Lung Diseases, Plocka 26 St, 01-138 Warsaw, Poland

E. Skopinska-Rozewska
Department of Pathology, Biostructure Center, Medical University of Warsaw, Banacha 1a St, 02-097 Warsaw, Poland

U. Demkow
Department of Laboratory Diagnostics and Clinical Immunology of the Developmental Age, Medical University of Warsaw, Marszalkowska 24 St, 00-576 Warsaw, Poland

M. Pokorski (ed.), *Respiratory Regulation - The Molecular Approach*,
Advances in Experimental Medicine and Biology 756, DOI 10.1007/978-94-007-4549-0_27,

Keywords Angiogenesis • Chronic inflammation • Interstitial lung disease • Angiotensin converting enzyme • Leukocytes

27.1 Introduction

Angiogenesis is currently recognized as a crucial step in the development of tumors and metastases (Saaristo et al. 2000). However, there is an increasing number of data suggesting a considerable role of angiogenesis in the pathogenesis of ILD, including granulomatosis, fibrosis, and vasculitis (Keane 2004; Tzouvelekis et al. 2006; Zielonka et al. 2010). Chronic inflammation and hypoxia, common disturbances in ILD, are strong stimuli for neovascularization (Wagner et al. 2008). VEGF is well known for its key role in tumor angiogenesis, while its contribution to neovascularization in ILDs is much less understood (Shibuya 2001). In this regard, data demonstrating a significant effect of angiotensin II (AT-II) on VEGF gene expression seem to be of considerable importance (Yoshiji et al. 2002a). AT-II, produced from AT-I by ACE, is known for its proangiogenic effect, like VEGF gene upregulation, tissue inhibitor of metalloproteinases-1 (TIMP-1) production and endothelial cells proliferation (Williams et al. 1995; Fujiyama et al. 2001). Moreover, experimental studies demonstrated that inhibition of ACE and therefore of AT-II synthesis produces a significant antiangiogenic effect (Yoshiji et al. 2004). Several ACE inhibitors at clinically comparable doses have been characterized as potent inhibitors of angiogenesis in experimental tumor development. The inhibition of AT-II by perindopril significantly suppressed VEGF expression in tumors (Yoshiji et al. 2002b). Therefore, while increased ACE activity appears to be a hallmark of active sarcoidosis, its precise role in neovascularization observed in sarcoid lungs is unclear (ATS/ERS/WASOG 1999). Increased ACE activity has been observed in other ILD patients (Grönhagen-Riska et al. 1978), still its biological function and diagnostic value has only been proven in sarcoidosis. The aim of this study was to examine the relationship between ACE activity in the sera of ILD patients and its effect on microvessel formation in an *in vivo* model of leukocyte-induced angiogenesis.

27.2 Methods

27.2.1 Study Population

The study protocol was approved by a local Ethics Committee and informed consent was obtained from each participant. The study population consisted of 123 ILD patients: 77 with sarcoidosis (SAR), 22 with idiopathic pulmonary fibrosis (IPF), and 16 with bird fanciers lung (BFL), eight with silicosis (SIL), and 14 healthy volunteers (Table 27.1). Patients receiving immunosuppressive treatment were excluded from the study. Sarcoidosis was diagnosed according to the ATS/ERS/WASOG standards (1999). Patients were stratified on the basis of chest radiographic staging into Stage I – 20 patients, in Stage II – 37 patients and in Stage III – 20 patients. The diagnosis of IPF was based on ATS criteria (2000). The diagnosis of BFL was based on clinical, radiological, functional, serological, BAL, and

Table 27.1 Characteristics of examined groups

	No. of subjects	Age (yr ± SD)	Female/Male	Smokers/Nonsmokers
Sarcoidosis	77	40.0 ± 11.5	31/46	19/58
IPF	22	62.5 ± 11.3	11/11	5/17
BFL	16	45.0 ± 16.2	9/7	5/11
Silicosis	8	62.5 ± 11.3	1/7	7/1
Healthy volunteers	14	36.2 ± 8.3	8/6	2/12

histopathological findings according to the Lacasse et al. (2003). The diagnosis of silicosis was based on clinical, radiological, and histopathological criteria, and occupational exposure to silica. A control group consisted of 14 healthy volunteers.

27.2.2 ACE Activity

Serum ACE activity was assayed by a colorimetric method with tripeptide N-(3-(2-furyl)acriloil)-L-fenylalanilglicilglicine (FAPGG) (Sigma Diagnostics, St. Louis, MA) at 345 nm using a spectrophotometric reader Elx800 (Biotec Instruments, USA). ACE activity was calculated as follows: ACE (U/l) = (Δ absorbance$_{ex}$/Δ absorbance$_{cont}$) x activity of calibrator, where Δ absorbance$_{ex}$ is Δ absorbance for examined sera during 5 min and Δ absorbance$_{cont}$ is Δ absorbance for calibrator during 5 min.

27.2.3 Mononuclear Cell Isolation and Incubation

Human peripheral blood mononuclear cells (MNC) were isolated from healthy donors' buffy-coat cells obtained from the Blood Donation Station in Warsaw, Poland, using a gradient technique. This method yielded an MNC preparation containing 10–15% monocytes and 85–90% lymphocytes, based on morphological criteria and myeloperoxidase staining. The MNC were incubated for 60 min at 37°C, 5% CO_2 in PBS enriched with serum (3:1) isolated from patients. Two control groups were prepared: in the first control, MNC were incubated in PBS supplemented with 25% of serum from health donors and in the second control, MNC were incubated only in PBS. Afterwards MNC were washed and suspended in Parker medium.

27.2.4 Leukocyte Induced Angiogenesis Assay

Protocols involving animals have been performed according to the Helsinki Convention for the use and care of animals and were approved by the respective Ethics Committee. Cutaneous angiogenesis assay was performed according to the method of Sidky and Auerbach (1975), with some modifications (Zielonka et al. 2010). MNC incubated with sera from ILD patients or healthy donors were inoculated intradermally (0.05 ml per one injection, with 5×10^5 cells, six injections per mouse, three mice for one tested sample) into regionally shaved Balb/c mice, anesthetized with chloral hydrate. The control group was injected MNC incubated with PBS only. After 72 h, the mice were killed with a lethal dose of Morbital (Biowet, Poland). Newly formed microvessels were identified and counted blindly by the same person UD with a dissection microscope (Nikon, Japan) at 6x magnification according to the Sidky and Auerbach criteria (1975). Results were expressed as the absolute number of the newly-formed microvessels or as the angiogenesis index (AI) calculated as a ratio: AI = (A_{ex}/A_{contr}), where A_{ex} number of new blood vessels formed upon induction by ILD patients sera and A_{contr} is number of new blood vessels formed upon induction by sera from healthy donors.

27.2.5 Statistical Analysis

Since the data followed a normal distribution, assessed with the Bartlett test, a *t*-test for independent samples was applied to determine differences between groups. The relationships between variables were examined by the Pearson correlation coefficient and $p < 0.05$ was used to indicate statistical significance. Analysis was performed using Statistica 6 for Windows package (StatSoft, Inc., Tulsa, OK).

27.3 Results

27.3.1 ACE Activity

The mean ACE activity was significantly higher in all examined groups compared with healthy controls (29 ± 8 U/L) (Fig. 27.1). The highest serum ACE activity was demonstrated in the silicosis group (94 ± 51 U/L), while the lowest in the BFL patients (45 ± 22 U/L). In both groups, ACE values were significantly different than those observed in the sarcoidosis patients (63 ± 34 U/L), while no differences were shown for the IPF group (59 ± 39 U/L).

27.3.2 Angiogenic Activity

MNC incubated with sera of each ILD patients' group demonstrated a considerably higher proangiogenic activity, as assessed by the number of newly formed microvessels, than the number of microvessels tallied after incubation with healthy volunteers' sera or with PBS ($p < 0.001$) (Fig. 27.2). The most pronounced proangiogenic effect was exerted by sera from the BFL group (17.2 ± 1.3). This effect was considerably stronger than stimulation induced by sera from the sarcoidosis (16.3 ± 1.5; $p < 0.05$), IPF (16.0 ± 0.9; $p < 0.05$), or silicosis patients (15.7 ± 0.4; $p < 0.01$). Moreover, sera from healthy volunteers' did augment the angiogenic activity of normal MNC (13.2 ± 0.9) as compared with PBS only (11.6 ± 1.2; $p < 0.001$).

Accordingly, the angiogenesis index reflecting proangiogenic activity of sera from the examined groups was significantly higher for BFL (1.3 ± 0.1) than for SAR (1.2 ± 0.1; $p < 0.001$), IPF (1.2 ± 0.1; $p < 0.001$), or SIL patients (1.1 ± 0.04; $p < 0.001$). Also, this index was considerably lower in the silicosis than those in the IPF ($p < 0.001$) and SAR patients ($p < 0.01$). The angiogenesis index for the PBS control group was significantly lower than in the other examined groups (0.9 ± 0.1; $p < 0.001$).

27.3.3 ACE – Angiogenesis Correlation

A negative correlation between the number of newly formed blood vessels and ACE serum activity was demonstrated for all examined ILD groups ($r = -0.42$; $p < 0.01$). The strongest correlation was observed in the sarcoidosis group ($r = -0.47$; $p < 0.01$). Similarly, a negative correlation between AI and ACE activity was also shown for all ILD patients ($r = -0.52$, $p < 0.01$) (Fig. 27.3), with the strongest correlations observed in the sarcoidosis ($r = -0.60$; $p < 0.001$) and silicosis patients ($r = -0.90$, $p < 0.001$).

27.4 Discussion

The present study demonstrates increased angiogenic activity of sera from ILD patients. We have previously demonstrated a significant correlation between the angiogenic activity of ILD patients' sera and the concentration of the serum tumor necrosis factor α (TNFα), although not with interleukin-6 (IL-6), IL-8, IL-12, or interferon γ (INFγ) (Zielonka et al. 2007a, b). An important role of angiogenesis in the ILD pathogenesis has been suggested (Tzouvelekis et al. 2006). However, the exact mechanisms have not yet been proposed. These results confirm that angiogenesis takes part not only in IPF or sarcoidosis but also in other ILD such as BLF and silicosis. Inflammatory and fibrotic

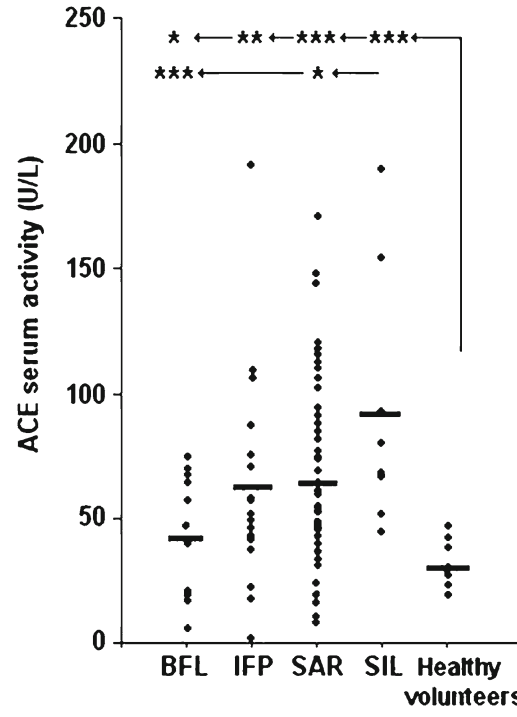

Fig. 27.1 ACE serum activity in patients with interstitial lung diseases and healthy volunteers. Mean values are indicated by *horizontal bars*, significant differences between groups are indicated by *arrows*; *p<0.05, **p<0.01, ***p<0.001

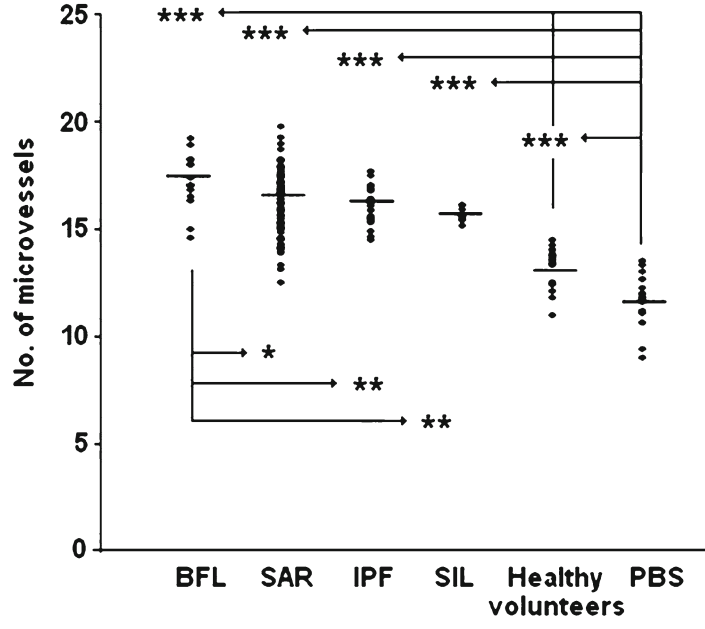

Fig. 27.2 Number of microvessels after injection of MNC preincubated with sera from ILD patients, healthy donors, and PBS. Mean values are indicated by *horizontal bars*, significant differences between groups are indicated by *arrows*

processes contribute to the pathogenesis of silicosis and the mechanism of mineral-induced pulmonary fibrosis appears to be similar to that involved in IPF or in a bleomycin model of fibrosis (Mossman and Churg 1998).

Our study gives a new insight into these processes. A negative correlation between the serum angiogenic and ACE activities demonstrated in all examined groups of ILD patients might suggest a new link between chronic inflammation, granuloma tissue, and neovascularization. Physiologically,

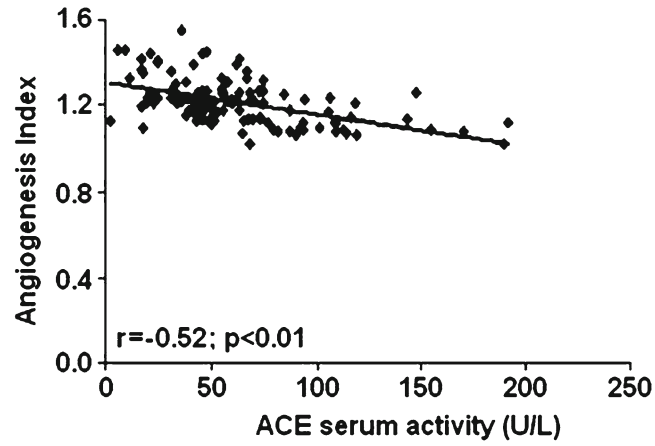

Fig. 27.3 Correlation between ACE serum level and angiogenesis index in ILD patients

ACE is a key enzyme in the renin-angiotensin system, converting angiotensin I into the potent vasopressor angiotensin II and also inactivating the vasodilator bradykinin (Hooper 1991). ACE produced by epithelioid cells is likely to be important both in mediating and modulating inflammation, primarily in granulomatous diseases (Gilbert et al. 1993). While ACE is involved in the pathogenesis of sarcoidosis, its serum level is also increased not only in pulmonary granulomatous diseases like tuberculosis, berylliosis (Brice et al. 1995), silicosis and asbestosis (Grönhagen-Riska et al. 1978), but also in extrathoracic granulomatous pathologies such as Gauchers' disease (Lieberman and Beutler 1976), leprosies and fungal infections (Lieberman and Rea 1977). Our data suggest its increased serum concentration in silicosis and IPF patients as well. In IPF studies, serum ACE has been generally shown within normal limits (Lieberman 1975). However, we believe that our IPF group consisting of patients with active progressing and untreated disease might only demonstrate a unique profile of ongoing inflammation. Hence, there is an increased ACE concentration in serum.

ACE is a critical physiologic regulator of blood pressure, inflammation, angiogenesis and is also a novel marker for identifying hemangioblasts differentiating from human embryonic stem cells (Zambidis et al. 2008). The participation of the renin-angiotensin system in neovascularization is important because ACE inhibitors are currently used for the treatment of hypertension and congestive heart failure. A negative correlation between serum ACE activity and angiogenic activity suggests that ACE inhibitors can stimulate neovascularization. Perhaps, a favorable effect of ACE inhibitors in cardiovascular diseases is related to the stimulation of neovascularization. The activation of vasculogenesis after antihypertensive drugs therapy such as the angiotensin-converting enzyme inhibitor (perindopril), and angiotensin type 1 receptor blocker (losartan) may participate in the reduction of major macro- and microvascular events observed in patients with stroke or type 2 diabetes (Patel et al. 2007).

Angiotensin II has multiple physiological effects. It has systemic (endocrine) and local (paracrine and autocrine) effects, favoring cell growth and differentiation through four types of receptors, of which types 1 and 2 (AT1 & AT2) are the most important (Escobar et al. 2004). Stimulation of AT1 leads to the activation of intracellular pathways that finally lead to vasoconstriction, inflammation and proliferation. The AT2 receptor effects are opposite to those of the AT1 effects. Endothelium plays a central role in the maintenance of vascular homeostasis and angiotensin II is one of the main effectors of endothelial dysfunction. ACE-2 has been identified as a critical negative modulator of angiotensin II bioactivity. However, the role of ACE-2 in vasculature remains unknown (Lovren et al. 2008). ACE-2 promoted capillary formation and neovessel maturation *in vivo* and reduced atherosclerosis in apolipoprotein E-knockout mice (Raizada and Ferreira 2007). Despite some similarities, ACE-2 is distinct from ACE.

Bradykinin induces dose-dependent endothelial sprout formation *in vitro* in the adult mouse heart only under hypoxia. The B2 receptor mediated sprouting that was induced by bradykinin and VEGF164, but did not mediate sprouting that was induced by the growth factor bFGF or PDGF-BB

(Sanchez de Miguel et al. 2008). Enalapril induces sprouting through both the B1 and B2 kinin receptors (Sanchez de Miguel et al. 2008). Both B2-receptor and B1-receptor agonist-induced angiogenesis requires nitric oxide biosynthesis (Sanchez de Miguel et al. 2008). This is of special interest since pharmacological inhibition of the ACE acts not only by reducing angiotensin II levels, but also by preventing enzymatic breakdown of kinins, suggesting that the kallikrein-kinin system is part of the ACE inhibition effects. The kallikrein-kinin system increases coronary blood flow, decreases infarct size and left ventricular remodelling post myocardial infarction (Westermann et al. 2008). ACE functions not only to convert angiotensin I to angiotensin II, but also to cleave bradykinin into inactive fragments. VEGF concentration is lower and ACE activity was significantly higher in the sera of patients with type 1 diabetes than in the sera of those with type 2 diabetes (Skopiński et al. 2001). Recently, Kozak et al. (2009) demonstrated that candesartan in an experimental model of stroke augments the ischemia-induced angiogenic state and provides long-term benefits. ACE inhibitors enhance myocardial capillarization (Hiller et al. 2010).

Conversely, it has been shown that ACE inhibitors may protect against cancer development (Lever et al. 1998). There is increasing evidence that angiotensin II and its receptor system are involved in angiogenesis, tumor growth and metastases in experimental models, suggesting the therapeutic potential of ACE inhibitors and AT1R blockers, used as antihypertensive drugs (Yoshiji et al. 2004). Recent studies have shown the activation of the local renin-angiotensin system in various tumor tissues, including the abundant generation of angiotensin II by ACE and the upregulation of type 1 angiotensin II receptor expression (Ino et al. 2006). It is hypothesized that angiotensin II may be involved in the regulation of tumor angiogenesis especially in receptor negative breast cancer by the regulation of angiogenesis associated genes *via* angiotensin II receptor type 1 (Herr et al. 2008). Perindopril inhibits VEGF-induced tumor growth (Yoshiji et al. 2002b). However, the inhibition of angiogenesis by captopril is not mediated by ACE inhibition, but by suppression of matrix metalloproteinase activity or production of angiostatin attributable to free thiol groups, which perindopril does not have (Gately et al. 1997). Sano et al. (2006) demonstrated that ACE expression in endothelial cells is negatively or positively regulated by Ang1 or VEGF, respectively, and the VEGF-mediated hyperpermeability is suppressed by angiotensin II type 1 receptor blocker. The dual effect of ACE inhibition on angiogenesis in type 1 diabetic mice was described by Ebrahimian et al. (2005). ACE inhibition improved neovascularization in the diabetic ischemic leg through activation of bradykinin signaling, whereas it reduced vessel growth in the diabetic retina through inhibition of an overactive angiotensin II pathway.

However, in ILDs the rationale for any therapeutic ACE-I application is quite vague at the moment. The exact contribution of neovascularization processes to ILDs development and progression is still unclear. Data concerning new vessels formation are not satisfactory, hence the outcome of pharmacological inhibition or stimulation of angiogenesis would be rather difficult to predict. We also do not know whether angiogenesis is helpful or detrimental for ILDs. The only well documented data come from the experimental thalidomide application (Carlesimo et al. 1995). Still, although shown clinically effective, this form of anti-angiogenic treatment was introduced only in patients resistant to other forms of anti-inflammatory therapy (Antoniou et al. 2007). We do not know yet whether there are too many or too few new vessels formed in pulmonary fibrosis and others ILDs. Further studies on the angiogenesis and its relationships to ACE and its inhibitors in ILD are needed.

Conflicts of interest: The authors declare no conflicts of interest in relation to this article.

References

Antoniou, K. M., Pataka, A., Bouros, D., & Siafakas, N. M. (2007). Pathogenetic pathways and novel pharmacotherapeutic targets in idiopathic pulmonary fibrosis. *Pulmonary Pharmacology & Therapeutics, 20*, 453–461.

ATS. (2000). Idiopathic pulmonary fibrosis: Diagnosis and treatment. International consensus statement. *American Journal of Respiratory and Critical Care Medicine, 16*, 646–664.

ATS/ERS/WASOG. (1999). Statement on sarcoidosis. *American Journal of Respiratory and Critical Care Medicine, 160*, 736–755.

Brice, E. A., Friedlander, W., Bateman, E. D., & Kirsch, R. E. (1995). Serum angiotensin-converting enzyme activity, concentration, and specific activity granulomatous disease, tuberculosis and COPD. *Chest, 107*, 706–710.

Carlesimo, M., Giustini, S., Rossi, A., Bonaccorsi, P., & Calvieri, S. (1995). Treatment of cutaneous and pulmonary sarcoidosis with thalidomide. *Journal of the American Academy of Dermatology, 32*, 866–869.

Ebrahimian, T. G., Tamarat, R., Diurez, C., Duriez, M., Levy, B. I., & Silvestre, J. S. (2005). Dual effect of angiotensin-converting enzyme inhibition on angiogenesis in type 1 diabetic mice. *Arteriosclerosis, Thrombosis, and Vascular Biology, 25*, 65–70.

Escobar, E., Rodríguez-Reyna, T. S., Arrieta, O., & Sotelo, J. (2004). Angiotensin II, cell proliferation and angiogenesis regulator: Biologic and therapeutic implications in cancer. *Current Vascular Pharmacology, 2*, 385–399.

Fujiyama, S., Matsubara, H., Nozawa, Y., Maruyama, K., Mori, Y., Tsutsumi, Y., Masaki, H., Uchiyama, Y., Koyama, Y., Nose, A., Iba, O., Tateishi, E., Ogata, N., Jyo, N., Higashiyama, S., & Iwasaka, T. (2001). Angiotensin AT(1) and AT(2) receptors differentially regulate angiopoietin-2 and vascular endothelial growth factor expression and angiogenesis by modulating heparin binding-epidermal growth factor (EGF)-mediated EGF receptor transactivation. *Circulation Research, 88*, 22–29.

Gately, S., Twardowski, P., Stack, M. S., Cundiff, D. L., Grella, D., Castellino, F. J., Enghild, J., Kwaan, H. C., Lee, F., Kramer, R. A., Volpert, O., Bouck, N., & Soff, G. A. (1997). The mechanism of cancer-mediated conversion of plasminogen to the angiogenesis inhibitor angiostatin. *Proceedings of the National Academy of Sciences of the United States of America, 94*, 10868–10872.

Gilbert, S., Steinbrech, D. S., Landas, S. K., & Hunninghake, G. W. (1993). Amounts of angiotensin-converting enzyme mRNA reflect the burden of granulomas in granulomatous lung disease. *American Review of Respiratory Disease, 148*(2), 483–486.

Gronhagen-Riska, C., Kurppa, K., Fyhrquist, F., & Selroos, O. (1978). Angiotensin-converting enzyme and lysozyme in silicosis and asbestosis. *Scandinavian Journal of Respiratory Diseases, 59*, 228–231.

Herr, D., Rodewald, M., Fraser, H. M., Hack, G., Konrad, R., Kreienberg, R., & Wulff, C. (2008). Potential role of renin-angiotensin-system for tumor angiogenesis in receptor negative breast cancer. *Gynecologic Oncology, 109*, 418–425.

Hiller, K. H., Ruile, P., Kraus, G., Bauer, W. R., & Waller, C. (2010). Tissue ACE inhibition improves microcirculation in remote myocardium after coronary stenosis: MR imaging study in rats. *Microvascular Research, 80*, 484–490.

Hooper, N. (1991). Angiotensin converting enzyme: Implications from molecular biology for its physiological functions. *The International Journal of Biochemistry, 23*, 641–647.

Ino, K., Shibata, K., Kajiyama, H., Nawa, A., Nomura, S., & Kikkawa, F. (2006). Manipulating the angiotensin system-new approaches to the treatment of solid tumors. *Expert Opinion on Biological Therapy, 6*, 243–255.

Keane, M. P. (2004). Angiogenesis and pulmonary fibrosis: Feast or famine? *American Journal of Respiratory and Critical Care Medicine, 170*, 207–209.

Kozak, A., Ergul, A., El-Remessy, A. B., Johnson, M. H., Machado, L. S., Elewa, H. F., Abdelsaid, M., Wiley, D. C., & Fagan, S. C. (2009). Candesartan augments ischemia-induced proangiogenic state and results in sustained improvement after stroke. *Stroke, 40*, 1870–1876.

Lacasse, Y., Selman, M., Costabel, U., Dalphin, J. C., Ando, M., Morell, F., Erkinjuntti-Pekkanen, R., Muller, N., Colby, T. V., Schuyler, M., Cormier, Y., & HP Study Group. (2003). Clinical diagnosis of hypersensitivity pneumonitis. *American Journal of Respiratory and Critical Care Medicine, 168*, 952–958.

Lever, A. F., Hole, D. J., Gillis, C. R., McCallum, I. R., McInnes, G. T., MacKinnon, P. L., Meredith, P. A., Murray, L. S., Reid, J. L., & Robertson, J. W. (1998). Do inhibitors of angiotensin-I-converting enzyme protect against risk of cancer? *The Lancet, 352*, 179–184.

Lieberman, J. (1975). Elevation of serum angiotensin converting enzyme (ACE) level in sarcoidosis. *The American Journal of Medicine, 59*, 365–372.

Lieberman, J., & Beutler, E. (1976). Elevation of serum angiotensin-converting enzyme in Gaucher's disease. *The New England Journal of Medicine, 294*, 1442–1444.

Lieberman, J., & Rea, T. H. (1977). Serum angiotensin-converting enzyme in leprosy and coccidioidomycosis. *Annals of Internal Medicine, 87*, 423–425.

Lovren, F., Pan, Y., Quan, A., Teoh, H., Wang, G., Shukla, P. C., Levitt, K. S., Oudit, G. Y., Al-Omran, M., Stewart, D. J., Slutsky, A. S., Peterson, M. D., Backx, P. H., Penninger, J. M., & Verma, S. (2008). Angiotensin converting enzyme-2 confers endothelial protection and attenuates atherosclerosis. *American Journal of Physiology. Heart and Circulatory Physiology, 295*, H1377–H1384.

Mossman, B. T., & Churg, A. (1998). Mechanisms in the pathogenesis of asbestosis and silicosis. *American Journal of Respiratory and Critical Care Medicine, 157*, 1666–1680.

Patel, A., MacMahon, S., Chalmers, J., Neal, B., Woodward, M., Billot, L., Harrap, S., Poulter, N., Marre, M., Cooper, M., Glasziou, P., Grobbee, D. E., Hamet, P., Heller, S., Liu, L. S., Mancia, G., Mogensen, C. E., Pan, C. Y., Rodgers, A., & Williams, B. (2007). Effects of a fixed combination of perindopril and indapamide on macrovascular and

microvascular outcomes in patients with type 2 diabetes mellitus (the ADVANCE trial): A randomised controlled trial. *The Lancet, 370*, 829–840.

Raizada, M. K., & Ferreira, A. J. (2007). ACE2: A new target for cardiovascular disease therapeutics. *Journal of Cardiovascular Pharmacology, 50*, 112–119.

Saaristo, A., Karpanen, T., & Alitalo, K. (2000). Mechanisms of angiogenesis and their use in the inhibition of tumor growth and metastasis. *Oncogene, 19*, 6122–6129.

Sanchez de Miguel, L., Neysari, S., Jakob, S., Petrimpol, M., Butz, N., Banfi, A., Zaugg, C. E., Humar, R., & Battegay, E. J. (2008). B2-kinin receptor plays a key role in B1-, angiotensin converting enzyme inhibitor-, and vascular endothelial growth factor-stimulated in vitro angiogenesis in the hypoxic mouse heart. *Cardiovascular Research, 80*, 106–113.

Sano, H., Hosokawa, K., Kidoya, H., & Takakura, N. (2006). Negative regulation of VEGF-induced vascular leakage by blockade of angiotensin II type 1 receptor. *Arteriosclerosis, Thrombosis, and Vascular Biology, 26*, 2673–2680.

Shibuya, M. (2001). Structure and function of VEGF/VEGF-receptor system involved in angiogenesis. *Cell Structure and Function, 26*, 25–35.

Sidky, Y. A., & Auerbach, R. (1975). Lymphocyte-induced angiogenesis: A quantitative and sensitive assay for the graft-versus-host reaction. *The Journal of Experimental Medicine, 141*, 1084–1100.

Skopiński, P., Sommer, E., Borowska, A., Hevelke, A., Rogala, E., & Skopińska-Rozewska, E. (2001). Angiotensin-converting enzyme activity and angiomodulatory effects of sera in patients with diabetic retinopathy. *International Journal of Clinical Pharmacology Research, 21*, 73–78.

Tzouvelekis, A., Anevlavis, S., & Bouros, D. (2006). Angiogenesis in interstitial lung diseases: A pathogenetic hallmark or a bystander? *Respiratory Research, 25*(7), 82.

Wagner, E. J., Sanchez, J., McClintock, J. Y., Jenkins, J., & Moldobaeva, A. (2008). Inflammation and ischemia-induced lung angiogenesis. *American Journal of Physiology. Lung Cellular and Molecular Physiology, 294*, L351–L357.

Westermann, D., Schultheiss, H. P., & Tschope, C. (2008). New perspective on the tissue kallikrein-kinin system in myocardial infarction: Role of angiogenesis and cardiac regeneration. *International Immunopharmacology, 8*, 148–154.

Williams, B., Baker, A. Q., Gallacher, B., & Lodwick, D. (1995). Angiotensin II increases vascular permeability factor gene expression by human vascular smooth muscle cells. *Hypertension, 25*, 913–917.

Yoshiji, H., Kuriyama, S., & Fukui, H. (2002a). Angiotensin-I-converting enzyme inhibitors may be an alternative anti-angiogenic strategy in the treatment of liver fibrosis and hepatocellular carcinoma. Possible role of vascular endothelial growth factor. *Tumour Biology, 23*, 348–356.

Yoshiji, H., Kuriyama, S., & Fukui, H. (2002b). Perindopril: Possible use in cancer therapy. *Anti-Cancer Drugs, 13*, 221–228.

Yoshiji, H., Kuriyama, S., Noguchi, R., & Fukui, H. (2004). Angiotensin-I converting enzyme inhibitors as potential anti-angiogenic agents for cancer therapy. *Current Cancer Drug Targets, 4*, 555–567.

Zambidis, E. T., Park, T. S., Yu, W., Tam, A., Levine, M., Yuan, X., Pryzhkova, M., & Péault, B. (2008). Expression of angiotensin-converting enzyme (CD143) identifies and regulates primitive hemangioblasts derived from human pluripotent stem cells. *Blood, 112*, 3601–3614.

Zielonka, T. M., Demkow, U., Filewska, M., Białas, B., Korczynski, P., Szopinski, J., Soszka, A., & Skopinska-Rozewska, E. (2007a). Angiogenic activity of sera from interstitial lung diseases patients in relation to IL-6, IL-8, IL-12 and TNFα serum level. *Central European Journal of Immunology, 32*, 53–60.

Zielonka, T. M., Demkow, U., Filewska, M., Golian-Geremek, A., Filewska, M., Zycinska, K., Bialas, B., Wardyn, K., & Skopinska-Rozewska, E. (2007b). TNFα and INFγ inducing capacity of sera from interstitial lung diseases patients in relation to its angiogenesis activity. *Journal of Physiology and Pharmacology, 58*(Suppl. 5), 767–780.

Zielonka, T. M., Demkow, U., Filewska, M., Radzikowska, E., Bialas, B., Filewska, M., Zycinska, K., Obrowski, M. H., Kowalski, J., Wardyn, K., & Skopinska-Rozewska, E. (2010). Angiogenic activity of sera from interstitial lung disease patients in relation to pulmonary function. *European Journal of Medical Research, 15*(Suppl. 2), 229–234.

Chapter 28
Development and Aging Are Oxygen-Dependent and Correlate with VEGF and NOS along Life Span

S. Zara, M. Pokorski, A. Cataldi, A. Porzionato, R. De Caro, J. Antosiewicz, and C. Di Giulio

Abstract During development and aging, vascular remodeling represents a critical adaptive response to modifications in oxygen supply to tissues. Hypoxia inducible factor (HIF) has a crucial role and is modulated by oxygen levels, with an age-dependent response in neonates, adult, and aged people. ROS are generated under hypoxic conditions and the accumulation of free radicals during life reduces the ability of tissues to their removal. In this immunohistochemical study we investigated the presence and localization of VEGF and iNOS in human carotid bodies (CB) sampled at autopsy from three children (mean age – 2 years), four adult young subjects (mean age – 44.3 years), and four old subjects (mean age – 67.3 years). VEGF immunoreactivity was significantly enhanced in CB tissues from the children (7.2 ± 1.2%) and aged subjects (4.7 ± 1.7%) compared with the young adults (1.4 ± 0.7%). On the other hand, iNOS immunoreactivity was enhanced in CB tissues from the children (0.4 ± 0.04%) and young adult subjects (0.3 ± 0.02%) compared with the old subjects (0.2 ± 0.02%). Prevention of oxygen desaturation, reducing all causes of hypoxemia from neonatal life to aging would decrease the incidence of diseases in the elderly population with lifespan extension.

Keywords Aging • Carotid body • Chemoreceptor • Hypoxia • Nitric oxide • VEGF

S. Zara
Department of Drug Sciences, University of Chieti, Via dei Vestini 31, 66100 Chieti, Italy

M. Pokorski
Department of Respiratory Research, Medical Research Center, Polish Academy of Sciences, Pawinskiego 5 St, 02-106 Warsaw, Poland

Department of Neuropsychology, Institute of Psychology, Opole University, Plac Staszica 1, 45-052 Opole, Poland

A. Cataldi
Department of Medicine and Ageing Sciences, University of Chieti, Via dei Vestini 31, 66100 Chieti, Italy

A. Porzionato • R. De Caro
Section of Anatomy, Department of Human Anatomy and Physiology, University of Padua, Poland

J. Antosiewicz
Department of Respiratory Research, Medical Research Center, Polish Academy of Sciences, Pawinskiego 5 St, 02-106 Warsaw, Poland

C. Di Giulio (✉)
Department of Neurosciences and Imaging, University of Chieti, Via dei Vestini 31, 66100 Chieti, Italy
e-mail: digiulio@unich.it

M. Pokorski (ed.), *Respiratory Regulation - The Molecular Approach*,
Advances in Experimental Medicine and Biology 756, DOI 10.1007/978-94-007-4549-0_28,

28.1 Introduction

Development and aging are strictly correlated as a result of cumulative oxidative damages to cells, derived from aerobic metabolism and influenced by environmental and genetic factors (Amicarelli et al. 1999; Babcock et al. 1992). Environmental factors include temperature, diet, exercise, and oxygen availability. To test if oxygen sensitive mechanisms related to NOS and VEGF are affected by age, we studied immunohistochemistry and structural correlates of carotid bodies collected from cadavers of infants, young adults, and aged subjects. We evaluated vascular endothelial growth factor (VEGF) and nitric oxide synthase (NOS) expression. The proteins are influential for angiogenesis and vasodilatation, respectively. NOS is known to catalyse the reaction of L-arginine into L-citrulline. NO behaves as a biological messenger molecule implicated in many physiological functions involving homeostatic adaptations and oxygen supply to tissues (Richmonds et al. 1999). Normally, acute hypoxia inhibits enzymatic activity, while in chronic hypoxia most enzymes, such as tyrosine hydroxylase or NOS, are stimulated, which represents a homeostatic defence mechanism (Di Giulio et al. 2000).

To test if oxygen sensitive CB mechanisms are affected in an age-dependent fashion, we studied the expression of VEGF and NOS, the two essential enzymes for tissue aging modulation, along the life axis in human CB.

28.2 Methods

The study was approved by a local Ethics Committee and was performed according to the Italian laws on autopsied human tissues (Porzionato et al. 2005).

The present immunohistochemical study investigates the expression and localization of VEGF and iNOS in human carotid bodies, sampled at autopsy from three children (mean age: 2 years ±66SD days), four young (mean age: 27.5 ± 3.4 years), and four old subjects (mean age: 73.5 ± 3.4 years). All subjects died of an accident's trauma and were all clinically without chronic pulmonary or cardiovascular diseases. Autopsies were performed between 18 and 78 h after death. Specimens were taken of the right carotid bifurcation, including 20 mm of the common carotid and 20 mm of the internal and external carotid arteries.

28.2.1 Light Microscopy Analysis and Immunohistochemistry

Tissues were fixed in 10% phosphate-buffered formalin for 72 h, dehydrated through ascending series of alcohols and xylene, and then paraffin embedded. Samples were de-waxed (xylene and alcohol in progressively lower concentrations) and 5 μm thick specimens were processed for Trichrome Mallory staining (Tricromica kit) (Bio Optica, Milano, Italy) to distinguish connective compartment from parenchyma.

In order to detect VEGF and iNOS proteins, immunohistochemistry was performed by means of Ultravision LP Detection System HRP Polymer & DAB Plus Chromogen (Lab Vision Thermo, CA, USA). Slides have been incubated in the presence of primary rabbit anti-VEGF and anti-iNOS antibodies (dilution 1:100) (Santa Cruz Biotechnology, CA, USA) and then in the presence of specific HRP-conjugated secondary antibodies. Peroxidase was developed using diaminobenzidine chromogen (DAB) and nuclei were hematoxylin counterstained. Negative controls were performed by omitting the primary antibody. Specimens were examined under light microscopy Leica DM 4000 equipped with a Leica DFC 320 camera (Leica Cambridge Ltd, Cambridge, UK) for computerized images.

28.2.2 Computerized Morphometry Measurements and Image Analysis

After digitalizing the images obtained from immunohistochemically stained sections, QWin Plus 3.5 software (Leica Cambridge Ltd, Cambridge, UK) was used to evaluate the VEGF and iNOS expressions. Image analysis of protein expression was performed through the quantification of the threshold area for immunohistochemical brown color per ten fields of light microscope observation. QWin Plus 3.5 assessments were logged into Microsoft Excel and processed for standard deviations and histograms. Differences between enzyme expressions in the age-groups studied were evaluated using a *t*-test and a linear regression analysis. $p < 0.05$ was taken as indicative of statistically significant difference.

28.3 Results

VEGF positive areas were significantly enhanced in carotid body specimens from the children ($7.2 \pm 1.2\%$) and aged subjects ($4.7 \pm 1.7\%$) compared with the young adults ($1.4 \pm 0.7\%$) (Fig. 28.1). On the other hand, iNOS expression was revealed higher in carotid body specimens from the children

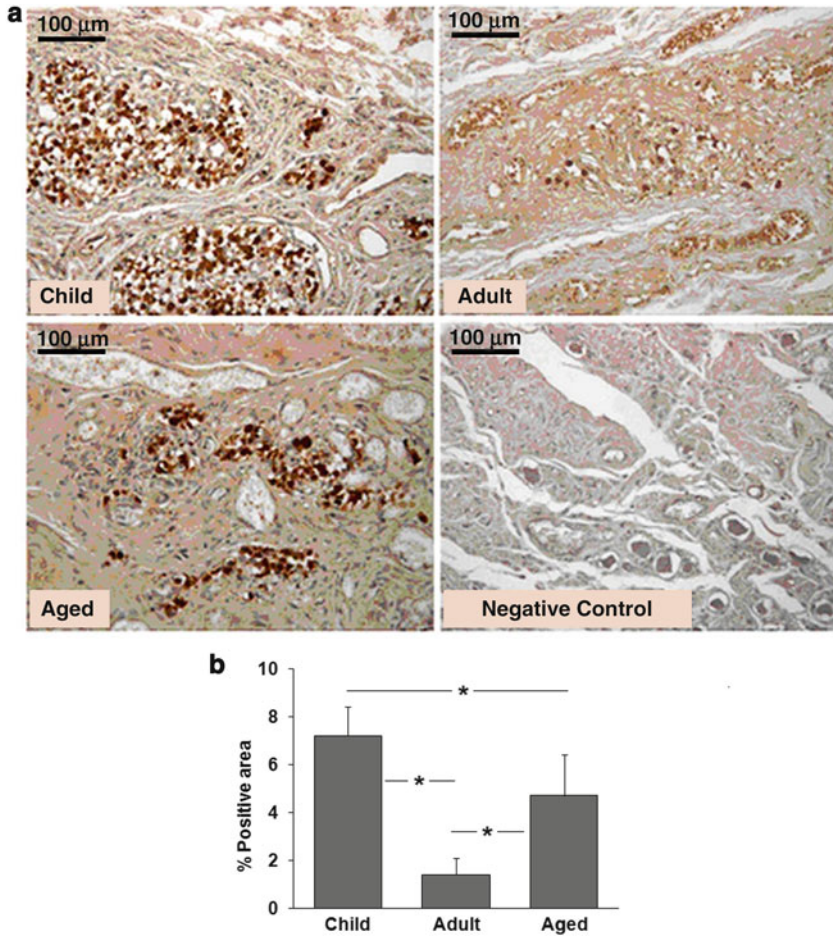

Fig. 28.1 (a) Immunohistochemical detection of VEGF expression in carotid bodies from child, adult, and aged subjects; **(b)** graphic representation of VEGF % positive area (means ± SD). Densitometric analysis was determined by direct visual counting of ten fields (mean values) for each of three slides per sample, magnification 40x. *Significant differences in VEGF between each of the three pairs of age-groups, all $p < 0.05$

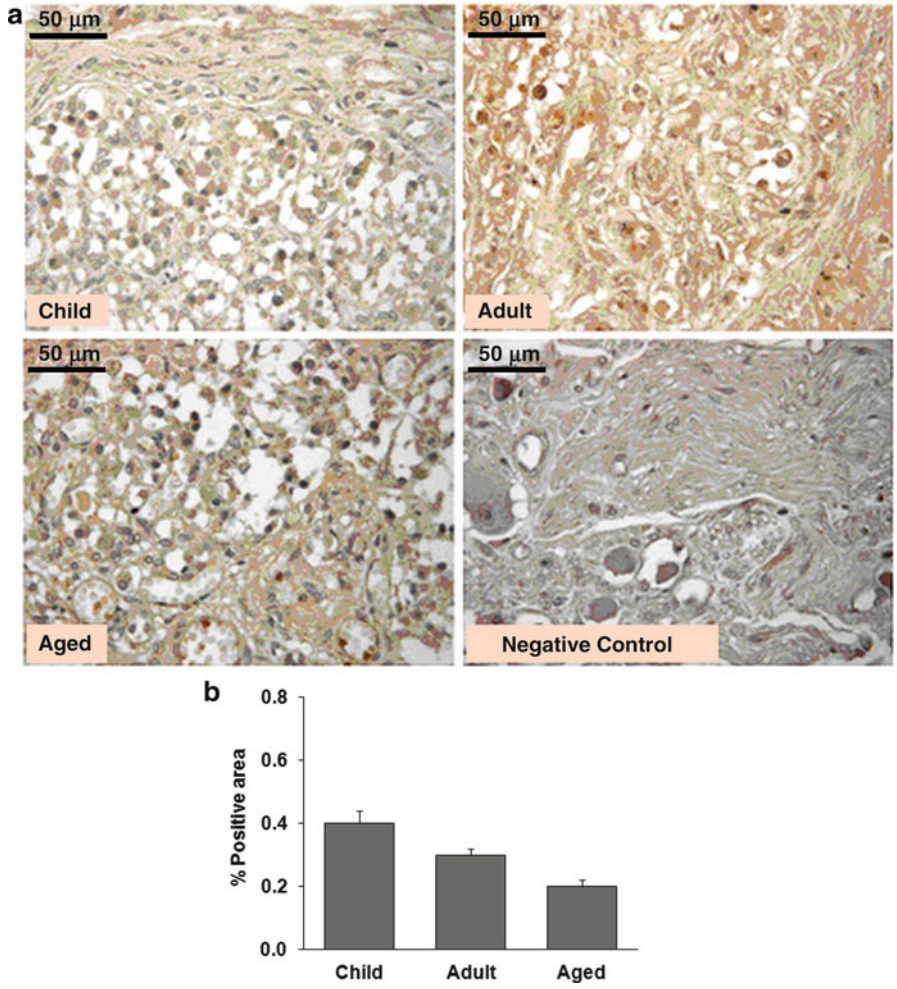

Fig. 28.2 **(a) Immunohistochemical detection of iNOS expression in carotid bodies** from child, adult, and aged subjects; **(b)** graphic representation of iNOS % positive area (means ± SD). Densitometric analysis was determined by direct visual counting of ten fields (mean values) for each of three slides per sample; magnification 40×. No significant differences among the age-groups were noted

and young adults (0.4 ± 0.04 and 0.3 ± 0.02%, respectively) compared with the 0.2 ± 0.02% in the aged subjects; but the differences here did not reach statistical significance (Fig. 28.2). Along with the evaluation of VEGF and iNOS expression, Mallory Trichrome staining was performed to estimate the proportions of CB parenchyma and interstitial tissue. We found a significant decrease in CB parenchymal area from child to old subject and a significant increase in intralobular connective tissue in the aged subjects compared with that in childhood (Fig. 28.3).

28.4 Discussion

The carotid body is an important organ for body homeostasis. Acute hypoxia increases chemosensory discharge, which is less evident during aging as well as during long-lasting hypoxia in the young (Lahiri et al. 2002). During development and aging, vascular remodeling represents a critical adaptive

a

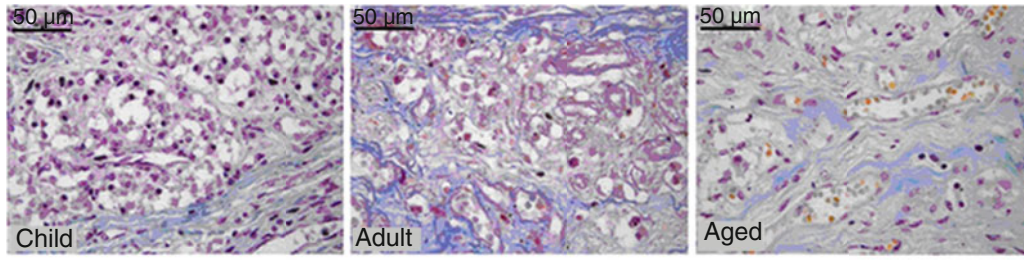

b

	Parenchyma area (%)	Interlobular connective tissue area (%)	Interlobular connective tissue area (%)
Child	84.8 ±7.2	75.9 ±6.3	69.8 ±0.5
Adult	12.0 ±0.9	15.5 ±1.5	14.8 ±1.2
Aged	3.2 ±0.4*	8.7 ±0.8	11.3 ±1.0**

Fig. 28.3 (a) Morphometric analysis of human carotid bodies from child, adult and, aged subjects performed on Trichrome Mallory stained slides. **(b)** Parenchyma, connective interlobular and intralobular compartment measurements expressed as % area (means ± SD), assessed by direct visual counting of ten fields for each of the three slides per five samples each.*Aged *vs.* child parenchyma % area, $p<0.05$; **Aged *vs.* child intralobular connective tissue % area, $p<0.05$

response to tissue hypoxia. Hypoxia inducible factor-1 (HIF-1α) is the regulator of oxygen homeostasis in tissues (Semenza 2009). It is a heterodimeric transcription factor that controls the induction of several genes involved in glycolysis, erythropoiesis, angiogenesis and vasodilatation when tissues are exposed to hypoxic conditions. Expression of VEGF and NOS in CB depends on age and hypoxia exposure (Di Giulio et al. 2005). When we say 'chronic hypoxia', we have to specify if we consider an intermittent situation, minutes, hours, days, weeks, or months of hypoxic exposure.

VEGF and NOS could be responsible for a reduction in the ventilatory response during chronic hypoxia and aging (Di Giulio et al. 2005). A lower expression of NOS during aging could explain a reduced CB hyperplastic effect due to hypoxia and decreased oxygen sensitive mechanisms. It is possible that oxygen keeps these factors in physiological ranges. Intermittent hypoxia can modulate the devolvement processes and accelerate aging, with HIF-1α likely playing a role during aging. In CB, HIF-1α is accumulated more at high altitude or during sleep disordered breathing characterized by intermittent hypoxia, which is mediated by increased generation of ROS. HIF-1α would be involved with NOS and VEGF in the developmental and aging processes. In aerobic organisms, more than 90% of the oxygen supply is used by cell mitochondria. Cells have developed a variety of enzymatic and non-enzymatic systems to convert ROS in less toxic species (Finkel and Holbrook 2000). Physiologically, antioxidant defences maintain ROS at harmless levels, preventing damage (Jamieson 1989). ROS are produced even at low oxygen levels, and the balance between different levels of oxygen supply and the metabolic demand leads to ROS formation. This balance is strictly correlated with a constant 'oxygen concentration'. ROS are alarm signals which could act on the gene expression factors during development and aging (Harman 1992). Mitochondrial activity for NOS expression might not be so important, but the interaction among tissue pH-CO_2 and O_2 could affect cell activity and oxygen consumption.

Although the chromophore theory of chemoreception still remains valid, alterations in the sensor structure mechanism could be affected by VEGF and NOS-1 which are important during development and aging. CB remains a model to study the development and aging processes and it could be a tool to clarify the modulation of cell metabolism and how preventing hypoxia we interfere with the aging

process. In other words, development and aging are physiologically correlated with the oxygen supply and metabolism, but how physical exercise or prevention of hypoxia would modulate the aging processes still remains an open question.

Acknowledgments JA supported by grant NN401153938 from the Polish Ministry of Science and Higher Education.

Conflicts of interest: The authors declare no conflicts of interest in relation to this article.

References

Amicarelli, F., Ragnelli, A. M., Aimola, P., Bonfigli, A., Colafarina, S., Di Ilio, C., & Miranda, M. (1999). Age-dependent ultrastructural alterations and biochemical response of rat skeletal muscle after hypoxic or hyperoxic treatments. *Biochimica et Biophysica Acta, 1453*, 105–114.

Babcock, M. A., Paterson, D. H., & Cunningham, D. A. (1992). Influence of ageing on aerobic parameters determined from a ramp test. *European Journal of Applied Physiology and Occupational Physiology, 65*, 138–143.

Di Giulio, C., Grilli, A., Ciocca, I., Macrì, M. A., Daniele, F., Sabatino, G., Cacchio, M., Da Porto, R., Di Natale, F., & Felaco, M. (2000). Carotid body NO-CO interaction and chronic hypoxia. *Advances in Experimental Medicine and Biology, 475*, 685–690.

Di Giulio, C., Cacchio, M., Bianchi, G., Rapino, C., & Di Ilio, C. (2005). Oxygen and life span: Chronic hypoxia and hyperoxia as models for studying VEGF, NOS and HIF during ageing. *Respiratory Physiology & Neurobiology, 147*, 31–38.

Finkel, T., & Holbrook, N. J. (2000). Oxidants, oxidative stress and the biology of ageing. *Nature, 408*, 239–247.

Harman, D. (1992). Free radical theory of aging: History. *Free Radical and Aging, 62*, 1–10.

Jamieson, D. (1989). Oxygen toxicity and reactive oxygen metabolites in mammals. *Free Radical Biology & Medicine, 7*, 87–108.

Lahiri, S., Di Giulio, C., & Roy, A. (2002). Lessons from chronic intermittent and sustained hypoxia at high altitudes. *Respiratory Physiology & Neurobiology, 130*, 223–233.

Porzionato, A., Macchi, V., Guidolin, D., Parenti, A., Ferrara, S.D., & De Caro, R. (2005). Histopathology of carotid body in heroin addiction. Possible chemosensitive impairment. *Histopathology, 46*, 296–306.

Richmonds, C. R., Boonyapisit, K., Kusner, L. L., & Kaminski, H. J. (1999). Nitric oxide synthase in aging rat skeletal muscle. *Mechanisms of Ageing and Development, 109*, 177–189.

Semenza, G. L. (2009). Regulation of oxygen homeostasis by hypoxia-inducible factor 1. *Physiology, 24*, 97–106.

Chapter 29
Sarcoidosis and Tuberculosis: A Connection to the Human Leukocyte Antigen System

A. Dubaniewicz, A. Zimmermann, M. Smigielska, M. Dubaniewicz-Wybieralska, G. Moszkowska, J. Wysocka, K. Adamczyk-Bak, J.M. Slominski, and P. Deeg

Abstract Infectious, genetic factors, and autoimmunity have been considered as potential causes of sarcoidosis (SA). Pathological similarities between SA and tuberculosis (TB) suggest *M. tuberculosis* antigen(s) as causative agent(s). Our published comparative analysis of the human leukocyte antigens (HLA) system in patients with SA or TB in the same ethnic group revealed that some antigens were connected with high risk of developing of SA or TB, but other were comparable in both patient populations. Is it possible that the predominating occurrence of HLA antigens characteristic for TB may cause tuberculosis in patients with SA? To answer this question we evaluated the HLA class I and II alleles frequency by PCR amplification with sequence-specific primers in three women with histopathologically proven pulmonary SA, who developed bacteriologically confirmed TB on a corticosteroids (CS) therapy. Analysis of HLA in every case separately revealed a trend for higher occurrence of both alleles predisposing and protecting from TB than SA, in comparison with healthy individuals in our previously mentioned HLA genotyping study. Overall, the number of alleles predisposing to TB was statistically greater than the number of alleles connected with a high risk of developing SA. Also, the frequency of protecting alleles was statistically higher for TB than for SA. Therefore, SA in

A. Dubaniewicz (✉) • M. Smigielska • K. Adamczyk-Bak • J.M. Slominski
Department of Pneumology, Gdansk Medical University, Debinki 7 St., Gdansk, Poland
e-mail: aduban@gumed.edu.pl

A. Zimmermann
Department of Nursing Management, Medical University of Gdansk, Gdansk, Poland

M. Dubaniewicz-Wybieralska
Department of Radiology, Gdansk Medical University, Gdansk, Poland

G. Moszkowska
Department of Clinical Immunology and Transplantology,
Gdansk Medical University, Gdansk, Poland

J. Wysocka
Department of Forensic Medicine, Gdansk Medical University,
Gdansk, Poland

P. Deeg
Department of Pneumology, Gdansk Medical University, Debinki 7 St.,
Gdansk, Poland

Deegenbergklinik Bad Kissingen Academic Teaching Hospital of the Julius
Maximilians University in Würzburg, Bad Kissingen, Germany

M. Pokorski (ed.), *Respiratory Regulation - The Molecular Approach*,
Advances in Experimental Medicine and Biology 756, DOI 10.1007/978-94-007-4549-0_29,

these patients developed at first, and the presence of additional environmental factors, e.g., age, CS might decrease an immune response and provoked TB. There is a possibility that the occurrence of HLA antigen more associated with high risk of developing TB than SA causes the development of tuberculosis in our patients with sarcoidosis.

Keywords Sarcoidosis • Tuberculosis • Genetic factors • Autoimmunity • Human leukocyte antigens system • Ethnicity

29.1 Introduction

Sarcoidosis (SA) is a granulomatous disorder of an unknown etiology. Infectious and genetic factors and autoimmunity have been considered as potential causes of SA (American Thoracic Society 1999). Due to similar clinical, radiological and histopathological pictures of sarcoidosis and tuberculosis (TB), *Mycobacterium tuberculosis* or mycobacterial antigen(s), e.g., A60, A85, KatG, SodA and heat shock proteins (Mtb-hsp) have been considered as infectious factors in the etiopathogenesis of SA (reviewed in Dubaniewicz 2010; Moller 2007). Some of these antigens are markers of latent TB during the dormant stage of *M. tuberculosis* (Yim and Selvaraj 2010). One-third of the world's population is believed to be infected with *M. tuberculosis*, but bacilli will reactivate and cause active TB only in 5–10% of individuals (Walzl et al. 2011). The mycobacterial hsp proteins expressed on the surface of antigen presenting cells (APCs) can be presented effectively to T- and B- lymphocytes in the context the human leukocytes antigens (HLA) class I and II antigens to induce specific immunity in SA or TB. It is possible that in genetically predisposed host (HLA and non-HLA), the presence of mycobacterial infection (Mtb-hsp, especially hsp16) may be involved in the development of (auto) immunity in SA (reviewed in Dubaniewicz et al. 2003, 2006).

The results of published analysis of polymorphisms of HLA class I and II antigens in different ethnic groups of patients with SA or TB in the world are inconsistent (Dubaniewicz et al. 2003, 2006; Dubaniewicz and Dubaniewicz 2005; Sato et al. 2010; Yim and Selvaraj 2010). That indicates the occurrence of HLA antigens characteristic for sarcoidosis only, for tuberculosis only, with some HLA being characteristic of both SA and TB. Thus, susceptibility to sarcoidosis or tuberculosis might have its cause in specific haplotypes of SA or TB patients in the same ethnic group (Dubaniewicz et al. 2003, 2006). In some cases, TB may coexist with SA, or develop before or after sarcoidosis.

The question arises whether the predominating occurrence of HLA alleles characteristic of only TB may cause tuberculosis in patients with SA? To this end we evaluated the frequency of HLA class I and II alleles in three women with pulmonary SA, who developed TB while being on corticosteroids therapy.

29.2 Methods

This article is based on 3 case reports of female subjects who presented to the hospital with unproductive chronic cough and other symptoms suggesting the possibility of SA. All patients were non-smokers, with no reported occupational exposures. Their medical and family history was negative for tuberculosis, autoimmune or other chronic disorders. They had no knowledge about previous contact with TB infected individuals and all were in good general physical condition. The study was performed in accordance with the Declaration of Helsinki for Human Research and the protocol was approved by an institutional Research Review Committee.

Case 1 In 2002, a 32 year-old woman presented with cough, erythema nodosum on the thighs, fever, and swelling and pain of bilateral wrists and ankles. Chest X-ray (CXR) revealed bilateral hilar lymphadenopathy (BHL) without pulmonary infiltration, corresponding to stage I SA. The patient was diagnosed with acute sarcoidosis presenting as Löfgren syndrome. The patient was treated with corticosteroids for 1 week (20 mg/day prednisone); the dose was tapered off over the following 3 weeks. Afterward, the patient did not turn up at the Outpatient Department for several years.

In 2010, the patient returned to the hospital with chronic cough, dyspnea, weight loss and mild fever (37.8°C). Blood pressure was 110/70, heart rate 100 bpm. During auscultation mild bilateral inspiratory crackles in the lower lung fields were recognized. A chest X-ray and a high resolution computer tomography (HRCT) revealed BHL with pulmonary infiltration (interstitial thickening with nodules and lymphadenopathy) corresponding to stage II SA. Bronchoscopy with broncho-alveolar lavage fluid (BALF) collection excluded neoplasmatic invasion or fibrosis. BALF analysis demonstrated a CD4/CD8 ratio of 5.1. BALF cultures and serology were negative for fungal and bacterial infection. A purified protein derivative (PPD) skin test was negative (<10 mm). Mediastinoscopy with lymph node biopsy revealed a non-caseating granuloma and a diagnosis of sarcoidosis was reinforced. Initial acid fast bacilli (AFB) microscopy was negative for *M. tuberculosis,* but 8 weeks later BALF cultures on the Löwenstein-Jensen medium were positive for *M. tuberculosis*. The patient was immediately referred to the Pomeranian Hospital for Infectious Diseases, where antituberculosis therapy was initiated.

Case 2 In 2007, a 55 year-old woman presented with cough lasting for 6 weeks. The patient had hypertension and lipid disorder in anamnesis, treated with a β-blocker and a statin. A HRCT revealed BHL with pulmonary infiltration corresponding to stage II SA. PPD skin test was negative. A consecutive open lung biopsy yielded a non-caseating granuloma and a diagnosis of sarcoidosis was made. Throughout the following years the patient was re-hospitalized several times for gastritis, hemoptysis, pulmonary non-specific infection and for diagnostic purposes. Throughout these visits the patients received antibiotic therapy for *Helicobacter pylori* and pulmonary non-specific infections (six times). The patients also received four times steroid therapy for relapse of sarcoidosis and was kept on a low dose (5 mg/d) steroid therapy till April 2010. During all these incidences of re-hospitalization, TB was excluded by AFB sputum and BALF microscopy and cultures.

In the autumn of 2010, the patient was admitted to the hospital with signs of a pulmonary infection including fever 38.4°C, hemoptysis, weight loss and productive cough. Blood pressure was 120/85 and heart rate of 110 bpm. Auscultation of the lungs revealed a decreased breath sounds over the lung periphery. A HRCT revealed pulmonary infiltration corresponding to stage III SA. Bronchoscopy was performed and sputum cultures were taken for TB culture. An initial AFB-microscopy was negative, but 6 weeks later the Löwenstein-Jensen medium BALF culture was positive for *M. tuberculosis* and the patient was referred to the Pomeranian Hospital for Infectious Diseases for antituberculosis therapy.

Case 3 In 1994, a 47 year-old woman presented with persistent cough lasting for 3 months. A PPD skin test was negative. Radiological examination revealed BHL corresponding to stage I SA. The patient had a history of arterial hypertension treated with a calcium channel blocker and an angiotensin converting enzyme inhibitor. A supraclavicular lymph node biopsy was performed which demonstrated non-caseating granulomas, and the diagnosis of SA was made. No initial steroid therapy was necessary. During the regular follow-up visits over the next 6 years, no further pulmonary changes were detected. In 2000, the patient was admitted to the hospital with exertion dyspnea, fatigue and fever (38.2°C). Blood pressure was 120/75 mmHg and heart rate was 100 bpm. A CXR demonstrated pulmonary infiltrations corresponding to stage III SA. Steroid therapy was initiated with prednisone 25 mg/day. Three months later, regression of the pulmonary changes were noted and steroid therapy was tapered off over the following 3 months. During the

Table 29.1 Comparison of clinical, radiological, histopathological, bacteriological, and laboratory features in tuberculosis and sarcoidosis

	Case 1	Case 2	Case 3
Age at SA diagnosis	32	55	47
Age at TB diagnosis	44	59	61
Löfgren syndrome (arthralgia, fever, erythema nodosum, hilar lymphadenopathy)	Yes	No	No
No. of relapses of SA at TB diagnosis	1	3	5
Steroid treatment during relapses of SA	Yes	Yes	Yes
Steroid treatment for SA at TB diagnosis	Yes	Yes	Yes
TB treatment	Successful	Successful	Successful
Organ involvement	Lung	Lung	Lung
Stage of SA at the 1st presentation	I	II	I
Stage of SA at TB diagnosis	II	II	II
Noncaseating granulomas in lymph nodes biopsy	+	+	+
Laboratory evaluation at SA and TB presentation:			
Blood count	Normal	Normal	Normal
CRP (N: 0.02–8.0 mg/l)	Normal	Normal	Normal
Erythrocyte sedimentation rate (N: 1–5 mm/h)	52	32	34
Hypercalciuria	No	No	No
Hypercalcemia	No	No	No
BALF analysis: CD4/CD8 ratio (in SA N: ≤3.5)			
Neutrophiles (%)	5.1	4.1	6.8
Lymphocytes (%)	19	18	20
Macrophages (%)	77	30	10
Monocytes (%)	3	11	0
Phagocytes (%)	1	9	4
Positive *M. tuberculosis* BALF culture	+	+	+
PPD test	Negative	Negative	Negative
Spirometry	Restrictive	Restrictive	Restrictive
Diffusing capacity of the lung for CO (in %)	78	72	75

following 4 years similar incidences re-occurred and each time steroid therapy was effective. The patient was thus kept on a low dose steroid therapy. At this stage, investigations toward TB, including AFB microscopy and the Löwenstein-Jensen medium cultures from BALF and PPD skin tests, were negative.

In 2007, the patient was admitted to the hospital due to a 4-month history of weight loss, fatigue, and fever. Auscultation of the lungs revealed slight crackles at the lower border of the right lung and an overall decrease in vesicular sounds over the lung periphery. A HRCT revealed BHL with pulmonary infiltration corresponding to stage II SA. An investigation towards tuberculosis was initiated but AFB-microscopy, the Löwenstein-Jensen medium cultures and PPD skin test were negative and the patient was treated for SA with 20 mg/day prednisone. After initial improvement lasting for 1 week, the general state of the patient worsened within the following 4 weeks, with no change in the CXR picture. During a diagnostic fiberoptic bronchoscopy, no macroscopic abnormalities were detected and BALF collection was performed for a second mycobacterial culture. Cultures for other bacteria and fungi were negative. Analysis for potential cancerous cells was negative as well. AFB-microscopy was positive and the following *M. tuberculosis* culture was reported to be positive 6 weeks later. The patient was referred to the Pomeranian Hospital for Infectious Diseases and antituberculosis therapy was initiated.

29.2.1 HLA Typing

Genomic DNA was extracted from 10 ml of peripheral blood from each individual using the salt extraction method. The HLA class I (A, B, C) and class II (DRB1 and DQ) typing was performed using PCR-SSP (Polymerase Chain Reaction with Sequence Specific Primers) 'low-resolution' (DYNAL) following the method of (Olerup and Zetterquist 1991). The alleles frequencies were compared using the Fisher test with the Yates' correction (STATISTICA vs. 9.0, STATSOFT, USA). Results were regarded as statistically significant at $p < 0.05$.

29.3 Results and Discussion

In this report we describe three patients who were initially diagnosed with a relapse of chronic sarcoidosis (Stage II–III) and were started on corticosteroid treatment, but who were subsequently found to have TB.

Analysis of HLA class I and II alleles polymorphism revealed in *Case 1*: HLA-A:*01,*26, B:*15,*40, C*01,*17, DRB1:*07,*13, DQB1:*02,*03, DQA1:*05,*05; in *Case 2*: HLA-A:*02,*24, B:*15,*40, C*03, *07, DRB1:*03,*07, DQB1:*02,*02, DQA1:*02,*05, and in *Case 3*: HLA-A:*01,*24, B:*15,*40, C*04,*07, DRB1:*11,*16, DQB1:*03,*05, DQA1:*01,*05.

For comparison of the distribution of HLA alleles among the three patients, we used data obtained from our previous genotyping study in a homogenous population of Polish, Caucasian patients with SA, TB, and healthy individuals (Dubaniewicz et al. 2003, 2006). The analysis of the genetic background of the patient from *Case 1* revealed that she did not have any alleles connected with a high risk of developing SA, but had one protecting allele (DQB1*03). Moreover, she had one TB predisposing HLA allele (B*15) and three alleles (DQB1*02; two DQA1*05) connected with a low risk of developing TB. The patient from *Case 2* neither had HLA alleles connected with SA development, nor alleles protecting from it, but had one allele (B*15) predisposing to TB and five alleles (A*02; two DQB1*02; DQA1*02; DQA1*05) protective for TB. Finally, the patient from *Case 3* had one HLA allele (DQA1*01) associated with SA susceptibility, but four other alleles (C*04; DRB1*16; DQB1*03; DQB1*05) that are bound with protection from this disorder. In addition, this subject had three alleles (B*15; DRB1*16; DQB1*05) predisposing to TB and another three (DRB1*11; DQA1*05) linked to a low risk of developing TB.

Taken together, among the HLA class I and II alleles in our three patients we noted the occurrence of one allele (DQA1*01) bound with a high risk of SA, five alleles (three B*15; DRB1*16; DQB1*05) connected with susceptibility to TB, five alleles (C*04; DRB1*16; two DQB1*03; DQB1*05) protecting from SA, and ten alleles (A*02; DRB1*11; three DQB1*02; four DQA1*05; DQA1*02) connected with a low risk of developing TB.

In each case taken separately, there was a trend for a higher number of alleles of both predisposing and protecting from TB than from SA, in comparison with healthy individuals. Overall, the number of alleles predisposing to TB was statistically greater than the number of alleles connected with a high risk of developing SA (5 *vs.* 1, $p = 0.009$). Also, the number of alleles bound with protection from a disease was statistically higher for TB than for SA (10 *vs.* 5 alleles, $p = 0.02$).

We also analyzed the frequency of HLA alleles in our three patients in the context of our above mentioned genotyping study comparing the occurrence of HLA class I and II in SA and TB patients (Dubaniewicz et al. 2003, 2006). In *Case 1* we detected three alleles, the frequency of which is higher in SA than TB (DRB1*13; two DQA1*05) and two alleles with a higher frequency of occurrence in TB than SA (B*15; DQB1*03). In *Case 2* we noted one allele with a higher occurrence in SA than TB (DQA1*05) and another one which is less frequent in SA than TB (B*15). In *Case 3* there were

three alleles (DRB1*11; DQA1*01; DQA1*05) which are more frequent in SA than TB and four alleles (B*15; DRB1*16; DQB1*03; DQB1*05) which are more frequent in TB than SA. In all cases taken together, the number of alleles more common in SA than TB equal that for the reverse (7 *vs*. 7 alleles). Also, in each case separately, the number of alleles with a higher occurrence in SA than TB and those that appeared more often in TB than SA were statistically equal (3 *vs*. 2 alleles, $p=0.78$ in *Case 1*, 1 *vs*. 1 allele in *Case 2*, and 3 *vs*. 4 alleles, $p=0.63$ in *Case 3*). These results point to the patients' well balanced susceptibility to both SA and TB.

According to our previously published analysis of HLA in Polish patients with Stage II SA, HLA-B5, B8, DRB1*15 and DQA1*01 were found significantly more frequently, whereas HLA-B13, B35, Cw4, DRB1*16, *04, *08, DQB1:*03, *04, *05, *06 and DQA1*03 were less common than in healthy individuals (Dubaniewicz et al. 2003, 2006). In TB patients, on the other hand, HLA-B15, Cw5, DRB1:*16,*14, DQB1*05, DQA1*03 were detected more often and HLA-A2, DRB1*11, DQB1*02, DQA1:*02, *05 less frequent than in controls. In addition, in Stage II SA, HLA-B5, B8, DRB1:*11, *13, *15, DQA1:*01, *05 were statistically more frequent and HLA-B13, B15, Cw4, DRB1:*04, *14, *16, DQB1:*03, *05, *06, DQA1*03 less common than in TB. The occurrence of other tested antigens was comparable for all three populations. It is worth noting that an opposite relation was found for the disease development risk associated with DRB1*16 and DQB1*05 allele present in Polish patients with SA or TB in comparison with healthy individuals. Both alleles were protective against SA and at the same time were risk factors for TB (Dubaniewicz et al. 2003, 2006).

Studies on the occurrence of HLA alleles in various ethnic groups revealed a significantly higher presence of HLA class I: A1, B8, B13, B27, Cw7 and HLA class II: DRB1:*03,*11,*12,*14,*15, DRw52, DQA1:*01,*03,*05 alleles than those of DRB1:*01, *04, *07, DQB1*05 alleles in SA patients (Morgenthau and Iannuzzi 2011; Sato et al. 2010). However, for TB susceptibility a strong connection was found for HLA genes located in locus B: HLA-B5, B8, B15, B18, B27, B35 and for Cw5, but also for DRB1:*15,*16, DQA1*01 and DQB1:*05, *06 alleles (Dubaniewicz et al. 2003, 2006; Yim and Selvaraj 2010). On the other hand, less frequent presence of RB1:*04,*07,*08,*11,*13,*14, DQA1*05 and DQB1:*02,*03,*04 alleles was noted in TB, compared with healthy individuals. In patients with both diseases, DRB1:*14,*15, DQA1*01 and DQB1:*05,*06 alleles were more frequent than in healthy subjects. It is also worth noting that in studies on various ethnic groups, the frequency of occurrence of DRB1:*04, *06,*08,*11 and DQB1:*03,*04 alleles were opposite in SA and TB patients, i.e., a positive correlation for developing SA and a negative for developing TB was found for those alleles (Goljan et al. 2000). As above mentioned, an opposite relation to SA and TB development was also found for HLA polymorphism in the Polish population of patients, although for different alleles (DRB1*16 and DQB1*05) (Dubaniewicz et al. 2003, 2006). Those observations indicate the possible reciprocal direction of associations between HLA polymorphism and the two diseases, depending on the patients' ethnic origin. However, some other studies (reviewed in Dubaniewicz et al. 2006) show no significant correlation of either SA or TB with DR and DQ haplotypes. Therefore, data from different ethnic or racial groups are not always consistent and some alleles that are protective for SA or TB in one population can be connected with a high risk of developing the disease in another (Sato et al. 2010; Yim and Selvaraj 2010).

The discrepancy between results obtained for different ethnic groups may be caused by specificity and sensitivity of applied methods, different frequencies of HLA class I and II subtypes, patterns of linkage disequilibrium and/or by different polymorphism of HLA residues and subsequent changes in antigen presentation during mycobacterial infection and/or autoimmune process.

The occurrence of certain HLA alleles is directly associated with changes in (auto)antigen(s) presentation to T lymphocytes and with following immune response, resulting in granuloma formation and organ dysfunction. It has been shown that DRB1*16 and DQB1*02 class II alleles, present in our patients (in *Case 3*, and in both *Case 1* and *Case 2*, respectively), interact with T-cells during mycobacterial ESAT-6 (early secretory antigen target) antigen recognition. Moreover, several epitopes

of *M. tuberculosis* antigens, e.g., hsp65 p2-12 peptide binding specifically to HLA coded by DRB1*03 allele, peptides p61-75 and p141-155 interacting mostly with DRB1*16 and DRB1*07 (present in *Case 1* and *Case 2*), and p501-515 interacting also with DRB1*16, were found to affect the regulation of the immunoreactivity of an individual during infection (reviewed in Dubaniewicz et al. 2005). The immunoreactivity of an organism to *M. tuberculosis* infection is regulated not only by hsp65, but also by other mycobacterial heat shock proteins – hsp16 and hsp70, which epitopes bind selectively to HLA-DRB1*01, DRB1*15,*16, DRB1*03, DRB1*04, DRB1*07, DRB4*01, DQA1*03 and DQB1*03 (allele present in *Case 1* and *Case 3*) (reviewed in Dubaniewicz 2010). Additionally, DQB1*05 (present in *Case 3*) has been found to influence the charge in the putative peptide binding pocket P9 of the DQ molecule, present in some individuals, and to be associated with the progression of TB by affecting the mycobacterial antigen presentation and down- regulating the immune response. Another study has found a strong association of DQB1*03 allele and no association of HLA-DR with immunosuppression in advanced TB (reviewed in Dubaniewicz et al. 2005). Kurian et al. (2004), however, noted that DRB1*03-positive TB patients have decreased the Th1 lymphocyte response in comparison with DRB1*03-nagative ones. Moreover, this allele is connected with decreased IFN-γ and TNF-α and increased TGF-β production, and hence with reduced Th1 response in patients with SA (Idali et al. 2006; Wahlstrom et al. 2001). In contrast to other genotyping studies (Idali et al. 2006; Sato et al. 2010), a high occurrence of DRB1*03 and DQB1*02 alleles in our patients correlated with chronic course of SA, and not with good prognosis Thus, it is possible that a low Th1 lymphocyte response associated with this particular haplotype together with a higher occurrence of HLA alleles predisposing to TB development, could induce TB. In contrast to this data, other authors have found that DRB1*03 and DQB1*03 alleles enhance the efficiency of the immune response to *M. tuberculosis*, while presenting mycobacterial hsp65 epitopes to T-cells. DRB1*03, DRB1*07 and DRB1*15,*16 has also been found to enhance Th1 activity due to *M. tuberculosis* MPB70 p8, p12 and p13 peptides presentation (reviewed in Dubaniewicz et al. 2005). Furthermore, DRB1*16 allele has been shown to elevate the level of circulating antibodies against 38kD protein of tubercle bacilli, and thus to enhance the immune response during TB. This is in agreement with the study performed by Khomenko et al. (1990), who have found in six ethnic groups of the Soviet Union that TB patients with DRB1*15,*16 allele have increased levels of IgG after PPD skin test. The authors also noted an association between dynamics of TB course and increased occurrence of DRB1*15,*16 and B15 (present in all the cases), and a decreased frequency of DRB1*03. The B15 antigen, along with other antigens from HLA locus B, is connected with TB development in various ethnic populations, including TB patients from Poland (reviewed in Dubaniewicz et al. 2005).

Some HLA alleles are additionally connected with the development of either acute or chronic form of SA. For example, DRB1*15,*16-positive and TNF-A2-negative patient's haplotype is connected with a chronic course of sarcoidosis and worse prognosis, present in our cases (Mrazek et al. 2005; Swider et al. 1999). DRB1*11 allele (present in *Case 3*) is strongly associated with a chronic course of SA and is correlated with the presence of *M. tuberculosis* DNA (Grosser et al. 2005). Furthermore, Grosser et al. (2005) have reported that the percentage of *M. tuberculosis*-positive SA patients was higher in a chronic course of the disease, in comparison with an acute form of it. The authors concluded that mycobacterial antigens can play a major pathogenic role in the chronic course of the disease (Grosser et al. 2005). In addition, some of HLA alleles, e.g., DRB1*03, DQB1*03, DQA1*05, and DQB1*02, which were present in our patients from *Cases 1–3,* can be associated with a high risk of the development of autoimmunological disorders (Plesner et al. 2002; Price et al. 1999; Sidney et al. 2002), and sarcoidosis is considered to be one such candidate due to molecular mimicry between human and mycobacterial hsp (Dubaniewicz 2010). DQB1*05 allele is said to contribute to the development of sarcoidosis and autoimmune manifestations (Papadopoulos et al. 2006).

The above outlined associations between mycobacterial antigens, HLA polymorphism, and the course of inflammation point to the complexity of the immune response to *M. tuberculosis* infection. Mycobacterial heat shock proteins, especially hsp16 and ESAT-6 are the antigens specific for the

dormant stage of TB and can be at play in the etiopathogenesis of sarcoidosis (reviewed in Dubaniewicz 2010). It is possible that in a host infected with *M. tuberculosis*, mycobacterial hsp develop a polar sarcoid (e.g., Löfgren syndrome) or a polar tuberculoid (e.g., chronic sarcoidosis), or other borderline forms of sarcoidosis or tuberculosis, depending on genetically different background of patients (e.g., HLA and non-HLA genes). In addition, the described HLA allele distribution between SA and TB in our cases points to the balance in patients' susceptibility to both diseases. In comparison with healthy individuals, SA patients who subsequently develop TB have more alleles connected with protection from TB than from SA. Hence, greater protection from developing TB, derived from the patients' genetic background, in conjunction with environmental factors may have resulted in the development of sarcoidosis as the first disorder. Due possibly to decreased immune response with low lymphoproliferation caused by age or inhibition of HLA class II antigen expression during treatment with corticosteroids (applied in all cases), β-blockers, statins, and calcium channel blockers (in 2 out of 3 cases), a higher number of HLA alleles predisposing to TB observed may have provoked tuberculosis (Livnat et al. 1987; Mach 2002; Messerli and Grossman 1998; Steffens and Mach 2004). Therefore, patients' genetic susceptibility should be considered in tailoring individual therapy. An analysis of patients' genetic background may protect from an excessive decline in his immune response during drug therapy and prevent from tuberculosis development, as SA and TB seem to be interconnected and may be caused by one agent – *M. tuberculosis* or its antigen(s).

Conflicts of interest: The authors declare no conflicts of interest in relation to this article.

References

American Thoracic Society. (1999). Statement on sarcoidosis. *American Journal of Respiratory and Critical Care Medicine, 160*, 736–755.

Dubaniewicz, A. (2010). Mycobacterium tuberculosis heat shock proteins and autoimmunity in sarcoidosis. *Autoimmunity Reviews, 9*(6), 419–424.

Dubaniewicz, A., & Dubaniewicz, A. (2005). Human Leukocyte antigens class I and class II: Associations and distribution in different ethnic groups of patients with pulmonary tuberculosis. *Current Respiratory Medicine Reviews, 1*(2), 117–121.

Dubaniewicz, A., Szczerkowska, Z., & Hoppe, A. (2003). Comparative analysis of HLA class I antigens in pulmonary sarcoidosis and tuberculosis in the same ethnic group. *Mayo Clinic Proceedings, 78*(4), 436–442.

Dubaniewicz, A., Moszkowska, G., & Szczerkowska, Z. (2005). Frequency of DRB1-DQB1 two-locus haplotypes in tuberculosis: Preliminary report. *Tuberculosis (Edinburgh, Scotland), 85*, 259–267.

Dubaniewicz, A., Dubaniewicz-Wybieralska, M., Moszkowska, G., Sternau, A., & Dubaniewicz, A. (2006). Comparative analysis of DR and DQ alleles occurrence in sarcoidosis and tuberculosis in the same ethnic group: Preliminary study. *Sarcoidosis, Vasculitis, and Diffuse Lung Diseases, 23*(3), 180–189.

Goljan, A., Puscinska, E., Sankowska, M., & Zielinski, J. (2000). Polymorphism of histocompatibility class II antigens coded with the DRB gene in familial sarcoidosis in Poland. *Pneumonologia i Alergologia Polska, 68*(11–12), 533–544.

Grosser, M., Luther, T., Fuessel, M., Bickhardt, J., Magdolen, V., & Baretton, G. (2005). Clinical course of sarcoidosis in dependence on HLA-DRB1 allele frequencies, inflammatory markers, and the presence of *M. tuberculosis* DNA fragments. *Sarcoidosis, Vasculitis, and Lung Diseases, 22*(1), 66–74.

Idali, F., Wiken, M., Wahlstrom, J., Mellstedt, H., Eklund, A., Rabbani, H., & Grunewald, J. (2006). Reduced Th1 response in the lungs of HLA-DRB1*0301 patients with pulmonary sarcoidosis. *European Respiratory Journal, 27*(3), 451–459.

Khomenko, A. G., Litvinova, V. I., Chukanovaa, V. P., & Pospelova, L. E. (1990). Tuberculosis in patients with various HLA phenotypes. *Tubercle, 71*(3), 187–192.

Kurian, S. M., Selvaraj, P., Reetha, A. M., Charles, N., & Narayanan, P. R. (2004). HLA-DR phenotypes and lymphocyte response to *M. tuberculosis* antigens in cures spinal tuberculosis patients and their contacts. *The Indian Journal of Tuberculosis, 51*, 71–75.

Livnat, S., Madden, K. S., Felten, D. L., & Felten, S. Y. (1987). Regulation of the immune system by sympathetic neural mechanisms. *Progress in Neuro-Psychopharmacology & Biological Psychiatry, 11*(2–3), 145–152.

Mach, F. (2002). Immunosuppressive effects of statins. *Atherosclerosis Supplements, 3*(1), 17–20.
Messerli, F. H., & Grossman, E. (1998). The calcium antagonist controversy: A posthumous commentary. *The American Journal of Cardiology, 82*(9B), 35R–39R.
Moller, D. R. (2007). Potential etiologic agents in sarcoidosis. *Proceedings of the American Thoracic Society, 4*(5), 465–468.
Morgenthau, A. S., & Iannuzzi, M. C. (2011). Recent advances in sarcoidosis. *Chest, 139*(1), 174–182.
Mrazek, F., Holla, L. I., Hutyrova, B., Znojil, V., Vasku, A., Kolek, V., Welsh, K. I., Vacha, J., du Bois, R. M., & Petrek, M. (2005). Association of tumor necrosis factor-α, lymphotoxin-α and HLA-DRB1 gene polymorphisms with Löfgren's syndrome in Czech patients with sarcoidosis. *Tissue Antigens, 65*(2), 163–171.
Olerup, O., & Zetterquist, H. (1991). HLA-DRB1*01 subtyping by allele-specific PCR amplification: A sensitive, specific and rapid technique. *Tissue Antigens, 37*(5), 197–204.
Papadopoulos, K. I., Wassmuth, R., Sponsel, T., Sjöberg, K., & Hallengren, B. (2006). Sarcoidosis and autoimmunity: Evidence of differential associations with HLA class II markers. *International Journal of Endocrinology and Metabolism, 4*, 13–18.
Plesner, A., Greenbaum, C. J., Gaur, L. K., Ernst, R. K., & Lernmark, A. (2002). Macrophages from high-risk HLA-DQB1*0201/*0302 type 1 diabetes mellitus patients are hypersensitive to lipopolysacharide stimulation. *Scandinavian Journal of Immunology, 56*(5), 522–529.
Price, P., Witt, C., Allcock, R., Sayer, D., Garlepp, M., Kok, C. C., French, M., Mallal, S., & Christiansen, F. (1999). The genetic basis for the association of the 8.1 ancestral haplotype (A1,B8,DR3) with multiple immunopathological diseases. *Immunology Reviews, 167*, 257–274.
Sato, H., Woodhead, F. A., Ahmad, T., Grutters, J. C., Spagnolo, P., van den Bosch, J. M., Maier, L. A., Newman, L. S., Nagai, S., Izumi, T., Wells, A. U., du Bois, R. M., & Welsh, K. I. (2010). Sarcoidosis HLA class II genotyping distinguishes differences of clinical phenotype across ethnic groups. *Human Molecular Genetics, 19*(20), 4100–4111.
Sidney, J., del Guercio, M. F., Southwood, S., & Sette, A. (2002). The HLA molecules DQA1*0501/B1*0201 and DQA1*0301/B1*0302 share an extensive overlap in peptide binding specificity. *Journal of Immunology, 169*(9), 5098–5108.
Steffens, S., & Mach, F. (2004). Anti-inflammatory properties of statins. *Seminars in Vascular Medicine, 4*(4), 417–422.
Swider, C., Schnittger, L., Bogunia-Kubik, K., Gerdes, J., Flad, H.-D., Lange, A., & Seitze, U. (1999). TNF-alpha and HLA-DR genotyping as potential prognostic markers in pulmonary sarcoidosis. *European Cytokine Network, 10*(2), 143–146.
Wahlstrom, J., Katchar, K., Wigzell, H., Olerup, O., Eklund, A., & Grunewald, J. (2001). Analysis of intracellular cytokines in $CD4^+$ and $CD8^+$ lung and blood T cells in sarcoidosis. *American Journal of Respiratory and Critical Care Medicine, 163*(1), 115–121.
Walzl, G., Ronacher, K., Hanekom, W., Scriba, T. J., & Zumla, A. (2011). Immunological biomarkers of tuberculosis. *Nature Reviews Immunology, 11*(5), 343–354.
Yim, J. J., & Selvaraj, P. (2010). Genetic susceptibility in tuberculosis. *Respirology, 15*(2), 241–256.

Chapter 30
Toll-Like Receptor-9 Polymorphisms in Sarcoidosis and Chronic Obstructive Pulmonary Disease

Stefan Pabst, Oxana Bradler, Adrian Gillissen, Georg Nickenig, Dirk Skowasch, and Christian Grohe

Abstract The etiology of inflammatory diseases of the lung like sarcoidosis and chronic obstructive pulmonary disease (COPD) is multifactorial. The main trigger for developing a COPD is tobacco smoking while exogenous factors causing sarcoidosis are unclear. In both diseases there is an underlying genetic susceptibility determining both the onset and the course of the diseases. Toll-like receptor (TLR)-9 plays an important role in innate immunity by recognizing bacterial CpG-DNA motifs. It is unclear whether single nucleotide polymorphisms (SNPs) in TLR-9 are able to alter the course of sarcoidosis or COPD, or raise the susceptibility for developing one of the disorders. We examined two SNPs in the promoter region of the TLR-9 gene (T1486C and T1237C) in 175 COPD patients (59% with a stable course of the disease, 41% with an instable course with more than 3 exacerbations over the last 3 years) and 166 sarcoidosis patients (19% with an acute and 81% with a chronic course of the disease lasting >2 years) comparing each group to 233 healthy controls. Polymerase chain reaction (PCR) and restriction fragment length polymorphism (RFLP) analysis was used for genotyping. The C-allele frequency of T1486C was significantly elevated in COPD patients ($p=0.008$). For T1237C there were no significant associations comparing the COPD cohort with the controls. In the sarcoidosis cohort, we could observe a significantly higher prevalence of the C-allele for T1237C in the chronic sarcoidosis cohort in comparison to the control group ($p=0.026$). For T1486 there no statistical association was observed. This is the first study showing an association between a SNP (T1486C) in the TLR-9 gene and the onset of COPD. Moreover, we could demonstrate that T1237C is able to alter the course of sarcoidosis as a disease-modifying gene. This study underlines that SNPs in TLR-9 might be involved in acquiring and maintaining lung diseases such as sarcoidosis and COPD.

Keywords COPD • Gene polymorphism • Sarcoidosis • TLR9 • Tobacco smoking

S. Pabst (✉) • O. Bradler • G. Nickenig • D. Skowasch
Medical Clinic II, Division of Pneumology, University Hospital of Bonn,
Sigmund-Freud-Str. 25, 53105 Bonn, Germany
e-mail: Stefan.pabst@ukb.uni-bonn.de

A. Gillissen
Department for Pulmonary Medicine, General Hospital Kassel,
Kassel, Germany

C. Grohe
Evangelische Lungenklinik Berlin-Buch,
Buch, Germany

M. Pokorski (ed.), *Respiratory Regulation - The Molecular Approach*,
Advances in Experimental Medicine and Biology 756, DOI 10.1007/978-94-007-4549-0_30,

30.1 Introduction

Sarcoidosis is an inflammatory granulomatous multisystem disorder, primarily affecting the lungs and lymph nodes. Other organs, including skin, heart, and liver may also be afflicted. The disease is characterized by noncaseating granulomas and an exaggerated cellular immune response caused by increased inflammatory activity of macrophages (Iannuzzi et al. 2007). The course of most sarcoidosis patients is short and favorable, but about 20% develop a chronic and prolonged disease, requiring treatment with corticosteroids. Up to 5% of all patients suffer severe complications such as lung fibrosis. The etiology remains unclear. Evidence suggests that it is the product of an unknown exogenous antigenic stimulus and an endogenous genetic susceptibility (Statement on sarcoidosis 1999).

Progressive airflow limitation due to chronic obstructive bronchitis and emphysema is the main characteristic of chronic obstructive pulmonary disease (COPD). COPD ranks fourth as a global cause of death and shows a worldwide increase both in morbidity and mortality (Murray and Lopez 1997). The most causative environmental factor for developing a COPD is tobacco smoke (Sandford and Paré 2000). However, not all smokers develop a COPD, indicating that other factors are at play. A genetic background also is supported by family studies (McCloskey et al. 2001).

Toll-like receptor (TLR)-9 recognizes bacterial CpG (cytosine-phosphodiester-guanine)-DNA motifs and therefore plays an important role in innate immunity (Hemmi et al. 2000). TLR-9 is ubiquitously expressed in cells of the human bronchial system and lung such as in bronchial epithelium (Mayer et al. 2007), alveolar macrophages, blood monocytes (Juarez et al. 2010), dendritic cells (Hemmi et al. 2000), and neutrophil granulocytes (Hayashi et al. 2003). Furthermore, it is suggested that TLR-9 plays an active role in the proliferation of activated CD4+ T cells (Chiffoleau et al. 2007).

In the present study we examined two single nucleotide polymorphisms (SNPs) in the promoter region of TLR-9: T1237C (rs5743836) and T1486C (rs187084). Both SNPs change protein products characterized for their downregulation of TLR-9 expression by luciferase reporter gene assays (Tao et al. 2007) and could be associated with autoimmune diseases such as atopic dermatitis (Novak et al. 2007) and asthma (Berghöfer et al. 2005). To evaluate genetic causes in the TLR-9 gene that influence the susceptibility or the course of COPD and sarcoidosis, we performed a genetic case-control study in two large Caucasian COPD and sarcoidosis cohorts.

30.2 Genotyping

30.2.1 Patient Population

The research was carried out in accordance with the Declaration of Helsinki of 1989 of the World Medical Association, and the study was approved by the Ethics Committee of Bonn, University School of Medicine, Germany/St. George Medical Center Leipzig, Germany. Written informed consent was obtained from each patient prior to their enrolment. Patients with severe medical disorders including malignancy and immunological disorders were excluded from the study. All patients were at least 18 years old.

COPD patients: 175 patients with COPD were recruited in the Department of Internal Medicine, Rheinische-Friedrich-Wilhelms University, Bonn, Germany, and the Department of Internal Medicine, St. George Medical Center Leipzig, Germany. The diagnosis of COPD was made according to the guidelines of the ATS/ERS (Celli and MacNee 2004). Blood samples were collected from two groups of patients with COPD. The first group comprised 72 patients with more than 3 hospitalizations over the last 3 years due to COPD exacerbations. This group was defined as ‘instable COPD’. Lung function

Table 30.1 Baseline characteristics of COPD patients and healthy controls

	COPD all	COPD stable	COPD instable	Controls
n	175	72	103	170
Sex (M/F)	115/60	45/27	70/33	77/93
Age (yr ± SD)	63.7 ± 10.7	63.0 ± 11.7	64.3 ± 10.0	62.3 ± 13.3
Packyears ± SD	33.9 ± 26.1	32.5 ± 25.5	34.9 ± 26.6	18.7 ± 8.4
Smoker (%)	73 (41.7%)	32 (44.4%)	41 (39.8%)	52 (30.6%)
Non-smoker (%)	18 (10.3%)	4 (5.6)	14 (13.6%)	20 (11.8%)
Ex-smoker (%)	84 (48.0%)	36 (50.0%)	48 (46.6%)	98 (57.6%)
FEV1%pred. ± SD	52.0 ± 20.8	58.5 ± 19.0	47.3 ± 0.9	97.9 ± 20.4
FEV1/FVC	59.3 ± 15.9	62.2 ± 15.3	57.2 ± 16.1	83.8 ± 26.5

Table 30.2 Baseline characteristics of sarcoidosis patients and healthy controls

	Sarcoidosis all	Sarcoidosis acute	Sarcoidosis chronic	Controls
n	166	32	134	233
Age (yr ± SD)	50.7 ± 13.6	42.8 ± 10.4	52.5 ± 12.4	48.6 ± 16.5
Sex (M/F)	74/92	14/18	60/74	111/122

in these subjects was measured before discharge. The second group included 103 outpatients with stable COPD. All body plethysmographic tests were performed according to the ATS/ERS criteria (Pellegrino et al. 2005). Smoking habit was defined as follows: non-smokers had never smoked; ex-smokers had smoked daily and given it up prior to entering the study. Smokers have smoked daily at the time of study. The amount of lifetime smoking was assessed as packyears (years of smoking x number of packs of 20 cigarettes per day). The baseline characteristics are shown in Table 30.1.

Sarcoidosis patients: 166 Caucasian patients with diagnosed sarcoidosis were included in the present study. They were recruited from the outpatient clinic of the Department of Internal Medicine, Rheinische-Friedrich-Wilhelms University, Bonn, Germany and from sarcoidosis peer-support groups nearby. Sarcoidosis was confirmed by biopsy evidence of noncaseating epitheloid cell granulomas in any organ and chest X-ray (posterior-anterior and lateral) abnormalities. Radiological staging was in accordance with ATS/ERS/WASOG Guidelines (Statement on sarcoidosis 2009). For statistical analysis, a 'chronic course' was defined as *either* having symptoms over at least 2 years *or* a minimum of two episodes in a lifetime. 'Acute sarcoidosis' was defined as only one episode of sarcoidosis prior to examination, which has completely resolved. The baseline characteristics are shown in Table 30.2.

Healthy controls: 233 healthy controls were selected in pre-engaging examinations at the University of Bonn, Germany. They were all residents of Germany. None had a history of lung disease or showed any symptoms of lung or other disease. Lung function tests were performed in all controls. All showed normal findings in laboratory examination, which included complete blood counts, urine analyses, hepatic enzyme activities and BUN levels. For comparison with the COPD cohort only 170 controls were selected for matching age and smoking status.

30.2.2 Methods

Peripheral venous blood samples of 9 ml were drawn from each patient by standard venous puncture. Each blood sample was collected in sterile tubes containing 15% K_3EDTA solution. DNA was isolated by salting out procedure described by Miller et al. (1988). Polymerase chain reaction (PCR) was used to determine the TLR9-genotypes (Table 30.3, Figs. 30.1 and 30.2). PCR was carried out in 25-µl reaction mixture containing 1 µg of genomic DNA, 1 µl of each 10 µM primer (MWG-Biotech, Ebersberg,

Table 30.3 Determination of the TLR-9 genotypes, sequences of primers as used for PCR and restriction fragment polymorphism analysis

Gene	SNP	Primers	Restriction enzyme	Fragments
TLR 9	**T1486C**	F: 5′TCCCAGCAGCAACAATTCATTA-3′	Afl II (37°C)	C-allele: 499 bp
	rs187084	R: 5′CTGCTTGCACTTGACTGTGT-3′		T-allele: 172 bp +327 bp
	T1237C	F: 5′ATGGGAGCAGAGACATAATGGA-3′	BstN I (60°C)	C-allele: 60 bp +48 bp +27 bp
	rs5743836	R: 5′CTGCTTGCACTTGACTGTGT-3′		T-alelle: 108 bp, 27 bp

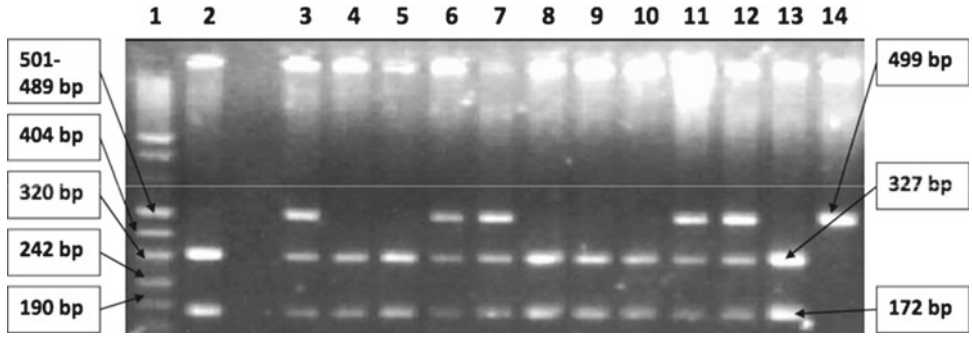

Fig. 30.1 Restriction fragments of T-1486C after enzymatic digestion with AflII; *line 1* – marker VIII; *lines 2, 4, 5, 8, 9, 10, and 13* – homozygous TT-genotype; *lines 3, 6, 7, 11, and 12* – heterozygous TC-genotype; *line 14* – homozygous CC-genotype

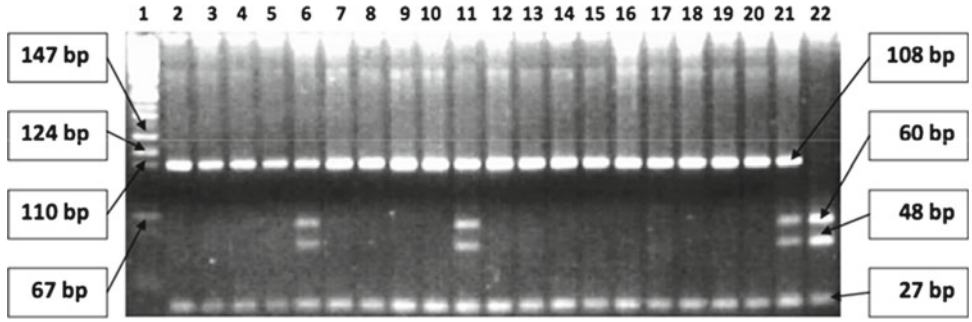

Fig. 30.2 Restriction fragments of T-1237C after enzymatic digestion with BstNI; *line 1* – marker VIII; *lines 2, 3, 4, 5, 7, 8, 9, 10, 12, 13, 14, 15, 16, 17, 18, 19, and 20* – homozygous TT-genotype; *lines 6, 11, and 21* – heterozygous TC-genotype; *line 22* – homozygous CC-genotype

Germany), 0.5 U Taq-polymerase (Invitrogen, Karlsruhe, Germany), 1 µl of each 1.25 mM base (Amersham, Braunschweig, Germany), 2.5 µl 10 × PCR-buffer (Invitrogen). The cycling condition both SNPs consisted of an initial cycle 95°C for 6 min in a thermocycler followed by 29 cycles (for rs5743836) or 34 cycles (for rs187084) denaturation with 95°C for 30 s, annealing with 62°C for 30 s and extension with 72°C for 60 s. A final synthesis step with 72°C for 10 min terminated the reaction.

SNP genotyping was performed by digestion with the restriction endonucleases AflII (rs187084, New England Biolabs, Frankfurt am Main, Germany) and BstNI (rs5743836, New England Biolabs),

respectively. The resulting fragments were separated on 3% MetaPhor agarose (Biozym, Hessisch Oldendorf, Germany) and stained with ethidium bromide (Fig. 30.2).

Statistical analysis was performed using software SPSS (version 13.0, Chicago, IL, USA). For each SNP, the distribution of genotypes was tested for differences between controls and stable/instable patients using Perason's chi-square test. The number of participants in the study led to a statistical power that ranged above 0.8.

30.3 Results

The baseline characteristics of COPD and sarcoidosis patients are displayed in Tables 30.1 and 30.2. The detailed results including the genotype distribution are presented in Table 30.3 (COPD) and Table 30.4 (sarcoidosis). In the COPD cohort, significant differences for T1486C were observed comparing all COPD patients to the healthy controls due to an elevated frequency of the mutated C-variant ($p=0.008$). No differences in between the COPD subgroups – stable *vs*. instable – could be detected for T1486C. However, each group compared to the controls showed significant results ($p=0.046$). No significant differences for T1237C were found comparing the COPD cohort with the controls.

In the sarcoidosis cohort, we demonstrated more C-alleles for T1237C compared to the controls with a significance in the chronic group ($p=0.026$). For T1486C, we only observed a trend toward increased C-allele frequency with equal distribution in the acute and the chronic group. However, statistical significance ($p=0.054$) was not reached (Table 30.5).

Table 30.4 Genotype distribution in the different COPD cohorts compared to healthy controls

	COPD all	COPD stable	COPD instable	Controls
T1486C				
TT	46 (26.3%)	20 (27.8%)	27 (26.2%)	66 (38.8%)
TC	103 (58.9%)	43 (59.7%)	59 (57.3%)	72 (42.4%)
CC	26 (14.9%)	9 (12.5%)	17 (16.5%)	32 (18.8%)
p[a]	**0.008**	**0.046**	**0.046**	
T1237C				
TT	125 (71.4%)	50 (69.4%)	75 (72.8%)	124 (72.9)
TC	46 (26.3%)	21 (29.2%)	25 (24.3%)	43 (25.3)
CC	4 (2.3%)	1 (1.4%)	3 (2.9%)	3 (1.8%)
p[a]	0.914	0.881	0.869	

[a]Compared to controls, significant results are printed in bold

Table 30.5 Genotype distribution in the different sarcoidosis cohorts compared to healthy controls

	Sarcoidosis all	Sarcoidosis acute	Sarcoidosis chronic	Controls
T1486C				
TT	57 (34.3%)	9 (28.1%)	48 (35.9%)	90 (38.6%)
TC	89 (53.6%)	18 (56.3%)	71 (53.0%)	99 (42.5%)
CC	20 (12.1%)	5 (15.6%)	15 (11.1%)	44 (18.9%)
p[a]	0.054	0.091	0.070	
T1237C				
TT	110 (66.3%)	23 (71.9%)	87 (64.9%)	175 (75.1%)
TC	54 (32.5%)	8 (25.0%)	46 (34.3%)	52 (22.3%)
CC	2 (1.2%)	1 (3.1%)	1 (0.8%)	6 (2.6%)
p[a]	0.056	0.923	**0.026**	

[a]Compared to controls, significant results are printed in bold

30.4 Discussion

This is the first study genotyping SNPs in the promoter region of TLR-9 in two large cohorts of patients with COPD and sarcoidosis comparing the genotype frequencies to a group of healthy controls. The results of the study suggest the T1486C SNP is a susceptibility gene for COPD, without acting as a disease modifying gene. In sarcoidosis, the T1237C polymorphism might operate as a disease modifying gene.

For both examined TLR-9 promoter polymorphisms, a functional relevance seems probably. By luciferase reporter gene assay, a significantly higher promoter activity of the (TT) genotype of T1237C (Novak et al. 2007) was demonstrated. In a different study, the C-allele was identified as a risk factor for the development of *H. pylori*-induced gastric precancerous lesion (Ng et al. 2010). Functional analysis of the SNP showed that carriage of the C-allele increased TLR-9 transcriptional activity driven mainly by activation of NF-kappaB. In COPD (Isajevs et al. 2011) and in sarcoidosis (Drent et al. 2001) higher NF-kappaB expression is found at the site of the disease. As we detected significantly more C-alleles in the cohort with a chronic disease, this could lead to higher TLR-9 expression in chronic sarcoidosis patients. However, this is only putative as neither NF-kappaB levels nor TLR-9 expression were studied.

Regarding genetic aspects, the results of a linkage study noted TLR-9 as a possible candidate gene for sarcoidosis (Schurmann et al. 2001), while a Dutch study showed no association between genetic variants and TLR9 in sarcoidosis population from the Netherlands (Veltkamp et al. 2010). However, the latter study did not look for different phenotypes of sarcoidosis. Therefore, our results with C1237T acting as a modifying SNP in sarcoidosis do not stand in contrast with the results of the Dutch study.

So far only two studies have examined the functionality of the TLR-9T-1486C SNP. Both studies showed that under basal conditions the C-allele of the TLR-9 T1486C SNP is associated with lower receptor expression (Tao et al. 2007; Elmaagacli et al. 2009). However, after stimulation of cells with CpG DNA, the C-allele in contrast to the T-allele resulted in a significant upregulation of TLR9 expression (Elmaagacli et al. 2009).

As we found significant more C-alleles in the COPD group a possible explanation would be that CpG DNA motifs as chronic inflammatory trigger cause upregulation of TLR-9 expression. As TLR-9 mediates cigarette smoke-induced release of proinflammatory CXCL8, this interaction may contribute to the accumulation of neutrophils and inflammation within the airways of smokers (Mortaz et al. 2010). A participation of TLR-9 SNPs in the pathogenesis of COPD has been examined only in one study before which could not find any association between the TLR-9 C1237T SNP and the risk for the development of COPD (Lazarus et al. 2003). A limitation in this study certainly is a relatively small sample size, comprising only 70 COPD patients.

In conclusion, we assume that polymorphisms in TLR-9 are a very promising target for further investigation in the context of inflammatory lung diseases such as COPD or sarcoidosis. As genetic studies are only hypothesis generating, prospective functional investigations in these cohorts are required to validate the genetic results.

Acknowledgments We thank Martina Lennarz for her excellent technical support and all participants for making this study possible.

Conflicts of interest: The authors declare no conflicts of interest in relation to this article.

References

Berghöfer, B., Frommer, T., König, I. R., Ziegler, A., Chakraborty, T., Bein, G., & Hackstein, H. (2005). Common human Toll-like receptor 9 polymorphisms and haplotypes: Association with atopy and functional relevance. *Clinical and Experimental Allergy, 35*, 1147–1154.

Celli, B. R., & MacNee, W. (2004). ATS/ERS Task force. Standards for the diagnosis and treatment of patients with COPD: A summary of the ATS/ERS position paper. *European Respiratory Journal, 23*, 932–946.

Chiffoleau, E., Heslan, J. M., Heslan, M., Louvet, C., Condamine, T., & Cuturi, M. C. (2007). TLR9 ligand enhances proliferation of rat CD4+ T cell and modulates suppressive activity mediated by CD4+ CD25+ T cell. *International Immunology, 19*, 193–201.

Drent, M., van den Berg, R., Haenen, G. R., van den Berg, H., Wouters, E. F., & Bast, A. (2001). NF-kappaB activation in sarcoidosis. *Sarcoidosis, Vasculitis, and Diffuse Lung Diseases, 18*, 50–56.

Elmaagacli, A. H., Koldehoff, M., & Beelen, D. W. (2009). Improved outcome of hematopoietic SCT in patients with homozygous gene variant of Toll-like receptor 9. *Bone Marrow Transplantation, 44*, 295–302.

Hayashi, F., Means, T. K., & Luster, A. D. (2003). Toll-like receptors stimulate human neutrophil function. *Blood, 102*, 2660–2669.

Hemmi, H., Takeuchi, O., Kawai, T., Kaisho, T., Sato, S., Sanjo, H., Matsumoto, M., Hoshino, K., Wagner, H., Takeda, K., & Akira, S. (2000). A Toll-like receptor recognizes bacterial DNA. *Nature, 408*, 740–745.

Iannuzzi, M. C., Rybicki, B. A., & Teirstein, A. S. (2007). Sarcoidosis. *The New England Journal of Medicine, 357*, 2153–2165.

Isajevs, S., Taivans, I., Svirina, D., Strazda, G., & Kopeika, U. (2011). Patterns of inflammatory responses in large and small airways in smokers with and without chronic obstructive pulmonary disease. *Respiration, 81*, 362–371.

Juarez, E., Nuñez, C., Sada, E., Ellner, J. J., Schwander, S. K., & Torres, M. (2010). Differential expression of Toll-like receptors on human alveolar macrophages and autologous peripheral monocytes. *Respiratory Research, 11*, 2.

Lazarus, R., Klimecki, W. T., Raby, B. A., Vercelli, D., Palmer, L. J., Kwiatkowski, D. J., Silverman, E. K., Martinez, F., & Weiss, S. T. (2003). Single-nucleotide polymorphisms in the Toll-like receptor 9 gene (TLR9): Frequencies, pairwise linkage disequilibrium, and haplotypes in three U.S. ethnic groups and exploratory case-control disease association studies. *Genomics, 81*, 85–91.

Mayer, A. K., Muehmer, M., Mages, J., Gueinzius, K., Hess, C., Heeg, K., Bals, R., Lang, R., & Dalpke, A. H. (2007). Differential recognition of TLR-dependent microbial ligands in human bronchial epithelial cells. *Journal of Immunology, 178*, 3134–3142.

McCloskey, S. C., Patel, B. D., Hinchliffe, S. J., Reid, E. D., Wareham, N. J., & Lomas, D. A. (2001). Siblings of patients with severe chronic obstructive pulmonary disease have a significant risk of airflow obstruction. *American Journal of Respiratory and Critical Care Medicine, 164*, 1419–1424.

Miller, S. A., Dykes, D. D., & Polesky, H. F. (1988). A simple salting out procedure for extracting DNA from human nucleated cells. *Nucleic Acids Research, 16*, 1215.

Mortaz, E., Adcock, I. M., Ito, K., Kraneveld, A. D., Nijkamp, F. P., & Folkerts, G. (2010). Cigarette smoke induces CXCL8 production by human neutrophils via activation of TLR9 receptor. *European Respiratory Journal, 36*, 1143–1154.

Murray, C., & Lopez, A. (1997). Mortality by cause for eight regions of the world: Global burden of disease study. *Lancet, 349*, 1269–1276.

Ng, M. T., Van't Hof, R., Crockett, J. C., Hope, M. E., Berry, S., Thomson, J., McLean, M. H., McColl, K. E., El-Omar, E. M., & Hold, G. L. (2010). Increase in NF-kappaB binding affinity of the variant C allele of the toll-like receptor 9–1237T/C polymorphism is associated with *Helicobacter pylori*-induced gastric disease. *Infection and Immunity, 78*, 1345–1352.

Novak, N., Yu, C. F., Bussmann, C., Maintz, L., Peng, W. M., Hart, J., Hagemann, T., Diaz-Lacava, A., Baurecht, H. J., Klopp, N., Wagenpfeil, S., Behrendt, H., Bieber, T., Ring, J., Illig, T., & Weidinger, S. (2007). Putative association of a TLR9 promoter polymorphism with atopic eczema. *Allergy, 62*, 766–772.

Pellegrino, R., Viegi, G., Brusasco, V., Crapo, R. O., Burgos, F., Casaburi, R., Coates, A., van der Grinten, C. P., Gustafsson, P., Hankinson, J., Jensen, R., Johnson, D. C., MacIntyre, N., McKay, R., Miller, M. R., Navajas, D., Pedersen, O. F., & Wanger, J. (2005). Interpretive strategies for lung function tests. *European Respiratory Journal, 26*, 948–968.

Sandford, A., & Pare, P. (2000). Genetic risk factors for chronic obstructive pulmonary disease. *Clinics in Chest Medicine, 21*, 633–643.

Schurmann, M., Reichel, P., Muller-Myhsok, B., Schlaak, M., Muller-Quernheim, J., & Schwinger, E. (2001). Results from a genome-wide search for predisposing genes in sarcoidosis. *American Journal of Respiratory and Critical Care Medicine, 164*, 840–846.

Statement on sarcoidosis. (1999). Joint Statement of the American Thoracic Society (ATS), the European Respiratory Society (ERS) and the World Association of Sarcoidosis and Other Granulomatous Disorders (WASOG) adopted by the ATS Board of Directors and by the ERS Executive Committee. *American Journal of Respiratory and Critical Care Medicine, 160*, 736–755.

Tao, K., Fujii, M., Tsukumo, S., Maekawa, Y., Kishihara, K., Kimoto, Y., Horiuchi, T., Hisaeda, H., Akira, S., Kagami, S., & Yasutomo, K. (2007). Genetic variations of Toll-like receptor 9 predispose to systemic lupus erythematosus in Japanese population. *Annals of the Rheumatic Diseases, 66*, 905–909.

Veltkamp, M., Van Moorsel, C. H., Rijkers, G. T., Ruven, H. J., Van Den Bosch, J. M., & Grutters, J. C. (2010). Toll-like receptor (TLR)-9 genetics and function in sarcoidosis. *Clinical and Experimental Immunology, 162*, 68–74.

Chapter 31
Association of Adiponectin Gene G276T Polymorphism with Atherogenic Indicators in Obese Children

Beata Pyrzak, Malgorzata Ruminska, Aneta Czerwonogrodzka-Senczyna, Anna Majcher, Alicja Wisniewska, Michal Brzewski, and Urszula Demkow

Abstract Adiponectin plays a protective role against atherosclerosis. Genetic investigation has revealed that G276T adiponectin gene polymorphism is related to adiponectin concentration and metabolic disturbances. The aim of the present study was to investigate the association of adiponectin gene G276T polymorphism with indices of atherosclerosis in obese children. We examined 159 children (125 obese and 34 non-obese). G276T of adiponectin gene polymorphism was identified using a PCR-RFLP method. The intima media thickness (IMT) was evaluated in 82 patients. In all children, the anthropometric indices, fasting plasma total cholesterol (TC), HDL and LDL cholesterol, triglycerydes (TG), C-reactive protein (CRP), and adiponectin were measured. Oral glucose tolerance test (OGTT) also was performed. We found that the obese patients presented with higher values of atherogenic indicators than the non-obese patients. The indicators positively correlated with CRP and lipid concentrations. Ninety one percent of obese children presented with elevated IMT which correlated with CRP. The children with GG genotype (GG + GT allele) had lower values of BMI, TC, and TG but higher adiponectin concentrations. The mean level of adiponectin was statistically decreased in the compared with the homozygous TT children. The other anthropometric and atherogenic indicators did not differ between these two sets of obese children. We conclude that adiponectin concentrations were decreased in children with polymorphism G276T in adiponectin gene. The study, however, failed to show significant associations between carotid IMT, lipid markers, blood pressure, or HOMA-IR in obese children.

Keywords Adiponectin • Atherosclerosis • Children • Genes • Polymorphism • Obesity • Intima media • Oral glucose tolerance

B. Pyrzak (✉) • M. Ruminska • A. Czerwonogrodzka-Senczyna • A. Majcher • A. Wisniewska
Department of Pediatric and Endocrinology, Warsaw Medical University,
Marszalkowska 24 St., 00-576 Warsaw, Poland
e-mail: beata.pyrzak@wum.edu.pl

M. Brzewski
Department of Pediatric Radiology, Warsaw Medical University, Warsaw, Poland

U. Demkow
Department of Laboratory Diagnostics and Clinical Immunology
of the Developmental Age, Warsaw Medical University,
Warsaw, Poland

M. Pokorski (ed.), *Respiratory Regulation - The Molecular Approach*,
Advances in Experimental Medicine and Biology 756, DOI 10.1007/978-94-007-4549-0_31,

31.1 Introduction

Adiponectin is secreted by white adipose tissue and exists as the most abundant adipokine in the human plasma. Adiponectin is dramatically up-regulated during adipogenesis and remains one of the most adipocyte-specific gene products identified to-date (Diez and Iglesias 2003). It is also known as ACRP30, apMI, adipoQ, and GBP28. Adiponectin is encoded by the ADIPOQ *gene* on chromosome 3q27, a region identified as susceptibility locus for the metabolic syndrome and T2DM by genome wide scans (Mori et al. 2002; Trujilio and Scerer 2005). Accumulating evidence shows that adiponectin regulates sensitivity for insulin, insulin resistance and β-cell dysfunction. Reduction of plasma/serum adiponectin levels is significantly related to the development of diabetes, obesity, and insulin resistance. Genetic studies have previously implicated the ADIPOQ locus as influencing variation in adiponectin levels (Heid et al. 2006; Pollin et al. 2005). Many studies have reported that single nucleotide polymorphisms (SNPs) in the adiponectin gene are associated with T2DM in different populations (Gibson and Froguel 2004, Hara et al. 2002). However, the results of these studies show strong racial and regional variations.

Experimental evidence suggests that adiponectin might play a protective role against atherosclerosis. Low plasma adiponectin has been reported in coronary heart disease and has correlated with some risk factors of cardiovascular diseases such as male sex, high blood pressure, obesity, and type 2 diabetes mellitus (Kazumi et al. 2002; Kondo et al. 2002). During the early phase of atherosclerosis, the macrophages secrete various cytokines and growth factors that promote smooth muscle cell's proliferation. Adiponectin has been shown to reduce the secretion of TNF-α by macrophages and to attenuate biological effects induced by TNF-α (Ouchi et al. 2001).

Adiponectin also inhibits the expression of intracellular adhesion molecule-1, endothelial cell adhesion molecule-1 and E-selectin in endothelial cells *in vitro* and prevents the attachment of monocytes to TNF-α prestimulated human aortic endothelial cell (Ouchi et al. 1999, 2001). The above outlined data suggest that this adipocyte-derived cytokine may exert anti-inflammatory and anti-atherogenic effects, especially on endothelial cells and macrophages, and may play a protective role in experimental models of vascular injury as well as in the early events of the atherosclerotic process. The relationship between plasma adiponectin level and various anthropometric and metabolic indices has been extensively studied in adults. Similarly in children and adolescents several studies suggest that plasma adiponectin can serve as an independent risk factor for the development of the metabolic syndrome, insulin resistance, or cardiovascular diseases later on in adulthood (Ogawa et al. 2005; Panagopoulou et al. 2008). Potentially, hypoadiponectinemia, together with other risk factors, may cause early progression of atherosclerosis in childhood and modulate the risk of cardiovascular diseases. The carotid artery intima media thickness (IMT) is an established, intermediate phenotype of atherosclerosis that has been used to monitor the development of pre-clinical atherosclerosis and to predict the onset of future cardiovascular events, such as myocardial infarction and stroke (Lorenz et al. 2007; O'Leary et al. 1999). IMT is an acknowledged morphological marker of early atherosclerosis and predictor of future cardiovascular events. This parameter can be measured non-invasively through the use of ultrasound imaging and enabling stratification of subjects into various risk classes.

The aim of this study was to investigate the association between adiponectin gene G276T polymorphism and plasma levels of adiponectin, IMT, lipids, HOMA-IR, and anthropometric measurements in obese children. We also studied whether selected risk factors for atherosclerosis (C-reactive protein) and lipid indicators are related to adiponectin levels.

31.2 Methods

The study protocol was approved by the Research and Ethics Committee of Warsaw Medical University in Warsaw, Poland. The examined group included 125 obese children and adolescents with simple obesity (62 girls and 63 boys) aged 11–18 (mean age 11.8 ± 3.3 years) sequentially recruited from

outpatients of the Pediatric Endocrinology Clinic at Children's Hospital of the Warsaw Medical University in Warsaw, Poland. There were no significant differences in age and sex among obese and non-obese children. A complete history was obtained and physical examination was carried out in all the participants.

The BMI was calculated as weight/height^2 (kg/m^2), BMI z-score adjusted for age and sex was calculated using normative data. Obesity was defined as a BMI z-score of more than +2. The BMI of all obese subjects was >95th percentile for age and sex reference values. The control group consisted of 34 healthy normal weight (BMI <85th percentile for age and sex reference values) children (17 girls and 17 boys) aged 11–18 years (mean age 13.5 ± 2.5). In 82 patients, the IMT was evaluated (67 obese and 15 non-obese children). All included children were free from any allergic disease, immune, and hematological disorders. Height (cm), weight (kg) and blood pressure were measured using standardized equipment. Waist circumference (cm) was measured and referred to percentile charts. Hip circumference (cm), WHR (waist-to-hip ratio) and the sum of the thickness of 3 and 10 skin and fat folds (mm) were measured and calculated. WHtR (waist-to-height ratio) was calculated. The percentage of fat tissue content measured in skin and fat folds on the arm and below the shoulder blade was calculated using Slaughter's equation (Slaughter et al. 1988). All children in the control group were at 25 percentile or less of the obesity measures. Hypertension was defined as a value of systolic and/or diastolic blood pressure ≥95th percentile for sex and age. Prehypertension was defined as a value of systolic and/or diastolic blood pressure from the 90 to 95th percentile. The IMT of the common carotid artery was determined using duplex ultrasonography. A value of IMT ≥0.5 mm was taken as abnormally increased.

31.2.1 Biochemical Tests

Oral glucose tolerance test (OGTT) in obese children included the measurements of glucose and insulin levels after a standard glucose load (1.75 g/kg, max 75 g) at 0, 30, 60, 90, 120 min after a prior 10–12-h fast. Insulin concentrations were measured by RIA (Radio-Immuno-Assay), plasma glucose level was measured using dry-chemistry method. Insulin resistance was estimated using the fasting plasma insulin homeostasis model assessment HOMA-IR [Gluk0min (mmol/l) × Ins0min (μU/ml):22.5].

Plasma total cholesterol (TC) and triglycerides (TG) were determined enzymatically on a Hitachi 912 analyzer (Roche Diagnostics). HDL cholesterol was measured using a homogenous method with polyethylene glycol-modified enzymes and alpha-cyclodextrin. LDL cholesterol was calculated by the Friedewald equation. C-reactive protein (CRP) was measured and the atherogenic indicators: TC/HDL, TG/HDL, non-HDL (TC minus HDL) were calculated. Adiponectin concentration were measured by RIA.

31.2.2 Genetic Tests

Genetic blood tests were performed in both groups of children. Genomic DNA was isolated using Genomic Midi AX isolation kit with ion-exchange membranes (A & A Biotechnology, Gdynia, Poland). Genotyping was done using polymerase chain reaction – restriction fragment length polymorphism analyses. Genomic DNA was amplified with specific flanking primers for 276G>T. The primers used for the PCR were: forward 5′-GGCCTCTTTCATCACAGACC-3′ and reverse 5′-AGATGCAGCAAAGCCAAAGT-3′. The amplified PCR product was digested with the addition BsmI enzymes (BioLabs, New England). The digested samples were separated by electrophoresis on 3% agarose gel and visualized. The identified genotypes were recognized according to the presence or absence of the enzyme restriction sites.

31.2.3 Statistical Analysis

The results were presented as means ± SD, minimum and maximum. The normality of data distribution was assessed by the Shapiro-Wilk test. A *t*-test for independent and non-independent samples was used to determine the intergroup differences. Pearson's χ^2 test was used to examine differences in characteristic variables and the distribution of genetic polymorphism between the two groups. In obese children, the odds ratio (OR) and 95% confidence interval (95%CI) were calculated to estimate the associations between polymorphic homozygous T and alleles G carriers. The Hardy-Weinberg equilibrium test was applied to evaluate genotype frequencies (Hosking et al. 2004). One-way analysis of variance ANOVA was used to investigate the relationship between the obesity measures, metabolic indices, IMT, adiponectin concentrations, and adiponectin gene polymorphisms. All analyses were performed using Statgraphics 9.0 plus and STATISTICA 9.0 software. Statistical significance was accepted at $p < 0.05$.

31.3 Results

Anthropometric and metabolic characteristics are presented in Table 31.1. The obese children had higher values of atherogenic indicators (TC/HDL: 4.6; TG/HDL: 3.65; non-HDL: 135.1 mg/dl) than the non-obese ones (TC/HDL: 2.6; TG/HDL: 1.5; non-HDL: 88.7 mg/dl, respectively ($p < 0.05$)). These indicators positively correlated with CRP ($p < 0.05$) and lipids (TC, LDL, HDL, TG). IMT amounted to 0.57 ± 0.12 mm in the obese children. In these children significant relations of the non-HDL ratio (TC minus HDL) to TC, TG, LDL, and TC/HDL were observed ($p < 0.05$). There were no differences between plasma lipids, IMT, or adiponectin concentrations between the obese and non-obese children.

The distribution of G276T of adiponectin gene polymorphism in the obese and non-obese children is presented in Fig 31.1. The frequency of alleles G and T in both groups was in HW equilibrium. The distribution of genotypes in the obese children was the following: GG (n = 45)–46.9%, GT (n = 34)–35.4%, TT (n = 17)–17.7%; and in the non-obese group: GG (n = 17)–47.2%, GT(n = 14)–38.9%, TT(n = 5)–13.9%. Homozygous TT carriers were more frequent in the obese than non-obese group: OR = 1.13 (95% C.I = 0.5–5.5), although the difference was not statistically significant $\chi^2 = 0.32$. The obese children were subdivided into two groups on the basis of the adiponectin genotypes (TT *vs.* GT + GG). The mean adiponectin serum levels were significantly lower in TT homozygous than in G (GG + GT) allele carriers in the obese group (ANOVA; F 6.25, $p < 0.01$).

The anthropometric indices, fasting plasma glucose (FPG), HOMA-IR, plasma lipids, lipid markers, IMT, systolic and diastolic blood pressure did not differ between the obese and non-obese children with TT genotype and carriers of G allele, irrespective of gender. The children with GG genotype had a lower body weight than the heterozygous GT: 59.8 ± 17.9 *vs.* 75.6 ± 25.0, $p = 0.02$. There were no significant differences between other anthropometric and metabolic indices, IMT, CRP, or adiponectin concentration. On the other hand, the children with GG genotype had decreases in body weight (59.8 ± 17.9 *vs.* 73.5 ± 24.2, $p = 0.01$), TC (162.3 ± 23.4 *vs.* 188.4 ± 11.6 mg/dl, $p = 0.008$), and TG (118.7 ± 57.9 *vs.* 185.0 ± 68.5 mg/dl, $p = 0.016$) and increases in adiponectin concentration (5.2 ± 2.4 *vs.* 9.8 ± 4.7 ng/ml, $p = 0.01$) compared with T allele carriers. The other indices FPG, HOMA-IR, lipids, IMT, and systolic and diastolic blood pressure did not differ between the obese children with gene polymorphism TT and wild homozygous GG.

The children with BMI z-score >6.0 (n = 6), compared with <6.0, had higher values of most of the anthropometric indices, especially of WHtR a characteristic parameter of central obesity (0.64 *vs.* 0.58, respectively, $p = 0.006$), IMT (0.65 ± 0.08 *vs.* 0.56 ± 0.08 mm, $p = 0.02$), and CRP

Table 31.1 Anthropometric and metabolic indices in obese and non-obese children

Anthropometric indices	Obese children (n = 125)	P<	Control group (n = 34)
Age (year)	11.8 ± 3.3	0.01	13.5 ± 2.5
Height (cm)	153.8 ± 17.2	0.05	161.8 ± 1.57
Body weight (kg)	71.7 ± 23.8	0.00001	49.9 ± 12.8
Body mass index (kg/m^2)	29.4 ± 5.1	0.00001	18.7 ± 2.6
SDS Body mass index (z-score)	3.8 ± 1.6	0.00001	–0.3 ± 0.7
Waist circumference (cm)	90.2 ± 12.3	0.00001	66.2 ± 7.7
Hip circumference (cm)	101.4 ± 13.6	0.00001	84.8 ± 9.4
Waist-to-hip ratio (WHR)	0.9 ± 0.1	0.00001	0.8 ± 0.1
Waist-to-height ratio (WHtR)	0.6 ± 0.1	0.00001	0.4 ± 0.0
Sum of 3 skinfold thickness (mm)	69.3 ± 12.9	0.00001	29.1 ± 12.3
Sum of 10 skinfold thickness (mm)	173.5 ± 27.7	NS	148.5 ± 27.6
% of body fat -Slaughter equation	33.8 ± 4.9	0.00001	20.6 ± 6.5
Total cholesterol (mg/dl)	176.8 ± 29.2	0.00001	150.0 ± 22.9
HDL (mg/dl)	44.1 ± 12.2	0.00001	57.5 ± 9.9
LDL (mg/dl)	104.2 ± 28.6	0.00001	74.9 ± 23.1
Triglycerides (mg/dl)	136.5 ± 70.2	0.001	79.7 ± 32.9
Glucose 0 min OGTT (mg/dl)	84.5 ± 10.5	NS	86.7 ± 11.5
Glucose 120 min OGTT (mg/dl)	123.0 ± 27.3	NS	115.0 ± 12.1
Insulin 0 min OGTT (μIU/ml)	16.0 ± 9.0	NS	11.2 ± 3.2
Insulin 120 min OGTT (μIU/ml)	100.4 ± 88.3	NS	94.8 ± 5.0
Adiponectin (ng/ml)	13.7 ± 5.9	0.01	16.7 ± 5.4
HOMA-IR	3.4 ± 2.1	NS	2.6 ± 1.0
CRP (mg/l)	0.5 ± 0.3	NS	0.4 ± 0.2
Systolic blood pressure (mmHg)	115.5 ± 11.6	NS	113.3 ± 9.5
Diastolic blood pressure (mmHg)	72.2 ± 8.9	NS	72.1 ± 9.2
non-HDL	135.1 ± 33.4	0.00001	88.7 ± 27.7
TC/HDL	4.59 ± 3.2	0.03	2.6 ± 0.7
TG/HDL	3.66 ± 2.9	0.01	1.5 ± 0.8
IMT (mm)	0.6 ± 0.1 (n = 67)	NS	0..5 ± 0.1(n = 15)

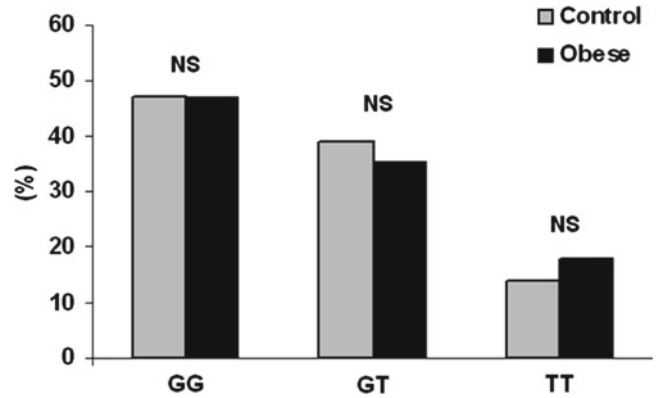

Fig. 31.1 Distribution of adiponectin genotypes in obese and non-obese children

(0.6 ± 0.4 *vs.* 0.4 ± 0.2 mg/l, p = 0.036). These children also had higher insulin concentrations (28.1 ± 16.4 *vs.* 15.3 ± 7.3 μIU/ml, p = 0.0007), HOMA-IR (6.2 ± 3.5 *vs.* 3.3 ± 1.9, p = 0.001), and decreased adiponectin concentrations (8.3 ± 1.6 *vs.* 16.5 ± 5.0 ng/ml, p = 0.001). In the children with extreme obesity, polymorphic changes of adiponectin gene were more frequent than in the non-obese group (3 carriers of GT and 3 carriers of TT genotype). IMT was increased in the obese children.

31.4 Discussion

In the present study we assessed whether adiponectin gene polymorphism at position +276 was associated with serum adiponectin concentration, insulin resistance or plasma lipids, the possible indices of subclinical atherosclerosis, in obese children. Several single-nucleotide polymorphisms (SNP) have been identified in adiponectin gene, including adipocyte, C1q, and collagen domain containing (ACDC). These genetic variations are associated with high risk of obesity, insulin resistance, type 2 diabetes (T2D), and other metabolic disturbances (Heid et al. 2006; Humphries et al. 2007). On the other hand, several other studies performed so far in the adult population show conflicting results regarding the association between these polymorphisms in regard to complex traits and to allele involved (Vozarova de Courten et al. 2005). The physiological mechanisms behind this genetic finding could be related to the effect of the ACDC SNP on the adiponectin level. Our present results, and data from other studies (Qi et al. 2005; Bouatia-Naji et al. 2005) are in favor of the association of obesity risk alleles 276GT with hipoadiponectinemia. Children with wild homozygous GG genotypes have a tendency toward higher values of adiponectin concentrations. In contrast, children with polymorphism TT have a tendency for hipoadiponectinemia. The limitations of our study include the possibility of false positive associations and a small sample size. Cieslak et al. (2011) in a group of 243 Polish children and adolescents with simple obesity found no consistent evidence for the association between obesity and the SNP in adiponectin gene. Those authors concluded that the SNPs tested (ADIPOQ: −11,377C > G, LEP: −2548C > T, 19A > G, RETN: −1300G > A, −1258C > T, and −420C > G) were not useful markers of childhood and adolescence obesity in the Polish population.

The relative contribution of genetic risk factors to the progression of subclinical atherosclerosis is poorly understood. It is likely that multiple variants are implicated in the development of atherosclerosis, but subtle genotypic and phenotypic differences are beyond the reach of the conventional case-control designs and the statistical procedures used in most association studies.

Adiponectin seems protective against atherosclerosis and the determination of its plasma levels may help assess the risk of coronary artery disease. A vasoprotective effect of adiponectin is supported by *in vitro* studies showing that adiponectin decreases the expression of adhesion molecules on the endothelial cells, suppresses the foam cell formation by macrophages, and inhibits vascular smooth muscle migration (Ouchi et al. 1999, 2001). However, the data concerning adiponectin plasma levels and increased IMT in obese adults as well as the association with mortality after cardiovascular events are contradictory (Jansson et al. 2003; Matsuda et al. 2004). In particular, the role of adiponectin at very early stages of atherosclerosis remains unclear, especially in children.

In the present study we failed to find a relation between adiponectin gene polymorphism at position +276 and subclinical atherosclerosis determined by the IMT measurements, CRP, and lipid indices in obese children. We noted just a tendency for higher values of total cholesterol concentrations and triglycerides in these children.

Monitoring the atherosclerotic changes in children has substantial limitations. Arnaiz et al. (2010) in a cross-sectional study in a group of 103 children determined BMI, waist circumference, percent fat mass, systolic and diastolic blood pressures, fasting lipid profile, glycemia and insulinemia, and CRP. These indices were compared to subclinical atherosclerosis determined by carotid intima media thickness and flow-mediated dilation of the brachial artery (FMD). Adiponectin correlated significantly with age, BMI, z-score BMI, waist circumference, systolic and diastolic blood pressures, HDL, insulinemia, and the HOMA index. No significant association between adiponectin and CRP, FMD, or IMT was found. When adjusting for sex, pubertal status, and the degree of obesity, the adiponectin levels correlated significantly with HDL cholesterol and the HOMA index. Those authors concluded that the adiponectin level is inversely related to the anthropometric indices of obesity and insulin resistance but is directly related to HDL levels. In our study, no relationship between subclinical atherosclerosis and adiponectic level was demonstrated. In obese children, the process of atheroclerosis occurs early, but any relation between the surrogate markers of atherosclerosis and various metabolic

indices is not straightforward. Moreover, in coronary artery disease-related case-control studies, individual SNPs seem to have only a minor role in predicting carotid IMT or its progression, when compared with the conventional risk factors (Fan et al. 2009; Samani et al. 2008). In fact, these variants are able to provide only a marginal and inconsistent improvement even in the discrimination of CHD cases or prediction of cardiovascular events (Cordell 2009; Arnaiz et al. 2010). In the present study, obese children demonstrated higher values of most of the anthropometric indices, notably of WHtR – a characteristic marker of central obesity, and of IMT, CRP, and lipids – noninvasive markers for early atherosclerotic changes. In children with morbid obesity, the polymorphism of adiponectin gene was more frequently detected than in non-obese children.

In summary, we showed that adiponectin concentrations are decreased in obese children with polymorphism G276T in adiponectin gene, but we did not find any significant relation of adiponectin to carotid IMT, lipid indices, blood pressure, or HOMA-IR. We submit that vascular changes in morbid obesity may occur already in childhood and can be connected to the examined polymorphism in adiponectin gene.

Conflicts of Interest: The authors declare no conflicts of interest in relation to this article.

References

Arnaiz, P., Acevedo, M., Barja, S., Aglony, M., Guzmán, B., Cassis, B., Carvajal, J., Moreno, M., Navarrete, C., & Berríos, X. (2010). Adiponectin levels, cardiometabolic risk factors and markers of subclinical atherosclerosis in children. *International Journal of Cardiology, 138*(2), 138–144.

Bouatia-Naji, N., Meyre, D., Lobbens, S., Séron, K., Fumeron, F., Balkau, B., Heude, B., Jouret, B., Scherer, P. E., Dina, C., Weill, J., & Froguel, P. (2005). ACDC/adiponectin polymorphisms are associated with severe childhood and adult obesity. *Diabetes, 55*(2), 545–550.

Cieslak, J., Skorczyk, A., Stachowiak, M., Szydłowski, M., Grzes, M., Paczynska, P., Skowronska, B., Majewska, K., Stankiewicz, W., Fichna, P., & Switoński, M. (2011). Polymorphisms in 5′-flanking regions of genes encoding adiponectin, leptin, and resistin are not associated with obesity of polish children and adolescents. *Molecular Biology Reports, 38*(3), 1793–1798.

Cordell, H. J. (2009). Genome-wide association studies: Detecting gene-gene interactions that underlie human diseases. *Nature Reviews Genetics, 10*, 392–404.

Diez, J. J., & Iglesias, P. (2003). The role of the novel adipocyte-derived hormone adiponectin in human disease. *European Journal of Endocrinology, 148*, 293–300.

Fan, Y. M., Raitakari, O. T., Kähönen, M., Hutri-Kähönen, N., Juonala, M., Marniemi, J., Viikari, J., & Lehtimäki, T. (2009). Hepatic lipase promoter C-480T polymorphism is associated with serum lipids levels, but not subclinical atherosclerosis: The Cardiovascular Risk in Young Finns Study. *Clinical Genetics, 76*, 46–53.

Gibson, F., & Froguel, P. (2004). Genetics of the APM1 locus and its contribution to type 2 diabetes susceptibility in French Caucasians. *Diabetes, 53*, 2977–2983.

Hara, K., Boutin, P., Mori, Y., Tobe, K., Dina, C., Yasuda, K., Yamauchi, T., Otabe, S., Okada, T., Eto, K., Kadowaki, H., Hagura, R., Akanuma, Y., Yazaki, Y., Nagai, R., Taniyama, M., Matsubara, K., Yoda, M., Nakano, Y., Tomita, M., Kimura, S., Ito, C., Froguel, P., & Kadowaki, T. (2002). Genetic variation in the gene encoding adiponectin is associated with an increased risk of type 2 diabetes in the Japanese population. *Diabetes, 51*(2), 536–540.

Heid, I. M., Wagner, S. A., Gohlke, H., Iglseder, B., Mueller, J. C., Cip, P., Ladurner, G., Reiter, R., Stadlmayr, A., Mackevics, V., Illig, T., Kronenberg, F., & Paulweber, B. (2006). Genetic architecture of the APM1 gene and its influence on adiponectin plasma levels and parameters of the metabolic syndrome in 1,727 healthy Caucasians. *Diabetes, 55*, 375–384.

Hosking, L., Lumsden, S., Lewis, K., Yeo, A., McCarthy, L., Bansal, A., Riley, J., Purvis, I., & Xu, C. (2004). Detection of genotyping errors by Hardy-Weinberg equilibrium testing. *European Journal of Human Genetics, 12*, 395–399.

Humphries, S. E., Cooper, J. A., Talmud, P. J., & Miller, G. J. (2007). Candidate gene genotypes, along with conventional risk factor assessment, improve estimation of coronary heart disease risk in healthy UK men. *Clinical Chemistry, 53*, 8–16.

Jansson, P. A., Pellme, F., Hammarstedt, A., Sandqvist, M., Brekke, H., Caidahl, K., Forsberg, M., Volkmann, R., Carvalho, E., Funahashi, T., Matsuzawa, Y., Wiklund, O., Yang, X., Taskinen, M. R., & Smith, U. (2003). A novel cellular marker of insulin resistance and early atherosclerosis in humans is related to impaired fat cell differentiation and low adiponectin. *The FASEB Journal, 17*, 1434–1440.

Kazumi, T., Kawaguchi, A., Sakai, K., Hirano, T., & Yoshino, G. (2002). Young men with high-normal blood pressure have lower serum adiponectin smaller LDL size, and higher elevated heart rate than that with optimal blood pressure. *Diabetes Care, 25*, 971–976.

Kondo, H., Shimomura, I., Matsukawa, Y., Kumada, M., Takahashi, M., Matsuda, M., Ouchi, N., Kihara, S., Kawamoto, T., Sumitsuji, S., Funahashi, T., & Matsuzawa, Y. (2002). Association of adiponectin mutation with type 2 diabetes. A candidate gene for the insulin resistance syndrome. *Diabetes, 51*, 2325–2328.

Lorenz, M. W., Markus, H. S., Bots, M. L., Rosvall, M., & Sitzer, M. (2007). Prediction of clinical cardiovascular events with carotid intima-media thickness: A systematic review and meta-analysis. *Circulation, 115*, 459–467.

Matsuda, M., Kawasami, F., Hamada, K., Kanda, Y., Saito, M., Eto, M., Matsuki, M., & Kaku, K. (2004). Impact of adiposity and plasma adipocytokines on diabetic angiopathies in Japanese Type 2 diabetic subjects. *Diabetic Medicine, 21*, 881–888.

Mori, Y., Otabe, S., Dina, C., Yasuda, K., Populaire, C., Lecoeur, C., Vatin, V., Durand, E., Hara, K., Okada, T., Tobe, K., Boutin, P., Kadowaki, T., & Froguel, P. (2002). Genome-wide search for type 2 diabetes in Japanese affected sib-pairs confirms susceptibility genes on 3q, 15q, and 20q and identifies two new candidate Loci on 7p and 11p. *Diabetes, 51*(4), 1247–1255.

O'Leary, D. H., Polak, J. F., Kronmal, R. A., Magnolio, T. A., & Burke, G. L. (1999). Carotid-artery intima and media thickness as a risk factor for myocardial infarction and stroke in older adults. Cardiovascular Health Study Collaborative Research Group. *The New England Journal of Medicine, 340*, 14–22.

Ogawa, Y., Kikuchi, T., Nagasaki, K., Hiura, M., Tanaka, Y., & Uchiyama, M. (2005). Usefulness of serum adiponectin level as a diagnostic marker of metabolic syndrome in obese Japanese children. *Hypertension Research, 28*, 51–57.

Ouchi, N., Kihara, S., Arita, Y., Maeda, K., Kuriyama, H., Okamoto, Y., Hotta, K., Nishida, M., Takahashi, M., Nakamura, T., Yamashita, S., Funahashi, T., & Matsuzawa, Y. (1999). Novel modulator for endothelial adhesion molecules: Adipocyte-derived plasma protein adiponectin. *Circulation, 100*, 2473–2476.

Ouchi, N., Kihara, S., Arita, Y., Nishida, M., Matsuyama, A., Okamoto, Y., Ishigami, M., Kuriyama, H., Kishida, K., Nishizawa, H., Hotta, K., Muraguchi, M., Ohmoto, Y., Yamashita, S., Funahashi, T., & Matsuzawa, Y. (2001). Adipocyte-derived plasma protein, adiponectin suppresses lipid accumulation and class A scavenger receptor expression in human monocyte-derived macrophages. *Circulation, 103*, 1057–1063.

Panagopoulou, P., Galli-Tsinopoulou, A., Fleva, A., Pavlitou-Tsiontsi, E., Vavatsi-Christaki, N., & Nousia-Arvanitakis, S. (2008). Adiponectin and insulin resistance in childhood obesity. *Journal of Pediatric Gastroenterology and Nutrition, 47*, 356–362.

Pollin, T. I., Tanner, K., O'connell, J. R., Ott, S. H., Damcott, C. M., Shuldiner, A. R., McLenithan, J. C., & Mitchell, B. D. (2005). Linkage of plasma adiponectin levels to 3q27 explained by association with variation in the APM1 gene. *Diabetes, 54*, 268–274.

Qi, L., Li, T., Rimm, E., Zhang, C., Rifai, N., Hunter, D., Doria, A., & Hu, F. B. (2005). The 276 polymorphism of the APM1 gene, plasma adiponectin concentration, a cardiovascular risk in diabetic men. *Diabetes, 54*, 1607–1610.

Samani, N. J., Raitakari, O. T., Sipila, K., Tobin, M. D., Schunkert, H., Juonala, M., Braund, P. S., Erdmann, J., Viikari, J., Moilanen, L., Taittonen, L., Jula, A., Jokinen, E., Laitinen, T., Hutri-Kähönen, N., Nieminen, M. S., Kesäniemi, Y. A., Hall, A. S., Hulkkonen, J., Kähönen, M., & Lehtimäki, T. (2008). Coronary artery disease-associated locus on chromosome 9p21 and early markers of atherosclerosis. *Arteriosclerosis, Thrombosis, and Vascular Biology, 28*, 1679–1683.

Slaughter, M. H., Lohman, T. G., Boileau, R. A., Horswill, C. A., Stillman, R. J., Van Loan, M. D., & Bemben, D. A. (1988). Skinfold equations for estimation of body fatness in children and youth. *Human Biology, 60*, 709–723.

Trujilio, M. E., & Scerer, P. E. (2005). Adiponectin-journey from an adipocyte secretory protein to biomarker of the metabolic syndrome. *Journal of Internal Medicine, 257*, 167–175.

Vozarova de Courten, B., Hanson, R. L., Funahashi, T., Lindsay, R. S., Matsuzawa, Y., Tanaka, S., Thameem, F., Gruber, J. D., Froguel, P., & Wolford, J. K. (2005). Common polymorphisms in the adiponectin gene ACDC are not associated with diabetes in Pima Indians. *Diabetes, 54*, 284–289.

Chapter 32
Relation of Fat-Mass and Obesity-Associated Gene Polymorphism to Fat Mass Content and Body Mass Index in Obese Children

Beata Pyrzak, Alicja Wisniewska, Anna Majcher, Andrzej Tysarowski, and Urszula Demkow

Abstract Fat mass content, fat distribution, and fat-mass and obesity associated (FTO) gene have been reported among a broad spectrum of genetic variation connected with body weight. The aim of our study was to investigate whether the T/A rs9939609 polymorphism of the FTO gene may influence obesity and metabolic indices in children. A 160 children were examined (136 obese and 24 non-obese). The anthropometric measurements and calculations included: height, weight, waist and hip circumference, sum of the thickness of 3 and 10 skin folds, % of fat content, % FAT- BIA , % LBM-BIA. BMI, SDS of BMI, WHR, and WHtR. Fasting plasma total cholesterol (TC), HDL and LDL-cholesterol, triglycerides (TG), oral glucose tolerance test (OGTT), and HOMA-IR were analyzed and the blood pressure were measured. The rs9939609 polymorphism of FTO gene was genotyped by allele-specific real-time polymerase chain- reaction (RT-PCR). We found that the mean concentrations of TC, TG, LDLC, and HOMA-IR were significantly higher, and HDL was lower in the obese than in non-obese children. The presence of TT, but not AA alleles, related to the percentage of fat content, BMI, and z-score of BMI. None of the other anthropometric indices did differ between the children with gene polymorphism and wild homozygous. In conclusion, rs9939609 polymorphism in the fat-mass and obesity-associated gene is associated with BMI and the percent of fat content in children.

Keywords Obesity associated gene • Polymorphism • Children • Oral glucose tolerance • Fat content

32.1 Introduction

Childhood obesity is increasing worldwide and is a risk factor for various disorders including type 2 diabetes, hypertension, cardiovascular disease, stroke, and cancer. Obesity is a major international public health and economic concern and has to do with environmental factors, such as low physical

B. Pyrzak (✉) • A. Wisniewska • A. Majcher
Department of Pediatric and Endocrinology, Warsaw Medical University,
Marszalkowska 24 St., 00-576 Warsaw, Poland
e-mail: beata.pyrzak@wum.edu.pl

A. Tysarowski
Department of Molecular Biology, The Maria Sklodowska-Curie Memorial Cancer Center and Institute of Oncology, Warsaw, Poland

U. Demkow
Department of Laboratory Diagnostics and Clinical Immunology of the Developmental Age, Warsaw Medical University, Warsaw, Poland

M. Pokorski (ed.), *Respiratory Regulation - The Molecular Approach*,
Advances in Experimental Medicine and Biology 756, DOI 10.1007/978-94-007-4549-0_32,

activity and overeating. However, genome-wide linkage and candidate gene association studies showed a relation of body mass index (BMI) and adiposity to variations in the fat-mass and obesity related locus FTO in adults and children (Karasawa et al. 2010; Sovio et al. 2011; Xi et al. 2010; Zimmermann et al. 2011). FTO is widely expressed in almost all tissues, but its exact role is unknown. FTO was first identified in the mouse by positional cloning (Peters 1999) as one of the genes within a 1.6 megabase deletion on chromosome 8 responsible for the Fused toes (Ft) phenotype (van der Hoeven 1994).

Mice homozygous for the deletion die mid-gestation and exhibit severe malformations of the head and face, central nervous system (CNS) developmental defects, randomized left-right asymmetry, polydactyly and growth retardation (van der Hoeven 1994; Gotz 2005; Anselme 2007). Heterozygotes display fused toes and enlargement of the thymus. However, no obesity or slimness was reported in these mice. Similar phenotype to that of Ft mice was seen in a human patient carrying a small chromosomal duplication on 16q12.2, a region that includes the FTO gene (Stratakis 2000). The discovery that this gene was associated with human obesity inspired further research aimed at elucidating its functional properties. Sequence analysis showed that FTO shares features with Fe(II) and 2-oxoglutarate (2OG) oxygenase. These enzymes catalyze oxidative reactions on multiple substrates using non-heme iron as a cofactor and 2OG as a co-substrate. Within this superfamily, FTO is most similar to the *Escherichia coli* enzyme AlkB and its eukaryotic homologs, which can repair DNA methylation damage by hydroxylation of methyl groups on the DNA leading to their removal. These data suggest that FTO might act as a demethylase (Gerken 2007; Sanchez-Pulido and Andrade-Navarro 2007; Fawcett and Barroso 2010). Human FTO and its vertebrate homologs are globular proteins that carry a nuclear localization signal and are unlikely to be targeted to membranes or organelles. That suggests that the nucleic acid demethylation activity of FTO might regulate the expression of genes involved in metabolism and that deregulation of this process might lead to obesity. Studies of mouse Fto and human FTO mRNA showed high levels of expression in the hypothalamic regions known to play important roles in the regulation of energy intake and expenditure, and suggest that the expression of FTO might be regulated by nutritional status (Fredriksson 2008; Gerken 2007). In the fasted state, mice exhibit a significant reduction in hypothalamic FTO mRNA expression compared with well-fed controls. This effect is not reversed by supplementation of the anti-starvation hormone leptin, which suggests that reduced hypothalamic FTO expression observed during fasting is independent of leptin level (Gerken 2007; Stratigopoulos 2008). Studies in mice suggest that FTO is down-regulated during fasting and up-regulated during feeding and these variations in FTO, resulting in decreased expression or activity, might provide a signal that promotes feeding and obesity. In contrast to the mouse data, FTO expression increases significantly in the hypothalamus of food-deprived and food-restricted rats (Fredriksson 2008); being likely strongly connected with circadian rhythmicity.

Further studies in FTO mouse models have shown that FTO knock-out mice develop postnatal growth retardation with a significant reduction of adipose tissue. The extreme leanness of FTO knock-out mice is a consequence of increased energy expenditure, despite decreased activity of animals and increased energy intake (Fischer et al. 2009). In humans, reports on the potential impact of FTO variants on dietary intake and energy expenditure have been inconsistent (Cecil et al. 2008; Hasselbalch et al. 2010; Haupt et al. 2009; Speakman et al. 2008).

Recently, the fat-mass and obesity-associated FTO gene was identified to be associated with obesity by several genome-wide association studies (Meyre et al. 2009). Because the FTO gene is highly polymorphic, several polymorphisms of the gene have been found to be associated with obesity or obesity phenotypes (Hotta et al. 2008; Rong et al. 2009). The rs9939609 FTO gene polymorphism has been most extensively studied and allele A was frequently associated with the obesity phenotype (Hotta et al. 2008; Rong et al. 2009). In the present study we examined the relation of FTO gene polymorphism rs9939609 to anthropometric indices in children.

32.2 Methods

The study protocol was approved by the Research and Ethics Committee of Warsaw Medical University in Warsaw, Poland. The examined group consisted of 136 obese children and adolescents with simple obesity (73 girls and 63 boys) aged 12–18 (mean age 12.5) years old sequentially recruited from outpatient of Endocrinology Clinic at Medical University of Warsaw's Children Hospital. There were no significant differences in age and sex among obese and non-obese children. A complete history was obtained and physical examination was carried out on all the participants.

The BMI (weight/height^2) of all obese subjects was >95th percentile for age and sex reference values. The control group consisted of 24 healthy children (11 girls and 13 boys) with normal body weight (BMI <85th percentile for age and sex reference values) aged 11–18 (mean age 13.8 years). All included children were free from any allergic disease, immune and hematological disorders. Height (cm), weight (kg) and systolic (SBP) and diastolic (DBP) blood pressure were measured using standardized equipment. The BMI was calculated as weight/height^2 (kg/m^2), BMI z-score adjusted for age and sex was calculated using normative data. Obesity was defined as a BMI z-score of more than +2. Waist circumference (cm) was measured and referred to the percentile charts. Hip circumference (cm), WHR (waist-to-hip ratio), waist-to-height ratio (WHtR), and the sum of the thickness of 3 and 10 skin and fat folds (mm) were measured. The percentage of fat tissue content measured in the skin and fat folds on the arm and below the shoulder blade was calculated using Slaughter's equation (Slaughter et al. 1988). Bioelectrical impedance analysis - BIA (% of fat FAT-BIA and % of lean LBM-BIA) on hand-to-leg in horizontal position was undertaken with a Maltron Body Fat-905. All children in the control group were at the 25th percentile or less of the obesity measures. Hypertension was defined as a value of systolic and/or diastolic blood pressure ≥95th percentile for sex and age. Prehypertension was defined as a value of systolic and/or diastolic blood pressure between the 90–95th percentile.

32.2.1 Biochemical Tests

Oral glucose tolerance test (OGTT) based on the measurements of glucose and insulin levels at 0, 30, 60, 90, 120 min after 10–12 h fast was performed with the use of a standard load of glucose (1.75 g/kg, max 75 g) in the group of obese children. The insulin concentration was measured by RIA (Radio-Immuno-Assay) and fasting plasma glucose (FPG) by a dry-chemistry method. Insulin resistance was estimated using the fasting plasma insulin homeostasis model HOMA-IR [Gluk0min (mmol/l) × Ins0min (μU/ml):22.5]. Plasma total cholesterol (TC) and triglycerides (TG) were determined enzymatically on a Hitachi 912 analyzer (Roche Diagnostics). HDL was measured using a homogenous method with polyethylene glycol-modified enzymes and alpha-cyclodextrin. LDL was calculated by the Friedewald equation.

32.2.2 Genetic Tests

The rs9939609 polymorphism of the FTO gene was genotyped by allele-specific real-time polymerase chain- reaction (RT-PCR). Genomic DNA was isolated using Genomic Midi AX isolation kit with ion-exchange membranes (A & A Biotechnology, Gdynia, Poland).

The primers and probes were part of the TaqMan MGB kit delivered by Applied Biosystems (Nr. 4351379 and C-30090620-10). The reaction was performed in the 7,500 Fast Real-Time PCR System (Applied Biosystems, Foster City, CA, USA) and fluorescence data were analyzed in genotyping

mode by the instrument's software v. 2.0.5. The final volume of the reaction mix was 20 μl with ~50 ng of DNA, 10 μl of 2 × TaqMan Universal PCR Master Mix (Applied Biosystems), 1 μl of TaqMan assay and filled with water to final volume. PCR condition: 10 min at 95°C for initial denaturation followed by 40 cycles of the following steps: 95°C for 15 s and 60°C for 1 min. PCR reaction was performed in MicroAmp Fast 96-Well Reaction Plate (0.1 ml) with MicroAmp® Optical Adhesive Film (Applied Biosystems).

32.2.3 Statistical Analysis

The results were presented as means ± SD, minimum and maximum. The normality of data distribution was assessed by the Shapiro-Wilk test. A *t*-test for independent and non-independent samples was used to determine intergroup differences. Logistic regression was used to investigate the relationship between the obesity measures, metabolic features and the examined polymorphisms. The proportional odds model was also used to obtain odds ratios for the association of each obesity measure with a given genotype. $\chi 2$ test was used to investigate the distribution of genetic polymorphism between the two groups and to determine relations between categorical variables. Statistical significance was accepted at $p < 0.05$. The Hardy-Weinberg equilibrium test was applied to evaluate genotype frequencies. The results were processed statistically using Statgraphics 9.0 plus and STATISTICA 9.0 software.

32.3 Results

The frequency of alleles A and T in both case and control groups were in HW (Hardy-Weinberg) equilibrium and were following: in the obese children TT-26%, AA-25%, and AT-49%; in control group TT-21%, AA-25%, and AT-54%. In the obese group, all auxological parameters assessing the extent of obesity were significantly elevated (Fig. 32.1).

In the obese children, analysis was carried out to test the association of FTO rs9939609 and obesity-related measures. The carriers of AA/AT had higher values of the weight, height, BMI, SDS BMI, waist and hip circumference, WHR, and percent of fat content compared with the TT homozygous, but the differences did not reach statistical significance. There was a tendency for a relation of single nucleotide polymorphisms (SNP) to BMI and to SDS BMI ($p = 0.07$ & $p = 0.06$)

We did not observe significant associations of TT or AA/AT with WHtR, % FAT-BIA, LBM-BIA, TC, HDL, LDL, TG, FPG, HOMA-IR, SBP, DBP (Table 32.1). We also tested the association of rs9939609 with anthropometric and metabolic indices between boys and girls and could not substantiate any differences.

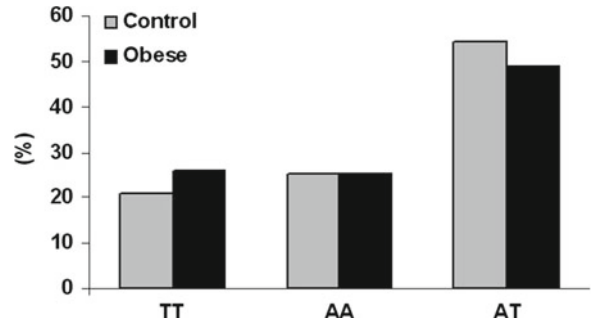

Fig. 32.1 Distribution of FTO genotypes in the obese and control groups

Table 32.1 Comparisons between TT *vs.* AA carriers and TT *vs.* AA/AT carriers

	TT (n = 36)	AA (n = 34)	p	AA/AT (n = 100)	p
Weight (kg)	71.0 ± 23.2	73.2 ± 28.9	NS	75.6 ± 23.0	NS
Height (cm)	156.6 ± 17.2	157.1 ± 15.7	NS	157.4 ± 15.9	NS
BMI	28.0 ± 3.9	30.4 ± 5.5	<0.05	29.7 ± 4.9	NS (0.07)
SDS BMI	3.3 ± 1.3	4.1 ± 1.8	<0.05	3.8 ± 1.5	NS (0.06)
Waist circum. (cm)	89.9 ± 13.7	92.2 ± 14.4	NS	91.3 ± 12.5	NS
Hip circum. (cm)	100.6 ± 12.2	104.8 ± 18.2	NS	104.3 ± 13.6	NS
WHR	0.9 ± 0.1	0.9 ± 0.1	NS	0.9 ± 0.1	NS
% fat content	32.9 ± 4.8	39.0 ± 4.8	p < 0.05	33.6 ± 5.0	NS
TC (mg/dl)	176.3 ± 32.12	184.1 ± 40.3	NS	182.7 ± 34.1	NS
HDL (mg/dl)	44.4 ± 8.8	41.2 ± 7.1	NS (0.07)	42.1 ± 8.3	NS
LDL (mg/dl)	117.6 ± 20.6	120.6 ± 24.6	NS	118.2 ± 28.2	NS
TG (mg/dl)	125.2 ± 25.1	134.2 ± 34.8	NS	136.4 ± 30.2	NS
FPG (mg/dl)	74.3 ± 11.2	75.4 ± 12.1	NS	76.0 ± 10.8	NS
HOMA-IR	3.4 ± 1.2	3.7 ± 1.1	NS (0.08)	3.5 ± 1.8	NS
SBP (mmHg)	105.6 ± 12.4	110.2 ± 24.6	NS	110.8 ± 20.2	NS
DBP (mmHg)	65.8 ± 8.8	66.2 ± 8.8	NS	66.2 ± 10.2	NS

Data are means ± SD. AA and AA/AT carriers were each compared with TT carriers. See Sect. 32.2 for acronyms

Analyzing the association between wild homozygous and AA genotypes we found that BMI, SDS BMI, and the percentage of fat content of AA genotype carriers were significantly higher compared with those in the TT genotype (BMI 28.1 ± 3.9 *vs.* 30.4 ± 5.5, p < 0.05; SDS BMI 3.3 ± 1.3 *vs.* 4.1 ± 1.8, p < 0.05; % of fat content 32.9 ± 4.8 *vs.* 39.0 ± 4.8, p < 0.05) (Table 32.1). A tendency for a lower value of HDL and elevated levels of HOMA-IR in AA homozygous compared with TT homozygous was noted. After adjustment for gender, MANOVA analysis did not show any differences between polymorphism of rs9939609 in the FTO gene and BMI, SDS BMI, and the percentage of fat content. In the control group, the patients subdivided into those with and without polymorphism did not show any differences in the anthropometric and metabolic indices.

32.4 Discussion

Previous studies of the FTO gene have found a highly significant association of the common SNP rs9939609 with BMI in several European populations and in children and adolescents in Asia (Xi et al. 2010). BMI is a convenient surrogate measure for obesity but it may be influenced by changes in height, bone mass, lean mass, and adiposity. In our study, we confirmed that the children carrying risk allele have a higher BMI and more adiposity than children with no A alleles. We did not investigate energy expenditure or energy intake, but several studies in children try to explain the role of this polymorphism in energy balance. The biological mechanisms behind this association are not yet fully understood. Functional investigations have suggested that this locus is likely involved in the hypothalamic regulation of appetite or energy expenditure and metabolic rate (Cecil et al. 2008; Speakman et al. 2008). Wardle et al. (2009) in a group of 131 children aged 4–5 tested the hypothesis that food intake would be associated with the FTO genotype status. The authors showed that children with two copies of the lower-risk FTO alleles have a lower BMI than those with one or two higher-risk alleles. They conclude that the T allele is protective against overeating by promoting responsiveness to internal signals of satiety. Sovio et al. (2011) in meta-analyzed associations between the FTO locus (rs9939609) and BMI in samples taken from children, aged from early infancy to 13 years of age, from eight

cohorts of European ancestry, found a positive association between additional minor (A) alleles and BMI from the 5.5 years olds onward, but an inverse association below the age of 2.5 years. They also found that carriers of minor alleles showed a lower BMI in infancy, earlier adiposity rebound (AR), and a higher BMI later in childhood. They confirmed the expected association between variations in rs9939609 and BMI in childhood, but only in the presence of an inverse association between the same variant and BMI in infancy. These results provide important information about the longitudinal gene effects and about the role of FTO in adiposity.

The influence of SNP of the FTO gene has also been shown to change over time. Probably it is connected with the timing of puberty. Rutters et al. (2011) investigated the relationship between SNP of the FTO gene (rs9939609) and obesity-related characteristics longitudinally during childhood and puberty in 101 children (58 boys and 43 girls). They concluded that the FTO A allele (rs9939609) is associated with the higher BMI, fat mass index, and leptin concentrations from the age of 12 years, whereas the associations show a dip at the age of 13–14 years and become stronger at the age of 17 years. The dip is presumably caused by the dominating endocrinological changes at mid-puberty. In the present study we found a relationship between gene polymorphism and the percentage of fat content, as assessed from the measurements of skin and fat folds on the arm and below the shoulder blade calculated using Slaughter's equation, which is dependent on the phase of puberty. We did not find any relationships between gene polymorphism and the waist or hip circumference; the measurements related to the trunk obesity. Juvenile obesity usually leads to obesity in adulthood which causes life threatening sequels such as diabetes, cardiovascular disease, hypertension, stroke, and cancer. Other authors have found such relationships as well. Mangge et al. (2011) have analyzed the single nucleotide polymorphism rs9939609 of FTO in 371 Styrian adolescents in relation to the degree of obesity, subcutaneous adipose tissue (SAT)-distribution determined by lipometry, and early metabolic and preatherosclerotic symptoms. The percentage of AA homozygotes for the rs9939609 SNP of FTO was significantly increased in obese adolescents. In that study, compared with the TT wild type, AA homozygotes showed significantly elevated values of SAT thickness at the trunk-located lipometer measurement points of the neck and frontal chest, of body weight, body mass index, waist, and hip circumference. No associations were found with carotis communis intima media thickness, systolic and diastolic blood pressure, ultrasensitive C-reactive protein (US-CRP), homocystein, total cholesterol, triglycerides, HDL cholesterol, oxidized LDL, fasted glucose, insulin, HOMA-index, liver transaminases, uric acid, adipokine-like resistin, leptin, and adiponectin.

In the present study we found a weak association between the examined polymorphism and HDL or HOMA–IR. We plan to screen these groups for the presence of overt metabolic and atherosclerotic disease symptoms later in life, and especially to study the clinical end points in the group of homozygotic rs9939609 carriers. The risk groups also will be a target for counseling concerning their future lifestyle. On the other hand, a study of Mook-Kanamori et al. (2011) has examined the effect of FTO genotype on body composition at the age of 6 months using skinfold thickness measurements and dual energy X-ray absorptiometry (DXA). That study was embedded in a population-based prospective cohort study from early fetal life onward. The FTO genotype was related to anthropometric measurements (weight and height), subcutaneous fat mass measured by skinfold thickness, and total, truncal, and peripheral fat mass and lean mass measured by DXA. Analyses for skinfold thickness and DXA were performed in 695 and 216 children, respectively. The authors found no significant differences between FTO genotypes in weight, height or BMI. Furthermore, the FTO genotype was not associated with skinfold thickness. Finally, they did not find any associations between the FTO genotype and body composition measures (fat and lean mass) assessed by DXA The authors concluded that longer follow-up studies are necessary to examine at what age and by which mechanisms the FTO genotype starts to influence fat mass and body composition.

Physical activity can be an important factor modifying the effect of FTO genotype. Scott et al. (2010) examined 1–5 years old children in the Growth, Exercise and Nutrition Epidemiological Study in preschoolers (GENESIS) (n = 1,980) and 11–18 years old Greek adolescents (n = 949). The authors

concluded that the FTO genotype effect was more pronounced in inactive than active males. Inactive males homozygous for the A allele had a higher mean BMI 3 kg/m^2 than T carriers. In this study, no significant association between the FTO genotype and adiposity was found. However, in a relatively large study of Jonsson et al. (2010), no evidence for the interaction between FTO and physical activity has been found.

In conclusion, in our study the FTO gene polymorphism rs9939609 was found to be associated with obesity. The limitations of this study include a small sample size and a limited statistical power. Although the analysis of the study seems sufficient to detect a relationship between FTO and obesity, it could not confirm the presence of relations between FTO and some metabolic parameters. These aspects require further research.

Conflicts of interest: The authors declare no conflicts of interest in relation to this article.

References

Anselme, I. (2007). Defects in brain patterning and head morphogenesis in the mouse mutant Fused toes. *Developmental Biology, 304*, 208–220.

Cecil, J. E., Tavendale, R., Watt, P., Hetherington, M. M., & Palmer, C. N. (2008). An obesity-associated FTO gene variant and increased energy intake in children. *The New England Journal of Medicine, 359*, 2558–2566.

Fawcett, K. A., & Barroso, I. (2010). The genetics of obesity: FTO leads the way. *Trends in Genetics, 26*, 266–274.

Fischer, J., Koch, L., Emmerling, C., Vierkotten, J., Peters, T., Brüning, J. C., & Rüther, U. (2009). Inactivation of the *Fto* gene protects from obesity. *Nature, 458*, 894–898.

Fredriksson, R. (2008). The obesity gene, FTO, is of ancient origin, up-regulated during food deprivation and expressed in neurons of feeding-related nuclei of the brain. *Endocrinology, 149*, 2062–2071.

Gerken, T. (2007). The obesity-associated FTO gene encodes a 2-oxoglutarate-dependent nucleic acid demethylase. *Science, 318*, 1469–1472.

Gotz, K. (2005). Homozygous Ft embryos are affected in floor plate maintenance and ventral neural tube pattering. *Developmental Dynamics, 233*, 623–630.

Hasselbalch, A. L., Angquist, L., Christiansen, L., Heitmann, B. L., Kyvik, K. O., & Sørensen, T. I. (2010). A variant in the fat mass and obesity-associated gene (FTO) and variants near the melanocortin-4 receptor gene (MC4R) do not influence dietary intake. *Journal of Nutrition, 140*, 831–834.

Haupt, A., Thamer, C., Staiger, H., Tschritter, O., Kirchhoff, K., Machicao, F., Häring, H. U., Stefan, N., & Fritsche, A. (2009). Variation in the FTO gene influences food intake but not energy expenditure. *Experimental and Clinical Endocrinology & Diabetes, 117*, 194–197.

Hotta, K., Nakata, Y., Matsuo, T., Kamohara, S., Kotani, K., Komatsu, R., Itoh, N., Mineo, I., Wada, J., Masuzaki, H., Yoneda, M., Nakajima, A., Miyazaki, S., Tokunaga, K., Kawamoto, M., Funahashi, T., Hamaguchi, K., Yamada, K., Hanafusa, T., Oikawa, S., Yoshimatsu, H., Nakao, K., Sakata, T., Matsuzawa, Y., Tanaka, K., Kamatani, N., & Nakamura, Y. (2008). Variations in the FTO gene are associated with severe obesity in the Japanese. *Journal of Human Genetics, 53*(6), 546–553.

Jonsson, A., Renström, F., Lyssenko, V., Brito, E. C., Isomaa, B., Berglund, G., Nilsson, P. M., Groop, L., & Franks, P. W. (2010). Assessing the effect of interaction between an FTO variant rs9939609 and physical activity on obesity in 15,925 Swedish and 2,511 Finish adults. *Diabetologia, 53*(6), 1244–1248.

Karasawa, S., Daimon, M., Sasaki, S., Toriyama, S., Oizumi, T., Susa, S., Kameda, W., Wada, K., Muramatsu, M., Fukao, A., Kubota, I., Kawata, S., Kayama, T., & Kato, T. (2010). Association of the common fat mass and obesity associated (FTO) gene polymorphism with obesity in a Japanese population. *Endocrine Journal, 57*(4), 293–301.

Mangge, H., Renner, W., Almer, G., Weghuber, D., Möller, R., & Horejsi, R. (2011). Rs9939609 variant of the fat mass and obesity-associated gene and trunk obesity in adolescents. *Journal of Obesity, 2011*, 186368.

Meyre, D., Delplanque, J., Chèvre, J. C., Lecoeur, C., Lobbens, S., Gallina, S., Durand, E., Vatin, V., Degraeve, F., Proença, C., Gaget, S., Körner, A., Kovacs, P., Kiess, W., Tichet, J., Marre, M., Hartikainen, A. L., Horber, F., Potoczna, N., Hercberg, S., Levy-Marchal, C., Pattou, F., Heude, B., Tauber, M., McCarthy, M. I., Blakemore, A. I., Montpetit, A., Polychronakos, C., Weill, J., Coin, L. J., Asher, J., Elliott, P., Järvelin, M. R., Visvikis-Siest, S., Balkau, B., Sladek, R., Balding, D., Walley, A., Dina, C., & Froguel, P. (2009). Genome-wide association study for early-onset and morbid adult obesity identifies three new risk loci in European populations. *Nature Genetics, 41*(2), 157–159.

Mook-Kanamori, D. O., Ay, L., Hofman, A., van Duijn, C. M., Moll, H. A., Raat, H., Hokken-Koelega, A. C., & Jaddoe, V. W. (2011). No association of obesity gene FTO with body composition at the age of 6 months. The generation R study. *Journal of Endocrinological Investigation, 34*(1), 16–20.

Peters, T. (1999). Cloning of Fatso (FTO), a novel gene deleted gene by the Fused toes (Ft) mouse mutation. *Mammalian Genome, 10*, 983–986.

Rong, R., Hanson, R. L., Ortiz, D., Wiedrich, C., Kobes, S., Knowler, W. C., Bogardus, C., & Baier, L. J. (2009). Association analysis of variation in/near FTO, CDKAL1, SLC30A8, HHEX, EXT2, IGF2BP2, LOC387761, and CDKN2B with type 2 diabetes and related quantitative traits in Pima Indians. *Diabetes, 58*(2), 478–488.

Rutters, F., Nieuwenhuizen, A. G., Bouwman, F., Mariman, E., & Westerterp-Plantenga, M. S. (2011). Associations between a single nucleotide polymorphism of the FTO gene (rs9939609) and obesity-related characteristics over time during puberty in a Dutch children cohort. *Journal of Clinical Endocrinology and Metabolism, 96*(6), E939–E942.

Sanchez-Pulido, L., & Andrade-Navarro, M. A. (2007). The FTO (fat mass and obesity associated) gene codes for a novel member of the non-heme dioxygenase superfamily. *BMC Biochemistry, 8*, 23.

Scott, R. A., Bailey, M. E., Moran, C. N., Wilson, R. H., Fuku, N., Tanaka, M., Tsiokanos, A., Jamurtas, A. Z., Grammatikaki, E., Moschonis, G., Manios, Y., & Pitsiladis, Y. P. (2010). FTO genotype and adiposity in children: Physical activity levels influence the effect of the risk genotype in adolescent males. *European Journal of Human Genetics, 18*(12), 1339–1343.

Slaughter, M. H., Lohman, T. G., Boileau, R. A., Horswill, C. A., Stillman, R. J., Van Loan, M. D., & Bemben, D. A. (1988). Skinfold equations for estimation of body fatness in children and youth. *Human Biology, 60*, 709–723.

Sovio, U., Mook-Kanamori, D. O., Warrington, N. M., Lawrence, R., Briollais, L., Palmer, C. N., Cecil, J., Sandling, J. K., Syvänen, A. C., Kaakinen, M., Beilin, L. J., Millwood, I. Y., Bennett, A. J., Laitinen, J., Pouta, A., Molitor, J., Davey Smith, G., Ben-Shlomo, Y., Jaddoe, V. W., Palmer, L. J., Pennell, C. E., Cole, T. J., McCarthy, M. I., Järvelin, M. R., & Timpson, N. J. (2011). Early growth genetics consortium. Association between common variation at the FTO locus and changes in body mass index from infancy to late childhood: The complex nature of genetic association through growth and development. *PLoS Genetics, 7*(2), e1001307.

Speakman, J. R., Rance, K. A., & Johnstone, A. M. (2008). Polymorphisms of the FTO gene are associated with variation in energy intake, but not energy expenditure. *Obesity (Silver Spring), 16*, 1961–1965.

Stratakis, C. A. (2000). Anisomastia associated with interstitial duplication of chromosome 16, mental retardation, obesity, dysmorphic facies, and digital anomalies: Molecular mapping of a new syndrome by fluorescent in situ hybridization and microsatellites to 16q13 (D16S419-D16S503). *The Journal of Clinical Endocrinology and Metabolism, 85*, 3396–3401.

Stratigopoulos, G. (2008). Regulation of Fto/Ftm gene expression in mice and humans. *American Journal of Physiology, 294*, R1185–R1196.

van der Hoeven, F. (1994). Programmed cell death is affected in the novel mouse mutant fused toes (Ft). *Development, 120*, 2601–2607.

Wardle, J., Llewellyn, C., Sanderson, S., & Plomin, R. (2009). The FTO gene and measured food intake in children. *International Journal of Obesity, 33*(1), 42–45.

Xi, B., Shen, Y., Zhang, M., Liu, X., Zhao, X., Wu, L., Cheng, H., Hou, D., Lindpaintner, K., Liu, L., Mi, J., & Wang, X. (2010). The common rs9939609 variant of the fat mass and obesity-associated gene is associated with obesity risk in children and adolescents of Beijing, China. *BMC Medical Genetics, 11*, 107.

Zimmermann, E., Skogstrand, K., Hougaard, D. M., Astrup, A., Hansen, T., Pedersen, O., Sørensen, T. I., & Jess, T. (2011). Influences of the common FTO rs9939609 variant on inflammatory markers throughout a broad range of body mass index. *PLoS One, 6*(1), e15958.

Chapter 33
Rapid Test for Influenza in Diagnostics

Teresa Jackowska, Monika Grzelczyk-Wielgorska, and Katarzyna Pawlik

Abstract In Poland no vaccines against influenza type A/H1N1 were available in the epidemic season 2009/2010. In our Department within 45 days (November-December 2009) 17 influenza suspected children (24%) were positive for influenza type A (QiuckVue Influenza A + B rapid tests). Of these 17 children, seven were hospitalized at the pediatric department. In six of them the presence of the A/H1N1v virus RNA was confirmed with real-time reverse transcription polymerase chain reaction (RT-PCR, Polymerase Chain Reaction). The initial presentation of influenza was unspecific. The possibility of performing the rapid test for influenza in the epidemic season proved to be very useful in the clinical diagnostics and management.

Keywords Influenza • A/H1N1v • Rapid test • Children • Vaccination

33.1 Introduction

The A/H1N1v pandemic influenza virus is a variant of the human A/H1N1 seasonal influenza virus circulating in the population since 1977 (World Health Organization 2009). It differs from the seasonal influenza virus in the content of a mixture of avian, swine and human viral influenza genetic material in the combination hitherto unprecedented in the world (World Health Organization 2009). The variant of the A/H1N1 virus was first identified in Mexico in April 2009 and since then has rapidly started to spread around the world.

A report of WHO of 30/04/2010 revealed about 17,919 deaths worldwide due to influenza caused by the A/H1N1v virus (World Health Organization 2010). Hence, WHO announced the pandemic of influenza on 11.06.2009 (World Health Organization 2009). In Poland, since the first A/H1N1v influenza case detection (06/05/2009) by the end of the reporting period (22.04.2010), within less than a year 2,535 A/H1N1v influenza cases were noted, including 181 deaths (Statement of the Chief Sanitary Inspector). The largest number of cases were registered in November and December 2009 (National Institute of Public Health 2010). The course of most cases was mild or moderate-severe.

T. Jackowska (✉) • M. Grzelczyk-Wielgorska • K. Pawlik
Department of Pediatrics, Medical Center of Postgraduate Education,
Marymoncka 99/103 St, Warsaw 01-813, Poland
e-mail: tjackowska@cmkp.edu.pl

M. Pokorski (ed.), *Respiratory Regulation - The Molecular Approach*,
Advances in Experimental Medicine and Biology 756, DOI 10.1007/978-94-007-4549-0_33,

The disease resolved spontaneously after 5–7 days. Most cases occurred in children and adolescents (80% did not exceed 30 years of age).

The most frequently described influenza complication is pneumonia, usually of mixed bacterial-viral etiology, which can lead to acute respiratory distress syndrome (Lee et al. 2009; Kumar et al. 2010). In children, neurological complications such as seizures (Centers of Disease Control and Prevention 2009), Rey's syndrome (Centers of Disease Control and Prevention 2009), acute encephalopathy (Centers of Disease Control and Prevention 2009; Gonzalez and Brust 2009; Fluss et al. 2010), and acute necrotizing encephalitis (Lyon et al. 2010) were reported.

33.2 Methods and results

33.2.1 Patients

This report describes data collected in accordance with the Declaration of Helsinki for human experimentation and it was approved by a local Ethics Committee.

In 2009/2010, in the Department of Pediatrics of the Medical Center of Postgraduate Education, in Warsaw, Poland, 102 QuickVue rapid diagnostic tests for influenza A and B were performed in children reporting to the Emergency Room with symptoms of 'influenza-like' respiratory tract infection (fever, rhinorrhea, cough, weakness, apathy). In 74 children, this test was performed within 45 days (from 4th November to 19th December 2009) and in 17 of them (24%) it was positive for influenza A.

Positive tests were noted in 6 boys and 11 girls aged two months to 17 years (median 7 years and 6 months). Five (30%) children did not require hospitalization and 12 (70%), due to severe course or belonging to a high risk group, required hospital treatment. Another five children, due to overcrowding, were sent to a hospital for infectious diseases.

Seven children were hospitalized in the pediatric department and in six of them the presence of viral A/H1N1v RNA was confirmed by polymerase chain reaction (RT-PCR). In one, a RT-PCR test was negative and the QuickVue rapid diagnostic test for influenza type A was positive.

At the ER all the influenza suspected children were tested with a QuickVue Influenza A + B rapid diagnostic test by BioMerieux, Poland. Nasopharyngeal swabs were taken. The cost of one test was approx. 13 Euro. All patients with a positive diagnostic test were taken swabs from both nasal passages and throat to detect the H1N1 virus RNA. The cost of the latter test was approx. 60 Euro.

33.2.1.1 Case 1

A 14-year-old girl (P.S.) was brought to the hospital following a triple loss of consciousness, which took place within 90 min. At the first fainting episode, just after waking up from a night sleep and standing upright, she sustained a head and face injury, knocking out two upper incisors. In anamnesis there was a history 2-day weakness, loss of appetite, and fever up to 39°C. On admission, she presented moderate-severe condition, poorly maintaining logic verbal contact, barely remained on her feet. Her physical examination revealed broken upper incisors, drying mucosa of the mouth, a white coating on the tongue, and a reddened softened throat. Heart rate was accelerated to 100 bpm and blood pressure was 100/60 mmHg. Meningeal symptoms were negative.

A differential white blood count revealed increased segmented neutrophils (5.2×10^3/μl; 86%), a slightly elevated value of C-reactive protein (CRP) to 17.4 mg/l and erythrocyte sedimentation rate (ESR) −50 mm after 1 h. A rapid diagnostic test for influenza type A was positive, and RT-PCR testing confirmed the presence of viral A/H1N1v RNA. Other tests were normal.

Oseltamivir was administered in a therapeutic dose (2 × 75 mg). On hospital Day 3, the girl stopped being febrile, her general condition improved. In her final laboratory findings, we observed the

normalization of CRP and ESR. However, she was leukopenic ($2.8 \times 10^3/\mu l$), with the predominance of lymphocytes ($1.7 \times 10^3/\mu l$, 58.6%). Following 5-day therapy with oseltamivir she was discharged home in very good condition.

33.2.1.2 Case 2

A 3.5-year-old girl (A.B.) was admitted to the hospital in moderate condition, with significant fatigue, lethargic, fever of 40°C, and wet cough for 5 days. On physical examination, abnormalities included macular rash on the skin of the lower limbs and trunk, excessive body temperature and a slight swelling of hand and wrist joints, and swollen eyelids. In addition, the symptoms of upper respiratory infection with vesicular murmur exacerbation and single rales at the base of both lungs were present. Prior to the admission, the girl received two doses of oral cefuroxime axetil. A month before she ran a course of chickenpox.

The white blood cell count was normal ($8.4 \times 10^3/\mu l$), with a slight predominance of lymphocytes ($5.4 \times 10^3/\mu l$, 60%). There were elevated levels of CRP – 62.8 mg/l and accelerated ESR – 90 mm after 1 h. Chest X-ray revealed bilateral bronchogenic parenchymal consolidation. A rapid test for influenza A was positive; RT-PCR confirmed the presence of viral A/H1N1v RNA.

Oseltamivir was administered in a therapeutic dose (2×45 mg) for 5 days. Given the high concentrations of inflammation markers, suspecting mixed viral-bacterial infection, intravenous amoxicillin with clavulanic acid was administered. From the 4th day of therapy, clinical improvement, fever, hand wrist and eyelid edema, and the auscultatory changes over the lung fields resolved. The patient's final peripheral blood smear was normal, CRP levels decreased (7.8 mg/l); however accelerated ESR (75 mm after 1 h) still persisted. After 7 days of therapy, the girl was discharged home in good condition.

33.2.1.3 Case 3

A 1.5-year-old boy (K.G.) was admitted to hospital due to 2-day-fever up to 40°C and a single syncope, with a loss of contact for about 3–5 s, followed by upper and lower limb tremors, and lip and hand cyanosis. A boy presented 3-day coryza and cough. His attending physician diagnosed pharyngitis and prescribed oral amoxicillin with clavulanic acid, which induced allergic symptoms (intense erythema on the cheeks and itchy skin). On admission, symptoms of respiratory tract infection (intensively reddened palatopharyngeal arches, profuse mucous secretions in the nasal passages) and atopic dermatitis were noted. Meningeal symptoms were negative and other organs were without any abnormalities.

In the full blood count, leucopenia ($3.5 \times 10^3/\mu l$) was found with granulocytopenia ($0.6 \times 10^3/\mu l$, 18.5%), slightly decreased platelet count ($124 \times 10^3/\mu l$). Other biochemical tests were normal. A rapid diagnostic test for influenza type A was positive, and RT-PCR confirmed the presence of viral A/H1N1v RNA.

Oseltamivir was administered in a therapeutic dose (2×30 mg) for 5 days. The boy's condition gradually improved, from the treatment Day 3, his fever resolved. His final blood count was normal ($4.4 \times 10^3/\mu l$ leucocytes, granulocytes $1.6 \times 10^3/\mu l$, and platelets $173 \times 10^3/\mu l$). After 6 days of hospitalization, the boy was discharged home in good condition.

33.2.1.4 Case 4

A 2.5-month-old male infant (I.N.) was referred to the hospital because of upper respiratory tract infection and suspected bilateral otitis media. For about 5 days, behavior changes, restlessness, worse appetite were observed. One day earlier, the boy started fever up to 39.3°C, had a dry cough and

watery coryza. On admission, symptoms of upper respiratory tract were present (rhinorrhea, a reddened and softened throat, bilaterally inflamed tympanic membrane).

Anemia (Hgb −10.3 g/dl) was found in the blood, with a white blood cell count at the lower limit of the norm (5.6×10^3/μl); the microscopic smear was normal. Other biochemical tests, including CRP levels were normal. The radiographic findings included peribronchial inflammatory consolidation in the middle-lower part of the right lung. A rapid diagnostic test for influenza type A was positive, and a RT-PCR test confirmed the presence of viral A/H1N1v RNA.

Oseltamivir was administered in a therapeutic dose (2 × 17.5 mg). However, on account on the child's age and inflammatory changes in the lungs antimicrobial treatment (amoxicillin with clavulanic acid) was added. From Day 2, there was an improvement of general condition, normalization of body temperature and appetite improvement. In final tests after 8-day therapy, an increase of white blood cells (7.5×10^3/μl) was noted; the patient, however, still remained anemic (Hgb – 9.7 g/dl). After 10 days of treatment, the boy was discharged home in good condition.

33.2.1.5 Case 5

A 2-month female infant (M.R.) was referred to hospital because of 1-day fever up to 39°C, malaise, drowsiness, aversion to food. A previously healthy child, pregnancy, and childbirth course were uneventful. In history, there were upper respiratory tract infections in her siblings. On admission tachycardia was found (150 bpm), bloated and tense abdomen, painful on palpation, and greenish, profuse, and liquid stools. There were no signs of the upper or lower respiratory tract infection.

Anemia (Hgb – 10.6 g/dl) was found in the blood, with a reduced white cell count (3.5×10^3/μl), granulocytopenia (0.5×10^3/μl, 18.5%), and a low blood platelet count (130×10^3/μl). In biochemical tests, there were elevated levels of CRP-19.7 mg/l and procalcitonin (PCT – 0.5 ng/ml; norm up to 0.5 ng/ml); other tests were normal. Chest X-ray was normal.

Lumbar puncture was not performed due to the lack of parental consent. Suspecting a generalized infection, however, the patient received ceftriaxone. On hospital Day 2 day, the girl continued fever, signs of upper respiratory tract infection appeared (abundant mucus in the nose, dry rales over the lungs fields). A rapid test for influenza was performed, which turned up positive for influenza A.

RT-PCR testing confirmed the presence of viral A/H1N1v RNA. Given the infant's age oseltamivir was administered in a therapeutic dose (2 × 11.25 mg) for 5 days, achieving very rapid improvement in clinical condition. From Day 3 on, the girl did not have fever, was active, and ate willingly, put on weight. Her final blood tests were normal, apart from persistent anemia (Hgb 10.0 g/dl).

33.2.1.6 Case 6

A 3.5-year-old boy (B.F.) was hospitalized in the department for several days because of recurrent, bilateral, exudative otitis, pharyngitis, and tonsillitis. Suddenly, on Day 8 of parenteral antibiotic therapy (amoxicillin with clavulanic acid), he started fever up to 39.4°C, gave a single loose stool. On physical examination, there were no abnormalities. However, in full blood count leucopenia (4.4×10^3/μl) was noted, with a left shift (bands 0.6×10^3/μl, 14%, segmented 2.9×10^3/μl, 66%). In addition, ESR was accelerated to 60 mm after 1 h. Other tests, including CRP, were normal. A rapid diagnostic test for influenza A was positive. RT-PCR testing confirmed the presence of viral A/H1N1v RNA.

Nosocomial A/H1N1v influenza virus infection was diagnosed. The patient received oseltamivir in a therapeutic dose (2 × 45 mg). The boy had fever for two consecutive days, vomited several times, gave loose stools, and required intravenous rehydration. Rotavirus, adenovirus, or norovirus infection was excluded. On the third day of antiviral therapy, fever stopped, his general condition improved.

In the final blood count, leucopenia ($4.0 \times 10^3/\mu l$) remained, microscopic smear was normal, and ESR decreased to 30 mm.

This patient apparently came down with an Nosocomial A/H1N1v influenza infection, despite the fact that other ill children were in isolation rooms with their parents, and medical staff followed the procedures of isolation.

33.2.1.7 Case 7

An 11-year-old girl (J.S.), with a positive history of bronchial asthma, was admitted to the emergency room due to 5-day dry, persisting cough, 1-day fever up to 39.5°C, and myalgia. Physical examination showed enlarged cervical and submandibular lymph nodes, reddened throat, and bilateral exacerbated vesicular murmur over the lung fields. Attention drew an intense, exhausting cough, greatly affecting speech.

The blood count revealed leucopenia ($3.5 \times 10^3/\mu l$), with the predominance of lymphocytes ($2.1 \times 10^3/\mu l$, 60%). Other biochemical blood tests, including CRP and ESR, and chest X-ray were normal. A rapid diagnostic test for influenza type A was positive, but RT-PCR testing did not detect A/H1N1v influenza virus RNA. Nonetheless, on the account of asthma in anamnesis and a season of increased influenza morbidity, the patient received oseltamivir (2×75 mg) for 5 days, plus steroids and beta-agonists by inhalation, gaining rapid clinical improvement. In the final blood cell count, performed after the completion of therapy, white blood cell count was normal ($5.1 \times 10^3/\mu l$), with a tendency to normalization of the microscopic smear (lymphocytes $2.6 \times 10^3/\mu l$, 50%). After the 6-day therapy, the girl was discharged in good condition.

Considering the clinical course, epidemiological data (a significant increase in influenza cases in this period), and a positive rapid test for influenza A, despite the lack of A/H1N1v virus confirmation by RT-PCR testing, we believed the girl had A/H1N1v influenza.

33.3 Discussion

In this report we presented the course of A/H1N1v influenza in seven children who were hospitalized in one of Warsaw's hospitals within only 45 days (November-December 2009) (Table 33.1). In Poland, by the decision of the Minister of Health, no A/H1N1v influenza vaccines had been purchased; therefore, influenza cases occurred in the unvaccinated population. As it appears from this case report,

Table 33.1 Abnormalities found in laboratory tests performed on admission in seven hospitalized children with the diagnosis of A/H1N1v influenza

Patient / Lab findings	Nr 1 (P. S.)	Nr 2 (A.B.)	Nr 3 (K.G.)	Nr 4 (I.N.)	Nr 5 (M.R.)	Nr 6 (B.F.)	Nr 7 (J.S.)
Hgb (g/dl)	12.5	11.4	12.7	10.3	10.6	12.4	13.9
WBC ($\times 10^3/\mu l$)	6.0	8.4	3.5	5.6	3.5	4.4	3.5
Gran. ($\times 10^3/\mu l$)	5.2	3.1	0.6	1.3	0.5	2.1	1.4
(%)	86	37.2	18.5	23.3	15.4	66	35.1
Limf. ($\times 10^3/\mu l$)	0.7	5.4	2.5	3.6	2.4	0.6	2.1
(%)	11.7	60	71.7	63.5	64.1	13.5	60
PLT ($\times 10^3/\mu l$)	175	266	124	302	130	319	211
CRP mg/l (norm to 2.8 mg/l)	17.4	62.8	0.7	1.1	19.7	0.4	0.6

the clinical picture of influenza caused by A/H1N1v virus among the hospitalized children had the following main features:

- high fever, 39–40°C, weakness, apathy, a loss of appetite;
- symptoms of respiratory tract infection (rhinorrhea, sore throat, cough), appearing concomitantly with fever or 1 day afterward;
- pneumonia in 2 out of the 7 hospitalized children (*Cases 2 & 4*);
- gastrointestinal symptoms (diarrhea, vomiting), predominating in 2 children (*Cases 5 & 6*);
- neurological manifestations (a loss of consciousness, seizures), predominating in 2 children (*Cases 1 & 3*);
- transient decrease in platelet count in 2 children (*Cases 3 & 5*);
- blood counts revealed leucopenia in 5 cases;
- CRP level elevated in 3 cases.

All hospitalized children were treated with oseltamivir (Tamiflu, Roche) in age- and weight-related therapeutic doses. The possibility of performing a rapid influenza test for influenza enabled an immediate implementation of antiviral therapy and quick improvement of patient clinical condition (Heinonen et al. 2010).

In cases of suspected mixed viral-bacterial infection (high levels of CRP, ESR, PCT) or radiologically confirmed pneumonia an antibiotic (amoxicillin with clavulanate or ceftriaxone) was administered. A decrease in fever and a significant relief of disease symptoms were observed from the 3rd day of therapy.

Within 45 days (November-December) 2009, in every fourth child reporting to the hospital emergency room with influenza-like symptoms, influenza type A was diagnosed. In this period, many children had to be referred to hospitals outside Warsaw due to overcrowding. We believe that during that period there was an increase in A/H1N1v influenza in Poland. Fortunately, the course of influenza was generally mild in children who were not from risk groups. The availability of a rapid diagnostic test for influenza in a potentially epidemic period was very useful, and its performance quick, easy and cost-effective in economic terms. The price of one test was approx. 13 Euro, while the RT-PCR testing for A/H1N1v influenza was 4.5 times more expensive. Furthermore, the result of a rapid test was immediate, while RT-PCR took a few days, which delayed administration of antiviral therapy.

A positive result of a rapid diagnostic test not only allows undertaking the optimal for the patient clinical decision but also enables to take epidemiological decisions (isolation of infected patients) in order to reduce the spread of infection both within and outside the department.

33.4 Conclusions

A/H1N1v influenza pandemic announced by WHO, was a challenge for the Polish and global health care systems in the 2009/2010 season. Subsequent publications and case reports are a source of medical expertise and a kind of preparation for next season of increased influenza incidence (Centers for Disease Control and Prevention 2010).

The presented cases demonstrate that not only adolescents but also little children are affected by A/H1N1 influenza, and the leading symptoms may be nonspecific or atypical, such as unconsciousness, seizures, vomiting, or diarrhea. Therefore, a quick diagnosis at the emergency room is extremely important to be able to provide appropriate treatment and limit the further spread of infection among people from the closest circle.

Our experience shows that rapid tests for influenza are extremely helpful in making these decisions and establishing an accurate diagnosis, yet cost-effective. The importance of immunization, especially among medical staff who is particularly vulnerable to infection must be emphasized, too.

Acknowledgments Supported by CMKP grant 501-1-1-19-49/2009.

Conflicts of interest: The authors declared no potential conflicts of interest.

References

Centers of Disease Control and Prevention. (2009). Neurologic complication associated with novel influenza A (H1N1) virus infection in children – Dallas, Texas, May 2009. *MMWR. Morbidity and Mortality Weekly Report, 58*, 773–778.

Centers for Disease Control and Prevention (2010). Influenza-associated pediatric mortality. http://www.cdc.gov/flu/weekly/. Updated 28 May 2010. Accessed 12 Apr 2010.

Fluss, J., Ferey, S., Menache-Starobinski, C., Delavelle, J., Van Bogaert, P., & Vargas, M. I. (2010). Mild influenza–associated encephalopathy/encephalitis with a reversible splenial lesion in Caucasian child with additional cerebellar features. *European Journal of Paediatric Neurology, 14*, 97–100.

Gonzalez, B. E., & Brust, D. G. (2009). Novel influenza A (H1N1) presenting as an acute encephalopathy in mother and daughter. *Clinical Infectious Diseases, 49*, 1966–1967.

Heinonen, S., Silvennoinen, H., Lehtinen, P., Vainionpää, R., Vahlberg, T., Ziegler, T., Ikonen, N., Puhakka, T., & Heikkinen, T. (2010). Early oseltamivir treatment of influenza in children 1–3 years of age: A randomized controlled trial. *Clinical Infectious Diseases, 51*, 887–894.

Kumar, S., Havens, P. L., Chusid, M. J., Willoughby, R. E., Jr., Simpson, P., & Henrickson, K. J. (2010). Clinical and epidemiologic characteristics of children hospitalized with 2009 pandemic H1N1 influenza A infection. *The Pediatric Infectious Disease Journal, 29*, 591–594.

Lee, C. W., Seo, J. B., Song, J. W., Lee, H. J., Lee, J. S., Kim, M. Y., Chae, E. J., Song, J. W., & Kim, W. Y. (2009). Pulmonary complication of novel influenza A (H1N1) infection: Imaging features in two patients. *Korean Journal of Radiology, 10*, 531–534.

Lyon, J. B., Remigio, C., Milligan, T., & Deline, C. (2010). Acute necrotizing encephalopathy in child with H1N1 influenza infection. *Pediatric Radiology, 40*, 200–205.

Reports on cases of infectious diseases and poisonings in Poland, National Institute of Public Health, National Institute of Hygiene (03.03.2010): http://pzh.gov.pl/epimeld

Statement of the Chief Sanitary Inspector: http://www.pis.gov.pl

World Health Organization (2009). Evolution of pandemic A (H1N1). http://www.who.int

World Health Organization (2010). Pandemic (H1N1) – update 98: http://www.who.int/csr/don/2010_04_30a/en/index.html

Chapter 34
Infections with A(H1N1)2009 Influenza Virus in Poland During the Last Pandemic: Experience of the National Influenza Center

M. Romanowska, I. Stefanska, S. Donevski, and L.B. Brydak

Abstract This study presents epidemiological and clinical data on non-sentinel patients considered by physicians as suspected to be infected with pandemic A(H1N1)2009 virus, from whom clinical specimens were sent for testing to the National Influenza Center, NIPH-NIH in Warsaw, Poland. Between April 28, 2009 and August 10, 2010, 988 (15.7%) out of the 6,311 specimens were tested by the National Influenza Center, including 798 from non-sentinel sources and 190 from sentinel influenza surveillance network. The non-sentinel specimens were tested by conventional RT-PCR to detect influenza A and in the case of positive specimens – one-step real-time RT-PCR to detect the pandemic virus A(H1N1)2009. In 145 (18.2%) cases, infections with the pandemic virus were confirmed, with the highest number in patients aged 15–25. In 45% of the confirmed cases, a history of travel to other countries was registered. The most common symptoms were fever ≥38°C (72.7%), cough (50%), sore throat, and myalgia (26.1%). In 40.7% of the swabbed patients, clinical and epidemiological criteria for the novel influenza A(H1N1)2009, set by the European Commission, were met. There were, however, specimens from persons without any reasonable indication for testing for the pandemic virus, specimens collected incorrectly, and documentation without basic information. These weaknesses resulted in unnecessary costs and overload of health care units. An improvement should be achieved in the area of communication between different pandemic players in the future. More attention is also needed to ensure that requirements and recommendations are known and used.

Keywords A(H1N1) virus • Influenza • Pandemic • Respiratory infection • Virus

M. Romanowska (✉) • S. Donevski
Department of Influenza Research, National Influenza Center, National Institute of Public Health-National Institute of Hygiene, Chocimska 24 St, Warsaw 00-791, Poland
e-mail: magdalena.machalaromanowska@gmail.com

I. Stefanska
Department of Fermentation Technology, Institute of Agricultural and Food Biotechnology, Rakowiecka 36 St, Warsaw 02-532, Poland

L.B. Brydak
Department of Influenza Research, National Influenza Center, National Institute of Public Health-National Institute of Hygiene, Chocimska 24 St, Warsaw 00-791, Poland

Faculty of Biology, Department of Microbiology and Immunology, Szczecin University, Waska 13 St, Szczecin 71-415, Poland

M. Pokorski (ed.), *Respiratory Regulation - The Molecular Approach*,
Advances in Experimental Medicine and Biology 756, DOI 10.1007/978-94-007-4549-0_34,

34.1 Introduction

On June 11, 2009, World Health Organization (WHO) declared the outbreak of influenza pandemic caused by the novel A(H1N1) virus of swine origin. In Europe, the first cases were confirmed in the United Kingdom and Spain in the end of April 2009 (ECDC 2010a). Since then, the National Influenza Center (NIC) in Poland, located at the Department of Influenza Research of the National Institute of Public Health-National Institute of Hygiene (NIPH-NIH) in Warsaw, Poland, immediately took necessary actions to manage this public health threat and as the first step to introduce appropriate methods of laboratory diagnostics. As of April 28, 2009 until the end of July 2009, the NIC was the only laboratory in Poland responsible for diagnostics of infections caused by the novel virus and authorized by WHO. Afterwards, testing was also performed by laboratories of 10 out of the 16 Voivodship Sanitary-Epidemiological Stations (VSESs) which successively received necessary equipment and became able to perform laboratory diagnostics of A(H1N1)2009 virus by PCR-based methods. Between April 28, 2009, when the first specimen was collected in Poland and August 10, 2010, when the end of the pandemic was announced by WHO, a total number of 6,311 specimens were tested all over the country. Infections with the pandemic A(H1N1)2009 influenza virus were confirmed in 2,378 cases (37.7%). The specimens were collected within the sentinel influenza surveillance system, but most of them originated from the non-sentinel sources, mainly hospitals. The NIC received and tested 988 out of the 6,311 specimens (15.7%), including 798 from the non-sentinel sources (80.8%) and 190 specimens from sentinel influenza surveillance network (19.2%).

The previous influenza pandemic occurred in 1968–1969, affected all age groups and was associated with one to four millions of deaths caused by A(H3N2) virus (WHO 2009b). Since 1997, there have been human infections with highly pathogenic avian influenza virus (HPAI) of A(H5N1) subtype with mortality reaching up to 60%. So far, all infections were due to direct contact with ill or dead birds or their feces, but sustained human-to-human transmission was not confirmed. In 1999, WHO prepared and published 'Influenza Pandemic Plan. The Role of WHO and Guidelines for National and Regional Planning' that emphasized the necessity to prepare national influenza pandemic preparedness plans by all member states (WHO 1999). The document was updated in 2005 (WHO 2005) and now is replaced by that of April 2009 (WHO 2009b). Since 1997, concerns of WHO and influenza experts regarding a possible pandemic outbreak were closely related to HPAI A(H5N1) virus. Therefore, the emergence of the novel A(H1N1) virus having pandemic potential in April 2009 was, to an extent, unexpected. The pandemic A(H1N1)2009 influenza virus is a reassortant of Eurasian avian-like swine A(H1N1) virus and North American swine A(H1N1) virus. The latter is a triple reassortant having genes of classical swine A(H1N1) virus, North American avian virus, and human influenza A(H3N2) virus (ECDC 2010b; Neumann and Kawaoka 2011). Consequently, the pandemic A(H1N1)2009 influenza virus has ribonucleic acid (RNA) segments coding neuraminidase (NA) and matrix protein (M) derived from the Eurasian avian-like swine influenza virus, segment coding polymerase PB1 derived from human seasonal influenza A(H3N2) virus, segments coding polymerase PA and polymerase PB2 derived from North American avian influenza virus, while the segment coding hemagglutinin (HA), nucleoprotein (NP), and non-structural protein (NS) derived from the North-American classical swine influenza virus (ECDC 2010b; Neumann and Kawaoka 2011). According to WHO reports, until August 1, 2010 over 214 countries worldwide were affected by the pandemic virus, and over 18,449 deaths were confirmed, including at least 4,879 in WHO EURO Region (WHO 2010a).

The aim of this study was to present epidemiological and clinical data on the 798 non-sentinel patients considered by physicians as suspected to be infected with pandemic A(H1N1)2009 virus, from whom clinical specimens were sent for testing to the NIC.

34.2 Methods

The data presented in this report include specimens collected between April 28, 2009 and August 10, 2010. In each case, a decision which patient should be swabbed was made by a physician. Detailed instructions regarding collection of clinical material, including its storage and transport, were prepared by the NIC and available on the website. Similarly, appropriate information was available on the website of the Chief Sanitary Inspectorate and the Ministry of Health. Phone information was also provided by the staff of the NIC and the National IHR Focal Point. Clinical materials were nasal and throat swabs, less often bronchoalveolar liquid, or tracheal washings. The NIC performed diagnostics of the pandemic influenza A(H1N1)2009 virus by nucleic acid amplification techniques. RNA was extracted from a specimen volume of 140 μL with QIAamp RNA Mini Viral Kit (Qiagen, Germany) according to the manufacturer's instruction. As the first step, conventional one-step reverse transcription-polymerase chain reaction (RT-PCR) assay was done to detect M gene of influenza virus A using Transcriptor One-Step RT-PCR Kit (Roche Diagnostics, Switzerland) and the following sets of primers: until December 2009 primers M30F (TTCTAACCGAGGTCGAAACG) and M264R2 (ACAAAGCGTCTACGCTGCAG) were used (WHO Collaborating Centre for Reference and Research on Influenza, National Institute of Infectious Diseases, Tokyo, Japan) and since December 2009 the modified primers were used: M30F2/08 (ATGAGYCTTYTAACCGAGGTCGAAACG) and M264R3/08 (TGGACAAANCGTCTACGCTGCAG) (WHO Collaborating Centre for Reference and Research on Influenza, National Institute of Infectious Diseases, Tokyo, Japan) (WHO 2009g). The temperature profile was the following: reverse transcription for 30 min at 50°C; inactivation of reverse transcriptase and initial denaturation for 7 min at 94°C; then 45 cycles of denaturation at 94°C for 10 s, annealing at 55°C for 30 s, and extension at 68°C for 55 s. The reaction was completed by a final extension at 68°C for 7 min. All specimens positive for influenza A were then tested by one-step real-time RT-PCR assay performed on the LightCycler 2.0 machine (Roche), using the protocol developed by the Centers for Disease Control and Prevention (CDC; Atlanta, USA) and SuperScript™III Platinum® One-Step Quantitative RT-PCR System (Invitrogen, USA) to detect HA gene of the pandemic influenza virus A(H1N1)2009 (WHO 2009a).

Data regarding individual patients were analyzed by sex, age, seasonal influenza vaccination status, symptoms of illness, and epidemiological and clinical criteria included into the case definition of the pandemic influenza A(H1N1)2009 (European Commission 2009).

34.3 Results

Data on the age of the swabbed patients, their sex, and the vaccination status is presented in Table 34.1. The highest proportion of specimens was received from patients aged 15–44 (61.7%, if patients of the unknown age were excluded). The specimens collected from men and women were relatively equally represented (47.7% *vs.* 52.3%). In 537 (67.3%) out of the 798 patients, information on the vaccination status against seasonal influenza in the epidemic season 2008/2009 or 2009/2010 was given by a physician. Among them, there were 7.3% of the vaccinated patients.

In 145 (18.2%) cases of 798 non-sentinel specimens, infections with the pandemic virus were confirmed. Most of the confirmed cases were found in the age group 15–25 years (42.8%). Similarly to the total number of specimens analyzed, the positive specimens were collected equally from men and women (51.0% *vs.* 49.0%). In the case of 99 patients, information on the vaccination status was known. Among them only 6.1% were vaccinated against seasonal influenza in the epidemic season 2008/2009 or 2009/2010. Detailed information is given in Table 34.2.

Table 34.1 Non-sentinel patients suspected to be infected with A(H1N1)2009 influenza virus from whom clinical specimens were collected and laboratory tested at the Dept. of Influenza Research, National Influenza Center, NIPH-NIH, between April 28, 2009 and August 10, 2010

	No. of patients	%
Age (year)		
0–4	37	4.6
5–14	102	12.8
15–25	269	33.7
26–44	209	26.2
45–64	127	15.9
≥65	31	3.9
Unknown	23	2.9
Gender		
Male	380	47.6
Female	417	52.3
Unknown	1	0.1
Vaccination against seasonal influenza in the epidemic season 2008/2009 or 2009/2010		
Yes	39	4.9
No	498	62.4
Unknown	261	32.7
Total	**798**	**100**

Table 34.2 Non-sentinel patients with laboratory confirmed infection with A(H1N1)2009 influenza virus from whom clinical specimens were collected and laboratory tested at the Dept. of Influenza Research, National Influenza Center, NIPH-NIH, between April 28, 2009 and August 10, 2010

	No. of patients	%
Age		
0–4	11	7.6
5–14	32	22.1
15–25	62	42.8
26–44	27	18.6
45–64	9	6.2
≥65	4	2.7
Unknown	0	0.0
Gender		
Male	74	51.0
Female	71	49.0
Unknown	0	0.0
Vaccination against seasonal influenza in the epidemic season 2008/2009 or 2009/2010		
Yes	6	4.1
No	93	64.1
Unknown	46	31.7
Total	**145**	**100**

The first laboratory-confirmed case in Poland was diagnosed on May 6, 2009 (week no. 19/2009). This specimen was collected from a woman aged 37 old who visited the USA and developed symptoms less than a week after the return to Poland.

The highest number of the non-sentinel specimens was received by the NIC in weeks 30–31/2009 (July 20, 2009–August 2, 2009). During summer holidays, i.e., between week 27/2009 (June 29,

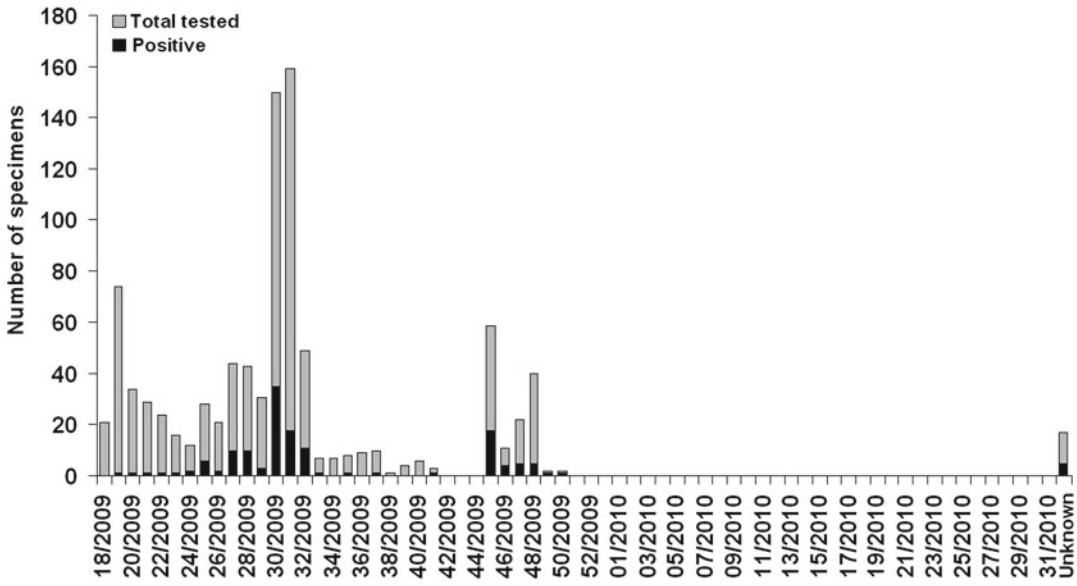

Fig. 34.1 Number of clinical specimens tested (n = 798) and positive (n = 145) for the pandemic influenza A(H1N1)2009 in different calendar weeks between April 27, 2009 and August 10, 2010

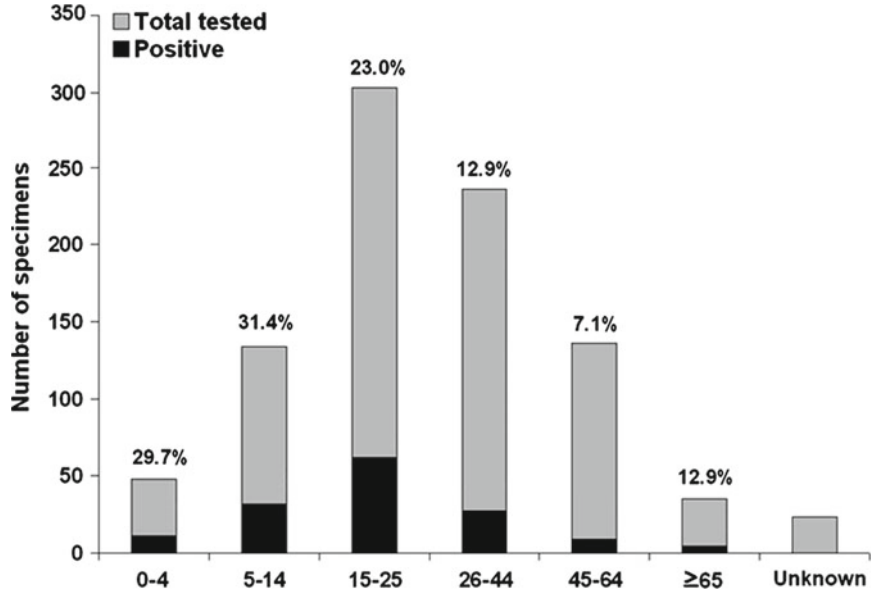

Fig. 34.2 Proportion of specimens positive for the pandemic influenza A(H1N1)2009 in different age groups

2009- July 5, 2009) and week 35/2009 (August 24–30, 2009), 52% of all specimens were collected. Since week 33/2009 (August 10–16, 2009), the number of specimens gradually decreased, although between week 45/2009 (November 2–8, 2009) and 48/2009 (November 23–29, 2009) an increase in the number of specimens was observed (Fig. 34.1).

A proportion of positive specimens among all specimens tested between the age groups ranged from 7.1% in the patients aged 45–64 to 31.4% in those aged 5–14 (Fig. 34.2).

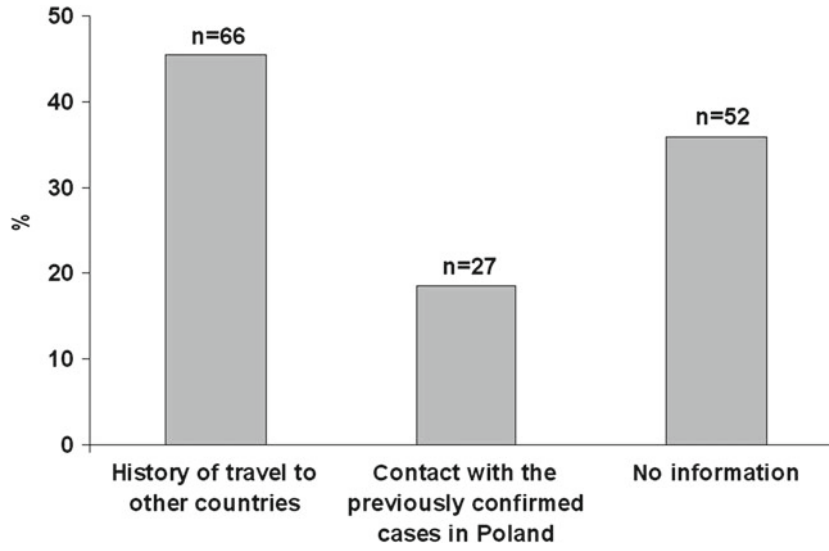

Fig. 34.3 Epidemiological data on the patients with laboratory confirmed A(H1N1)2009 infection (n = 145)

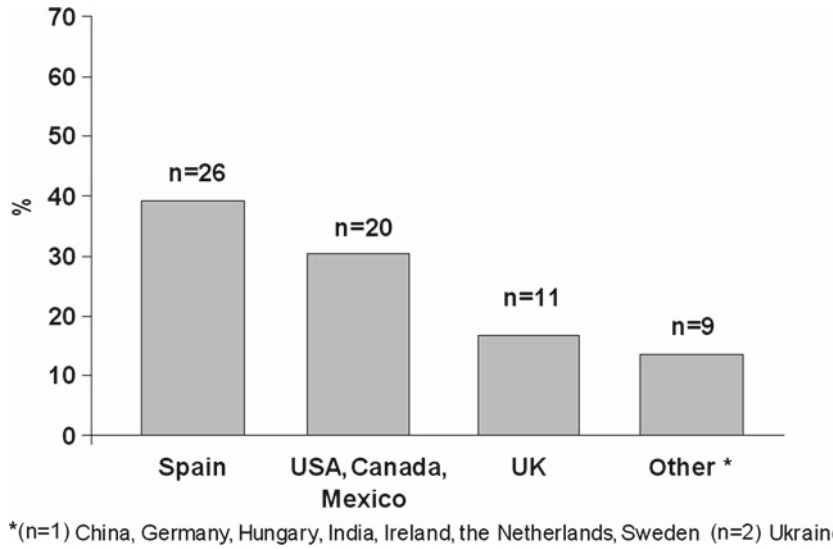

Fig. 34.4 Proportion of patients visiting different countries in whom A(H1N1)2009 infection was laboratory confirmed after their return to Poland (n = 66)

In 45.5% of patients with laboratory confirmed infection with A(H1N1)2009 influenza virus, a history of travel to other countries was registered (Fig. 34.3). Among them, almost 40% returned from Spain and 30% visited the USA and/or Canada or Mexico (Fig. 34.4).

Information on the clinical symptoms was available for 88 out of the 145 patients with laboratory confirmed A(H1N1)2009 infection. Among them, the most common symptoms were fever ≥38°C (72.7% of patients), cough (50.0%), sore throat (26.1%), myalgia (26.1%), and coryza (20.5%) (Table 34.3).

Table 34.3 Clinical symptoms in patients with laboratory confirmed infection with A(H1N1)2009 influenza virus (n = 145) from whom clinical specimens were collected and laboratory tested at the Dept. of Influenza Research, National Influenza Center, NIPH-NIH, between April 28, 2009 and August 10, 2010

Symptom	No. of patients	%
Fever ≥38°C	64	44.1
Subfebrile body temperature	5	3.4
Cough	44	30.3
Sore throat	23	15.9
Myalgia	23	15.9
Coryza	18	12.4
Malaise	10	6.9
Headache	9	6.2
Chills	6	4.1
Abdominal pain	3	2.1
Lack of appetite	2	1.4
Vomiting	4	2.8
Dyspnea	2	1.4
Conjunctivitis	2	1.4
Nausea	2	1.4
Diarrhea	1	0.7
Sinusitis	1	0.7
Lacrimation	1	0.7
Stomatitis	1	0.7
Dizziness	1	0.7
No symptoms (contact with the confirmed case)	7	4.8
No specific data available	57	39.3

40.7% of all swabbed patients met the European Commission's (EC 2009) clinical and epidemiological criteria for novel influenza A(H1N1)2009. When the population of patients was broke down to infected and non-infected persons, 56% (56 out of the 75) of those with confirmed infection and 38.1% (167 out of the 438) of those with not confirmed infection met these criteria. Detailed data for all swabbed patients are presented in Table 34.4.

34.4 Discussion

The results presented in this article indicate two different aspects of the influenza pandemic A(H1N1)2009 in Poland. The first is the similarity of the infection picture to that in other countries, while the second reveals weaknesses in the response to a pandemic situation which should be treated as a lesson for the future.

Since the first information on the emergence of the novel influenza virus in Europe, the NIC started preparations for the diagnosis of infections caused by this pathogen. A formal cooperation was maintained with WHO and the European Centre for Disease Prevention and Control (ECDC) and there were informal contacts with the members of the WHO Global Influenza Surveillance Network (GISN) and the European Influenza Surveillance Network (EISN). Certainly, cooperation with the most important national bodies was also in place, including the Ministry of Health, the Chief Sanitary Inspectorate, and the Government Center for Security. The NIC regularly participated in the meetings

Table 34.4 Clinical and epidemiological criteria of the novel influenza A(H1N1)2009 case (European Commission 2009) met in patients from whom clinical specimens were collected and laboratory tested at the Dept. of Influenza Research, National Influenza Center, NIPH-NIH, between April 28, 2009 and August 10, 2010

Criteria met[a]	All patients	%	Infected patients	%	Non-infected patients	%
Clinical & epidemiological	209	26.2	42	29.0	167	25.6
Only epidemiological	240	30.1	28	19.3	212	32.5
Only clinical	14	1.8	0	0.0	14	2.1
Epidemiological criteria met, but no information on clinical criteria	72	9.0	24	16.6	48	7.4
Clinical criteria met, but no information on epidemiological criteria	41	5.1	11	7.6	30	4.6
Epidemiological criteria not met and no information on clinical criteria	8	1.0	0	0.0	8	1.2
Clinical criteria not met and no informa tion on epidemiological criteria	28	3.5	5	3.4	23	3.5
Neither epidemiological nor clinical criteria met	14	1.7	0	0.0	14	2.1
No information on clinical and epidemio logical criteria	172	21.6	35	24.1	137	21.0
Total	798	100	145	100	653	100

[a]*EC* epidemiological criteria met when at least one of the following three occurred in 7 days before disease onset: (1) close contact to a confirmed case of novel influenza A(H1N1) virus infection while the case was ill, (2) traveling to an area where sustained human-to-human transmission of novel influenza A(H1N1) was documented, and (3) working in a laboratory where samples of the novel influenza A(H1N1) virus were tested

EC clinical criteria met when one of the following three occurred: (1) fever >38°C and signs and symptoms of acute respiratory infection, (2) pneumonia (severe respiratory illness), and (3) death from unexplained acute respiratory illness

of the National Influenza Pandemic Committee providing scientific background and advice on the interventions or recommendations that should be prepared for physicians, laboratory workers, and the community. In the first step, the NIC prepared detailed instructions regarding the collection of clinical specimens (types of specimens, technical ways of their collection, the optimal time for specimen collection, storage and transport conditions, etc.) that were available on the website of the NIPH-NIH and on other relevant websites. Moreover, staff of the NIC was able to respond to any questions regarding the diagnostics of the pandemic virus and in the first months of the pandemic, until the end of July 2009, this type of information, along with the diagnostics, was given to all interested parties on a 24-h basis. Most of the specimens (80.8%) tested by the NIC were from outside the sentinel influenza surveillance network, i.e. , mainly from hospitals. This resulted from the recommendations of the Minister of Health, the National Adviser for the Infectious Diseases, the National Adviser for Epidemiology, and other members of the National Influenza Pandemic Committee. According to them, all patients meeting clinical criteria and epidemiological criteria of the infection with the novel influenza virus A(H1N1)2009 had to be admitted to hospital infectious wards and the hospitals were responsible for the specimen collection and sending for laboratory testing. Since August 3, 2009, the above recommendations were modified and patients not severely ill were treated at home. This change of the recommendations also explained a decrease of the number of specimens received by the NIC since week 33/2009 (August 10–16, 2009). This decrease also resulted from the fact that laboratories of the VSESs gradually became able to perform laboratory diagnostics of A(H1N1)2009 virus. Thus, since August 2009, the NIC played mainly a role of a national reference laboratory verifying questionable results and coordinating the sentinel influenza surveillance system. It is interesting that following the decrease above outlined, a secondary increase in the number of non-sentinel specimens between weeks 45–48/2009 was observed. This situation could be partially associated with a significant

increase of the number of influenza-like illness (ILI) cases in the Ukraine in November 2009 and a recommendation of the National Influenza Pandemic Committee in Poland to intensify tracing of the suspected cases in the voivodships bordering the Ukraine (WHO 2009f). Nevertheless, in first part of November 2009, twofold to almost fourfold increase of the ILI incidence was registered in the whole of Poland compared with the last week of October 2009 (107.8 ILI cases/100,000 between 8th and 15th of November 2009 *vs.* 65.5 ILI cases/100,000 between November 1–7, 2009 *vs.* 27.8 cases/100,000 between October 23–31, 2009) (National Institute of Public Health-National Institute of Hygiene and Chief Sanitary Inspectorate 2009a, b, c).

This study shows that adolescents and young adults were the most frequently affected subjects; 48.2% of confirmed cases in the 15–25 years old and only 2.7% in the ≥65 years old group. This finding is consistent with the observations made in most of other countries (WHO 2009c). Metaanalysis performed by Khandaker et al. (2011) on data pooled from five studies from the United Kingdom, Germany, Peru, the USA, and Saudi Arabia showed that 64% of the confirmed cases were in patients aged 10–29. The authors also show that the highest proportion of positive cases among all specimens collected in a given age group was present in patients up to 25 years of age (29.7% of positive specimens in 0–4 years old; 31.4% in 5–14 years old, and 23% in 15–25 years old subjects).

This higher rate of infections at younger age and lower in the elderly are not surprising as HA glycoprotein of the A(H1N1)2009 pandemic virus is more similar to HA glycoprotein of the 1918 pandemic virus and its close descendants than to the seasonal influenza viruses A(H1N1) circulating recently (Garten et al. 2009; Greenbaum et al. 2009; Krause et al. 2010; Smith et al. 2009; Xu et al. 2010). This was also confirmed by the seroepidemiological studies showing that people aged >60 years have pre-existing cross-reactive specific antibodies to the pandemic virus A(H1N1)2009 (Booy et al. 2011; Hancock et al. 2009; Ikonen et al. 2010; Miller et al. 2010; Rizzo et al. 2010, WHO 2009d, 2010b). The finding of this study that the most affected group was patients aged up to 25 may also be related to summer holidays. During 9 weeks of the holiday time, 52% of all non-sentinel specimens from a 67-week long period of analysis were collected. The present study shows that 45.5% of infected patients had a history of travel to other countries earlier affected by the pandemic influenza virus. It is also a reasonable assumption that young people were more likely to travel than older ones. It is also known that at least to mid-August 2009 all confirmed influenza cases in Poland, i.e., those diagnosed at the NIC and VSESs laboratories were imported or linked with the imported cases. A similar situation was observed in other European countries, while a sustained virus transmission at a national level was observed in Spain, Germany, and the United Kingdom.

An equal frequency of infection in either sex, a fairly mild course, and the presence of gastrointestinal symptoms in about 14% of cases seen in the present study are all in accord with the observations made in other studies (Khandaker et al. 2011; Neumann and Kawaoka 2011; WHO 2009c, e). We also analyzed vaccination status of the swabbed patients regarding seasonal influenza vaccination in the epidemic season 2008/2009 and 2009/2010. These seasonal vaccines did not provide any protection against the A(H1N1)2009 pandemic virus. Nevertheless, it was interesting to find out how many of the swabbed patients were vaccinated with the seasonal vaccine, especially taking into account a strong interest of the community in acquiring the pandemic vaccine, on the one hand, and a low seasonal influenza vaccination rate in the general Polish population, on the other hand. The results show that barely 7.3% of the swabbed patients were vaccinated. The vaccination rate was no different among the positive cases, amounting to 6.1%. These values are similar to the seasonal influenza vaccination rates registered for a few epidemic seasons in the total population in Poland. In the epidemic season 2008/2009 barely 5.2% of the total Polish population was vaccinated against influenza, in 2009/2010 – 5.5%, and in 2010/2011 – 5.0% (Brydak 2010, 2011). According to the European Union's Council Recommendation 2009/1019/EU of December 22, 2009, all member states should prepare and implement national, regional, and local plans or appropriate policies to improve seasonal influenza vaccination coverage to be able to achieve a target of 75% vaccination coverage in the older age groups and, if possible, also in other risk groups and healthcare workers, preferably by the season

2014/2015 (European Council 2009). In Poland, there is no specific national program for human seasonal influenza. There is a National Health Program prepared for the years 2007–2015 and one of its strategic objectives is to increase the effectiveness of prevention against infectious diseases and infections. One of the priorities of this program is to reduce the incidence of infectious diseases that are preventable by vaccinations. Nevertheless, influenza is not mentioned in the program by name (National Health Program for years 2007–2015). A low interest in influenza prophylaxis causes that there is still much to do to increase influenza vaccination coverage in Poland.

Considering the emergence of the pandemic influenza virus A(H1N1)2009, the ECDC prepared, on the request of the EC, a case definition for the illness caused by this pathogen, including clinical, epidemiological, and laboratory criteria (European Commission 2009). The definition determines that a case under investigation is any person meeting both clinical and epidemiological criteria. Certainly, the use of this case definition has been important, particularly in the first months of the pandemic when there was no sustained transmission of the virus observed and the majority of the cases were imported. The results of this study show that the above case definition has not been known or used by many physicians who collected clinical specimens and sent it to the NIC. Both types of criteria were met in 40.7% of the swabbed patients. It is also known that among patients with the laboratory confirmed infection, clinical and epidemiological criteria were met in 56.0% of them, while among non-infected patients – in 38.1% of them. These results confirm that collection of specimens from patients meeting both types of criteria could increase a probability to single out persons really infected with the pandemic virus. The EC case definition was available in Polish on the most important websites providing information to physicians and the community during the pandemic, and in the recommendations prepared for physicians by the Minister of Health, the National Adviser for the Infectious Diseases and the National Adviser for Epidemiology. Therefore, there is a question of whether distribution of this information was poor and ineffective or physicians just did not use the information in practice. The problem was repeatedly discussed during the meetings of the National Pandemic Committee. There is a probability that physicians acted under strong pressure put out by patients and consequently tried to avoid any negative reactions. Nevertheless, testing the specimens collected from patients who did not meet both epidemiological and clinical criteria resulted in unnecessary costs and overload of laboratory staff and healthcare workers. Even when transmission of the pandemic virus was already sustained and confirmed in the Polish community, laboratory diagnostics should be performed for patients meeting clinical criteria and preferably for patients from the risk groups or with a severe course of the disease, according to WHO recommendations (WHO 2009h). The experience of the NIC shows that some specimens have been collected from asymptomatic patients, e.g., from seven healthcare workers from the same hospital department who had no symptoms, but had contact with a confirmed case. Moreover, these healthcare workers asked the NIC to perform diagnostics for influenza A(H1N1)2009 and for influenza B, despite the fact that in the confirmed case infection with the pandemic variant was diagnosed. This examples show the lack of knowledge on the nature of influenza viruses, even among healthcare workers.

Beside specimens collected from persons without any reasonable indication for laboratory testing for the pandemic virus, there have also been specimens collected incorrectly, e.g., those with too much volume of transport medium, collected too late after the onset of symptoms, stored for too long a time, or with attached documentation without basic information on the patient and/or physician who ordered the testing. Specific data on such issues were not presented in the present article. However, these weaknesses also resulted in unnecessary costs, waste of valuable time, and overload of health care units and the staff of the NIC. It is unjustified that after the end of the pandemic was announced by WHO, i.e., since August 2010 through the epidemic season 2010/2011, physicians kept on sending specimens to the NIC asking to perform diagnostics only for the pandemic virus A(H1N1)2009. They excluded from the diagnostics the influenza virus B and other respiratory viruses causing influenza-like illnesses such as respiratory syncytial virus, parainfluenza viruses, human metapneumovirus, coronaviruses, adenoviruses, or rhinoviruses which all can be detected in one PCR reaction by using

multiplex commercially available kits, e.g., Labopass™ RV detection kit (Cosmo), ResPlex II Plus Panel RUO (Qiagen), Seeplex RV12 ACE Detection kit (Seegene), or Seeplex RV15 OneStep ACE Detection kit (Seegene) (Brunstein et al. 2008; Do et al. 2011; Kim et al. 2009; Lee et al. 2010; Roh et al. 2008; Yoo et al. 2007).

There are some limitations of this study. The problem was that specific clinical and epidemiological information was not provided by physicians for all the swabbed patients. Nevertheless, available data presented in this study show that the picture of the infections caused by the pandemic A(H1N1)2009 influenza virus in Poland was similar to that in other countries and point to a few key elements that have to be improved before the outbreak of the next influenza pandemic. These elements are the need for rapid and effective communication between different pandemic players, effective access to timely, concise, and legible information and the recommendations to increase the seasonal influenza vaccination rates.

Conflicts of interest: The authors declare no conflicts of interest in relation to this article.

References

Booy, R., Khandaker, G., Heron, L. G., Yin, J., Doyle, B., Tudo, K. K., Hueston, L., Gilbert, G. L., Macintyre, C. R., & Dwyer, D. E. (2011). Cross-reacting antibodies against the pandemic (H1N1) 2009 influenza virus in older Australians. *The Medical Journal of Australia, 194*, 19–23.

Brunstein, J. D., Cline, Ch. L., McKinney, S., & Thomas, E. (2008). Evidence from multiplex molecular assays for complex multipathogen interactions in acute respiratory infections. *Journal of Clinical Microbiology, 46*(1), 97–102.

Brydak, L. B. (2010). Influenza – A disease of the 21st century. *Sepsis, 3*(4), 301–306. Article in Polish.

Brydak, L. B. (2011). Influenza – A family disease. *Family Medicine and Primary Care Review, 13*(2), 281–286. Article in Polish.

Do, A. H. L., van Doorn, H. R., Nghiem, M. N., Bryant, J. E., Do, Q. H., Van, T. L., Tran, T. T., Wills, B., Vo, M. H., Vo, C. K., Nguyen, M. D., Farrar, J., Tran, T. H., & de Jong, M. D. (2011). Viral etiologies of acute respiratory infections among hospitalized Vietnamese children in Ho Chi Minh City, 2004–2008. *PLoS One, 6*(3), e18176. 1–9.

European Council. (2009). Council Recommendation of 22 December 2009 on seasonal influenza vaccination (2009/1019/EU). *Official Journal of the European Union* 2009, L 348, 29.12.2009, pp. 71–72, http://eur-lex.europa.eu/LexUriServ/LexUriServ.do?uri=OJ:L:2009:348:0071:0072:EN:PDF

European Centre for Disease Prevention and Control (2010a). *European 2009 influenza pandemic timeline, 11 August, ECDC Influenza Programme* (pp. 1–11). http://www.ecdc.europa.eu/en/healthtopics/H1N1/Documents/110810_2009_pandemic_European_Timeline.pdf

European Centre for Disease Prevention and Control. (2010b). ECDC special report. The 2009 A(H1N1) pandemic in Europe. A review of the experience. Nov 2010 (pp. 1–48). http://www.ecdc.europa.eu/en/publications/Publications/101108_SPR_pandemic_experience.pdf

European Commission. (2009). Commission Decision of 30 April 2009 amending Decision 2002/253/EC laying down case definitions for reporting communicable diseases to the Community network under Decision No 2119/98/EC of the European Parliament and of the Council (2009/363/EC)'. *Official Journal of the European Union* 2009, L 110, 1.5.2009, pp. 58–59, http://eur-lex.europa.eu/LexUriServ/LexUriServ.do?uri=OJ:L:2009:110:0058:0059:EN:PDF

Garten, R. J., Davis, C. T., Russell, C. A., Shu, B., Lindstrom, S., Balish, A., Sessions, W. M., Xu, X., Skepner, E., Deyde, V., Okomo-Adhiambo, M., Gubareva, L., Barnes, J., Smith, C. B., Emery, S. L., Hillman, M. J., Rivailler, P., Smagala, J., de Graaf, M., Burke, D. F., Fouchier, R. A., Pappas, C., Alpuche-Aranda, C. M., López-Gatell, H., Olivera, H., López, I., Myers, C. A., Faix, D., Blair, P. J., Yu, C., Keene, K. M., Dotson, P. D., Jr., Boxrud, D., Sambol, A. R., Abid, S. H., St George, K., Bannerman, T., Moore, A. L., Stringer, D. J., Blevins, P., Demmler-Harrison, G. J., Ginsberg, M., Kriner, P., Waterman, S., Smole, S., Guevara, H. F., Belongia, E. A., Clark, P. A., Beatrice, S. T., Donis, R., Katz, J., Finelli, L., Bridges, C. B., Shaw, M., Jernigan, D. B., Uyeki, T. M., Smith, D. J., Klimov, A. I., & Cox, N. J. (2009). Antigenic and genetic characteristics of swine-origin 2009 A(H1N1) influenza viruses circulating in humans. *Science, 325*(5937), 197–201.

Greenbaum, J. A., Kotturi, M. F., Kim, Y., Oseroff, C., Vaughan, K., Salimi, N., Vita, R., Ponomarenko, J., Scheuermann, R. H., Sette, A., & Peters, B. (2009). Pre-existing immunity against swine-origin H1N1 influenza viruses in the general human population. *Proceedings of the National Academy of Sciences United States of America, 106*(48), 20365–20370.

Hancock, K., Veguilla, V., Lu, X., Zhong, W., Butler, E. N., Sun, H., Liu, F., Dong, L., DeVos, J. R., Gargiullo, P. M., Brammer, T. L., Cox, N. J., Tumpey, T. M., & Katz, J. M. (2009). Cross-reactive antibody responses to the 2009 pandemic H1N1 influenza virus. *The New England Journal of Medicine, 361*(20), 1945–1952.

Ikonen, N., Strengell, M., Kinnunen, L., Osterlund, P., Pirhonen, J., Broman, M., Davidkin, I., Ziegler, T., & Julkunen, I. (2010). High frequency of cross-reacting antibodies against 2009 pandemic influenza A(H1N1) virus among the elderly in Finland. *European Surveillance*, *15*(5), 16–23. http://www.eurosurveillance.org/images/dynamic/EE/V15N05/V15N05.pdf

Khandaker, G., Dierig, A., Rashid, H., King, C., Heron, L., & Booy, R. (2011). Systematic review of clinical and epidemiological features of the pandemic influenza A (H1N1) 2009. *Influenza and Other Respiratory Viruses, 5*(3), 148–156.

Kim, S. R., Ki, C. S., & Lee, N. Y. (2009). Rapid detection and identification of 12 respiratory viruses using dual priming oligonucleotide system-based multiplex PCR assay. *Journal of Virological Methods, 156*(1–2), 111–116.

Krause, J. C., Tumpey, T. M., Huffman, C. J., McGraw, P. A., Pearce, M. B., Tsibane, T., Hai, R., Basler, C. F., & Crowe, J. E., Jr. (2010). Naturally occurring human monoclonal antibodies neutralize both 1918 and 2009 pandemic influenza A (H1N1) viruses. *Journal of Virology, 84*(6), 3127–3130.

Lee, J.-H., Chun, J.-K., Kim, D. S., Park, Y., Choi, J. R., & Kim, H.-S. (2010). Identification of adenovirus, influenza virus, parainfluenza virus, and respiratory syncytial virus by two kinds of multiplex polymerase chain reaction (PCR) and a shell vial culture in pediatric patients with viral pneumonia. *Yonsei Medical Journal, 51*(5), 761–767.

Miller, E., Hoschler, K., Hardelid, P., Stanford, E., Andrews, N., & Zambon, M. (2010). Incidence of 2009 pandemic influenza A H1N1 infection in England: A cross-sectional serological study. *The Lancet, 375*(9720), 1100–1108.

National Health Programme for years. (2007–2015). *Enclosure to the resolution of the Cabinet No. 90/2007 of 15 May 2007*. http://www.mz.gov.pl/wwwfiles/ma_struktura/docs/zal_urm_npz_90_15052007p.pdf

National Institute of Public Health-National Institute of Hygiene and Chief Sanitary Inspectorate. (2009a*). Epidemiological reports. Influenza and influenza-like illness in Poland*. 23–31 Oct 2009. *10D*(30), 117–120. http://www.pzh.gov.pl/oldpage/epimeld/grypa/2009/I_09_10D.pdf

National Institute of Public Health-National Institute of Hygiene and Chief Sanitary Inspectorate. (2009b). *Epidemiological reports. Influenza and influenza-like illness in Poland*. 1–7 Nov 2009'. *11A*(31), 121–124. http://www.pzh.gov.pl/oldpage/epimeld/grypa/2009/I_09_11A.pdf

National Institute of Public Health-National Institute of Hygiene and Chief Sanitary Inspectorate. (2009c). *Epidemiological reports. Influenza and influenza-like illness in Poland*. 8–15 Nov 2009. *11B*(32), 125–128. http://www.pzh.gov.pl/oldpage/epimeld/grypa/2009/I_09_11B.pdf

Neumann, G., & Kawaoka, Y. (2011). The first influenza pandemic of the new millennium. *Influenza and Other Respiratory Viruses, 5*, 157–166.

Rizzo, C., Rota, M. C., Bella, A., Alfonsi, V., Declich, S., Caporali, M. G., Ranghiasci, A., Lapini, G., Piccirella, S., Salmaso, S., & Montomoli, E. (2010). Cross-reactive antibody responses to the 2009 A/H1N1v influenza virus in the Italian population in the pre-pandemic period. *Vaccine, 28*(20), 3558–3562.

Roh, K. H., Kim, J., Nam, M. H., Yoon, S., Lee, C. K., Lee, K., Yoo, Y., Kim, M. J., & Cho, Y. (2008). Comparison of the Seeplex reverse transcription PCR assay with the R-mix viral culture and immunofluorescence techniques for detection of eight respiratory viruses. *Annals of Clinical and Laboratory Science, 38*(1), 41–46.

Smith, G. J., Vijaykrishna, D., Bahl, J., Lycett, S. J., Worobey, M., Pybus, O. G., Ma, S. K., Cheung, C. L., Raghwani, J., Bhatt, S., Peiris, J. S., Guan, Y., & Rambaut, A. (2009). Origins and evolutionary genomics of the 2009 swine-origin H1N1 influenza A epidemic. *Nature, 459*(7250), 1122–1125.

World Health Organization. (1999). *Influenza pandemic plan. The Role of WHO and guidelines for national and regional planning*. WHO/CDS/CSR/EDC/99.1, Geneva, Switzerland, Apr 1999. http://www.who.int/csr/resources/publications/influenza/whocdscsredc991.pdf

World Health Organization. (2005). *WHO global influenza preparedness plan. The role of WHO and recommendations for national measures before and during pandemics*. WHO/CDS/CSR/GIP/2005.5, Geneva, Switzerland. http://www.who.int/csr/resources/publications/influenza/WHO_CDS_CSR_GIP_2005_5.pdf

World Health Organization. (2009a). *CDC realtime RTPCR (rRTPCR) protocol for detection and characterization of swine influenza* (version 2009). 28 Apr 2009, revision 2 (6 Oct 2009)', http://www.who.int/csr/resources/publications/swineflu/CDCRealtimeRTPCR_SwineH1Assay-2009_20090430.pdf

World Health Organization. (2009b). Pandemic influenza preparedness and response. WHO guidance document. Apr 2009, http://whqlibdoc.who.int/publications/2009/9789241547680_eng.pdf

World Health Organization. (2009c). New influenza A (H1N1) virus: Global epidemiological situation, June 2009. *The Weekly Epidemiological Record*, *84*(25), 249–260. http://www.who.int/wer/2009/wer8425.pdf

World Health Organization. (2009d). Global influenza surveillance network: Laboratory surveillance and response to pandemic H1N1 2009. *The Weekly Epidemiological Record*, *84*(36), 361–372. http://www.who.int/wer/2009/wer8436.pdf

World Health Organization. (2009e). Epidemiological summary of pandemic influenza A (H1N1) 2009 virus – Ontario, Canada, June 2009. *The Weekly Epidemiological Record*, *84*(47), 485–492. http://www.who.int/wer/2009/wer8447.pdf

World Health Organization. (2009f). *Pandemic (H1N1) 2009, Ukraine – update 1*, 3 Nov 2009'. http://www.who.int/csr/don/2009_11_03/en/index.html#

World Health Organization. (2009g). *WHO information for laboratory diagnosis of pandemic (H1N1) 2009 virus in humans – revised*. 23 Nov 2009. http://www.who.int/csr/resources/publications/swineflu/WHO_Diagnostic_RecommendationsH1N1_20090521.pdf

World Health Organization. (2009h). *Clinical management of human infection with pandemic (H1N1) 2009: Revised guidance*. 1–15 Nov 2009. http://www.who.int/csr/resources/publications/swineflu/clinical_management_h1n1.pdf

World Health Organization. (2010a). *Pandemic (H1N1) 2009 – update 112*. WHO, 6 Aug 2010. http://www.who.int/csr/don/2010_08_06/en/index.html

World Health Organization. (2010b). Seroepidemiological studies of pandemic influenza A (H1N1) 2009 virus. *The Weekly Epidemiological Record*, *85*(24), 229–236. http://www.who.int/wer/2010/wer8524.pdf

Xu, R., Ekiert, D. C., Krause, J. C., Hai, R., Crowe, J. E., Jr., & Wilson, I. A. (2010). Structural basis of preexisting immunity to the 2009 H1N1 pandemic influenza virus. *Science, 328*(5976), 357–360.

Yoo, S. J., Kuak, E. Y., & Shin, B. M. (2007). Detection of respiratory viruses with two-set multiplex reverse transcriptase-PCR assay using a dual priming oligonucleotide system. *The Korean Journal of Laboratory Medicine, 27*(6), 420–427.

Chapter 35
Immune Response to Influenza Vaccine in Hemodialysis Patients with Chronic Renal Failure

Agnieszka Mastalerz-Migas, Andrzej Steciwko, and Lidia B. Brydak

Abstract Chronic renal failure and dialysis belong to contraindications to vaccination with live vaccines. The objective of this study was to evaluate the humoral response to influenza vaccination consisting of the formation of antibodies against hemagglutinin and neuraminidase in patients undergoing chronic hemodialysis due to chronic renal failure. The study included 173 patients treated at a dialysis station in the Silesian region in Poland. The patients were assigned to the following groups: Group A-71 hemodialysis patients, mean age 65.4 ± 14.5 years; mean time of dialysis therapy 38.9 ± 31.7 months, vaccinated against influenza; Group B-39 hemodialysis patients, mean age 64.0 ± 13.5 years; mean time of dialysis therapy 45.0 ± 45.2 months, not vaccinated against influenza; and Group C-63 healthy patients, mean age 44.1 ± 21.2 years, vaccinated against influenza – control group. The vaccinated patients (Groups A & C) received a single dose of Agrippal influenza vaccine (Novartis) containing hemagglutinin from three strains of the influenza virus: A/Brisbane/59/2007 (H1N1), A/Brisbane/10/2007 (H3N2), and B/Brisbane/60/2008. The serological response to vaccination was assessed from antihemagglutinin (anti-HA) and antineuraminidase antibody assays (anti-NA). We found that the protection level of antibodies (protection rate) against H1 was only 40% among the vaccinated hemodialysis patients, as opposed to 65% in controls. The level of anti-H3 antibodies was similar in both groups of vaccines; 68% in dialysis patients and 75% in controls. The level of anti-HB antibodies was higher in the dialysis patient than in controls; 70% *vs.* 38%, respectively. The response rate to H1 antigen a month after vaccination was almost twice lower in the hemodialysis patients than in healthy controls vaccinated against influenza; 37% *vs.* 65%, respectively. We conclude that there is a rather insufficient serological response in the group of hemodialysis patients vaccinated with a single dose of influenza vaccine.

Keywords Chronic kidney disease • Hemagglutinin • Hemodialysis • Influenza vaccine • Neuraminidase

A. Mastalerz-Migas (✉) • A. Steciwko
Department of Family Medicine, Wroclaw Medical University, Syrokomli 1 St., Wroclaw 51-141, Poland

Public Higher Professional Medical School, Opole, Poland
e-mail: agamigas@op.pl

L.B. Brydak
Department of Influenza Research, National Influenza Center, National Institute of Public Health – National Institute of Hygiene, Warsaw, Poland

Department of Microbiology and Immunology, Faculty of Biology, University of Szczecin, Szczecin, Poland

M. Pokorski (ed.), *Respiratory Regulation - The Molecular Approach*,
Advances in Experimental Medicine and Biology 756, DOI 10.1007/978-94-007-4549-0_35,

35.1 Introduction

Chronic kidney disease is a challenge for medicine. It is estimated that the prevalence of chronic kidney disease is 11% in the general population, which means that the problem may affect more than four million people in Poland. The number of dialyzed patients increased from 497 in 1981 to 13,513 in 2004 in Poland, representing about a 27-fold increase. Any infection, including influenza, can cause exacerbation of the disease – or even death. Hence the emphasis should be placed on appropriate treatment, especially on the prevention of infections such as influenza. Progression of chronic renal failure and production of uremic toxins impair humoral and cellular immunity, aggravated by the process of hemodialysis which predisposes these patients to the occurrence of generalized, severe bacterial or viral infections. Chronic renal failure and dialysis belong to contraindications to vaccination with live vaccines. However, administration of an inactivated split or subunit vaccine against influenza is effective and safe for that group of patients, although publications on influenza vaccination in this adult patient group are sparse (Jordan et al. 1973; Nikoskelainen et al. 1982; Gilbertson et al. 2003; Janus et al. 2008).

The objective of this study was to evaluate the humoral response to influenza vaccination consisting of antibody production against hemagglutinin and neuraminidase in patients undergoing chronic hemodialysis due to chronic renal failure.

35.2 Methods

The study was approved by the Bioethics Committee of the Medical Academy of Wroclaw, Poland. All patients enrolled into the study provided written informed consent. The study was conducted in the epidemic season 2009/2010.

The study included 173 patients treated in the Dialysis Station in the cities of Opole and Nysa and in the Primary Health Care Clinic in the city of Wroclaw, Poland. The patients were assigned to the following study groups:

- Group A: 71 hemodialyzed patients (48 men, 23 women), mean age 65.4 ± 14.5 years; mean time of dialysis therapy 38.9 ± 31.7 months – these patients were vaccinated against influenza;
- Group B: 39 hemodialyzed patients (22 men, 17 women), mean age 64.0 ± 13.5 years; mean time of dialysis therapy 45.0 ± 45.2 months – these patients did not agree to be vaccinated against influenza and constituted a comparison group for Group A;
- Group C: 63 healthy patients (22 men, 41 women), mean age 44.1 ± 21.2 years; these patients were vaccinated against influenza and constituted a control group.

The vaccinated patients (Groups A & C) received a single dose of Agrippal influenza vaccine (Novartis, UK) which is a subunit vaccine type containing the viral surface glycoproteins – hemagglutinin and neuraminidase. One dose of vaccine contained 15 μg of hemagglutinin from three different strains of influenza virus: A/Brisbane/59/2007 (H1N1), A/Brisbane/10/2007 (H3N2), and B/Brisbane/60/2008 in a volume of 0.5 ml. The vaccine was administered into the deltoid muscle. The patients were instructed to report any symptoms of infection of the respiratory tract occurring with high fever in order to diagnose influenza in the epidemic season of 2009/2010 ending as of March 2010.

Ten milliliters of blood for clot were taken twice from each vaccinated patient: before the vaccination and 1 month afterward. Blood samples also were drawn from the non-vaccinated patients at the same time interval to obtain sera for immunological studies. Pending the collection of all samples, the sera were stored frozen at −70°C.

To obtain serological responses to the vaccination, antihemagglutinin (anti-HA) and antineuraminidase assays (anti-NA) were performed. The level of anti-HA antibodies was determined using the hemagglutination inhibition tests (HAIT). After the removal of non-specific hemagglutination

inhibitors, appropriate assays were performed. Anti-HA antibody titre for a specific virus strain was assumed to be the highest serum dilution in which agglutination of blood cells was inhibited.

Humoral responses to hemagglutinin (H1, H3, and HB) were assessed based on the following parameters:

- geometric mean of antibody titres (GMT) before and after vaccination against influenza
- mean increase in antibody titres (mean fluorescence intensity, MFI) before and after vaccination against influenza
- protective rate – expressed in the percentage of people with antibody assays ≥1:40 before and after vaccination against influenza
- response rate – expressed in the percentage of people who had at least fourfold increase in antibody titres after vaccination

The level of anti-NA antibodies was determined using the neuraminidase activity inhibition test (NI). In accordance with the procedure, the titre of antibodies against neuraminidase (subtypes N1, N2 and NB) was considered to be a dilution of serum that resulted in 50% inhibition of neuraminidase activity. Humoral responses to neuraminidase (N1, N2, and NB) were assessed based on the following parameters:

- geometric mean of antibody titres (GMT) before and after vaccination against influenza
- mean increase in antibody titres (mean fluorescence intensity, MFI) after vaccination against influenza.

35.3 Results

The results of humoral responses to influenza vaccination in the groups studied are shown in Tables 35.1 and 35.2. Antihemagglutinin antibody titers were significantly higher 1 month after vaccination in the vaccinated hemodialyzed patients and healthy controls, Groups A & C. The geometric mean titer (GMT) increased from 1.75 to 13.74 for antigen H1, from 4.09 to 53.46 for antigen H3, and from 2.83 to 39.25 for antigen HB in Group A. The increases of GMT in Group C

Table 35.1 Antihemagglutinin antibodies H1, H3, and HB in response to influenza vaccination in hemodialyzed patients in the epidemic season of 2009/2010

		Geometric mean antibody titres (GMT)		Mean increase in antibody levels (MFI)	Protective level (%)		Response rate (%)
Antigen	Group	Before vaccination	1 month after vaccination	1 month after vaccination	Before vaccination	1 month after vaccination	1 month after vaccination
A/Brisbane/59/2007 (H1N1)	A	1.75	13.74	7.86	1.41	39.44	36.62
	B	1.43	1.63	1.15	4.23	4.23	0.00
	C	1.95	38.01	19.47	0.00	64.79	64.79
A/Brisbane/10/2007 (H3N2)	A	4.09	53.46	13.07	14.08	67.61	66.20
	B	2.16	2.68	1.24	4.23	7.04	2.82
	C	4.75	61.89	13.04	0.00	74.65	70.42
B/Brisbane/60/2008	A	2.83	39.25	13.85	7.04	70.42	67.61
	B	1.66	1.56	0.94	0.00	2.82	0.00
	C	2.88	30.05	10.45	0.00	38.03	38.03

Antibody titre was the highest serum dilution in which agglutination of blood cells was inhibited
A – hemodialyzed patients, vaccinated (n = 71)
B – hemodialyzed patients, non-vaccinated (n = 39)
C – healthy group, vaccinated (n = 63)

Table 35.2 Antineuraminidase antibodies N1, N2, and NB in response to influenza vaccination in hemodialyzed patients in the epidemic season of 2009/2010

Antigen	Group	Geometric mean antibody titres (GMT)		Mean increase in antibody levels (MFI)
		Before vaccination	1 month after vaccination	1 month after vaccination
A/Brisbane/59/2007 (H1N1)	A	4.58	55.75	12.17
	B	1.49	2.76	1.86
	C	1.95	38.01	19.47
A/Brisbane/10/2007 (H3N2)	A	11.03	51.06	4.63
	B	1.48	3.06	2.07
	C	4.75	61.89	13.04
B/Brisbane/60/2008	A	10.10	47.68	4.72
	B	1.34	2.21	1.64
	C	2.88	30.05	10.45

Antibody titre was a dilution of serum that resulted in 50% inhibition of neuraminidase activity
A – hemodialyzed patients, vaccinated (n = 71)
B – hemodialyzed patients, non-vaccinated (n = 39)
C – healthy group, vaccinated (n = 63)

were from 1.95 to 38.01 for H1, from 4.75 to 61.89 for H3, and from 2.88 to 30.05 for HB. The mean fluorescence intensity (MFI) of anti-HA antibody levels after vaccination amounted to 7.86 for antigen H1, 13.07 for antigen H3, and 13.85 for antigen HB in Group A. In Group C, MFI amounted to 19.47 for H1, 13.04 for H£, and 10.45 for HB. In group B (not vaccinated), MFI amounted to 1.15 for H1, 1.24 for H3, and 0.94 for HB. The protection rate (the post-vaccination percentage of patients with protective anti-HA antibody titers 40) increased from 1.41% to 39.44% for antigen H1, from 14.08% to 67.61% for antigen H3, and from 7.04% to 70.42% for antigen HB in Group A. The protection rate in group C increased from 0% to 64.79% for antigen H1, 75.65 for antigen H3, and 38.03% for antigen HB in group C. In Group B, the protection rate did not increase significantly. The response rate, i.e., a percentage of patients with at least a four-fold increase of anti-HA antibody titers after vaccination, amounted to 36.62% for antigen H1, 64.79% for antigen H3, and 67.61% for antigen HB in Group A. The response rate in Group C after vaccination amounted to 64.79% for antigen H1, 70.42% for antigen H3, and 38.03% for antigen HB. In Group B, the response rate amounted to 0 for H1, 2.82 for H3, and 0 for HB.

Antineuraminidase antibody titers were significantly higher after vaccination than before it in Groups A & C. The GMT increased from 4.58 to 55.75 for antigen N1, from 11.03 to 51.06 for antigen N3, and from 10.10 to 47.68 for antigen NB in Group A. The increases in GMT were from 1.95 to 38.01 for N1, from 4.75 to 61.89 for N3, and from 2.88 to 30.05 NB in Group C. In Group B (not vaccinated), GMT changed from 1.49 to 2.76 for N1, from 1.48 to 3.06 for N3, and from 1.34 to 2.21 for NB. The MFI of anti-NA antibody levels after vaccination amounted to 12.17 for antigen N1, 4.63 for antigen N3, and 4.72 for antigen NB in Group A. It amounted to 19.47 for N1, 13.04 for N3, and 10.45 for NB in Group C. In Group B (not vaccinated), MFI amounted to 1.86 for N1, 2.07 for N3, and 1.64 for NB.

35.4 Discussion

Previous reports on influenza vaccination in groups at high risk and serious complications from influenza, including patients with a history of leukemia during maintenance chemotherapy or at different times after its completion, after splenectomy, in patients with hemophilia, HIV-infected

patients, children with bronchopulmonary dysplasia, patients with breast cancer, lymphoma or Wegener's disease are encouraging (Brydak and Machala 2000; Brydak et al. 2000, 2001; Wyzgal et al. 2002). These patients produced protective levels of antibodies and the vaccine turned out to be safe for them. At the same time, these reports confirm the validity of influenza vaccination in patients in higher risk groups, which is clearly stressed by the Advisory Committee on Immunization Practices, WHO, and other international scientific medical associations (ACIP 2001).

Among patients with chronic diseases, the recommendations for influenza vaccination should notably concern asthma, COPD, coronary disease, diabetes, and chronic kidney disease. Patients with chronic renal failure, particularly during dialysis therapy, are at high risk of exposures to infective agents and a severe course of infection, both viral and bacterial. Hence, the importance of prevention of infection through immunization vaccinations is stressed. Vaccination against influenza of these patients cannot be underestimated, as the course and complications of the disease may be fatal. However, it is well known that the immune response, both humoral and cellular, in such patients is impaired and in many cases the question arises of whether the vaccine will sufficiently produce protective antibody titres (Cappel et al. 1983). The reports are scanty and their results are divergent, which does not allow a comprehensive assessment of the issue. Patients with chronic renal failure treated conservatively, dialysis patients (hemodialysis, peritoneal dialysis), and patients after kidney transplantation have been studied. The studies however were conducted in small patient groups and not always included a complete evaluation of the humoral response in terms of antibodies against neuraminidase and hemagglutinins. Cavdar et al. (2003) have compared the humoral response (only H3N2) after influenza vaccination in 23 hemodialysis patients with 26 patients with cardiac disease and normal renal function and found the response was comparable in both treatment groups. Antonen et al. (2000) have compared hemodialysis (n = 42), peritoneal dialysis patients (n = 15), and those with chronic renal failure treated conservatively (n = 20) with cardiac patients with normal renal function (n = 31). The authors demonstrate a weaker humoral response in hemodialysis patients and the ones treated conservatively compared with the other groups. Beyer et al. (1988) have shown significant differences in the levels of antibodies produced against H1N1 antigens (low titres) and H3N2 (high titres) in patients on hemodialysis.

The main protective effect of influenza vaccination is related to antibody response to HI antigen of the virus. Protection studies have shown that anti-hemagglutinin antibody titres ≥40 can be considered as the safety threshold beyond which a serious influenza infection is rather unlikely. According to the statement of the Committee for Proprietary Medicinal Products and the Commission of the European Community, after influenza vaccination the protection rate (protective level of antibodies) should amount to at least 70% of the vaccinees and the response rate should be at least 40% of the vaccinees.

In our study, the protection rate against H1 was only 40% among the vaccinated hemodialysis patients, as opposed to 65% in the control group of healthy subjects. The level of antibodies against H3 antigen was similar in these two groups of subjects (68% of patients on dialysis and 75% of healthy patients) and that against HB antigen was higher in the dialysis group; 70% *vs.* 38% in healthy subjects. The response rate to H1 antigen at 1 month after vaccination was almost twice lower in the hemodialysis group than that in healthy subjects vaccinated against influenza; 37% *vs.* 65%, respectively.

35.5 Conclusion

The study demonstrates a rather insufficient serological response in the group of hemodialysis patients vaccinated with a single dose of influenza vaccine.

Acknowledgments Supported by a research fellowship within the 'Development program of Wroclaw Medical University' funded by the European Social Fund, Human Capital, National Cohesion Strategy no. UDA-POKL.04.01.01-00-010/08-01.

Conflicts of interest: The authors declared no conflicts of interest in relation to this article.

References

Advisory Committee on Immunization Practices. (2001). Prevention and control of influenza. *MMWR Morbidity and mortality weekly report, 50*, 1–46.

Antonen, J. A., Hannula, P. M., Pyhälä, R., Saha, H. H., Ala-Houhala, I. O., & Pasternack, A. I. (2000). Adequate seroresponse to influenza vaccination in dialysis patients. *Nephron, 86*(1), 56–61.

Beyer, W. E., Versluis, D. J., Kramer, P., Diderich, P. P., Weimar, W., & Masurel, N. (1988). Trivalent influenza vaccine in patients on haemodialysis: Impaired seroresponse with differences for A-H3N2 and A-H1N1 vaccine components. *Nephron, 49*(1), 16–19.

Brydak, L. B., & Machala, M. (2000). Humoral immune response to influenza vaccination in patients from high risk groups. *Drugs, 60*(1), 35–53.

Brydak, L. B., Roszkowska-Blaim, M., Machala, M., Leszczyńska, B., & Sieniawska, M. (2000). Antibody response to influenza immunization in two consecutive epidemic seasons in patients with renal diseases. *Vaccine, 18*(28), 3280–3286.

Brydak, L. B., Roszkowska-Blaim, M., Machala, M., Leszczyńska, B., & Sieniawska, M. (2001). Immunological response to influenza vaccination in children with renal failure. *Nephrology, Dialysis, Transplantation, 16*(3), 643–644.

Cappel, R., Van Beers, D., Liesnard, C., & Dratwa, M. (1983). Impaired humoral and cell-mediated immune responses in dialyzed patients after influenza vaccination. *Nephron, 33*, 21–25.

Cavdar, C., Sayan, M., Sifil, A., Artuk, C., Yilmaz, N., Bahar, H., & Camsari, T. (2003). The comparison of antibody response to influenza vaccination in continuous ambulatory peritoneal dialysis, hemodialysis and renal transplantation patients. *Scandinavian Journal of Urology and Nephrology, 37*(1), 71–76.

Gilbertson, D. T., Unruh, M., McBean, A. M., Kausz, A. T., Snyder, J. J., & Collins, A. J. (2003). Influenza vaccine delivery and effectiveness in end-stage renal disease. *Kidney International, 63*(2), 738–743.

Janus, N., Vacher, L.-V., Karie, S., Ledneva, E., & Deray, G. (2008). Vaccination and chronic kidney disease. *Nephrology, Dialysis, Transplantation, 23*, 800–807.

Jordan, M. C., Rousseau, W. E., Tegtmeier, G. E., Noble, G. R., Muth, R. G., & Chin, T. D. (1973). Immunogenicity of inactivated influenza virus vaccine in chronic renal failure. *Annals of Internal Medicine, 79*(6), 790–794.

Nikoskelainen, J., Väänänen, P., Forsström, J., & Kasanen, A. (1982). Influenza vaccination in patients with chronic renal failure. *Scandinavian Journal of Infectious Diseases, 14*(4), 245–251.

Wyzgal, J., Brydak, L. B., Zygier, D., Paczek, L., Rowinski, W., & Grochowiecki, T. (2002). Study on efficacy of influenza vaccination in renal allograft recipients. *Transplantation Proceedings, 34*(2), 572–575.

Chapter 36
Co-Infections with Influenza and Other Respiratory Viruses

I. Stefanska, M. Romanowska, S. Donevski, D. Gawryluk, and L.B. Brydak

Abstract Clinicians often do not consider the presence of more than one viral etiologic agent in respiratory infection, and in many cases they order diagnostics for influenza viruses or recently even only for A(H1N1)2009 virus. However, in a substantial number of patients with a respiratory tract disease, co-infection with various viral pathogens has been confirmed. Although the association between the occurrence of co-infection and substantially higher severity of disease is still unclear, a rapid and proper diagnostics of wide spectrum of viral respiratory pathogens reveals an accurate picture of the disease and is essential for appropriate therapeutic management and control of infection. In the present study we reported five cases of multiple respiratory infection in hospitalized immunosuppressed patients: two double infections with influenza virus (IV) type A/respiratory syncytial virus (RSV) type A and IV type A/coronavirus (CoV) OC43, one infection with four viruses – IV type A/RSV type A and B/CoV OC43, and two cases of mixed infections caused by five viral agents – IV type A and B/RSV type A and B/ parainfluenza type 3 or CoV OC43. Each patient had an underlying chronic disease and received immunosuppressive treatment. Despite a low number of tested specimens, our study shows that the inclusions of multiplex PCR methods for diagnostics of respiratory tract infections and the extension of diagnostic strategies by clinicians to detect viruses other than influenza are very important and make a contribution to identifying the true rate of co-infections and their correlation with the clinical symptoms and severity of disease.

Keywords Infection • Influenza • Diagnostics • Multiplex PCR • Respiratory viruses

I. Stefanska (✉) • M. Romanowska • S. Donevski
Department of Influenza Research, National Influenza Center, National Institute
of Public Health-National Institute of Hygiene, Chocimska 24 St., 00-791 Warsaw, Poland

Department of Fermentation Technology, Institute of Agricultural and Food Biotechnology,
Rakowiecka 36 St., 02-532 Warsaw, Poland
e-mail: i.stefanska@gmail.com

D. Gawryluk
Third Department of Pulmonary Diseases, National Tuberculosis and Chest Diseases Research Institute,
Plocka 26 St, 01-138 Warsaw, Poland

L.B. Brydak
Department of Influenza Research, National Influenza Center, National Institute
of Public Health-National Institute of Hygiene, Chocimska 24 St., Warsaw 00-791, Poland

Department of Microbiology and Immunology, Faculty of Biology,
University of Szczecin, Waska 13 St, 71-415 Szczecin, Poland

M. Pokorski (ed.), *Respiratory Regulation - The Molecular Approach*,
Advances in Experimental Medicine and Biology 756, DOI 10.1007/978-94-007-4549-0_36,

Abbreviations

AdV	adenovirus
ALRI	acute low respiratory tract infection
ARI	acute respiratory tract infection
CDC	Centers for Disease Control and Prevention
CMV	cytomegalovirus
C. pneumo	*Chlamydia pneumoniae*
CTX	cyclophosphamide
CVEV	coxsackie virus/echovirus family
EV	enteroviruses
hBoV	human bocavirus
hCoV	human coronavirus
hMPV	human metapneumovirus
hRV	human rhinovirus
IV	influenza virus
IV-A	influenza virus type A
IV-B	influenza virus type B
IV-C	influenza virus type C
M. pneumo	*Mycoplasma pneumoniae*
PCR	polymerase chain reaction
PIV	parainfluenza virus
PIV-1	parainfluenza virus type 1
PIV-2	parainfluenza virus type 2
PIV-3	parainfluenza virus type 3
PIV-4	parainfluenza virus type 4
RSV	respiratory syncytial virus
RSV-A	respiratory syncytial virus type A
RSV-B	respiratory syncytial virus type B
RT-PCR	reverse transcription-polymerase chain reaction

36.1 Introduction

Human respiratory tract infections represent a major public health problem because they are associated with a high rate of hospitalization, significant morbidity, and mortality. They thus cause a considerable financial burden on the health-care system throughout the world. The elderly and immunocompromised subjects with medical conditions are especially at high risk of developing severe course of infection and various complications. The most common respiratory viruses are influenza virus type A (IV-A) and B (IV-B), respiratory syncytial virus type A (RSV-A) and B (RSV-B), parainfluenza virus type 1, 2 and 3 (PIV-1, -2, -3), human rhinoviruses (hRV), human metapneumoviruses (hMPV), adenoviruses (AdV), human coronaviruses (hCoV), human bocavirus (hBoV) and enteroviruses (EV) (Do et al. 2011).

Infectious respiratory diseases caused by different viruses are characterized by a wide range of similar respiratory symptoms from mild cold to severe pneumonia. This makes the clinical distinction between different agents involved in infection very difficult. Although the high rates of infection with more than one respiratory virus have been reported, especially in children (Table 36.3), the real number of co-infections is undoubtedly underestimated, mainly due to sensitivity of diagnostic methods

used and limited number of tested viruses. In majority of cases the most likely or casual viral agents are tested first and the diagnostics stops with a detection of the primary relevant infectious agent. Meanwhile rapid, reliable, and accurate identification of every viral pathogen involved in infection is crucial for patient management, surveillance, and control of infection, including the prevention of nosocomial transmission.

Widespread use of PCR-based methods and their excellent sensitivity and specificity contributed to a great improvement of diagnostics of respiratory infections. While single PCR assay enables a detection of only one target, the multiplex molecular methods provide a simultaneous detection of multiple viruses in the single reaction and thus give a more accurate diagnosis of causative pathogens and provide a better understanding of the etiology of infection. The main advantages of using multiplex reactions are time saving and reducing the use of reagents and specimens, and consequently the cost of analysis. The Seeplex RV Detection Kit (Seegene Inc., Korea), used in our study, is a qualitative multiplex assay that detects 12 respiratory viruses including 11 types of RNA and one type of DNA virus: IV-A, IV-B, RSV-A, RSV-B, PIV-1, PIV-2, PIV-3, hRV, hMPV, Adv, hCoV OC43 and combined hCoV 229E/NL63. The assay uses dual priming oligonucleotide (DPO™) technology, which prevents non-specific amplification (it generates consistently high specificity by blocking the extension of non-specifically primed templates). The primers were designed for highly conserved regions in viral genome.

In the epidemic season 2010/2011, the National Influenza Centre in Poland received 140 specimens (paid diagnostics) from hospitalized patients with respiratory tract infection, including 49 specimens from severe cases (i.e., patients from intensive care units, with pneumonia, respiratory failure, immunocompromised patients). In the majority of these specimens, hospitals required only detection of influenza viruses (IV-A and IV-B (n = 29) or IV-A and subtype A(H1N1)2009 (n = 93)). Testing of specimens not only for influenza, but also other respiratory viruses was commissioned only for 18 patients. In these cases the multiplex Seeplex™ RV12 ACE Detection Kit was used to detect 12 respiratory viruses. In our paper, we present five cases of multiple infections caused by various respiratory viruses in immunocompromised patients.

36.2 Methods

All respiratory specimens (nasopharyngeal swabs) were suspended in 500 μl of physiological saline solution (within several hours after samples collection). Viral nucleic acid was extracted from 140 μl of sample using the QIAamp Viral RNA Mini Kit (Qiagen, Germany), according to the manufacturer's instructions. The elution was performed with 60 μl of elution buffer. cDNA was synthesized by using First Strand cDNA Synthesis Kit with random hexamer primers (Fermentas, Lithuania). Reverse transcription reactions were performed in a final volume of 20 μl with 1 μl of random hexamers, 5 μl of water, 5 μl of total nucleic acids extracted from clinical specimen, 4 μl of 5× RT Buffer, 2 μl of dNTP Mix (10 mM each), 1 μl of RiboLock™ RNase Inhibitor and 2 μl of M-MuLV Reverse Transcriptase. After incubation for 5 min at 25°C, reverse transcription reactions were carried out for 60 min at 45°C, followed by inactivation of reverse transcriptase for 5 min at 70°C.

The next step was multiplex reaction with using the Seeplex™ RV12 ACE Detection Kit (Seegene, Inc., Korea) containing A and B sets of primer. Both panels were performed in 20 μl reaction volumes in accordance with the supplied protocols. The internal amplification control for detection of inhibitor of PCR, positive control (a mixture of 12 pathogens and internal control clones from the manufacturer as a template) and negative control (sterilized water instead of a template) were included in each reaction. After amplification, the obtained PCR products were analyzed by electrophoresis in 2% agarose gel stained with GelRed™ 10,000× solution. The respiratory viruses were identified by

comparison of amplicons with bands included in the positive control and molecular size marker for set A or B provided by the manufacturer and consisting of seven bands with the same length as PCR products for internal control and six appropriate viruses.

The results positive for influenza type B were confirmed by further analysis by one-step real-time RT-PCR assay according to CDC rRT-PCR Protocol (version 2007) and those positive for influenza A were tested by RealTime ready Influenza A/H1N1 Detection Set (Roche Diagnostics, Switzerland) with using primer set only for detection of type A (M2). Specimens with laboratory results indicative RSV- A or/and RSV-B were confirmed by one-step RT-PCR using Transcriptor One-Step RT-PCR Kit (Roche Diagnostics, Switzerland) and primers: 5' – TGTTATAGGCATATCATTGA – 3' and 5' – TTAACCAGCAAAGTGTTAGA – 3' described by Gröndahl et al. (1999). Amplification was carried out in a 25 μl reaction volume, including 5 μl of 5 × Transcriptor buffer, 0.4 μM of each primer, 0.5 μl of enzyme, 5 μl of extracted template and water to a final volume. Cycling reaction was performed in a Veriti™ 96-Well Thermal Cycler (Applied Biosystems Inc., USA) as follows: a single cycle of reverse transcription for 30 min. at 50°C and reverse transcriptase inactivation and initial denaturation for 7 min at 94°C, than 45 cycles of denaturation at 94°C for 10 s, annealing at 55°C for 30 s and extension at 68°C for 55 s. After the last cycle, the reaction was completed by a final extension at 68°C for 7 min. Amplification products (20 μl) were separated in 1.5% agarose gel stained with GelRed™ 10,000× solution in 1 × TAE buffer. GeneRuler™ 100 bp DNA Ladders was used for estimating the molecular size weight of the obtained bands (Fermentas, Lithuania). Clinical specimens, isolated nucleic acids, and cDNA were stored at −70°C.

36.3 Results

Ten out of the 18 respiratory specimens were positive for at least one respiratory virus. Single infections were found in five cases and were caused by IV-A (three cases) and RSV-B (two cases). Co-infections (infections with two or more viruses) were found in five patients: double infections were identified in two cases, one patient was co-infected with four different viral pathogens, and in other two patients multiple infections caused by five viral agents was detected. Table 36.1 shows the pathogens involved in multiple infections.

Four co-infected patients (P1, P2, P3, and P4) were hospitalized in the same hospital and Department. The swabs were collected on the 4th of March 2011 (from patients P1 and P2) and the 11th of March 2011 (from patients P3 and P4). Patient 5 was hospitalized in another hospital and the swab was collected on the 3rd of February 2011. All five patients were immunosuppressed, including one child (4-year-old boy) and have different underlying chronic diseases (Table 36.2). Only two patients (P1 and P3 with co-infections caused by IV-A, IV-B and three other viruses) developed symptoms of acute respiratory infection with signs of bronchial obturation and they required longer antiviral therapy. One of them (P1) was mechanically ventilated for 3 days. The condition of the remaining patients was medium or good. Three patients received oseltamivir, one oseltamivir and then zanamivir, one patient received antibiotics and no antiviral drugs. The condition of two patients after therapy was medium, although one of them received oseltamivir. In this patient mixed infection with five viral agents: IV-A, IV-B, RSV-A, RSV-B, and PIV-3 were confirmed.

Monoplex PCR with different primer sets for detection of IV-A, IV-B and RSV-A/B (without identification of subtype) showed the results consistent with multiplex Seeplex PCR. In case of Patient 2, a second specimen (bronchoalveolar lavage) was collected on the 23rd of March 2011 and the result was positive for RSV-B and negative for the other pathogens, including IV-A and RSV-A, which were detected in the previous specimen.

Table 36.1 Type of detected co-infection

Virus detected		
2 viral agents:		
1.	Influenza type A Respiratory syncytial virus type A	Patient 2 (P2)
2.	Influenza type A Coronavirus OC43	Patient 5 (P5)
4 viral agents:		
1.	Influenza type A Respiratory syncytial virus type A Respiratory syncytial virus type B Coronavirus OC43	Patient 4 (P4)
5 viral agents:		
1.	Influenza type A Influenza type B Respiratory syncytial virus type A Respiratory syncytial virus type B Parainfluenza type 3	Patient 1 (P1)
2.	Influenza type A Influenza type B Respiratory syncytial virus type A Respiratory syncytial virus type B Coronavirus OC43	Patient 3 (P3)

36.4 Discussion

Conventional methods of diagnostics of viral respiratory infections base mainly on virus isolation by cell culture, antigen detection, and serological assays. Cell culture has been considered as the gold standard for virus diagnosis but is not adapted to all medically important respiratory viruses. In contrast to this method, PCR permits rapid detection of viruses that are difficult to culture or have not been well replicated *in vitro*, such as hMPV, hCoV NL63 and hRV, with excellent sensitivity and specify (Calvo et al. 2008). Additionally, viruses present in specimens may considerably differ with viral loads and rate of replication, and this would make the detection of slowly replicating pathogens difficult. Therefore, numerous studies have been developed over recent years to evaluate the PCR-based methods for detection and typing/subtyping of respiratory viruses (Templeton et al. 2004; Bellau-Pujol et al. 2005; Gunson et al. 2005; Wu et al. 2008). When a viral infection is taken into consideration, because of very similar and nonspecific clinical symptoms caused by various respiratory viruses, the list of possible etiologic agents is very long. In contrast to monoplex PCR reaction, the use of multiplex PCR allows detecting various respiratory pathogens in a single reaction, including the identification of the type and the detection of co-infections with multiple agents, which could be missed by the monoplex reaction. The introduction of multiplex PCR to routine diagnostics revealed a higher prevalence of co-infections than has previously been reported by conventional techniques (Freymuth et al. 1997). A review of the literature indicates that the rate of co-infections may range from approximately 15 to as high as 50% of all positive specimens (Table 36.3). The majority of papers presenting the results of molecular assays for simultaneous detection of respiratory viruses and mixed infections focus on pediatric patients, infants, and young children in whom viral shedding in the respiratory tract is usually much higher. In these patients, the respiratory syncytial viruses were the most common pathogen occurred in respiratory viral co-infection, the next most often identified viruses in mixed infection were hRV, PIV, hMPV, and others. There also are observed co-infections with different subtypes of influenza A virus (Pajak et al. 2011).

Table 36.2 Characteristics of patients with diagnosed co-infections

	Patient 1	Patient 2	Patient 3	Patient 4	Patient 5
Age/sex	58/female	33/female	70/female	40/male	4/male
Medical conditions	Wegener's granuloma with affecting of central nervous system, deep lymphocytopenia, and 3 months earlier the pulmonary embolism	Wegener's granuloma and Takayasu disease, lymphocytopenia	Dermatomyositis with interstitial pulmonary disease	Allergic pulmonary alveolitis	Hemosiderosis
Therapy	Immunosuppressive therapy (CTX)	Immunosuppressive therapy (CTX, prednisone)	Glucocorticoid therapy	Glucocorticoid therapy	Immunosuppressive therapy (encorton)
Symptoms	Severe course of infections with pneumonia, respiratory failure and pancytopenia	No symptoms of acute respiratory infection	Typical influenza-like illness with malaise, fever and cough	No symptoms of acute respiratory infection	No symptoms of acute respiratory infection; intensified cough, tachypnea and decrease of carbonation
Received antiviral treatment	Oseltamivir (2×75 mg) for 5 days, than oseltamivir (2×150 mg) for 11 days	Oseltamivir (2×75 mg) for 5 days	Oseltamivir (2×75 mg) for 6 days, than zanamivir (2×5 mg) for 6 days	Oseltamivir (2×75 mg) for 11 days	No treatment (only antibiotics)
Condition of patients before/ after therapy	Severe, mechanical ventilation for 3 days/ medium	Good/good	Medium/good	Medium/good	Medium/medium
Other laboratory tests and results	Culture of bronchial secretion– *Acinetobacter baumanii*; stool culture– *Clostridium difficile*	PCR positive for CMV (bronchial secretion); the culture of bronchial secretion – negative results	Culture of sputum-negative results	Culture of bronchial secretion – negative results	Culture of throat swab– negative result; the culture of bronchial secretion– *Streptococcus pneumoniae*

Table 36.3 Review of literature regarding co-infections

Reference	Tested pathogens	The number of co-infections (percentage of all positive specimens)	The number of pathogens detected per sample	Co-infections rates by respiratory viral pathogens	Study group
Freymuth et al. (1997)	IV-A; RSV; PIV-1, -2; PIV-3; hRV; Adv	50 (28.2%)	Double infection, $n=50$	RSV = 90.0%; PIV-1/2/3 = 40.0% (PIV-3 = 34.0%); AdV = 28.0%; IV-A = 24.0%; hRV = 18.0%	277 hospitalized infants
Bellau-Pujol et al. (2005)	IV-A; IV-B; IV-C; RSV; PIV-1; PIV-2; PIV-3; PIV-4; hMPV; hRV; hCoV OC43/229E	33 (20.6%)	Double infection, $n=30$ Three pathogens, $n=3$	hRV = 81.8%; RSV = 42.4%; hMPV = 39.4%; PIV-1/2/3 = 27.3% (PIV-3 = 21.2%); hCoV OC43, IV-A/B = 6.1%	203 from hospitalized children
Yoo et al. (2007)	IV-A; IV-B; RSV-A; RSV-B; PIV-1; PIV-2; PIV-3; hMPV; hRV; AdV; hCoV OC43; hCoV 229E/NL63	16 (14.3%)	Double infection, $n=15$ Three pathogens, $n=1$	RSV-A/B = 81.3%; PIV = 62.5%; hMPV = 18.8%[a]	200 children ≤5 years old
Brunstein et al. (2008)	IV-A; IV-B; RSV-A; RSV-B; PIV-1; PIV-2; PIV-3; PIV-4; hMPV; hRV; AdV; CVEV; bacterial pathogens[b]	475 (40.4%)	Double infection, $n=371$ Three pathogens, $n=89$ Four pathogens, $n=14$ Five pathogens, $n=1$	No data of this type available	1,742 patients with ARI (80% pediatric and 20% adult)
Calvo et al. (2008)	IV-A; IV-B; IV-C; RSV; PIV-1; PIV-2; PIV-3; PIV-4; hMPV; hRV; AdV; hCoV 229E/OC43; EV	86 (17.4%)	Double infection, $n=70$ Three pathogens, $n=12$ Four pathogens, $n=4$	RSV-A/B = 79.1%; AdV = 43.0%; hRV = 30.2%; hMPV = 22.1%; IV-A = 18.6%; EV = 10.5%; IV-C, PIV-1/2/3/4 = 9.3%; hCoV = 1.2%	749 hospitalized children under 24 months of age with ALRI
Roh et al. (2008)	IV-A; IV-B; RSV-A; RSV-B; PIV-1; PIV-2; PIV-3; hMPV; hRV; AdV; hCoV OC43; hCoV 229E/NL63	7 (21.2%)	Double infection, $n=7$	AdV = 57.1%; IV-B, hRV = 28.6%; RSV-A, RSV-B, PIV-1, PIV-3, hCoV = each 14.3%	50 patients with ARI, (45 children, 5 adults)
Kim et al. (2009)	IV-A; IV-B; RSV-A; RSV-B; PIV-1; PIV-2; PIV-3; hMPV; hRV; AdV; hCoV OC43; hCoV 229E/NL63	13 (17.1%)	Double infection, $n=12$ Three pathogens, $n=1$	RSV-A/B = 69.3%, PIV-1/2/3 = 84.7%; hRV, AdV = 23.1%; IV-B = 7.7%	92 patients (86 children, 6 adults)
Lee et al. (2010)	IV-A; IV-B; RSV-A; RSV-B; PIV-1; PIV-2; PIV-3; hMPV; hRV; AdV; hCoV OC43; hCoV 229E/NL63; hBoV; EV	30 (29.1%)	Double infection, $n=25$ Three pathogens, $n=4$ Four pathogens, $n=1$	RSV-A/B = 90.0%; hMPV = 33.3%; hRV = 20%; IV-A/B = 16.7%; PIV-3 = 16.7%; AdV = 16.7%; hCoV 229E/NL63 = 13.3%; hCoV OC43 = 10.0%; PIV-1 = 3.3%	220 pediatric patients with ALRI

(continued)

Table 36.3 (continued)

Reference	Tested pathogens	The number of co-infections (percentage of all positive specimens)	The number of pathogens detected per sample	Co-infections rates by respiratory viral pathogens	Study group
Meerhoff et al. (2010)	IV-A; IV-B; RSV-A; RSV-B; PIV-1, PIV-2; PIV-3; PIV-4; hMPV; hRV; AdV; hCoV; BoV; *M. pneumo; C. pneumo*	45 (47.9%)	Double infection, $n = 25$ Three pathogens, $n = 17$ Four pathogens, $n = 2$ Five pathogens, $n = 1$	BoV = 91%; RSV = 72%; hCoV = 71%; hMPV = 60%; hRV = 57%[a]	98 infants
Richard et al. (2008)	IV-A/B; RSV-A/B; PIV-1/2/3/4; hCoV NL63; hRV; EV	44 (25.4%)	Double infection, $n = 44$	RSV-A/B = 81.8%; hRV = 50.0%; hMPV = 18.2%; EV = 13.6%; IV-A/B, hCoV NL63 = 11.4%	180 hospitalized infants with bronchiolitis
Nascimento et al. (2010)	IV-A; IV-B; RSV; PIV-1; PIV-2; PIV-3; hMPV; hRV; AdV; hCoV NL63/HKU1; hBoV; EV	34 (47.2%)	Double infection, $n = 22$ Three pathogens, $n = 8$ Four pathogens, $n = 4$	RSV = 67.6%; hRV = 61.8%; EV = 44.1%; hMPV, BoV = 23.5%; PIV-3 = 17.6%; hCoV = 5.1%; IV-A, PIV-1 = 2.9%	77 infants with acute bronchiolitis
Do et al. (2011)	IV-A; IV-B; RSV-A; RSV-B; PIV-1; PIV-2; PIV-3; hMPV; hRV; AdV; hCoV OC43; hCoV 229E, NL63; hBoV; EV	62 (27.9%)	Double infection, $n = 55$ Three pathogens, $n = 6$ Four pathogens, $n = 1$	BoV = 43.5%; IV-A/B = 33.9%; RSV-A/B = 33.9%; hCoV NL63 = 25.8%; EV = 24.2%; AdV = 19.4%; PIV-1/2/3 = 12.9%; hRV = 9.7%; hMPV = 8.1%	309 children (2–13 year old) with ARI

Abbreviations: *ARI* acute respiratory tract infection, *ALRI* acute low respiratory tract infection, *IV* influenza virus: A (IV-A), B (IV-B) and C (IV-C), *RSV* respiratory syncytial virus: type A (RSV-A) and type B (RSV-B), *PIV* parainfluenza virus: type 1 (PIV-1), type 2 (PIV-2), typa 3 (PIV-3) and type 4 (PIV-4), *hMPV* human metapneumovirus, *hRV* human rhinovirus, *AdV* adenovirus, *hCoV* human coronavirus, *hBoV* human bocavirus, *EV* enteroviruses, *CVEV* coxsackie virus/echovirus family, *M. pneumo Mycoplasma pneumoniae, C. pneumo Chlamydia pneumoniae*

[a] Co-infections rates by the most common viral pathogen

[b] *Haemophilus influenza* (all types); *Haemophilus influenzae* (strains a, b, c and d); *Haemophilus influenzae* (strains e and f); *Mycoplasma pneumoniae*; *Chlamydia pneumoniae*; *Legionella pneumophila*; *Streptococcus pneumoniae*; *Neiseria meningitidis*

The Seeplex™ RV Detection Kit has recently been found as a good tool for the detection of multiple infections caused by common respiratory viruses (Yoo et al. 2007; Do et al. 2011), with sensitivity higher than viral culture assays (Drews et al. 2008; Roh et al. 2008; Kim et al. 2009; Lee et al. 2010). Our findings confirmed that co-infections are not a rare occurrence, particularly in immunocompromised patients with medical conditions receiving immunosuppressive therapy. Nevertheless, a limitation of this study is a low number of tested specimens (18 specimens) that does not allow making more significant observations, especially the comparison of clinical and epidemiological features between patients with single infection and patients with multiple infections.

A rapid and accurate identification of etiologic agents involved in a respiratory infection is of essential clinical value. This may support the physician's decision regarding the selection of appropriate treatment and a prompt use of antiviral drugs, such as neuraminidase inhibitors in case of influenza infections, for a patient, the exposed family members, or contact persons. Clinicians are inclined to use antibiotics in cases when the etiological agent of infection is not identified. Therefore, in spite of lack of specific antiviral drugs and the symptomatic and supportive treatment in majority of respiratory viral infections, a rapid detection of viral pathogen may help avoid an inappropriate use of antibiotics. Moreover, the multiplex methods that enable detection of a broad spectrum of common viral pathogens are clinically desirable in case of specific groups of patients: children, the elderly, and immunocompromised individuals who tend to have prolonged virus shedding and who are at increased risk of serious complications and mortality. Such tests allow detecting agents not primarily expected in a patient.

Another important aspect of the identification of mixed infections is that the presence of more than one pathogen may influence the course of infection; although the exact clinical significance of mixed infection remains unclear (Paranhos-Baccalà et al. 2008). In numerous studies that have described co-infections, no clinical differences among patients with single and multiple infections are reported, including the severity of disease, clinical signs of infection, their intensity, or duration of hospital stays (Brouard et al. 2000; Lee et al. 2010; Nascimento et al. 2010). In contrast, Calvo et al. (2008) reported that infants with co-infections of RSV and one or more other respiratory pathogens have a significantly higher incidence of fever and the duration of hospitalization was longer in comparison to infants infected only with RSV. In the study of Richard et al. (2008), a significant correlation between dual viral infection and increased severity in bronchiolitis was found and infants with co-infections were at 2.7 times higher risk for admission to the pediatric intensive care unit than those with single infections. The other significant factors that bore on the severity of infection were: age (<42 days), premature birth, and the underlying chronic disease. There were no statistically significant differences between host conditions, duration of assisted ventilation or of supplemental oxygen administration, and duration of hospitalization (Richard et al. 2008). Certainly, further studies for a better understanding of these various interactions and the clinical differences between single and multiple respiratory viral infections need to be carried out.

Brunstein et al. (2008) suggested the occurrence of pathogen co-suppression, when infection with one pathogen reduces a risk for infection with others. Such interactions have been observed for the following viruses: RSV and IV; RSV-A and RSV-B; RSV and PIV; hRV and RSV/IV. However, in the present study we identified four cases of simultaneous infections with RSV and IV. Two of these cases were caused by RSV-A and RSV-B and one by both types of RSV and PIV. These four co-infected patients (P1, P2, P3 and P4) were hospitalized in the same unit, multiple infections were caused by four different combinations of only six viruses (IV-A in four patients, IV-B in two patients, RSV-A in four patients, RSV-B in three patients, hCoV OC43 in two patients, and PIV-3 in one patient) and all specimens were collected during 1 week, which all suggests a high probability of nosocomial transmissions. Additionally, in the case of Patient 2, the second specimen collected after an interval of 19 days was negative for IV-A and RSV-A but positive for RSV-B.

The present study has some limitation. In electrophoretic gel patterns of PCR products obtained for patients with co-infections, the intensity of bands was variable, with some faint bands. Due to excellent sensitivity of PCR and its very low detection limit (even several copies per reaction, including

non-replicated viruses), weak positive results may be related not with active but passing infection (Calvo et al. 2008). Especially in children and immunosuppressed patients, shedding of a low concentration of viruses from a previous infection would be expected. This may be relevant for the interpretation of multiple infections and for the role of particular pathogens in the clinical picture of disease. The identified presence of viral agents does not exclude the possibility of concomitant infection caused by bacterial pathogens. In our study, in Patients 2, 3, and 4 cultures of bronchial secretion or sputum gave all negative results. In Patient 1, culture of bronchial secretion was positive for *Acinetobacter baumanii* and in Patient 5 it was positive for *Streptococcus pneumoniae* but that from a throat swab was negative.

36.5 Conclusions

In conclusion, our findings show that in case of hospitalized patients with respiratory tract infection, especially with severe infections observed in children, elderly, and immunocompromised patients who are susceptible to serious complications, the simultaneous detection of multiple viral agents is advisable and more reliable than detection of only influenza viruses. This enables to reveal an accurate picture of the disease and thus is essential for the control of infection, including the nosocomial transmission, prioritizing diagnostic and improvement of both preventive and therapeutic managements. Identifying the accurate etiology of infection also allows the physician to determine better prognosis and to inform patients about the measures that should be implemented to limit the spread of infections to other persons.

Conflicts of interest: The authors declare no conflicts of interest in relation to this article.

References

Bellau-Pujol, S., Vabret, A., Legrand, L., Dina, J., Gouarin, S., Petitjean-Lecherbonnier, J., Pozzetto, B., Ginevra, C., & Freymuth, F. (2005). Development of three multiplex RT-PCR assays for the detection of 12 respiratory RNA viruses. *Journal of Virological Methods, 126*(1–2), 53–63.

Brouard, J., Freymuth, F., Varbet, A., Jokic, M., Guillois, B., & Duhamel, J. F. (2000). Viral co-infections in immunocompetent infants with bronchiolitis: Prospective epidemiologic study. *Archives of Pediatrics, 7*(Suppl. 3), 531–535.

Brunstein, J. D., Cline, C. L., McKinney, S., & Thomas, E. (2008). Evidence for multiplex molecular assay for complex multipathogen interactions in acute respiratory infections. *Journal of Clinical Microbiology, 46*(1), 97–102.

Calvo, C., García-García, M. L., Blanco, C., Vázquez, M. C., Frías, M. E., Pérez-Breña, P., & Casas, I. (2008). Multiple simultaneous viral infections in infants with acute respiratory tract infections in Spain. *Journal of Clinical Virology, 42*(3), 268–272.

Do, A. H. L., van Doorn, H. R., Nghiem, M. N., Bryant, J. E., Hoang, T. Ht., Do, Q. H., Van, T. L., Tran, T. T., Wills, B., Nguyen, V. Cv., Vo, M. H., Vo, C. K., Nguyen, M. D., Farrar, J., Tran, T. H., & de Jong, M. D. (2011). Viral etiologies of acute respiratory infections among hospitalized Vietnamese children in Ho Chi Minh City. 2004–2008. *PLoS One, 6*(3), e18176.

Drews, S. J., Blair, J., Lombos, E., DeLima, C., Burton, L., Mazzulli, T., & Low, D. E. (2008). Use of the Seeplex RV Detection kit for surveillance of respiratory viral outbreaks in Toronto, Ontario, Canada. *Annals of Clinical and Laboratory Science, 38*(4), 376–379.

Freymuth, F., Vabret, A., Galateau-Salle, F., Ferey, J., Eugene, G., Petitjean, J., Gennetay, E., Brouard, J., Jokik, M., Duhamel, J.-F., & Guillois, B. (1997). Detection of respiratory syncytial virus, parainfluenza virus 3, adenovirus and rhinovirus sequences in respiratory tract of infants by polymerase chain reaction and hybridization. *Clinical and Diagnostic Virology, 8*(1), 31–40.

Gröndahl, B., Puppe, W., Hoppe, A., Kühne, A., Weigl, J. A. I., & Schmitt, H. J. (1999). Rapid identification of nine microorganisms causing acute respiratory tract infections by single-tube multiplex reverse transcription-PCR: Feasibility study. *Journal of Clinical Microbiology, 37*(1), 1–7.

Gunson, R. N., Collins, T. C., & Carman, W. F. (2005). Real-time RT-PCR detection of 12 respiratory viral infections in four triplex reactions. *Journal of Clinical Virology, 33*(4), 341–344.

Kim, S. R., Ki, C. S., & Lee, N. Y. (2009). Rapid detection and identification of 12 respiratory viruses using dual priming oligonucleotide system-based multiplex PCR assay. *Journal of Virological Methods, 156*(1–2), 111–116.

Lee, J. H., Chun, J. K., Kim, D. S., Park, Y., Choi, J. R., & Kim, H. S. (2010). Identification of adenovirus, influenza virus, parainfluenza virus, and respiratory syncytial virus by two kinds of multiplex polymerase chain reaction (PCR) and shell vial culture in pediatric patients with viral pneumonia. *Yonsei Medical Journal, 51*(5), 761–767.

Meerhoff, T. J., Houben, M. L., Coenjaerts, F. E., Kimpen, J. L., Hofland, R. W., Schellevis, F., & Bont, L. J. (2010). Detection of multiple respiratory pathogens during primary respiratory infection: Nasal swab versus nasopharyngeal aspirate using real-time polymerase chain reaction. *European Journal of Clinical Microbiology and Infectious Diseases, 29*(4), 365–371.

Nascimento, M., Souza, A. V., Ferreira, A. V., Rodrigues, J. C., Abramovici, S., & Silva Filho, L. V. (2010). High rate of viral identification and coinfections in infants with acute bronchiolitis. *Clinics (São Paulo, Brazil), 65*(11), 1133–1137.

Pajak, B., Stefanska, I., Lepek, K., Donevski, S., Romanowska, M., Szeliga, M., Brydak, L. B., Szewczyk, B., & Kucharczyk, K. (2011). Rapid differentiation of mixed influenza A/H1N1 virus infections with seasonal and pandemic variants by multitemperature single-stranded conformational polymorphism analysis. *Journal of Clinical Microbiology, 49*(6), 2216–2221.

Paranhos-Baccalà, G., Komurian-Pradel, F., Richard, N., Vernet, G., Lina, B., & Floret, D. (2008). Mixed respiratory virus infections. *Journal of Clinical Virology, 43*(4), 407–410.

Richard, N., Komurian-Pradel, F., Javouhey, E., Perret, M., Rajoharison, A., Bagnaud, A., Billaud, G., Vernet, G., Lina, B., Floret, D., & Paranhos-Baccalà, G. (2008). The impact of dual infection in infants admitted to a pediatric intensive care unit associated with severe bronchiolitis. *Pediatric Infectious Disease Journal, 27*(3), 1–6.

Roh, K. H., Kim, J., Nam, M. H., Yoon, S., Lee, C. K., Lee, K., Yoo, Y., Kim, M. J., & Cho, Y. (2008). Comparison of the Seeplex reverse transcription PCR assay with the R-mix viral culture and immunofluorescence techniques for detection of eight respiratory viruses. *Annals of Clinical and Laboratory Science, 38*(1), 41–46.

Templeton, K. E., Scheltinga, S. A., Beersma, M. F., Kroes, A. C., & Claas, E. C. (2004). Rapid and sensitive method using multiplex real-time PCR for diagnosis of infections by influenza A and B viruses, respiratory syncytial virus, and parainfluenza viruses 1, 2, 3, and 4. *Journal of Clinical Microbiology, 42*(4), 1564–1569.

Wu, C., Cheng, X., He, J., Lv, X., Wang, J., Deng, R., Long, Q., & Wang, X. (2008). A multiplex real-time RT-PCR for detection and identification of influenza viruses A and B and subtypes H5 and N1. *Journal of Virological Methods, 148*(1–2), 81–88.

Yoo, S. J., Kuak, E. Y., & Shin, B. M. (2007). Detection of 12 respiratory viruses with two-set multiplex reverse transcriptase-PCR assay using a dual priming oligonucleotide system. *The Korean Journal of Laboratory Medicine, 27*(6), 420–427.

Chapter 37
Flow Cytometry in Detection of Abnormalities of Natural Killer Cell

K. Popko, I. Malinowska, E. Gorska, A. Stelmaszczyk-Emmel, and U. Demkow

Abstract The population of natural killer (NK) cells is very heterogeneous and plays a role in the immune system. Several NK cells subpopulations are recognized, differing in phenotype, cytokine release and cytotoxic ability. Different expression of biologically relevant molecules on the surface of NK cells may indicate their multiple functions. The activity of NK cells has mainly to do with their cytotoxic nature. A complete analysis of NK cells function requires application of many tests because a defect may be present at different stages of the cytotoxic process, from signal transduction through lysosome degranulation to target cells destruction. Flow cytometry is actually one of the best methods for the identification of NK cells and tracking their defects.

Keywords Immunodeficiency • Cytotoxicity • Immune system • Natural killer cells • Perforin

37.1 Introduction

37.1.1 Role and Diversity of NK Cells

Normal function of the immune system depends on the proper proportion and efficiency of immunocompetent cells of different lineages. One crucial cell population maintaining the immunological homeostasis is the natural killer (NK) cell lineage. The major role of NK cells is rejection of tumors, destruction of invading pathogens and of the organism's own cells that may be autoreactive. The main action of NK cells is antibody-independent spontaneous cytotoxicity. NK cells also play a regulative role in the immune system by releasing a broad range of cytokines.

Disorders affecting function or the number of NK cells may destabilize the immune system and lead to uncontrolled proliferation of pathologically changed cells. As a consequence, tumors and

K. Popko (✉) • E. Gorska • A. Stelmaszczyk-Emmel • U. Demkow
Department of Laboratory Diagnostics and Clinical Immunology of Developmental Age,
Medical University of Warsaw, Marszalkowska 24 St., Warsaw 00-576, Poland
e-mail: aksiak@interia.pl

I. Malinowska
Department of Pediatrics, Hematology and Oncology, Medical University of Warsaw,
Marszalkowska 24 St., Warsaw 00-576, Poland

M. Pokorski (ed.), *Respiratory Regulation - The Molecular Approach*,
Advances in Experimental Medicine and Biology 756, DOI 10.1007/978-94-007-4549-0_37,

autoimmunization may arise. The NK cell population is heterogenic. Several subpopulations may be recognized, differing in phenotype, cytokine release and cytotoxic ability. In healthy subjects, five NK cell populations may be defined: $CD56^{bright}$ $CD16^{-}$, $CD56^{bright}$ $CD16^{dim}$, $CD56^{dim}$ $CD16^{-}$, $CD56^{dim}$ $CD16^{bright}$, $CD56^{-}$ $CD16^{bright}$. Under normal conditions, the subpopulations $CD56^{dim}$ $CD16^{-}$ and $CD56^{-}$ $CD16^{bright}$ are in the minority and the $CD56^{bright}$ $CD16^{-}$ and $CD56^{bright}$ $CD16^{dim}$ are dominant. Among many important differences between NK cell subpopulations some are worth mentioning. The $CD56^{bright}$ cells lack KIR receptors (killer cell immunoglobulin-like receptors) and ILT2 (immunoglobulin-like transcript 2), in opposition to the $CD56^{dim}$ subpopulation in which the molecules listed above can be found in abundance. On the other hand, CD94/NK2A receptors, which play a major role as inhibitory receptors, could be found in the majority of the $CD56^{bright}$ cells and rarely on the $CD56^{dim}$ cells. Numerous differences in expressions of biologically relevant molecules on the surface and within the different subpopulations of NK cells may indicate their multiple functions. There is evidence that the $CD56^{dim}$ cells show higher cytotoxic activity in comparison with $CD56^{bright}$ cells (Cooper et al. 2001a, b). There is also a higher amount of perforins and granzymes in their cytoplasmic granules. Furthermore, these cells are able to form more conjugates with K562 target cells. High expression of CD16 molecules on their surface enables more effective reactions of antibody dependent cytotoxicity. On the other hand, the $CD56^{bright}$ cells are the most effective in cytokine production (IFN-gamma, TNF-alpha, GM-CSF, IL-10, IL-13) (Wilk et al. 2008).

Taking all these findings into consideration, the assessment of subpopulations of NK cells seems of importance, because relevant change in one of the subpopulations may modify or even highly affect physiological role and function of all NK cells.

37.1.2 Defects in NK Cell Function

There are rather rare disorders in which NK cells are absent, deficient, or dysfunctional, in the absence of any other identifiable immunodeficiency, genetic or iatrogenic disorders which could affect NK cells. NK cell disorders are characterized clinically by susceptibility to severe and recurrent infection with *Herpes viruses*, including *Varicella zoster virus* (VZV), *Herpes simplex virus* (HSV) I and II, *Epstein-Barr virus* (EBV), and *Cytomegalovirus* (CMV). There is also a marked susceptibility in some patients to *Human Papilloma Viruses* infections (Biron et al. 1999; Mossman and Ashkar 2005; Notarangelo and Mazzolari 2006). The background of these deficiencies is diverse and often complicated as it involves genetic abnormalities, impaired signal transduction, and consequently loss of cytotoxic abilities.

One of the most severe disorders resulting from impairment of NK cell function is hemophagocytic lymphohistiocytosis (HLH). This disease may lead to uncontrolled hyperactivation of macrophages which phagocytose erythrocytes, leucocytes, platelets and their precursors within bone marrow, liver and lymph nodes. As a consequence, patients suffer from fever, advanced pancytopenia and hepatosplenomegaly. The disorder is life-threatening and often the only successful treatment is bone marrow transplantation (Fishman 2000; Henter et al. 2007; Lackner et al. 2008).

In most cases of genetically determined familial form of HLH, mutations impairing the production of perforins occur, thus lytic action of NK cells is disturbed. In this case, elimination of pathogens is impossible and concurrently the immunological system is turned on for a constant and uncontrolled stimulation. As a result of inflammatory cytokine and growth factor actions, macrophage activation and proliferation occurs. Macrophages infiltrate internal organs: bone marrow, liver, spleen, lymph nodes, CNS and heart. This leads to phagocytosis of hematopoetic cells and systemic inflammatory response syndrome (SIRS) development (Horne et al. 2008; Vastert et al. 2009). Macrophage activation syndrome (MAS) clinically resembles the familial form of HLH. In both cases, the most common factor that triggers hemophagocytic syndrome is usually viral infection, especially EBV or CMV.

Patients suffering form MAS also show a lower number of NK cells or perforin secreting cells in the bloodstream. Impaired release of perforins can be detected in CD8 lymphocytes as well. Defects in cytotoxicity of NK cells and CD8 lymphocytes are commonly detected in MAS and HLH (Grom et al. 2004; Villanueva et al. 2005).

37.1.3 The Aim of the Present Report

Flow cytometry is one of the most useful tools in the evaluation of NK cells function. This method enables tracking of the defects appearing at various stages of cells action and activation. Numerous tests with individual modifications and applications have been designed and described (Alter et al. 2004; Aktas et al. 2009; Betts et al. 2003; Brenan and Parish 1988; Bryceson et al. 2005, 2010; Byrd et al. 2007; Chung et al. 2009; Chrysofakis et al. 2004; Epling-Burnette et al. 2007; Fauriat et al. 2007; Garcia-Iglesias et al. 2009; Hersperger et al. 2008; Kim et al. 2007; Mattis et al. 1997; Morissette et al. 2007; Papadopoulos et al. 1994; Perez et al. 2004; Perfetto et al. 2006; Piet et al. 2011; Sivori et al. 1999; Zimmer et al. 2005). The aim of this publication is to present the tests most commonly used for the analysis of NK cells. These tests are based on widely accepted protocols with our own modifications.

37.2 Proposed Diagnostic Scheme for NK Cells Evaluation

Screening of NK cell function is based on the cytotoxicity test. However, this test does not detect the location of defects. NK cells contain high concentrations of cytolytic granules in their cytoplasm. These lytic vesicles contain a number of cytolytic proteins such as perforin and granzyme, designed to induce death in target cells upon release. Identification of the content of intracellular granules is an important part of the diagnostics. It may be performed through the evaluation of perforin and granzymes intracellular expression. Subsequent to the activation, NK cells rapidly release granules at the immunological synapse inducing death of the target cell. Lining the membrane of these cytolytic granules is the lysosomal-associated membrane protein-1 (CD107a and CD107b). Therefore, degranulation can be assessed by evaluation of the surface CD107a and CD107b expression.

The influence of cytokines on NK cells function and immune system balance cannot be ignored. Useful knowledge supporting diagnostics of NK cells defects can be gained by evaluation of relevant cytokines production and secretion.

37.2.1 Flow Cytometric Cytotoxicity Test

Cytotoxic activity is the most relevant function of NK cells. Cytotoxicity test is commonly used to assess cytotoxic activity of NK cells. It enables accurate measurements of lymphocyte or NK cells cytotoxic activity against target cells, but proper identification of presumptive pathology is impossible. The most commonly referenced test which is based on usage of radioactive chromium, as an indicator of target cells, creates nowadays a big technical problem for numerous laboratories. Using radioactive chemical components requires specialized, highly qualified and certified isotopic laboratory. The method applying flow cytometry which was described by many authors seems to be the best alternative (Brenan and Parish 1988; Kim et al. 2007; Mattis et al. 1997; Papadopoulos et al. 1994; Perfetto et al. 2006). In this method, staining with radioactive chromium is replaced with various fluorescence

stains. Flow cytometry gives a broad operating range with diverse modifications and applications. It allows for simultaneous identification of expression of many surface or/and intracellular antigens, receptors or other factors present or appearing during the incubation of the effector cells with appropriate target cells.

37.2.1.1 Methods

1. Separation of PBMS from anticoagulated, heparinized blood by density gradient centrifugation (Histopaque 1077, Sigma-Aldrich). After separation, cells are diluted twice in PBS (phosphate buffered saline) and ones in RPMI 1,640 culture media (Lonza) supplemented with 10% FCS (Fetal Calf Serum), 4 mM of L-glutamine, 1% of 1M HEPES Buffer and 8 μg/ml antibiotic (Sigma-Aldrich, St. Louis, MO). After the last washing PBMS are suspend at final concentration 4 mln/ml.
2. Preparation of K562 cells. Target cells are harvested from the culture (RPMI as mentioned above), washed twice in PBS and diluted in RPMI media in a final concentration of 1 mln/ml.
3. Target cells (K562) are labeled with fluorescent dye DiO_{18} (3.3'-dioctadecyloxacarbocyanine perchlorate; Sigma-Aldrich, St. Louis, MO). DiO_{18} is incorporated almost irreversibly into a cell membrane *via* two C_{18} alkyl chains (Brenan and Parish 1988, Mattis et al. 1997). 24 μg/ml (10 μl from the stock), is added to 1 mln of K562 cells suspend in 1 ml of RPMI media and incubated in 37°C, 5% CO_2 for 30 min. After incubation, cells are washed three times in PBS and ones in RPMI and suspended in concentration 1 mln/ml.
4. Separated PBMS are cultured with target K562 cells in four sterile tubes: effector (E) cells to target (T) cells ratio 40:1, E:T 10:1, control with effector PBMC without target K562 cells, control with target K562 without PBMC. Final reaction volume is 200 μl.
5. The culture is derived 4 h in incubator in humidified, 37°C, 5% CO_2 atm.
6. After 4 h, tubes are taken out from the incubator and a propidium iodide (PI) (intracellular DNA staining) is added to the culture. The tubes are placed back into the incubator for 30 min. PI is taken up by the DNA of the cells that have been killed. After 30-min incubation, tubes with the cell suspensions are removed from the incubator and put into the flow cytometer. The ratio of dead cells to live cells at the different proportions effector to target cells is determined.

Live target (K562) cells show only DiO_{18} fluorescence (Fig. 37.1a, b; field D4), dead target cells shoved both DiO_{18} and PI fluorescence (Fig. 37.1a, b; field D2). The percentage of dead target cells is calculated according to the formula: dead cells × 100%/total number of target cells. Specific lysis is present as: the percentage of dead target cells (with effector cells) subtracted dead target cells (without effector cells).

37.2.2 Degranulation Analysis

The surface expression of antigens CD107a and CD107b on activated NK cells is strictly related to their cytotoxic ability. CD107a (LAMP1 – Lysosome Associated Membrane Proteins 1) and CD107b (LAMP2) could be found within the lysosomal membrane. As a result of NK cell stimulation, degranulation occurs and lysosomal proteins CD107 are dislocated into cell membrane (Aktas et al. 2009; Alter et al. 2004; Bryceson et al. 2005, 2010). Detection of these markers on the cell surface confirms cytotoxic activation. Impaired CD107a or/and CD107b expression on the surface of cell membrane of activated NK cells may reflect errors in degranulation process. Infrequently impaired degranulation results from an immunodeficiency syndrome connected with genetic mutation or polymorphisms and leads to hyperactivation of immune system. More often this dysfunction is of low clinical significance. The flow cytometry method allows to identify cases when genetic test can be reasonable.

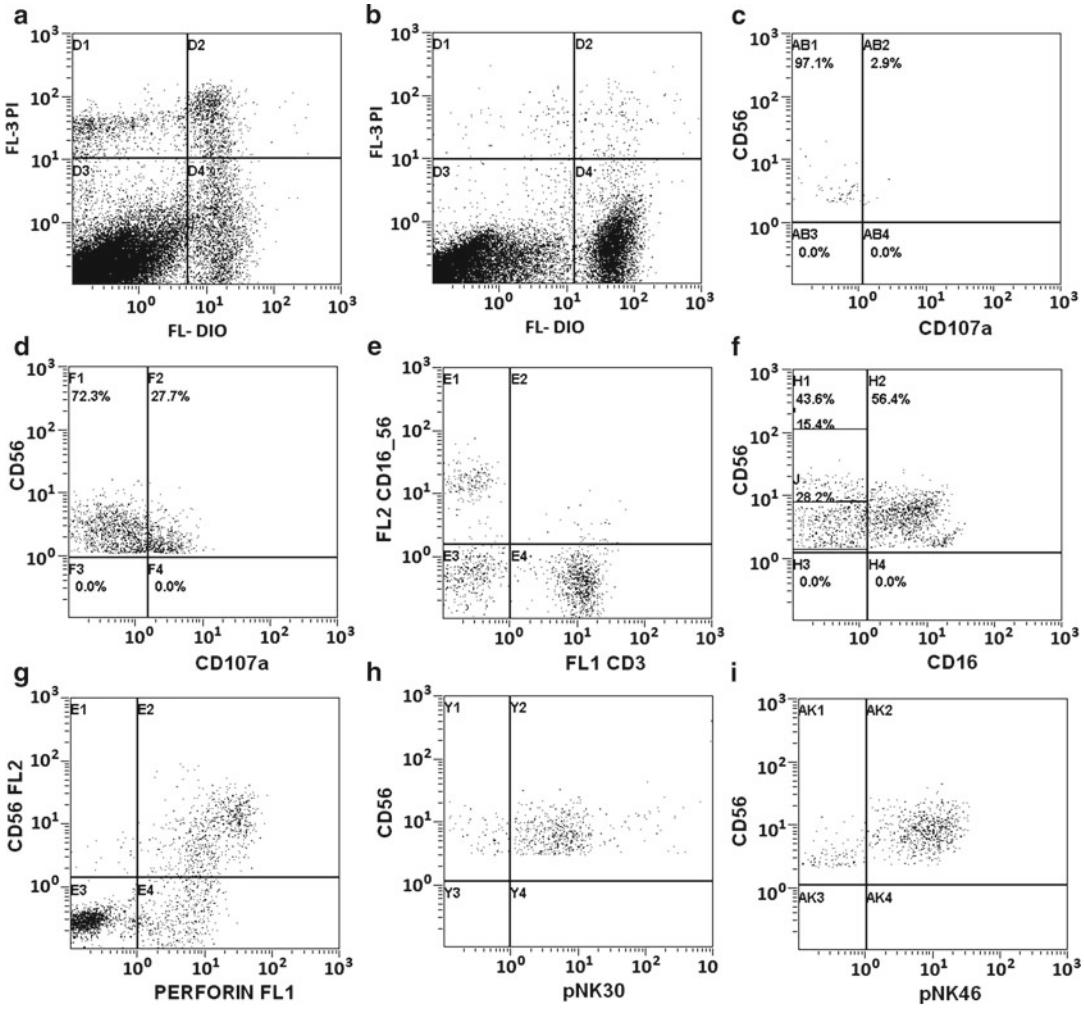

Fig. 37.1 (**a**) **Cytotoxicity test results – normal cytotoxic activity,** (**b**) **Cytotoxicity test results – depressed cytotoxic activity.** In *both panels*: D1 – dead PI stained cells, D2 – dead PI and DiO_{18} stained K562 cells, D3 – unstained cells, and D4 – live DiO_{18} stained K562 cells. (**c**) **Expression of CD107a antigen** on the surface of non-stimulated NK cells. (**d**) **Expression of CD107a antigen** on the surface of NK cells after stimulation with K562 target cells. (**e**) **Expression of NK cells CD56CD16 antigens** on the surface of whole blood mononuclear cells (**f**) **Percentages of NK cell subpopulations in PBMC** isolated from human whole blood cells: H1 – 43.6% NK CD56, J – 28.2% $CD56^{dim}$, I –15.4% $CD56^{bright}$, H2 – 56.4% – NK CD56+CD16+. (**g**) **Intracellular expression of perforin** in whole blood NK cells: E2 – 93%. (**h**) **Expression of activating pNK30 receptor** on the surface of peripheral blood NK cells: Y1 – 14%, Y2 – 86%. (**i**) **Expression of activating pNK46 receptor** on the surface of peripheral blood NK cells: AK1 – 8%, AK2 – 92%

37.2.2.1 Methods

Separation of PBMS from anticoagulated, heparinized blood is performed by density gradient centrifugation (Histopaque 1077; Sigma-Aldrich, St. Louis, MO). After separation, cells are diluted twice in PBS (phosphate buffered saline) and once in RPMI 1,640 culture media (Lonza) supplemented with 10% FCS (Fetal Calf Serum Sigma-Aldrich) and 4 mM of L-glutamine, 1% of 1M HEPES Buffer, and 8 μg/ml of antibiotic (Sigma-Aldrich, St. Louis, MO). After the last washing, PBMS are suspended in RPMI media at a final concentration 4 mln/ml.

1. Preparation of K562 cells. Target cells are harvested from the culture (RPMI as mentioned above), washed twice in PBS and diluted in RPMI media at a final concentration of 1 mln/ml.
2. Incubation of PBMC with 10 μl of ready-to-use monoclonal antibodies solution (anti CD107a fluorescein isothiocyanate (FITC)-conjugated, anti D107b FITC and CD16 phycoerythrin (PE)-conjugated, CD56 phycoerythrin-cyanine (PE-Cy5)-conjugated, Becton Dickinson) immediately after isolation without stimulation as a negative control.
3. Separated PBMS are cultured with not stained target K562 cells in three sterile tubes, effector (E) cells to target (T) cells ratio 10:1. The final reaction volume is 200 μl.
4. The culture is for 1 h in incubator in humidified, 37°C, 5% CO_2 atm.
5. After the incubation, 4 μl monensin containing reagent (Golgi Stop, Becton Dickinson) is added to each tube and they are placed again in the incubator for 3–5 h.
6. After incubation, probes are stained with 10 μl of ready-to-use monoclonal antibodies solution (anti-CD107a FITC, anti-CD107b FITC, and anti-CD16 PE, CD56 PE-Cy5, Becton Dickinson) and incubated for 20 min, after which the probes are fixed with 100 μl of 2% formalin solution and filled with PBS to a total volume 500 μl.
7. The probes are analyzed in the flow cytometer Cytomix FC 500 Beckman Coulter. (Fig. 37.1c, d). Compensation matrixes are generated manually upon acquisition.

37.2.3 Flow Cytometry Analysis of Subpopulations of NK Cells

It is well known that the number of circulated whole blood NK cells has a direct impact on the cytotoxicity range. In most cases, a great decrease in the NK cell population is related to the presence of impaired cytotoxicity. Relevant changes in the proportion of different subpopulations of NK cells may modify or even highly affect their physiological role and the homeostasis of the immune system. Therefore, the assessment of subpopulations of NK cells seems to be important.

37.2.3.1 Methods

Whole blood leukocytes (4 mln/ml) are incubated with 10 μl of ready-to-use monoclonal antibodies solutions: anti CD3 FITC, anti CD16CD56 PE, anti CD56 PE-Cy5, anti CD16 PE (Becton Dickinson), protected from light, 20 min at room temp. After staining, erythrocytes are lysed with 500 μl of OptiLyse C reagent (Beckman Coulter). Probes are analyzed in the flow cytometer Cytomix FC 500 Beckman Coulter (Fig. 37.1e, f).

37.2.4 Evaluation of Intracellular Expression of Perforin in NK Cells

Perforin, constitutively expressed by NK cells, is a cytotoxic molecule responsible for the induction of apoptosis of target cells. Genetic mutations in the perforin gene lead to impaired or even completely inhibited production of the protein and in consequence become a reason of severe immune deficiencies. A flow cytometry method designed for intracellular perforin identification provides preliminary information about perforin expression. This test allows to recognize individuals with a presumable defect in perforin production and to qualify them to highly specialized, complicated, and precise genetic tests. However, it has to be taken into consideration that decreased or sometimes increased expression of intracellular perforin may be connected not only with genetic abnormalities but also with the presence of several chronic infections, including HIV or HCV (Hersperger et al. 2008; Morissette et al. 2007; Par et al. 2006; Perez et al. 2004; Portales et al. 2003).

37.2.4.1 Methods

Whole blood leukocytes as well as isolated PBMC are stained with 10 µl of monoclonal anti-CD4, anti-CD8 and anti-CD56 antibodies, 20 min protected from light (Becton Dickinson) to identify surface expression of population specific antigens. Then, cells are permeabilized for 15 min with 100 µl of IntraPrep 1 permabilization reagent (Beckman Coulter). After incubation, probes are washed once in 4 ml of PBS, then 100 ml of IntraPrep reagent 2 is added to each tube and incubated for 5 min. After 5-min incubation, 10 µl of second, intracellular mouse anti-human perforin antibodies (Becton Dickinson) are added and incubated for 20 min. The probes are then washed with 4 ml of PBS, fixed with 100 µl of 2% formalin solution (Sigma Aldrich, St. Louis, MO) and filled with PBS to a final volume of 500 µl. Probes are analyzed in the flow cytometer Cytomix FC 500 Beckman Coulter (Fig. 37.1g). The expression of intracellular perforin analyzed in samples from patients has to be related to the result obtained at the same time in a sample of blood taken from a healthy donor.

37.2.5 Analysis of Surface Activating Receptors on Resting and Activated NK Cells

The induction of NK cells cytolytic function is regulated by the expression of diverse surface receptors. These receptors are able either to inhibit or enhance NK cells reactivity (Mc Queen and Parham 2002; Vitale et al. 2003). The interaction of inhibitory receptors with their ligands leads to self-tolerance. On the other hand, virus-infected or tumor cells which have lost their HLA Class I antigens undergo killing. Actually, only three natural cytotoxicity triggering receptors have been proposed as specific for NK cells. These are NKp30, NKp44 and NKp46. Upon interaction with their ligands (which are still unidentified) on target cells, these receptors activate NK cells cytotoxicity (Srivastava and Srivastava 2006). Two of them: NKp30 and NKp46 are constitutively presented on the membrane of NK cells and the third NKp44 is expressed after cell activation. It has to be taken into consideration that loss or decreased expression of these receptors may lead to impaired activation and in consequence blockage of NK cells action (Byrd et al. 2007; Garcia-Iglesias et al. 2009; Sivori et al. 1999). This hypothesis was confirmed in some publications. NK cells from patients suffering from myelocytic/monocytic acute myeloid leukemia exhibit poor cytolytic functions due to deficient expression of NKp30, NKp44, and NKp46 receptors (Fauriat et al. 2007). In patients with myelodysplastic syndromes the expression of activating NK cell receptors (NKG2D and NKp30) decreases as the disease progresses to myeloid leukemia (Epling-Burnette et al. 2007).

37.2.5.1 Methods

Whole blood leukocytes (4 mln/ml) are stained with 10 µl of ready-to-use monoclonal antibodies anti CD3 FITC, anti-NKp30 PE, anti-NKp46 PE and anti-CD56 PE-Cy5 (Becton Dickinson) and incubated for 20 min in room temperature, protected from light. After staining, erythrocytes are lysed with 500 µl of OptiLyse C reagent (Beckman Coulter). Probes are analyzed in flow cytometer Cytomix FC 500 Beckman Coulter (Fig. 37.1h, i).

Acknowledgments Supported by grant 0989/B/P01/2011/40 form the Polish National Center of Science and Funds for Scientific Research 1WW /N/2010.

Conflicts of interest: The authors declare no conflicts of interest in relation to this article.

References

Aktas, E., Kucuksezer, U. C., Bilgic, S., Erten, G., & Deniz, G. (2009). Relationship between CD107a expression and cytotoxic activity. *Cellular Immunology, 254*, 149–154.

Alter, G., Malenfant, J. M., & Altfeld, M. (2004). CD107a as a functional marker for the identification of natural killer cell activity. *Journal of Immunological Methods, 294*, 15–22.

Betts, M. R., Brenchley, J. M., Price, D. A., De Rosa, S. C., Douek, D. C., Roederer, M., & Koup, R. A. (2003). Sensitive and viable identification of antigen-specific CD8+ T cells by a flow cytometric assay for degranulation. *Journal of Immunological Methods, 281*, 65–78.

Biron, C. A., Nguyen, K. B., Pien, G. C., Cousens, L. P., & Salazar-Mather, T. P. (1999). Natural killer cells in antiviral defense: Function and regulation by innate cytokines. *Annual Review of Immunology, 17*, 189–220.

Brenan, M., & Parish, C. R. (1988). Automated fluorometric assay for T cell cytotoxicity. *Journal of Immunological Methods, 112*, 121–123.

Bryceson, Y. T., March, M. E., Domingo, F., Barber, D. F., Ljunggren, H. G., & Long, E. O. (2005). Cytolytic granule polarization and degranulation controlled by different receptors in resting NK cells. *The Journal of Experimental Medicine, 202*, 1001–1012.

Bryceson, Y. T., Yenan, T., Fauriat, C., Nunes, J. M., Wood, S. M., Bjorkstrom, N. K., Long, E. O., & Ljunggren, H. G. (2010). Functional analysis of human NK cells by flow cytometry. *Methods in Molecular Biology, 612*, 335–352.

Byrd, A., Hoffmann, S. C., Jarahian, M., Momburg, F., & Watzl, C. (2007). Expression analysis of the ligands for the natural killer cell receptors NKp30 and NKp44. *PLoS One, 2*, e1339–e1347.

Chrysofakis, G., Tzanakis, N., Kyriakoy, D., Tsoumakidou, M., Tsiligiani, M., & Siafakas, N. M. (2004). Perforin expression and cytotoxic activity of sputum $cd8^{+}$ lymphocytes in patients with COPD. *Chest, 125*, 71–76.

Chung, A. W., Rollman, E., Center, R. J., Kent, S. J., & Stratov, I. (2009). Rapid degranulation of NK cells following activation by HIV-specific antibodies. *Journal of Immunology, 182*, 1202–1210.

Cooper, M. A., Fehniger, T. A., Turner, S. C., Chen, K. S., Bobak, A., Gheheri Ghayur, T., Carson, W. E., & Caliguri, M. A. (2001a). Human natural killer cells: A unique innate immunoregulatory role for the $CD56^{bright}$subset. *Blood, 97*, 3146–3151.

Cooper, M. A., Fehniger, T. A., & Caligiuri, M. A. (2001b). The biology of human natural killer-cell subset. *Trends in Immunology, 11*, 633–640.

Epling-Burnette, P. K., Bai, F., Painter, J. S., Rollison, D. E., Salih, H. R., Krusch, M., Zou, J., Ku, E., Zhong, B., Boulware, D., Moscinski, L., Wei, S., Djeu, J. Y., & List, A. F. (2007). Reduced natural killer (NK) function associated with high-risk myelodysplastic syndrome (MDS) and reduced expression of activating NK receptors. *Blood, 109*, 4816–4824.

Fauriat, C., Just-Landi, S., Mallet, F., Arnoulet, C., Sainty, D., Olive, D., & Costello, R. T. (2007). Deficient expression of NCR in NK cells from acute myeloid leukemia: Evolution during leukemia treatment and impact of leukemia cells in NCRdull phenotype induction. *Blood, 109*, 323–330.

Fishman, D. N. (2000). Hemophagocytic syndromes and infection. *Emerging Infectious Diseases, 6*, 601–608.

Garcia-Iglesias, T., del Toro-Arreola, A., Albarran-Somoza, B., del Toro-Arreola, S., Sanchez-Hernandez, P. E., Ramirez-Dueñas, M. G., Balderas-Peña, L. M. A., Bravo-Cuellar, A., Ortiz-Lazareno, P. O., & Daneri-Navarro, A. (2009). Low NKp30, NKp46 and NKG2D expression and reduced cytotoxic activity on NK cells in cervical cancer and precursor lesions. *BMC Cancer, 9*, 186–193.

Grom, A. A., Villaneuva, J., Lee, S., Goldmuntz, E. A., Passo, M. H., & Filipowich, A. (2004). Natural killer cell dysfunction: A common pathway in systemic-onset juvenile rheumatoid arthritis, macrophage activation syndrome, and hemophagocytic lymphohistiocytosis? *Arthritis and Rheumatism, 50*, 689–698.

Henter, J. I., Horne, A., Arico, M., Egeler, R. M., Filipovich, A. H., & Imashuku, S. (2007). Review HLH-2004: Diagnostic and therapeutic guidelines for hemophagocytic lymphohistiocytosis. *Pediatric Blood & Cancer, 48*, 124–131.

Hersperger, A. R., Makedonas, G., & Betts, M. R. (2008). Flow cytometric detection of perforin upregulation in human CD8 T cells. *Cytometry Part A, 73*, 1050–1057.

Horne, A. C., Goransdotter-Rame, K., Rudd, E., Zheng, C., Wali, Y., al-Lamki, Z., Gurgey, A., Yalman, N., Nordenskjold, M., & Henter, J. I. (2008). Characterization of PRF1, STX1 and UNC13D genotype-phenotype correlations in familial hemophagocytic lymphohistiocytosis. *British Journal of Haematology, 43*, 75–83.

Kim, G. G., Donnenberg, W. S., Donnenberg, A. D., Gooding, W., & Whiteside, T. L. (2007). A novel multiparametric flow cytometry-based cytotoxicity assay simultaneously immunophenotypes effector cells: Comparisons to a 4 h ^{51}Cr-release assay. *Journal of Immunological Methods, 325*, 51–66.

Lackner, H., Urban, C., Sovinz, P., Benesch, M., Moser, A., & Schwinger, W. (2008). Hemophagocytic lymphohistiocytosis as severe adverse event of antineoplastic treatment in children. *Haematologica, 93*, 291–294.

Mattis, A. E., Bernhardt, G., & Lipp Forster, M. R. (1997). Analyzing cytotoxic T lymphocyte activity: A simple and reliable flow cytometry-based assay. *Journal of Immunological Methods, 204*, 135–142.

Mc Queen, K. L., & Parham, P. (2002). Variable receptors controlling activation and inhibition of NK cells. *Current Opinion in Immunology, 14*, 615–621.

Morissette, M. C., Parent, J., & Milot, J. (2007). Perforin, granzyme B, and FasL expression by peripheral blood T lymphocytes in emphysema. *Respiratory Research, 8*(1), 62–70.

Mossman, K. L., & Ashkar, A. A. (2005). Herpesviruses and the innate immune response. *Viral Immunology, 18*, 267–281.

Notarangelo, L. D., & Mazzolari, E. (2006). Natural killer cell deficiencies and severe varicella infection. *The Journal of Pediatrics, 148*, 563–564.

Papadopoulos, N. G., Dedoussis, G. V., Spanakos, G., Gritzapis, A. D., Baxevanis, C. N., & Papamichail, M. (1994). An improved fluorescence assay for the determination for lymphocyte mediated cytotoxicity using flow cytometry. *Journal of Immunological Methods, 177*, 101–111.

Par, G., Berki, T., Palinkas, L., Balogh, P., Szereday, L., Halasz, M., Szekeres-Bartho, J., Miseta, A., Hegedus, G., Mozsik, G., Hunyady, B., & Par, A. (2006). Immunology of HCV infection: The causes of impaired cellular immune response and the effect of antiviral treatment. *Orvosi Hetilap, 147*, 591–600.

Perez, O. D., Mitchell, D., Jager, G. C., & Nolan, G. P. (2004). LFA-1 signaling trough p44/42 is coupled to perforin degranulation in CD56+CD8+ natural killer cells. *Blood, 104*, 1083–1093.

Perfetto, S. P., Chattopadhyay, P. K., Lamoreaux, L., Nguyen, R., Ambrozak, D., Koup, R. A., & Roederer, M. (2006). Amine reactive dyes: An effective tool to discriminate live and dead cells in polychromatic flow cytometry. *Journal of Immunological Methods, 313*, 199–208.

Piet, B., de Bree, G. J., Smids-Dierdorp, B. S., van der Loos, C. M., Remmerswaal, E. B., von der Thusen, J. H., van Haarst, J. M., Eerenberg, J. P., Ten Brinke, A., van der Bij, W., Timens, W., van Lier, R. A., & Jonkers, R. E. (2011). $CD8^+$ T cells with an intraepithelial phenotype upregulate cytotoxic function upon influenza infection in human lung. *The Journal of Clinical Investigation, 121*, 2254–2263.

Portales, P., Reynes, J., Rouzier-Panis, R., Baillat, V., Clot, J., & Corbeau, P. (2003). Perforin expression in T cells and virological response to PEG-interferon alpha2b in HIV-1 infection. *AIDS, 17*, 505–511.

Sivori, S., Pende, D., Bottino, C., Marcenaro, E., Pessino, A., Biassoni, R., Moretta, L., & Moretta, A. (1999). NKp46 is the major triggering receptor involved in the natural cytotoxicity of fresh or cultured human NK cells. Correlation between surface density of NKp46 and natural cytotoxicity against autologous, allogeneic or xenogeneic target cells. *European Journal of Immunology, 29*, 1656–1666.

Srivastava, B. I., & Srivastava, M. D. (2006). Expression of natural cytotoxicity receptors NKp30, NKp44 and NKp46 mRNAa and proteins by human hematopoietic cells. *Leukemia Research, 30*, 37–46.

Vastert, S. J., van Wijk, R., D'Urbano, L. E., de Vooght, K. M., de Jager, W., Ravelli, A., Magni-Manzoni, S., Insalaco, A., Cortis, E., van Solinge, W. W., Prakken, B. J., Wulffraat, N. M., de Benedetti, F., & Kuis, W. (2009). Mutations in the perforin gene can be linked to macrophage activation syndrome in patients with systemic onset juvenile idiopathic arthritis. *Rheumatology, 49*, 441–449.

Villanueva, J., Lee, S., Giannini, E. H., Graham, T. B., Passo, M. H., Filipovich, A., & Grom, A. A. (2005). Natural killer cell dysfunction is a distinguishing feature of systemic onset juvenile rheumatoid arthritis and macrophage activation syndrome. *Arthritis Research & Therapy, 7*, R30–R37.

Vitale, M., Falco, M., Castriconi, R., Parolini, S., Zambello, R., Semenzato, G., Biassoni, R., Bottino, C., Moretta, L., & Moretta, A. (2003). Identification of NKp80, a novel triggering molecule expressed by human NK cells. *European Journal of Immunology, 31*, 233–242.

Wilk, E., Kalippke, K., Buyny, S., Schmidt, R. E., & Jacobs, R. (2008). New aspects of NK cell subset identification and inference of NK cells regulatory capacity by assessing functional and genomic profiles. *Immunobiology, 213*, 271–283.

Zimmer, J., Andrès, E., & Hentges, F. (2005). NK cell subsets and CD107a mobilization assay. *Leukemia, 19*, 1849–1851.

Chapter 38
sVEGF R1 and Tie-2 Levels During Chemotherapy of Lung Cancer Patients

R.M. Mroz, M. Korniluk, B. Panek, M. Ossolinska, and E. Chyczewska

Abstract Angiogenesis plays important role in tumor growth and development. Protein ligands and their receptor tyrosine kinases are crucial in tumor related angiogenesis. Ligand/receptor systems such as vascular endothelial growth factor (VEGF), and tyrosine kinase with immunoglobulin-like and epidermal growth factor homology domains (Tie) family play important role in this phenomenon. The aim of this study was to evaluate the concentration of soluble receptor of VEGF (sVEGF R1) and Tie-2 domain in plasma of lung cancer patients before and after chemotherapy. Forty four lung cancer patients, 11 with small lung cancer (SCLC), 5 females and 6 males (mean age 60.2, range 39–72 years), and 33 patients with non-small cell lung cancer (N-SCLC), 6 females and 27 males (mean age 61.9, range 42–78 years) received four courses of chemotherapy. Control group consisted of 44 patients with COPD, 4 females and 40 males (mean age 37.1, 18–60 years). In all cases clinical partial response was achieved. Both sVEGF R1 and Tie-2 concentrations were elevated in cancer group before treatment compared with control: sVEGF (pg/ml): 60.7 and 66.2 *vs.* 48.8 and Tie-2 (ng/ml): 37.3 and 37.5 *vs.* 30.7 in SCLC and N-SCLC *vs.* C, respectively. Treatment decreased sVEGF R1 (pg/ml): 66.7 *vs.* 11.6 ($p < 0.05$) and 66.2 *vs.* 14.39 ($p < 0.001$), and Tie-2 (ng/ml): 37.3 *vs.* 26.3 ($p < 0.05$) and 37.5 *vs.* 25.7 ($p < 0.001$) in SCLC and N-SCLC, respectively. We conclude that VEGF R1and Tie-2 receptors may play important role in lung cancer development and their receptor concentrations may reflect the patients' response to treatment.

Keywords Angiogenesis • Lung cancer • Small cell lung cancer • Non-small cell lung cancer • VEGF – Epidermal growth factor • Pharmacotherapy • Tyrosine kinase

38.1 Introduction

It is well established now that angiogenesis, the growth of new blood vessels is required for development and progression of solid tumors (Phillips et al. 1976; Risau 1987). The importance of angiogenesis specifically in lung carcinogenesis is supported by a large body of research, including studies

R.M. Mroz (✉) • M. Korniluk • B. Panek • M. Ossolinska • E. Chyczewska
Department of Lung Diseasess, Bialystok Medical University, Zurawia 14, Bialystok, Bialystok, Poland
e-mail: robmroz@wp.pl

M. Pokorski (ed.), *Respiratory Regulation - The Molecular Approach*,
Advances in Experimental Medicine and Biology 756, DOI 10.1007/978-94-007-4549-0_38,

demonstrating altered expression of proangiogenic factors such as vascular endothelial growth factor (VEGF) (Phillips et al. 1976; Shibuya et al. 1994). Moreover, inhibition of tumor growth with angiogenesis inhibitors and correlations between tumor blood vessel density and both tumor characteristics, metastases, and clinical outcome supports idea of targeting angiogenesis factors as a new anticancer treatment strategies (Sharma et al. 2011). VEGF-A, also known as vascular permeability factor (VPF) plays a fundamental role in physiological and pathophysiological forms of angiogenesis and regulation of endothelial cell differentiation (Berse et al. 1992; Le et al. 1993; Senger et al. 1993). VEGF normal function is to create new blood vessels during embrionic development, new blood vessels after injury, muscle following exercise, and new vessels to bypass blocked vessels. Many studies have shown that VEGF is a key proangiogenic factor that is overexpressed in all solid tumors, acting through its receptors VEGFR1 and VEGFR2 (Sharma et al. 2011). Protein ligands and their receptor tyrosine kinases are crucial in tumor related angiogenesis. Ligand /receptor systems such as VEGF, and tyrosine kinase with immunoglobulin-like and epidermal growth factor homology domains (Tie) family play important role in this phenomenon. Tie-2 receptor on endothelial cells is activated through binding of angiopoietins. Angiopoietin-1 (Ang-1) and angiopoietin-2 (Ang-2) have been identified as ligands with different effector functions of the vascular assembly and maturation-mediating receptor tyrosine kinase Tie-2 (Saharinen et al. 2011). Ang-1 is responsible for the integrity of the endothelium, whereas Ang-2, together with VEGF stimulates angiogenic responses, or, by acting alone, targets blood vessels for regression. The aim of this study was to evaluate the concentration of soluble receptor of VEGF (sVEGF R1) and Tie-2 domain in plasma of lung cancer patients before and after chemotherapy.

38.2 Methods

The study was performed in conformity with the Declaration of Helsinki for Human Experimentation and the protocol was approved by a local Ethics Committee.

The study group consisted of 44 lung cancer patient (11 patients with small cell lung cancer (SCLC), 5 females and 6 males (mean age 60.2, range 39–72 years), and 33 patients with non-small cell lung cancer (N-SCLC), 6 females and 27 males (mean age 61.9, range 42–78 years)). All 11 SCLC patients were current smokers (mean pack/years: 32, min-max: 10–50 pack/years). In N-SCLC group, there were 31 current (94%) and two ex-smokers (6%) with smoking history of 30 pack/years ranging from 12 to 50 pack/years). All SCLC patients represented extensive disease (ED) clinical stage. N-SCLC group consisted of 15 patients at clinical stage IIIB and 18 patients at clinical stage IV of the disease. In SCLC group chemotherapy was carried out in a 21-day cycle using cis-platin at a dose of 100 mg/m^2 on day 1 and etoposid at a dose of 100 mg/m^2 on days 1–3 of the cycle. In N-SCLC patients chemotherapy was carried out in a 21-day cycle using cis-platin at a dose of 100 mg/m^2 on day 2 and gemcytabine at a dose of 1,000 mg/m^2 on days 1 and 8 of the cycle. sVEGF R1 and Tie-2 measurements were carried out before and after chemotherapy. The control group consisted of 44 patients with COPD, 4 females and 40 males (mean age 37.1, 18–60 years). There were seven (16%) current smokers, and 37 (84%) non smokers (mean pack/years = 2, min-max 0–30). Clinical response to therapy was calculated by X-ray and CT scans before and after chemotherapy. Serum samples, obtained from the whole blood of patients with lung cancer before and after four cycles of chemotherapy, were used as the study material. To exclude the possible interference of chemotherapy, subsequent blood samples were obtained at least 28 days after the last administration of cytotoxic drugs. Blood serum was stored at −80°C immediately after separation by centrifugation (3,000 rpm) until the assay was performed. At the first stage, blood samples were taken to assess sVEGF R1 and Tie-2 after complete diagnostics of lung cancer had been made, including X-ray and CT of the chest, bronchoscopy with H + P examination, bronchial biopsy (BB), or transbronchial needle aspiration biopsy (TBNA). The clinical analysis comprised the evaluation of clinical staging of NSCLC (TNM, AJCC),

and the performance stage according to Zubrod. The response to therapy was estimated according to the WHO criteria. All patients underwent basic laboratory tests and accessory investigations (ultrasonography of the abdominal cavity). Next, blood samples were collected to determine the concentrations of sVEGF R1 and Tie-2 to evaluate impact of chemotherapy.

Serum sVEGF R1 was analyzed with a Quantikine Kit and Tie-2 concentrations were determined by means of an enzyme-linked immunosorbent assay (ELISA) method (R&D System, Minneapolis, USA). All specimens were assayed in duplicates. The serum concentrations of sVEGF R1 and Tie-2 were reported as pg/ml, and ng/ml, respectively.

Statistical analysis was performed using Statistica 9.0 software (Stat Soft Inc., Tulsa, USA). K-S test was used for normality. All parametrical data was calculated by a I-test. Non-parametrical Mann Whitney test was used for sVEGF and Tie measurements. Results are presented as means ± SD. A value of $p < 0.05$ was considered to be the level of statistical significance.

38.3 Results

We found partial clinical response (PR) in all cancer patients. In the SCLC group, although elevated, both Tie-2 and sVEGF R1 did not reach statistical significance ($p = 0.36$ and $p = 0.07$, respectively) (Fig. 38.1a, b). Serum levels of both sVEGF R1 and Tie-2 were significantly higher in the N-SCLC patients before treatment compared with control ($p = 0.03$ and $p = 0.05$, respectively) (Fig. 38.1c, d). After four cycles of chemotherapy, we found a significant decrease of sVEGF R1 and Tie-2 in the SCLC group ($p = 0.03$ and $p = 0.05$, respectively) (Fig. 38.2a, b). The levels of both molecules also were significantly lower after chemotherapy in the N-SCLC group ($p = 0.001$ and $p = 0.001$, respectively) (Fig. 38.2c, d). Referring to the clinical stage of N-SCLC, sVEGF R1 levels tended to be higher in

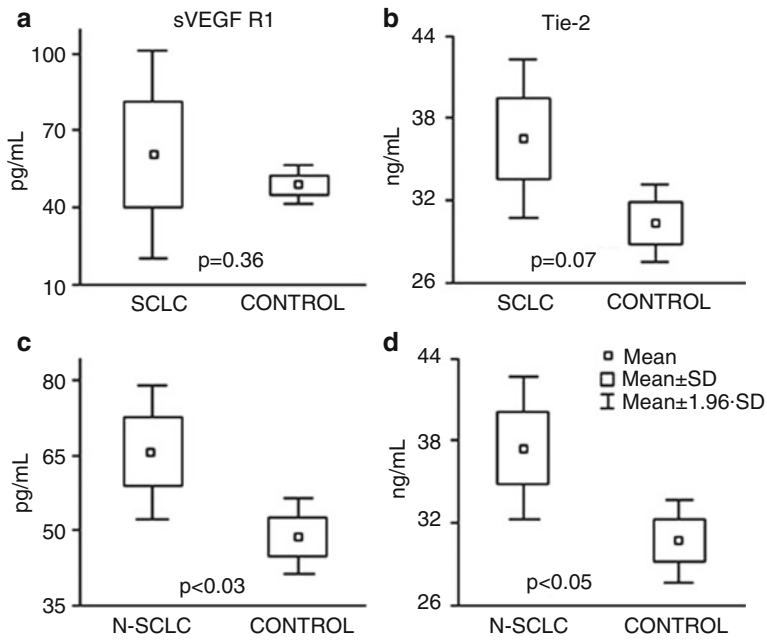

Fig. 38.1 sVEGF R1 and Tie2 in small cell (SCLC) and non-small cell lung cancer (N-SCLC). (**a**) SCLC sVEGF R1 before treatment compared with control, (**b**) SCLC Tie-2 before treatment compared with control, (**c**) N-SCLC sVEGF R1 before treatment compared with control, and (**d**) N-SCLC Tie-2 before treatment compared with control

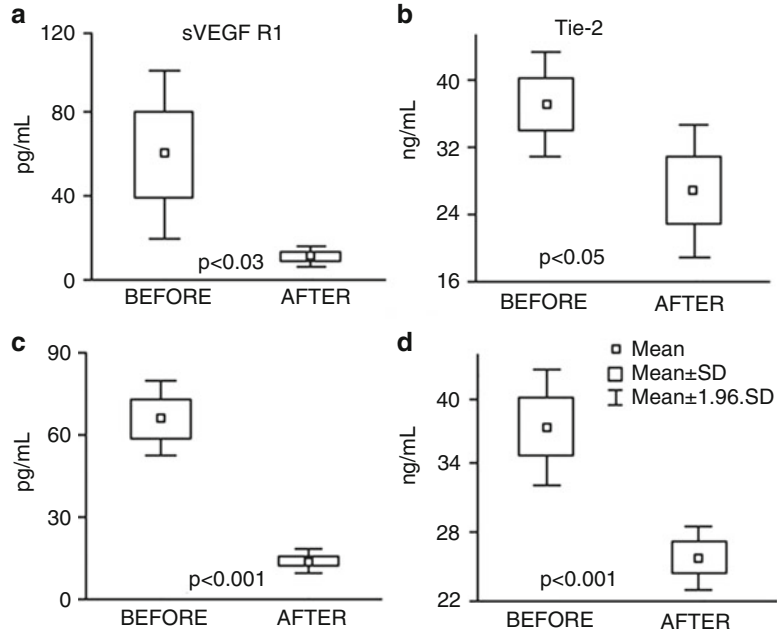

Fig. 38.2 Treatment influence on sVEGF R1 and Tie2. (**a**) SCLC sVEGF R1 before and after treatment, (**b**) SCLC Tie-2 before and after treatment, (**c**) N-SCLC sVEGF R1 before and after treatment, and (**d**) N-SCLC Tie-2 before and after treatment

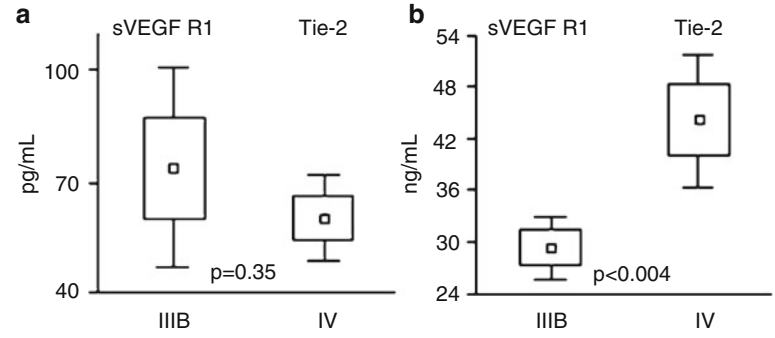

Fig. 38.3 sVEGF R1 and Tie-2 in N-SCLC before treatment; (**a**) stage IIIB (**b**) stage IV

group IIIB, whereas Tie-2 levels were significantly higher in stage IV of the disease ($p=0.35$ and $p=0.004$, respectively) (Fig. 38.3a, b). Chemotherapy significantly lowered the levels of both molecules, irrespective of disease stage ($p=0.003$ and $p=0.003$, for stage IIIB, respectively) (Fig. 38.4a, b) and ($p=0.001$ and $p=0.003$, for stage IV, respectively) (Fig. 38.4c, d).

38.4 Discussion

In this study we confirmed previous observations of increased plasma sVEGF R1 and Tie-2 levels in lung cancer patients (Sartelet et al. 2004). It is also consisted with previous findings in N-SCLC and SCLC patients reported by our group (Swidzinska et al. 2004a; Naumnik et al. 2009). Although the

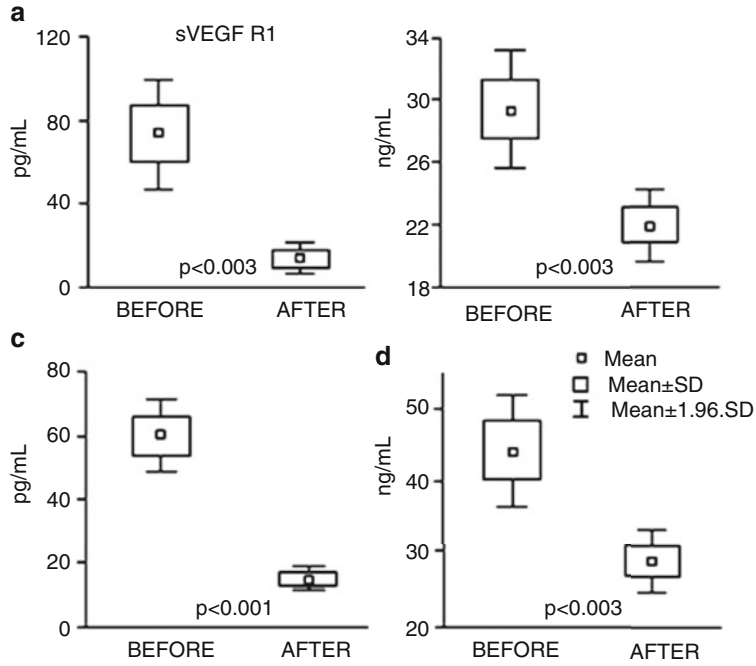

Fig. 38.4 Comparison of sVEGF R1 and Tie-2 according to clinical stages of N-SCLC before and after treatment. (**a**) Stage IIIB – sVEGF R1, (**b**) Stage IIIB – Tie-2, (**c**) Stage IV – sVEGF R1, and (**d**) Stage IV – Tie-2

predominant body of evidence is based on N-SCLC findings, increased plasma levels of VEGF in SCLC are also reported by others (Tas et al. 2006). In our study the elevation of sVEGF R1 and Tie-2 was found in advanced clinical stage of the disease. This is consistent with findings of Lissoni et al. (2003) who studied patients with metastatic lung and colon carcinoma. Beinert et al. (1999) found that plasma VEGF level elevation may be dependent on previous radiotherapy due to VEGF activation by an oxidative stress. After chemotherapy, in all our patients we found a partial clinical response and decrease of both studied molecules. This is consistent with previous findings of our group (Swidzinska et al. 2004b; Naumnik et al. 2009). Elevated VEGF and Tie-2 levels have been mainly reported in N-SCLC with minority of reports addressing the SCLC patients (Dowell et al. 2004). Ustuner et al. (2008) found that low serum VEGF concentration may be a independent prognostic factor in SCLC patients, suggesting that surveillance of VEGF and its receptors to predict chemotherapy response may not be useful. Whether the levels of serum VEGF and its receptors VEGFR-1 and VEGFR-2 would be valuable in detecting treatment modalities of SCLC needs to be further explored. All patients presented with advanced clinical stage of disease and elevated levels of VEGF and Tie-2. The levels of both molecules decrease after chemotherapy. This is consistent with the findings of others. Lissoni et al. (2003) found that higher plasma levels of VEGF before and after cis-platin-based chemotherapy correlated with poor prognosis, suggesting that changes in VEGF levels during chemotherapy may represent a useful biomarker to predict the effect of chemotherapy in terms of tumor response and survival in patients with metastatic solid neoplasms. Jantus-Lewintre et al. (2011) suggested that a combination of VEGF-A and sVEGFR-2 can be used as an independent prognostic biomarker in advanced N-SCLC. In contrast, Ludovini et al. (2004) found that VEGF weakly correlated with regulators of apoptosis and could not be independent predictive factor for resistance to cis-platin-based chemotherapy and prognostic for survival. Chorostowska-Wynimko et al. (2009) found that VEGF levels decreased following neoadjuvant therapy with subsequent significant up-regulation after surgery. Moreover, post-surgery serum VEGF strongly correlated with TGF-beta concentration. VEGF and Tie-2 are some of the key elements of recently introduced targeted anticancer therapy. An et al. (2012)

suggested that improved survival in patients with lower posttreatment plasma VEGF levels treated with bevacizumab plus chemotherapy may predict clinical benefit early in the course of therapy. Kanashiro et al. (2007) found decreased VEGF R1 levels after therapy with antagonists of growth hormone releasing hormone and bombesin in non-small cell lung cancer. Hu et al. (2010) developed a novel gene delivery system targeting Tie-2 for cancer gene therapy. Stacher et al. (2009) investigated several factors of the VEGF-signaling pathway and Tie-2 in epitheloid hemangioendotheliomas and primary pulmonary epitheloid angiosarcomas by means of immunohistochemistry using antibodies against VEGF family and Tie-2. Based on their findings the authors suggested a new therapeutic option in the therapy of pulmonary vascular tumors by blockade of the ligands or their receptors. These and other findings support further studies on the role of VEGF and Tie-2 as key elements of tumor related angiogenesis. Based on our findings we conclude that plasma levels of sVEGF R1 and Tie-2 may be useful biomarkers to predict the effect of chemotherapy in terms of tumor response and survival in lung cancer patients.

Conflicts of interest: The authors declare no conflicts of interest in relation to this article.

References

An, S. J., Huang, Y. S., Chen, Z. H., Su, J., Yang, Y., Chen, J. G., Yan, H. H., Lin, Q. X., Yang, J. J., Yang, X. N., Zhou, Q., Zhang, X. C., & Wu, Y. L. (2012). Posttreatment plasma VEGF levels may be associated with the overall survival of patients with advanced non-small cell lung cancer treated with bevacizumab plus chemotherapy. *Medical Oncology, 29*(2), 627–632.

Beinert, T., Binder, D., Oehm, C., Ziemer, S., Priem, F., Schweigert, M., Stuschke, M., Fleischhacker, M., Siebert, G., Mergenthaler, H. G., Werner, T. G., Sezer, O., & Possinger, K. (1999). Increased levels of vascular endothelial growth factor in bronchoalveolar lavage of patients with bronchial carcinoma effect of tumor activity and oxidative stress due to radio-chemotherapy? *European Journal of Medical Research, 4*(8), 328–334.

Berse, B., Brown, L. F., Van de Water, L., Dvorak, H. F., & Senger, D. R. (1992). Vascular permeability factor (vascular endothelial growth factor) gene is expressed differentially in normal tissues, macrophages, and tumors. *Molecular Biology of the Cell, 3*(2), 211–220.

Chorostowska-Wynimko, J., Zaleska, J., Chabowski, M., Szpechcinski, A., Zych, J., Rudzinski, P., Langfort, R., Orlowski, T., & Roszkowski-Sliz, K. (2009). Neoadjuvant therapy affects tumor growth markers in early stage non-small-cell lung cancer. *European Journal of Medical Research, 14*(Suppl 4), 42–44.

Dowell, J. E., Amirkhan, R. H., Lai, W. S., Frawley, W. H., & Minna, J. D. (2004). Survival in small cell lung cancer is independent of tumor expression of VEGF and COX-2. *Anticancer Research, 24*(4), 2367–2373.

Hu, A., Wu, X., Li, Z., Wang, H., Li, J., Yao, M., Chen, X., Qu, S., Xu, Y., & Gu, J. (2010). A novel gene delivery system targeting Tie2 for cancer gene therapy. *Anticancer Research, 30*(6), 1999–2004.

Jantus-Lewintre, E., Sanmartín, E., Sirera, R., Blasco, A., Sanchez, J. J., Tarón, M., Rosell, R., & Camps, C. (2011). Combined VEGF-A and VEGFR-2 concentrations in plasma: diagnostic and prognostic implications in patients with advanced NSCLC. *Lung Cancer, 74*(2), 326–331.

Kanashiro, C. A., Schally, A. V., Zarandi, M., Hammann, B. D., & Varga, J. L. (2007). Alterations of EGFR/HER, angiogenesis and apoptosis pathways after therapy with antagonists of growth hormone releasing hormone and bombesin in non-small cell lung cancer. *International Journal of Oncology, 30*(4), 1019–1028.

Le, Q. A., Duval, D., & Tobelem, G. (1993). Tumor angiogenesis. *Baillière's Clinical Haematology, 6*(3), 711–730.

Lissoni, P., Rovelli, F., Malugani, F., Brivio, F., Fumagalli, L., & Gardani, G. S. (2003). Changes in circulating VEGF levels in relation to clinical response during chemotherapy for metastatic cancer. *The International Journal of Biological Markers, 18*(2), 152–155.

Ludovini, V., Gregorc, V., Pistola, L., Mihaylova, Z., Floriani, I., Darwish, S., Stracci, F., Tofanetti, F. R., Ferraldeschi, M., Di, C. L., Ragusa, M., Daddi, G., & Tonato, M. (2004). Vascular endothelial growth factor, p53, Rb, Bcl-2 expression and response to chemotherapy in advanced non-small cell lung cancer. *Lung Cancer, 46*(1), 77–85.

Naumnik, W., Chyczewska, E., & Ossolinska, M. (2009). Serum levels of angiopoietin-1, angiopoietin-2, and their receptor tie-2 in patients with nonsmall cell lung cancer during chemotherapy. *Cancer Investigation, 27*(7), 741–746.

Phillips, P., Steward, J. K., & Kumar, S. (1976). Tumor angiogenesis factor (TAF) in human and animal tumors. *International Journal of Cancer, 17*(5), 549–558.

Risau, W. (1987). Endothelium, angiogenesis and metastasis. *Onkologie, 10*(4), 260–262.

Saharinen, P., Eklund, L., Pulkki, K., Bono, P., & Alitalo, K. (2011). VEGF and angiopoietin signaling in tumor angiogenesis and metastasis. *Trends in Molecular Medicine, 17*(7), 347–362.

Sartelet, H., Decaussin, M., Devouassoux, G., Nawrocki-Raby, B., Brichon, P. Y., Brambilla, C., & Brambilla, E. (2004). Expression of vascular endothelial growth factor (VEGF) and its receptors (VEGF-R1 [Flt-1] and VEGF-R2 [KDR/Flk-1]) in tumorlets and in neuroendocrine cell hyperplasia of the lung. *Human Pathology, 35*(10), 1210–1217.

Senger, D. R., Van de Water, L., Brown, L. F., Nagy, J. A., Yeo, K. T., Yeo, T. K., Berse, B., Jackman, R. W., Dvorak, A. M., & Dvorak, H. F. (1993). Vascular permeability factor (VPF, VEGF) in tumor biology. *Cancer and Metastasis Reviews, 12*(3–4), 303–324.

Sharma, P. S., Sharma, R., & Tyagi, T. (2011). VEGF/VEGFR pathway inhibitors as anti-angiogenic agents: Present and future. *Current Cancer Drug Targets, 11*(5), 624–653.

Shibuya, M., Seetharam, L., Ishii, Y., Sawano, A., Gotoh, N., Matsushime, H., & Yamaguchi, S. (1994). Possible involvement of VEGF-FLT tyrosine kinase receptor system in normal and tumor angiogenesis. *Princess Takamatsu Symposia, 24*, 162–170.

Stacher, E., Gruber-Mosenbacher, U., Halbwedl, I., Dei Tos, A. P., Cavazza, A., Papotti, M., Carvalho, L., Huber, M., Ermert, L., & Popper, H. H. (2009). The VEGF-system in primary pulmonary angiosarcomas and haemangioendotheliomas: New potential therapeutic targets? *Lung Cancer, 65*(1), 49–55.

Swidzinska, E., Ossolinska, M., Naumnik, W., Izycki, T., Kucejko, W., & Chyczewska, E. (2004). Circulating VEGF and its soluble receptor sVEGFR-1 in patients with lung cancer. *Pneumonologia i Alergologia Polska, 72*(9–10), 389–394.

Tas, F., Duranyildiz, D., Oguz, H., Camlica, H., Yasasever, V., & Topuz, E. (2006). Serum vascular endothelial growth factor (VEGF) and interleukin-8 (IL-8) levels in small cell lung cancer. *Cancer Investigation, 24*(5), 492–496.

Ustuner, Z., Saip, P., Yasasever, V., Vural, B., Yazar, A., Bal, C., Ozturk, B., Ozbek, U., & Topuz, E. (2008). Prognostic and predictive value of vascular endothelial growth factor and its soluble receptors, VEGFR-1 and VEGFR-2 levels in the sera of small cell lung cancer patients. *Medical Oncology, 25*(4), 394–399.

Chapter 39
Reliable Detection of Rare Mutations in EGFR Gene Codon L858 by PNA-LNA PCR Clamp in Non-small Cell Lung Cancer

Michal Skronski, Joanna Chorostowska-Wynimko, Ewa Szczepulska, Adam Szpechcinski, Piotr Rudzinski, Tadeusz Orlowski, and Renata Langfort

Abstract PNA-LNA PCR clamp real-time PCR method represents allele-specific approach to mutation analysis of EGFR gene in NSCLC. Due to its unique design, it is characterized by exceptionally high specificity and sensitivity but also allows detection of rare or not specifically-targeted EGFR mutations within examined exons, otherwise undetectable by other mutation-specific fluorescent probes. We herein present two cases of rare mutations revealed by PNA-LNA PCR clamping of NSCLC samples referred for routine EGFR gene molecular diagnostics. In one, the EGFR gene L858 codon mutation was detected by standard PNA-LNA PCR clamping, subsequently reconfirmed and characterized by direct sequencing of allele specific amplification products as the missense mutation c.2572C>A (p.L858M) paired with L861Q mutation on the same allele (*in cis*). In the second sample, low quality FFPE material from pleural biopsy, c.2573C>T missense mutation (p.L858P) was revealed. Still, repeated DNA analysis by PNA-LNA PCR clamp and direct sequencing demonstrated low level of mutant allele existing in a total allele pool suggesting rather artifactual c.2572C>T transition, a phenomenon quite frequent in low-volume FFPE samples upon fixation procedures. In conclusion, superior sensitivity and unique design of PNA-LNA PCR clamping are crucial for its excellent diagnostic effectiveness. As we demonstrated, the method allows detecting rare EGFR mutations, although it increases the risk of detection of a very low signal, e.g., generated by a small pool of mutated allele. Therefore, applicability of PNA-LNA PCR clamp product for the direct sequencing reevaluation is of key importance enabling reliable validation of results.

Keywords EGFR mutations • Non-small cell lung cancer • PNA-LNA PCR clamp • Rare mutations • Sequencing

M. Skronski • J. Chorostowska-Wynimko (✉) • A. Szpechcinski
Laboratory of Molecular Diagnostics and Immunology, National Institute of Tuberculosis and Lung Diseases, 26 Plocka St, Warsaw 01-138, Poland
e-mail: j.chorostowska@gmail.com

E. Szczepulska • R. Langfort
Department of Pathology, National Institute of Tuberculosis and Lung Diseases, 26 Plocka St, Warsaw 01-138, Poland

P. Rudzinski • T. Orlowski
Department of Surgery, National Institute of Tuberculosis and Lung Diseases, 26 Plocka St, Warsaw 01-138, Poland

M. Pokorski (ed.), *Respiratory Regulation - The Molecular Approach*,
Advances in Experimental Medicine and Biology 756, DOI 10.1007/978-94-007-4549-0_39,

39.1 Introduction

Molecular methods comprise currently an important part of routine diagnostic in lung adenocarcinoma patients as the detection of EGFR gene activating mutations within cancer genome is a prerequisite for successful therapy with EGFR tyrosine kinase inhibitors. More than 90% of detected EGFR somatic mutations in human lung cancer are located within exon 19 as in-frame microdeletions (45.7–55.7%), mainly as 15-nucleotide deletion p.E746_A750del15 and in exon 21, as point missense mutation L858R (41.0–43.3%) (Prudkin and Wistuba 2006; Sharma et al. 2007).

It is of crucial importance that the methods employed for detection of EGFR mutations are sufficiently specific and sensitive to provide consistent, reliable and rapid diagnosis (Chorostowska-Wynimko and Szpechcinski 2007). Direct sequencing is the gold standard for any mutation analysis within human genomic DNA. It is also utilized by many laboratories for EGFR mutation identification, despite its limited effectiveness. In non-small cell lung cancer (NSCLC) samples with a low-quality DNA or not-abounding with cancer cells (<50%) prevail. Supplementary methods, like microdissection, are then recommended (Pirker et al. 2010), which increases the costs and the time-load of work. In formalin-fixed paraffin-embedded (FFPE) samples, even those rich with cancer cells, DNA quality is frequently affected by formalin fixation procedures and a low-level mutation signal in direct sequencing fluorogram might be confused with background noise and not recognized.

Meanwhile, molecular probes-based PCR assays are fast, relatively cost-effective, and characterized by high specificity and sensitivity. Real-time PCR-based methods are mutation-specific, consequently do not allow detection of any given mutation within exons 18–21. Still, the most important from clinical and therapeutic point of view might be revealed effectively. The literature demonstrates a high concordance of these methods with standard direct sequencing in resected NSCLC specimens. The PNA-LNA PCR clamp real-time PCR method represents allele-specific approach to mutation analysis and due to its unique design is characterized by exceptionally high specificity and sensitivity (Nagai et al. 2005). High affinity and specificity of PNA oligomers for complementary DNA sequence and their resistance to exonucleolytic activity of DNA polymerase result in inhibition of wild type allele PCR amplification in tumor-derived DNA. At the same time EGFR mutant allele, if present, is preferentially amplified, thus detection sensitivity is remarkably increased (Fig. 39.1). Moreover, LNA modifications improve specificity of hydrolysis probes binding to target DNA sequence. This quality is of key importance for ultra-sensitive detection of point mutations. In addition, PNA-LNA PCR clamp is the only real-time PCR method that allows positive confirmation/reevaluation of its product by direct sequencing, if necessary. Besides, PNA-LNA PCR clamp due to its unique design allows detection of rare or not specifically-targeted EGFR mutations within examined exons, otherwise undetectable by other mutation-specific fluorescent probes.

In the current report we present two cases demonstrating high sensitivity and specificity of PNA-LNA PCR clamp method allowing reliable detection of rare mutations in EGFR gene L858 codon.

39.2 Methods

The study was performed in conformity with the 1989 Declaration of Helsinki for human research and the protocol was accepted by a local Ethics Committee.

39.2.1 Sample 1

Tissue material from resected lung adenocarcinoma was referred for EGFR gene mutation analysis. Specimen was incubated in RT for 24 h in tissue preserving medium and subsequently frozen at −80°C until further analysis. Next, sample was homogenized and DNA extracted with GeneMATRIX Tissue

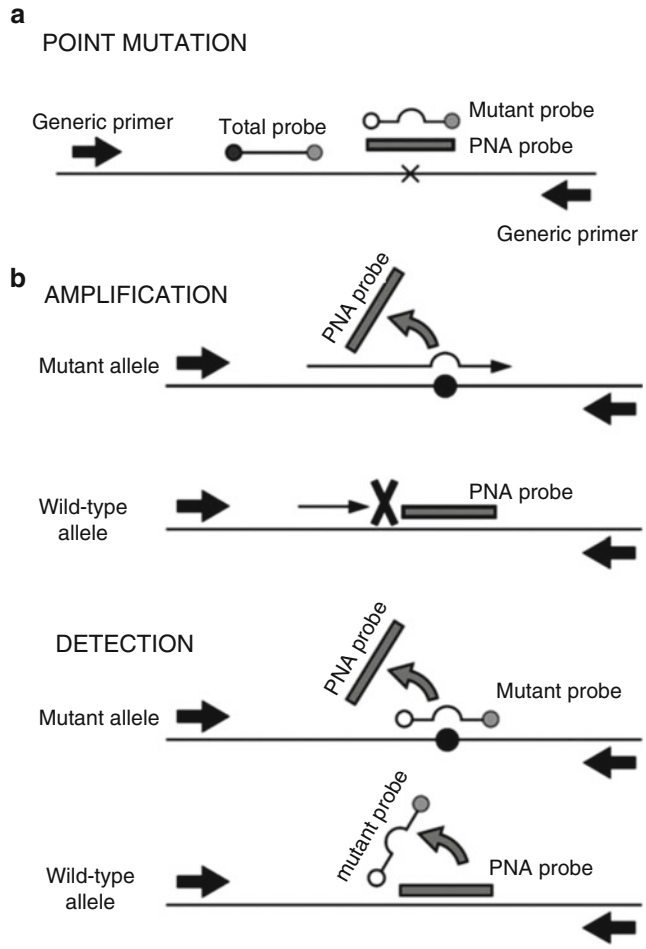

Fig. 39.1 PNA-LNA PCR clamp system for detection of point mutation. (**a**) Amplification of region of interest with generic primers is detected by a total probe. PNA probe and mutant probe are located at mutation site; (**b**) during amplification, PNA binds with high specificity and affinity to wild-type sequence only. No signal from the mutant probe and a high level of amplification detected, despite the presence of PNA oligomer in the reaction mixture, indicate the presence of rare or unknown mutation (Nagai et al. 2005)

DNA Isolation Kit (EURx, Gdansk, Poland) Afterwards, PNA-LNA PCR clamp real time assay was performed with 200 nmol/L of each forward and reverse primer specific to exon 21 sequence (Genomed SA, Warsaw, Poland), creating 191 bp PCR product 5 μmol/L of PNA 14-mer (clamp primer) binding to wild type sequence (Panagene, South Korea) and 100 nmol/L of both total and L858R fluorescent hydrolysis probes containing LNA bases (Eurogentec, Belgium) (Nagai et al. 2005). For every PNA-LNA PCR clamp (PNA+) reaction, similar procedure without the addition of PNA oligomer was performed as amplification control.

PNA-LNA PCR clamp reactions were run with 2x Universal Probe Master Mix (Roche) in 20 μl of reaction volume using LightCycler 480 II thermal cycler (Roche). PCR cycling was 45 cycles of 15 s at 95°C and 45 s at 56°C. Results were analyzed with software provided by Roche with LightCycler 480 II. A second derivative and endpoint genotyping analysis of fluorescence results were performed. The sample was considered mutation positive if ΔCp and/or ΔEF (endpoint fluorescence) values were lower than the level of a fluorescence signal for 1% of heterozygous mutant DNA control.

PNA-LNA PCR clamp reaction and control reaction products were purified from deoxynucleotides, primers, fluorescent probes and PNA oligomers using GeneMATRIX PCR/DNA Clean-Up Purification Kit (EURx, Gdansk, Poland). Both forward and reverse strand were sequenced by BigDye Terminator Kit (Applied Biosystems) and capillary electrophoresis system ABi 3130xl Genetic Analyzer (Applied Biosystems; Genomed, Warsaw, Poland). Sequence fluorograms were analyzed with FinchTV sequence viewer (Geospiza) and MutationSurveyor ver.3.97 software (SoftGenetics).

39.2.2 Sample 2

Tissue material from pleural biopsy with histologically confirmed content of lung adenocarcinoma cells, estimated by an experienced pathologist as 35%, was referred for EGFR gene mutation analysis.

DNA was extracted by QiaAMP FFPE tissue DNA isolation kit (Qiagen, Hilden, Germany) and amplified by PCR reaction with outer primers. Due to poor amplification, nested PCR reaction and nested real-time PNA-LNA PCR clamp assay were performed.

PCR pre-amplification reaction: 5 μl of undiluted tissue DNA and of 2x PCR Ready Mix (Sigma), 500 nmol/L of both F and R primers (Genomed SA, Warsaw, Poland) flanking EGFR exon 21 and appropriate DDW quantity were used for final reaction volume of 20 μl. PCR primers designed as described elsewhere (Molina-Vila et al. 2008). PCR pre-amplification reactions were performed on PTC-200 thermal cycler (BioRad) with 25 cycles of 30 s at 95°C, 30 s at 59°C, and 1 min at 72°C. In all nested PCR reactions, 5 μl of first PCR product was diluted with DDW 1:1000. Nested PCR reaction mixture: 2xPCR Ready Mix (Sigma, St. Louis, MO), 500 nmol/L of both F and R nested primers flanking EGFR exon 21 and appropriate DDW quantity were used for final reaction volume of 20 μl. Reactions were performed on PTC-200 thermal cycler (BioRad) with 30 cycles of 30 s in 95°C, 30 s at 59°C and 1 min at 72°C. Next, PCR products of all reactions were subjected to electrophoresis in 2% agarose gel and visualized in UV light by ethidium bromide staining.

For Sanger direct sequencing purposes, PCR products were enzymatically purified with ExoSAP-IT kit (GE Healthcare) according to the manufacturer's instructions. For amplification of both PNA-LNA PCR clamp and normal PCR purified products, 5 pM of a forward or reverse primer was added. PNA-LNA PCR clamp reactions and direct sequencing were performed and analyzed as described above.

39.3 Results

In order to comprehensively evaluate and compare PNA + and PNA-PCR clamp reactions for DNA sample, Cp values and EF signal were analyzed. Cp value represents the so called crossing point, i.e., the maximum value for the second derivative analysis of fluorescence curves, while endpoint fluorescence signal indicates the level of wild-type or mutant allele endpoint PCR amplification. Differences in Cp and EF values for PNA + and PNA- reactions were referred as ΔCp and ΔEF, respectively. Both, ΔCp and ΔEF were matched with respective data from internal control reactions performed in samples containing DNA from heterozygous L858R/wt H1975 cell line intermixed with wild-type allele (1%, 10% and 100%).

39.3.1 Sample 1

Total probe detected amplification of PCR product with no corresponding positive signal from L858R probe. Both, ΔCp (Table 39.1a, Fig. 39.2a) and ΔEF (Table 39.1b, Fig. 39.2b) for PNA + and PNA- reaction strongly implied unidentified mutation within the analyzed exon. In order to identify variation

Table 39.1 Sample 1 (**a**) total probe ΔCp and (**b**) ΔEF for both PNA+and PNA− reactions implies mutation within PNA binding sequence in exon 21 of EGFR gene. Undiluted mutant DNA (100%), 1:10, and 1:100 of mutant to wild-type ratio (10% and 1%, respectively) and wild-type only DNA provide internal control of analyzed sample amplification and therefore mutation presence; (**a**) ΔCp – difference between PNA-LNA PCR clamp and PNA- control reaction Cp values and (**b**) ΔEF – difference in endpoint fluorescence signal in 45th cycle of PNA-LNA PCR clamp reaction and PNA- control reaction

a	Cp PNA+	Cp PNA−	ΔCp	**b**	PNA+	PNA−	ΔEF
Sample 1	24.72	23.18	1.54		3.74	3.80	0.06
H1975 100%	26.55	25.93	0.62		4.10	4.12	0.02
H1975 10%	30.01	27.82	2.19		4.48	4.85	0.37
H1975 1%	33.61	28.06	5.55		4.08	4.53	0.45
wt	37.37	28.14	9.23		3.24	4.74	1.50

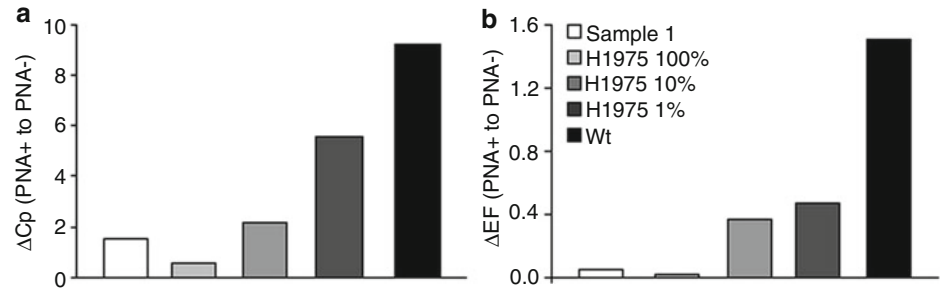

Fig. 39.2 (**a**) **ΔCp and** (**b**) **ΔEF values from PNA-LNA PCR clamp assay for Sample 1 DNA and controls** containing different amount of heterozygous L858R DNA intermixed with wild-type. Undiluted mutant DNA (100%), 1:10 and 1:100 of mutant to wild-type ratio (10% and 1%, respectively), and wild-type only DNA provide internal control of the analyzed sample amplification and therefore of the mutation presence; *ΔCp* difference between PNA+and PNA- Cp values, *ΔEF* difference in endpoint fluorescence signal in 45th cycle of PNA-LNA PCR clamp reaction and PNA-control

in PNA clamp binding region (codons 856–860), bidirectional Sanger sequencing of PNA-LNA PCR clamp reaction and of the control reaction (no PNA clamp oligomer) products were performed. Double mutation c.2572C>A (L858M)+c.2582T>A (L861Q) was identified in both samples. Still, analysis of PNA (−) reaction product showed a heterozygous sequence for both mutations (Fig. 39.3a), while in allele-specific PNA (+) reaction product, a homozygous sequence for both c.2572C>A (L858M) and c.2582C>A (L861Q) mutations was present (Fig. 39.3b).

39.3.2 Sample 2

In PNA-LNA PCR clamp reaction, ΔCp and ΔEF values for Sample 2 DNA and controls were analyzed. Total probe detected the amplification of PCR product with no corresponding positive signal from L858R probe. While no consistent ΔCp between PNA+and PNA- reactions was observed (Table 39.2a, Fig. 39.4a), ΔEF (difference in the total probe endpoint fluorescence values between PNA+and PNA- reaction) allowed sample identification as mutation positive (Table 39.2b, Fig. 39.4b). The presence of unidentified variation in PNA clamp binding region (codons 856–860) was verified by bidirectional Sanger sequencing of allele-specific clamped PCR reaction. Cytosine to Thymine transition signal in position c.2573 of EGFR gene was detected, but only in PNA+reaction product sequence (Fig. 39.5a, b). Sample analysis was repeated. In the second PNA-LNA PCR clamp reaction,

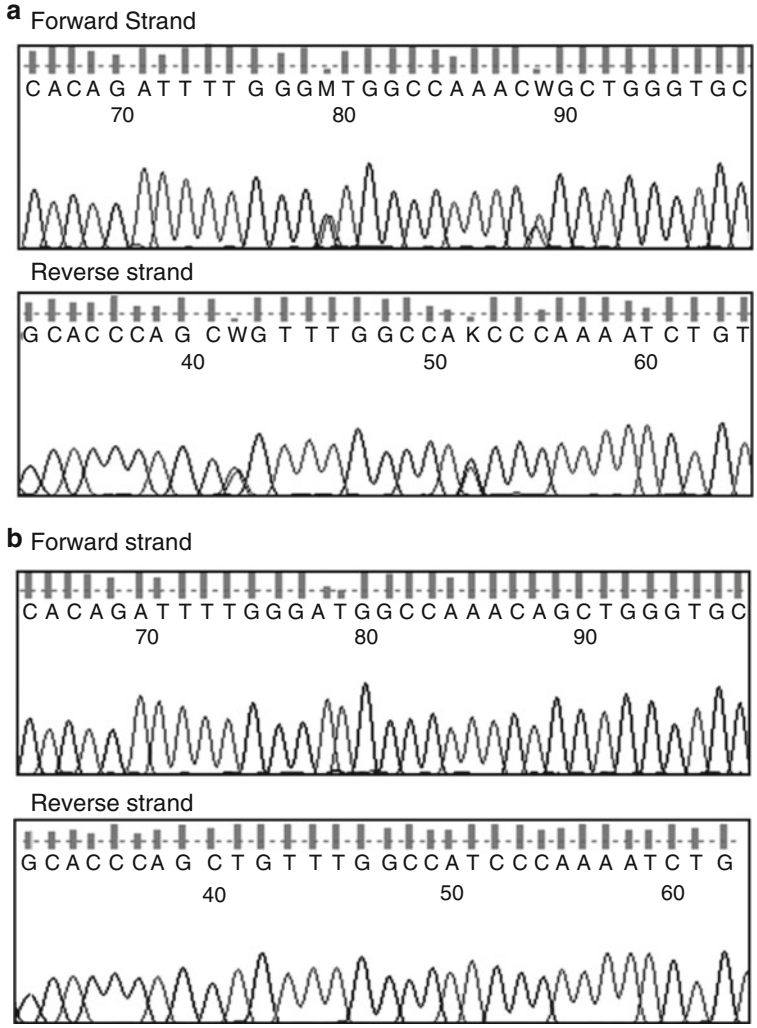

Fig. 39.3 Direct sequencing of PCR reaction product (a) and of PNA-LNA PCR clamp product (b) demonstrate heterozygous c.2572C>A and c.2582T>A mutations in Sample 1 DNA. L858M + L861Q double mutation was detected both in forward and reverse strands

endpoint fluorescence of the total probe was consistent with the previous results (Table 39.3a, Fig. 39.6a) while the second derivative analysis repeatedly showed a mutation negative signal (Table 39.3b, Fig. 39.6b). Additionally, PNA-LNA PCR clamp product sequencing revealed a low mutated nucleotide signal in reaction with a forward primer only (Fig. 39.7).

39.4 Discussion

In the present study we demonstrate the effectiveness of a PNA-LNA PCR clamp method in detection of rare point mutations within the L858 codon of EGFR gene. The method, apart from being highly specific and sensitive towards most frequent EGFR gene activating mutations, offers an additional advantage which may be important for both clinical and scientific purposes.

The PNA-LNA PCR clamp is the only real-time PCR method allowing sequence analysis of a reaction product. Thus, upon receiving the inconsistent signaling from total and L858R mutation specific probe it

Table 39.2 Sample 2 (**a**) total probe ΔCp for both PNA + and PNA- reactions implies no mutation within PNA binding sequence in EGFR gene exon 21 and (**b**) total probe ΔEF indicates mutation in PNA binding sequence of EGFR gene exon 21

a	Cp PNA +	Cp PNA –	ΔCp	**b**	EFPNA +	EFPNA –	ΔEF
Sample 2	30.83	24.25	6.58		2.89	3.21	0.32
H1975 100%	27.39	26.82	0.57		3.43	3.55	0.12
H1975 10%	31.03	28.66	2.37		3.38	3.68	0.30
H1975 1%	35.03	29.30	5.73		3.05	3.47	0.42
wt	–	29.17	–		2.04	3.48	1.44

Abbreviations as in Table 39.1

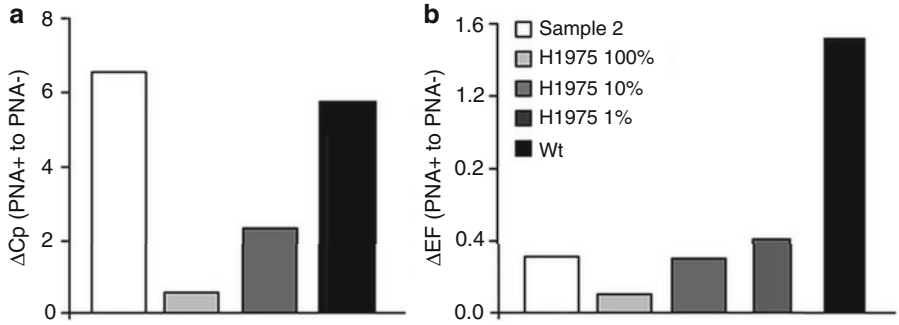

Fig. 39.4 (**a**) **ΔCp values from PNA-LNA PCR clamp assay for Sample 2 DNA** and controls containing different amount of heterozygous L858R/wt H1975 cell line DNA intermixed with wild-type and (**b**) **ΔEF values from PNA-LNA PCR clamp assay for Sample 2 DNA** and controls containing different amount of heterozygous L858R DNA intermixed with wild-type. Abbreviations as in Fig. 39.2a, b, respectively

was possible to reconfirm the real-time PCR results by direct sequencing and reveal two missense mutations c.2572C>A(p.L858M) and c.2573C>T (p.L858P). In the current literature, there are only few reports concerning both L858M and L858P mutations, all of them diagnosed by Sanger sequencing (Tam et al. 2006; Chen et al. 2011; Wu et al. 2011). It is due to the fact that most molecular probes-based PCR methods detect only limited number of specific mutations, whereas direct sequencing reveals all abnormalities within the analyzed sequence, including rare and unknown mutations. As mentioned above, in this aspect the PNA-LNA PCR clamp offers a unique opportunity of its product reanalysis by sequencing.

Meanwhile, most known clinically relevant EGFR activating mutations are clustered in mutational hotspots within exon 19 and 21. Consequently, the PNA-LNA PCR clamp is the only PCR based method enabling both fast and reliable EGFR gene mutation diagnosis and sensitive detection of rare mutation if combined with direct sequencing. In addition, in routine laboratory diagnostics it is considerably more cost- and time effective (basic wild-type/mutation genotyping on isolated tumor DNA in less than 2–3 h) than Sanger sequencing (usually 2–3 days). Therefore, in our opinion, the PNA-LNA PCR clamp is an optimal method for the detection of EGFR mutations. Our data strongly suggest that the PNA-LNA PCR clamp method allows detecting any mutation in PNA clamp binding sequences (14–18 nt) located in most variable locations of exons 18–21.

Interestingly, in one of the presented cases L858M mutation was paired with L861Q mutation (c. 2582T>A). A similar observation was previously demonstrated only by Tam et al. (2006). Likewise, reported frequency of double EGFR gene mutations in exons 18–21 is rather low 3–13% (Zhang et al. 2007; Tam et al. 2006). Most often, double mutations were found *in cis* form, i.e., both

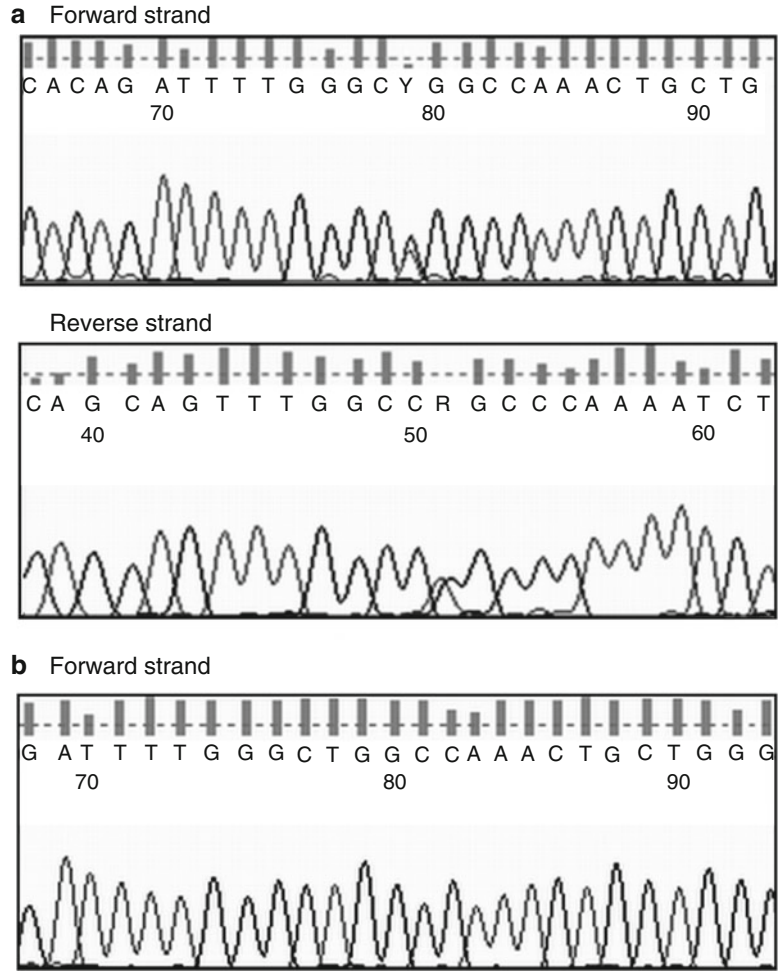

Fig. 39.5 (**a**) **Direct sequencing of PNA-LNA PCR clamp product** demonstrates both c.2573T>mutation and wild type allele in Sample 2 DNA; mutation was present in both forward and reverse strands. (**b**) **Direct sequencing of PCR reaction product** demonstrates presence of wild-type sequence only in Sample 2 DNA; Reaction was repeated

Table 39.3 Sample 2 (**a**) total probe ΔCp in repeated PNA-LNA PCR clamp analysis demonstrates no consistent differences within PNA binding sequence in EGFR gene exon 21 and (**b**) total probe ΔEF in repeated PNA-LNA PCR analysis demonstrates no consistent differences between both reactions

a	Cp PNA +	Cp PNA −	ΔCp	**b**	PNA +	PNA −	ΔEF
Sample 2	27.86	19.46	8.40		3.17	3.42	0.25
H1975 10%	30.93	28.69	2.24		3.34	3.38	0.04
H1975 1%	34.62	29.47	5.15		2.99	3.34	0.35
wt	38.01	29.44	8.57		2.31	3.35	1.24

Abbreviations as in Table 39.1a, b, respectively

wild type and mutated alleles were present. Tam et al. (2006) confirmed L858M and L861Q double mutations within the same allele (*in cis*) by subcloning and direct sequencing cDNA of EGFR transcript isolated from tumor tissue. In both cases, the second allele was wild-type. As the PNA-LNA PCR clamp method preferentially amplifies L858 codon mutant allele but not L861 codon mutant allele, we were able to detect both mutations within the same gene copy. Sequencing of the PNA(−) PCR

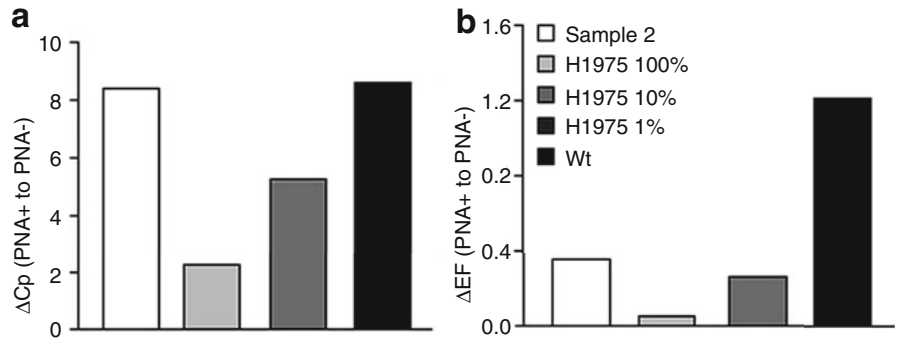

Fig. 39.6 ΔCp (a) and ΔEF (b) values from repeated PNA-LNA PCR clamp assay for Sample 2 DNA and controls containing different amount of heterozygous L858R DNA intermixed with wild-type. Abbreviations as in Fig. 39.2a, b, respectively

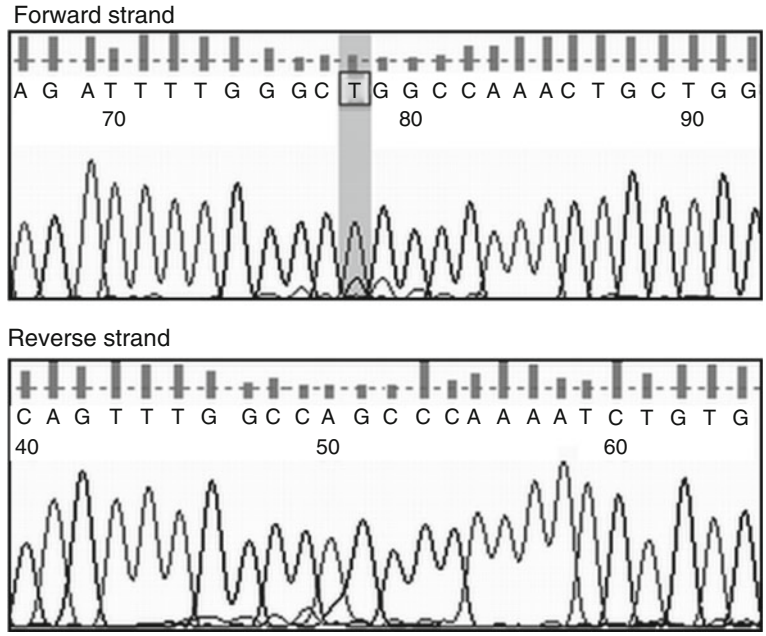

Fig. 39.7 Direct sequencing of repeated PNA-LNA PCR clamp reaction product demonstrates both low level of c.2573T>mutation signal and wild type allele in Sample 2 DNA; mutation was present in forward strand, but not in reverse strand

reaction product revealed heterozygous genotype for both L858M and L861Q mutations strongly suggesting that the other allele was wild-type.

Clinical relevance of L858M and L861Q double mutation is unknown. However, according to the literature, L861Q up-regulates EGFR kinase domain activation and decreases receptor sensitivity towards reversible TKI (Kancha et al. 2011). In L858M mutation, non-polar leucine is switched into the non-polar methionine, hence any significant structural changes within the EGFR protein structure would be unlikely.

In contrast to the mutations discussed above, preliminary results of the PNA-LNA PCR clamp and direct sequencing molecular analysis suggesting the c.2572C>T missense transition in Sample 2 were

not consistently confirmed by the repeated sample evaluation. While L858P mutation was detected by two independent PCR assays, thus proving that low level of mutant allele existed within total allele pool, the direct sequencing analyses were not similar. Although L858P mutation was reported by Wu et al. (2011), we believe that c.2572C>T transition revealed in this particular sample was most likely artifactual. The material referred for molecular analysis consisted of low-volume FFPE tissue and provided only low-concentrated and poorly amplifiable DNA sample. Although the PNA-LNA PCR clamp method allows a reliable examination of low-quality materials, DNA from FFPE samples, in particular small ones, are prone to PCR amplification of artifactual mutations. Formalin fixation strongly affects DNA quality, generating, e.g., cytosine and adenine deaminations. An error rate for Taq polymerase in amplification of DNA reported for FFPE samples was much higher than its standard base miscorporation frequency. It has been implied that Taq polymerase, incorporates A instead of G located opposite to damaged cytosine leading to G>A transitions and consequently C>T artifactual changes (so-called 'A-rule') (Williams et al. 1999). Likewise, deamination of adenine results in hypoxanthine residues and in A→G/T→C transitions (Marchetti et al. 2006).

Consequently, it should be emphasized that superior sensitivity of the PNA-LNA PCR clamping, crucial for its unique diagnostic effectiveness, increases the risk of a very low signal detection, e.g., generated by a small pool of mutated allele. In an experimental setting, the PNA-LNA PCR clamp method has shown exceptional sensitivity in detecting mutant allele at the wild-type background with 1:2,000 ratio (1 allele in 1,000 of diploid human genome copies) (Nagai et al. 2005). Its reliability has been also demonstrated in clinics. Tanaka et al. (2007, 2010) evaluated the EGFR mutation status in variety of cytological specimens (bronchoscopy specimens, pleural effusion, sputum, and pericardial effusion) and in paraffin-embedded tissues with 97% sensitivity and 100% specificity. Therefore, the reliable method validation and good quality, and a repetitive intralaboratory control of final results are prerequisite for the successful EGFR mutation diagnostics.

Conflicts of interest: The authors declare no conflicts of interest in relation to this article.

References

Chen, C., Jiang, X. L., Zhan, C. C., & Li, K. (2011). Correlation of genes associated with drug response to prognosis of large cell lung carcinoma. *Chinese Journal of Cancer, 30*, 497–504.

Chorostowska-Wynimko, J., & Szpechcinski, A. (2007). The impact of genetic markers on the diagnosis of lung cancer: A current perspective. *Journal of Thoracic Oncology, 2*, 1044–1051.

Kancha, R. K., Peschel, C., & Duyster, J. (2011). The epidermal growth factor receptor-L861Q mutation increases kinase activity without leading to enhanced sensitivity toward epidermal growth factor receptor kinase inhibitors. *Journal of Thoracic Oncology, 6*, 387–392.

Marchetti, A., Felicioni, L., & Buttitta, F. (2006). Assessing EGFR mutations. *The New England Journal of Medicine, 354*(5), 526–528.

Molina-Vila, M. A., Bertran-Alamilo, J., Reguart, N., Taron, M., Castella, E., Ljatjos, M., Costa, C., Mayo, C., Pradas, A., QueralT, C., Botia, M., Perez-Cano, M., Carrasco, E., Tomas, M., Mate, J. L., Moran, T., & Rosell, R. (2008). A sensitive method for detecting EGFR mutations in non-small cell lung cancer samples with few tumor cells. *Journal of Thoracic Oncology, 5*, 1224–1235.

Nagai, Y., Miyazawa, H., Huqun, Tanaka, T., Udagawa, K., Kato, M., Fukuyama, S., Yokote, A., Kobayashi, K., Kanazawa, M., & Hagiwara, K. (2005). Genetic heterogeneity of the epidermal growth factor receptor in non-small cell lung cancer cell lines revealed by a rapid and sensitive detection system, the peptide nucleic acid-locked nucleic acid PCR clamp. *Cancer Research, 65*, 7276–7282.

Pirker, R., Herth, F. J., Kerr, K. M., Filipits, M., Taron, M., Gandara, D., Hirsch, F. R., Grunenwald, D., Popper, H., Smit, E., Dietel, M., Marchetti, A., Manegold, C., Schirmacher, P., Thomas, M., Rosell, R., Cappuzzo, F., & Stahel, R. (2010). Consensus for EGFR mutation testing in non-small cell lung cancer: Results from a European workshop. *Journal of Thoracic Oncology, 5*, 1706–1713.

Prudkin, L., & Wistuba, I. I. (2006). Epidermal growth factor receptor abnormalities in lung cancer. Pathogenetic and clinical implications. *Annals of Diagnostic Pathology, 10*, 306–315.

Sharma, S. V., Bell, D. W., Settleman, J., & Haber, D. A. (2007). Epidermal growth factor receptor mutations in lung cancer. *Nature Reviews Cancer, 7*, 169–181.

Tam, I. Y., Chung, L. P., Suen, W. S., Wang, E., Wong, M. C., Ho, K. K., Lam, W. K., Chiu, S. W., Girard, L., Minna, J. D., Gazdar, A. F., & Wong, M. P. (2006). Distinct epidermal growth factor receptor and KRAS mutation patterns in non-small cell lung cancer patients with different tobacco exposure and clinicopathologic features. *Clinical Cancer Research, 12*, 1647–1653.

Tanaka, T., Nagai, Y., Miyazawa, H., Koyama, N., Matsuoka, S., Sutani, A., Huqun Udagawa, K., Murayama, Y., Nagata, M., Shimizu, Y., Ikebuchi, K., KanazawA, M., Kobayashi, K., & Hagiwara, K. (2007). Reliability of the peptide nucleic acid-locked nucleic acid polymerase chain reaction clamp-based test for epidermal growth factor receptor mutations integrated into the clinical practice for non-small cell lung cancers. *Cancer Science, 98*, 246–252.

Tanaka, T., Matsuoka, M., Sutani, A., Gemma, A., Maemondo, M., Inoue, A., Okinaga, S., Nagashima, M., Oizumi, S., Uematsu, K., Nagai, Y., Moriyama, G., Miyazawa, H., Ikebuchi, K., Morita, S., Kobayashi, K., & Hagiwara, K. (2010). Frequency of and variables associated with the EGFR mutation and its subtypes. *International Journal of Cancer, 126*, 651–655.

Williams, C., Ponten, F., Moberg, C., Söderkvist, P., Uhlen, M., Ponten, J., Sitbon, G., & Lundeberg, J. (1999). A high frequency of sequence alterations is due to formalin fixation of archival specimens. *American Journal of Pathology, 155*, 1467–1471.

Wu, S. G., Yang, C. H., Yu, C. J., Lee, J. H., Hsu, Y. C., Chang, Y. L., Shih, J. Y., & Yang, P. C. (2011). Good response to pemetrexed in patients of lung adenocarcinoma with epidermal growth factor receptor (EGFR) mutations. *Lung Cancer, 72*, 333–339.

Zhang, G. C., Lin, J. Y., Wang, Z., Zhou, Q., Xu, C. R., Zhu, J. Q., Wang, K., Yang, X. N., Chen, G., Yang, J. J., Huang, Y. J., Liao, R. Q., & Wu, Y. L. (2007). Epidermal growth factor receptor double activating mutations involving both exons 19 and 21 exist in Chinese non-small cell lung cancer patients. *Clinical Oncology (Royal College of Radiologists), 19*, 499–506.

Chapter 40
Neurological Paraneoplastic Syndromes in Lung Cancer Patients

P. Stefens-Stawna, T. Piorunek, H. Gabryel-Batura, W. Kozubski, and S. Michalak

Abstract Lung cancer is recognized among the most frequent causes of paraneoplastic neurological syndromes (PNS). Neurological syndromes in subjects with systemic malignancy remain a clinical and diagnostic challenge. The aim of the study was to evaluate the frequency of NPS, their clinical manifestation and association with onconeural antibodies in patients with lung cancer. Fifty patients hospitalized with the diagnosis of PNS participated in the study. Neurological evaluation consisted of the Rankin scale (mRS), the Barthel index (BI), and testing for the presence of onconeural antibodies by means of indirect immunofluorescence, as screening, and Western blotting as confirmation. The majority of lung cancer patients (64%) aged 62 ± 10 had NPS symptoms. Their neurological condition and daily living activities were reasonable: mRS (1.0; 0.0–4.0) and BI (100; 7.4–100) scores. Classical PNS were found in 30% of cases and included sensory neuropathy (16%), paraneoplastic cerebellar degeneration (12%) as the most frequent symptoms. Autoimmune reaction was observed in 42% of lung cancer patients and in 20% was represented by well-characterized onconeural antibodies. Anti-Hu antibody was identified as the most frequent. In conclusion, PNS signs in lung cancer patients have both classical and non-classical features. In the course of SCLC only well-characterized onconeural antibodies were identified. The presence of well-characterized onconeural antibodies is strongly associated with classical features of PNS.

Keywords Lung cancer • Onconeural antibodies • Paraneoplastic neurological syndromes • Malignancy • Barthel index • Sensory neuropathy • Autoimmune reaction

P. Stefens-Stawna • W. Kozubski
Department of Neurology, University of Medical Sciences, Poznan, Poland

T. Piorunek • H. Gabryel-Batura
Department of Pulmonology, Allergology and Respiratory Oncology,
University of Medical Sciences, Poznan, Poland

S. Michalak (✉)
Department of Neurochemistry and Neuropathology, University of Medical Sciences,
49 Przybyszewskiego St., Poznan 60-355, Poland
swami622@gmail.com

Neuroimmunological Unit, Polish Academy of Sciences,
Poznan, Poland

M. Pokorski (ed.), *Respiratory Regulation - The Molecular Approach*,
Advances in Experimental Medicine and Biology 756, DOI 10.1007/978-94-007-4549-0_40,

40.1 Introduction

Clinical manifestations caused by indirect effects of systemic malignancy, with exclusion of metastases, compression or infiltration, are paraneoplastic neurological syndromes (PNS). Currently used diagnostic criteria take into consideration two important notions: classical paraneoplastic neurological syndromes and well-characterized onconeural antibodies (Graus et al. 2004). Limbic encephalitis, paraneoplastic cerebellar degeneration, Lambert-Eaton myasthenic syndrome, subacute sensory neuropathy, opsoclonus/myoclonus syndrome, and dermatomyositis are recognized as classical PNS, because their presence strongly suggests association with malignancy. Detection of anti-Hu, anti-Yo, anti-Ri, anti-Ma/Ta, anti-CRMP-5, anti-amphiphysin antibodies enables a definite PNS diagnosis, even if the underlying malignancy is not identified. For that reason, such a group of antibodies was described as 'well-characterized' (Graus et al. 2004). However, the definite PNS diagnosis is also possible if neurological deficit has non-classical features in a patient with already diagnosed cancer. On the other hand, by means of indirect immunofluorescence used as a screening test for detection of onconeural antibodies, a spectrum of positive reactions can be observed including: anti-Tr, anti-myelin, anti-myelin-associated glycoprotein (anti-MAG), anti-glutamic acid decarboxylase (anti-GAD), anti-neuroendothelium, anti-gangliosides or anti-glial fibrillary acid protein (anti-GFAP). The clinical significance of not well-characterized antibodies remains unclear. Currently, accepted hypothesis of the immune-mediated pathomechanism of paraneoplastic neurological syndromes focuses on the cell-mediated response. However, onconeural antibodies are widely used in laboratory PNS diagnosis. There are data indicating that humoral response may be less an important pathomechanism in the development of PNS. First, the majority of target antigens have intracellular localization that theoretically makes them inaccessible to antibodies. In animal models, a passive transfer of immunoglobulins from patients with PNS leads to the finding that onconeural antibodies are not the only cause of PNS (Tanaka et al. 1994). Second, clinical studies show that treatment with intravenous immunoglobulins may not always be effective, which underscores the complexity of the PNS pathomechanisms. In lung cancer with a coexisting Lambert-Eaton myasthenic syndrome with paraneoplastic cerebellar degeneration, immunomodulating treatment leads to improvement of myasthenic symptoms, while the cerebellar signs persist (Graus et al. 2002). The cell-mediated immune response may be more important in the PNS pathogenesis. The profile of cells detected in cerebrospinal fluid ($CD8^+$, $CD4^+$ lymphocytes, NK cells, and B lymphocytes) of patients with 'anti-Hu' syndrome, associated frequently with small-cell lung cancer (SCLC), indicates the role of T lymphocytes and natural killer cells (de Graaf et al. 2008). Cytotoxic effects of $CD8^+$ T cells, mediating non-apoptotic death of neurons, suggest that the presence of onconeural antibodies may be considered as a bystander effect (Bernal et al. 2002). On the other hand, experimental studies suggest the non-immune-mediated mechanisms involved in indirect effects of systemic malignancy on the nervous system (Michalak et al. 2006a, b, 2007). Blood–brain barrier disruption has also been shown as an important component of the PNS pathology (Greenlee et al. 1995; Michalak et al. 2010). Lung cancer is recognized as one of the most frequent malignancy associated with classical and non-classical paraneoplastic neurological syndromes (Gozzard and Maddison 2010).

With the above outlined background in mind we have undertaken the study on paraneoplastic neurological syndromes in lung cancer patients. The aim of the study was to evaluate the frequency, clinical PNS manifestation, and association with well-characterized onconeural antibodies and other autoimmune reactions in such patients.

40.2 Methods

The study protocol was accepted by the Ethics Committee of the University of Medical Sciences in Poznan, Poland and each recruited participant gave the informed consent.

Fifty consecutive lung cancer patients (28 males, 22 females, ratio 1.3:1), mean age 62 ± 10 years, with the PNS diagnosis hospitalized in the Department of Pulmonology, Allergology and Respiratory Oncology, at Poznan University of Medical Science and at a Neurological Clinic participated in the study. Neurological examination and evaluation were performed by a neurologist with the use of a modified Rankin scale (mRS) and Barthel index (BI). Testing for the presence of onconeural antibodies was performed by means of indirect immunofluorescence, as a screening, and Western blotting (EUROIMMUN, Germany), as confirmatory test in all cases. Neuroimaging, neurophysiological, cerebrospinal fluid examination, and other laboratory tests were performed as required for differential diagnosis.

Data were presented as means ± SD. The distribution of results was analyzed with the D'Agostino-Pearson test. The differences between variables with the Gaussian distribution were evaluated with a variance ratio test (F-test) and in case of non-Gaussian distribution, with a non-parametric Mann–Whitney *U* test. Statistical analysis was performed with the use of licensed MedCalc software.

40.3 Results

The demographic and clinimetric data of patients are showed in Table 40.1. No statistically significant differences in the age, mRs and BI index scores were found between the male and female patients with lung cancer.

In 64% of the lung cancer patients we found signs of neurological deficits (Fig. 40.1). Classical paraneoplastic neurological syndromes were diagnosed in 30% of patients and included sensory neuropathy (16%), paraneoplastic cerebellar degeneration (12%), and the Lambert-Eaton myasthenic syndrome (2%). Coexisting PNS manifested in 4% of the subjects: in 2% sensory neuropathy coexisted with limbic encephalitis and paraneoplastic cerebellar degeneration and in another 2% limbic encephalitis was associated with neuropathy. Non-classical PNS manifested as a motor neuron disease (8%), upper motor neuron syndrome (8%), neuropathy (6%), sensomotoric neuropathy (4%), polymyositis (2%), dementia (2%), and bulbar syndrome (2%).

Autoimmune reaction was detected in 42% of lung cancer patients (Fig. 40.2) and in 20% was represented by well-characterized antibodies. Among these antibodies, anti-Hu antibody was found in 16% of subjects; but only in 2% as a single antibody, in 12% as one of two antibodies, and in 2% as one of three coexisting antibodies. Anti-Hu antibody coexisted in 6% of cases with anti-amphiphysin and in 4% with anti-Ma/Ta antibodies. In 2% of patients, anti-amphiphysin was a single antibody and in 6% as one of two antibodies. Anti-Ri was found in 2% as a single one and in 2% as one of two coexisting antibodies. Anti-Ma/Ta was detected only as coexisting antibodies: in 2% of patients as one of two and in 2% as one of three antibodies. Also, anti-CV-2 was found only as one of three coexisting antibodies in 2% of cases.

Autoimmunity not related to the well-characterized antibodies included anti-Myelin associated glycoprotein (anti-MAG) (6%), anti-myelin (4%), anti-neuroendothelium (4%), anti-glial fibrillary acid protein (anti-GFAP) (2%), and anti-nuclear antibodies (ANA) (2%).

Table 40.1 Demographic and clinimetric data of lung cancer patients

	Total	Males	Females
Age (years)	62 ± 10	67 ± 10	57 ± 9
mRS (median; interquartile range)	1.0 0.0–4.0	1.0 1.0–2.0	2.0 1.0–2.0
BI (median; interquartile range)	100.0 7.4–100	100.0 88.8–100	97.50 90.0–100

Values are means ± SD

mRS modified Rankin scale, *BI* Barthel Index

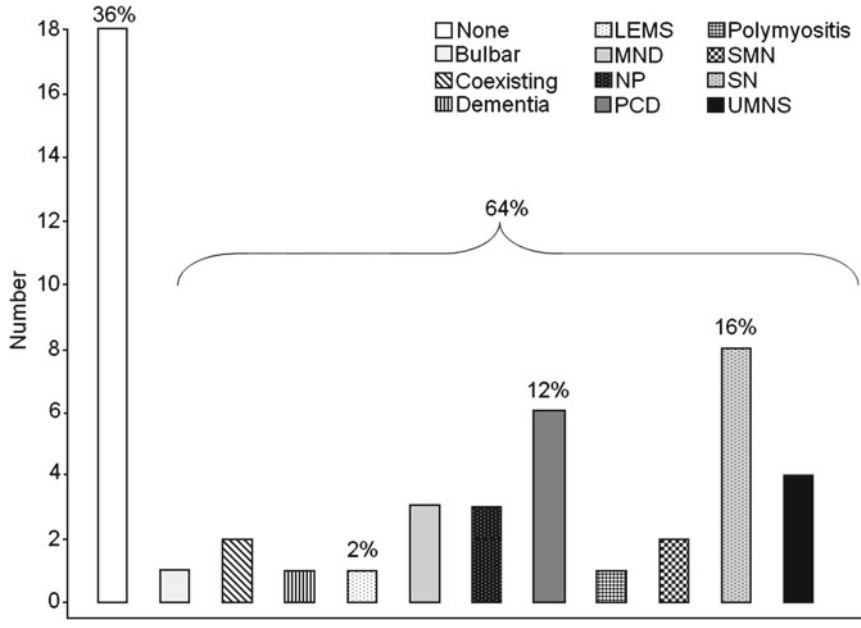

Fig. 40.1 Paraneoplastic neurological syndromes in lung cancer patients. *LEMS* Lambert-Eaton myasthenic syndrome, *MND* motor neuron disease, *NP* neuropathy, *PCD* paraneoplastic cerebellar degeneration, *SMN* sensomotoric neuropathy, *UMNS* upper motor neuron syndrome

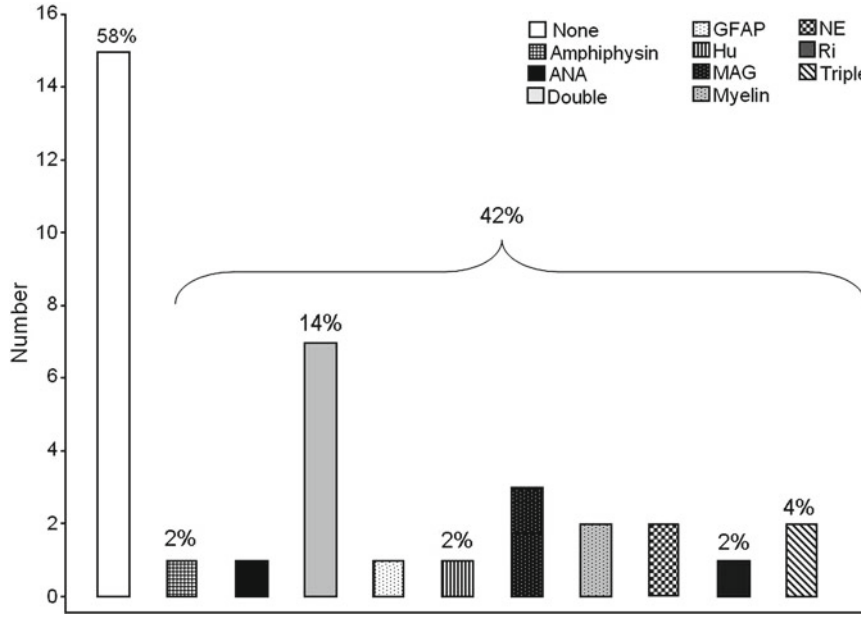

Fig. 40.2 Spectrum of antibodies detected in lung cancer patients. *ANA* antinuclear antibodies, *GFAP* antiglial fibrillary acid protein, *MAG* antimyelin associated glycoprotein, *NE* antineuroendothelium

Among the small-cell lung cancer patients (14 cases), 50% manifested symptoms of both classical and non-classical PNS associated only with the presence of the well-characterized onconeural antibodies. In the non-SCLC patients (20 cases), 65% had symptoms of classical as well as non-classical

Table 40.2 Associations between types of lung cancer, PNS and antibodies

Type of cancer	PNS	Antibody
SCLC	50% (PCD/SN/UMNS)	6% (coexisting anti-Hu & anti-amphiphysin)
Non-SCLC	65%	10% (anti-Hu/ anti-amphiphysin/ anti-Ma/Ta)
	(PCD/LE/SN/N/UMNS)	40% (anti-MAG/anti-GFAP/anti-myelin/ anti-neuroendothelium/ANA)
Non-defined	75%	31% (anti-Hu/anti-Ri/anti-Ma/Ta/ anti-CV2/)
	(LEMS/SN/LE/Dementia/ MND/N/Polymyositis/Bulbar)	19% (anti-aquaporin/anti-MAG/ anti-myelin/anti-neuroendothelium)

PNS and both well-characterized onconeural antibodies and not well-characterized antibodies were detected (Table 40.2). The patients with non-defined histological types of lung cancer (16 cases) presented a spectrum of classical (75%) and non-classical PNS associated with both well-characterized and not-well-characterized antibodies (Table 40.2). An interesting observation in the last group was the Lambert-Eaton myasthenic syndrome coexisting anti-Hu and anti-aquaporin antibodies. Sixty seven percent of patients with well-characterized antibodies manifested signs of classical PNS which were observed just in 27% of cases with not well-characterized antibodies.

40.4 Discussion

In the present study on paraneoplastic neurological syndromes we noted a high prevalence of indirect effects of malignancy on the nervous system in lung cancer patients. Clinical manifestations observed in small-cell lung cancer as well as in non-small-cell lung cancer or not defined neoplasms had clinical features of classical and non-classical PNS. An important observation was the association of small-cell lung cancer only with coexisting well-characterized onconeural antibodies (anti-Hu and anti-amphiphysin). In other groups of lung cancer patients, a broad spectrum of antibodies was found. Our study showed a high prevalence of coexisting antibodies, with anti-Hu as the most frequent antibody. This finding is in concordance with the results from other studies. Monstad et al. (2009) in a study on onconeural antibodies in patients with various types of tumors also found anti-Hu as the most frequent antibody (22.5%) in lung cancer. This percentage is higher than that observed in the present study (16%); however, both studies were concerned with different populations of patients. Monstad et al. (2009) selected only small-cell lung cancer subjects. Small-cell lung cancer patients formed the largest group with onconeural antibodies (28.5%) among other malignancies. In that study a spectrum of onconeural antibodies identical to those found in the present study was observed in lung cancer patients and included anti-amphiphysin, anti-Ri and anti-Ma/Ta. Monstad et al. (2009) also found one case with anti-Yo antibodies; the case not observed in our patients. A percentage of coexisting antibodies reported by the authors was similar to that found in the present study, as also were double antibodies in lung cancer patients more frequent than in other types of tumors. Other studies on antibodies in lung cancer patients identified anti-Hu (Graus et al. 1985; Monstad et al. 2004), anti-Ri (Pittock et al. 2003; Knudsen et al. 2006), anti-CV2 (Yu et al. 2001; Monstad et al. 2008), and anti-amphiphysin (Antoine et al. 1999; Pittock et al. 2005). Among other antibodies detected in lung cancer, anti-SOX (Tschernatsch et al. 2010), anti-VGCC (anti-voltage gated calcium channels) (Monstad et al. 2004), anti-AMPA (Lai et al. 2009), anti-GABA (Lancaster et al. 2010), and anti-aquaporin (Pittock and Lennon 2008) were observed. Anti-aquaporin antibodies are currently used for the diagnosis of neuromyelitis optica and their paraneoplastic context has not been widely studied.

In our study one of the patients with the Lambert-Eaton myasthenic syndrome had both anti-Hu and anti-aquaporin antibodies in the course of lung cancer. The prevalence of anti-aquaporin antibodies can be underestimated in clinical settings, because the laboratory tests are not widely used.

In the group of patients with well-characterized antibodies we found a high prevalence of classical PNS. In a study by Monstad et al. (2009), no neurological deficit was observed in small-cell lung cancer patients with onconeural antibodies; however, the authors did not exclude the possibility of minor signs and a limitation of that study was that the patients were not examined by a neurologist. In our study, all patients were examined by a qualified neurologist and neuroimaging, neurophysiological examination or other specific diagnostic procedures were ordered if needed for differential diagnosis.

Among classical PNS, the Lambert-Eaton myasthenic syndrome is strongly associated with lung cancer, as 50–60% of these patients have underlying small-cell lung cancer (O'Neill et al. 1988). Lung cancer has also been identified as the most frequent cause of paraneoplastic limbic encephalitis (Gultekin et al. 2000). Other associations between classical PNS and lung cancer include: paraneoplastic cerebellar degeneration, subacute sensory neuropathy, chronic gastrointestinal pseudo-obstruction, opsoclonus-myoclonus syndrome (Gozzard and Maddison 2010). However, also non-classical PNS manifestations have been reported in the course of lung cancer: brainstem encephalitis, acquired peripheral nerve hyperexcitability syndrome or stiff person syndrome (Gozzard and Maddison 2010). In our study we observed both classical and non-classical PNS, but the strong association between classical PNS and well-characterized onconeural antibodies is particularly noteworthy.

40.5 Conclusions

To conclude paraneoplastic neurological syndromes are associated with majority of lung cancers and may have both classical and non-classical features. In small-cell lung cancer patients only well-characterized onconeural antibodies were identified. In other groups of patients both well-characterized and other autoantibodies were detected as well as coexistance of antibodies was observed. The presence of well-characterized onconeural antibodies is strongly associated with classical features of PNS.

Conflicts of interest: The authors declare no conflicts of interest in relation to this article.

References

Antoine, J. C., Absi, L., Honnorat, J., Boulesteix, J. M., de Brouker, T., Vial, C., Butler, M., De Camilli, P., & Michel, D. (1999). Antiamphiphysin antibodies are associated with various paraneoplastic neurological syndromes and tumors. *Archives of Neurology, 56*, 172–177.

Bernal, F., Graus, F., Pifarre, A., Saiz, A., Benyahia, B., & Ribalta, T. (2002). Immunohistochemical analysis of anti-Hu-associated paraneoplastic encephalomyelitis. *Acta Neuropathologica, 103*, 509–515.

de Graaf, M., de Beukelaar, J., Bergsma, J., Kraan, J., van den Bent, M., Klimek, M., van Norden, Y., Kusuma, A., Smitt, P. S., & Gratama, J. W. (2008). B and T cell imbalances in CSF of patients with Hu-antibody associated PNS. *Journal of Neuroimmunology, 195*, 164–170.

Gozzard, P., & Maddison, P. (2010). Which antibody and which cancer in which paraneoplastic syndromes? *Practical Neurology, 10*, 260–270.

Graus, F., Cordon-Cardo, C., & Posner, J. B. (1985). Neuronal antinuclear antibody in sensory neuronopathy from lung cancer. *Neurology, 35*, 538–543.

Graus, F., Lang, B., & Pozo-Rosich, P. (2002). P/Q type calcium channel antibodies in paraneoplastic cerebellar degeneration with lung cancer. *Neurology, 59*, 764–766.

Graus, F., Delattre, J. Y., Antoine, J. C., Dalmau, J., Giometto, B., Grisold, W., Honnorat, J., Sillevis Smitt, P., Vedeler, Ch, Verschuuren, J. J., Vincent, A., & Voltz, R. (2004). Paraneoplastic Neurological Syndrome Euronetwork.

Recommended diagnostic criteria for paraneoplastic neurological syndromes. *Journal of Neurology Neurosurgery and Psychiatry, 75*, 1135–1140.

Greenlee, J. E., Burns, J. B., Rose, J. W., Jaeckle, K. A., & Clawson, S. (1995). Uptake of systemically administered human anticerebellar antibody by rat Purkinje cells following blood–brain barrier disruption. *Acta Neuropathologica, 89*, 341–345.

Gultekin, S. H., Rosenfield, M. R., Voltz, R., Eichen, J., Posner, J. B., & Dalmau, J. (2000). Paraneoplastic limbic encephalitis: Neurological symptoms, immunological findings and tumour association in 50 patients. *Brain, 7*, 1481–1494.

Knudsen, A., Monstad, S. E., Dorum, A., Lonning, P. E., Salvesen, H. B., Drivsholm, L., Aarseth, J. H., & Vedeler, C. A. (2006). Ri antibodies in patients with breast, ovarian or small cell lung cancer determined by a sensitive immunoprecipitation technique. *Cancer Immunology, Immunotherapy, 55*, 1280–1284.

Lai, M., Hughes, E. G., Peng, X., Zhou, L., Gleichman, A. J., Shu, H., Matà, S., Kremens, D., Vitaliani, R., Geschwind, M. D., & Bataller, L. (2009). AMPA receptor antibodies in limbic encephalitis alter synaptic receptor location. *Annals of Neurology, 65*, 424–434.

Lancaster, E., Lai, M., Peng, X., Hughes, E., Constantinescu, R., Raizer, J., Friedman, D., Skeen, M. B., Grisold, W., Kimura, A., Ohta, K., Iizuka, T., Guzman, M., Graus, F., Moss, S. J., Balice-Gordon, R., & Dalmau, J. (2010). Antibodies to the GABA(B) receptor in limbic encephalitis with seizures: Case series and characterisation of the antigen. *Lancet Neurology, 9*, 67–76.

Michalak, S., Wender, M., & Michalowska-Wender, G. (2006a). Cachexia-induced cerebellar degeneration: Involvement of serum TNF and MCP-1 in the course of experimental neoplastic disease. *Acta Neurobiologiae Experimentalis (Wars), 66*, 113–122.

Michalak, S., Adamczewska-Goncerzewicz, Z., & Szczech, J. (2006b). ATPases and lipid peroxidation in the rat sciatic nerve in the course of experimental neoplastic disease. *Experimental and Molecular Pathology, 8*, 92–99.

Michalak, S., Ambrosius, W., Osztynowicz, K., & Kozubski, W. (2007). ATP-ases activities, lipids and heat shock protein 70 kDa in spinal cord in rats with experimental neoplastic disease. *Research Journal of Medical Science, 1*, 199–208.

Michalak, S., Wender, M., Michalowska-Wender, G., & Kozubski, W. (2010). Blood–brain barrier breakdown and cerebellar degeneration in the course of experimental neoplastic disease. Are circulating cytokine-induced neutrophil chemoattractant-1 (CINC-1) and −2 alpha (CINC-2 alpha) the involved mediators? *Folia Neuropathologica, 48*, 93–103.

Monstad, S. E., Drivsholm, L., Storstein, A., Aarseth, J. H., Haugen, M., Lang, B., Vincent, A., & Vedeler, C. A. (2004). Hu and voltage-gated calcium channel (VGCC) antibodies related to the prognosis of small-cell lung cancer. *Journal of Clinical Oncology, 22*, 795–800.

Monstad, S. E., Drivsholm, L., Skeie, G. O., Aarseth, J. H., & Vedeler, C. A. (2008). CRMP5 antibodies in patients with small-cell lung cancer or thymoma. *Cancer Immunology, Immunotherapy, 57*, 227–232.

Monstad, S. E., Knudsen, A., Salvesen, H. B., Aarseth, J. A., & Vedeler, Ch. A. (2009). Onconeural antibodies in sera from patients with various types of tumours. *Cancer Immunology, Immunotherapy, 58*, 1795–1800.

O'Neill, J. H., Murray, N. M. F., & Newsom-Davis, J. (1988). The Lambert–Eaton myasthenic syndrome. A review of 50 cases. *Brain, 111*, 577–596.

Pittock, S. J., & Lennon, V. A. (2008). Aquaporin-4 autoantibodies in a paraneoplastic context. *Archives of Neurology, 65*, 629–632.

Pittock, S. J., Lucchinetti, C. F., & Lennon, V. A. (2003). Anti-neuronal nuclear autoantibody type 2: Paraneoplastic accompaniments. *Annals of Neurology, 53*, 580–587.

Pittock, S. J., Lucchinetti, C. F., Parisi, J. E., Benarroch, E. E., Mokri, B., Stephan, C. L., Kim, K. K., Kilimann, M. W., & Lennon, V. A. (2005). Amphiphysin autoimmunity: Paraneoplastic accompaniments. *Annals of Neurology, 58*, 96–107.

Tanaka, K., Tanaka, M., Onodera, O., Igarashi, S., Miyatake, T., & Tsuji, S. (1994). Passive transfer and active immunization with the recombinant leucine-zipper (Yo) protein as an attempt to establish an animal model of paraneoplastic cerebellar degeneration. *Journal of Neurological Sciences, 127*, 153–158.

Tschernatsch, M., Singh, P., Gross, O., Gerriets, T., Kneifel, N., Probst, C., Malas, S., Kaps, M., & Blaes, F. (2010). Anti-SOX1 antibodies in patients with paraneoplastic and non-paraneoplastic neuropathy. *Journal of Neuroimmunology, 226*, 177–180.

Yu, Z., Kryzer, T. J., Griesmann, G. E., Kim, K., Benarroch, E. E., & Lennon, V. A. (2001). CRMP-5 neuronal autoantibody: Marker of lung cancer and thymoma-related autoimmunity. *Annals of Neurology, 49*, 146–154.

Chapter 41
Cardiovascular Side Effects of Aminophylline in Meconium-Induced Acute Lung Injury

D. Mokra, I. Tonhajzerova, J. Mokry, M. Petraskova, M. Hutko, and A. Calkovska

Abstract As inflammation plays an important role in the pathogenesis of neonatal meconium aspiration syndrome (MAS), anti-inflammatory agents including inhibitors of phosphodiesterases (PDE) are increasingly used in the treatment. To evaluate side effects of PDE inhibitors, this study analyzed changes in blood pressure, heart rate (HR) and heart rate variability (HRV) during and after intravenous aminophylline in the animal model of MAS. Oxygen-ventilated rabbits were given meconium intratracheally (25 mg/ml, 4 ml/kg) or saline. Thirty minutes later, the animals were treated by intravenous aminophylline (Syntophyllin, 2 mg/kg) or saline (sham-treated controls). A second dose of the treatment was given 2 h later. During (5 min) and immediately after (5 min) the treatment, and during 5 h after the treatment, mean blood pressure in the femoral artery (MAP), HR and HRV were evaluated. In meconium-instilled animals, increases in MABP, HR, and HRV were observed already 5 min after aminophylline administration, while in saline-instilled animals aminophylline increased HR and caused inconsistant changes in HRV parameters compared to sham-treated animals. Within 5 h after the treatment administration, MAP, HR, and HRV parameters gradually returned to the initial values. Concluding, intravenous aminophylline may lead to acute cardiovascular changes. Thus, if aminophylline is used for treatment of MAS, its possible cardiovascular effects should be considered, particularly in patients with cardiovascular instability.

Keywords Meconium • Aspiration • Aminophylline • Phosphodiesterase • Cardiovascular system • Inflammation • Heart rate variability

41.1 Introduction

Meconium aspiration syndrome (MAS) is a serious cause of respiratory insufficiency in the term and post-term newborns. Aspirated meconium may cause airway obstruction, dysfunction of pulmonary surfactant, inflammation, pulmonary vasoconstriction and lung edema. In the treatment of the disease,

D. Mokra (✉) • I. Tonhajzerova • M. Petraskova • M. Hutko • A. Calkovska
Department of Physiology, Jessenius Faculty of Medicine, Comenius University,
Mala Hora 4, Martin SK-03601, Slovakia
e-mail: mokra@jfmed.uniba.sk

J. Mokry
Department of Pharmacology, Jessenius Faculty of Medicine, Comenius University, Martin, Slovakia

M. Pokorski (ed.), *Respiratory Regulation - The Molecular Approach*,
Advances in Experimental Medicine and Biology 756, DOI 10.1007/978-94-007-4549-0_41,

anti-inflammatory agents, e.g., inhibitors of phosphodiesterases have been increasingly used (Shekerdemian et al. 2002; Korhonen et al. 2004; Bassler et al. 2006), besides the use of exogenous surfactant and pulmonary vasodilators (Mokra and Mokry 2010). Although administration of PDE inhibitors may lead to valuable improvement in lung functions, it may be associated with severe cardiovascular effects (Minton and Henry 1996; Fakioglu et al. 2004). Paradoxically, despite a growing use of PDE inhibitors for treatment of MAS, there is no information up to now on their possible side effects on cardiovascular function in MAS. It is also alarming that acute cardiovascular changes caused by the treatment may be critical for meconium-aspirated newborns with cardiovascular instability, who represent a big portion of patients with MAS.

The aim of this pilot study was to investigate an influence of intravenous administration of the non-selective PDE inhibitor aminophylline on cardiovascular functions in saline- and meconium-instilled rabbits during and after aminophylline, and within 5 h after its administration. To assess acute cardiovascular changes, blood pressure in femoral artery, heart rate, and heart rate variability were evaluated.

41.2 Methods

41.2.1 Design of Experiments

The animals used in experiments were cared for in accordance with the Guide for Care and Use of Experimental Animals and the design of experiments was approved by a local Ethics Committee of Jessenius Faculty of Medicine in Martin, Slovakia. Adult rabbits (chinchilla) of 2.5 ± 0.3 kg were anesthetized with intramuscular ketamine (20 mg/kg; Narketan, Vétoquinol, UK) and xylazine (5 mg/kg; Xylariem, Riemser, Germany), followed by continuous infusion of ketamine (20 mg/kg/h). Tracheotomy was performed and catheters were inserted into a femoral artery and the right atrium for blood sampling, and into a femoral vein to administer anesthetics. The animals were then paralyzed with pipecuronium bromide (0.3 mg/kg; Arduan, Gedeon Richter, Hungary) and subjected to pressure-controlled ventilator (Beat-2, Chirana, Slovakia). All animals were ventilated with a frequency of 30/min, fraction of inspired oxygen (FiO_2) of 0.21, inspiration time Ti 50%, peak inspiratory pressure (PIP) to keep a tidal volume (V_T) between 7 and 9 ml/kg and no positive end-expiratory pressure (PEEP) at this stage of experiment.

After stabilization, cardiopulmonary parameters were recorded and the blood gases were analyzed. Then, the rabbits obtained intratracheally 4 ml/kg of suspension of human meconium (Mec; 25 mg/ml) or saline (Sal). From this moment on, the animals were ventilated with FiO_2 1.0 and PEEP 0.3 kPa. In the meconium-instilled animals, respiratory failure developed within 30 min, defined as >30% decrease in dynamic lung-thorax compliance (C_{dyn}) and $PaO_2 < 10$ kPa at FiO_2 1.0. After recording the parameters, 0.5 and 2.5 h after meconium or saline instillation the animals received intravenously two doses of aminophylline (Amin; 2.0 mg/kg each, diluted in saline up to a total volume of 1 ml; Syntophyllin, Hoechst-Biotika, SR) (Mec + Amin group, n = 6, and Sal + Amin group, n = 4) or the same volume of saline (referred to as sham-treated animals; Mec + Sal group, n = 6, and Sal + Sal group, n = 4). Aminophylline or saline was given over a period of 5 min. Immediate cardiovascular changes associated with treatment were evaluated during the 5-min interval of drug administration (A1 for the first dose and A2 for the second dose) and within 5-min post-administration interval (PA1 for the first dose and PA2 for the second dose) (Fig. 41.1). All animals were oxygen-ventilated for additional 5 h after the first dose of treatment and cardiovascular parameters were recorded at 0.5, 1, 2, 3, 4, and 5 h to investigate early effects of the treatment. At the end of experiments, animals were killed by an overdose of anesthetics.

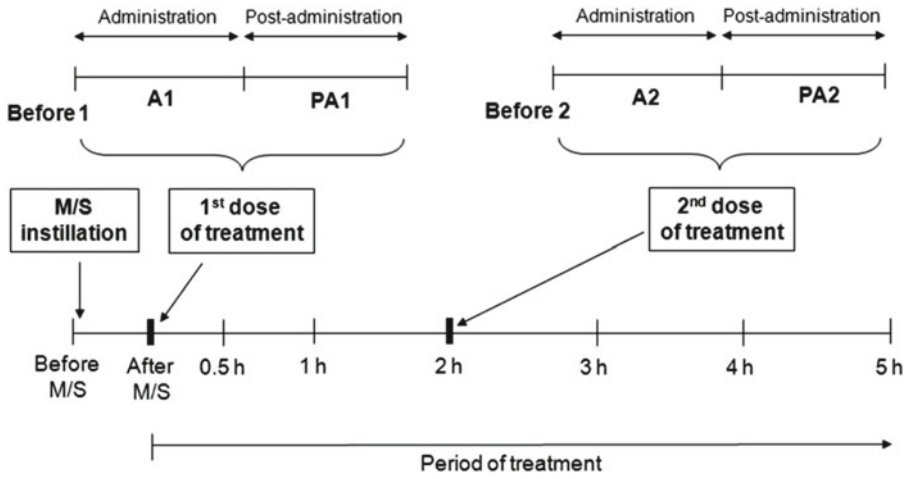

Fig. 41.1 Scheme of treatment administration and measurements during experiments

41.2.2 Evaluations of Cardiopulmonary Parameters

Tracheal airflow and V_T were measured by a Fleisch head connected to a pneumotachograph. Airway pressure was registered *via* a pneumatic catheter placed in the tracheal tube and connected to electromanometer. C_{dyn} was calculated as a ratio between V_T adjusted per kg and airway pressure gradient (PIP-PEEP).

Systolic (SBP) and diastolic (DBP) blood pressures were measured *via* a catheter in the femoral artery connected to electromanometer, and the mean arterial blood pressure (MAP) was calculated as MAP = DP + 1/3 (SP–DP). Heart rate (HR) was obtained from ECG recorded by subcutaneous electrodes.

Heart rate variability (HRV) expressing fluctuations of the heart rate around its average value is a sensitive marker of activity of the autonomic (parasympathetic and sympathetic) control mechanisms of the heart (Moguilevski et al. 1996). HRV was evaluated using computer system (VariaPulse TF3, Sima Media, Czech Republic). Parameter of time analysis, mean squared successive difference (MSSD), and spectral powers in low frequency (LF: 0.05–0.15 Hz) and high frequency (HF: 0.15–2.0 Hz) bands were evaluated.

Data were tested for normality of distribution by Kolmogorov-Smirnov test. Since distribution of some HRV variables (spectral powers) was extremely skewed, logarithmic transformation data was used to improve normality before statistical analysis was performed. Then, between-group differences were analyzed by ANOVA with a *post-hoc* LSD test. Within-group differences were evaluated by a Wilcoxon test. A $p < 0.05$ was considered statistically significant. Data are expressed as means ± SE.

41.3 Results

Body weight and initial values of all cardiopulmonary parameters were comparable between the groups before intratracheal instillation of meconium/saline. Analysis of the 5-min long interval of the first dose of treatment administration (A1) and of the 5-min long interval immediately after the administration (PA1) showed an acute increase in MAP and HR in both aminophylline-treated groups (Mec + Amin and Sal + Amin), while changes in MAP were more obvious in Mec + Amin group and

Table 41.1 Mean arterial blood pressure, heart rate, and heart rate variability parameters before, during (A) and immediately post-administration (P) of the first (1) and second (2) dose of treatment

	Before 1	A1	PA1	Before 2	A2	PA2
Mean arterial blood pressure (MAP, kPa)						
Sal + Sal	8.2 ± 0.8	8.5 ± 0.9	9.0 ± 1.0*	8.8 ± 0.8	8.6 ± 0.9	8.7 ± 0.9
Sal + Amin	7.2 ± 0.2	7.7 ± 0.4	8.5 ± 0.7*	7.3 ± 0.6	7.5 ± 0.8	8.3 ± 0.9
Mec + Sal	8.5 ± 0.7	8.3 ± 0.7	8.3 ± 0.7**	7.5 ± 0.5	7.6 ± 0.5	7.8 ± 0.4*
Mec + Amin	8.0 ± 0.4	9.1 ± 0.8	**11.4 ± 0.8**	8.3 ± 0.8	9.5 ± 1.2	**10.1 ± 1.0**
Heart rate (HR, bpm)						
Sal + Sal	211 ± 11	215 ± 10	210 ± 8*	230 ± 16	230 ± 17	229 ± 17
Sal + Amin	234 ± 17	247 ± 21	**253 ± 17**	255 ± 29	265 ± 31	264 ± 27
Mec + Sal	214 ± 14	212 ± 11	208 ± 10*	232 ± 17	234 ± 16	234 ± 16
Mec + Amin	212 ± 8	226 ± 10	223 ± 9	216 ± 10	227 ± 12	222 ± 19
Log HF (ms^2)						
Sal + Sal	0.4 ± 0.1	0.4 ± 0.2**	0.6 ± 0.1**	0.3 ± 0.3	0.4 ± 0.2	0.5 ± 0.2*
Sal + Amin	**−0.8 ± 0.2**	**−1.7 ± 0.4**	−0.5 ± 0.5***	−0.7 ± 0.8	−0.8 ± 0.6	0.2 ± 0.9**
Mec + Sal	0.7 ± 0.2*	0.3 ± 0.2**	0.4 ± 0.3***	0.5 ± 0.1*	0.4 ± 0.1*	0.9 ± 0.1*
Mec + Amin	0.6 ± 0.5*	0.2 ± 0.3**	**2.4 ± 0.4**	1.1 ± 0.2**	0.7 ± 0.4*	**2.3 ± 0.5**
MSSD (ms^2)						
Sal + Sal	1.8 ± 0.5	1.6 ± 0.7	1.5 ± 0.6***	2.0 ± 0.1	1.9 ± 0.1	1.9 ± 0.1*
Sal + Amin	1.4 ± 0.4	1.3 ± 0.4	1.3 ± 0.1***	1.1 ± 0.7	1.7 ± 0.5	2.3 ± 1.0*
Mec + Sal	2.4 ± 0.5	3.8 ± 0.8	3.0 ± 0.7***	1.5 ± 0.2	2.3 ± 0.4	2.5 ± 0.7*
Mec + Amin	2.5 ± 0.4	5.9 ± 3.1	**8.2 ± 1.2**	1.4 ± 0.8	7.3 ± 1.2	**9.3 ± 1.5**

Mec meconium, *Sal* saline, *Amin* aminophylline, *Log HF* logarithmic expression of spectral power in high frequency band, *MSSD* mean squared successive difference
For Mec + Amin and Sal + Amin (indicated by bold) *vs.* other groups: $^{*}p < 0.05$; $^{**}p < 0.01$; $^{***}p < 0.001$

those in HR more visible in Sal + Amin group. A similar trend to increase MAP and HR was also observed during and after administration of the second dose of treatment (intervals A2 and PA2) 2 h later (Table 41.1).

Together with increases in MAP and HR we observed an increase in the two selected parameters of HRV: logarithmic expression of spectral power in high frequency band (log HF) and mean squared successive difference (MSSD), which are markers of vagal (parasympathetic) regulation of heart activity. Both of them increased already during, and particularly 5 min after administration of aminophylline, explicitely in the meconium-instilled animals (Table 41.1). At the end of experiments, the values of MAP, HR, and HRV gradually returned to the levels comparable with the sham-treated controls (Table 41.2).

41.4 Discussion

Treatment with anti-inflammatory drugs, e.g., inhibitors of phosphodiesterases (PDE), may be associated with serious adverse effects. This study was performed to evaluate short-term cardiovascular effects of non-selective PDE inhibitor aminophylline in the condition of experimental MAS. The results showed that intravenous administration of aminophylline may lead to acute increase in blood pressure, heart rate, and heart rate variability.

Aminophylline is a mixture of theophylline and ethylenediamine, improving theophylline water-solubility. Aminophylline as a representant of methylxanthines acts as a non-selective PDE inhibitor increasing cAMP and cGMP and decreasing concentrations of intracellular calcium, acetylcholine,

Table 41.2 Mean arterial blood pressure, heart rate, and heart rate variability parameters before and after intratracheal meconium/saline (M/S) instillation and hourly after treatment administration

	Before M/S	After M/S	1 h	3 h	5 h
Mean arterial blood pressure (MAP, kPa)					
Sal + Sal	9.6 ± 0.5	9.4 ± 0.6	9.4 ± 0.8	9.9 ± 0.4*	10.4 ± 0.7
Sal + Amin	9.4 ± 0.3	8.4 ± 0.4	8.4 ± 1.0	**7.6 ± 0.8**	9.0 ± 1.4
Mec + Sal	8.9 ± 0.2	9.2 ± 0.6	9.4 ± 0.6	8.8 ± 0.5	8.9 ± 0.8
Mec + Amin	9.3 ± 0.4	8.9 ± 0.7	10.0 ± 0.7	9.1 ± 0.8	9.6 ± 0.5
Heart rate (HR, bpm)					
Sal + Sal	200 ± 11	213 ± 8	214 ± 6*	233 ± 13	242 ± 12
Sal + Amin	207 ± 13	222 ± 17	**255 ± 27**	267 ± 29	260 ± 21
Mec + Sal	201 ± 7	206 ± 7	208 ± 6*	234 ± 8	244 ± 11
Mec + Amin	191 ± 16	207 ± 10	229 ± 21	234 ± 21	247 ± 24
Log HF (ms^2)					
Sal + Sal	−0.51 ± 0.22	−0.23 ± 0.39	−0.41 ± 0.66*	0.06 ± 0.14*	−0.49 ± 0.37
Sal + Amin	−0.04 ± 1.20	−0.69 ± 0.42	−0.65 ± 0.74*	−0.76 ± 0.76**	−0.16 ± 0.63
Mec + Sal	−0.30 ± 0.22	−0.32 ± 0.32	0.09 ± 0.29*	−0.01 ± 0.30**	0.21 ± 0.41
Mec + Amin	−0.17 ± 0.16	−0.55 ± 0.34	**1.13 ± 0.23**	**1.43 ± 0.16**	0.65 ± 0.36
MSSD (ms^2)					
Sal + Sal	2.93 ± 0.76	1.44 ± 0.32	1.42 ± 0.46*	1.48 ± 0.34***	1.50 ± 0.29
Sal + Amin	3.26 ± 1.10	1.44 ± 0.35	3.51 ± 1.96	1.24 ± 0.48***	3.46 ± 2.38
Mec + Sal	2.84 ± 0.41	1.91 ± 0.41	1.79 ± 0.40*	1.12 ± 0.16***	1.93 ± 0.61
Mec + Amin	3.01 ± 0.73	2.03 ± 0.76	**5.87 ± 1.94**	**5.52 ± 1.52**	3.80 ± 2.18

Mec meconium, *Sal* saline, *Amin* aminophylline, *Log HF* logarithmic expression of spectral power in high frequency band, *MSSD*: mean squared successive difference

For Mec + Amin and Sal + Amin (indicated by bold) *vs.* other groups: *$p < 0.05$; **$p < 0.01$; ***$p < 0.001$

and monoamines, which results in bronchodilation and vasodilation, and several other anti-inflammatory effects. In addition, aminophylline acts also as a competitive antagonist of adenosine receptors and some actions, e.g., bronchodilation, are mediated also through these mechanisms (Barnes 2003; Salari et al. 2005).

Besides therapeutic effects, cardiovascular effects of aminophylline such as tachycardia, hypertension, and generation of extrasystoles were described previously (Gilman et al. 1990; Marks et al. 1999). In our study, intravenous administration of aminophylline increased arterial blood pressure, heart rate, and HRV; the last effect concerned predominantly parasympathetic activity. These changes were observed in meconium-instilled rabbits already during the time of aminophyline administration, but they were even more expressed immediately after completion of administration, while increased HRV lasted for several hours after administration of the first dose of aminophylline. Similar results were previously found also in ventilated newborns with severe RDS (Kibblewhite and Sleigh 1996), where i.v. aminophylline increased heart rate and some parameters of HRV, particularly the spectral power in HF band. Administration of aminophylline increased heart rate and cardiac output and influenced vascular resistance also in various animal models (Spalding et al. 2000; Takahashi et al. 2000). We may presume that some of cardiovascular effects may be caused by inhibition of PDE, as increase of cAMP in smooth muscle cells and myocardium shows positive chronotropic and inotropic effects (Mirossay and Mojzis 2006). In addition, theophylline increases levels of circulating catecholamines (Hirota et al. 2001; Barnes 2005). On the other side, changes in HRV and generation of arrhythmias may also be caused by antagonism with adenosine receptors (Barnes 2003). Agonists of A_1 adenosine receptors decrease heart rate and blood pressure *via* A_1 receptors in the periphery; however, little is known on the participation of central A_1 receptors in this action. Little also is known about A_{2A} receptors, where agonists of A_{2A} receptors increase the heart rate (Schindler et al. 2005).

Considering cardiovascular effects of aminophylline, an interesting finding is its different action in meconium-instilled *vs*. saline-instilled (i.e., healthy) animals. Stronger effects on the blood pressure and heart rate variability in animals with MAS and, on the other hand, a stronger effect on heart rate in saline-instilled controls may indicate a contribution of various substances, mediators and possibly also of ROS released during inflammation and hypoxemia in the processes of cardiovascular regulation (Hoover et al. 2000; Malave et al. 2003; Murray 2003). Similarly, higher cardiovascular responsibility to intravenous dexamethasone was previously observed in meconium- than in saline-instilled animals (Mokra et al. 2008).

In conclusion, intravenous administration of aminophylline increased blood pressure, heart rate, and heart rate variability in meconium-instilled rabbits during and immediately after the drug administration, while changes in HRV were observed for hours after aminophylline treatment. Therefore, possible acute cardiovascular effects of aminophylline should be kept in mind when aminophylline is considered to be used for treatment of MAS, particularly in patients with cardiovascular instability.

Acknowledgments Authors thank D. Kuliskova and J. Neuschlova for technical assistance. Study was supported by Project "Center of Excellence in Perinatology Research (CEPV II)"No. 26220120036, co-financed from EU sources.

Conflicts of interest: The authors declare no conflicts of interest in relation to this article.

References

Barnes, P. J. (2003). Theophylline. New perspectives for an old drug. *American Journal of Respiratory and Critical Care Medicine, 167*, 813–818.

Barnes, P. J. (2005). Theophylline in chronic obstructive pulmonary disease. New horizons. *Proceedings of the American Thoracic Society, 2*, 334–339.

Bassler, D., Choong, K., McNamara, P., & Kirpalani, H. (2006). Neonatal persistent pulmonary hypertension treated with milrinone: Four case report. *Biology of the Neonate, 89*, 1–5.

Fakioglu, H., Gelvez, J., Torbati, D., Glover, M. L., Olarte, J. L., Camacho, M. T., & Wolfsdorf, J. (2004). Aminophylline therapy during endotoxemia in anesthetized spontaneously breathing rats. *Pharmaceutical Research, 49*, 45–50.

Gilman, A. G., Rall, T. W., Nies, A. S., & Taylor, P. (Eds.). (1990). *Goodman and Gilman's the pharmacological basis of therapeutics* (Vol. 8, p. 625). New York: Pergamon Press.

Hirota, K., Yoshioka, H., Kabara, S., Kudo, T., Ishihara, H., & Matsuki, A. (2001). A comparison of the relaxant effects of olprinone and aminophylline on methacholine-induced bronchoconstriction in dogs. *Anesthesia and Analgesia, 93*, 230–233.

Hoover, D. B., Chang, Y., Hancock, J. C., & Zhang, L. (2000). Actions of tachykinins within the heart and their relevance to cardiovascular disease. *Japanese Journal of Pharmacology, 84*, 367–373.

Kibblewhite, D. P., & Sleigh, J. W. (1996). Heart rate variability in premature neonates pre- and postmethylxanthine administration. *Paediatric Anaesthesia, 6*, 399–403.

Korhonen, K., Kiuru, A., Svedstrom, E., & Kaapa, P. (2004). Pentoxyfylline reduces regional inflammatory and ventilatory disturbances in meconium-exposed piglet lungs. *Pediatric Research, 56*, 901–906.

Malave, H. A., Taylor, A. A., Nattama, J., Deswal, A., & Mann, D. L. (2003). Circulating levels of tumor necrosis factor correlate with indexes of depressed heart rate variability. A study in patients with mild-to-moderate heart failure. *Chest, 123*, 716–724.

Marks, B. L., Katz, L. M., Haky, J. E., Foss, W. M., & Torok, D. J. (1999). Spectral analysis of heart rate variability and pulmonary responses to topical applications of a 2% aminophylline-based thigh cream. *International Journal of Obesity, 23*, 198–202.

Minton, N. A., & Henry, J. A. (1996). Acute and chronic human toxicity of theophylline. *Human and Experimental Toxicology, 15*, 471–481.

Mirossay, L., & Mojzis, J. (2006). *Basic pharmacology and pharmacotherapy* (Vol. 1, p. 535). Kosice: Equilibria. in Slovakian.

Moguilevski, V. A., Shiel, L., Oliver, J., & McGrath, B. P. (1996). Power spectral analysis of heart-rate variability reflects the level of cardiac autonomic activity in rabbits. *Journal of the Autonomic Nervous System, 58*, 18–24.

Mokra, D., & Mokry, J. (2010). *Meconium aspiration syndrome: From pathomechanisms to treatment* (Vol. 1, p. 130). New York: Nova Science Publishers.

Mokra, D., Tonhajzerova, I., Mokry, J., Drgova, A., Petraskova, M., Calkovska, A., & Javorka, K. (2008). Rapid cardiovascular effects of dexamethasone in rabbits with meconium-induced acute lung injury. *Canadian Journal of Physiology and Pharmacology, 86*(11), 804–814.

Murray, D. R. (2003). What is "heart rate variability" and is it blunted by tumor necrosis factor? *Chest, 123*, 664–667.

Salari, P., Mojtahedzadeh, M., Najafi, A., Sadraie, S., Bahaadini, K., Moharreri, M., Hadavand, N., & Abdollahi, M. (2005). Comparison of the effect of aminophylline and low PEEP vs. high PEEP on EGF concentration in critically ill patients with ALI/ARDS. *Journal of Clinical Pharmacy Therapeutics, 30*, 139–144.

Schindler, C. W., Karcz-Kubicha, M., Thorndike, E. B., Muller, C. E., Tella, S. R., Ferre, S., & Goldberg, S. R. (2005). Role of central and peripheral adenosine receptors in the cardiovascular responses to intraperitoneal injections of adenosine A1 and A2A subtype receptor agonists. *British Journal of Pharmacology, 144*, 642–650.

Shekerdemian, L. S., Ravn, H. B., & Penny, D. J. (2002). Intravenous sildenafil lowers pulmonary vascular resistance in a model of neonatal pulmonary hypertension. *American Journal of Respiratory and Critical Care Medicine, 165*, 1098–1102.

Spalding, M. B., Ala-Kokko, T. I., Kiviluoma, K., Ruskoaho, H., & Alahuhta, S. (2000). The effect of aminophylline on right heart function in young pigs after ligation of the right coronary artery. *Pharmacology and Toxicology, 86*, 192–194.

Takahashi, S., Fujii, Y., Hoshi, T., Inomata, S., Miyabe, M., & Toyooka, H. (2000). Modifications of the hemodynamic consequences of theophylline intoxication with landiolol in halothane-anesthetized dogs. *Canadian Journal of Anaesthesia, 47*, 265–272.

Chapter 42
Proteomic Analysis of the Carotid Body: A Preliminary Study

C. Di Giulio, S. Angelucci, C. Di Ilio, E. Eleuterio, F. Di Giuseppe, M. Sulpizio, V. Verratti, M. Pecyna, and M. Pokorski

Abstract We present a proteomic analysis of the rat carotid body (CB) preparation by comparison between normoxia and hypoxia. Proteomic investigation would be helpful to identify the stress-induced protein during hypoxia and to know what O_2 species are being sensed by CB cells. Adult Wistar rats were used, one group was kept in room air (21% O_2) as control, and the other was kept in a Plexiglas chamber for 12 days in chronic hypoxia (10–11% inspired oxygen). A total protein extract for each lysated tissue was separated using a broad pH range no-linear IPG strip (3–10) and the second dimension was performed on a 9–16% polyacrylamide gel. Exposure to hypoxia for 12 days produced significant changes in protein expression, providing an initial insight into the mechanism underlying differences in susceptibility to hypoxia. Further investigation is needed to have an overview of the specific set of proteins present in the CB and the functions of such proteins in signal transduction and adaptation during hypoxia.

Keywords Carotid body • Chemoreceptor • Chronic hypoxia • Proteomics • Signal transduction

42.1 Introduction

Cellular PO_2 is maintained within a narrow range in mammals by transportation of O_2 by ventilation and circulation to cells, for which O_2 sensing and supply must be strategically controlled. Although O_2 is sensed by almost all cells, the most efficient and timely sensing takes place in the carotid body (CB), for the global benefit of the rest of the body. CB is localized close to the heart and chemoreceptor cells sense O_2 with each inspiration in a few seconds, so that the signal can

C. Di Giulio (✉) • V. Verratti
Department of Neurosciences and Imaging, University of Chieti, Via dei Vestini 31, 66100 Chieti, Italy
e-mail: digiulio@unich.it

S. Angelucci • C. Di Ilio • E. Eleuterio • F. Di Giuseppe • M. Sulpizio
Department of Biomedical Science, University of Chieti, Via dei Vestini 31, 66100 Chieti, Italy

M. Pecyna
Faculty of Pedagogics, The Academy of Management and Administration,
Ozimska 63 St., 45-368 Opole, Poland

M. Pokorski (✉)
Department of Respiratory Research, Medical Research Center,
Polish Academy of Sciences, Pawinskiego 5, 02-106 Warsaw, Poland

M. Pokorski (ed.), *Respiratory Regulation - The Molecular Approach*,
Advances in Experimental Medicine and Biology 756, DOI 10.1007/978-94-007-4549-0_42,

be carried nearly instantaneously by chemoreceptor afferents to the brain. The respiratory and cardiovascular brainstem regions evoke reflex responses in a feedback manner by the next inspiration, so that expiration eliminates CO_2 and O_2 is taken up according to the current metabolic needs (Barnard et al. 1987). This feedback control system operates breath by breath to sustain the life. Oxygen tension affects a series of physiological functions, influencing the expression of several enzymes. In some tissue, hypoxia inhibits enzymatic activity and in others it increases it. This apparent dual-effect is related to the oxygen tension and the response is influenced acutely or chronically by the processes of enzyme synthesis and degradation. At the molecular level, cellular responses to chronic cellular hypoxia involve, besides reduced enzymatic activity, changes in DNA-protein interaction leading to alterations in gene expression (Bunn and Poyton 1996; Kietzman et al. 2000). The regulation of the genes encoding proteins depends upon accurate sensing of PO_2 and transduction of the signal that actives hypoxia inducible factor-1 (HIF-1), a heterodimeric protein composed of α and β subunits. HIF-1α is the key protein regulating cellular responses to hypoxia (Lahiri et al. 2007). It is a factor that controls the induction of genes involved in glycolysis, erythropoiesis, angiogenesis, and vasodilatation when tissues are exposed to hypoxic conditions (Prabhakar and Overholt 2000; Lopez-Barneo et al. 2001).

At the plasma membrane, O_2 sensing takes place instantaneously involving ion channels and heme proteins (Wenger and Bauer 2000; Lahiri et al. 2002). The newly formed HIF will be stabilized in hypoxia and then it will dimerize with HIF-β subunit, which presents independently of the PO_2, to form a complex that moves into the nucleus (Semenza 2001). The hypotheses concerning the mechanisms of sensitivity to low oxygen concentration are many; some authors propose a mechanism linked to a hypothetical heme protein 'sensor' located in the plasma membrane, others put forward 'acid hypothesis' which suggests a role of the membrane hydrogen ion pump acting in concert with changing oxygen levels, still others turn to the hypothesis of a metabolic sensor related to changes in the intracellular ATP levels, increased Ca^{2+} influx, and consequently also chemosensory discharge which is relayed to the brain. Although the chromophore theory of chemoreception still remains valid, alterations in the sensor structure could be affected by HIF-1α, VEGF, and NOS-1. Proteomic identification of novel proteins for studying the interaction between pathways involving increased metabolism and induction of stress-induced proteins in response to chronic or intermittent hypoxia will help clarify how chronic hypoxia *per se* promotes a remodelling of the structure and function of the cardio-respiratory system, the brain, and other organs. Cell growth, differentiation, aging, and death are, in general, related to a series of factors including oxygen consumption. Therefore, in the present study we investigated the effects of 12-day exposure to chronic hypoxia on carotid body protein pattern. We reasoned that proteomic analysis could give a fresh insight into the pathways sensing changes in oxygen and could help resolve, still enigmatic, carotid body mechanisms engaged in the adaptation to hypoxia.

42.2 Methods

42.2.1 Hypoxic Treatment

Two groups of Wistar rats weighting 250–400 g were used, according to the guidelines of the Declaration of Helsinki. The study protocol was accepted by a local Ethics Committee. One group (four rats) was kept in room air (21% O_2) as a control group; the other was kept in a Plexiglas chamber for 12 days in chronic hypoxia (10–12% inspired oxygen). The chamber was recirculated with a pump; CO_2 was removed from the chamber air with baralyme and continuously monitored by a capnograph. Boric acid was mixed with the litter to minimize the emission of urinary ammonia.

42.2.2 Proteomic Analysis

The total protein extract for each lysated tissue were separated using a broad pH range no linear IPG strip (3–10) and the second dimension was performed on a 9–16% polyacrylamide gel (Angelucci et al. 2006, 2010). The lysated samples were loaded onto commercial 4–7 IPG strip and the second dimension was performed on a 9–16% acrylamide gel. Analytical gels were stained with ammoniacal silver nitrate, while gels used for MALDI-TOF MS protein identification were silver-stained without glutaraldehyde. After staining, gels were scanned with a MagicScan scanner (GE Healthcare, formerly Amersham Biotech, Uppsala, Sweden) in transparency mode at 800 dpi and the TIFF images were stored. Once digitized, the gel images were analyzed with Image Master 2D platinum software, 6.0 versions (GE Healthcare, formerly Amersham Biotech, Uppsala, Sweden). A positional gel calibration was carried out by using a 2D calibration method included in the analysis package that calculates the position of protein spots in terms of their isoelectric point (pI) and molecular weight (MW) values. On average, 67 and 45 protein spots were detected for normoxia and hypoxia samples, respectively. The quantity of each spot was normalized with respect to the total spot volume detected in the gel. Relative spot volumes were determined by modeling the optical density in individual spot segments using a two-dimensional Gaussian analysis (Angelucci et al. 2010).

42.3 Results

Exposure to hypoxia for 12 days produced significant changes in the expression of proteins, providing an initial insight into the mechanisms underlying differences in susceptibility to hypoxia at different age. These results indicate that proteins involved in the glycolytic pathway are down-regulated, whereas glycolytic enzymes and deaminases involved in ATP and AMP production were up-regulated by ~50%. This would be consistent with recent reports that protein synthesis plays a crucial role in modulating the phosphorylation of pyruvate dehydrogenase, inactivating it and blocking mitochondrial activity, and thus preserving cells from ROS damage and consequent apoptosis. Hypoxia also down-regulated other enzymes involved in protein synthesis. The results of our quantitative analysis showed that exposure to hypoxia for 12 days produced more than 1.5-fold increases in the expression of 10/70 protein and decreases of 16/70 protein.

42.4 Discussion

The oxygen-gradient diffusion at the capillary tissue level is essential for the cellular survival (Chandel and Schumaker 2000). Maintenance of oxygen homeostasis in the arterial blood is mediated by reflexes sensitive to oxygen decrease and by release of several factors. The CBs are the sensory organs to detect systemic hypoxia. These minute organs respond in a few second time required for an initial transduction step involving the O_2 sensor and changing protein content or activity. Chronic hypoxia stimulates cellular growth and metabolism; CBs show hypertrophy of type I cells, increase in catecholamine synthesis, and decreases in density of K^+ ion channels.

The regulation of genes encoding proteins depends upon accurate sensing of PO_2 and activation HIF that is a key protein regulating cellular responses to hypoxia (Semenza 2009). HIF regulates several genes including endothelin (ET-1) and VEGF. To better understand chemoreception we need to know what O_2 species are being sensed by cells and how cells sense oxygen. It would be helpful to have an overview of the specific set of proteins present in the CB and the functions of

such proteins in signal transduction and adaptation during hypoxia. Chemosensitive cells located in the CB play a fundamental role for the survival in hypoxic conditions; their stimulation increases discharge frequency in the afferents fibers running to the brainstem respiratory network, leading to an increase in ventilation. The mechanisms of responses to acute and chronic hypoxia are not necessarily the same. Chronic effects involve new syntheses of proteins initiated by some specific mechanisms. During chronic hypoxia, ventilatory adaptation is a homeostatic reaction that tends to compensate the hypoxia. The resulting immediate hyperventilation seems to involve both peripheral and central mechanism. During altitude acclimatization period, ventilation tends to return to the basal value, the increase in ventilation persist for weeks and tends to adapt with time. This phenomenon has also been seen in patients suffering from cyanotic congenital heart diseases or lung disease with a reduction of the hypoxic ventilatory response. The attenuated ventilatory response during chronic hypoxia is a useful process to reduce the energy cost necessary to maintain hyperventilation trough carotid body modifications.

Chronic hypoxia, a common link of many illnesses, induces adaptations in the tissues geometry. In particular, the structure of the CB modifies in chronic hypoxia and with age due to an increase in the extracellular matrix, alterations in the volume of mitochondria, and rearrangements of intracellular organelles (Di Giulio et al. 2009). During chronic hypoxia, CB hypertrophy is less evident in the aged than young CB, which is probably related to a reduced release of growth factors during aging (Di Giulio et al. 2003). Furthermore, such a reduction in hypertrophy could be due to general protein structural changes occurring during aging.

The body reacts to hypoxia by NO-modulated HIF-1α-mediated expression of hypoxia-inducible genes to maintain an adequate O_2 flux to tissues and to optimize metabolic processes. Introducing a proteomic approach (Jin et al. 2004) to study the functional significance of the regulation of protein synthesis in the adaptation to hypoxia would help clarify the way of prevention of tissue damage resulting from ROS and would optimize metabolic control; in effect making active life possible even in extreme conditions. The present results may also have a bearing on human physiopathology, particularly on aging. During chronic hypoxia, NOS activity increases, and nitric oxide-mediated inhibition of chemosensory discharge would take part in the mitigation of the ventilatory adaptation to hypoxia. Moreover, chronic hypoxia increases neuroglobin (Ngb) in CB (Di Giulio et al. 2006). The physiological role of Ngb is not well understood, but the protein is thought to participate in such processes as oxygen transport, oxygen storage, and nitric oxide detoxification. Similar to hemoglobin, Ngb may act as a respiratory protein by reversibly binding gaseous ligands (NO and O_2) *via* the Fe-containing porphyrin ring. Proteomics seems to open a new valuable avenue of research to elucidate the oxygen sensitive molecular mechanisms.

Acknowledgments This paper is dedicated to the memory of Prof. Sukhamay Lahiri, for his example in science and in life.

Conflicts of interest: The authors declare no conflicts of interest in relation to this article.

References

Angelucci, S., Ciavardelli, D., Di Giuseppe, F., Eleuterio, E., Sulpizio, M., Tiboni, G. M., Giampietro, F., Palombo, P., & Di Ilio, C. (2006). Proteome analysis of human follicular fluid. *Biochimica et Biophysica Acta, 11*(1764), 1775–1785.

Angelucci, S., Marchisio, M., Di Giuseppe, F., Pierdomenico, L., Sul pizio, M., Eleuterio, E., Lanuti, P., Sabatino, G., Miscia, S., & Di Ilio, C. (2010). Proteome analysis of human Wharton's jelly cells during *in vitro* expansion. *Proteome Science, 26*, 8–18.

Barnard, P., Andronikou, S., Pokorski, M., Smatresk, N., Mokashi, A., & Lahiri, S. (1987). Time-dependent effect of hypoxia on carotid body chemosensory function. *Journal of Applied Physiology, 63*, 685–691.

Bunn, A. F., & Poyton, R. O. (1996). Oxygen sensing and molecular adaptation to hypoxia. *Physiological Reviews, 76*, 839–885.

Chandel, N. S., & Schumaker, P. T. (2000). Cellular oxygen sensing mechanisms: Old questions, new insight. *Journal of Applied Physiology, 88*, 1880–1889.

Di Giulio, C., Cacchio, M., Bianchi, G., Rapino, C., & Di Ilio, C. (2003). Carotid body as a model for aging studies: Is there a link between oxygen and aging? *Journal of Applied Physiology, 95*, 1755–1758.

Di Giulio, C., Bianchi, G., Cacchio, M., Artese, L., Piccirilli, M., Verratti, V., Valerio, R., & Iturriaga, R. (2006). Neuroglobin, a new oxygen binding protein is present in the carotid body and increases after chronic intermittent hypoxia. *Advances in Experimental Medicine and Biology, 580*, 15–19.

Di Giulio, C., Antosiewicz, J., Walski, M., Petruccelli, G., Verratti, V., Bianchi, G., & Pokorski, M. (2009). Physiological carotid body denervation during aging. *Advances in Experimental Medicine and Biology, 648*, 257–263.

Jin, K., Mao, X. O., & Greenberg, D. A. (2004). Proteomic analysis of neural hypoxia in vitro. *Neurochemical Research, 29*, 1123–1128.

Kietzman, T., Fandrey, J., & Acker, H. (2000). Oxygen radicals as messengers in oxygen-dependent gene expression. *News in Physiological Sciences, 15*, 2202–2209.

Lahiri, S., Di Giulio, C., & Roy, A. (2002). Lesson from chronic intermittent and sustained hypoxia. *Respiratory Physiology & Neurobiology, 130*, 223–233.

Lahiri, S., Antosiewicz, J., & Pokorski, M. (2007). A common oxygen sensor regulates the sensory discharge and globes cell HIF-1α in the rat carotid body. *Journal of Physiology and Pharmacology, 58*(Suppl.5), 327–334.

Lopez-Barneo, J., Pardal, R., & Ortega-Sanez, P. (2001). Cellular mechanisms of oxygen sensing. *Annual Review of Physiology, 63*, 259–287.

Prabhakar, N. R., & Overholt, J. L. (2000). Cellular mechanisms of oxygen sensing at the carotid body: Heme proteins and ion channels. *Respiration Physiology, 122*, 209–221.

Semenza, G. L. (2001). HIF-1 O_2 and the 3 PHDs: How animal cells signal hypoxia to the nucleus. *Cell, 107*, 1–3.

Semenza, G. L. (2009). Regulation of oxygen homeostasis by hypoxia-inducible factor-1. *Physiology, 24*, 97–106.

Wenger, R. H., & Bauer, C. (2000). Oxygen sensing: 'Hydroxy' translates 'oxy'. *News in Physiological Sciences, 15*, 195–196.

Chapter 43
Effects of Body Positions on Respiratory Muscle Activation During Maximal Inspiratory Maneuvers

M.O. Segizbaeva, M.A. Pogodin, and N.P. Aleksandrova

Abstract We evaluated the maximal mouth inspiratory pressure and the EMG patterns of major respiratory and accessory muscles used in the generation of voluntary inspiratory maneuvers during different body positions. Ten healthy subjects (F/M-4/6), the mean age 22.0 ± 0.6 years, participated in the study. The maximal inspiratory mouth pressure (MIP) during Müller's maneuver was measured from residual volume in the standing, sitting, right-sided (RSL) and left-sided lying (LSL), supine, and head-down-tilt (HDT) (−30° relatively horizon) positions. EMG of the diaphragmatic (D), parasternal (PS), sternocleidomastoid (SM), and genioglossus (GG) muscles were assessed in each body position. The baseline MIP was 105.3 ± 12.0 in men and 59.9 ± 10.1 cmH_2O in women in the standing position and did not appreciable differ in the other positions, except the HDT where it was lower by 23 and 27% in men and women, respectively ($P < 0.05$). During Müller's maneuver, diaphragmatic EMG activity also was similar in all the body positions, but it was significantly enhanced in the HDT. In contrast, PS EMG showed the highest level of activation in the standing position, taken as the control, reference level, and was lower in the HDT. Activation of SM during the maneuver was near the control in the sitting position, lower in the supine (79%), RSL (85%), LSL (80%), and HDT (72%) positions ($P < 0.05$). GG EMG was significantly greater during maximal inspiratory effort in the supine and HDT positions (125 and 130%, respectively), while it was lower in the sitting, LRS, and LLS positions (76, 57, and 43%) compared with standing ($P < 0.05$). We conclude that the inspiratory pressure generated during Müller's maneuver is a reflection of complex interactions between several muscle groups during changes in body positions.

Keywords Body position • EMG • Inspiratory pressure • Respiratory muscles • Müller's maneuver

43.1 Introduction

The function of inspiratory muscles is to create a negative pressure in the thorax, and the most widely used measure of inspiratory muscle strength is the pressure generated in the mouth during a maximal voluntary maneuver (Black and Hyatt 1969; Enright et al. 1994). Maximal inspiratory mouth pressure (MIP or P_{Imax}) is a simple and noninvasive index of inspiratory muscle strength (ATS/ERS Statement 2002).

M.O. Segizbaeva (✉) • M.A. Pogodin • N.P. Aleksandrova
Laboratory of Respiration Physiology, I.P. Pavlov Institute of Physiology RAN, St. Petersburg, Russia
e-mail: marina@infran.ru

M. Pokorski (ed.), *Respiratory Regulation - The Molecular Approach*,
Advances in Experimental Medicine and Biology 756, DOI 10.1007/978-94-007-4549-0_43,

The measurement of respiratory muscle force is important in the diagnosis of respiratory muscle weakness or dysfunction and in the evaluation of therapeutic effects (Troosters et al. 2005; Decramer et al. 1994; Lagri and Tobin 2003). The pressure generated depends on the age, sex and body mass index (Black and Hyatt 1969; Sachs et al. 2009; Evans and Whitelaw 2009) in healthy subjects and on lung function parameters and blood gas tensions in COPD patients (Heijdra et al. 1994). Mechanical factors such as the lung volume at which maximal inspiratory efforts are performed, and the velocity of shortening of muscles may influence MIP (Nava et al. 1993). It is possible to influence the length of inspiratory muscles in normal subjects by changing position from standing to sitting, supine, and especially the head-down tilt. The diaphragm will then be displaced upwards by the abdominal content, and will achieve a more advantageous position on the length-tension curve. The relationship between the force generated by different respiratory muscles and their activity may change during inspiratory efforts performed during different body positions, resulting from specific recruitment patterns of respiratory muscles. The relative contribution of different muscles to the generation of maximal inspiratory effort (Müller's maneuver) and their electrical activity during this voluntary maneuver in different body positions has not been fully investigated.

The objectives of the present study were to evaluate the effect of body position on maximal inspiratory pressure and to determine the relative activity and pattern of recruitment of four major inspiratory and accessory muscles: diaphragm, parasternal, sternocleidomastoid, and genioglossus in healthy subjects.

43.2 Methods

43.2.1 Subjects

The study was approved by a local Ethics Committee and conducted in accordance with the ethical standards of the Helsinki Declaration for Human Experimentation. All subjects were familiarized with the experimental procedures, and gave informed consent. Ten healthy, nonsmoking subjects (F/M-4/6) participated in the study. Their mean age was 22.0 ± 0.6 years, Anthropometric data for men: height 172.1 ± 4.2 cm, weight 72.6 ± 3.5 kg, vital capacity (VC) 4.2 ± 0.5 l and for women: height 163.2 ± 2.4 cm, weight 52.1 ± 2.3 kg, VC 3.5 ± 0.6 l. All of them had no cardiorespiratory and neuromuscular disorders and had ventilatory function within normal limits. None of the subjects had a previous experience in performing the maximal inspiratory maneuver nor were aware of the aims of the study.

43.2.2 Maximal Inspiratory Pressure Measurements

Maximal inspiratory mouth pressure (MIP) was measured with a portable device (PowerBreath, UK) in accordance with ATS/ERS Statement (ATS/ERS Statement 2002). MIP was recorded at the mouth during a quasi-state short maximal inspiration against occluded airways (Müller's maneuver). The maneuver was performed at residual volume (RV) (Troosters et al. 2005). The subjects had a nose clip in place during the maneuver. Each participant was instructed to expire slowly and completely as far as possible, to seal lips firmly around the mouthpiece and then to perform a maximal inspiratory effort. The subjects were verbally encouraged by the operators to achieve a maximal effort. To prevent closure of the glottis and to avoid significant pressure generation by the muscles of the cheek and buccal muscles, a small leak was present in the equipment. The pressure obtained reflects the pressure generated only by the respiratory muscles (ATS/ERS Statement 2002; Troosters et al. 2005). For the sake of convenience, MIP was expressed in positive values.

43.2.3 EMG Recording

The electromyograms (EMG) of the diaphragm (EDI), parasternal (EPS), sternocleidomastoid (ESM), and genioglossus (EGG) were obtained with surface electrocardiographic electrodes (ARBO, TYCO Healthcare Group LP, Germany). The skin was cleaned with an abrasive. The surface EDI was recorded by electrodes applied to the skin over the seventh and eighth intercostal spaces close to the upper rib edge. The EMG of the stemocleidomastoid (ESM) was obtained with electrodes positioned longitudinally over the middle third of the muscle on the right side of the neck, while the parasternal muscle EMG (EPS) was recorded with electrodes placed in the second right intercostal space close to the sternum. The EMG of the genioglossus (EGG) was obtained from two electrodes placed longitudinally on the underside of the chin at 5 and 10 mm from the inferior margin of the mandible after having checked that minimal inspiratory electrical activity was present during spontaneous breathing. All the EMGs were amplified and continuously recorded on a six channel recorder (Biograph, Russia). EMGs were displayed and visualized simultaneously. All the data were stored on PC for future analysis. To quantify the EMG, the signals were filtered (30 Hz–1,000 kHz) and integrated on a moving-time-average basis with a time constant of 150 ms. The peak amplitude of integrated EMG was measured for each inspiratory muscle during valid Müller's maneuver in all body positions. The amplitude was measured in arbitrary units and then expressed as a percentage of the maximum reached during Müller's maneuver in the standing position.

43.2.4 Study Design

Two researchers performed all the testing using the same equipment for all sessions. Thus, the same instructions, explanations, and encouragement were given to all subjects. Since Müller's maneuver was unfamiliar to participants, it was carefully explained. The researcher first demonstrated the correct maneuver. Then, each participant was asked to perform a few maximal inspiratory efforts in order to adopt for the correct performance of this test. After placement of all skin electrodes, the subject was asked to perform maneuver and maximal inspiratory pressure was measured. Maximal inspiratory efforts were maintained for 3–4 s separated by at least 1 min between efforts. For each body position, the subject performed a minimum of five maneuvers until two maximal pressure values were obtained which did not differ by more than 5%; the higher of the two was chosen for analysis. The maneuvers were performed in different positions in successive order with a resting period of 10 min in-between.

Six different positions were used:

1. Chair sitting: The subject sat in a chair with no armrests and was instructed not to slouch forward nor lean to either side. The chair had a fixed, padded back that was at 90° to the seat.
2. Standing: The subject adopted a comfortable stance.
3. Supine: The subject was positioned lying on his back on a padded tilt table (horizon). A little pillow was placed under the head.

4–5. Side lying: The subject was positioned lying on the right side, then on the left side on a padded tilt table. A pillow was placed under the head.

6. Head down: The subject was positioned as for the back lying position on a padded tilt table which was lowered, so that the subject's body was at a 30° angle, with the head lower than the feet.

Each subject was placed into the first position (1) and allowed to rest in this position for 5 min. After completing MIP testing in this position, subjects moved into the next successively assigned position (from 2 to 6). Testing would be terminated if the subject was too fatigued to continue or was unable to perform the test correctly.

43.2.5 Data Analysis

Data are presented as means ± SE. Those EMGs which corresponded to the higher MIP were chosen for analysis. Differences between MIP as well as the peak integrated EMGs during Müller's maneuver in the sitting, supine, RSL, LSL, and head-down positions were compared with data in the standing position (control, taken for 100%) with a *t*-test. The criterion for statistical significance was taken as $P<0.05$.

43.3 Results

43.3.1 Respiratory Muscle Force and Effect of Body Position

The mean MIP values in different body positions are presented in Fig. 43.1. For the six male subjects, MIP ranged from 88 to 119 cmH_2O (mean – 105.3 cmH_2O) in the standing position. For the four female subjects, the corresponding ranges were 46–79 cmH_2O (mean – 59.9 cmH_2O) in this position. These values are approximately in the normal range for males found by others (Leech et al. 1983; Sachs et al. 2009; Hautmann et al. 2000), but are somehow lower for females (Charfi et al. 1991; Sachs et al. 2009; Hautmann et al. 2000; Windisch et al. 2004). Sitting and both side-lying MIPs were similar to the standing MIP values in men and women (Fig. 43.1). The supine position resulted in lower values of MIP in both men and women, but there were no significant differences between the standing and supine MIPs. HDT led to results which were lower by 23% in men and 27% in women compared with those in the standing position ($P<0.05$).

43.3.2 Electromyographic Responses

We were able to obtain inspiratory EMG activity of all muscles during quiet breathing in all subjects. Also, appreciable phasic inspiratory activity during voluntary maximal inspiration against closed

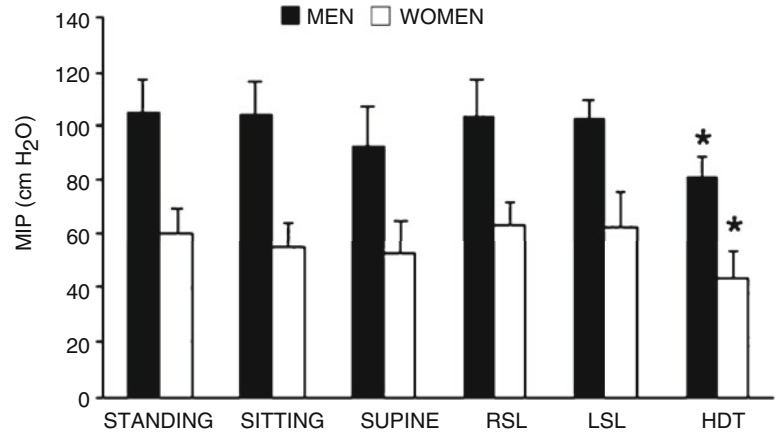

Fig. 43.1 Effects of body position on maximal inspiratory pressures measured at the mouth (MIP, cmH_2O) in male and female subjects with normal respiratory function. *RSL* right-sided lying, *LSL* left-sided lying, *HDT* head down tilt; *$P<0.05$ compared with the standing position

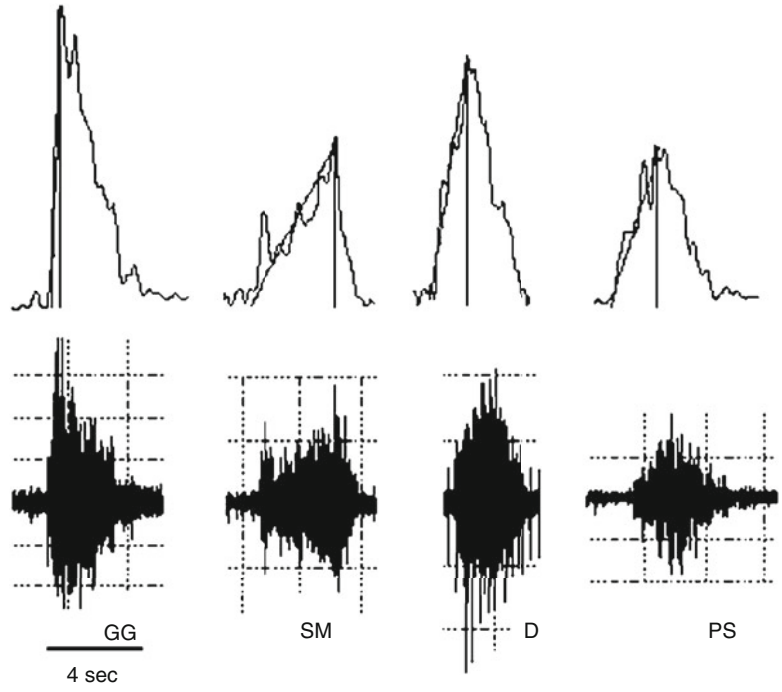

Fig. 43.2 Individual example of raw and moving-time averaged (time constant 150 ms) electromyograms of the diaphragm (*D*), intercostal parasternal (*PS*), sternocleidomastoid (*SM*), and genioglossus (*GG*) muscles during Müller's maneuver (in arbitrary units)

airways was obtained in all subjects in different body positions (Fig. 43.2). Diaphragmatic EMG recorded with surface electrodes mainly reflects the activity of the costal part, while the esophageal electrodes measure mainly activity in the crural part of the diaphragm. It has been shown that there is a good agreement between these two measurements, which suggests that activation of the two parts is similar in the tests used to measure maximal respiratory muscle strength. Surface electrodes may, therefore, provide viable information about diaphragm activity, which circumvents the not always acceptable for the subject issue of the introduction of a catheter through the nose (Nava et al. 1993). Integrated electrical activity of each muscle was expressed as a percentage of its value in the standing position, taken as 100%. The peak magnitude of diaphragmatic EMG activity during Müller's maneuver tended to increase in the sitting, RSL, and LSL positions ($P > 0.05$), but was significantly greater than that in the control before the maneuver by 121% in the supine and 139% in the HDT positions ($P < 0.05$) (Fig. 43.3). As illustrated in Fig. 43.3, the lower-than-control values for EPS were always achieved during Müller's maneuver in all body positions, especially in HDT (70%) compared with control ($P < 0.05$). When changing the position from standing to sitting, supine, RSL, and LSL, the values of ESM during the maximal inspiratory effort were all lower than those in the control by approximately 20%. The ESM values obtained during the inspiratory maneuver in HDT were lower by 28% compared with the standing position ($P < 0.05$). Body position significantly affected the EGG achieved by normal subjects during maximal inspiratory efforts. As shown in Fig. 43.3, Müller's maneuver produced the greatest EGG amplitude in the supine (125%) and HDT (130%) positions ($P < 0.05$), and less so, although still significantly, in sitting, RLS, and LSL positions ($P < 0.05$), amounting to 76, 57, and 43% of control, respectively.

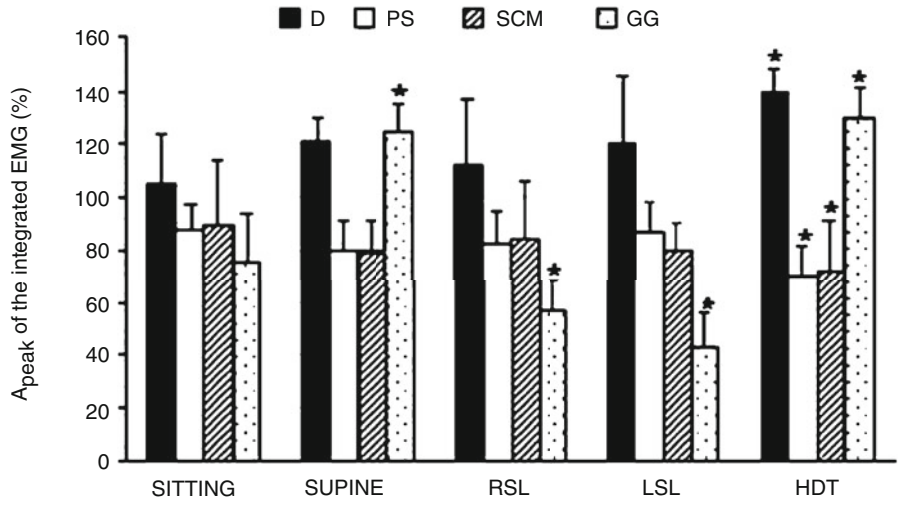

Fig. 43.3 Mean peak amplitudes of the integrated EMG of the diaphragm (*D*), intercostal parasternal (*PS*), sternocleidomastoid (*SM*), and genioglossus (*GG*) muscles during Müller's maneuver in the sitting, supine, right sided-lying (*RSL*), left sided-lying (*LSL*), and head down tilt (*HDT*) positions. The peak amplitude of EMGs was expressed as a percentage of the maximal values achieved during Müller's maneuver in the standing position. *RSL* right-sided lying, *LSL* left-sided lying, *HDT* head down tilt; *P < 0.05 compared with the standing position

43.4 Discussion

The purpose of this study was twofold. We sought to assess the effects of postural changes on the maximal inspiratory pressure and to compare the magnitude of the diaphragm and accessory inspiratory muscle activities evoked by a maximal, voluntarily increased drive to these muscles under different body positions, and finally to assess the relationship between the EMG and maximal inspiratory mouth pressure.

It is known that gender (Black and Hyatt 1969), age (Troosters et al. 2005), weight (BMI), and high (Wilson et al. 1984) are factors influencing inspiratory muscle force in normal subjects. In order to exclude the effects of these factors, to standardize conditions, and to evaluate exclusively the effect of postural changes on MIP we divided the subjects into the male and female groups. The subjects of either gender were of the similar age and had similar weight and high. The mean values of MIP obtained in Müller's maneuver in females appeared to be relatively lower than those reported in the literature (Charfi et al. 1991; Sachs et al. 2009; Hautmann et al. 2000; Windisch et al. 2004). The discrepancy may be related to a rather small number of female subjects in our study. Besides, in contrast to most previous studies, our subjects were naive and untrained, and it is known that higher values can only be achieved after specific muscle coordination training (Hawkes et al. 2007). Moreover, other individual features such as elastic recoil pressure of the respiratory system (Badr et al. 2002) and physical fitness (our unpublished results) also can influence the maximal respiratory pressure. When changing body position from standing to sitting, supine, RSL, and LSL, there were no significant alterations in maximal inspiratory pressure in both male and female subjects. But the supine position led to results which were lower than those in the standing position ($P > 0.05$), and the HDT led to results which were significantly lower than those all other positions ($P < 0.05$).

It has been shown in COPD patients that changes in body position may significantly influence MIP. Leaning forward, for example, may result in higher inspiratory pressures (O'Nelly and McCarthy 1983), while measurements obtained in the recumbent positions show lower pressures (Nava et al. 1993). In healthy subjects, some studies show that the standing, sitting and supine positions have no

significant influence on the result of the MIP measurement (Fiz et al. 1990), but other authors have found that MIP were lower in the supine position (Koulouris et al. 1989). Our results are in line with the last finding. The effect of HDT on maximal inspiratory pressure has not previously been described. Due to the limited data available and the lack of previous research it was hard to accurately compare the supine and HDT with other positions. There are data that maximal expiratory pressure is significantly lower in the supine and especially in HDT (−20° relatively horizon) positions compared with other positions (Badr et al. 2002).

In our study, the head down position had the lowest mean MIP in both male and female groups. One of the possible explanations for the diminished performance in this position is lack of practice (Badr et al. 2002). Not often do people find themselves in such a position in their everyday live. All the subjects of our study stated that they felt "uncomfortable" in the head down position. This may further limit their performance in this position. On the other hand, changes in muscle mechanics might influence MIP when changing from standing to supine and HDT. Gravity pulls the abdominal content caudally, increasing the vertical diameter of the thorax in the standing position (Castile et al. 1982). In the HDT, the abdominal content pushes the diaphragm up into the thoracic cavity, raising the diaphragm length and decreasing functional residual capacity (FRC) relative to the standing condition. The diaphragm length is then in a more optimal part of the length-tension relationship curve and may generate a higher intrathoracic pressure. At the same time, the diaphragm should displace abdominal content during inspiratory effort, overcoming the additional loading in HDT. So, the possible explanation of decreased MIP values in the head down position might be that the diaphragm is overloaded by abdominal content displacement during maximal inspiratory effort. And despite the diaphragm being at a more favorable position in the length-tension curve, increased force generated by it apparently cannot compensate for this mechanical load. Besides, the length of all other muscles may become less optimal in the supine and HDT positions; consequently a lower MIP is seen. For example, McCool and Leith (1987) have suggested that expiratory muscles attain their optimal length during standing. It is possible that decreased phasic activity of the sternocleidomastoid, parasternal, intercostal, and other accessory as well as expiratory muscles contributes to a decrease in MIP in the supine (Druz and Sharp 1981; Estenne et al. 1985; Heijdra et al. 1994) and HDT positions. To verify this supposition, we investigated the relationship between electrical activity and mechanical responses during Müller's maneuver.

The voluntary maximal inspiratory effort is a maneuver requiring activation, recruitment, and coordination of different muscle groups (Koulouris et al. 1989). In the present study, the trend of changes in peak integrated EMG of all muscles was similar in both groups of subjects in all body positions; therefore the data of male and female groups were combined (Fig. 43.3). We found that the difference in diaphragmatic EMG between the standing and HDT positions showed a trend toward being greater during Müller's maneuver. In contrast, supine and especially HDT positions elicited a decrease in peak inspiratory activity of the parasternal and sternocleidomastoids muscles during this maneuver compared to the standing position. These results confirm the possibility of decreased MIP in HDT because of a significant lower-than-control activation of PS and SCM. So, the diaphragm can be maximally activated during the voluntary inspiratory maneuver but other accessory muscles need not be activated fully in HDT.

The pattern of respiratory muscle activity suggests the existence of a possible hierarchy or coordination of muscle recruitment – specific muscle groups recruit in a particular order, when subject performs maximal inspiratory maneuver in different body positions. The diaphragm is maximally active during the voluntary inspiratory effort in all body positions, but in HDT. PS and SM, accessory muscles, acting in synergism with the diaphragm, are not necessarily active to the same extent.

The genioglossus is a major dilator muscle of upper airways. GG does not participate in the generation of maximal inspiratory pressure, but contributes to stabilization of airway patency. This muscle showed a significant dependence of its activation on postural changes during Müller's maneuver. It was minimally active during side-lying positions. The maximal activation of GG was obtained in supine and HDT

positions in all subjects. Upper airway dilator muscles are activated in phase with the respiratory cycle generated by the central nervous system. Studies have shown that non-physiological upper airway mechanoreceptive stimuli (e.g., rapidly imposed pulses of negative pressure) also activate these muscles. Such reflexes may become activated during conditions that alter airway resistance in order to stabilize airway patency (Akahoshi et al. 2001).

It is known that premotor drive from multiple descending pathways, i.e., from the motor cortex for voluntary respiratory tasks, including Müller's maneuver, may be integrated at the spinal cord (Aminoff and Sears 1971; Bellingham 1999). This may be due to direct, oligosynaptic pathways from the motor cortex to the diaphragm and intercostal motoneurons (Gandevia and Plassman 1988) or from local spinal reflexes. At the spinal level, all inputs acting on motoneurons and interneurons, including spinal reflexes, can be coordinated to produce the appropriate motor output (Bellingham 1999). The mechanism that generates the gradient of diaphragm and parasternal intercostal motoneuron output in both voluntary and involuntary efforts is also likely to occur at the spinal cord rather than medulla (DiMarco and Kowalski 2009; Kowalski and DiMarco 2009). Changes in the output of diaphragm and parasternal intercostal motoneurons during inspiratory efforts reveal an interplay between multiple descending drives to these motoneurons, and it is possible that these premotor drives are integrated at spinal interneurons and motoneurons (Hudson et al. 2010).

We conclude that the pressure generated during Müller's maneuver is a reflection of complex interactions between several muscle groups and changes in body positions from standing to supine and HDT might activate different muscles, resulting in a lower maximal inspiratory mouth pressure.

Conflicts of interest: The authors declare no conflicts of interest in relation to this article.

References

Akahoshi, T., White, D. P., Edwards, J. K., Beauregard, J., & Shea, S. A. (2001). Phasic mechanoreceptor stimuli can induce phasic activation of upper airway muscles in humans. *The Journal of Physiology, 531*, 677–691.

Aminoff, M. J., & Sears, T. A. (1971). Spinal integration of segmental, cortical and breathing inputs to thoracic respiratory motoneurons. *The Journal of Physiology, 215*, 557–575.

ATS/ERS. (2002). ATS/ERS statement on respiratory muscle testing. *American Journal of Respiratory and Critical Care Medicine, 166*, 518–624.

Badr, C., Elkins, M. R., & Ellis, E. R. (2002). The effect of body position on maximal expiratory pressure and flow. *The Australian Journal of Physiotherapy, 48*, 95–102.

Bellingham, M. C. (1999). Synaptic inhibition of cat phrenic motoneurons by internal intercostal nerve stimulation. *Journal of Neurophysiology, 82*, 1224–1232.

Black, L. F., & Hyatt, R. E. (1969). Maximal respiratory pressures: Normal values and relationships to age and sex. *American Review of Respiratory Disease, 99*, 696–702.

Castile, R., Mead, J., Jackson, A., Wohl, M. E., & Stokes, D. (1982). Effects of posture on flow volume curve configuration in normal humans. *Journal of Applied Physiology, 53*, 1175–1183.

Charfi, M. R., Matran, R., Regnard, J., Richard, M. O., Champeau, J., Dall'ava, J., & Lockhart, A. (1991). Maximal ventilatory pressure through the mouth in adults: Normal values and explanatory variables. *Revue des Maladies Respiratoires, 8*, 367–374.

Decramer, M., Lacquet, L. M., Fagard, R., & Rogiers, P. (1994). Corticosteroids contribute to muscle weakness in chronic airflow obstruction. *American Journal of Respiratory and Critical Care Medicine, 150*, 11–16.

DiMarco, A. F., & Kowalski, K. E. (2009). High frequency spinal cord stimulation of inspiratory muscles in dogs: A new method of inspiratory muscle pacing. *Journal of Applied Physiology, 107*, 662–669.

Druz, W. S., & Sharp, J. T. (1981). Activity of respiratory muscles in upright and recumbent humans. *Journal of Applied Physiology, 51*, 1552–1561.

Enright, P. L., Kronmal, R. A., Manolio, T. A., Schenker, M. B., & Hyatt, R. E. (1994). Respiratory muscle strength in the elderly: Correlates and reference values; Cardiovascular Health Study Research Group. *American Journal of Respiratory and Critical Care Medicine, 149*, 430–438.

Estenne, M., Yernault, J. C., & de Troyer, A. (1985). Rib cage and diaphragm-abdomen compliance in humans: Effects of age and posture. *Journal of Applied Physiology, 59*, 1842–1848.

Evans, J. A., & Whitelaw, W. A. (2009). The assessment of maximal respiratory mouth pressures in adults. *Respiratory Care, 54*, 1348–1359.

Fiz, J. A., Texido, A., Izquierdo, J., Ruiz, J., Roig, J., & Morera, J. (1990). Postural variation of the maximum inspiratory and expiratory pressure in normal subjects. *Chest, 97*, 313–314.

Gandevia, S. C., & Plassman, B. L. (1988). Responses in human intercostal and truncal muscles to motor cortical and spinal stimulation. *Respiration Physiology, 73*, 325–337.

Hautmann, H., Hefele, S., Schotten, K., & Huber, R. M. (2000). Maximal inspiratory mouth pressures in healthy subjects: What is the lower limit of normal? *Respiratory Medicine, 94*, 689–693.

Hawkes, E. Z., Nowicky, A. V., & McConnell, A. K. (2007). Diaphragm and intercostal surface EMG and muscle performance. *Respiratory Physiology & Neurobiology, 155*, 213–219.

Heijdra, Y. F., Dekhuijzen, P. N. R., van Herwaarden, C. L. A., & Folgering, H. T. M. (1994). Effect of body position, hyperventilation, and blood gas tension on maximal respiratory pressures in patients with chronic obstructive pulmonary disease. *Thorax, 49*, 453–458.

Hudson, A. L., Butler, J. E., Gandevia, S. C., & De Troyer, A. (2010). Interplay between the inspiratory and postural functions of the human parasternal intercostal muscles. *Journal of Neurophysiology, 103*, 1622–1629.

Koulouris, N., Mulvey, D. A., Laroche, C. M., Goldstone, J., Moxham, J., & Green, M. (1989). The effect of posture and abdominal binding on respiratory pressures. *The European Respiratory Journal, 2*, 961–965.

Kowalski, K. E., & DiMarco, A. F. (2009). Distribution of inspiratory drive to the external intercostal muscles during high frequency spinal cord stimulation. *American Journal of Respiratory and Critical Care Medicine, 179*, A4211. Abstract.

Lagri, F., & Tobin, M. J. (2003). Disorders of the respiratory muscles. *American Journal of Respiratory and Critical Care Medicine, 168*, 10–48.

Leech, J. A., Chezzo, H., Stevens, D., & Becklake, M. R. (1983). Respiratory pressures and function in young adults. *The American Review of Respiratory Disease, 128*, 17–23.

McCool, F. D., & Leith, D. E. (1987). Pathophysiology of cough. *Clinics in Chest Medicine, 8*, 189–195.

Nava, S., Ambrosino, N., Crotti, P., Fracchia, C., & Rampulla, C. (1993). Recruitment of some respiratory muscles during three maximal inspiratory manoeuvres. *Thorax, 48*, 702–707.

O'Nelly, S., & McCarthy, D. S. (1983). Postural relief of dyspnoea in severe chronic airflow limitation: Relationship to respiratory muscle strength. *Thorax, 38*, 595–600.

Sachs, M. C., Enright, P. L., Stukovsky, K. D. H., Jiang, R., & Barr, R. G. (2009). Performance of maximum inspiratory pressure tests and maximum inspiratory pressure reference equations for 4 race/ethnic groups. *Respiratory Care, 54*, 1321–1328.

Troosters, T., Gosselink, R., & Decramer, M. (2005). Respiratory muscle assessment. In R. Gosselink & H. Stam (Eds.), *Lung function testing* (European respiratory monograph, Vol. 31, pp. 57–71). Wakefield: European Respiratory Society Journals Ltd., Sheffield, UK.

Wilson, S. H., Cooke, N. T., Edwards, R. N. T., & Spiro, S. G. (1984). Predicted normal values for maximal respiratory pressures in Caucasian adults and children. *Thorax, 39*, 535–538.

Windisch, W., Henning, E., Sorichter, S., Hamm, H., & Griee, C. P. (2004). Peak or plateau maximal inspiratory mouth pressure: Which is best? *The European Respiratory Journal, 23*, 708–713.

Index

M. Pokorski (ed.), *Respiratory Regulation - The Molecular Approach*,
Advances in Experimental Medicine and Biology 756, DOI 10.1007/978-94-007-4549-0,